NUSANTARA BIOSCIENCE

ISEA JOURNAL OF BIOLOGICAL SCIENCES

| Nusantara Biosci | vol. 17 | no. 2 | pp. 185-374 | November 2025 |
| ISSN 2087-3948 | E-ISSN 2087-3956|

Triticum aestivum L. photo by Hans Hillewaert

Society for
Indonesian Biodiversity

Sebelas Maret University
Surakarta

Published semiannually

PRINTED IN INDONESIA

ISSN 2087-3948 E-ISSN 2087-3956

NUSANTARA
BIOSCIENCE
ISEAJournal of Biological Sciences
| Nusantara Biosci | vol. 17 | no. 2 | pp. 185-374 |Nov 2025 |
|ISSN 2087-3948| E-ISSN 2087-3956|

PUBLISHER: Smujo International

ASSOCIATION: Society for Indonesian Biodiversity

INSTITUTION: School of Graduates, Sebelas Maret University, Surakarta

FIRST PUBLISHED: 2009

ADDRESS:
Bioscience Program, School of Graduates, Sebelas Maret University
Jl. Ir. Sutami 36A Surakarta 57126, Indonesia. Tel. & Fax.: +62-271-663375, email: editors@smujo.id

ONLINE: smujo.id/nb

List of reviewers: https://smujo.id/nb/reviewers

Society for Indonesian Biodiversity **Sebelas Maret University Surakarta**

Published by Smujo International for The Society for Indonesian Biodiversity and Sebelas Maret University Surakarta

GUIDANCE FOR AUTHORS

Aims and Scope ***Nusantara Bioscience*** (Nusantara Biosci) encourages submission of manuscripts dealing with all aspects of biological sciences that emphasize issues germane to biological and nature conservation; especially for the research conducted in the Islands of the Southeast Asian reign or Nusantara, but also from around the world.

Article types The journal seeks original full-length: (i) **Research papers**, (ii) **Reviews**, and (iii) **Short communications**. Original research manuscripts are limited to 8,000 words (including tables and figures) or proportional to articles in this publication number. Review articles are also limited to 8,000 words, while Short communications should be less than 2,500 words, except for pre-study.

Submission: The journal only accepts online submissions through the open journal system **(https://smujo.id/nb/about/submissions)** or, for login problems, email the editors at unsjournals@gmail.com (or editors@smujo.id). Submitted manuscripts should be the original works of the author(s). Please ensure that the manuscript is submitted using the template, which can be found at (https://biodiversitas.mipa.uns.ac.id/D/template.doc). The manuscript must be accompanied by a cover letter containing the article title, the first name and last name of all the authors, and a paragraph describing the claimed novelty of the findings versus current knowledge. Please also provide a list of five potential reviewers in your cover letter. They should come from outside your institution and better from three different countries. Submission of a manuscript implies the submitted work has not been published (except as part of a thesis or report, or abstract) and is not being considered for publication elsewhere. When a group writes a manuscript, all authors should read and approve the final version of the submitted manuscript and its revision; and agree on the submission of manuscripts for this journal. All authors should have made substantial contributions to the concept and design of the research, acquisition of the data and its analysis, drafting the manuscript, and correcting the revision. All authors must be responsible for the work's quality, accuracy, and ethics.

Ethics Author(s) must be obedient to the law and/or ethics in treating the object of research and pay attention to the legality of material sources and intellectual property rights.

Copyright If the manuscript is accepted for publication, the author(s) still hold the copyright and retain publishing rights without restrictions. For the new invention, authors must manage its patent before publication.

Open Access The journal is committed to free-open access that does not charge readers or their institutions for access. Readers are entitled to read, download, copy, distribute, print, search, or link to the full texts of articles, as long as not for commercial purposes. The license type is CC-BY-NC-SA.

Acceptance Only articles written in US English are accepted for publication. Manuscripts will be reviewed by editors and invited reviewers (double-blind review) according to their disciplines. Authors will generally be notified of acceptance, rejection, or need for revision within 1 to 2 months of receipt. Manuscripts will be rejected if the content does not align with the journal scope, does not meet the standard quality, is in an inappropriate format, or contains complicated grammar, dishonesty (i.e., plagiarism, duplicate publications, fabrication of data, citations manipulation, etc.), or ignoring correspondence in three months. The primary criteria for publication are scientific quality and significance. **Uncorrected proofs** will be sent to the corresponding author by system or email as .doc or .docx files for checking and correcting typographical errors. The corrected proofs should be returned in 7 days to avoid publication delays. The accepted papers will be published online in chronological order at any time but printed at the end of each month.

Charges Publishing costs waiver is granted to foreign (non-Indonesian) authors who first publish the manuscript in this journal. However, other authors are charged USD 150 (IDR 2,100,000). **Reprint** Authors or other parties may freely download and distribute. However, a printed request will be charged, especially regarding postal charges.

Manuscript preparation Manuscript is typed on A4 (210x297 mm^2) paper size, in a single column, single space, 10-point (10 pt) Times New Roman font. The margin text is 3 cm from the top, 2 cm from the bottom, and 1.8 cm from the left and right. Smaller lettering sizes can be applied in presenting tables and figures (9 pt). Word processing program or additional software can be used; however, it must be PC compatible, use the template, and be Microsoft Word based (.doc or .rtf; not .docx). **Scientific names** of species (incl. subspecies, variety, etc.) should be written in italics, except in italicized sentences. Scientific names (genus, species, author) and cultivar or strain should be mentioned completely for the first time mentioning it in the body text, especially for taxonomic manuscripts. The genus name can be shortened after the first mention, except in early sentences, or where this may generate confusion; name of the author can be eliminated after the first mention. For example, *Rhizopus oryzae* L. UICC 524 can be written hereinafter as *R. oryzae* UICC 524. Using trivial names should be avoided. **Biochemical and chemical nomenclature** should follow the order of the IUPAC-IUB. For DNA sequences, it is better to use Courier New font. Standard chemical abbreviations can be applied for common and clear used, for example, completely written butilic hydroxyl toluene (BHT) to be BHT hereinafter. **Metric measurements** should use IS denominations, and other systems should use equivalent values with the denomination of IS mentioned first. A dot should not follow abbreviations like g, mg, mL, etc. Minus index (m^{-2}, L^{-1}, h^{-1}) suggested being used, except in things like "per-plant" or "per-plot." **Mathematical equations** can be written down in one column with text; in that case, they can be written separately. **Numbers** one to ten are written in words, except if it relates to measurement, while values above them are written in number, except in early sentences. The fraction should be expressed in decimal. In the text, it should be used "%" rather than "percent." Avoid expressing ideas with complicated sentences and verbiage/phrasing, and use efficient and effective sentences.

The title of the article should be written in compact, clear, and informative sentence, preferably not more than 20 words. Name of author(s) should be completely written, especially for the first and the last name. **Name and institution** address should also be completely written with street name and number (location), postal code, telephone number, facsimile number, and email address. We choose local names in Bahasa Indonesia for universities in Indonesia. The mention of "strata" program, should be avoided. Manuscript written by a group, author for correspondence along with address is required (marked with "♥"). **The title page** (first page) should include title of the article, full name(s), institution(s) and address(es) of the author(s); the corresponding authors detailed postage and e-mail addresses (P), and phone (O) and fax numbers (O).

Abstract A concise abstract is required (about 200 words). The abstract should be informative and state briefly the aim of the research, the principal results and major conclusions. An abstract is often presented separately from the article, thus it must be able to stand alone (completely self-explanatory). References should not be cited, but if essential, then cite the author(s) and year(s). Abbreviations should be avoided, but if essential, they must be defined at their first mention. **Keywords** are about five words, covering scientific and local name (if any), research themes, and special methods used; and sorted from A to Z. **Abbreviations** (if any): All important abbreviations must be defined at their first mention there. **Running title** is about five words.

Introduction is about 600 words, covering the aims of the research and provide an adequate background, avoiding a detailed literature survey or a summary of the results. **Materials and Methods** should emphasize on the procedures and data analysis. **Results and Discussion** should be written as a series of connecting sentences, however, for a manuscript with long discussion should be divided into subtitles. Thorough discussion represents the causal effect mainly explains why and how the results of the research were taken place, and do not only re-express the mentioned results in the form of sentences. **Concluding** sentence should be given at the end of the discussion. **Acknowledgements** are expressed in a brief; all sources of institutional, private and corporate financial support for the work must be fully acknowledged, and any potential conflicts of interest are noted.

Figures and Tables of a maximum of three pages should be clearly presented. The title of a picture is written down below the picture, while the title of a table is written above the table. Colored figures can only be accepted if the information in the manuscript can lose without those images; the chart is preferred to use black and white images. The author could consign any picture or photo for the front cover, although it does not print in the manuscript. All images property of others should be mentioned the source. Author is suggested referring to Wikipedia for international boundaries and Google Earth for satellite imagery. If not specifically mentioned, it is assumed to refer to these sources. **There is no appendix**, all data or data analysis is incorporated into Results and Discussions. For broad data, it can be displayed on the website as a supplement.

References Preferably 80% of it comes from scientific journals published in the last 10 years. In the text, give the author names followed by the year of publication and arrange from oldest to newest and from A to Z; in citing an article written by two authors, both of them should be mentioned; however, for three and more authors only the first author is mentioned followed by et al. For example, Saharjo and Nurhayati (2006) or (Boonkerd 2003a, b, c; Sugiyarto 2004; El-Bana and Nijs 2005; Balagadde et al. 2008; Webb et al. 2008). Extent citation should be avoided, as shown with the word "cit." Reference to unpublished data and personal communication should not appear in the list but should be cited in the text only (e.g., Rifai MA 2007, pers. com. (personal communication); Setyawan AD 2007, unpublished data). In the reference list, the references should be listed in alphabetical order. Names of journals should be abbreviated. Always use the standard abbreviation of a journal's name according to the **ISSN List of Title Word Abbreviations** (www.issn.org/2-22661-LTWA-online.php). Please include DOI links for journal papers. The following examples are for guidance.

Journal:

Saharjo BH, Nurhayati AD. 2006. Domination and composition structure change at hemic peat natural regeneration following burning; a case study in Pelalawan, Riau Province. Biodiversitas 7: 154-158. DOI: 10.13057/biodiv/d070213.

The usage of "et al." in long author lists will also be accepted:

Smith J, Jones M Jr, Houghton L et al. 1999. Future of health insurance. N Engl J Med 965: 325-329. DOI: 10.10007/s002149800025.

Book:

Rai MK, Carpinella C. 2006. Naturally Occurring Bioactive Compounds. Elsevier, Amsterdam.

Chapter in the book:

Webb CO, Cannon CH, Davies SJ. 2008. Ecological organization, biogeography, and the phylogenetic structure of rainforest tree communities. In: Carson W, Schnitzer S (eds.). Tropical Forest Community Ecology. Wiley-Blackwell, New York.

Abstract:

Assaeed AM. 2007. Seed production and dispersal of *Rhazya stricta*. 50th annual symposium of the International Association for Vegetation Science, Swansea, UK, 23-27 July 2007.

Proceeding:

Alikodra HS. 2000. Biodiversity for development of local autonomous government. In: Setyawan AD, Sutarno (eds.). Toward Mount Lawu National Park; Proceeding of National Seminary and Workshop on Biodiversity Conservation to Protect and Save Germplasm in Java Island. Universitas Sebelas Maret, Surakarta, 17-20 July 2000. [Indonesian]

Thesis, Dissertation:

Sugiyarto. 2004. Soil Macro-invertebrates Diversity and Inter-Cropping Plants Productivity in Agroforestry System based on Sengon. [Dissertation]. Universitas Brawijaya, Malang. [Indonesian]

Information from the internet:

Balagadde FK, Song H, Ozaki J, Collins CH, Barnet M, Arnold FH, Quake SR, You L. 2008. A synthetic *Escherichia coli* predator-prey ecosystem. Mol Syst Biol 4: 187. DOI: 10.1038/msb.2008.24. www.molecularsystembiology.com.

NUSANTARA
BIOSCIENCE
| Nusantara Biosci | vol. 17 | no. 2 | pp. 185-374 | Nov 2025|
| ISSN 2087-3948 | E-ISSN 2087-3956|
ISEAJournal of Biological Sciences

Stand structure, diversity, and carbon stock assessment of Lake Duluti Forest Reserve in Tanzania **185-193**
UPENDO SHWAIBU MFINANGA, EZEKIEL EDWARD MWAKALUKWA

Effect of tannin and amino acid supplementation on growth, digestibility, and blood parameters in heifer calves **194-201**
LU'LU' NABILA SALSABILA, AINISSYA FITRI, FAJAR EDY MARETNO SITANGGANG, IDAT GALIH PERMANA, WARTIKA ROSA FARIDA, DWITAMI ANZHANY, RONI RIDWAN

Destructive sampling-based allometric equations for biomass and carbon estimation in *Acacia* hybrid plantations in Southeastern Vietnam **203-217**
NGUYEN THI HA, TRAN QUANG BAO, NGUYEN THANH TUAN, DIEGO I. RODRÍGUEZ-HERNÁNDEZ, NGUYEN TIEN DUNG, TRAN THI NGOAN

Morphological characterization and correlation of seed, fruit, and seedling of *Horsfieldia iryaghedhi* (Gaertn.) Warb. **218-225**
INDRIANI EKASARI, SAHROMI, PUTRI KESUMA WARDHANI

Fatty acid profile of *Chlorella sorokiniana* InaCC M8 grown in tofu wastewater for biofuel potential **226-234**
DEVY SUSANTY, LUSI NURUL SAFITRI, RICSON PEMIMPIN HUTAGAOL, ADE AYU OKSARI, NURLELA

Effect of temperature on rice (*Oryza sativa*) seedling disease incidence and severity in Bangladesh **235-242**
MD. TANBIR RUBAYET, FARHANA PRODHAN, MD. ABDULLAH AL MAMUN, MD. ABDUL KADER, MD. MOTAHER HOSSAIN, MD. MAHIDUL ISLAM MASUM, MUHAMMAD ZIAUL HOQUE, MD. MIZANUR RAHMAN, JATISH CHANDRA BISWAS

Effect of light and media composition on growth and stomatal density of *Phalaenopsis amboinensis* **243-252**
MUHAMMAD ALANWARI NUGRAHA, DWI MURTI PUSPITANINGTYAS, HARYANTO

Dengue virus and *Plasmodium* coinfection among febrile patients in Osun State, Nigeria **253-258**
BABAJIDE B. AJAYI, KEHINDE S. OLAITAN, OLUWATOBA F. OWOYOMI, SUNDAY E. ONI, AKINWALE M. AKINLABI, ELIZABETH O. ARO, DAVID O. OGBOLU

Bamboo diversity, ecological structure, and utilization in the riparian ecosystem of the Upper Bengawan Solo River, Central Java, Indonesia **259-276**
FIKA NUR APRILIA, FRANSISCA AMELIA KARTIKA ARDHYANTI, GHAZY AQILA SHANDY PRABOWO, HANA PARAMESTI, ANA SHOLEKAH ASZAR, CHEE KONG YAP, AHMAD DWI SETYAWAN

Assessing tourist experience and willingness to pay for biodiversity conservation at Mongkrang Hill, Mount Lawu, Central Java, Indonesia **277-288**
ARDITA AYU WULANDARI, ARUM NUR MUKARROMAH, ASFI DZIHNI, ATIKAH KHOIRIYAH AZZAM, ANGGUN DERISTANI, SUNARTO, AHMAD DWI SETYAWAN

Gamma-ray irradiation induced polymorphism in *Echinacea purpurea* revealed by RAPD markers **289-297**
AGUSTINA PUTRI CAHYANINGSIH, NITA ETIKAWATI, AHMAD YUNUS

Phylogeny and recombination of papaya begomoviruses in Northern and Central-East India **298-312**
AARSHI SRIVASTAVA, VINEETA PANDEY, RAKESH KUMAR VERMA, AVINASH MARWAL, RAMWANT GUPTA, MUHAMMAD SHAFIQ SHAHID6, R. K. GAUR

Effect of phosphorus and potassium on growth and yield parameters and disease incidence of potato **313-321**
MOHAMMAD SAIDUL ISLAM, ABU ASHRAF KHAN, MD. TANBIR RUBAYET, MD. MOYNUL HAQUE, MD. ABDUL KARIM, ISMAIL HOSSAIN MIAN

Updated information on qualitative leaf anatomical characters of *Eusideroxylon zwageri* Teijsm. and Binn. from East Kalimantan **322-336**
ASIH PERWITA DEWI, TRI Y.I. WULANSARI, SENI K. SENJAYA, DEBY ARIFIANI, IRVAN F. WANDA, YUNITA LISNAWATI, SUNARDI, APRILIANA D. PRAWESTRI, IRFAN MARTIANSYAH, EVANA, RIZKY D. SATRIO, ANJALI M.N.K. HARTONO, SUYOKO, ADE Y. YUSWANDI, MUHAMMAD SYUKUR, DEA K. SARI, CHIKA A. RASYL

Diversity of urban street tree communities in Semarang District, Indonesia **337-354**
ARDHIAN ABDUL MADJID, ARDITA AYU WULANDARI, ASFI DZIHNI, MARIO PINTOR DAVID SIMANJUNTAK, SAFIRA CHAIRUNISA, ARU DEWANGGA, WIDHI HIMAWAN, INOCENCIO E. BUOT JR, AHMAD DWI SETYAWAN

Invasion dynamics and elevational range expansion of insects in tropical agricultural landscapes of Wonosobo, Central Java, Indonesia **355-374**
SIBRINA SALSABILA, ROI ANDRIANTO, SYARIFAH HASNA ROSYIDA, SAKINA ENOVA RAHMADHANI, QUROTUL AINIA, ARU DEWANGGA, AHMAD DWI SETYAWAN

THIS PAGE INTENTIONALLY LEFT BLANK

NUSANTARA BIOSCIENCE
Vol. 17, No. 2, pp. 185-193
November 2025

ISSN: 2087-3948
E-ISSN: 2087-3956
DOI: 10.13057/nusbiosci/n170201

Stand structure, diversity, and carbon stock assessment of Lake Duluti Forest Reserve in Tanzania

UPENDO SHWAIBU MFINANGA, EZEKIEL EDWARD MWAKALUKWA♥
Department of Ecosystems and Conservation, College of Forestry, Wildlife and Tourism, Sokoine University of Agriculture. PO. Box 3010, Chuo Kikuu, Morogoro, Tanzania. Tel./fax.: +255-23-2604648, ♥email: ezedwa@sua.ac.tz

Manuscript received: 19 March 2025. Revision accepted: 18 June 2025.

Abstract. *Mfinanga US, Mwakalukwa EE. 2025. Stand structure, diversity, and carbon stock assessment of Lake Duluti Forest Reserve in Tanzania. Nusantara Bioscience 17: 185-193.* For a successful conservation of biodiversity in a particular forest, assessment of its status and underlying threats is important. Estimation of carbon stocks locked up in the forest is also key in designing the required climate change mitigation options. However, there is limited information on the biodiversity status and carbon storage potential of many forest reserves in Tanzania. This study assessed the tree and shrub species diversity, composition, stand structure, and carbon stock potential of the Lake Duruti Forest Reserve (LDFR). Data were collected from 40 systematically established concentric plots (0.071 ha each) covering a total forest area of 26.24 ha. A total of 48 tree and shrub species were recorded, comprising both adult individuals (DBH ≥ 5 cm) and regenerants (DBH < 5 cm), representing 25 plant families. Adult individuals accounted for 42 species from 23 families, while regenerants included 22 species from 15 families. The Shannon-Wiener diversity index (H′) was 3.21 for adults and 2.80 for regenerants, indicating high species diversity. The mean stem density of adult trees was 197 ± 97 stems ha^{-1}, with a basal area of 16.27 ± 7.30 m^2 ha^{-1}. The estimated above-ground carbon stock was 79.24 ± 35.31 Mg C ha^{-1}, while below-ground carbon stock was 30.86 ± 12.77 Mg C ha^{-1}. The absence of visible anthropogenic disturbance suggests effective conservation measures are in place. These findings highlight the ecological stability and carbon sequestration potential of LDFR and highlight the need for strategic planning to enhance biodiversity conservation and carbon stock management.

Keywords: Catchment forests, climate change, eco-tourism, vegetation composition, volcanic lakes

INTRODUCTION

Tanzania is globally recognized for its exceptional biodiversity, iconic tourist attractions, and significant role in global conservation efforts (URT 2021a). The country's protected areas, under central government jurisdiction, cover approximately 307,800 km^2—equivalent to 32.5% of the total land area (NAFORMA 2015; URT 2021a). These areas include 21 National Parks, 29 Game Reserves, 23 Game Controlled Areas, the Ngorongoro Conservation Area, 22 Nature Forest Reserves, various other forest reserves, and marine parks and reserves (URT 2015; NAFORMA 2015; URT 2021a). Additionally, about 1.4 million hectares of gazetted catchment forests contribute to the network of protected landscapes (NAFORMA 2015).

These protected areas are crucial not only for biodiversity conservation and climate change mitigation but also as key revenue generators through tourism. Tourism contributes approximately 17% to Tanzania's national GDP and accounts for 25% of total export earnings, making it a cornerstone of the national economy (URT 2021a). Serengeti National Park, for example, generates over 53% of Tanzania National Parks revenue and is globally known for the Great Migration. However, the revenue potential of other protected areas remains underexplored.

In 2022, the Tanzania Forest Services Agency (TFS) reported increased tourist visits to the country's nature forest reserves, collecting approximately USD 550,000 from 242,824 visitors (Ract et al. 2024). This highlights growing interest in eco-tourism beyond traditional wildlife safaris. Nevertheless, limited awareness of the biodiversity and attractions within forest reserves continues to constrain revenue generation from these sites. The availability of ecological and biodiversity information is therefore critical to promoting eco-tourism and attracting a broader spectrum of visitors (URT 1998; URT 2021b).

Lake Duluti Forest Reserve (LDFR), located in the Arumeru District of the Arusha Region, is one such underutilized catchment forest reserve (Iddi 1998; NAFORMA 2015). The reserve, notable for its ecological, hydrological, and cultural significance, contains a central volcanic lake that serves as a key tourist attraction. It also supports a variety of ecologically important flora and fauna (TFS 2022). However, no previous study has documented the plant species composition or carbon storage potential of LDFR. The absence of such information may have contributed to its lower profile among tourist destinations in northern Tanzania, consequently limiting the revenue potential for TFS, the agency responsible for its management.

This study was conducted to assess the forest condition and carbon storage potential of the Lake Duluti Forest Reserve. The findings aim to fill critical knowledge gaps and enhance public awareness of the ecological functions of tropical moist forests, particularly their role in climate change mitigation. Specifically, the study aimed to: (i) assess tree and shrub species diversity and composition in

LDFR; (ii) determine the stand structure (stem density, basal area, and diameter distribution) of tree and shrub species; (iii) evaluate the regeneration status of tree and shrub species; and (iv) estimate the above- and below-ground carbon stocks within LDFR.

MATERIALS AND METHODS

Study area

Lake Duluti Forest Reserve (LDFR) is a protected catchment forest managed by the Tanzania Forest Services Agency (TFS) under the Ministry of Natural Resources and Tourism (TFS 2022). The reserve is located in Akheri Ward, Arumeru District, approximately 14 km from Arusha City, at coordinates 3°23′S and 36°47′E and an elevation of 1,290 meters above sea level (Lovett and Pócs 1993; TFS 2022) (Figure 1). The site is accessible via a 1.3 km road from Tengeru Township off the Arusha-Moshi highway. LDFR was initially gazetted under Government Notice No. 314 on 2 July 1965. Following a resurvey in 2017, the reserve boundaries were revised and officially updated in Government Notice No. 694 of 28 August 2020 (Map JB No. 2774) to incorporate previously excluded forest areas (TFS 2022). The total area of the reserve, including the lake, is approximately 86.24 ha. Lake Duluti occupies about 60 ha, while the surrounding forest spans approximately 26.24 ha (Lovett and Pócs 1993). The lake, a volcanic crater, has an estimated depth of 700 meters. Despite its volcanic origin, the water is non-saline, suggesting that rainfall is the primary source of recharge. It remains full throughout the year, sustained by underground springs, with no visible surface inflows or outflows.

The local climate is characterized by oceanic rainfall and continental temperatures, with an annual average precipitation of approximately 1,100 mm. Mean monthly maximum temperatures reach 21°C in March, and minimum temperatures drop to about 17°C in July (Lovett and Pócs 1993). The forest structure is largely influenced by groundwater availability. Submontane forest thrives in areas 5-10 m above the lake level and 20-50 m from the shore, where groundwater is abundant. On the upper slopes, where groundwater is limited, dry montane forest dominates. Additionally, a floating island of *Cyperus papyrus* L. has formed along the lake's northern shoreline (Lovett and Pócs 1993). The reserve serves as a vital water source for the Tengeru settlement, the Agricultural Training Institute, and adjacent coffee farms through a water plant situated on the eastern lake edge. LDFR also holds significant recreational value, attracting eco-tourism activities such as canoeing and sport fishing. The forest reserve supports a variety of wildlife, including small mammals like the vervet monkey (*Cercopithecus aethiops* subsp. *pygerythrus*), blue monkey (*Cercopithecus neumanni*), black-and-white colobus (*Colobus guereza* Rüppell, 1835), and marsh mongoose (*Ichneumia albicauda* (G.Cuvier, 1829)). LDFR also provides an important breeding habitat for birds. Common avian species observed include the white-faced whistling duck (*Dendrocygna viduata* (Linnaeus, 1766)), chestnut weaver (*Ploceus rubiginosus* Rüppell, 1840), bronze mannikin (*Lonchura cucullata* (Swainson, 1837)), and little swift (*Apus affinis* (J.E.Gray, 1830)).

LDFR is bordered by Patandi Village, which has an estimated population of 6,070. The local economy primarily depends on agriculture and livestock keeping, although some residents are also engaged in cultural eco-tourism and the sale of forest products such as honey harvested from homesteads (TFS 2022).

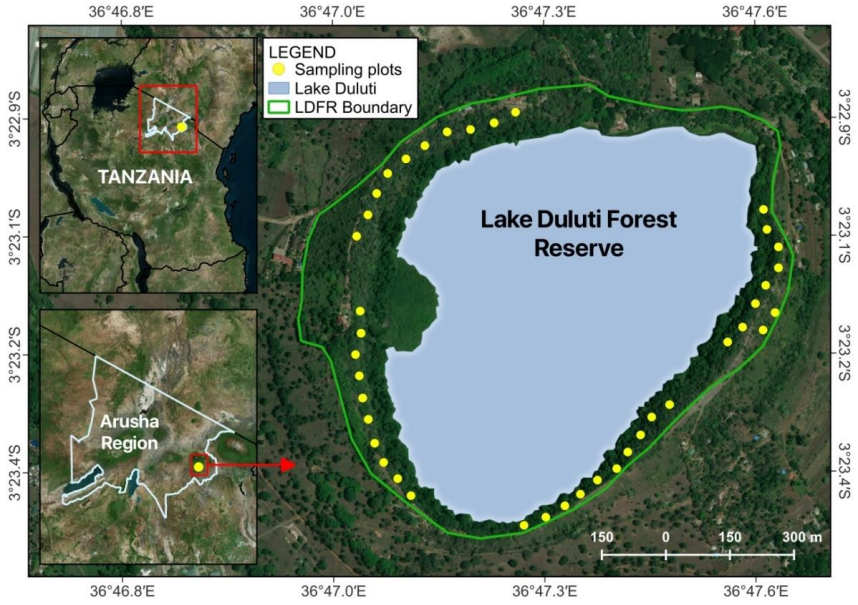

Figure 1. Map of Arusha region, Tanzania, showing the location of the Lake Duluti Forest Reserve (RDFR) and the layout of sample plots in the reserve (filled yellow circles)

Data collection

A systematic sampling design was employed for ecological data collection. Forty circular sample plots, each with a 15 m radius, were established at intervals of 50 m both within and between transect encircling the lake. In each plot, vegetation data were collected using concentric subplots of different radii, based on Diameter at Breast Height (DBH) classes: Within a 2 m radius: all regenerants with DBH < 5 cm were identified, counted, and recorded; within a 5 m radius: all trees and shrubs with DBH ≥ 5 cm and < 10 cm were measured, identified, and recorded; within a 10 m radius: all individuals with DBH ≥ 10 cm and < 20 cm were recorded similarly; within a 15 m radius: all trees and shrubs with DBH ≥ 20 cm were measured and recorded. Plot coordinates and elevations were recorded using a handheld GPS device.

Data analysis

The collected data were analyzed for species richness, composition, diversity, stem density, basal area, and estimation of above- and below-ground biomass and carbon stocks. Species richness was determined by compiling a comprehensive list of plant species across all sample plots. Species diversity was calculated using the Shannon-Wiener diversity index ($H' = -\Sigma pi \ln Pi$), where Pi is the proportion individuals belonging to the i^{th} species (Kent 2012). The species Importance Values Index (IVI) was calculated as the sum of the relative frequency, relative density, and relative basal area (Kent and Coker 1992). Stem density (number of stems per hectare) was calculated using the formula: $N = (n/a_i)$, where n is the number of individuals in a plot, and a_i is the area of plot (ha). Basal area (m^2 ha^{-1}) was calculated from the DBH measurement using the formula: $G = (G_i/n)$, where G_i is the basal area of a plot (m^2 ha^{-1}), and n = number of sample plots.

The allometric models developed by Masota et al. (2016) for lowland and humid montane forests were employed to estimate both above-ground and below-ground biomass of the forest. Subsequently, the biomass values were converted into carbon stock per hectare by applying a carbon conversion factor of 0.49, as recommended by Manyanda et al. (2020). The resulting carbon stocks were expressed in megagrams of carbon per hectare (Mg C ha^{-1}).

The following equations were applied for biomass estimation:

Total tree above-ground biomass (kg) = $0.9635 \times DBH^{1.9440}$ (n = 60, RMSE (kg) = 1020.3, $R^2 = 0.80$, MPE (%) = 0.0).

Total tree below-ground biomass (kg) = $7.5811 \times DBH^{1.16801}$ (n = 29, RMSE (kg) = 312.7, R^2=0.71, MPE (%) = 2.0).

Where DBH refers to the diameter at breast height (cm), RMSE denotes the root mean square error, R^2 indicates the coefficient of determination and MPE represents the mean percentage error.

RESULTS AND DISCUSSION

Species richness and composition

A total of 48 tree and shrub species of both adults (≥ 5 cm Dbh) and regenerants (< 5 cm Dbh) belonging to 25 plant families and 41 genera were identified and recorded in the forest (Tables 1 and 2). Trees contributed the most to the identified species (83%), while shrubs contributed the least (17%). Tree species accounted for the majority of observations (83%), whereas shrubs contributed only 17%. The most represented plant families were Fabaceae and Moraceae, each with five species. These were followed by Euphorbiaceae, Meliaceae, Rubiaceae, and Rutaceae, which each comprised three species. The remaining families generally contained one or two species.

For adult individuals (DBH ≥ 5 cm), a total of 290 trees were measured, with diameters ranging from 5 to 160 cm. These individuals represented 42 species across 23 families and 36 genera (Table 1). As with the total count, tree species dominated (83%), while shrubs remained a minority (17%). Fabaceae and Moraceae remained the most prevalent families, each with five species. Additional common families among adults included Anacardiaceae, Euphorbiaceae, Meliaceae, and Rutaceae, each represented by three species (Table 1). The three most ecologically dominant adult species, based on the Importance Value Index (IVI), were *Bridelia micrantha* (Hochst.) Baill. (42.5%), *Ficus sycomorus* L. (34.4%), and *Sorindeia madagascariensis* (Spreng.) DC. (22.8%) (Table 1). In contrast, the least represented species in the reserve were *Cedrela odorata* L. (0.9%), *Garcinia* sp. (0.9%), and *Obetia radula* (Baker) B.D.Jacks. (0.7%). On average, five species were recorded per sampling plot, with species richness per plot ranging from 2 to 8. The species accumulation curve (Figure 2) reached an asymptote, suggesting that the sampling effort was adequate to capture the majority of tree and shrub species present in the forest.

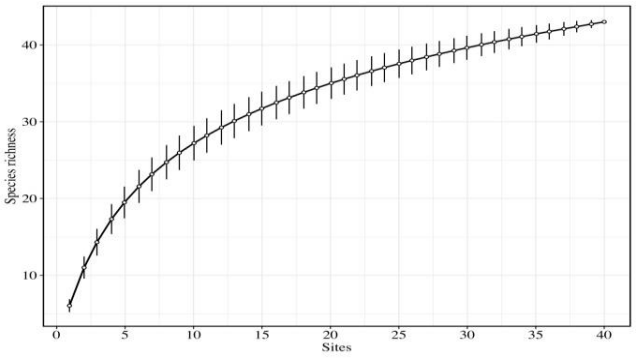

Figure 2. Species accumulation curve of tree species in the Lake Duluti Forest Reserve, Arumeru District in Tanzania. The curve depicts the expected number of species as a function of the sampled area, with the upper and lower bounds representing the 95% confidence intervals

Table 1. Checklist of adult tree and shrub species with Dbh ≥ 5 cm sorted by IVI identified in the Lake Duluti Forest Reserve, Arumeru district, Tanzania

Botanical name	Family	Habit	Frequency (%)	*H'	Rf (%)	RDe (%)	RDo (%)	IVI	Density (stems ha^{-1})	Basal area (m^2ha^{-1})	AGC (Mg C ha^{-1})	BGC (Mg C ha^{-1})
Bridelia micrantha (Hochst.) Baill.	Phyllanthaceae	Tree	65	0.28	12.9	12.8	16.7	42.5	19±4	1.91±0.42	9.43±2.05	3.95±0.70
Ficus sycomorus L.	Moraceae	Tree	40	0.20	8.0	6.0	20.5	34.4	8±2	4.83±1.24	22.85±5.84	5.12±1.19
Sorindeia madagascariensis DC.	Anacardiaceae	Tree	40	0.21	8.0	8.4	6.4	22.8	16±7	1.31±0.71	6.44±3.44	2.68±1.11
Newtonia buchananii (Baker) G.C.C.Gilbert & Boutique	Fabaceae	Tree	27.5	0.13	5.5	6.8	6.3	18.5	9±3	0.88±0.52	4.21±2.45	1.37±0.50
Drypetes gerrardii Hutch.	Putranjivaceae	Tree	30	0.18	6.0	7.4	3.1	16.5	19±8	0.42±0.14	2.16±0.71	1.67±0.60
Trichilia emetica (Forssk.) Vahl	Meliaceae	Tree	30	0.16	6.0	4.8	4.3	15.0	7±2	0.78±0.33	3.81±1.61	1.52±0.51
Albizia gummifera (J.F.Gmel.) C.A.Sm.	Fabaceae	Tree	27.5	0.16	5.5	3.6	4.0	13.1	7±2	0.71±0.26	3.43±1.27	1.50±0.53
Turraea robusta Gürke	Meliaceae	Shrub	20	0.13	4.0	5.0	2.8	11.8	7±3	0.23±0.10	1.18±0.51	0.82±0.32
Deinbollia kilimandscharica Taub.	Sapindaceae	Shrub	15	0.11	3.0	4.3	2.2	9.5	11±6	0.21±0.09	1.08±0.48	0.82±0.34
Allophylus africanus P.Beauv.	Sapindaceae	Shrub	15	0.10	3.0	4.5	1.9	9.3	12±7	0.22±0.11	1.23±0.54	0.94±0.39
Psychotria capensis subsp. *riparia* (K.Schum. & K.Krause) Verdc.	Rubiaceae	Shrub	12.5	0.09	2.5	5.5	1.2	9.1	15±7	0.08±0.04	0.43±0.20	0.66±0.30
Croton megalocarpus Hutch.	Euphorbiaceae	Tree	15	0.15	3.0	3.4	2.5	8.9	10±5	0.31±0.12	1.58±0.63	1.09±0.45
Ficus sur Forssk.	Moraceae	Tree	12.5	0.07	2.5	2.3	3.0	7.7	2±1	0.50±0.29	2.41±1.39	0.73±0.36
Albizia petersiana (Bolle) Oliv.	Fabaceae	Tree	7.5	0.12	1.5	2.6	3.4	7.5	5±3	0.45±0.30	2.24±1.48	1.05±0.68
Trilepisium madagascariense DC.	Moraceae	Tree	12.5	0.09	2.5	3.4	1.6	7.5	9±7	0.14±0.07	0.73±0.35	0.56±0.25
Cordia africana Lam.	Boraginaceae	Tree	12.5	0.08	2.5	0.9	2.3	5.7	2±1	0.89±0.64	4.19±2.99	0.98±0.54
Rauvolfia caffra Sond.	Apocynaceae	Tree	12.5	0.08	2.5	1.2	1.7	5.4	2±1	0.23±0.11	1.17±0.53	0.54±0.23
Cussonia holstii Harms ex Engl.	Araliaceae	Tree	7.5	0.06	1.5	1.9	1.7	5.0	3±2	0.09±0.06	0.46±0.32	0.31±0.19
Strychnos sp.	Loganiaceae	Tree	10	0.10	2.0	2.2	0.5	4.7	8±5	0.07±0.04	0.38±0.20	0.45±0.23
Ficus lutea Vahl	Moraceae	Tree	7.5	0.05	1.5	0.8	2.1	4.4	1±1	0.21±0.13	1.05±0.66	0.38±0.23
Spathodea campanulata P.Beauv.	Bignonaceae	Tree	5	0.05	1.0	0.8	2.0	3.7	1±1	0.37±0.28	1.80±1.33	0.52±0.36
Dombeya rotundifolia (Hochst.) Planch.	Malvaceae	Tree	7.5	0.05	1.5	0.9	1.0	3.4	2±1	0.08±0.05	0.41±0.23	0.25±0.14
Ozoroa insignis Delile	Anacardiaceae	Tree	5	0.05	1.0	1.1	1.2	3.3	2±1	0.11±0.10	0.56±0.49	0.28±0.23
Vangueria infausta Burch.	Rubiaceae	Shrub	7.5	0.05	1.5	1.0	0.8	3.3	2±1	0.04±0.02	0.21±0.13	0.19±0.11
Tabernaemontana ventricosa Hochst. ex A.DC.	Apocynaceae	Tree	7.5	0.05	1.5	1.1	0.3	2.9	2±1	0.04±0.02	0.20±0.12	0.20±0.11
Sarcomelicope simplicifolia (Endl.) T.G.Hartley	Rutaceae	Tree	5	0.03	1.0	1.4	0.3	2.7	4±3	0.04±0.03	0.22±0.15	0.25±0.18
Combretum molle R.Br. ex G.Don	Combretaceae	Tree	5	0.05	1.0	0.7	0.8	2.6	1±1	0.06±0.04	0.32±0.23	0.19±0.14
Celtis africana Burm.f.	Cannabaceae	Tree	5	0.03	1.0	0.4	0.9	2.3	1±0	0.08±0.06	0.38±0.32	0.17±0.13
Albizia chinensis (Osbeck) Merr.	Fabaceae	Tree	2.5	0.03	0.5	0.6	0.9	2.0	1±1	0.09±0.09	0.45±0.45	0.20±0.20
Manilkara sp.	Sapotaceae	Tree	2.5	0.02	0.5	0.2	0.8	1.5	0±0	0.08±0.08	0.37±0.37	0.14±0.14
Senna siamea (Lam.) H.S.Irwin & Barneby	Fabaceae	Tree	2.5	0.03	0.5	0.5	0.4	1.4	2±2	0.02±0.02	0.11±0.11	0.12±0.12
Commiphora eminii Engl.	Burseraceae	Tree	2.5	0.02	0.5	0.3	0.5	1.3	0±0	0.08±0.08	0.41±0.41	0.14±0.14
Rhus natalensis Bernh.	Anacardiaceae	Shrub	2.5	0.02	0.5	0.6	0.2	1.3	3±3	0.02±0.02	0.13±0.13	0.17±0.17
Ficus thonningii Blume	Moraceae	Tree	2.5	0.02	0.5	0.1	0.6	1.2	0±0	0.54±0.54	2.53±2.53	0.43±0.43
Calodendrum capense (L.f.) Thunb.	Rutaceae	Tree	2.5	0.02	0.5	0.5	0.1	1.1	1±1	0.01±0.01	0.04±0.04	0.05±0.05
Clausena anisata (Willd.) Hook.f.	Rutaceae	Shrub	2.5	0.02	0.5	0.4	0.1	1.0	1±1	0.01±0.01	0.05±0.05	0.05±0.05
Croton sylvaticus Hochst.	Euphorbiaceae	Tree	2.5	0.02	0.5	0.4	0.1	1.0	0±0	0.03±0.03	0.15±0.15	0.08±0.08
Euphorbia candelabrum Welw.	Euphorbiaceae	Tree	2.5	0.02	0.5	0.3	0.2	1.0	1±1	0.01±0.01	0.07±0.07	0.07±0.07
Trema orientale (L.) Blume	Ulmaceae	Tree	2.5	0.02	0.5	0.5	0.0	1.0	1±1	0.01±0.01	0.03±0.03	0.04±0.04
Cedrela odorata Ruiz & Pav.	Meliaceae	Tree	2.5	0.02	0.5	0.2	0.2	0.9	0±0	0.01±0.01	0.06±0.06	0.04±0.04
Garcinia sp.	Clusiaceae	Tree	2.5	0.02	0.5	0.1	0.3	0.9	0±0	0.03±0.03	0.15±0.15	0.08±0.08
Obetia radula (Baker) Baker ex B.D.Jacks.	Urticaceae	Tree	2.5	0.02	0.5	0.2	0.0	0.7	1±1	0.02±0.02	0.11±0.11	0.09±0.09
Total			**502.5**	**3.21**	**100**	**100**	**100**	**300**	**197 ± 97**	**16.27 ± 7.30**	**79.17 ± 35.31**	**30.86 ± 12.77**

Note: * H' = Shannon-Wiener diversity index, Rf = Relative frequency, RDe= Relative density, RDo= Relative dominance (basal area), IVI = Importance Value Index, AGC = Above Ground Carbon (mean ± SE), BGC = Below Ground Carbon (mean ± SE), Plot size = 15 m radius. SE = Standard error

The 42 species belonging to 23 plant families recorded in this study from 40 concentric sample plots represent a lower species richness than those reported by several comparable studies. For example, Mwakalukwa et al. (2023a) recorded 54 species from 29 families using 23 plots of 0.071 hectares in the dry evergreen montane forest of the Essimingor Nature Forest Reserve in Tanzania. Similarly, Sitati et al. (2014) reported 75 species from 100 plots of 0.02 hectares in the Gelai Forest Reserve, also in Tanzania. Daba et al. (2022) documented 68 species across 33 families using 100 plots of 0.04 hectares in the Afromontane Forest of Southwest Ethiopia. Furthermore, Noumi (2015) reported 146 species from 41 families using 60 plots of 0.1 hectares in Cameroon. In contrast, the current study's species richness exceeds that reported by Teshager et al. (2018), who identified 32 species from 20 families using 40 plots of 0.02 hectares in the Weiramba Forest, Ethiopia. The relatively lower species count in the present study may be attributed to differences in sampling intensity, including total area surveyed, number of plots, and plot sizes, which were generally higher in the aforementioned studies.

Species diversity

The Shannon-Wiener diversity index (H') for tree and shrub species with diameter at breast height equal to or greater than five centimeters in the LDFR was calculated as 3.21 (Table 1). The species contributing most to this diversity index were *B. micrantha* (0.28), *S. madagascariensis* (0.21), and *F. sycomorus* (0.20). This H' value is lower than those reported by Kacholi et al. (2015) in the moist forest of Uluguru Nature Forest Reserve, Tanzania (H' = 4.03), Mwaluseke et al. (2023) from the dry evergreen forest of Lendikinya Forest Reserve, Tanzania (H' = 3.46), and Noumi (2015) in Cameroon (H' = 4.96). However, it is higher than those documented in other studies. For example, Teshager et al. (2018) reported an H' of 2.3 in a moist forest in Ethiopia, Mwakalukwa et al. (2023a) reported an H' of 2.7 in the Essimingor Nature Forest Reserve, Sitati et al. (2014) recorded an H' of 2.8 in the Gelai Forest Reserve, and Mwakalukwa and Masisi (2024) found an H' of 2.91 in the Rau Catchment Forest Reserve, a lowland groundwater forest in Tanzania.

According to Magurran (2004) and Noumi (2015), Shannon-Wiener index values typically range from 1.5 to 4.9 and rarely exceed 5. Ecosystems with values above 2 are generally considered to have moderate to high diversity. Therefore, the H' value of 3.21 in this study indicates that the LDFR supports a high level of species diversity among its tree and shrub populations. This relatively high diversity may be attributed to the low levels of disturbance observed in the forest.

Stand structure

The stem density and basal area for adult trees and shrubs with diameter at breast height equal to or greater than five centimeters in the LDFR were 197 ± 97 stems per hectare and 16.27 ± 7.30 square meters per hectare, respectively (Table 1). The species contributing most to stem density included *Drypetes gerrardii* Hutch. (19 ± 8 stems per hectare), *B. micrantha* (19 ± 4 stems per hectare), *S. madagascariensis* (16 ± 7 stems per hectare), and *Psychotria riparia* (15 ± 7 stems per hectare). Regarding basal area, *F. sycomorus* was the most dominant species, contributing 4.83 ± 1.24 square meters per hectare, followed by *B. micrantha* with 1.91 ± 0.42 square meters per hectare and *S. madagascariensis* with 1.31 ± 0.71 square meters per hectare. The stem density distribution by size class exhibited a reverse J-shaped pattern (Figure 3), which is characteristic of healthy regenerating forests. In contrast, the basal area distribution followed a normal J-shaped curve, with trees exceeding 70.1 centimeters in diameter contributing the most to the mean basal area of the forest (Figure 4).

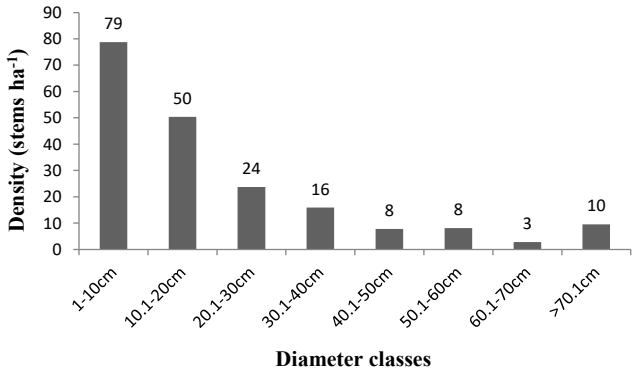

Figure 3. Distribution of density

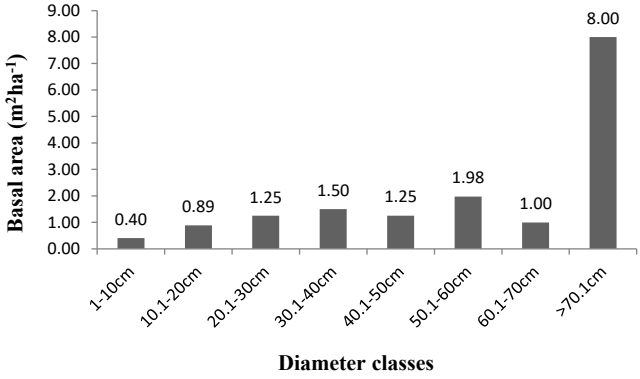

Figure 4. Distribution of basal area per hectare for trees and shrubs with ≥ 5 cm Dbh by diameter classes in Lake Duluti Forest Reserve, Arumeru District, Tanzania (n = 40)

The total mean stem density of adult individuals (dbh ≥ 5 cm) recorded in this study was 197 ± 97 stems ha^{-1}, which is considerably lower than values reported from other forest reserves in East Africa. For instance, Mwakalukwa et al. (2023a) reported 288 ± 173 stems ha^{-1} in Essimingor Nature Forest Reserve, while Sitati et al. (2014) and Sitati et al. (2016) recorded 377 stems ha^{-1} and 435 stems ha^{-1} in Gelai and Ketumbeine Forest Reserves, respectively. Similarly, Kacholi et al. (2015) documented 390 stems ha^{-1} in the Uluguru Nature Forest Reserve, and Gebeyehu et al. (2019) reported stem densities ranging from 365.6 to 664.1 stems ha^{-1}, with a mean of 636.5 stems ha^{-1} across five Ethiopian forests. In western Cameroon, Noumi (2015) found a mean stem density of 544 stems ha^{-1}. Conversely, the stem density in this study exceeded the values reported by Mwakalukwa et al. (2023b) (190 ± 117 stems ha^{-1}) from the Lolkisale Village Land Forest Reserve and by Mwakalukwa and Masisi (2024), who recorded 185 ± 81 stems ha^{-1} in the lowland groundwater forest of Rau Catchment Forest Reserve. The relatively lower stem density observed in Lake Duruti Forest Reserve (LDFR) suggests that it is among the few moist, submontane, dry evergreen forests in Tanzania with lower stocking rates. This might be attributed to site-specific factors such as extensive water cover, which potentially limits the availability of terrestrial habitat for tree establishment. In contrast, higher stem densities in other forests could be linked to microclimatic conditions that enhance species establishment and survival.

With respect to basal area, the mean value recorded in LDFR was 16.27 ± 7.30 m² ha^{-1} for adult individuals (dbh ≥ 5 cm). This is higher than the 11.47 ± 7.23 m² ha^{-1} reported by Mwakalukwa et al. (2023a) for Essimingor, 7.68 ± 5.17 m² ha^{-1} reported by Mwakalukwa et al. (2023b) for Lolkisale, and 11.42 ± 5.41 m² ha^{-1} reported for Lendikinya Forest Reserve (Mwaluseke et al. 2023). However, it remains lower than the 23.05 ± 12.37 m² ha^{-1} observed by Mwakalukwa and Masisi (2024) in Rau Catchment Forest Reserve, 24 m² ha^{-1} reported by Kacholi et al. (2015) for Uluguru Nature Forest Reserve, and 26.87 m² ha^{-1} reported by Sitati et al. (2014) for Gelai Forest Reserve. Furthermore, Sitati et al. (2016) reported 30.49 ± 2.3 m² ha^{-1} from Ketumbeine, while higher values were recorded by Teshager et al. (2018) (32.10 m² ha^{-1}), Noumi (2015) (52.72 m² ha^{-1}), Mialla (2002) (69.3 ± 1.6 m² ha^{-1}), and Tynsong et al. (2022), who documented a mean of 61.72 ± 4.82 m² ha^{-1} in tropical evergreen forests of India. The relatively low stem density in LDFR likely accounts for its moderate basal area. In other studies, higher basal areas may be attributed to greater stem densities and the presence of more individuals in higher dbh classes, which substantially contribute to overall basal area values.

Regeneration

Regeneration status of tree and shrub species (dbh < 5 cm) in LDFR is summarized in Table 2. A total of 22 species representing 15 plant families and 20 genera were recorded. Of these, tree species constituted 77%, while shrub species accounted for 23%. The most dominant families were Fabaceae and Rubiaceae, each represented by three species. Ebenaceae, Loganiaceae, and Rutaceae followed, each with two species. The remaining families contributed one species each. The most frequently encountered regenerants were *D. gerrardii* (35%), *Newtonia buchananii* (Baker) G.C.C.Gilbert & Boutique (20%), *Psychotria capensis* subsp. *riparia* (K.Schum. & K.Krause) Verdc. (20%), and *Celtis africana* Burm.fil. (20%), which also significantly contributed to the Shannon-Wiener diversity index (H′) and stem density values.

Table 2. Checklist of tree and shrub species of regenerants with DBH of < 5 cm sorted by density identified in Lake Duluti Forest Reserve, Arumeru District, Tanzania

Botanical name	Family	Habit	Frequency (%)	*H'	Density (stems ha^{-1})
Drypetes gerrardii Hutch.	Putranjivaceae	Tree	35	0.29	855±223
Newtonia buchananii (Baker) G.C.C. Gilbert & Boutique	Fabaceae	Tree	20	0.21	537±269
Albizia gummifera (J.F.Gmel.) C.A.Sm.	Fabaceae	Tree	17.5	0.19	418±185
Sorindeia madagascariensis (Spreng.) DC.	Anacardiaceae	Tree	17.5	0.19	279±132
Sarcomelicope simplicifolia (Endl.) T.G.Hartley	Rutaceae	Tree	15	0.17	279±123
Psychotria capensis subsp. *riparia* (K. Schum. & K. Krause) Verdc.	Rubiaceae	Shrub	20	0.21	259±100
Strychnos mitis S.Moore	Loganiaceae	Tree	2.5	0.05	199±199
Celtis africana Burm.fil.	Cannabaceae	Tree	20	0.21	199±68
Clausena anisata (Willd.) Hook.fil.	Rutaceae	Shrub	10	0.13	159±86
Trichilia emetica (Forssk.) Vahl	Meliaceae	Tree	12.5	0.15	159±71
Albizia petersiana (Bolle) Oliv.	Fabaceae	Tree	5	0.08	139±98
Tabernaemontana ventricosa Hochst. ex A.DC.	Apocynaceae	Tree	12.5	0.15	139±63
Diospyros abyssinica (Hiern) F.White	Ebenaceae	Tree	5	0.08	99±82
Strychnos sp.	Loganiaceae	Tree	7.5	0.11	80±48
Vangueria infausta Burch.	Rubiaceae	Shrub	7.5	0.11	80±48
Deinbollia kilimandscharica Taub.	Sapindacea	Shrub	5	0.08	40±28
Euclea divinorum Hiern	Ebenaceae	Tree	5	0.08	40±28
Flacourtia indica (Burm.fil.) Merr.	Salicaceae	Tree	5	0.08	40±28
Trilepisium madagascariense DC.	Moraceae	Tree	5	0.08	40±28
Antidesma sp.	Phyllanthaceae	Tree	2.5	0.05	20±20
Commiphora eminii Engl.	Burseraceae	Tree	2.5	0.05	20±20
Rothmannia sp.	Rubiaceae	Shrub	2.5	0.05	20±20
Total			**235**	**2.80**	**4,100 ± 1,967**

Note: * Shannon-Wiener diversity index (H'), plot size = 2 m radius

The calculated Shannon-Wiener diversity index (H') for regenerants was 2.80, indicating high species diversity among young individuals in the reserve. The mean stem density of regenerants was 4,098 ± 1,966 stems ha^{-1}, which is notably higher than values reported in comparable forest ecosystems. For instance, Mwakalukwa et al. (2023a) reported 736 ± 621 stems ha^{-1} for regenerants (dbh < 5 cm) in Essimingor Nature Forest Reserve, while Teshager et al. (2018) recorded 1,635 stems ha^{-1} for seedlings and 1,116 stems ha^{-1} for saplings in Weiramba Forest, Ethiopia. These results suggest that despite the relatively low adult stem density, LDFR exhibits a high regeneration potential. The abundance of regenerants may reflect favorable microsite conditions, reduced anthropogenic disturbance, or successful reproductive strategies of dominant species, highlighting the ecological importance of LDFR as a viable forest system capable of sustaining long-term regeneration and resilience.

Biomass and carbon storage

The mean above-ground biomass and carbon stock potential of trees and shrubs with a Diameter at Breast Height (DBH) ≥ 5 cm in the Lake Duruti Forest Reserve (LDFR) were estimated at 158.48 ± 70.61 Mg ha^{-1} and 79.24 ± 35.31 Mg C ha^{-1}, respectively. Correspondingly, the mean below-ground biomass and carbon stock potential for the same category of individuals were 61.73 ± 25.54 Mg ha^{-1} and 30.86 ± 12.77 Mg C ha^{-1} (Table 1; Figure 5). Species contributing most significantly to above-ground carbon stocks were also those with the highest basal area, namely *F. sycomorus* (22.85 ± 5.84 Mg C ha^{-1}), *B. micrantha* (9.43 ± 2.05 Mg C ha^{-1}), and *S. madagascariensis* (6.44 ± 3.44 Mg C ha^{-1}). These same species were also dominant contributors to below-ground carbon stocks: *F. sycomorus* (5.12 ± 1.19 Mg C ha^{-1}), *B. micrantha* (3.95 ± 0.70 Mg C ha^{-1}), and *S. madagascariensis* (2.68 ± 1.11 Mg C ha^{-1}) (Table 1). Biomass and carbon distribution across diameter classes revealed that individuals with DBH > 70.1 cm accounted for the largest share of the mean biomass and carbon stocks within the forest (Figure 5).

The total mean above-ground carbon stock (AGC) for trees and shrubs with DBH ≥ 5 cm in the Lake Duruti Forest Reserve (LDFR) was 79.24 ± 35.31 Mg C ha^{-1}. This value exceeds estimates reported from several other tropical forests. For instance, Swai et al. (2014) documented 48.4 ± 8.0 Mg C ha^{-1} from the Hanang Mountain Forest, while Shirima et al. (2015) recorded 54.30 ± 5.84 Mg C ha^{-1} from montane forests and miombo woodlands in Tanzania. Similarly, Mwakalukwa et al. (2023a) reported 56.93 ± 34.60 Mg C ha^{-1} in the dry evergreen forest of Essimingor Nature Forest Reserve, and Mwakalukwa et al. (2023b) found a much lower value of 19.55 ± 13.38 Mg C ha^{-1} in the Lolkisale Village Land Forest Reserve, North-East Tanzania. Mwaluseke et al. (2023) reported the lowest among these, with 16.04 ± 7.7 Mg C ha^{-1} from the Lendikinya Forest Reserve. In contrast, the AGC stock reported in this study is lower than some of the highest values recorded in other regions. Mwakalukwa and Masisi (2024) reported 107.48 ± 61.28 Mg C ha^{-1} from the lowland groundwater forest of Rau Catchment Forest Reserve in Tanzania. Even higher values have been reported from Ethiopia, including 180.18 ± 17.19 Mg C ha^{-1} and 106.71 ± 7.64 Mg C ha^{-1} in dry evergreen Afromontane forests (Asrat et al. 2022), and 191.6 ± 19.7 Mg C ha^{-1} across five Afromontane forests (Gebeyehu et al. 2019). Daba et al. (2022) reported 203.80 ± 12.38 Mg C ha^{-1} from a tropical forest in Southwest Ethiopia while, in India, Naveenkumar et al. (2017) recorded a range of 99-216 Mg C ha^{-1} from a tropical dry forest.

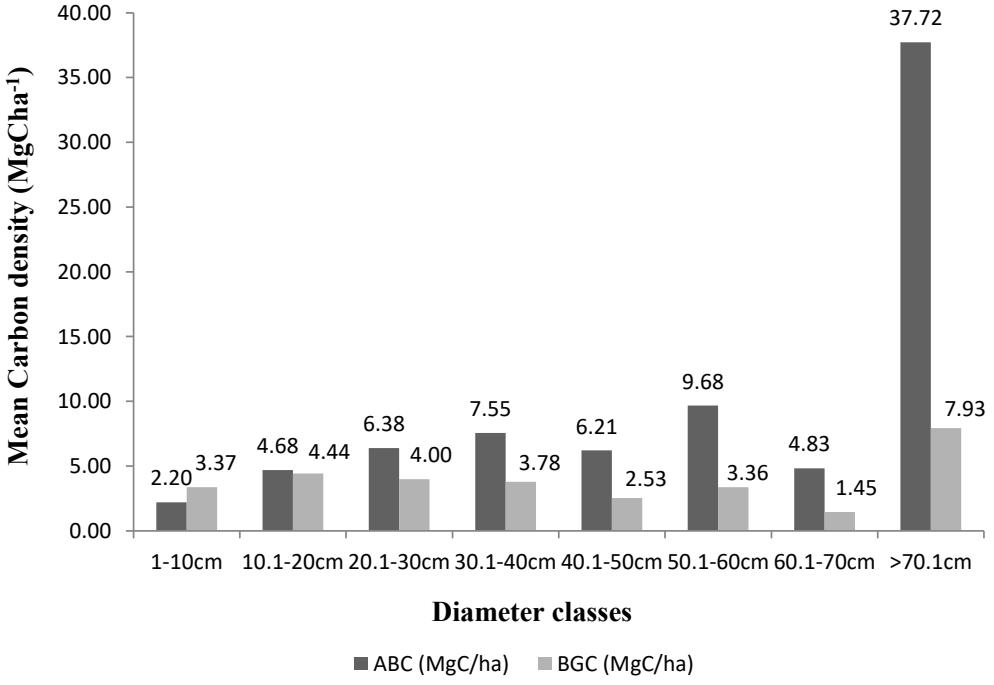

Figure 5. Distribution of both above and below-ground means carbon density for trees and shrubs with ≥ 5 cm DBH by diameter classes in the Lake Duluti Forest Reserve, Arumeru District, Tanzania (n = 40)

Regarding Below-Ground Carbon (BGC) density, the mean value of 30.86 ± 12.77 Mg C ha^{-1} reported in this study falls within the range observed in comparable ecosystems. It is slightly lower than the 34.71 ± 19.72 Mg C ha^{-1} reported by Mwakalukwa et al. (2023a) for the Essimingor Nature Forest Reserve. However, it is higher than values reported by Mwakalukwa and Masisi (2024), who documented 21.50 ± 12.26 Mg C ha^{-1} for the Rau Catchment Forest Reserve, and significantly exceeds the 3.91 ± 2.68 Mg C ha^{-1} recorded by Mwakalukwa et al. (2023b) for the Lolkisale Village Land Forest Reserve.

The variation in carbon stock values between studies can largely be attributed to differences in forest structure, particularly the size distribution of trees. Forests with many large trees generally exhibit higher biomass and carbon density. In contrast, a dominance of small trees tends to lower overall carbon stocks (Mauya and Madundo 2021). Other contributing factors include differences in terrain, climate, and methodological approaches—particularly the choice of allometric models used for biomass estimation.

Despite the relatively low stem density of adult trees (≥ 5 cm DBH), the LDFR stores considerable amounts of carbon in both above- and below-ground pools. The diameter of trees recorded ranged from 5 to 160 cm, with a notable proportion of large trees: 67% of the 290 trees measured had a DBH ≥ 20 cm, while 33% were < 20 cm. These findings highlight the ecological importance of large-diameter trees in carbon sequestration. To obtain a comprehensive estimate of total carbon storage, further quantification of additional carbon pools—such as soil, litter, deadwood, grasses, and herbs—is strongly recommended.

In conclusion, this study highlights the exceptional biodiversity and carbon storage potential of the Lake Duruti Forest Reserve. A total of 42 woody species were identified, and the species diversity index (H′ = 3.21) suggests a floristically rich and heterogeneous ecosystem. Compared to other tropical forests, both in Tanzania and beyond, LDFR demonstrates relatively high above- and below-ground carbon stock values, largely driven by the presence of large trees. The high number of regenerants also reflects a healthy forest regeneration dynamic, indicative of long-term ecological stability. Together, the forest's structural composition, species richness, and significant carbon sequestration capacity highlight its conservation value.

To ensure the continued protection of this important ecosystem, the development and implementation of a comprehensive forest management plan is essential. Such a strategy would not only promote biodiversity conservation but also maintain and potentially enhance existing carbon stocks. This calls for immediate and coordinated conservation efforts involving local communities, stakeholders, and policymakers, to secure the long-term ecological and climate-regulating functions of LDFR.

ACKNOWLEDGEMENTS

The author would like to thank the Tanzania Forest Services Agency (TFS) staff at Lake Duruti Forest Reserve for assisting with data collection. Mr. Gabriel Laizer is acknowledged for assisting with tree and shrub species identifications, Mr. Jofrey Jacob for assisting with data processing and analysis, and Mr. Sami Madundo for assisting with the preparation of the study site map.

REFERENCES

Asrat F, Soromessa T, Bekele T, Kurakalva RM, Guddeti SS, Smart DR, Steger K. 2022. Effects of environmental factors on carbon stocks of dry evergreen afromontane forests of the Choke Mountain Ecosystem, Northwestern Ethiopia. Intl J For Res 2022 (1): 9447946. DOI: 10.1155/2022/9447946.

Daba DE, Dullo BW, Soromessa T. 2022. Effect of forest management on carbon stock of tropical moist afromontane forest. Intl J For Res 2022 (1): 3691638. DOI: 10.1155/2022/3691638.

Gebeyehu G, Soromessa T, Bekele T, Teketay D. 2019. Carbon stocks and factors affecting their storage in dry afromontane forests of Awi Zone, North-western Ethiopia. J Ecol Environ 43: 7. DOI: 10.1186/s41610-019-0105-8.

Iddi S. 1998. Eastern Arc Mountains and their national and global importance. J East Afr Nat Hist 87 (1): 19-26. DOI: 10.2982/0012 8317(1998)87[19:EAMATN]2.0.CO;2.

Kacholi DS, Whitbread AM, Worbes M. 2015. Diversity, abundance, and structure of tree communities in the Uluguru forests in the Morogoro region, Tanzania. J For Res 26 (3): 557-569. DOI: 10.1007/s11676 015-0078-0.

Kent M, Coker P. 1992. Vegetation Description and Analysis. A Practical Approach. John Wiley and Sons, New York.

Kent M. 2012. Vegetation Description and Analysis, A Practical Approach, 2nd edition. Wiley-Blackwell, John Wiley & Sons, Hoboken, NJ, USA.

Lovett JC, Pocs T. 1993. Assessment of the Condition of the Catchment Forest Reserves: A Botanical Appraisal, Government Printers, Dar es Salaam.

Magurran AE. 2004. Measuring Biological Diversity. Blackwell Publishing, Oxford.

Manyanda BJ, Nzunda EF, Mugasha WA, Malimbwi RE. 2020. Estimates of volume and carbon stock removals in Miombo Woodlands of Mainland Tanzania. Intl J For Res 2020 (1): 4043965. DOI: 10.1155/2020/4043965.

Masota AM, Bollandsås OM, Zahabu E, Eid T. 2016. Allometric Biomass and Volume Models for Lowland and Humid Montane Forests. In: Malimbwi RE, Eid T, Chamshama SAO (eds.). Allometric Tree Biomass and Volume Models in Tanzania. Department of Forest Mensuration and Management, Sokoine University of Agriculture, Tanzania.

Mauya EW, Madundo S. 2021. Above-ground biomass and carbon stock of usambara tropical rainforests in Tanzania. Tanz J For Nat Conserv 90 (2): 63-82.

Mialla YS. 2002. Participatory Forest Resource Assessment and Zonation in Monduli Catchment Forest Reserve, Arusha, Tanzania [Dissertation]. Sokoine University of Agriculture, Morogoro. [Tanzania]

Mwakalukwa EE, Masisi B. 2024. Diversity, structure, and carbon storage of Rau catchment forest reserve in Moshi District, Tanzania. Asian J For 9 (1): 1-11. DOI: 10.13057/asianjfor/r090101.

Mwakalukwa EE, Mwakisu A, Madundo S, Maliondo SMS. 2023b. Vegetation composition, diversity, stand structure, and carbon storage of Lolkisale Village Land Forest Reserve in the Northeastern part of Tanzania. Nusantara Biosci 15: 79-90. DOI: 10.13057/nusbiosci/n150109.

Mwakalukwa EE, Mwakisu A, Maliondo SMS. 2023a. Woody species diversity, composition, structure and carbon storage of a dry evergreen montane forest of Essimingor Nature Forest Reserve in Tanzania. Intl J Trop Drylands 7 (1): 26-36. DOI: 10.13057/tropdrylands/t070104.

Mwaluseke ML, Mwakalukwa EE, Maliondo SMS. 2023. Vegetation composition, diversity, stand structure and carbon stock of a dry

evergreen montane forest of Lendikinya forest reserve in Tanzania. Biodiversitas 24 (1): 551-562. DOI: 10.13057/biodiv/d240164.

NAFORMA. 2015. National Forest Resources Monitoring and Assessment of Tanzania Mainland. Ministry of Natural Resources and Tourism, Tanzania. Ministry for Foreign Affairs of Finland & Food and Agriculture Organisation of the United Nations.

Naveenkumar J, Arunkumar KS, Sundarapandian SM. 2017. Biomass and carbon stocks of a tropical dry forest of the Javadi Hills, Eastern Ghats, India. Carbon Manag 8 (5-6): 351-361. DOI: 10.1080/17583004.2017.1362946.

Noumi E. 2015. Floristic structure and diversity of a tropical sub-montane evergreen forest, in the Mbam Minkom Massif (Western Yaoundé). J Biol Life Sci 6 (1): 149-193. DOI: 10.5296/jbls.v6i1.7028.

Ract C, Burgess ND, Dinesen L, Sumbi P, Malugu I, Latham J, Anderson L, Gereau RE, Gonçalves de Lima M, Akida A, Nashanda E, Shabani Z, Tango Y, Mteleka S, Santos Silayo D, Mwangi J, Lyatuu G, Platts PJ, Rovero F. 2024. Nature Forest Reserves in Tanzania and their importance for conservation. PLoS ONE 19 (2): e0281408. DOI: 10.1371/journal.pone.0281408.

Shirima DD, Totland Ø, Munishi PKT, Moe SR. 2015. Relationships between tree species richness, evenness and above-ground carbon storage in montane forests and miombo woodlands of Tanzania. Basic Appl Ecol 16 (3): 239-249. DOI: 10.1016/j.baae.2014.11.008.

Sitati N, Gichohi N, Lenaiyasa P, Maina M, Warinwa F, Muruthi P, Sumba DS, Mandima J. 2016. Tree species diversity and dominance in Ketumbeine Forest Reserve, Tanzania. J Biodivers Manag For 5: 3. DOI: 10.4172/2327 4417.1000161.

Sitati N, Gichohi N, Lenaiyasa P, Millanga P, Maina M, Warinwa F, Muruthi P. 2014. Tree species diversity and dominance in Gelai Forest Reserve, Tanzania. J Energy Nat Resour 3 (3): 31-37. DOI: 10.11648/j.jenr.20140303.12.

Swai G, Ndangalasi HJ, Munishi PKT, Shirima DD. 2014. Carbon stocks of Hanang forest, Tanzania: An implication for climate mitigation. J Ecol Nat Environ 6 (3): 90-98. DOI: 10.5897/JENE2013.0418.

Teshager Z, Argaw M, Eshete A, Gebew Z. 2018. Woody species diversity, structure and regeneration status in Weiramba forest of Amhara region, Ethiopia: Implications of managing forests for biodiversity conservation. J Nat Sci Res 8 (5): 16-31.

TFS (Tanzania Forest Services Agency). 2022. Five years management plan for lake Duluti forest reserve 2022/23 - 2026/27 (Draft). Ministry of Natural Resources and Tourism.

Tynsong H, Dkhar M, Tiwari BK. 2022. Tree diversity and vegetation structure of the tropical evergreen forests of the southern slopes of Meghalaya, North East India. Asian J For 6 (1): 22-36. DOI: 10.13057/asianjfor/r060104.

URT (United Republic of Tanzania). 1998. The National Forest Policy. Forestry and Beekeeping Division. Ministry of Natural Resource and Tourism. Dar es Salaam.

URT (United Republic of Tanzania). 2015. National Biodiversity Strategy and Action Plan (NBSAP) 2015 2020. Vice President's Office, Division of Environment, United Republic of Tanzania, Dar es salaam.

URT (United Republic of Tanzania). 2021a. The Budget Speech for the Ministry of Natural Resources and Tourism in the year 2022/2023. Minister for Natural Resources and Tourism. Dodoma.

URT (United Republic of Tanzania). 2021b. National Forest Policy Implementation Strategy (2021-2031). United Republic of Tanzania. Ministry of Natural Resources and Tourism.

NUSANTARA BIOSCIENCE
Vol. 17, No. 2, pp. 194-201
November 2025

ISSN: 2087-3948
E-ISSN: 2087-3956
DOI: 10.13057/nusbiosci/n170202

Effect of tannin and amino acid supplementation on growth, digestibility, and blood parameters in heifer calves

LU'LU' NABILA SALSABILA[1], AINISSYA FITRI[2,♥], FAJAR EDY MARETNO SITANGGANG[1], IDAT GALIH PERMANA[1], WARTIKA ROSA FARIDA[2], DWITAMI ANZHANY[2], RONI RIDWAN[2]

[1]Department of Nutrition and Feed Science, Graduate School of Institut Pertanian Bogor. Jl. Raya Dramaga, Bogor 16680, West Java, Indonesia
[2]Research Centre for Applied Zoology, National Research and Innovation Agency. Jl. Raya Bogor KM. 46, Bogor 16911, West Java, Indonesia.
Tel.: +62-811-1933-3639, ♥email: aini002@brin.go.id

Manuscript received: 25 March 2025. Revision accepted: 3 August 2025.

Abstract. *Salsabila LN, Fitri A, Sitanggang FEM, Permana IG, Farida WR, Anzhany D, Ridwan R. 2025. Effect of tannin and amino acid supplementation on growth, digestibility, and blood parameters in heifer calves. Nusantara Bioscience 17: 194-201.* Nutritional management during the growth phase of heifer calves is crucial for optimal performance and health. Tannins and amino acids have shown potential benefits in ruminant nutrition through improved protein utilization and antimicrobial properties. This study aimed to evaluate the effect of tannins (1% DM), amino acids (0.3% DL-methionine + 0.7% L-lysine), and their mixture on heifer calves' performance and metabolic indicators. To achieve the objective, a 4 × 4 Latin square design was used with 4 calves (109.00 ± 18.17 kg of body weight), each receiving 4 treatments in 4 periods. The treatment period lasted 14 days, including 10 days for diet adaptation and 4 days for sample collection. The basal diet was a Total Mixed Ration (TMR) consisting of 20 kg/d of forage and 2 kg/d of concentrate. Treatments included: P1 (control, TMR only), P2 (TMR + 1% dry matter intake (DMI) tannin), P3 (TMR + 1% DMI amino acids), and P4 (TMR + 1% DMI tannin and 1% DMI amino acids). The results showed that individual supplementation in P2 (0.66 kg/h/d) and P3 (0.73 kg/h/d) had higher Average Daily Gain (ADG) compared to P1 (0.54 kg/h/d) and P4 (0.41 kg/h/d) ($p < 0.05$). Feed efficiency in P2 (2.65%) and P3 (3.02%) is higher than in P1 (2.49%) and P4 (1.74%) ($p < 0.05$). Although nutrient intake did not differ, Crude Protein (CP) intake in the P1 (0.32 kg/day) was lower than in the P2 (0.44 kg/day), P3 (0.39 kg/day), and P4 (0.40 kg/day) ($p < 0.05$). Plasma protein and cholesterol levels were lower in the P1 (7.07 g/dL; 94.14 mg/dL) than those (7.46-7.62 g/dL; 125.98-149.85 mg/dL, respectively) ($p < 0.05$). Overall, supplementation of 1% DMI tannin or amino acids alone improved the performance without compromising hematological profiles and blood metabolites.

Keywords: Amino acids, blood protein, calves, performance, tannin

INTRODUCTION

Efficiently managing dairy calves, especially in milk production, is crucial for the long-term success of dairy farming (van Niekerk et al. 2020). The importance of managing replacement heifers is often overlooked, especially in high mortality and morbidity rates. Mortality rates of calves can be substantially high, particularly in developing areas, with approximately 35% (Li et al. 2011). High morbidity and mortality rates cause substantial economic losses, contradicting animal welfare and food safety. Growth and mortality rates in calves have proven to be suitable indicators for health assessment. High growth rates also show proper nutrition and feeding, as insufficient nutrition will inhibit immunity, leading to disease and mortality (Tautenhahn et al. 2020). In Indonesia, the yearly rate of calf births ranges from 52-67%, while calf mortality rates range from 8 to 48%, deemed very high (Talib et al. 2003). Common health issues in calves include respiratory diseases, gastrointestinal disorders, and nutritional deficiencies, which can lead to stunted growth and increased mortality rates (McGuirk and Peek 2014).

Nutritional management is one of the primary concerns in the growth phase of the heifer calves. This is because insufficient nutrition can inhibit the growth rate, disrupt reproductive growth, and hinder the immunity of the calves (Tautenhahn et al. 2020; van Niekerk et al. 2020). The transition to solid feed has been proven effective through significant metabolic changes. For instance, calves must adapt from a carbohydrate-rich diet to one that includes more complex nutrients, which affects their blood biochemical profiles and overall health (Nagy et al. 2014; Khan et al. 2016). Around 4 to 6 weeks, ruminal fermentation and absorption will develop in calves (Mirzaei-Alamouti et al. 2025). Moreover, calves weaned early without adequate solid feed intake tend to reduce growth rates, increase susceptibility to illness, and impact overall digestive health (Bhatti et al. 2012; Benetton et al. 2019; Hao et al. 2021). The stress associated with weaning and dietary changes is inevitable. Therefore, effective management of nutrition strategies is essential to mitigate risks and promote better health outcomes for calves.

Feed supplements can enhance performance and increase livestock growth (Abitante et al. 2024). Tannins and amino acids have beneficial effects on calves' health and performance. Tannins are a heterogeneous group of polyphenols, serving as secondary metabolites in plants that are synthesized in response to biotic and abiotic stressors. These compounds also have properties such as antioxidant, antimicrobial, anthelmintic, anti-inflammatory, and antimethanogen (Fraga-Corral et al. 2021; Fitri et al. 2022;

Boukrouh et al. 2024). Previous studies explained that supplementing tannin in ruminant diets with moderate levels (0.2-0.6% dry matter (DM) in steers and 10 g/day in calves) has been associated with improved performance and reductions in both gastrointestinal parasitism and nitrogen pollution (Dell'Anno et al. 2024). Moreover, the addition 1% chestnut-tannin extract in piglets' diets and 6 g/day of tannin extract in preweaning calves' diet improved gut health through antibacterial properties and reduced incidence of diarrhea, whereas feed intake and the average daily gain were unaffected (Girard et al. 2018; Dell'Anno et al. 2024). Tannin supplementation has also been reported to improve growth rates in post-weaning calves by enhancing the colonization of beneficial microbiota that play a key role in the development and function of the gastrointestinal tract, which is subsequently associated with increased body weight and improved feed efficiency in growing ruminants (Hassan et al. 2020; Al Rharad et al. 2025). Feed processing techniques have been developed to minimize undegradable protein and increase the direct delivery of amino acids to the small intestine (Mirzaei-Alamouti et al. 2025), particularly using tannin to protect amino acids.

Essential amino acids, such as lysine and methionine, are crucial for protein synthesis and overall growth (Montout et al. 2021). Supplementing diets with lysine and methionine enhanced growth performance and immune function, reducing the incidence of illness in livestock (Montout et al. 2021). However, Silva et al. (2021) found that lysine and methionine (17 and 5.3 g/d) supplemented in the solid concentrate calves' diet detrimentally affect the animals' performance and metabolism. This might be because the amino acids are quickly degraded in the rumen, causing inefficient absorption (Schwab and Broderick 2017).

Although the potential benefits of tannin and amino acids supplementation have been investigated, a limited number of studies have investigated the combination of tannin and amino acids in post-weaned calves. Tannins can bind proteins and form tannin-amino acid complexes, reducing excessive protein degradation in the rumen and improving protein utilization. Under the acidic conditions of the abomasum, these complexes dissociate, increasing the amount of bypass protein that reaches the small intestine (Lorenz et al. 2014).

Based on the background above, this study aimed to address the knowledge gap by assessing the influence of tannin, amino acids, and their combination on performance, nutrient intake, digestibility, and blood metabolites in heifer calves. It was hypothesized that the supplementation of tannin, amino acids, and their mixture would increase average daily gain, protein digestibility, and immune profile, as shown by the blood metabolites.

MATERIALS AND METHODS

Experimental design and animals

Four Friesian Holstein post-weaned heifer calves (109.00 ± 18.17 kg of live weight, aged 6 to 7 months) were used for the experiment conducted at PT Sumber Citarasa Alam, Ciawi, Bogor, Indonesia. The animal used in this experiment was approved by the Animal Care and Use Committee of the Ethical Clearance, BRIN (Number: 004/KE.02/SK/01/2024). A Latin square design with 4 treatments and 4 replications was used. Each experimental period consisted of 10 days for diet adaptation and 4 days for data and sample collection. The sample size was determined based on data from the previous period of calves.

Treatment and feeding management

Calves were given a Total Mixed Ration (TMR) consisting of 20 kg/day of fresh forage and 2 kg/day of commercial concentrate (as fed basis). Diets were offered twice daily at 0900 and 1700, with ad libitum access to drinking water. The diets were supplemented with tannin, amino acids, and a mixture of tannin and amino acids. The experimental treatments were: P1: Control ration (TMR only), P2: TMR + 1% tannin (DM of diet), P3: TMR + 1% amino acids (0.3% DL-methionine and 0.7% L-lysine, DM of diet), P4: TMR + 1% tannin + 1% amino acids.

Tannin, amino acids, and a mixture of tannin and amino acids were added on top and then mixed into the TMR. The tannin used was a commercial extract from the Chestnut tree (Hydrolyzable tannin, Saviolife, Italy), while the amino acids were DL-methionine and L-lysine (PT Cheil Jedang, Indonesia).

Feed analysis

Representative samples of the TMR for each treatment were collected daily and composited by treatment and period. Samples were dried at 60°C for 48 hours and analyzed for dry matter (DM), organic matter (OM), ash, crude protein (CP), ether extract (EE), and crude fiber (CF) according to AOAC (1995) procedures. The nutrient composition of rations is presented in Table 1.

Growth performance

Growth performance in this study was evaluated based on average daily gain (ADG) and feed efficiency. The calves were weighed on 1 and 14 of each period (14-day intervals), before their morning feeding using a digital livestock scale. Average daily gain (ADG) was calculated using the following formula:

ADG (kg/head/day) = [final weight (kg) - initial weight (kg)] / 14 days

Table 1. Composition of the nutrient composition of the ration

Nutrient composition	P1	P2	P3	P4
Dry matter (DM, %)	21.25	20.18	24.65	22.53
Organic matter (% DM)	86.40	86.43	83.32	86.88
Ash (% DM)	13.60	13.57	16.68	13.12
Crude protein (% DM)	10.02	12.54	12.58	12.99
Ether extract (% DM)	1.13	0.83	0.84	0.87
Crude fiber (% DM)	26.12	28.91	29.05	29.04

Note: P1: control (TMR only), P2: TMR + 1% tannin (DM of diet), P3: TMR + 1% amino acids (0.3% DL-methionine and 0.7% L-lysine, DM of diet), P4: TMR + 1% tannin + 1% amino acid supplementation

While feed efficiency was calculated using the following formula:

Feed efficiency (%) = ADG (kg/head/day) / dry matter intake (kg/day)

Nutrient intake and digestibility

Offered feed and feces of individual calves were weighed and sampled every day from day 10 to 14 on each experimental period (5-day collection at the end of each period). Fecal samples were collected daily (24-hour collection) and 10% composited by treatment and period. All samples were dried in the oven at 60°C for 48 hours, ground finely, and kept until analyzed. The samples were analyzed for dry matter (DM), organic matter (OM), crude protein (CP), ether extract (EE), and crude fiber (CF) content using the in vitro method (AOAC 1985). Subsequently, nutrient intake was calculated based on the feed intake and nutrient composition, following the formula below:

Nutrient intake (kg/head/day) = [%nutrient in feed × feed offered (kg/day)] - [%nutrient in refusal × feed refused (kg/day)]

While the following formula calculates nutrient digestibility:

Nutrient digestibility (%) = [(nutrient intake - nutrient in fecal) / nutrient intake] × 100%

The nutrients intake and digestibility measured included the DM, OM, CP, EE, and CF.

Blood metabolites and haematological

Blood samples were collected on day 14 in an EDTA vacuum blood collection tube, which was stored in a cooler box container for a while and brought to the laboratory for analysis. Haematological analysis measured were erythrocytes, hemoglobin, hematocrit, and leukocytes. Initially, blood tests were performed using the automated hematology analyzer (NIHON KOHDEN CelltacEs Automated Hematology Analyzer, Japan), which took approximately 18 to 27 µL. Blood metabolites analysis measured in this experiment were glucose, triglyceride, blood urea nitrogen (BUN), cholesterol, and protein. The analysis was calculated based on the general procedure of KIT reagents. Samples were analyzed using a colorimetric enzymatic method with KIT reagents brand GLORY DIAGNOSTICS (Spain). After obtaining the absorbance, the blood metabolite value was calculated by dividing the sample absorbance value by the standard absorbance value.

Statistical analysis

The study used a Latin square design with 4 treatments and 4 replications. Data were analyzed using the Analysis of Variance (ANOVA) method with SAS software, followed by Duncan's Further Test. Significance was declared at $p < 0.05$ and trends toward a significant difference at $0.05 < p < 0.10$.

RESULTS AND DISCUSSION

Performance of the calves

Table 2 shows a significant difference in average daily gain (ADG) and feed efficiency ($p < 0.05$). Based on the results, supplementation of tannin (P2) and amino acid (P3) had a higher ADG and feed efficiency than the control, with the highest values found in the P3 treatment. Meanwhile, the P4 treatment had the lowest ADG and feed efficiency compared to other treatments. Tannin and amino acid supplementation did not affect the fresh daily intake, which ranged between 13.65 and 17.14 kg/head/day, and there was no significant difference between treatments.

Nutrient intake

As shown in Table 3, the treatments did not affect intake of DM, OM, EE, and CF ($p > 0.05$). However, CP intake was significantly higher in P2 (0.44 kg/d), P3 (0.39 kg/d), and P4 (0.40 kg/d) compared to the control (P1: 0.32 kg/d, $p < 0.05$).

Table 2. Performance in female Friesian Holstein dairy calves

Parameters	Treatment				SEM	*p-value*
	P1	P2	P3	P4		
Average daily gain (kg/head/day)	0.54^{ab}	0.66^{bc}	0.73^{c}	0.41^{a}	0.04	0.015
Fresh daily intake (kg/head/day)	14.86	17.14	13.65	14.68	0.49	0.086
Feed efficiency (%)	2.49^{ab}	2.65^{b}	3.02^{b}	1.74^{a}	0.17	0.036

Note: Means in the same row with different superscripts differ significantly ($p < 0.05$); Note: P1: control (TMR only), P2: TMR + 1% tannin (DM of diet), P3: TMR + 1% amino acids (0.3% DL-methionine and 0.7% L-lysine, DM of diet), P4: TMR + 1% tannin + 1% amino acid supplementation, SEM: Standard Error Mean

Table 3. Nutrient intake in female Friesian Holstein dairy calves

Parameters (kg/head/day)	P1	P2	P3	P4	SEM	*p-value*
Dry matter intake	3.16	3.51	3.37	3.31	0.09	0.584
Organic matter intake	2.73	3.04	2.80	2.87	0.08	0.559
Crude protein intake	0.32^{a}	0.44^{b}	0.39^{b}	0.40^{b}	0.01	0.021
Ether extract intake	0.04	0.03	0.03	0.03	0.00	0.079
Crude fiber intake	0.82	1.02	0.98	0.96	0.03	0.118

Note: Means in the same row with different superscripts differ significantly ($p < 0.05$); Note: P1: control (TMR only), P2: TMR + 1% tannin (DM of diet), P3: TMR + 1% amino acids (0.3% DL-methionine and 0.7% L-lysine, DM of diet), P4: TMR + 1% tannin + 1% amino acid supplementation, SEM: Standard Error Mean

Table 4. Digestibility nutrient in female Friesian Holstein dairy calves

Parameters (%)	P1	P2	P3	P4	SEM	*p-value*
Dry matter digestibility	68.91	64.90	68.55	60.25	1.86	0.262
Organic matter digestibility	72.88	70.17	72.78	64.40	1.66	0.164
Crude protein digestibility	58.79	66.70	68.76	67.06	2.13	0.216
Ether extract digestibility	66.40	66.04	72.10	58.08	2.44	0.308
Crude fiber digestibility	74.56	68.62	69.14	61.62	1.88	0.081

Note: Means in the same row with different superscripts differ significantly ($p < 0.05$); Note: P1: control (TMR only), P2: TMR + 1% tannin (DM of diet), P3: TMR + 1% amino acids (0.3% DL-methionine and 0.7% L-lysine, DM of diet), P4: TMR + 1% tannin + 1% amino acid supplementation, SEM: Standard Error Mean

Table 5. Hematology in female Friesian Holstein dairy calves

Parameters	P1	P2	P3	P4	SEM	*p-value*	Normal range*
Erythrocytes (10^6/µL)	9.74	9.32	9.72	10.65	0.40	0.521	5.0-10.0
Leukocytes (10^3/µL)	12.81	22.75	22.71	31.91	2.79	0.068	4.0-12.0
Haemoglobin (g%)	9.28	9.91	9.54	10.53	0.35	0.487	8.0-15.0
Haematocrit (%)	34.48	33.09	35.64	38.91	1.12	0.391	24.0-46.0

Note: Means in the same row with different superscripts differ significantly ($p < 0.05$); *) Normal ranges according to Latimer et al. (2011), P1: control (TMR only), P2: TMR + 1% tannin (DM of diet), P3: TMR + 1% amino acids (0.3% DL-methionine and 0.7% L-lysine, DM of diet), P4: TMR + 1% tannin + 1% amino acid supplementation, SEM: Standard Error Mean

Table 6. Blood metabolites in female Friesian Holstein dairy calves

Parameters	P1	P2	P3	P4	SEM	*p-value*	Normal range*
Glucose (mg dL^{-1})	86.10	85.40	88.51	84.70	1.34	0.749	40.0-100.0
Triglyceride (mg dL^{-1})	29.41	27.39	27.02	29.04	1.04	0.889	17.0-30.0
BUN (mg dL^{-1})	29.44	20.97	29.38	32.74	2.03	0.388	10.0-25.0
Protein (g dL^{-1})	7.07^{a}	7.58^{b}	7.46^{b}	7.62^{b}	0.07	0.012	6.0-8.0
Cholesterol (mg dL^{-1})	94.14^{a}	125.98^{b}	138.59^{bc}	149.85^{c}	5.98	0.001	80.0-170.0

Note: Means in the same row with different superscripts differ significantly ($p < 0.05$); *) Normal ranges according to Latimer et al. (2011) and Mitruka et al. (1977); BUN: blood urea nitrogen; P1: control (TMR only), P2: TMR + 1% tannin (DM of diet), P3: TMR + 1% amino acids (0.3% DL-methionine and 0.7% L-lysine, DM of diet), P4: TMR + 1% tannin + 1% amino acid supplementation; SEM: Standard Error Mean

Nutrient digestibility

Table 4 shows no significant differences in nutrient digestibility in all treatments ($p > 0.05$). However, CF digestibility was lower in P4 (61.62%) compared to other treatments ($p = 0.081$).

Hematological and blood metabolites

The treatment effect on blood hematology, including erythrocytes, leukocytes, hemoglobin, and hematocrit, is presented in Table 5. The results show no significant differences in the hematological blood ($p > 0.05$).

The effect of treatment on blood metabolites, including glucose, triglyceride, blood urea nitrogen (BUN), protein, and cholesterol, is presented in Table 6. All treatments had no significant differences in glucose, triglyceride, and BUN in all treatments ($p > 0.05$). However, blood protein levels were significantly higher in supplemented treatments (P2: 7.58 g/dL, P3: 7.46 g/dL, P4: 7.62 g/dL) compared to the control (P1: 7.07 g/dL, $p < 0.05$). Cholesterol levels were significantly elevated in all supplemented groups compared to the control ($p < 0.01$), with the highest levels observed in P4 (149.85 mg/dL), followed by P3 (138.59 mg/dL) and P2 (125.98 mg/dL), compared to P1 (94.14 mg/dL).

Discussion

Performance of the calves

Average daily gain (ADG) in this study ranged from 0.41 kg/head/day to 0.73 kg/head/day. The normal range of ADG of 6-to-7-month-old calves varied from 0.4 kg/head/day to 0.9 kg/head/day, reported by Gitau et al. (1994). The supplementation of amino acid (P3: 0.73 kg/head/day) had the highest ADG. Amino acids, particularly methionine, are crucial for the growth of all animals and basic life functions (Vázquez-Añón et al. 2006) and can increase ADG (Zhou et al. 2016). Adding amino acids lysine and methionine increased the availability of methionine and lysine in the intestine, post-ruminal segment, and the entire gastrointestinal tract (Mazinani et al. 2020), thereby contributing to increased feed efficiency and average daily gain (Zhou et al. 2016). In this study, tannin supplementation (P2: 0.66 kg/head/day) in the ration increased ADG due to improved feed efficiency. Adding tannins in ruminant feed can improve feed efficiency by increasing the amount of rumen undegradable protein (Ma et al. 2024). Tannin-protein complexes formed at near-neutral pH (3.5-7.5) help more protein avoid breaking down in the rumen and release protein at a pH less than 3.5 (Jones and Mangan 1977). Furthermore, the protein is released and digested in the

small intestine (Ma et al. 2024). In previous studies, tannin supplementation in calves increased average daily gain (Soleiman and Kheiri 2018). However, supplementation with tannin-amino acids (P4) exhibited low. Supplementing tannin-amino acids in monogastrics it could decrease the absorption of essential amino acids (especially methionine) and reduce the animals' growth (Reed 1995). Moreover, tannins interfere with protein digestion by inhibiting the activity of proteases (Bhat et al. 2013; Jing et al. 2021), pectinases, amylases, cellulases, and lipases (Bhat et al. 2013), thereby decreasing nutritional digestibility in the rumen (Zhang et al. 2019a). This suggests that the rumen in young calves is still developing during the transition phase, which could make nutrient digestion less efficient than in adult ruminants (Hassan et al. 2020; Schwarzkopf et al. 2022). This could explain part of the lower ADG and feed efficiency observed in the P4.

The highest feed efficiency was found in amino acids supplementation (P3: 3.02%) and tannin supplementation (P2: 2.65%), although daily fresh intake remained relatively the same in all treatments. Based on the calculation, lower feed intake balanced with high average daily gain would lead to more feed efficiency (Krueger et al. 2010). Additionally, the presence of amino acids in the diet effectively promoted significant body weight gain, showing good feed efficiency (Niroumand et al. 2020). The increase in feed efficiency in tannin supplementation ration caused by lower protein degradation and CH_4 emissions (Orzuna-Orzuna et al. 2021). This indirectly increased the utilization of protein and energy in the calves. However, supplementation of tannin-amino acid (P4: 1.74%) reduced feed efficiency. Lower feed efficiency is indirectly caused by the formation of excessive tannins and proteins, which interfere with absorption and digestion. Incorrect levels of tannins and proteins can lead to growth suppression in livestock (Ojo 2022). Based on meta-analysis, hydrolyzable tannin (HT) has an adverse effect, causing inactivation of ruminal microorganisms, inhibiting the action of a microbial deaminase only at doses between 101 and 200 g/kg DM (Brutti et al. 2023). Still, the HT doses in this study, 0.91 g/kg, were lower and did not produce a lethal effect.

Nutrient intake

The CP intake in this study was significantly higher in the added supplementation compared to the control treatment. CP intake was linked to higher protein levels in the feed. According to Negesse et al. (2001), Katangole and Yan (2020), feeding with more protein could lead to more CP intake, and if animals eat enough, it might help with digestion, which can improve average daily gain (Etman et al. 2020). Sharma et al. (2020) also mentioned feeding more protein could help calves grow faster.

On the other hand, in P4, CP intake was higher, and ADG was lower. This was probably because of the complex formation of tannins and amino acids, which is difficult to break down. Tannins can react with many nitrogen-based compounds, including amino acids (Adamcyzk et al. 2017), and are more reactive when the amino acids have bigger molecular sizes and more amine groups (Adamcyzk et al. 2011). Lysine has two amine groups and methionine has one (Adamcyzk et al. 2017). As phenolic compounds, tannins showed the ability to bind and the high bond strength between tannin and protein (Besharati et al. 2022). In this study, different results for ADG were caused by the changes in how the supplements acted chemically. Moreover, the various levels of bond strength will modify the enzyme activity (Adamcyzk et al. 2017). Therefore, it is suggested that tannin-amino acid chemistry is crucial and requires further consideration.

Nutrient digestibility

The DM, OM, CP, EE, and CF digestibility in this study were within the normal range (Coutinho et al. 2014; Sarker et al. 2019; Geberemariyam et al. 2020; Suryani et al. 2020). Tannins can influence proteins and starch degradation (Besharati et al. 2022). Hydrolyzable tannins have more potentially adverse effects compared to condensed (Zhang et al. 2019b). However, small doses used in this study did not significantly affect the nutrient digestibility. Previous studies suggested that concentrations higher than 5% would limit nutrient digestibility (Atiku et al. 2016). Adding hydrolyzable tannin from chestnuts up to 2% did not really affect DM and OM breakdown in the rumen based on an in vitro study (Sadarman et al. 2019). Also, giving amino acids (2.0 mL/100 kg BW) might help improve how well nutrients are digested (Abdel-Raheem et al. 2022). However, in this study, adding 1% amino acids did not significantly affect how nutrients were digested, although it showed a significant effect compared to the control treatment.

There was a bit of a trend toward higher CP digestibility and lower CF digestibility when tannins, amino acids, or both were added. Tannins added to the feed have been shown to decrease rumen undegradable protein, thereby increasing nitrogen and protein to be used more (Orzuna-Orzuna et al. 2021). The lower CF digestibility was caused by the tannin-protein complex, which affected fiber digestion in the P4 group (Besharati et al. 2022). Amino acids like lysine and methionine have also been said to lower fiber digestion in calves compared to the control (Mudgal et al. 2018). However, young calves don't have a fully developed rumen, so fiber digestion is lower (Metiya et al. 2023). Since there were no significant differences in nutrient digestibility between the treatments, adding tannins, amino acids, or both did not change overall digestibility much.

Hematological and blood metabolites

Erythrocytes, hemoglobin, and hematocrit levels were within the normal range, indicating that the animals were in good health, according to Latimer et al. (2011), and the treatments in the diets did not affect the hematological profiles in this study. This response might be due to the relatively short period (14 days), which may not have been sufficient to express treatment effects fully. The added supplementation contributed to an increase in leukocytes and the adaptation process of the calves. Similarly, Ma et al. (2024) reported that adding 0.5 and 1% tannin increased leukocytes, serving as a protective mechanism and enhancing the organism's defense against potential threats (Naidenko and Mikhail 2020).

In this study, glucose levels were still in the normal range, according to Latimer et al. (2011), and blood triglyceride levels also fell within the normal range, according to Brito et al. (2021). However, BUN levels were a bit high, which is above the normal range, according to Latimer et al. (2011). This suggested the nitrogen in the feed was not being used efficiently. BUN levels are often used to check how well animals use nitrogen; nevertheless, calves with higher BUN levels could keep their body condition during cold weather (Tshuma et al. 2014). When animals fed with a lot of protein, especially the kind that breaks down in the rumen, BUN levels can increase because of the extra nitrogen in the blood (Xia et al. 2018). Adding tannins to the feed might help protect protein, allowing it to break down later in the gut, where the animal can better use it.

Protein levels in this study were within the normal range, as reported by Latimer et al. (2011). Blood protein levels are directly proportional to the amount of protein the livestock consumes. This is consistent with the findings of Schwab and Broderickt (2017), protein is converted into amino acids and will be transported through the blood. Mitruka et al. (1977) reported cholesterol levels in the normal range. Cholesterol levels increased with the added supplementation.

Furthermore, a high-protein diet can reduce total cholesterol in the blood of growing calves (Croccodrilli et al. 1970). This finding was not in line with the current study. Water-insoluble fats must bind to proteins, allowing the formation of low-density lipoproteins, which transport cholesterol from the liver to tissues (Laka et al. 2022). However, as a health marker in calves, there is a need to monitor blood cholesterol levels. Cholesterol deficiency in calves can cause diarrhea, leading to mortality (Otter and Hateley 2017).

In conclusion, the addition of individual tannins and amino acids at 1% DMI of calves' diets showed a significant effect compared to the control treatment, reduced fresh daily intake, resulting in higher average daily gain, improved feed efficiency, and increased CP utilization, without impairing calves' health. Adding the tannin-amino acids mixture produced intermediate effects, suggesting an antagonistic interaction. However, this combination shows potential for improving nutrient digestibility and protein utilization in young calves. Further studies should focus on the tannin-amino acids ratio to maximize these benefits and avoid negative interactions.

ACKNOWLEDGEMENTS

The authors would like to thank the National Research and Innovation Agency through the Endowment Fund for Education Agency (LPDP) for funding the research named Riset dan Inovasi untuk Indonesia Maju (RIIM) program Batch 3 (Grant Number B-840/II.7.5/FR.06/5/2023 and B-977/III.5/FR.06.00/5/2023). The authors would like to thank PT Sumber Citarasa Alam for their support.

REFERENCES

Abdel-Raheem SM, Mohamed GAE, Monzaly HMA, Farghaly MM. 2022. The effects of dietary eubiotics or intravenous amino acid infusions on nutrient digestibility, rumen fermentation, performance and blood parameters of buffalo calves under subtropical climatic conditions. Slov Vet Res 60 (Suppl 25): 259-270. DOI: 10.26873/svr-1588-2022.

Abitante G, Leme PR, de Paula Carlis MS, Ramírez-Zamudio GD, Gomes BIP, de Andrade LB, Goulart RS, Pugliesi G, Saran Netto A, Dahlen CR, Silva SL. 2024. Effects of early weaning on performance and carcass quality of Nellore young bulls. Animals (Basel) 14 (5): 779. DOI: 10.3390/ani14050779.

Adamczyk B, Adamczyk S, Smolander A, Kitunen V. 2011. Tannin acid and Norway spruce condesed tannins can precipitate various organic nitrogen compounds. Soil Biol Biochem 43 (3): 628-637. DOI: 10.1016/j.soilbio.2010.11.034.

Adamczyk B, Simon J, Kitunen V, Adamczyk S, Smolander A. 2017. Tannins and their complex interaction with different organic nitrogen compounds and enzymes: Old paradigms versus recent advances. ChemistryOpen 6 (5): 610-614. DOI: 10.1002/open.201700113.

Al Rharad A, El Aayadi S, Avril C, Souradjou A, Sow F, Camara Y, Hornick JL, Boukrouh S. 2025. Meta-analysis of dietary tannins in small ruminant diets: Effects on growth performance, serum metabolites, antioxidant status, ruminal fermentation, meat quality, and fatty acid profile. Animals (Basel) 15 (4): 596. DOI: 10.3390/ani15040596.

AOAC. 1985. Official Method of Analysis. Association of Official Analytical Chemists, Washington.

Atiku A, Oladipo OO, Forcados GE, Usman AS, Mancha MD. 2016. Anti-nutritional and phytochemical profile of some plants grazed upon by ruminants in North Central Nigeria during the dry season (January to April). Intl J Livest Prod 7 (4): 19-23. DOI: 10.5897/ijlp2015.0268.

Benetton JB, Neave HW, Costa JHC, von Keyserlingk MAG, Weary DM. 2019. Automatic weaning based on individual solid feed intake: Effects on behavior and performance of dairy calves. J Dairy Sci 102 (6): 5475-5491. DOI: 10.3168/jds.2018-15830.

Besharati M, Maggiolino A, Palangi V, Kaya A, Jabbar M, Eseceli H, De Palo P, Lorenzo JM. 2022. Tannin in ruminant nutrition: Review. Molecules 27 (23): 8273. DOI: 10.3390/molecules27238273.

Bhat TK, Kannan A, Singh B, Sharma OP. 2013. Value addition of feed and fodder by alleviating the antinutritional effects of tannins. Agric Res 2 (3): 189-206. DOI: 10.1007/s40003-013-0066-6.

Bhatti SA, Ali A, Nawaz H, McGill D, Sarwar M, Afzal M, Khan MS, Ehsanullah, Amer MA, Bush R, Wynn PC, Warriach HM. 2012. Effect of pre-weaning feeding regimens on post-weaning growth performance of Sahiwal calves. Animal 6 (8): 1231-1236. DOI: 10.1017/s1751731112000250.

Boukrouh S, Noutfia A, Moula N, Avril C, Louvieaux J, Hornick JL, Cabaraux JF, Chentouf M. 2024. Growth performance, carcass characteristics, fatty acid profile, and meat quality of male goat kids supplemented by alternative feed resources: Bitter vetch and sorghum grains. Arch Anim Breed 67: 481-492. DOI: 10.5194/aab-67-481-2024.

Brito RF, França AFS, Pansani AP, Castro CH, Colugnati DB, Souza LF, Rabelo LA, Nunes-Souza V, Xavier CH, Oliveira GA, Corrêa DS, Ramos AT, Macedo LM, Ferreira RN. 2021. Performance and serum parameters of calves (*Bos taurus*) subject to milk restriction associated with supplementation with 2-hydroxy-4-(methylthio) butanoic acid. J Anim Sci 99 (6): skab104. DOI: 10.1093/jas/skab104.

Brutti DD, Canozzi MEA, Sartori ED, Colombatto D, Barcellos JOJ. 2023. Effects of the use of tannins on the ruminal fermentation of cattle: A meta-analysis and meta-regression. Anim Feed Sci Tech 306: 115806. DOI: 10.1016/j.anifeedsci.2023.115806.

Coccodrilli Jr GD, Chandler PT, Polan CE. 1970. Effects of dietary protein on blood lipids of the calf with special reference to cholesterol. J Dairy Sci 53 (11): 1627-1631. DOI: 10.3168/jds.s0022-0302(70)86448-7.

Coutinho DA, Branco AF, Santos GT, Osmari MP, Teodoro AL, Diaz TG. 2014. Intake, digestibility of nutrients, milk production and composition in dairy cows fed on diets containing cashew nut shell liquid. Acta Sci 36: 311-316. DOI: 10.4025/actascianimsci.v36i3.23512.

Dell'Anno M, Frazzini S, Ferri I, Tuberti S, Bonaldo E, Botti B, Grossi S, Sgoifo Rossi CA, Rossi L. 2024. Effect of dietary supplementation of chesnut and quebracho tannin supplementation on neonatal diarrhoea in preweaning calves. Antioxidants (Basel) 13 (2): 237. DOI: 10.3390/antiox13020237.

Etman KEI, El-Nahrawy MM, El-Sayed FA, Ghoniem AH, Sayed SK, Farag ME. 2020. Effect of probiotic bacteria or enzymes supplementation on productive performance of fatting Friesian steers. J Anim Poult Prod 11 (9): 353-358. DOI: 10.21608/jappmu.2020.118214.

Fitri A, Yanza YR, Jayanegara A, Ridwan R, Astuti WD, Sarwono KA, Fidriyanto R, Rohmatussolihat R, Widyastuti Y, Obitsu T. 2022. Divergence effects between dietary Acacia and Quebracho tannin extracts on nutrient utilization, performance, and methane emission of ruminants: A meta-analysis. Anim Sci J 93 (1): e13765. DOI: 10.1111/asj.13765.

Fraga-Corral M, Otero P, Cassani L, Echave J, Garcia-Oliveira P, Carpena M, Chamorro F, Lourenço-Lopes C, Prieto MA, Simal-Gandara J. 2021. Traditional applications of tannin-rich extracts supported by scientific data: Chemical composition, bioavailability and bioaccessibility. Foods 10 (2): 251. DOI: 10.3390/foods10020251.

Geberemariyam T, Getu K, Mulugeta W, Dereje F, Aeimro K, Mesfin D, Betlehem M, Endale Y. 2020. Feed intake and growth performance of Jersey Calves in maize stover silage based total mixed ration. J Biol Agric Healthc 10: 9-13. DOI: 10.7176/jbah/10-17-02.

Girard M, Thanner S, Pradervand N, Hu D, Ollagnier C, Bee G. 2018. Hydrolysable chestnut tannins for reduction of post-weaning diarrhea: Efficacy on an experimental ETEC F4 model. PLoS One 13 (5): e0197878. DOI: 10.1371/journal.pone.0197878.

Gitau GK, McDermott JJ, Adams JE, Lissemore KD, Walter-Toews D. 1994. Factors influencing calf growth and daily weight gain on smallholder dairy farms in Kiambu District, Kenya. Prev Vet Med 21 (2): 179-190. DOI: 10.1016/0167-5877(94)90006-x.

Hao Y, Xing M, Gu X. 2021. Research progress on oxidative stress and its nutritional regulation strategies in pigs. Animals (Basel) 11 (5): 1384. DOI: 10.3390/ani11051384.

Hassan FU, Arshad MA, Ebeid HM, Rehman MS, Khan MS, Shahid S, Yang C. 2020. Phytogenic additives can modulate rumen microbiome to mediate fermentation kinetics and methanogenesis through exploiting diet-microbe interaction. Front Vet Sci 7: 575801. DOI: 10.3389/fvets.2020.575801.

Jing H, Huang X, Jiang C, Wang L, Du X, Ma C, Wang H. 2021. Effects of tannic acid on the structure and proteolytic digestion of bovine lactoferrin. Food Hydrocoll 117: 106666. DOI: 10.1016/j.foodhyd.2021.106666.

Jones WT, Mangan JL. 1977. Complexes of the condensed tannins of sainfoin (*Onobrychis viciifolia* scop.) with fraction 1 leaf protein and with submaxillary mucoprotein, and their reversal by polyethylene glycol and pH. J Sci Food Agric 28 (2): 126-136. DOI: 10.1002/jsfa.2740280204.

Katangole CB, Yan T. 2020. Effect of varying dietary crude protein level on feed intake, nutrient digestibility, milk production, and nitrogen use efficiency by lactating Holstein-Friesian cows. Animals 10 (12): 2439. DOI: 10.3390/ani10122439.

Khan MA, Bach A, Weary DM, von Keyserlingk MAG. 2016. Invited review: Transitioning from milk to solid feed in dairy heifers. J Dairy Sci 99 (2): 885-902. DOI: 10.3168/jds.2015-9975.

Krueger WK, Gutierrez-Bañuelos H, Carstens GE, Min BR, Pinchak WE, Gomez RR, Anderson RC, Krueger NA, Forbes TD. 2010. Effects of dietary tannin source on performance, feed efficiency, ruminal fermentation, and carcass and non-carcass traits in steers fed a high-grain diet. Anim Feed Sci Technol 159 (1-2): 1-9. DOI: 10.1016/j.anifeedsci.2010.05.003.

Laka K, Makgoo L, Mbita Z. 2022. Cholesterol-lowering phytochemicals: Targeting the mevalonate pathway for anticancer interventions. Front Genet 13: 841639. DOI: 10.3389/fgene.2022.841639.

Latimer KS, Mahaffey EA, Prasse KW. 2011. Duncan and Prasse's Veterinary Laboratory Medicine: Clinical Pathology 5th edn. John Wiley and Sons Inc., West Sussex.

Li YL, McAllister LTA, Beauchemin KA, He ML, McKinnon JJ, Yang WZ. 2011. Substitution of wheat dried distillers grains with solubles for barley grain or barley silage in feedlot cattle diets: Intake, digestibility, and ruminal fermentation. J Anim Sci 89 (8): 2491-2501. DOI: 10.2527/jas.2010-3418.

Lorenz MM, Alkhafadji L, Stringano E, Nilsson S, Mueller-Harvey I, Udén P. 2013. Relationship between condensed tannin structures and their ability to precipitate feed proteins in the rumen. J Sci Food Agric 94: 963-968. DOI: 10.1002/jsfa.6344.

Ma M, Enomoto Y, Takashaki T, Uchida K, Chambers JK, Goda Y, Yamanaka D, Takashaki SI, Kuwahara M, Li J. 2024. Study of the effects of condensed tannin additives on the health and growth performance of early-weaned piglets. Animals 14 (16): 2337. DOI: 10.3390/ani14162337.

Mazinani M, Naserian AA, Rude BJ, Tahmasbi AM, Validesh R. 2020. Effect of feeding rumen protected amino acids on the performance of feedlot calves. J Adv Vet Anim Res 7 (2): 229-233. DOI: 10.5455/javar.2020.g414.

McGuirk SM, Peek SF. 2014. Timely diagnosis of dairy calf respiratory disease using a standardized scoring system. Anim Health Res Rev 15 (2): 145-147. DOI: 10.1017/S1466252314000267.

Metiya A, Vahora S, Patel A, Patel J. 2023. Effect of supplementing rumen-protected methionine and lysine with lower crude protein diet on apparent digestibility and rumen fermentation of crossbred female calves. Pharma Innov J 12 (11): 1777-1781.

Mirzaei-Alamouti H, Salehi S, Khani M, Vazirigohar M, Aschenbach JR. 2025. Changes in ruminal fermentation and growth performance in calves after increasing ruminal undegradable protein at two different time points pre-weaning. Animals 15 (6): 804. DOI: 10.3390/ani15060804.

Mitruka BM, Rawnsley HM, Vadehra BV. 1977. Clinical Biochemical and Hematological Reference Values in Normal Experimental Animals. Masson Publ., NewYork.

Montout L, Poullet N, Bambou JC. 2021. Systematic review of the interaction between nutrition and immunity in livestock: Effect of dietary supplementation with synthetic amino acids. Animals (Basel) 11 (10): 2813. DOI: 10.3390/ani11102813.

Mudgal V, Saxena N, Mohan C, Jain S, Kumar K, Sharma ML, Kumar R. 2018. Precision feeding approach affecting growth, nutrient utilization, feed conversion efficiency and economics of feeding weaned Murrah buffalo calves. Indian J Anim Sci 88: 80-83. DOI: 10.56093/ijans.v88i10.84151.

Nagy O, Tóthová C, Kováč G. 2014. Age-related changes in the concentrations of serum proteins in calves. J Appl Anim Res 42 (4): 451-458. DOI: 10.1080/09712119.2013.875918.

Naidenko SV, Mikhail VA. 2020. Size matters: Zoo data analysis shows that the white blood cell ratio differs between large and small felids. Animals (Basel) 10 (6): 940. DOI: 10.3390/ani10060940.

Negesse T, Rodehutscord M, Pfeffer E. 2001. The effect of dietary crude protein level on intake, growth, protein retention and utilization of growing male Saanen kids. Small Rumin Res 39 (3): 243-251. DOI: 10.1016/s0921-4488(00)00193-0.

Niroumand M, Ganjkhanlou M, Rezayazdi K. 2020. Supplementation of Holstein dairy calves fed two levels of crude protein with methionine and lysine. S Afr J Anim Sci 50 (3): 442-451. DOI: 10.4314/sajas.v50i3.11.

Ojo MA. 2022. Tannins in foods: Nutritional implications and processing effects of hydrothermal techniques on underutilized hard-to-cook legume seeds-a review. Prev Nutr Food Sci 27 (1): 14-19. DOI: 10.3746/pnf.2022.27.1.14.

Orzuna-Orzuna JF, Dorantes-Iturbide G, Lara-Bueno A, Mendoza-Martínez GD, Miranda-Romero LA, Hernández-García PA. 2021. Effects of dietary tannins' supplementation on growth performance, rumen fermentation, and enteric methane emissions in beef cattle: A meta-analysis. Sustainability 13 (13): 7410. DOI: 10.3390/su13137410.

Otter A, Hateley G. 2017. Blood cholesterol concentrations in dairy calves. Vet Record 180 (2): 52-52. DOI: 10.1136/vr.j122.

Reed JD. 1995. Nutritional toxicology of tannins and related polyphenols in forage legumes. J Anim Sci 73: 1516-1528. DOI: 10.2527/1995.7351516x.

Sadarman S, Ridla M, Nahrowi N, Ridwan R, Harahap RP, Nurfitriani RA, Jayanegara A. 2019. Physical quality of soy sauce waste silage with tannin additives from acacia (*Acacia mangium* Wild.) and other additives. Jurnal Peternakan 16 (2): 66-75. DOI: 10.24014/jupet.v16i2.7418. [Indonesian]

Sarker NR, Yeasmin D, Habib MA, Tabassum F. 2019. Feeding effect of total mixed ration on milk yield, nutrient intake, digestibility and rumen environment in Red Chittagong Cows. Asian J Med Biol Res 5 (1): 71-77. DOI: 10.3329/ajmbr.v5i1.41048.

Schwab CG, Broderick GA. 2017. A 100-year review: Protein and amino acid nutrition in dairy cows. J Dairy Sci 100 (12): 10094-10112. DOI: 10.3168/jds.2017-13320.

Schwarzkopf S, Kinoshita A, Hüther L, Salm L, Kehraus S, Südekum KH, Huber K, Dänicke S, Frahm J. 2022. Weaning age influences indicators of rumen function and development in female Holstein calves. BMC Vet Res 18 (1): 102. DOI: 10.1186/s12917-022-03163-1.

Sharma B, Nimje P, Tomar SK, Dey D, Mondal S, Kundu SS. 2020. Effect of different fat and protein levels in calf ration on performance of Sahiwal calves. Asian-Australas J Anim Sci 33 (1): 53-60. DOI: 10.5713/ajas.18.0604.

Silva JT, Miqueo E, Torrezan TM, Rocha NB, Slanzon GS, Virginio Júnior GF, Bittar CMM. 2021. Lysine and methionine supplementation for dairy calves is more accurate through the liquid than the solid diet. Animals (Basel) 11 (2): 332. DOI: 10.3390/ani11020332.

Soleiman P, Kheiri F. 2018. The effect of different levels of tannic acid on some performance traits in holstein dairy calves. Iran J Appl Anim Sci 8 (1): 19-23.

Suryani NN, Suarna IW, Mahardika IG, Sarini SP, Doloksaribu L. 2020. Energy and nitrogen retention of Bali Heifers (*Bos sondaicus*) fed diet containing different energy protein level. TERNAK TROPIKA J Trop Anim Prod 21 (1): 69-76. DOI: 10.21776/ub.jtapro.2020.021.01.9.

Talib C, Entwistle K, Siregar A, Turner SB, Lindsay D. 2003. Survey of population and production dynamics of Bali cattle and existing breeding programs in Indonesia. ACIAR Proceedings. Australian Centre for International Agricultural Research. 2003. [Australia]

Tautenhahn A, Merle R, Muller KE. 2020. Factors associated with calf mortality and poor growth of dairy heifer calves in northeast Germany. Prev Vet Med 184: 105154. DOI: 10.1016/j.prevetmed.2020.105154.

Tshuma T, Holm DE, Fosgate GT, Lourens DC. 2014. Pre-breeding blood urea nitrogen concentration and reproductive performance of Bonsmara heifers within different management systems. Trop Anim Health Prod 46 (6): 1023-1030. DOI: 10.1007/s11250-014-0608-3.

van Niekerk JK, Fischer-Tlustos AJ, Wilms JN, Hare KS, Welboren AC, Lopez AJ, Yohe TT, Cangiano LR, Leal LN, Steele MA. 2020. ADSA Foundation Scholar Award: New frontiers in calf and heifer nutrition-From conception to puberty. J Dairy Sci 104 (8): 8341-8362. DOI: 10.3168/jds.2020-20004.

Vázquez-Añón M, Kratzer D, González-Esquerra R, Yi IG, Knight CD. 2006. A multiple regression model approach to contrast the performance of 2-hydroxy-4-methylthio butanoic acid and DL-Methionine supplementation tested in broiler experiments and reported in the literature. Poult Sci 85 (4): 693-705. DOI: 10.1093/ps/85.4.693.

Xia C, Aziz Ur Rahman M, Yang H, Shao T, Qiu Q, Su H, Cao B. 2018. Effect of increased dietary crude protein levels on production performance, nitrogen utilisation, blood metabolites and ruminal fermentation of Holstein bulls. Asian-Australas J Anim Sci 31 (10): 1643-1653. DOI: 10.5713/ajas.18.0125.

Zhang J, Xu X, Cao Z, Wang Y, Yang H, Azarfar A, Li S. 2019a. Effect of different tannin sources on nutrient intake, digestibility, performance, nitrogen utilization, and blood parameters in dairy cows. Animals (Basel) 9 (8): 507. DOI: 10.3390/ani9080507.

Zhang R, Chen J, Mao X, Qi P, Zhang X. 2019b. Anti-inflammatory and anti-aging evaluation of pigment-protein complex extracted from *Chlorella pyrenoidosa*. Mar Drugs 17 (10): 586. DOI: 10.3390/md17100586.

Zhou Z, Bulgari O, Vailati-Riboni M, Trevisi E, Ballou MA, Cardoso FC, Luchini DN, Loor JJ. 2016. Rumen-protected methionine compared with rumen-protected choline improves immunometabolic status in dairy cows during the peripartal period. J Dairy Sci 99 (11): 8956-8969. DOI: 10.3168/jds.2016-10986.

NUSANTARA BIOSCIENCE
Vol. 17, No. 2, pp. 203-217
November 2025

ISSN: 2087-3948
E-ISSN: 2087-3956
DOI: 10.13057/nusbiosci/n170218

Destructive sampling-based allometric equations for biomass and carbon estimation in *Acacia* hybrid plantations in Southeastern Vietnam

NGUYEN THI HA[1], TRAN QUANG BAO[2,♥], NGUYEN THANH TUAN[3], DIEGO I. RODRÍGUEZ-HERNÁNDEZ[4], NGUYEN TIEN DUNG[5], TRAN THI NGOAN[1]

[1]Vietnam National University of Forestry at Dongnai. Dong Nai Province, Vietnam
[2]Department of Forestry, Ministry of Agriculture and Rural Development. Ba Dinh District, Hanoi, Vietnam. Tel: +84-94-5043274, ♥email: baofuv@vnuf.edu.vn
[3]Faculty of Silviculture, Vietnam National University of Forestry. Dong Nai Campus, Bien Hoa 810000, Dong Nai, Vietnam
[4]School of Biological Sciences, University of Bristol. 24 Tyndall Avenue, Bristol, BS8 1TQ, UK
[5]La Nga - Dong Nai Forestry Company Limited, Dong Nai Province, Vietnam

Manuscript received: 26 September 2024. Revision accepted: 18 August 2025.

Abstract. *Ha NT, Bao TQ, Tuan NT, Rodríguez-Hernández DI, Dung NT, Ngoan TT. 2025. Destructive sampling-based allometric equations for biomass and carbon estimation in* Acacia *hybrid plantations in Southeastern Vietnam. Nusantara Bioscience 16: 203-217.* This study developed accurate allometric equations for estimating aboveground and belowground biomass, as well as carbon stocks, for *Acacia* hybrid (*Acacia mangium* × *Acacia auriculiformis*) plantations in Southeastern, Vietnam. A dataset of 45 destructively sampled trees with varying ages and diameter classes was used to validate the models. The fresh biomass of the four tree components (stem, branches, leaves, and roots) was measured for a total of 180 samples. Samples were oven-dried at 105°C for stems and branches, and 80°C for leaves, to determine their biomass. Linear and non-linear equations were employed to model both individual tree and stand-level dry biomass (AGB: aboveground biomass, BGB: belowground biomass, TGBG: total biomass), and carbon stocks (AGC: aboveground carbon, BGC: belowground carbon, TGC: total carbon). Diameter at breast height (DBH), tree height (H), stand density (SD), and stand age (A) were included as predictor variables. The best-fitting models were selected based on coefficients of determination (R^2), sum of squared errors (SEE), mean absolute error (MAE), sum of squared residuals (SSR), correction factors (CF), mean absolute percentage error (MAPE), and root mean square error (RMSE), with R^2 values greater than 0.895 and RMSE values less than 0.363. The results revealed strong relationships between aboveground and belowground biomass, and logarithmic functions of DBH and tree height were found to be good predictors for all biomass components. The key equations are: ln(AGB) = -3.03805 + 0.586847*ln(DBH*H) + 1.58329*ln(DBH); ln(BGB) = -0.597955 + 0.485409*ln(DBH)^2; ln(TGB) = -2.65453 + 2.11674*ln(DBH) + 0.57522*ln(H). Among the variables, DBH was found to be particularly effective in estimating BGB. At the stand level, total biomass (TSB) has a significant correlation with stand density, mean diameter, and stand height, as shown in the following equation: Ln(TSB) = -9.85561 + 1.09128*ln(SD) + 1.96789*ln(D_s) + 0.608831*ln(H_s). These models provide foresters with valuable tools for estimating biomass and carbon accumulation in *Acacia* hybrid plantations. The total carbon stock of the *Acacia* hybrid population in the study area ranged from 29.0 tons/ha to 313.3 tons/ha. This information can support carbon accounting efforts and contribute to Vietnam's initiatives for carbon reduction and climate change mitigation.

Keywords: *Acacia mangium* × *auriculiformis*, allometric modeling**,** carbon stock, destructive sampling, Southeast Asia reforestation

INTRODUCTION

Forest ecosystem plays a large part in mitigating climate change through the sequestration of atmospheric carbon dioxide (CO) and acting as immense carbon sinks under initiatives such as REDD+ (Reducing Emissions from Deforestation and Forest Degradation) (Rizvi et al. 2015; Pham et al. 2019). Tropical rainforests are vital, containing about 25% of the carbon in terrestrial biomass and soils and generating about 34% of the global terrestrial primary production (Dixon et al. 1994). Carbon storage capacity varies tremendously with forest type, site quality, and species (Siraj and Teshome 2017; Tuan et al. 2022). Accurate estimation of aboveground biomass (AGB), belowground biomass (BGB), and overall carbon stocks is therefore essential to comprehending and managing forest carbon cycles (Magerl et al. 2019; Anderson-Teixeira et al. 2021).

Since the 1970s, endeavors like the International Biological Program (IBP) and national forest inventories have encouraged biomass and carbon quantification (Brown and FAO 1997). The first studies by Brown and Lugo (1982) estimated that tropical forests hold 46% of the terrestrial ecosystem carbon, 11% of which is stored in soils. Subsequent studies have estimated biomass in the United States (Jenkins et al. 2003), Australia (NFI 2003), China (Liu et al. 2016; Luo et al. 2020), and other forests (Huy et al. 2016; Salunkhe et al. 2018). Plantation forests are also under the limelight for their relatively high biomass accretion rates, and studies have been carried out on the likes of *Eucalyptus* (Prabha et al. 2023), *Hevea brasiliensis* (Dabi et al. 2021), and *Rhizophora* in Vietnam (Phan et al. 2019; Vinh et al. 2019). Forests around the world hold an estimated 296.2 billion tons of carbon, with the most being stored in South America, followed by Africa, then Europe and Asia (FAO 2015).

Estimation methods of biomass are generally destructive or non-destructive. Destructive methods, involving felling and weighing the trees, are accurate but costly, time-consuming, and disturbance-causing for the environment. Non-destructive methods like allometric models and remote sensing are cost-saving and convenient for large-scale applications (Salunkhe et al. 2018; Schettini et al. 2022). Allometric models relating the diameter, height, and wood density of the tree to biomass are particularly helpful in carbon storage estimation at various scales (Chave et al. 2014).

Studies on *Acacia mangium* and *Acacia auriculiformis* in Bangladesh, Malaysia, Japan, and China have given valuable biomass information (Adam and Jusoh 2018; Zhang et al. 2018). Nevertheless, studies on *Acacia* hybrids (*Acacia mangium* × *Acacia auriculiformis*) in Vietnamese conditions are few. Models tend to use DBH or DBH and height only and ignore variables such as stand density, age, and wood density, which can significantly improve accuracy (Chave et al. 2014; Paul et al. 2016).

Vietnam has about 14 million hectares of forest cover, accounting for 42% of its land area. Plantation forests occupy 4.7 million hectares, with 2.35 million hectares of *Acacia* hybrids dominating more than half of the plantation forest (MARD, 2020). These *Acacia* hybrid plantations are highly valued for rapid growth, short rotation cycles, high productivity, and high carbon sequestration potential (Dinh Kha and Huy Thinh 2017; Adam and Jusoh 2018). They also play an essential role in Vietnam's climate change response, notably achieving the net-zero emission target by 2050 (MONRE 2022). Participation in UN-REDD and the establishment of Measurement, Reporting, and Verification (MRV) systems require region- and species-specific biomass models. However, most apply Tier 1 default values or generic simplified equations that may not be site-specific (IPCC 2006; Pham et al. 2019).

There are over 2,000 hectares of *Acacia* hybrid plantation owned by La Nga Forestry Company in Southeastern Vietnam, yet no localized allometric models exist. Current models (e.g., Bao and Phuc 2018) fail to include site-specific variables, reducing accuracy and practicability.

The research addresses these gaps by developing site-specific allometric models to predict AGB, BGB, and total carbon stores of *Acacia* hybrids in Southeastern Vietnam. Models are developed at the tree and stand levels, incorporating key structural and ecological characteristics. The outcome is expected to enhance forest carbon accounting, aid climate-related forestry policy, and improve global schemes such as REDD+ that promote sustainable forest management and carbon offset schemes.

MATERIALS AND METHODS

Study site and species

The research was conducted at La Nga Forestry Company, Dinh Quan District, Dong Nai Province, Southeastern Vietnam (Figure 1). The area covers about 14,658.55 ha of planted forest, with the geographical coordinates ranging from 11° to 11° 23' latitude and 107° to 107° 22' longitude. The area experiences a subequatorial tropical monsoon climate, with an average annual temperature of 25°C, average rainfall of 3,293 mm, and average annual humidity of 83%. It is located in the transitional zone from the South Central Highlands to the plains. It consists of undulating hills with a maximum elevation of 272 m and a minimum of 60 m. The soil types at the company are grey basalt (16%), red basalt (13%), reddish-yellow ferralitic developed on schist (62%), and alluvial (9%). In 2020, the planted forest in the study site was 14,658.55 hectares, and approximately 2,071 hectares with plantations of *Acacia* hybrid, ranging in age from 1 to 10 years old (MARD 2020).

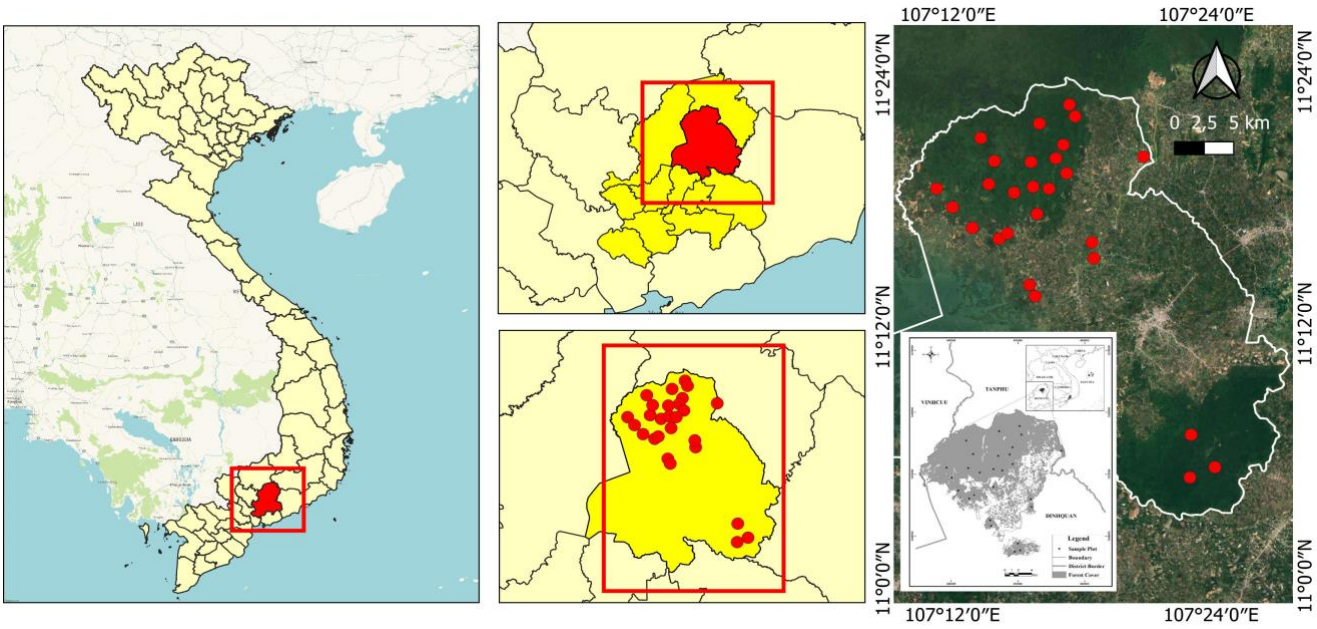

Figure 1. Geographic location of the study area and the sample plots (black stars) where trees of *Acacia* hybrid were harvested

Tree sampling

Tree sampling for *Acacia* hybrid individuals was carried out in forest plantations between 2 and 10 years old, respectively. In this study, we employed the destructive method by felling down trees of different diameters and stand age classes. Specifically, 45 healthy individuals, with diameters at breast height (DBH) ranging from 4 to 22 cm (ages 2 to 10 years), were destructively sampled. The number of sampled trees was stratified by age, with a minimum of three trees per age class. Consequently, the number of trees sampled at each age ranged from three trees (age 8) to six trees (ages 3, 4, 5, and 10) (Table S1). The DBH of each tree was calculated from the measured stem circumference using a diameter tape, with an accuracy of ±1.0 cm. Tree height was measured using a Criterion RD 1000 hypsometer, with a precision of ±0.1 m. These trees were weighed and measured to calculate their fresh biomass for four components: leaves, branches, stems, and roots (Figure 2).

Figure 2. Tree harvesting and destructive sampling showing the separation of each tree component: A. Leaves, B. Branches, C. Stems, and D. Roots with stumps

In total, 180 samples were collected from the 45 trees, with each tree providing four samples (leaves, branches, stems, and roots). Belowground biomass (BGB) was assessed by excavating and weighing coarse roots (>2 mm in diameter). Fine roots (<2 mm) were excluded from sampling due to difficulties in separation and measurement, particularly under field conditions. Root, stem, and branch samples weighed approximately 0.5 to 1.0 kg, while leaf samples weighed between 0.2 and 0.5 kg. The samples were then transported to the laboratory and oven-dried for at least 72 hours at 105°C for stems, branches, and roots, and at 80°C for leaves (Brown and FAO 1997; Chave et al. 2014). After drying, the samples were reweighed to determine the dry to fresh biomass ratio, which was used to calculate the dry biomass for each plant part. Carbon content was analyzed using a TOC/TN analyzer (HT 1300) on a total of 36 dry biomass samples, with 4 samples from each age group at the laboratory of the Southern Academy of Forest Sciences.

Above- and belowground biomass and carbon estimation

In this study, we utilized 20 candidate models to estimate the biomass or carbon content of individual trees and stands (Table S2). The dependent variable (Y) is the biomass or carbon of individual trees or stands, while the independent variables (X) include two key tree dimensions: diameter at breast height (DBH, cm) and tree height (H, m), and two stand characteristics: stand density (SD) and stand age (A). Including tree dimensions (DBH, H) together with stand-level factors (SD, A) provides a comprehensive approach for estimating biomass and carbon stocks, enhancing the accuracy and reliability of forest carbon quantification. In order to evaluate the performance of developed H-DBH models, the data were randomly divided into a training dataset (80%) and a validation dataset (20%). The analysis process was performed using R software (version 4.2.2) with the support of library packages such as Metrics, dplyr, ggplot2, and readxl.

To address potential multicollinearity, we have included a correlation matrix and calculated the variance inflation factor (VIF) for all predictor variables. Variables with VIF values greater than 10 were excluded to reduce multicollinearity and enhance model robustness. Finally, we used several criteria to select the most appropriate models for estimating individual tree and stand biomass, as outlined below:

Coefficient of determination (R^2): In general, the function is considered optimal when R^2 is higher for at least 50%. However, there are cases where the highest R^2 does not correspond to the most suitable model, so it is necessary to rely on other statistical criteria described below.

Verification of model and model parameters: It is required that both the model and its parameters are statistically significant ($p < 0.05$).

Sum of Squares Error (SEE), Mean Absolute Error (MAE), and Sum of Squared Residuals (SSR): The equation is considered best when these three indices are minimized.

Correction Factors (CF): Referencing works by Cao and Li (2019).

$$CF = \exp(RSE^2 / 2) \quad (1)$$

Where: RSE denotes the residual standard error. The model is considered optimal when the Correction Factor (CF) approaches 1.

Mean Absolute Percentage Error (MAPE): This metric is used to test the applicability of the equations and evaluate the level of deviation and average fluctuation of the estimated values produced by the model compared to actual observations.

$$MAPE = \frac{100}{n} \sum_{i=1}^{n} \frac{|Yo - Ye|}{Yo} \quad (2)$$

Where: Y_e: predicted observations, Y_o: actual observations; n: the number of observations.

AIC (Akaike information criteria) and BIC (Bayesian Information Criterion):

$$AIC = -n \cdot \ln(RMSE^2) + 2p \quad (3)$$

$$BIC = -n \cdot \ln(RMSE^2) + p * \ln(n) \quad (4)$$

Where: n: the number of observations, p: number of model parameters to be estimated, RMSE: Root mean square error.

Models with a higher coefficient of determination (R^2), and lower values for SSR, SEE, MAE, MAPE, RMSE, and CF, along with statistically significant parameters ($p<0.05$), were selected as the best-fitting biomass allometric equations, fit statistics of non-linear regression analysis also including AIC (Akaike information criteria), and BIC (Bayesian Information Criterion). Information criteria are important measures for selecting non-linear models because they provide a quantitative measure of how well a particular model fts the data. These criteria allow for the selection of the most appropriate non-linear model. Therefore, this study deployed these criteria for further validation of the selected model. The lower ft statistic values indicate a better-ft model.

Additionally, to assess the influence of individual observations on model performance, we calculated Cook's distance and leverage values for all regression models. Observations with a Cook's distance greater than 1.0 were considered potentially influential, and high-leverage points were identified based on the standard leverage threshold $2p/n$, where p is the number of predictors and n is the number of observations (Baba et al. 2021).

RESULTS AND DISCUSSION

Allometric equations for estimating the biomass and carbon stocks of individual tree

Biomass equations for individual tree

Based on 20 candidate models, we developed 12 of the most effective allometric equations for estimating aboveground biomass (AGB), belowground biomass (BGB), and total ground biomass (TGB). All these equations were modeled as a function of diameter at breast height (DBH), tree height (H), age (A), and stand densities (SD). Models with a higher coefficient of determination (R^2), and lower values for SSR, SEE, MAE, MAPE, RMSE, AIC, BIC and CF, along with statistically significant parameters ($p<0.05$), were

selected as the best-fitting biomass allometric equations. The selected models are highlighted in bold (Table 1, Table S3).

The results of the correlation analysis and statistical indices indicate that the equations are all statistically significant and have high coefficients of determination (R^2>0.96), with uniform coefficients of determination within allowable limits. This demonstrates a very close relationship between the factors considered. For the AGB estimation model, Model (4), which is a two-dimensional logarithmic model with two factors, has the highest R^2 (0.99). It also has a relatively small estimated standard error, mean absolute error, and correction factor (CF). The RMSE, AIC, BIC for Model (4) is the smallest (Figure 3), and all equation parameters are significant (p<0.001). Therefore, Model (4) is suitable for estimating aboveground biomass for individual trees of *Acacia* hybrid.

For the BGB estimation model, the results in Table 1, Figure 3, and Table S3 indicate that all four models exhibit high R^2 coefficients, ranging from 0.886 to 0.901. In addition, the SEE, MAE, AIC, BIC and SSR errors are all minimal. Notably, Model (6) demonstrates the smallest AIC, BIC for test dataset. Consequently, Model (6) was selected for the estimation of BGB for individual *Acacia* hybrids.

Similarly, the results in Table 1, Figure 3, and Table S3 show that the relationship between the total biomass of *Acacia* hybrid individuals and the investigated factors is very close, with a high coefficient of determination (ranging from 0.780 to 0.988). The SSR, SEE, and MAE errors were also all very small, indicating an adequate model fit. Among the models, Model (12) has the highest level of R^2 (0.988 for train dataset and 0.974 for test dataset) and the lowest of AIC and BIC.

Figure 4 shows the correlation and residual error between the observed values and estimated values from the model. The residual error measures how much each observed value deviates from the model built using all observed data. In the error case shown in Figure 4, most of the residuals are less than 0.5, with only a few estimated residuals larger than 0.5 but not exceeding 1.

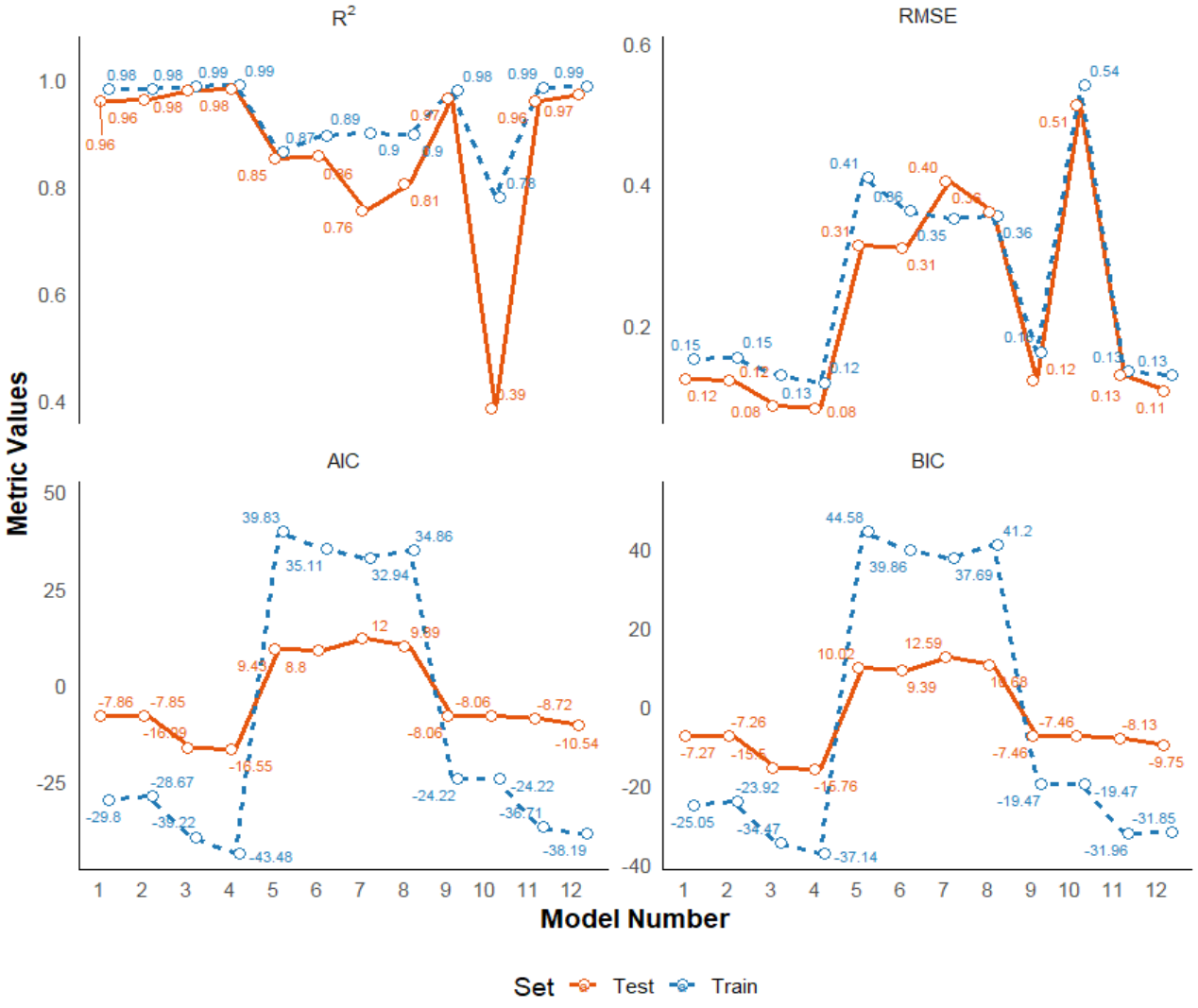

Figure 3. Goodness-of-fit statistics of the most effective models for estimating biomass at the individual tree level. The statistic values are shown for both training and testing datasets

Table 1. The most effective models for estimating individual tree biomass

Component	No.	Allometric equations	Model parameters		
			a	b	c
AGB	1	AGB= exp(a + b*ln(DBH))	-2.42702**	2.56912**	
	2	$ln(AGB) = (a + b*ln(ln(DBH)))^2$	0.540346**	1.59586**	
	3	$ln(AGB) = a + b*ln(DBH^2*H)$	-3.37784**	0.952494**	
	4	ln(AGB) = a + b*ln(DBH*H) + c*ln(DBH)	-3.03805***	0.586847***	1.58329***
BGB	5	$BGB = (a + b*DBH^2)^2$	1.44278*	0.0126791**	
	6	$ln(BGB) = a + b*ln(DBH)^2$	-0.597955***	0.485409***	
	7	$log(BGB) = a + b*log(DBH^2*H)$	-4.15561**	0.862991**	
	8	log(BGB) = a + b*log(DBH*H) + c*log(DBH)	-3.70196**	0.37481***	1.70517**
TGB	9	TGB = exp(a+ b*ln(DBH))	-2.0556*	2.50782**	
	10	ln(TGB) = exp(a + b*ln(DBH))	-0.0188452*	1.57559*	
	11	$ln(TGB) = a + b*ln(DBH^2*H)$	-2.98404**	0.929806**	
	12	ln(TGB) = a+ b*ln(DBH) + c*ln(H)	-2.65453***	2.11674***	0.57522***

Note: Regression models are more suitable for biomass prediction and are printed in bold, AGB: Aboveground dry biomass, BGB: Belowground dry biomass, DBH: Diameter at breast height, H: Tree height, TGB: Total dry biomass. *significant at P<0.05; **significant at P<0.005 level; ***significant at P<0.001 level

Carbon equations for individual tree

Developing a carbon estimation model contributes to carbon storage monitoring and quantifying the environmental value of forests. Carbon estimation models with high coefficient of determination and small errors are summarized and presented in Table 2 and Table S4.

The analysis of the correlation and model error of terrestrial carbon estimates reveals a strong connection between terrestrial carbon stocks and the investigated factors. The coefficient of determination is notably high (ranging from 97.5% to 99.0%), and the model parameters are statistically significant, with coefficients of variation and errors within acceptable limits. Model (15) shows the smallest error compared to MAPE (MAPE=9.62%), while model (14) has the largest MAPE (15.38%). Consequently, model (15) is deemed suitable for estimating aboveground carbon for *Acacia* hybrid (refer to Table 2, Figure 5 and Table S4).

Similarly, testing various functions with statistical criteria to select optimal variables and functions for estimating underground carbon shows that underground biomass carbon has a strong relationship with diameter at breast height. As shown in Table 2, Figure 5 and Table S4, the coefficients of determination of the four models are all relatively high (>86.6%). Models (17) and (18) exhibit the highest MAPE, at 36.13% and 28.09%, respectively. However, Model (20) has the highest coefficient of determination (0.901) and the lowest value of RMSE, AIC and BIC, at 0.352, 32.94, and 37.69, respectively. Therefore, Model (20) is suitable for estimating belowground carbon for *Acacia* hybrid trees.

Since the components of a tree (stem, branches, bark, leaves, roots) are closely related, biomass and carbon for components that are difficult to measure directly below ground can be estimated from models with different predictor variables (Kenzo et al. 2020; Handavu et al. 2021; Annighöfer et al. 2022), or from the relationship between aboveground and belowground biomass carbon (Bieluczyk et al. 2023). Therefore, equation (20) enables the rapid estimation of belowground carbon based on tree growth variables, such as diameter at breast height.

Carbon sequestration is now a recognized forest management mechanism, supported by economic mechanisms at the macro level, primarily due to the "Carbon Credits" initiative. Developing a forest tree carbon estimation model is thus valuable for forest management planning and calculating energy reserves in forest biomass. The error and correlation analysis of the models (Table 2, Figure 5 and Table S4) indicates that the coefficients of determination are very high (97.36% to 98.71%), demonstrating a strong relationship between total tree carbon and the investigation factors D and H. Additionally, the errors are small and within permissible limits. Model (23) records the highest coefficient of determination (98.8%) and the smallest error compared to MAPE (9.77%). Model (22) has the highest MAPE value (15.04%) and the lowest coefficient of determination (96.50%). Hence, model (23) is suitable for estimating the carbon of *Acacia* hybrid.

Figure 6 illustrates the correlation and residual error between observed values and estimated carbon values from the model. Similar to the biomass estimation model, the residual error is assessed to compare each observed value against the model built using all observed data. Most residuals are less than 2, with only a few estimated residuals exceeding 2 but not surpassing 5.

Allometric equations for estimating the biomass plantations

By testing various types of functions that relate biomass to investigation factors and basic growth of the forest stand, we explored single-variable functions, multi-variable functions, and combinations of variables to select the most optimal model for estimating biomass in a population. The variables tested in these functions included: Stand diameter (Ds), stand height (Hs), stand age (A) and stand density (SD).

The results of constructing a biomass estimation model for an *Acacia* hybrid forest stand are summarized in Table 3. The results of error analysis and the correlation between biomass and investigated factors in an *Acacia* hybrid forest stand show that the coefficients of determination of the models are very high, ranging from 94.12% to 99.31%

(Table 3). This demonstrates a close relationship between forest biomass and the investigated factors such as DBH, H, N, and A. The models and their parameters are all significant at a 99% confidence level. Additionally, the errors (SSR, SEE, MAE) are small. Model (28) has the highest coefficient of determination (>99%) and the smallest error compared to MAPE (4.99%) (refer to Table 3, and Figure 7). Hence, model (28) is the most suitable for estimating the total biomass of *Acacia* hybrid forests.

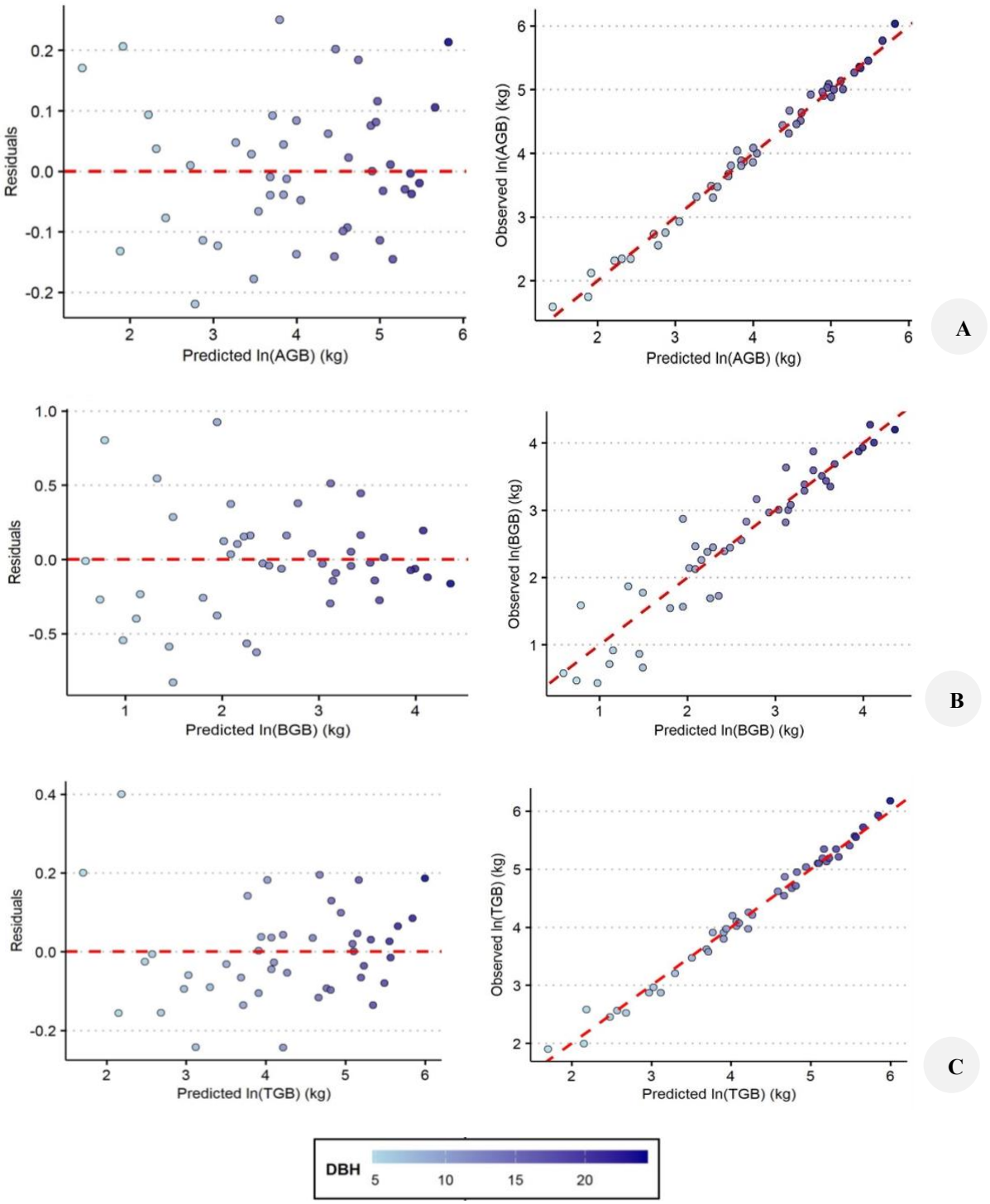

Figure 4. Scatter plots illustrating the comparison between individual tree biomass of *Acacia* hybrid obtained from field measurements and our estimation method. A. Aboveground dry biomass, B. Belowground dry biomass, C. Total dry biomass

Table 2. The most effective models for estimating carbon stocks of *Acacia* hybrid individual tree

Component	No	Allometric equations	Model parameters		
			a	b	c
AGC	13	AGC = exp(a + b*ln(DBH))	--3.14061**	2.56921**	
	14	AGC = exp(a+ b*sqrt(DBH))	-2.0804**	1.50233*	
	15	ln(AGC) = a+b *ln(DBH) + c*ln(H)	-3.75174***	2.17016***	0.586943**
	16	ln(AGC) = a+ b*ln(DBH^2*H)	-4.09147	0.952527	
BGC	17	BGC = (a + b* DBH^2)^2	1.00944***	0.00887663***	
	18	BGC = (a+ b* DBH)^2	-0.504757**	0.250682*	
	19	ln(BGC) = a+ b*ln(DBH) +c*ln(H)	-4.42019**	2.08145**	0.375082*
	20	ln(BGC) = a+ b*ln(DBH^2*H)	-4.87416*	0.863603**	
TGC	21	TGC = exp(a+ b*ln(DBH))	-2.76832**	2.50757**	
	22	TGC = (a+ b* DBH)^2	-1.55574*	0.614246*	
	23	ln(TGC) = a+ b*ln(DBH) + c*ln(H)	-3.36645**	2.11701***	0.574454***
	24	ln(TGC) = a+ b*ln(DBH^2*H)	-3.69657**	0.929702**	

Note: regression models are more suitable for biomass prediction, are printed in bold, AGC: Aboveground carbon, BGC: Belowground carbon, DBH: Diameter at breast height, H: Tree height, TGC: Total carbon, *significant at P<0.05; **significant at P<0.005 level; ***significant at P<0.001 level

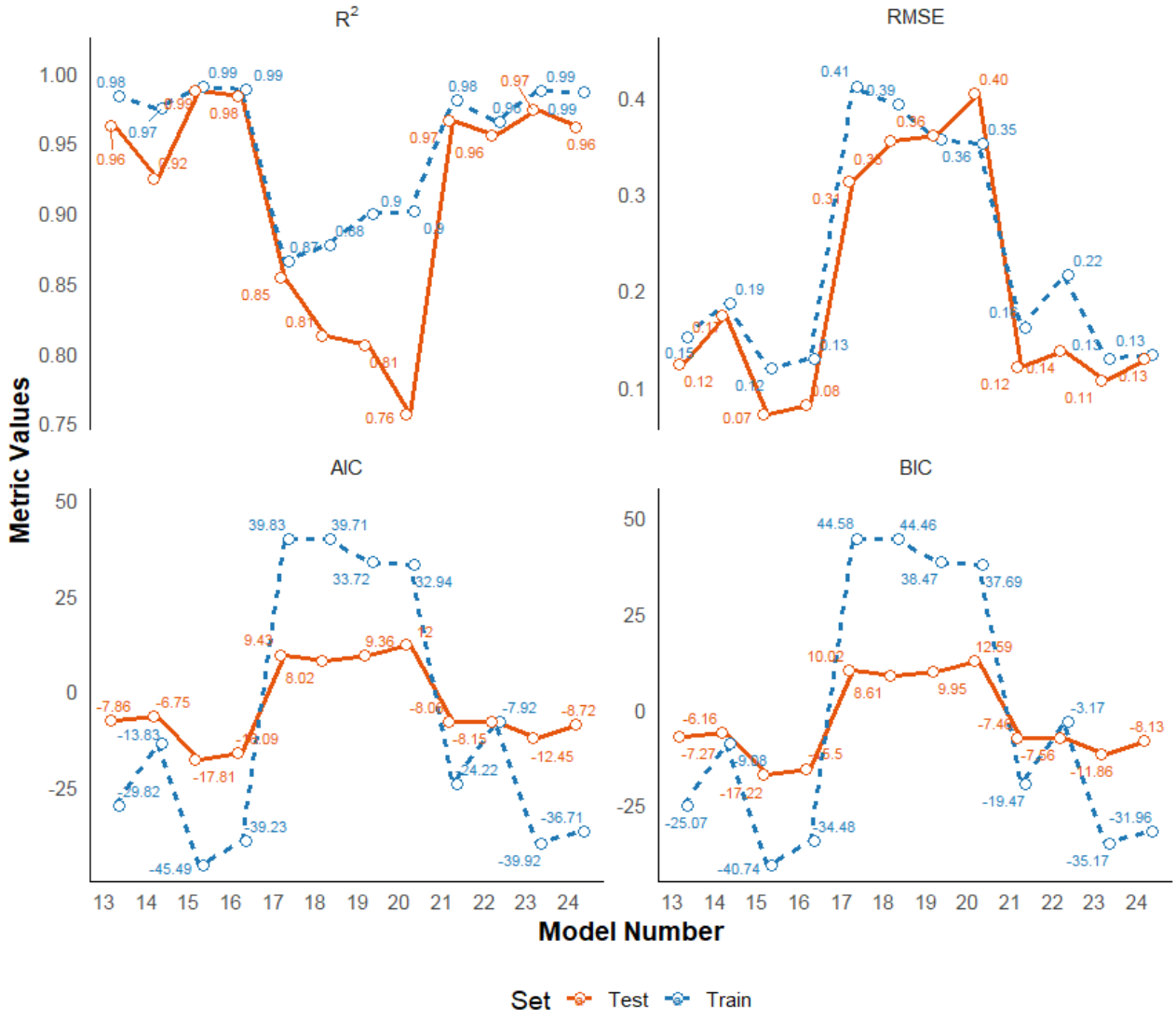

Figure 5. Goodness-of-fit statistics of the most effective models for estimating carbon at the individual tree level. The statistic values are shown for both training and testing datasets

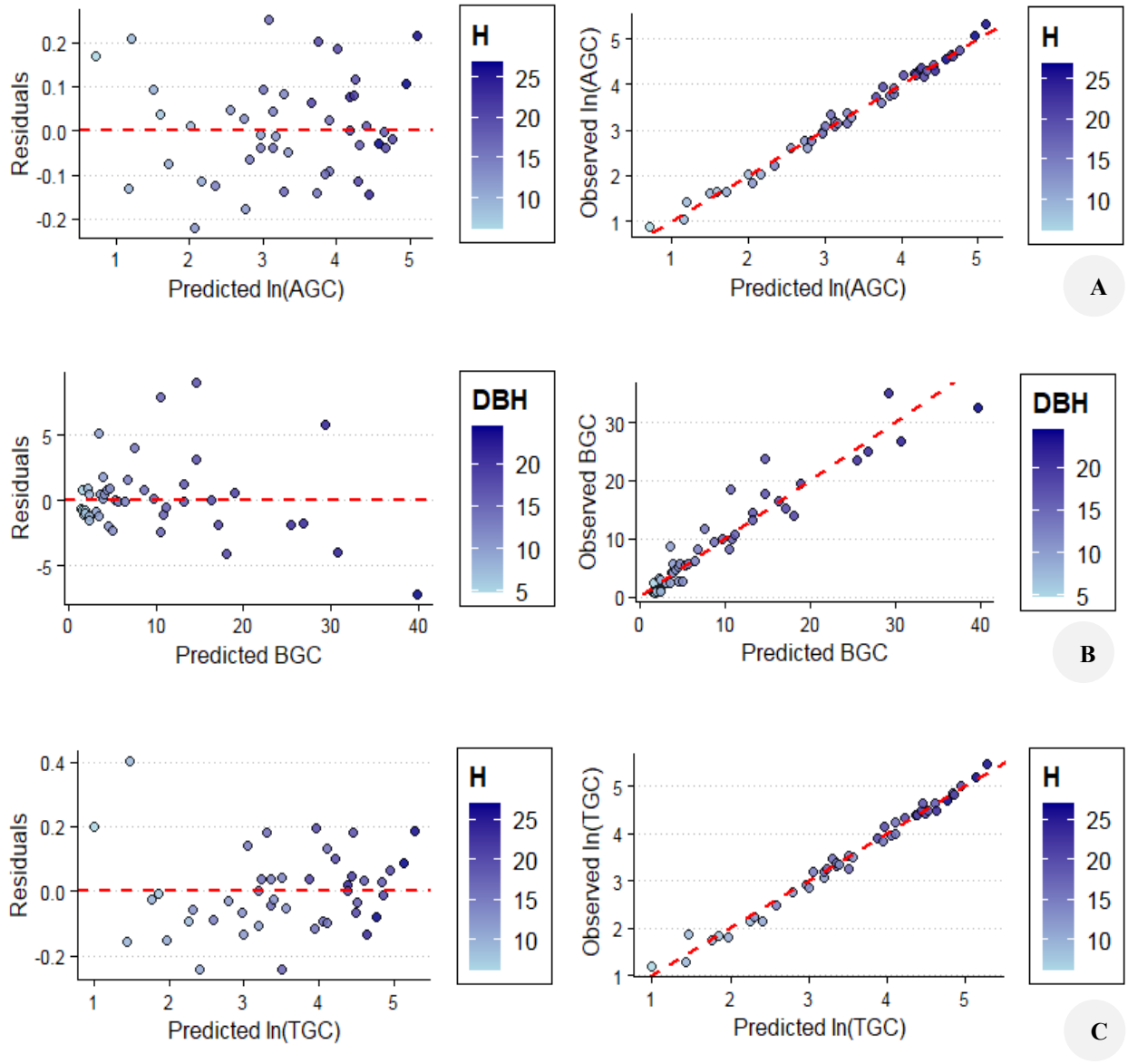

Figure 6. Correlation and bias of the *Acacia* hybrid carbon estimation model. A. Aboveground carbon, B. Belowground dry carbon, C. Total dry carbon. Note: All carbon values are expressed in kg

Table 3. Models for estimating total stand BGB of *Acacia* hybrid plantations

No.	Allometric equations	Model evaluation statistics					
		R^2	SSR	SEE	MAE	MAPE	CF
25	Ln(TSB) = -10.8046 + 1.21052*ln(SD) + 2.65308*ln(D_s)	98.89	0.22	0.08	0.06	6.01	1.00
26	Ln(TSB) = -11.3581 + 1.48312*ln(SD* D_s) + 0.836347*ln(A)	94.12	1.15	0.18	0.14	12.72	1.02
27	Ln(TSB) = -9.94382 + 0.22143*ln(A) + 2.33323*ln(D_s) + 1.14724*ln(SD)	99.29	0.14	0.06	0.05	5.05	1.00
28	Ln(TSB) = -9.85561 + 1.09128*ln(SD) + 1.96789*ln(D_s) + 0.608831*ln(H_s)	99.31	0.14	0.06	0.05	4.99	1.00

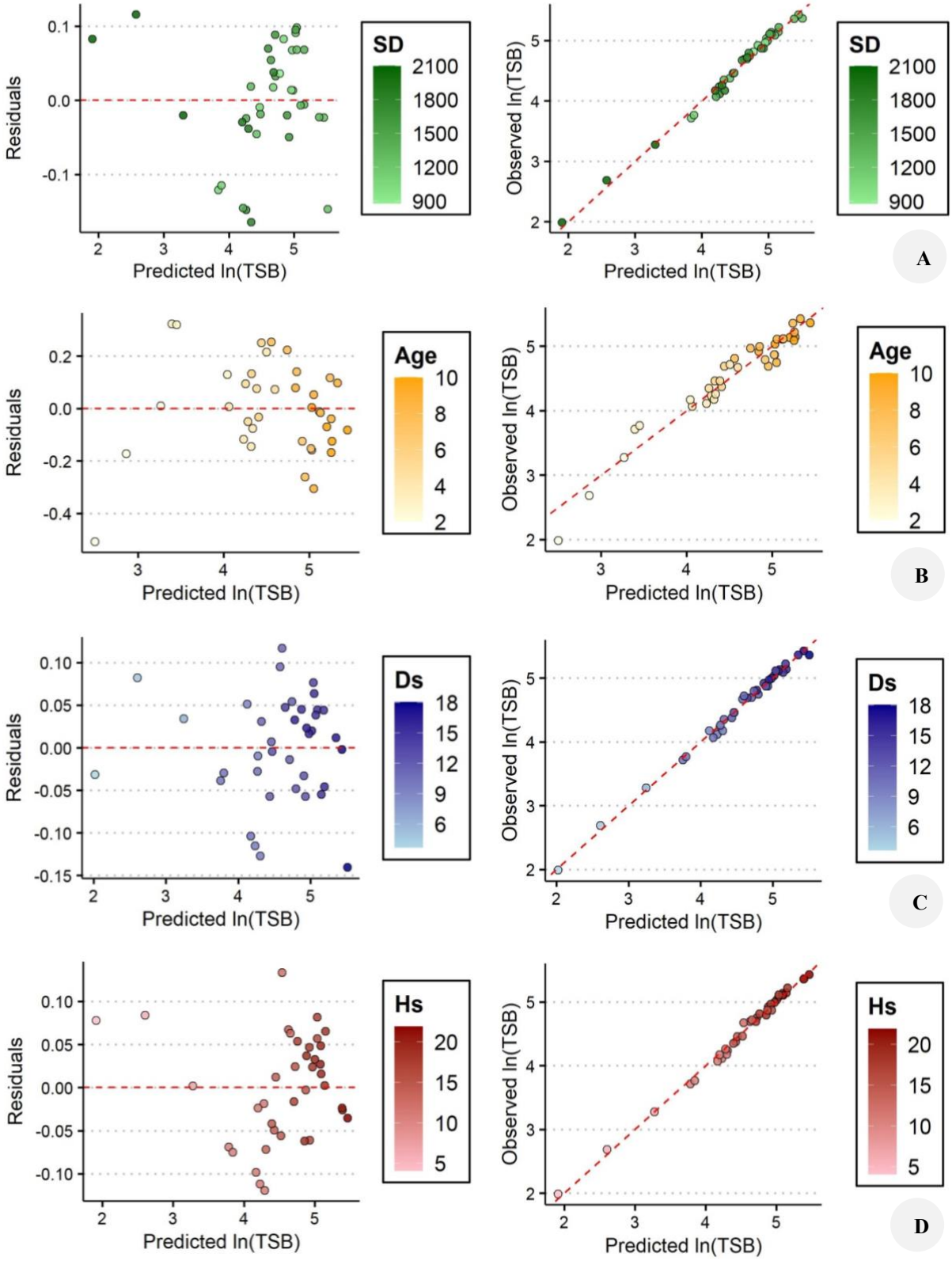

Figure 7. Comparison of four logarithmic regression models for estimating the stand biomass of *Acacia* hybrid (TSB). A. Model 25, B. Model 26, C. Model 27, D. Model 28. TGB: the stand biomass of *Acacia* hybrid (ton/ha), D_s: Stand diameter (cm), Hs: Stand height (m), A: Stand age (years), SD: stand density (trees/ha)

Discussion

First, using allometric equations to estimate forest biomass and carbon stocks is a highly accurate and reliable method, and it has been repeatedly applied worldwide (Chave et al. 2014; Paul et al. 2016; Doan et al. 2025). Second, this study employs a combination of exponential and log-linear functions to estimate biomass and carbon. Many domestic and international studies have found that these, along with linear functions, are common functional forms for biomass estimation (Anitha et al. 2015; Bao and Phuc 2018; Brahma et al. 2021; Cabrera-Ariza et al. 2021).

The criteria for selecting the best-fit model for each biomass component included R^2, Mean Absolute Error (MAE), Correction Factor (CF), Sum of Squared Residuals (SSR), and mean absolute percentage error (MAPE). While most studies rely on the R^2 coefficient for function selection, some incorporate MAE and SRR criteria as well (Anitha et al. 2015; Huy et al. 2016; Paul et al. 2016; Nguyenthi 2017; Bao and Phuc 2018). Additionally, some studies consider Correction Factor (CF) and Sum of Squared Errors (SEE) (Bao and Phuc 2018; Altanzagas et al. 2019; Levan et al. 2020) and Mean Absolute Percentage Error (MAPE) (Nguyenthi 2017; Tashi et al. 2017; Pothong et al. 2022). These criteria are widely used for selecting suitable functions to estimate forest biomass and carbon accumulation.

Regarding the variables used to estimate biomass and carbon, the biomass and carbon equation refers to the relationship between the biomass and carbon of a tree (or its parts such as trunk, branches, leaves, roots) with one or more investigation variables (such as diameter, height, wood weight, density) (Luo et al. 2020; Aneseyee et al. 2021; Cabrera-Ariza et al. 2021). This study estimates the biomass and carbon of individual *Acacia* hybrid trees using an equation that includes either diameter or height, or both D and H. For estimating biomass and carbon of *Acacia* hybrid plantations, many variables such as D, H, N, A, and combinations of D and H, D, H, and N were used. The results show that models estimating total biomass and carbon can use variables such as diameter, height, density, and age. Specifically, *Acacia* hybrid biomass and carbon have a closer relationship with the two factors D and H than with just D. Additionally, the research indicates that using more variables such as density, diameter, and height yields, more accurate results than using a single variable.

A synthesis of 5,924 forest biomass estimation equations in China shows that 43.5% of the equations are based on a single predictor (diameter or height), while 56.5% are based on two predictors (diameter and height) or a combination of both. Among these, diameter at breast height is the most commonly used variable in biomass equations (96.8%) (Luo et al. 2020). The use of the diameter variable in biomass equations is also common in Europe, India, Indonesia, and Africa, with 46%, 48%, 55%, and 63%, respectively (Anitha et al. 2015; Brahma et al. 2021). This preference is due to the ease of measuring diameter in practice and its suitability for estimating forest biomass and carbon (Anitha et al. 2015).

In general, many research projects on biomass and carbon have been conducted using various methods, with the commonly used method based on the correlation equation between biomass and investigated criteria of standard trees or plantations. Some authors confirm that tree biomass and carbon depend closely on tree trunk diameter, thus building a correlation function with diameter at breast height (Solomon et al. 2017; Adam and Jusoh 2018; Aneseyee et al. 2021). However, other authors assert that biomass and carbon also depend on tree height, thereby using both diameter and height for better estimation results (Huy et al. 2016; Abich et al. 2019).

According to Altanzagas et al. (2019), tree biomass and carbon can be estimated from predictor variables such as diameter, height, and wood density. The above results show that forest tree biomass and carbon have a close relationship with the investigated factors D, H, N, and A. Therefore, biomass and carbon can be estimated from the variables D, or a combination of D and H, or a combination of D, H, and N. This approach is consistent with the scientific and practical basis of many national and international studies conducted on woody plants, trees, and shrubs in plantations (Huy et al. 2016; Nguyenthi 2017; Abich et al. 2019; Altanzagas et al. 2019; Handavu et al. 2021; Bieluczyk et al. 2023).

This study will be used to inform the development and deployment of climate mitigation programs, including REDD+, the Clean Development Mechanism (CDM), and voluntary offset markets. *Acacia* hybrid stands and other forest plantations have become more trusted components of national greenhouse gas (GHG) inventories and carbon sequestration activities in Vietnam (Pham et al. 2019). The allometric models developed here provide convenient methods for predicting aboveground and belowground biomass with more precision, which is required to calculate carbon credits and monitor changes over time. The result of this study also supports Tier 2 methods under IPCC guidelines by being regionally calibrated models, reducing uncertainty less than default emission factors (IPCC 2006). Besides, these models can also be integrated into project-level Monitoring, Reporting, and Verification (MRV) systems, satisfying Vietnam's updated Nationally Determined Contributions (NDCs) and forest-based climate solution commitment (MONRE 2022). With the growth of the voluntary carbon market in Southeast Asia, especially with interest in nature-based solutions, solid biomass equations such as here will be essential for enabling scientifically valid and financially viable forest carbon projects (Hamrick and Gallant 2017).

In conclusion, we developed 10 suitable allometric equations to accurately estimate the biomass and carbon stocks of individual trees and plantations of *Acacia* hybrid in Southeastern Vietnam. Among these, the linear logarithmic function with two factors DBH and tree height was the most appropriate for estimating the total biomass and total carbon stocks of *Acacia* hybrids. Additionally, a single-factor linear function with independent DBH as predictor variable was suitable for estimating total biomass and BGB of *Acacia* hybrid. The study also demonstrated the relationship between AGB and BGB using a correlation function, with the predictor variable being biomass or AGC. Whereas the biomass and carbon for the *Acacia* hybrid

at stand-level were estimated using a linear logarithmic model with three predictor variables: DBH, H, and stem density, in the form: Ln(TSB) = -9.85561 + 1.09128*ln(SD) + 1.96789*ln(Ds) + 0.608831*ln(Hs). With these findings, foresters charged with managing this forest type can now implement these models to more accurately estimate the biomass and carbon accumulation over time of *Acacia* hybrid in a more accurate way. To apply these models in practice, users need to measure one or more of the following variables in the field such as DBH, H. Once these parameters are recorded, users can substitute the measured values into the corresponding biomass or carbon equation (e.g., for aboveground biomass, belowground biomass, or total biomass) provided in this study. The output will yield an estimate of dry biomass (kg) or carbon stock (kg/tree) for each individual tree. This study emerges as the foundation for accurately calculating the total fresh biomass and carbon stocks of *Acacia* hybrid forests in Southeastern Vietnam and benefits the country to meet its carbon reduction goals. However, this study also has limitations. Although the allometric models demonstrated high predictive power within the sample plantations managed by La Nga Forestry Company in Southeastern Vietnam, caution should be exercised when applying them to other regions. Additionally, moisture content may vary across seasons and tree ages, especially in leaf tissues, potentially affecting the accuracy of dry biomass estimation despite the use of oven-drying protocols. Variability in *Acacia* clone types, soil characteristics, climate, and silvicultural practices may affect tree allometry and model accuracy. Therefore, we recommend local model calibration and/or the inclusion of site-specific random effects before broader application. Further studies should validate and refine these models across diverse ecological zones to enhance their applicability.

ACKNOWLEDGEMENTS

We would like to thank La Nga Forestry Company Limited, Vietnam, for generously granting permission to conduct this study. The authors would also like to thank our colleagues and the staff of La Nga Forestry Company Limited for their support in data collection. Additionally, we express our appreciation to the editorial team and the anonymous reviewers for their valuable comments and suggestions.

REFERENCES

Abich A, Mucheye T, Tebikew M, Gebremariam Y, Alemu A. 2019. Species-specific allometric equations for improving aboveground biomass estimates of dry deciduous woodland ecosystems. J For Res 30 (5): 1619-1632. DOI: 10.1007/s11676-018-0707-5.

Adam NS, Jusoh I. 2018. Allometric model for predicting aboveground biomass and carbon stock of *Acacia* plantations in Sarawak, Malaysia. BioResources 13: 7381-7394. DOI: 10.15376/biores.13.4.7381-7394.

Altanzagas B, Luo Y, Altansukh B, Dorjsuren C, Fang J, Hu H. 2019. Allometric equations for estimating the above-ground biomass of five forest tree species in Khangai, Mongolia. Forests 10 (8): 661. DOI: 10.3390/f10080661.

Anderson-Teixeira KJ, Herrmann V, Banbury Morgan R, Bond-Lamberty B, Cook-Patton SC, Ferson AE, Muller-Landau HC, Wang MMH. 2021. Carbon cycling in mature and regrowth forests globally. Environ Res Lett 16 (5): 053009. DOI: 10.1088/1748-9326/abed01.

Aneseyee AB, Soromessa T, Elias E, Feyisa GLJCB. 2021. Allometric equations for selected *Acacia* species (*Vachellia* and *Senegalia* genera) of Ethiopia. Carbon Balance Manag 16: 34. DOI: 10.1186/s13021-021-00196-1.

Anitha K, Verchot LV, Joseph S, Herold M, Manuri S, Avitabile V. 2015. A review of forest and tree plantation biomass equations in Indonesia. Ann For Sci 72: 981-997. DOI: 10.1007/s13595-015-0507-4.

Annighöfer P, Mund M, Seidel D, Ammer C, Ameztegui A, Balandier P, Bebre I, Coll L, Collet C, Hamm T, Huth F, Schneider H, Kuehne C, Löf, Mary Petritan A, Catalin Petritan I, Peter S, Jürgen B. 2022. Examination of aboveground attributes to predict belowground biomass of young trees. For Ecol Manag 505: 119942. DOI: 10.1016/j.foreco.2021.119942.

Baba AM, Midi H, Adam MB, Rahman NHA. 2021. Detection of influential observations in spatial regression model based on outliers and bad leverage classification. Symmetry 13: 2030. DOI: 10.3390/sym13112030.

Bao TQ, Phuc VT. 2018. Biomass and CO_2 sequestration of *Acacia* hybrid plantation in Ba Ria Vung Tau Province. J For Sci 2: 69-75. [Vietnamese]

Bieluczyk W, Asselta FO, Navroski D, Gontijo JB, Venturini AM, Mendes LW, Simon CP, de Camargo PB, Tadini AM, Martin-Neto L, Bendassolli JA, Rodrigues RR, van der Putten WH, Tsai SM. 2023. Linking above and belowground carbon sequestration, soil organic matter properties, and soil health in Brazilian Atlantic Forest restoration. J Environ Manag 344: 118573. DOI: 10.1016/j.jenvman.2023.118573.

Brahma B, Nath AJ, Deb C, Sileshi GW, Sahoo UK, Das AK, 2021. A critical review of forest biomass estimation equations in India. Tree For People 5: 100098. DOI: 10.1016/j.tfp.2021.100098.

Brown S, FAO. 1997. Estimating Biomass and Biomass Change of Tropical Forests: A Primer, FAO FORESTRY PAPER 134. A Forest Resources Assessment publication, Rome.

Brown S, Lugo AE. 1982. The storage and production of organic matter in tropical forests and their role in the global carbon cycle. Biotropica 14 (3): 161-187. DOI: 10.2307/2388024.

Cabrera-Ariza A, Valdés S, Gilabert H, Santelices-Moya RE, Alonso-Valdés M. 2021. Allometric models for estimating aboveground biomass in short rotation crops of *Acacia* species in two different sites in Chile. Forests 12 (12): 1767. DOI: 10.3390/f12121767.

Cao L, Li H. 2019. Analysis of error structure for additive biomass equations on the use of multivariate likelihood function. Forests 10 (4): 298. DOI: 10.3390/f10040298.

Chave J, Réjou-Méchain M, Búrquez A, Chidumayo E, Colgan MS, Delitti WB, Duque A, Eid T, Fearnside PM, Goodman RC. 2014. Improved allometric models to estimate the aboveground biomass of tropical trees. Glob Chang Biol 20: 3177-3190. DOI: 10.1111/gcb.12629.

Dabi H, Bordoloi R, Das B, Paul A, Tripathi OP, Mishra BP. 2021. Biomass, carbon stock and soil physicochemical properties in plantation of East Siang district, Arunachal Pradesh, India. Environ Chall 4: 100191. DOI: 10.1016/j.envc.2021.100191.

Dinh Kha L, Huy Thinh H. 2017. Research and development of *Acacia* hybrids for commercial planting in Vietnam. Vietnam J Sci Technol Eng 59 (1): 36-42. DOI: 10.31276/VJSTE.59(1).36.

Dixon RK, Solomon A, Brown S, Houghton R, Trexier M, Wisniewski J. 1994. Carbon pools and flux of global forest ecosystems. Science 263 (5144): 185-190. DOI: 10.1126/science.263.5144.185.

Doan TNM, Vu VM, Ruano I, Bravo F. 2025. Disentangling the relationship of aboveground biomass, structure and tree diversity in a mixed *Acacia* plantation in Northern Vietnam. Eur J For Res 144: 941-961. DOI: 10.1007/s10342-025-01776-3.

FAO [Food and Agriculture Organization]. 2015. Global Forest Resources Assessment 2015, Food and Agriculture Organization of the United Nations, Rome.

Hamrick K, Gallant M. 2017. Unlocking Potential: State of the Voluntary Carbon Markets 2017. Forest Trends. https://www.forest-trends.org/publications/unlocking-potential/.

Handavu F, Syampungani S, Sileshi GW, Chirwa PWC. 2021. Aboveground and belowground tree biomass and carbon stocks in the miombo woodlands of the Copperbelt in Zambia. Carbon Manag 12 (3): 307-321. DOI: 10.1080/17583004.2021.1926330.

Huy B, Poudel KP, Temesgen H. 2016. Aboveground biomass equations for evergreen broadleaf forests in South Central Coastal ecoregion of Viet Nam: Selection of eco-regional or pantropical models. For Ecol Manag 376: 276-283. DOI: 10.1016/j.foreco.2016.06.031.

IPCC [Intergovernmental Panel on Climate Change]. 2006. Guidelines for National Greenhouse Gas Inventories. Agriculture, Forestry and Other Land Use. Forest Land. https://www.ipcc-nggip.iges.or.jp/public/2006gl/pdf/4_Volume4/V4_04_Ch4_Forest_Land.pdf#page=17&zoom=100,92,514.

Jenkins JC, Chojnacky DC, Heath LS, Birdsey RA. 2003. National-scale biomass estimators for United States tree species. For Sci 49 (1): 12-35. DOI: 10.1093/forestscience/49.1.12.

Kenzo T, Himmapan W, Yoneda R, Tedsorn N, Vacharangkura T, Hitsuma G, Noda I. 2020. General estimation models for above- and below-ground biomass of teak (*Tectona grandis*) plantations in Thailand. For Ecol Manag 457: 117701. DOI: 10.1016/j.foreco.2019.117701.

Levan C, Buimanh H, Tope BOO, Xu X, Nguyenminh T, Lak C, Nebiyou L, Wang J, Buivan T. 2020. Biomass and carbon storage in an age-sequence of *Acacia mangium* plantation forests in Southeastern region, Vietnam. For Syst 29 (2): 65-80. DOI: 10.5424/fs/2020292-16685.

Liu Y, Li S, Sun X, Yu X. 2016. Variations of forest soil organic carbon and its influencing factors in east China. Ann For Sci 73: 501-511. DOI: 10.1007/s13595-016-0543-8.

Luo Y, Wang X, Ouyang Z, Lu F, Feng L, Tao J. 2020. A review of biomass equations for China's tree species. Earth Syst Sci Data 12 (1): 21-40. DOI: 10.5194/essd-12-21-2020.

Magerl A, Le Noë J, Erb KH, Bhan M, Gingrich S. 2019. A comprehensive data-based assessment of forest ecosystem carbon stocks in the US 1907-2012. Environ Res Lett 14 (12): 125015. DOI: 10.1088/1748-9326/ab5cb6.

MARD [Ministry of Agriculture and Rural Development]. 2020. Promulgation of the state of National forests. Ministry of Agriculture and Rural Development No. 1558/QĐ-BNN-TCLN, Ha Noi, Viet Nam.

MONRE [Ministry of Natural Resources and Environment]. 2022. Updated Nationally Determined Contribution (NDC) of Vietnam. Ministry of Natural Resources and Environment, Vietnam. https://unfccc.int/sites/default/files/NDC/2022-11/Viet%20Nam_NDC_2022_Eng.pdf

NFI [National Forest Inventory]. 2003. Australia's State of the Forests Report 2003, National Forest Inventory, Bureau of Rural Sciences, Canberra.

Nguyenthi H. 2017. Study on building Allometric equations for estimating the biomass and carbon stocks of mangrove forests based on the application of Remote Sensing and GIS in Ca Mau Province. [Doctoral Dissertation]. Vietnam Forestry University, Ha Noi.

Paul KI, Roxburgh SH, Chave J et al. 2016. Testing the generality of above-ground biomass allometry across plant functional types at the continent scale. Glob Chang Biol 22 (6): 2106-2124. DOI: 10.1111/gcb.13201.

Pham TT, Hoang TL, Nguyen DT, Dao TLC, Ngo HC, Pham VH. 2019. The context of REDD+ in Vietnam: Drivers, agents and institutions [2nd edition]. CIFOR Occasional Paper No. 196. Center for International Forestry Research (CIFOR), Bogor. DOI: 10.17528/cifor/007402.

Phan SM, Nguyen HTT, Nguyen TK, Lovelock C. 2019. Modelling above ground biomass accumulation of mangrove plantations in Vietnam. For Ecol Manag 432: 376-386. DOI: 10.1016/j.foreco.2018.09.028.

Pothong T, Elliott S, Chairuangsri S, Chanthorn W, Shannon DP, Wangpakapattanawong P. 2022. New allometric equations for quantifying tree biomass and carbon sequestration in seasonally dry secondary forest in northern Thailand. New For 53:17-36. DOI: 10.1007/s11056-021-09844-3.

Prabha ACS, Rajkamal A, Senthivelu M, Pragadeesh S. 2023. Carbon stock in biomass of important plantations in the southern zone of Tamil Nadu, India. Ecol Environ Conserv 29 (2): 688-692. DOI: 10.53550/EEC.2023.v29i02.022.

Rizvi A, Baig S, Barrow E, Kumar C. 2015. Synergies between climate mitigation and adaptation in forest landscape restoration, Global Forest and Climate Change Programme, International Union for Conservation of Nature, Gland, Switzerland.

Salunkhe O, Khare PK, Kumari R, Khan ML. 2018. A systematic review on the aboveground biomass and carbon stocks of Indian forest ecosystems. Ecol Processes 7: 17. DOI: 10.1186/s13717-018-0130-z.

Schettini BLS, Jacovine LAG, Torres CMME, Carneiro ACO, Castro RVO, Villanova PH, de Rocha SJSS, Rufino MPMX, de Oliveira Neto SN, de Morais Júnior VTM. 2022. Use of destructive and non-destructive methodologies to estimate stem biomass accumulation and carbon stock in an eucalyptus forest. Revista Árvore 46: e4611. DOI: 10.1590/1806-908820220000011.

Siraj KT, Teshome BB. 2017. Potential difference of tree species on carbon sequestration performance and role of forest based industry to the environment (Case of Arsi Forest Enterprise Gambo District). Environ Pollut Clim Chang 1: 2-10. DOI: 10.4172/2573-458X.1000132.

Solomon N, Birhane E, Tadesse T, Treydte AC, Meles K. 2017. Carbon stocks and sequestration potential of dry forests under community management in Tigray, Ethiopia. Ecol Processes 6: 20. DOI: 10.1186/s13717-017-0088-2.

Tashi S, Keitel C, Singh B, Adams M. 2017. Allometric equations for biomass and carbon stocks of forests along an altitudinal gradient in the eastern Himalayas. Forestry: Intl J For Res 90 (3): 445-454. DOI: 10.1093/forestry/cpx003.

Tuan NT, Rodríguez-Hernández DI, Tuan VC, Quy NV, Obiakara MC, Hufton J. 2022. Effects of tree diversity and stand structure on above-ground carbon storage in evergreen broad-leaved and deciduous forests in Southeast Vietnam. Dendrobiology 88: 38-55. DOI: 10.12657/denbio.088.003.

Vinh TV, Marchand C, Linh TCK, Vinh DD, Allenbach M. 2019. Allometric models to estimate above-ground biomass and carbon stocks in *Rhizophora apiculata* tropical managed mangrove forests (Southern Viet Nam). For Ecol Manag 434: 131-141. DOI: 10.1016/j.foreco.2018.12.017.

Zhang H, Duan H, Song M, Guan D. 2018. The dynamics of carbon accumulation in *Eucalyptus* and *Acacia* plantations in the Pearl River delta region. Ann For Sci 75: 40. DOI: 10.1007/s13595-018-0717-7.

Table S1. Number of destructively sampled trees

No.	Age (years)	DBH (cm)	H (m)
1	2	4.77	6.2
2	2	5.25	9.5
3	2	6.53	10.7
4	2	6.68	8.1
5	2	7.8	9.2
6	3	6.05	10
7	3	7.96	11
8	3	9.24	12.5
9	3	9.87	13.5
10	3	12.42	14.5
11	3	10.19	12.5
12	4	7.32	12.8
13	4	9.87	15.5
14	4	10.51	15.7
15	4	15.92	16.7
16	4	11.3	12
17	4	12.1	13
18	5	5.41	9
19	5	10.51	16.5
20	5	11.15	16.6
21	5	17.2	20.4
22	5	13.1	13
23	5	16.07	15.8
24	6	11.46	15
25	6	21.66	19
26	6	14.8	16.5
27	6	15.44	16.8
28	7	7.96	15
29	7	13.38	21
30	7	17.83	21
31	7	17.83	20
32	7	18.78	18.4
33	8	9.87	17
34	8	14.01	20.6
35	8	19.42	19
36	9	10.83	17
37	9	16.24	24.5
38	9	22.61	27
39	9	21.33	20.7
40	10	11.78	17.6
41	10	17.2	22
42	10	18.47	24
43	10	19.11	27
44	10	26.43	29
45	10	22.28	20.7

Table S2. Models are used to estimate the biomass and carbon of individual trees or plantations

No.	Equations
1	$Y = (a + b.x)^2$
2	$Y = 1/(a + b/x)$
3	$Y = a + b.\log x$
4	$Y = a + b.x^2$
5	$Y = a + b.x + c.x^2$
6	$Y = a + b.x.z$
7	$Y = a + b.x.z^2$
8	$Y = a + b.x^2.z$
9	$Y = a + b.x + c.x^2.z$
10	$Y = a + b.z + c.x^2.z$
11	$Y = (a + b.\text{sqrt}(x))^2$
12	$Y = \text{sqrt}(a + b.x^2)$
13	$Y = \exp(a + b.x)$
14	$Y = a.x^b$
15	$Y = a.\exp(-b.x^{-c})$
16	$\log Y = a + b.\log x + c.\log z$
17	$\log Y = a + b.\log(x.z)$
18	$\log Y = a + b.\log(x^2.z)$
19	$\log Y = a + b.\log(x.z^2)$
20	$\log Y = a + b.\log x + c.\log(x.z)$

Table S3. Goodness-of-fit statistics of the most effective models for estimating biomass at the individual tree level

Train dataset									
Model	**R2**	**SSR**	**SEE**	**MAE**	**MAPE**	**CF**	**RMSE**	**AIC**	**BIC**
Model 1	0.984	0.822	0.155	0.125	12.191	1.011	0.151	-29.800	-25.050
Model 2	0.983	0.857	0.159	0.125	12.152	1.012	0.154	-28.670	-23.920
Model 3	0.988	0.600	0.133	0.108	10.911	1.008	0.129	-39.220	-34.470
Model 4	0.990	0.504	0.122	0.099	9.860	1.007	0.118	-43.480	-37.140
Model 5	0.866	6.061	0.422	0.308	36.149	1.088	0.410	39.830	44.580
Model 6	0.895	4.745	0.374	0.269	27.896	1.068	0.363	35.110	39.860
Model 7	0.901	4.459	0.362	0.259	26.914	1.064	0.352	32.940	37.690
Model 8	0.899	4.557	0.366	0.255	26.424	1.065	0.356	34.860	41.200
Model 9	0.980	0.945	0.167	0.131	12.846	1.013	0.162	-24.220	-19.470
Model 10	0.780	10.507	0.556	0.457	38.076	1.157	0.540	-24.220	-19.470
Model 11	0.987	0.645	0.138	0.104	10.282	1.009	0.134	-36.710	-31.960
Model 12	0.988	0.597	0.132	0.100	9.761	1.008	0.129	-38.190	-31.850
Test dataset									
	R2	**SSR**	**SEE**	**MAE**	**MAPE**	**CF**	**RMSE**	**AIC**	**BIC**
Model 1	0.962	0.138	0.141	0.103	10.534	1.008	0.124	-7.860	-7.270
Model 2	0.964	0.130	0.136	0.096	9.833	1.007	0.120	-7.850	-7.260
Model 3	0.982	0.065	0.096	0.064	6.690	1.004	0.085	-16.090	-15.500
Model 4	0.983	0.061	0.093	0.067	6.984	1.003	0.082	-16.550	-15.760
Model 5	0.854	0.880	0.355	0.226	24.633	1.050	0.313	9.430	10.020
Model 6	0.857	0.859	0.350	0.230	25.429	1.049	0.309	8.800	9.390
Model 7	0.756	1.467	0.458	0.298	35.401	1.085	0.404	12.000	12.590
Model 8	0.806	1.170	0.409	0.260	30.774	1.067	0.361	9.890	10.680
Model 9	0.966	0.131	0.137	0.108	11.157	1.007	0.121	-8.060	-7.460
Model 10	0.387	2.371	0.582	0.440	33.259	1.141	0.513	-8.060	-7.460
Model 11	0.961	0.151	0.147	0.102	10.670	1.008	0.130	-8.720	-8.130
Model 12	0.974	0.101	0.120	0.082	8.550	1.006	0.106	-10.540	-9.750

Table S4. Goodness-of-fit statistics of the most effective models for estimating carbon at the individual tree level

Train dataset									
Model	**R2**	**SSR**	**SSE**	**MAE**	**MAPE**	**CF**	**RMSE**	**AIC**	**BIC**
Model 13	0.984	0.821	0.155	0.125	12.184	1.011	0.151	-29.820	-25.070
Model 14	0.975	1.261	0.193	0.147	14.323	1.018	0.187	-13.830	-9.080
Model 15	0.990	0.516	0.123	0.098	9.623	1.007	0.120	-45.490	-40.740
Model 16	0.988	0.603	0.133	0.110	11.031	1.008	0.129	-39.230	-34.480
Model 17	0.866	6.057	0.422	0.308	36.130	1.088	0.410	39.830	44.580
Model 18	0.877	5.548	0.404	0.277	28.086	1.080	0.393	39.710	44.460
Model 19	0.899	4.557	0.366	0.255	26.389	1.065	0.356	33.720	38.470
Model 20	0.901	4.459	0.362	0.259	26.885	1.064	0.352	32.940	37.690
Model 21	0.980	0.945	0.167	0.131	12.847	1.013	0.162	-24.220	-19.470
Model 22	0.965	1.688	0.223	0.160	15.038	1.024	0.217	-7.920	-3.170
Model 23	0.988	0.597	0.133	0.100	9.767	1.008	0.129	-39.920	-35.170
Model 24	0.987	0.645	0.138	0.104	10.286	1.009	0.134	-36.710	-31.960

Test dataset									
Model	**R2**	**SSR**	**SSE**	**MAE**	**MAPE**	**CF**	**RMSE**	**AIC**	**BIC**
Model 13	0.962	0.138	0.141	0.103	10.539	1.008	0.124	-7.860	-7.270
Model 14	0.925	0.271	0.197	0.151	15.380	1.015	0.174	-6.750	-6.160
Model 15	0.987	0.047	0.082	0.059	6.116	1.003	0.072	-17.810	-17.220
Model 16	0.983	0.060	0.093	0.062	6.399	1.003	0.082	-16.090	-15.500
Model 17	0.854	0.879	0.354	0.226	24.624	1.050	0.313	9.430	10.020
Model 18	0.812	1.129	0.402	0.253	31.087	1.065	0.354	8.020	8.610
Model 19	0.806	1.169	0.409	0.260	30.746	1.067	0.360	9.360	9.950
Model 20	0.757	1.465	0.458	0.298	35.366	1.085	0.404	12.000	12.590
Model 21	0.966	0.131	0.137	0.108	11.154	1.007	0.121	-8.060	-7.460
Model 22	0.956	0.171	0.157	0.115	12.351	1.010	0.138	-8.150	-7.560
Model 23	0.974	0.101	0.120	0.082	8.551	1.006	0.106	-12.450	-11.860
Model 24	0.961	0.151	0.147	0.102	10.672	1.008	0.130	-8.720	-8.130

NUSANTARA BIOSCIENCE
Vol. 17, No. 2, pp. 218-225
November 2025

ISSN: 2087-3948
E-ISSN: 2087-3956
DOI: 10.13057/nusbiosci/n170204

Morphological characterization and correlation of seed, fruit, and seedling of *Horsfieldia iryaghedhi*

INDRIANI EKASARI[1,♥], SAHROMI[2], PUTRI KESUMA WARDHANI[2]

[1]Research Center of Biota Systems, National Research and Innovation Agency. Jl. Raya Jakarta-Bogor Km. 46, KST Soekarno, Cibinong, Bogor 16911, West Java, Indonesia. Tel.: +62-21-87907604, ♥email: indriani.ekasari@brin.go.id

[2]Research Center of Applied Botany, National Research and Innovation Agency. Jl. Raya Jakarta-Bogor Km. 46, KST Soekarno, Cibinong, Bogor 16911, West Java, Indonesia

Manuscript received: 2 May 2025. Revision accepted: 4 September 2025.

Abstract. *Ekasari I, Sahromi, Wardhani PK. 2025. Morphological characterization and correlation of seed, fruit, and seedling of* Horsfieldia iryaghedhi*. Nusantara Bioscience 17: 218-225. Horsfieldia iryaghedhi* is a critically endangered species from the Myristicaceae family. Examining seed, fruit, and seedling morphology of the species is crucial, as generative propagation remains the only known conservation method. Therefore, this study aimed to determine the morphological characterization of the seed, fruit, and seedling of *H. iryaghedhi* and to analyse the correlation between seed, fruit, and seedling traits. This study was conducted at the Bogor Botanical Garden, utilizing five plant collections. The examined morphological traits included length, width, and weight of the seed, as well as fruit height, root collar diameter, and the number of leaves for the seedling. The results showed that the length, width, and weight of the fruit were 39.64±2.48 mm, 30.04±1.98 mm, and 20.33±3.60 g, respectively. Overall, the correlation between seed and fruit parameters indicates that one trait influences the other. The low variability in fruit and seed traits, despite being obtained from mother trees of different origins, has implications for the species' genetic diversity. The mean for seedling height is 106.74±32.78 cm, and the mean of collar diameter is 1.27±0.64 mm. Height and root collar diameter seedling traits were found to be closely related in 24-month-old seedlings. Understanding the ecology of seedling growth is essential for developing developmental strategies to conserve biodiversity and restore natural habitats. In conclusion, the variability in fruit and seed traits is exhibited by plants obtained from mother trees of different origins. The trees in the Bogor Botanical Gardens study site are mother trees, and this is extremely important for the future sustainable population of this species.

Keywords: Endangered species, Indonesia, Myristicaceae, plant traits, species conservation

INTRODUCTION

Horsfieldia iryaghedhi (Gaertn.) Warb. belongs to the Myristicaceae family and is frequently used for its medicinal properties in its native regions (Arrijani 2005; Waman et al. 2021). It is a woody tree species with a trunk ranging from 5 to 25 meters in height and up to 50 cm in diameter at breast height. The leaves are arranged alternately in two vertical rows, chartaceous, with petioles measuring between 1.5 and 3 cm in length; the blade shape ranges from ovate-elliptical to oblong-lanceolate, base rounded to attenuate, and apex acute to acuminate. The fruit is a one-seeded follicle, ellipsoid in shape, yellow-brown in color, and covered with dense, brown-yellow, stellate hairs; the pericarp thickness ranges from 1.5 to 3 mm. *H. iryaghedhi* flowers and bears fruit throughout the year, thriving in lowland rainforests, humid soils—sometimes with silt roots—wet evergreen forests, and disturbed forest ecosystems, from sea level up to an altitude of 500 meters (Wulijarni-Soetjipto 2001). This species is native to Sri Lanka (POWO 2024) and is widely distributed across South-east Asia, including Malaysia, Singapore, and Java.

The seed fat of *H. iryaghedhi* is used as an ingredient in candle production (van der Vossen 2001), while its flowers have been recognized as medicinal materials in Sri Lankan tradition since ancient times (Kankanamalage et al. 2014). Although several studies have investigated changes in species composition, stand structure, and geographical distribution, as well as phenotypic diversity and chemical composition across different habitats, only a few have explored the physiological responses of seeds, fruits, and seedlings. Given that *H. iryaghedhi* is either extinct in the wild or critically endangered (IUCN 2025), conservation efforts must prioritize protection within its native habitat, alongside ex-situ conservation measures such as botanical gardens.

Ex situ conservation involves relocating living plants or seeds from their native habitats to controlled environments to protect them from natural or human-induced threats (Zhao et al. 2022; Junaedi et al. 2023). Bogor Botanical Garden (BBG) is an ex-situ conservation area in Indonesia, maintaining over 12,370 accessions that encompass 3,555 species, 1,202 genera, and 191 families (Ariati et al. 2019). These collections are planted on an 87-hectare land area in the center of Bogor City, West Java Province, Indonesia. This Botanical Garden focuses on collections originating from Indonesia and abroad, and it conserves lowland humid and wet plant species (Wanda et al. 2022). Given the limited space available for expanding the BBG species collection, a planting strategy was implemented that allowed only a few trees of each species to be planted in the garden. These trees were chosen from the best growing

seedlings, after which the origin of the seedlings or seeds was recorded, and their growth (including phenology) was frequently observed. This phenology helps restoration practitioners and endangered plant conservationists determine when to collect *H. iryaghedhi* fruits or seeds.

Many studies utilize morphological descriptors to differentiate among plant genetic resources (Poljak et al. 2021, 2024, 2025; Vidaković et al. 2024, 2025). Leaf morphometry is frequently employed to describe phenotypic diversity (Wanda et al. 2022; Puntieri and González 2023). However, in the context of this study, seeds and fruits hold even greater significance due to their essential role in plant conservation. Seed traits provide valuable insights for both taxonomic and functional differentiation. Beyond classification, seeds serve as the foundation of plant production (Drvodelić et al. 2025), food security (Yadav et al. 2024), ecological restoration (Leger et al. 2024), and the long-term persistence of sexually propagated species (Tumpa et al. 2021), as they directly influence germination success and seedling vigor. Seedling establishment, however, depends on a complex interplay of intrinsic seed attributes and environmental conditions (Sari et al. 2021; Nantongo et al. 2022). Among those attributes, seed mass is a reliable indicator of stored reserves available for early growth. Heavier seeds from the same mother tree and same species typically exhibit higher germination rates and produce more robust seedlings than lighter seeds, allowing them to withstand resource-limited environments and ultimately accelerate early growth (Nantongo et al. 2022).

Seedlings are a crucial component of plant populations, representing a vital stage in the life cycle of plants. The successful dispersal and maintenance of plant populations rely on seedling regeneration (Liu et al. 2019). Additionally, height-collar diameter correlations have been analyzed for gymnosperm and angiosperm trees and seedlings in China (Tumpa et al. 2021). Compared to mature trees, seedlings tend to exhibit greater height growth relative to stem diameter and possess higher height–diameter allometric exponents (Zhang et al. 2020).

This study aimed to characterize the morphological features of *H. iryaghedhi*'s seeds, fruits, and seedlings, as well as to analyze the correlations between seed, fruit, and seedling traits.

MATERIALS AND METHODS

Study area

This study was conducted between August and October 2023 at BBG in Indonesia (Figure 1). BBG is situated on 87 ha of land in the center of Bogor City, West Java, Indonesia (6°35'51.46"S, 106°47'58.45"E), at an altitude of 230-270 m above sea level. Bogor has a tropical climate, with an average temperature ranging from 25-27.4°C, an average humidity of 80%, and an annual rainfall of 3.658 mm/year (Safarinanugraha et al. 2018; Wanda et al. 2022), and the soil type is primary Latosol (a type of soil formed from weathered volcanic rock).

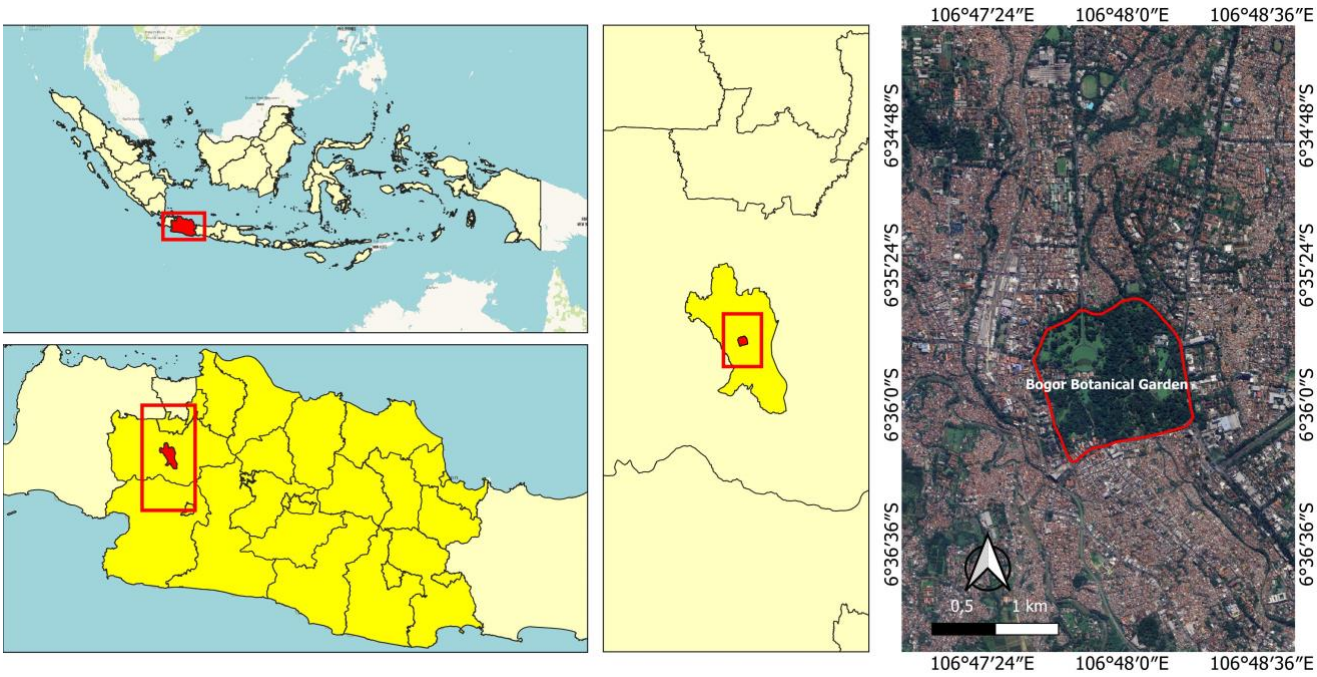

Figure 1. Study site of *Horsfieldia iryaghedhi* in Bogor Botanical Garden, Bogor City, West Java, Indonesia

Plant materials

The BBG conserved nine *Horsfieldia iryaghedhi* trees, eight from Sri Lanka and one from Papua (Ariati et al. 2019). Of these, only five trees were mature and fruiting during the study, all of which originated from Sri Lanka. Tree height (m), diameter at breast height (DBH, cm), and botanical location of each numbered tree were recorded and used in the selection process. Height, DBH, and crown diameter were measured using a hypsometer and diameter tape, respectively (Table 1). Ultimately, five trees were sampled for fruit collection at the site. The selected trees showed no signs of pests or disease, had straight, circular stems with large diameters, fine horizontal branches, and produced an abundance of fruit.

According to phenology data from the BBG registration department, in previous years, *H. iryaghedhi* flowered from January to July, producing mature fruit. By August, when this study was conducted, the availability of mature fruit had declined, leaving only 27 viable samples for testing. In comparison to other *Horsfieldia* species, the ripened seeds of *H. kingii* in north-east India are available from February to April (Datta and Rane 2013). In contrast, those of *Horsfieldia hainanensis* in Yunnan Province, China, are available from April to May (Liu et al. 2024). These fruit samples were carefully selected and randomly collected. To prevent heat exposure and maintain freshness, the collected fruit was stored in cloth bags. The seeds were then transported to the laboratory on the same day for further processing. After selecting mature fruit from the twigs, a cutting test was performed to assess freshness, with selected fruit characterized by yellow-brownish peels.

Data collection

A total of 27 fruits of *H. iryaghedhi* were measured for three major morphological traits, including weight, length, and width (diameter). Seeds were collected from the peeled fruits, and then their length and width were measured using a digital caliper, while their weight was determined with a digital scale. The single-seed weight was measured using a precision balance with an accuracy of 0.01 g.

In addition to observing the physical properties of fruits and seeds, this study also observed 24-month-old *H. iryaghedhi* seedlings grown under uniform nursery conditions with no shade. These seedlings were planted in similar soil environments, maintaining consistent growth vigor and canopy structure. A total of 52 seedlings were evaluated for height, basal diameter, and leaf count. Seedling height was measured to the nearest millimeter using a ruler, basal diameter was recorded with digital calipers, and collar diameter was measured to the nearest 0.1 mm using a digital caliper.

Data analysis

Descriptive, correlation, and regression analyses were performed using MS Excel for Windows 11. Regression analyses were performed to observe the correlation between all treatments concerning seed, fruit, and seedling performance parameters.

RESULTS AND DISCUSSION

A total of five *Horsfieldia iryaghedhi* trees, each over 40 years old, were measured for this study. The height of these trees ranged from 8 to 23.9 m, while their diameter at breast height varied from 52.23 to 184.08 m. The crown diameter spanned from 5.2 to 8.9 m (Table 1). The mean wind velocity and air temperature recorded were 1.68±0.27 m/s and 34±1.34ºC, respectively. These trees were planted along the edge of the lake in the BBG, mirroring their natural habitat within the wet tropical biome (POWO 2024).

Variability of seeds, fruits, and seedlings of *Horsfieldia iryaghedhi*

All morphological traits of seeds (length, width, and weight), fruits (length, width, and weight), and seedlings (height, root collar diameter, and number of leaves) were examined to ensure standard parametric test assumptions were met before analysis. Detecting seed size can impact production, breeding, storage, and transportation, while also enhancing quality (Yin et al. 2023). Seed weight in this study ranged from 2.90 g to 8.80 g, with a mean of 5.57±1.27 g (Table 2). The mean seed length and diameter were 28.17±2.08 mm and 19.37±2.23 mm, respectively. In general, larger seeds result in heavier seedlings with more resources being dedicated to seedling development (Nantongo et al. 2022). Therefore, this study recommends that heavier seeds will have a better germination rate and produce more vigorous seedlings than lighter ones. This also improves seedling survival up to the period of leaf growth, reducing reliance on seed stores (Naruangsri et al. 2023; Barczyk et al. 2024) for photosynthesis.

Table 1. Characteristics of *Horsfieldia iryaghedhi* trees sampled for fruit and seed collection in Bogor Botanical Garden, Indonesia

Location in the garden	Height (m)	Diameter breast height (cm)	Crown diameter (m)	Wind velocity (m/s)	Temp (ºC)	Air humidity (%)
IV. G. 155	23.9	26.11	7.7	1.2	32.8	42
XIII. F. 6	8.0	24.84	5.2	1.8	33.7	46
XIII. 9 (o)	15.9	92.04	8.9	1.8	34.5	45
XIII. 11	11.5	48.73	7.9	1.8	33	43
XIII. 11 a	11.5	35.67	6.6	1.8	36	41
Mean	14.16	45.47	7.26	1.68	34	43.4
SD	6.12	27.72	1.41	0.27	1.30	2.07
CV	0.43	0.61	0.19	0.16	0.04	0.05

Note: SD: Standard deviation; CV: Coefficient of variation

Under optimal conditions, resources are primarily allocated to plant growth and the production of large seeds to store more nutrients, thereby enhancing the seedling's ability to respond to adverse conditions. Seed size, a functional trait, has implications for seedling germination, survival, and recruitment. According to reports, seedlings developed from large seeds tend to exhibit a higher growth capacity (Martínez-González et al. 2021).

The length, diameter, and weight of mature fruit ranged from 32.80 to 43.60 mm, 24.60 to 33.90 mm, and 10.90 to 26.10 g, respectively, with mean values of 39.64±2.48 mm, 30.04±1.98 mm, and 20.33±3.60 g. According to Martínez-González et al. (2021), seeds serve as the fundamental propagation unit for the majority of trees. Variability in seed and fruit size can be primarily attributed to genetic diversity within the sample population. Morphological variability in plants is a crucial mechanism that enables species to adapt to their immediate environment. Plant populations often occupy large areas, continuous or disjoint, in which the pressures on individuals can differ significantly. Under such conditions, different populations and individuals can exhibit considerable variation in phenotypic and genetic diversity (Vidaković et al. 2024). However, the location of fruit on the tree, as well as differing microclimatic conditions within the canopy and soil, can also contribute to variability in fruit development within the same tree. Seeds, as a generative propagation material, are essential to understanding their variability in conservation strategy for *H. iryaghedhi*. This study found low variability in fruits and seeds collected from five mother trees of *H. iryaghedhi* in the BBG, despite the mother trees originating from different locations (Papua and Sri Lanka). *H. iryaghedhi* planted in the BBG did not exhibit any differences in terms of height, breast-height diameter, or crown diameter due to any environmental conditions. The low CV (CV<1) suggested that there was essentially no difference in growth across the five mother trees (Table 1).

The lowest seedling height recorded was 82.60 cm, while the highest reached 143.70 cm. The overall mean values for seedling height, collar diameter, and number of leaves were 106.74±32.78 cm, 1.27±0.64 mm, and 17.54±12.23, respectively. Certain seedling traits, particularly those related to conservation (e.g., biomass) and resource acquisition (e.g., foliar area), play a crucial role in life-cycle strategies. These traits may exhibit similarities across both tropical rainforests and tropical dry forests. Limited information on the percentage of *H. iryaghedhi* seed germination necessitates conservation issues for this genus. However, seedling management in the nursery until the appropriate planting period is critical. According to a previous study, *Horsfieldia hainanensis* has a successful regeneration rate of 0.4-5.6% in its natural habitat between the ages of 0 and 4 years, due to pathogen and herbivore attacks (Liu et al. 2019). This implies that seedling maintenance in the nursery is necessary to preserve this species. Seedlings taller than 200 cm have reasonably good survival prospects because they escape ungulate browsing at this height (Waller et al. 2020).

This study found that all seeds and fruits used in the experiment exhibited a proportionate oval form. A shorter diameter and a longer length characterized the overall shape of the seeds and fruits. Seed and fruit weight correlated with the weight of ripe fruit, including the seed, peel, and flesh. Shape is an essential factor in many respects (Drvodelić et al. 2025), and when *H. iryaghedhi* fruit can be domesticated, it will be more appealing to customers. According to previous research, seeds of the Myristicaceae family, including *H. iryaghedhi*, are relatively large (Arrijani 2005). The mean seeds found in this study were comparatively bigger when compared to those of *H. glabra* (Waman et al. 2021), with a seed length of 27.4 cm, a seed width of 16.2 cm, and a seed weight of 3.7 g, and *H. hainanensis* (Liu et al. 2024) with a seed weight of 5-6 g. Seedling growth may be hindered if seeds are uniform in size and shape. Moreover, seed size has a significant impact on growth traits, with seedlings from larger seeds generally exhibiting superior performance in terms of height, biomass, leaf number, and foliar area (Martínez-González et al. 2021). For ecological purposes, the fruit and seed of *H. iryaghedhi* are relatively large and heavy, meaning their natural distribution tends to be close to the parent tree. Consequently, when the species is introduced to the natural environment, human intervention may be required to facilitate dispersal (Ekasari et al. 2025).

Correlation between seed and fruit parameters (length, width, and weight)

The correlation between seed length, width, and weight is presented in Table 3. A positive correlation was observed among these parameters, with the lowest significant positive correlation found for the seed length parameter, which is the correlation between seed width and seed length ($r=0.52$, $p<0.001$) within the medium category. In addition, the highest positive correlation for the seed length parameter was observed between seed length and fruit weight ($r=0.83$, $p<0.001$), which falls within the very strong category. It is suggested that the seed length increases with the fruit weight. This study demonstrates that seed length parameters are linearly correlated with other seed and fruit parameters. The strong correlation indicates that commonly measured seed traits—length, width, and weight—have a genetic basis (Dicko et al. 2019).

Among all parameter associations, fruit weight and length exhibited the strongest correlation ($r=0.88$, $p<0.001$). The analysis of 27 seeds revealed correlations ranging from medium to very strong, except the low correlation between fruit width and seed width ($r=0.27$, $p<0.001$). The findings of this study suggest that the width of *H. iryaghedhi* seeds is not linearly related to fruit width, but is linearly related to the other parameters in the seeds and fruit. Furthermore, this study suggests that the morphological traits of the analyzed seeds can be used to predict one parameter based on another, opening up new possibilities for predictive plant morphology. Fruit and seed morphological traits are highly correlated, suggesting that factors affecting fruit also influence seed proportionally. A previous study demonstrated a positive and significant correlation between the fruit

weight, length, and width of *Entandrophragma bussei* in Tanzania (Andrew et al. 2021).

Correlation between seedling parameters (height, collar diameter, and number of leaves)

The seedling parameters showed a medium correlation with height (r=0.42, p<0.001) and root collar diameter parameters (r=0.51, p<0.001). Only the correlation for root collar diameter and height parameters was strong (r=0.76, p 0.001). This study suggests that the two parameters (seedling height and root collar diameter) have a strong correlation for 24-month-old seedlings of *H. iryaghedhi* at the BBG nursery (Table 7). Many countries apply morphological attributes to evaluate seedling quality, including height and root collar diameter. Seedling age is one of the primary quantitative morphological attributes (Mataruga et al. 2023; Naruangsri et al. 2023). The height tends to increase faster than the root collar diameter at the seedling stage, with growth standards varying depending on the container size in the nursery (Zhang et al. 2020; Mataruga et al. 2023).

The number of leaves parameter has a medium correlation with seedling height and root collar diameter. This result implies that the condition of 24-month-old *H. iryaghedhi* seedlings was defined by seedling height and root collar diameter, having a medium correlation with the number of leaves surviving and growing in the nursery. Tree species may optimize growth strategies in response to environmental conditions by reducing the risk of bending or falling while also maximizing efficiency in using the most limited resources (Zhang et al. 2020), such as limited root growth space due to polybags or containers, or competition for sunlight. Furthermore, plants allocate a higher proportion of biomass to leaves and a larger root collar diameter in nutrient-rich environments where above-ground competition for light is intense. In nutrient-poor environments, where below-ground competition prevails, plants allocate a higher proportion of their resources to roots (Nantongo et al. 2022).

Root collar diameter parameter is influential for the survival of *H. iryaghedhi* species groups and has proven to be more indicative than the height parameter. This trait may serve as a better indicator of energy reserves for the seedling during its next growth phase. It is also typically more closely correlated to both total and below-ground seedling biomass. Aside from seedling height, root collar diameter is another good predictor of future plantation success (Bayala et al. 2009; Jones et al. 2023).

Survival often varies among sites and seedlings of different sizes, as growth is notoriously responsive to local conditions. It frequently takes time to progress through vulnerable-size classes, which can be either short-term or long-term (Waller et al. 2024). The strong correlation between height and root collar diameter parameters (r=0.76, p<0.001) in 24-month-old *H. iryaghedhi* seedlings highlights differences in seedling development and survival. Meanwhile, a previous study found that the growth of seedling height was directly related to the number of leaves but inversely proportional to the increase in root collar diameter (Nantongo et al. 2022). Examining differences in seedling development and survival will help determine the trait with limited regeneration parameters.

Table 2. Distribution of seed, fruit, and seedling of *Horsfieldia iryaghedh*i collection of Bogor Botanical Garden, Indonesia

Parameters	Minimum	Maximum	Mean	SD	CV (%)
Seed length (mm)	23.10	31.10	28.17	2.08	0.07
Seed diameter (mm)	16.40	29.10	19.37	2.23	0.11
Seed weight (g)	2.90	8.80	5.57	1.27	0.23
Fruit length (mm)	32.80	43.60	39.54	2.48	0.06
Fruit diameter (mm)	24.60	33.90	30.04	1.98	0.06
Fruit weight (g)	10.90	26.10	20.33	3.60	0.18
Seedling height (cm)	82.60	143.70	106.74	32.78	0.31
Root collar diameter (mm)	0.73	1.88	1.27	0.64	0.51
Number of leaves	7.00	36.00	17.54	12.23	0.71

Note: SD: Standard deviation; CV: Coefficient of variation

Table 3. The correlation coefficient between the length, width, and weight of fruit and seed parameters of *Horsfieldia iryaghedhi*

Parameters	Seed length	Seed width	Seed weight	Fruit length	Fruit width	Fruit weight
Seed length	1	***	***	***	***	***
Seed width	0.52	1	***	***	ns	***
Seed weight	0.74	0.59	1	***	***	***
Fruit length	0.81	0.56	0.55	1	***	***
Fruit width	0.65	0.27	0.40	0.67	1	***
Fruit weight	0.83	0.50	0.53	0.88	0.83	1

Note: 0.000-0.199: Very low, 0.200-0.399: Low, 0.40-0.599: Medium, 0.600-0.799: Strong, 0.800-1.000: Very strong. Source: (Sugiyono 2010). ***: p>0.001, ns: non-significant

Table 4. Correlation between height, root collar diameter, and number of leaves on seedling parameters of *Horsfieldia iryaghedhi*

Seedling parameters	Height	Collar diameter	Number of leaves
Height	1	***	***
Root collar diameter	0.76	1	***
Number of leaves	0.42	0.51	1

Note: 0.000-0.199: Very low, 0.200-0.399: Low, 0.40-0.599: Medium, 0.600-0.799: Strong, 0.800-1.000: Very strong. Source: (Sugiyono 2010). ***: p>0.001, ns: non-significant

Understanding the ecology of seedling growth is essential not only for gaining knowledge about plant community processes and succession, but also for developing strategies to conserve biodiversity and restore natural habitats (Susanto et al. 2016). Therefore, seedlings need to be monitored in the field, as environmental traits that are suitable for seed germination may not be ideal for seedling or adult plant development, which generates a conflict between seed and seedling development (Nantongo et al. 2022).

Conservation efforts and their implications in this study

The species *H. iryaghedhi* remains largely unknown, particularly in Indonesia, and is currently classified as a garden collection at the BBG in West Java and the Purwodadi Botanical Garden (PBG) in East Java (Junaedi et al. 2023). Its utilization has received minimal attention. Given that this species is critically endangered and possesses medicinal properties, it is essential to implement appropriate conservation strategies, such as planting it as a collection plant in botanical gardens. Currently, generative propagation via seed is the only known method for conserving the Myristicaceae family, with limited research on vegetative propagation. Since this species is classed as severely endangered, effective genetic conservation measures must be considered in the future, such as seed conservation starting from determining the seed collection protocol, seed sorting, seed testing, seed germination, intensive care in the nursery, and the reintroduction protocol if this species is replanted into its natural habitat.

This study found a strong correlation between the fruit and seed traits of *H. iryaghedhi*; therefore, seed conservation should begin with selecting healthy and normal-sized fruits to obtain seeds of similar size (normal size). Twenty-four-month-old seedlings in the BBG nursery are not yet ready to be planted in their natural habitat, as they have a mean height of 106±32.74 cm, which is less than 2 m. Seedlings with above 2 m are thought to be more resistant to the underpressure of sunlight, have bigger roots to get nutrients, and are pathogen-resistant. Another case for *H. kingii* is that low tree densities, sporadic and supra-annual fruiting, skewed sex ratios, and possible pollination limitations may result in low fruit and seed availability for this species, as well as the effects of anthropogenic disturbances, deforestation, and climate change, placing them at greater risk in their natural habitat (Datta and Rane 2013).

This study was limited to one fruiting year, and there is no previous literature on the morphology of *H. iryaghedhi* fruits collected from BBG and PBG. Future studies could investigate whether changes in seed morphology occur from year to year, influenced by environmental conditions and fruit position on the tree, allowing for additional multivariate analysis, such as principal component analysis (PCA) or other cluster analysis. In addition to being a collection plant at BBG, the *H. iryaghedhi* collection planted in PBG in East Java can be explored further if used as genetic material, given that the two sites present different conditions. This highlights the need for a comprehensive conservation approach, including intensive phenological studies from the flowering stage to the fruit maturation. Selecting fruit and seeds with proportional shape and larger size from the same population will enhance quality and promote future growth (Martínez-González et al. 2021). Although this study was constrained by the limited number of seeds and trees analyzed, it provides valuable insights into the morphology and characteristics of seeds, fruits, and seedlings, which can be easily altered for future research or practical field applications. Collaboration between nursery practitioners and field managers is essential to identify plant traits that support the survival of *H. iryaghedhi* seedlings. Practitioners should also provide nursery workers with additional insights on habitat conditions and contribute observations regarding reforestation efforts and the success of different seedling varieties. This is crucial for producers to enhance seed quality, taking into account the findings and recommendations (Mataruga et al. 2023).

In conclusion, *H. iryaghedhi*'s seed and fruit traits were predicted using length, width, and weight parameters, revealing a positive correlation among all tested traits. All traits examined at BBG showed low variability despite being obtained from mother trees from different origins. Additionally, height and root collar diameter traits were found to be closely related in 24-month-old seedlings, with the root collar diameter increasing with seedling height. However, only a minimal correlation was found between the number of leaves and either seedling height or root collar diameter. Given that *H. iryaghedhi* is critically endangered, further efforts are necessary to enhance both in situ and ex-situ conservation strategies. The BBG is an important site that serves as a source of propagation material for growing new seedlings and transplanting them to similar sites within the BBG. It is essential to understand that the trees in BBG are mother trees, and this is extremely important for the future population of this species, as they would be one of the primary sources of seeds for *H. iryaghedhi*.

ACKNOWLEDGEMENTS

The authors are grateful to the Director of the Research Center for Plant Conservation, Botanic Gardens and Forestry-BRIN (National Research and Innovation Agency-Republic of Indonesia), for supporting this study, as well as to Erica Tira Mutia and Novita Dyah Wulandari for their assistance

with data sampling. The author contributions are as follows: Indriani Ekasari: conceptualization, data analysis, visualization, and manuscript improvement; Sahromi: conceptualization, data collection, and manuscript revision; Putri Kesuma Wardhani: review and editing. This study did not receive any specific grant from funding agencies in the public, commercial, or not-for-profit sectors. The authors declare no conflict of interest regarding the publication of this article.

REFERENCES

Andrew SM, Kombo SA, Chamshama SAO. 2021. Diversity in fruit and seed morphology of wooden banana (*Entandrophragma bussei* Harms ex Engl.) populations in Tanzania. Tree For People 5: 100095. DOI: 10.1016/j.tfp.2021.100095.

Ariati SR, Astuti RS, Supriyatna I, Yuswandi AY, Setiawan A, Saftaningsih D, Pribadi DO. 2019. An Alphabetical List of Plant Species Cultivated in The Bogor Botanic Gardens, Bogor: Center for Plant Conservation Botanic Gardens. Indonesian Institute of Sciences, Bogor, Indonesia.

Arrijani A. 2005. Review: Biology and conservation of genus *Myristica* in Indonesia. Biodiversitas 6: 147-151. DOI: 10.13057/biodiv/d060216.

Barczyk MK, Acosta-Rojas DC, Espinosa CI, Schleuning M, Neuschulz EL. 2024. Seedling recruitment of small-seeded and large-seeded species in forests and pastures in southern Ecuador. Basic Appl Ecol 75: 44-52. DOI: 10.1016/j.baae.2024.01.005.

Bayala J, Dianda M, Wilson J, Ouédraogo SJ, Sanon K. 2009. Predicting field performance of five irrigated tree species using seedling quality assessment in Burkina Faso, West Africa. New For 38 (3): 309-322. DOI: 10.1007/s11056-009-9149-4.

Datta A, Rane A. 2013. Phenology, seed dispersal and regeneration patterns of *Horsfieldia kingii*, a rare wild nutmeg. Trop Conserv Sci 6 (5): 674-689. DOI: 10.1177/194008291300600507.

Dicko A, Natta AK, Biaou HSS, Akossou A. 2019. Assessing morphological traits variation and fruit production of *Lophira lanceolata* (Ochnaceae) in Benin. Am J Plant Sci 10 (6): 1048-1060. DOI: 10.4236/ajps.2019.106076.

Drvodelić D, Španjol E, Vuković M, i Jemrić T. 2025. Medlar (*Mespilus germanica* L.) fruit morphology depending on fruit size. Šumarski List 149 (3-4): 115-126. DOI: 10.31298/sl.149.3-4.1.

Ekasari I, Lailati M, Nurlaeni Y, Puspanti A, Mufida YR. 2025. Seed morphology and seedling growth modeling for *Litsea cordata* and *Sloanea sigun* in Java montane forests. Intl J Des Nat Ecodynamics 20 (3): 547-554. DOI: 10.18280/ijdne.200310.

IUCN. 2025. https://iucnredlist.org.

Jones PD, Sabo AE, Forrester JA, Mladenoff DJ, McDill ME. 2023. Northern hardwood seedlings respond to a complex of environmental factors when deer herbivory is limited. For Ecol Manag 527: 120600. DOI: 10.1016/j.foreco.2022.120600.

Junaedi DI, Nasution T, Putri DM, Iryadi R, Lestari R, Kurniawan V, Pratiwi RA, Handayani A, Sudarmono. 2023. Threatened exotic species of botanical gardens: Application of trait-based naturalized species risk scoring assessment. S Afr J Bot 152: 321-331. DOI: 10.1016/j.sajb.2022.11.046.

Kankanamalage TNM, Dharmadasa RM, Abeysinghe DC, Wijesekara RGS. 2014. A survey on medicinal materials used in traditional systems of medicine in Sri Lanka. J Ethnopharmacol 155 (1): 679-691. DOI: 10.1016/j.jep.2014.06.016.

Leger E, Agneray A, Baughman O, Brummer E, Erickson T, Hufford K, Kettenring K. 2024. Integrating evolutionary potential and ecological function into agricultural seed production to meet demands for the decade of restoration. Restor Ecol 32 (8): e13543. DOI: 10.1111/rec.13543.

Liu X, He Y, Xiao Y, Wang Y, Jiang Y, Jiang Y. 2019. Soil seed burial and competition with surrounding plants determine the emergence and development of seedling of the endangered species *Horsfieldia hainanensis* Merr. in China. Sci Rep 9: 17970. DOI: 10.1038/s41598-019-54644-7.

Martínez-González I, Velázquez-Rosas N, Pineda-López MdelR, Ruiz-Guerra B, Sánchez-Velásquez LR. 2021. The role of seed size in the performance of *Ceiba aesculifolia* seedling subjected to foliar damage. Acta Oecol 112: 103772. DOI: 10.1016/j.actao.2021.103772.

Mataruga M, Cvjetković B, De Cuyper B et al. 2023. Monitoring and control of forest seedling quality in Europe. For Ecol Manag 546: 121308. DOI: 10.1016/j.foreco.2023.121308.

Nantongo JS, Mudondo S, Oluk R, Agaba H, Gwali S. 2022. Variation in seed and seedling traits of the different ethno-varieties of jackfruit, a potential fruit tree species for food security. Tree For People 9: 100303. DOI: 10.1016/j.tfp.2022.100303.

Naruangsri K, Tiansawat P, Elliott S. 2023. Differential seed removal, germination and seedling growth as determinants of species suitability for forest restoration by direct seeding - A case study from northern Thailand. For Ecosyst 10: 100133. DOI: 10.1016/j.fecs.2023.100133.

Poljak I, Šatović Z, Vidaković A, Tumpa K, Idžojtić M. 2024. Population variability of rosemary willow (*Salix eleagnos* Scop.) based on leaf morphometry: Evidence of small and large-leaf morphotypes. Šumarski List 148 (5-6): 219-236. DOI: 10.31298/sl.148.5-6.1.

Poljak I, Tumpa K, Vidaković A, Šatović Z, Liber Z, Jezic M, Ćurković-Perica M, Idžojtić M. 2025. Morphological variability of fruits and leaves allows delimitation between cultivated and wild chestnuts and their natural crosses. Genet Resour Crop Evol 72 (4): 3953-3968. DOI: 10.1007/s10722-024-02195-w.

Poljak I, Vahčić N, Vidaković A, Tumpa K, Žarković I, Idžojtić M. 2021. Traditional sweet chestnut and hybrid varieties: Chemical composition, morphometric and qualitative nut characteristics. Agronomy 11 (3): 516. DOI: 10.3390/agronomy11030516.

POWO [Plants of The World Online]. 2024. Plants of The World Online. Royal Botanic Gardens Kew. www.powo.kew.org.

Puntieri J, González AM. 2023. Are the anatomical traits of stems and leaves good indicators of habitat specificity in closely related Myrtaceae species from Patagonia? Acta Bot Bras 37: e20230019. DOI: 10.1590/1677-941X-ABB-2023-0019.

Safarinanugraha D. Gunawan A. Mugnisjah WQ. 2018. The development of Bogor Botanic Garden design from 1817 to 2017 base on spatial and functional. IOP Conf Ser: Earth Environ Sci 179 (1): 012026. DOI: 10.1088/1755-1315/179/1/012026.

Sari N, Silverman E, Reiland D, Wehner TC. 2021. Seed characterization and correlations between seed and cotyledon properties in *Lagenaria* spp. Accessions. HortScience 56 (2): 185-192. DOI: 10.21273/HORTSCI15569-20.

Sugiyono. 2010. Metode Penelitian Kuantitatif, Kualitatif, dan R&D [Quantitative, Qualitative Research Methods, and Research and Development]. Alfabet, Bandung, Indonesia.

Susanto D, Ruchiyat D, Sutisna M, Amirta R. 2016. Flowering, fruiting, seed germination and seedling growth of *Macaranga gigantea*. Biodiversitas 17 (1): 192-199. DOI: 10.13057/biodiv/d170128.

Tumpa K, Vidaković A, Drvodelić D, Šango M, Idžojtić M, Perković I, Poljak I. 2021. The effect of seed size on germination and seedling growth in sweet chestnut (*Castanea sativa* mill.). Forests 12 (7): 858. DOI: 10.3390/f12070858.

van der Vossen HUB. 2001. Plant Resources of South-East Asia 14: Vegetables Oil and Fat. Backhuys, Leiden.

Vidaković A, Benić L, Mrvičić I, Pešut E, Jakšić V, Poljak I. 2024. Morphological variation in blackthorn (*Prunus spinosa* L.) populations in the Northwestern part of the Balkan Peninsula - Absence of geographical and environmental structure. Acta Soc Bot Pol 93: 187157. DOI: 10.5586/asbp/187157.

Vidaković A, Radunić M, Poljak I. 2025. Variation in chemical composition and fruit morphometric traits of almond-leaved pear (*Pyrus spinosa* Forssk.) natural populations. Genet Resour Crop Evol 72: 1495-1510. DOI: 10.1007/s10722-024-02059-3.

Waller DM, Riege DA, Alverson WS. 2024. The regeneration ratio: Combining seedling growth and mortality data to predict regeneration success. For Ecol Manag 556: 121737. DOI: 10.1016/j.foreco.2024.121737.

Waman AA, Bohra P, Roy TK, Shivashankara KS. 2021. Seed morphological and biochemical studies in certain wild nutmegs. Trees 35 (3): 939-945. DOI: 10.1007/s00468-021-02091-1.

Wanda IF, Rachmadiyanto AN, Oksari AA. 2022. Leaf morphometric and chlorophyll content study of bisbul (*Diospyros discolor* Willd.) at the Bogor Botanical Garden. J Trop Biodivers Biotechnol 7 (2): jtbb72565. DOI: 10.22146/jtbb.72565.

Wulijarni-Soetjipto NJPCM. 2001. *Horsfieldia iryaghedhi* (Gaertn.) Warb. In: van der Vossen HAM, Umali BE (eds). Plant Resources of South-East Asia No 14: Vegetable oils and fats. PROSEA Foundation, Bogor, Indonesia.

Yadav A, Garg S, Kumar S, Alam B, Arunachalam A. 2024. A review on genetic resources, breeding status and strategies of dragon fruit. Genet Resour Crop Evol 72 (3): 2511-2531. DOI: 10.1007/s10722-024-02123-y.

Yin H, Xie B, Chen B, Ma J, Chen J, Zhou Y, Han X, Xiong Z, Yu Z, Huang F. 2023. Detection of moisture content and size of pumpkin seed based on hyperspectral reflection and transmission imaging techniques. J Food Compost Anal 124: 105651. DOI: 10.1016/j.jfca.2023.105651.

Zhang WP, Zhao L, Larjavaara M, Morris EC, Sterck FJ, Wang GX. 2020. Height-diameter allometric correlations for seedling and trees across China. Acta Oecol. 108: 103621. DOI: 10.1016/j.actao.2020.103621.

Zhao X, Chen H, Wu J, Ren H, Wei J, Ye P, Si Q. 2022. Ex-situ conservation of threatened higher plants in Chinese botanical gardens. Glob Ecol Conserv 38: e02206. DOI: 10.1016/gecco.2022.e02206.

NUSANTARA BIOSCIENCE
Vol. 17, No. 2, pp. 226-234
November 2025

ISSN: 2087-3948
E-ISSN: 2087-3956
DOI: 10.13057/nusbiosci/n170205

Fatty acid profile of *Chlorella sorokiniana* InaCC M38 grown in tofu wastewater for biofuel potential

DEVY SUSANTY[1,♥], LUSI NURUL SAFITRI[1], RICSON PEMIMPIN HUTAGAOL[1], ADE AYU OKSARI[2], NURLELA[1]

[1]Department of Chemistry, Faculty of Mathematics and Natural Sciences, Universitas Nusa Bangsa. Jl. Sholeh Iskandar, Cibadak, Tanah Sereal, Bogor 16166, West Java, Indonesia. Tel./fax.: +62-251-7592051, ♥email: dvsusanty@gmail.com

[2]Department of Biology, Faculty of Mathematics and Natural Sciences, Universitas Nusa Bangsa. Jl. Sholeh Iskandar, Cibadak, Tanah Sereal, Bogor 16166, West Java, Indonesia

Manuscript received: 5 March 2025. Revision accepted: 9 October 2025.

Abstract. *Susanty D, Safitri LN, Hutagaol RP, Oksari AA, Nurlela. 2025. Fatty acid profile of* Chlorella sorokiniana *InaCC M38 grown in tofu wastewater for biofuel potential. Nusantara Bioscience 17: 226-234. Chlorella sorokiniana* Shihira & Krauss, 1965 is a microalgae that can grow in tofu liquid waste medium by utilizing the nutrients in the waste in the form of carbon (C), nitrogen (N), phosphorus (P), and potassium (K). This research aims to determine the lipid content and fatty acid compounds contained in *C. sorokiniana* cultured in 25, 30, and 35% Tofu Liquid Waste (TLW) medium using two extraction methods. In this study, the growth of *C. sorokiniana* on TLW medium was determined by calculating the cell density of *C. sorokiniana* using a hemocytometer, and the biomass was collected by centrifuging. *Chlorella sorokiniana* was cultivated for seven days. Lipid extraction was performed using maceration and a combined ultrasonic-assisted extraction (UAE)–maceration method. Biomass and lipid yields, as well as fatty acid methyl esters (FAME) profiles, were analyzed using GC–MS. *Chlorella sorokiniana* grows well on 30% TLW medium with a dry biomass weight of 0.45 g/L on day 7; extraction using the combined method extracted more fatty acid compounds than the maceration method. Lipid yield using the extraction by combined extraction method had more excellent results (4.61%) than the maceration method (3.82%). The fatty acid composition of *C. sorokiniana* extracted by combination extraction consists of 11 types of Saturated Fatty Acids (SFA), two types of Monounsaturated Fatty Acids (MUFA), and two types of Polyunsaturated Fatty Acids (PUFA). The Saturated fatty acid most commonly contained in *C. sorokiniana* was palmitic acid, which could be applied as biodiesel. *Chlorella sorokiniana* cultured in 30% TLW has a higher percentage of SFA (56.58%) with less PUFA, making it more potential for biodiesel.

Keywords: *Chlorella sorokiniana*, fatty acid, maceration, medium, ultrasound-assisted extraction

INTRODUCTION

Lipids from microalgae are commercial compounds in various industries, such as nutritional products, pharmaceuticals, and biodiesel (Sun et al. 2018). The utilization of lipids from microalgae is related to their fatty acid composition. Several studies state that omega-3 and omega-6 fatty acids are essential for pharmaceutical and nutritional needs (Perdana et al. 2021), while palmitic and oleic acids are the primary fatty acids for biodiesel (Sun et al. 2018). The development of microalgae as a lipid source must consider culture costs. Waste medium is a solution to reduce costs for microalgae production.

The use of municipal wastewater for the cultivation of *Acutodesmus obliquus* CN01 and *Desmodesmus maximus* CN06 showed high lipid productivity in *D. maximus* CN06 (3.43 mg/L.day), which mainly consisted of hexadecanoic acid (C16:0) and oleic acid (C18:1), making it suitable for biodiesel (Purba et al. 2022). *Scenedesmus obliquus* cultured in Chinese city wastewater yielded a lipid yield of 0.367 gL^{-1}, indicating its feasibility for biodiesel production (Han et al. 2021). *Chlorella vulgaris* Beij. grown in wastewater with higher light intensity show nitrogen and phosphorus consumption of 75%, with oleic acid as the highest fatty acid, so it has the potential to be a source of biodiesel (Nzayisenga et al. 2020). *Monoraphidium braunii* was cultured in the waste medium, produced high lipid productivity of 5.26 mg L^{-1} day^{-1} (El-Sheekh et al. 2023).

One of the microalgae that is known to be able to grow in waste medium is *Chlorella sorokiniana* Shihira & Krauss, 1965. The growth of *C. sorokiniana* has been studied in real wastewater (RWW) (Rani and Ojha 2021), unsterilized domestic wastewater (Bulynina et al. 2023), cassava wastewater (Padri et al. 2025), cooking cocoon wastewater (Xue et al. 2021), wastewater from the industrial processing of instant coffee (WIC) (Melo et al. 2022), chicken broiler waste medium (Susanty and Oksari 2020), and tofu liquid waste (Mursandi et al. 2022). Tofu liquid waste (TLW) contains carbon, nitrogen, and phosphorus, so that it can be used as a source of nutrition for the microalgae *C. sorokiniana*. The growth of *C. sorokiniana* at TLW medium concentrations of 15, 20, 25, and 30% shows that 30% TLW medium provides the best growth (Mursandi et al. 2022) but has yet to show optimal results. Further research needs to be conducted to determine the optimum medium concentration by testing the growth of *C. sorokiniana* on 25, 30, and 35% TLW medium.

Growth medium can influence fatty acids in microalgae. *Chlorella sorokiniana* cultured on PE-001

medium showed the presence of palmitic acid, palmitoleic acid, stearic acid, oleic acid, and linoleic acid (Qiu et al. 2017). *Chlorella sorokiniana* cultured in Tris-acetate-phosphate medium (TAP) with ascorbic acid and Iron III Chloride ($FeCl_3$) showed the C16 and C18 fatty acids, but in different amounts (Ammar et al. 2021). *Chlorella sorokiniana* cultured mixotrophically using DWW medium yielded a total lipid of 0.433±0.060 g/g DW (Hamidian and Zamani 2022). The use of TLWas a culture medium for *C. sorokiniana* has been studied. However, the fatty acids have not been studied based on the concentration of the medium used.

The extraction method used also influences the fatty acids extracted from microalgae biomass. This research was carried out in two ways: by maceration and a combination of ultrasound-assisted extraction (UAE) and maceration. *Chlorella sorokiniana* has strong cell walls with a complex matrix composed of carbohydrates, polypeptides, and glycoproteins (Kim et al. 2024), so the process of destroying microalgae cell walls is necessary. The UAE method provides a cavitation wave effect that helps the process of destroying the microalgae matrix, making the extraction process more effective (Shevelyuhina et al. 2022). Combining UAE and maceration extraction needs to be compared with maceration to determine the difference in the yield of extracted lipids and fatty acids profile. Research regarding the identification of fatty acid compounds of *C. sorokiniana* cultured from TLW medium needs to be carried out to determine the fatty acid composition of *C. sorokiniana* cultured at different TLW medium concentrations and different extraction methods. The fatty acid profile of *C. sorokiniana* cultured in various concentrations of TLW medium and extraction using a combination of UAE and maceration is a novelty of this research. This study aims to examine lipid productivity and fatty acid profiles at TLW concentrations and extraction.

MATERIALS AND METHODS

Study area

Chlorella sorokiniana inaCC M38 is an isolate purchased from the inaCC BRIN collection. Tofu liquid waste used as culture medium was obtained from tofu factories in the Ciriung area, Bogor District, West Java, Indonesia. In this study, the cultivation of *C. sorokiniana* was carried out on tofu liquid waste medium with three concentration variations, namely 25, 30, and 25%. *Chlorella sorokiniana* biomass was extracted using two extraction methods, namely maceration and combined maceration with UAE, to compare lipids and fatty acids.

Nutrient analysis of tofu liquid waste

In this study, the tofu liquid waste was used as a culture medium for *C. sorokiniana*. Macronutrients in the form of carbon (C), nitrogen (N), phosphorus (P), and potassium (K) contained in tofu liquid waste are tested first based on SNI 19-7030-2004.

Preparation of tofu liquid waste medium

The material used as a medium for *C. sorokiniana* is tofu liquid waste that is taken from tofu pressing. Tofu liquid waste was taken by homogenizing the waste and measuring the pH before being used as a culture medium. Variations in TLW medium concentration were 25, 30 and 35%. The medium was added to NaOH 2N solution until it reached a neutral pH of 7 (Mursandi et al. 2022).

Cultivation of the microalgae *Chlorella sorokiniana*

Cultivation of the microalgae *C. sorokiniana* was carried out in TLW medium with concentrations of 25, 30, and 35%, and sterilization was carried out using an autoclave at a temperature of 121°C, pressure of 1 atm for 15 minutes. *Chlorella sorokiniana* was cultured in sterile LCT medium with an initial density of $\pm 10^5$ cells/mL. Cultivation was carried out at 30°C and light intensity from two TL lamps (2,300 lux) (Mursandi et al. 2022). The remaining waste after cultivation is disposed of in a collection of organic waste for which the laboratory has prepared a collection tank.

Calculation of *Chlorella sorokiniana* cell abundance

Chlorella sorokiniana cells were taken with a pipette and then observed under a microscope with a magnification of 40×10. The abundance of *C. sorokiniana* cells was counted with three repetitions. The abundance of *C. sorokiniana* cells was calculated using an improved Neubauer hemocytometer. Cell abundance was determined by counting microalgae cells in 5 small boxes (Mursandi et al. 2022).

Cell density (cells/mL) N = Total number of cells × 10^4

Chlorella sorokiniana biomass collection

Harvesting or collection of *C. sorokiniana* microalgae biomass was carried out on day 7 (during optimum growth). *Chlorella sorokiniana* biomass was harvested by separating the medium from the microalgae using a centrifuge at a speed of 3,600 rpm for 3 minutes. The biomass was dried at room temperature for 24 hours until dry biomass was obtained (Mursandi et al. 2022).

Lipid extraction of *Chlorella sorokiniana*

Chlorella sorokiniana biomass was extracted using a combined method of Ultrasonic-Assisted Extraction (UAE) and maceration. The sample was added with n-hexane solvent (Sivaramakrishnan and Incharoensakdi 2019) in a ratio of 1:10 (w/v). The sample was put into an ultrasonic device for an extraction process for 90 minutes at a frequency of 42 KHz at room temperature. After the sample was sonicated, it was continued with maceration for 24 hours and stirred using a shaker. After the extraction process was complete, filtering was carried out using filter paper to separate the extraction results from the resulting dregs. The solvent was removed using a rotary evaporator until no more solvent drips. The remaining solvent is evaporated using a water bath.

Lipid content (%) = (lipid weight)/(sample weight) × 100%

Esterification process of *Chlorella sorokiniana*

The esterification process begins by placing the sample into a boiling flask and mixing it with 5 mL of 1% sulfuric acid dissolved in methanol. The mixture was then heated using a reflux condenser for 1 hour. After the mixture had cooled, 20 mL of distilled water and 5 mL of n-hexane were added to the solution. The methyl ester is then taken by evaporating the hexane fraction of the mixture.

Identification of fatty acid methyl ester (FAME) of *Chlorella sorokiniana*

The fatty acid compounds in *C. sorokiniana* extract were identified using Gas Chromatography-Mass Spectrometry (GC-MS), carried out on the optimal yield of *C. sorokinian*a microalgae oil extract by injecting one µL of sample solution into the GC-MS. The mobile phase used is ultra high purity (UHP) helium, while the stationary phase used is an RTX 5 column, which is non-polar, containing 5% diphenyl and 95% dimethylpolysiloxane.

Data analysis

Cell growth analysis was done by making a growth curve between cultivation time and cell density. The dry biomass of *C. sorokiniana* was compared among three LCT medium concentration treatments. Data analysis of the influence of TLW concentration on biomass by one-way ANOVA statistical test and Duncan Multiple Range Test (DMRT) test using IBM SPSS version 23. The fatty acids identified from the GC-MS results were compared using the extraction method and the culture medium concentration.

RESULTS AND DISCUSSION

Tofu liquid waste nutrition

Tofu liquid waste is a by-product of tofu production, which is still rich in organic substances. The use of this waste has been researched as plant fertilizer because of the presence of elements N, P, and K. The right amount of N, P, and K will promote growth, but if it is excessive, it will have a negative impact, so appropriate concentrations are needed (Kurniawan et al. 2024). Tofu Liquid Waste (TLW) can be used as a culture medium because it contains good nutrients for the growth of *C. sorokiniana* (Mursandi 2022). Table 1 shows that the availability of nutrients (carbon, nitrogen, phosphorus, and potassium) in TLW is relatively high. *C. sorokiniana* can reduce 78.82% nitrate and 88.17% phosphate in dairy wastewater (DWW) (Hamidian and Zamani 2022).

Tofu liquid waste is a by-product of tofu production, which is still nutrient-rich. The availability of nutrients in the medium influences the rate of microalgae productivity because microalgae utilize nutrients as a source for their body's metabolism (Ziganshina et al. 2022). Nitrogen plays a role in the formation of amino acid compounds, lipids, and chlorophyll (Negi et al. 2015; Toumi and Politaeva 2021). Potassium plays a role in the process of photosynthesis and affects cell density (He et al. 2020).

The growth and biomass of *Chlorella sorokiniana*

TLW contains carbon and nitrogen in high concentrations (Table 1). TLW dilution was conducted to see the limits of *C. sorokiniana*'s growth ability. At the three TLW dilution concentrations (25, 30, and 35%), *C. sorokiniana* could adapt and grow well immediately. This condition is indicated by the cell density, which directly increases on the first day of cultivation. However, at 25% TLW, the cell division ability of *C. sorokiniana* began to decrease on the fourth day, caused by the amount of nutrients being more limited than in the other two concentrations. The 30% TLW provides good growth with more cell density than 25 and 35% TLW (Figure 1). Nutrient availability at 30% TLW provides more appropriate growth with the highest cell density on day 7 (4.89×10^5 cells/mL) with a dry biomass of 0.45 g/L.

TLW generally contains nitrogen as ammonium (Nuryoto et al. 2025). The growth of *C. sorokiniana* at 35% TLW was lower than at 30% TLW. The presence of high levels of ammonium can be toxic to cells. Free ammonium can induce reactive oxygen species (ROS formation) in cells, inhibiting cell growth (Shen et al. 2020). Cell density correlates with the biomass produced. The high cell density of *C. sorokiniana* at 30% TLW provides a high biomass (Table 2).

Lipid yield and fatty acid profile of *Chlorella sorokiniana*

The highest lipid yield was obtained from *C. sorokiniana*, cultured at 30% TLW, and extracted using a combined extraction method (Figure 2). Extraction by sonication utilizes ultrasonic waves so that the solvent exposed to these waves experiences an increase in density; the molecules approach each other and become denser. Increasingly larger cavitation bubbles often accompany this process. The collision between the microalgae cell wall and the solvent medium caused by ultrasonic vibrations opens the pores in the cell wall. As a result, the components contained in microalgae can more easily dissolve into the solvent through a diffusion process (Shevelyuhina et al. 2022). Microalgae cells have thick and rigid cell walls, so the combination of UAE and maceration gives optimal results for lipids. There are also more types of fatty acid compounds extracted using the combined UAE and maceration extraction method compared to only the maceration method (Figure 3). The process of breaking down microalgae cell walls with the help of sonication produces a more diverse fatty acid composition (twelve types of saturated fatty acids and four types of unsaturated fatty acids) than the maceration method (5 types of saturated fatty acids and two types of unsaturated fatty acids). These results are almost the same as previous research, which identified 19 different types of fatty acids (Djamaludin and Chamidah 2021).

The extract obtained from the combined extraction method contains higher lipid yield percentages than the maceration method. Microalgae cells have thick and rigid cell walls. Hence, the combination of UAE and maceration gives a higher lipid yield percentage than the maceration method. The research results showed that extraction,

starting with breaking down the cell walls using ultrasound, produced an extract with higher amounts of fatty acids. Chlorella has the characteristics of a strong cell wall (Widyaningrum and Prianto 2021), so special treatment is required to break down the cell wall, enhancing the diffusion of molecules inside the cell with an extraction solvent.

Extraction using the combined method yielded a greater variety of extracted fatty acids compared to maceration (Figure 3). Monounsaturated fatty acids were extracted using the combined extraction method. The percentage of saturated fatty acids was higher in the combined extraction method compared to the maceration method (Figure 4). The extraction method can affect the profile of the extracted fatty acids (Pérez-Barradas et al. 2023). The percentage of saturated fatty acids was higher in the combined extraction method with myristic acid. The palmitic acid extracted using the maceration method was higher than that extracted using the combined method. Maceration extraction showed a higher content of unsaturated fatty acids, potentially resulting in a lower cetane number for biodiesel use.

Identification of fatty acid compounds in *C. sorokiniana* cultured at different TLW medium concentrations was chosen based on the optimal results of the extraction method, namely, using a combination of UAE extraction and maceration. *Chlorella sorokiniana* cultured at 30% TLW produces more diverse types of saturated fatty acids than those cultured at 25 and 35% TLW (Figure 5). The dominant fatty acids in *C. sorokiniana* cultured at all variations in TLW concentrations were C16:0 and C18:2. These results are comparable to other studies on fatty acids in *Chlorella* (Table 3).

The 9,12-octadecadienoic acid (C18:2) is identified in *C. sorokiniana* that was cultured in TLW 25 and 35%. Another form of C18:2 identified in *C. sorokiniana* is 10,13-octadecadienoic acid, which is also found in *C. vulgaris* (Morowvat and Ghasemi 2016). *Chlorella sorokiniana* cultured at 25 and 35% TLW showed the presence of 7,10-Hexadecadienoic acid. This fatty acid was identified in *Chlorella* (Fernandes and Cordeiro 2020). The stearic acid (C18:0) and palmitoleic acid (C16:1) were only identified in *C. sorokiniana* cultured in 30% TLW medium.

Table 1. Nutrition contained in tofu liquid waste

Component	Content (mg/L)
Organic Carbon (C)	1,136
Nitrogen (N)	5,879
Phosphorus (P)	74.4
Potassium (K)	437.1

Table 2. Biomass (dry weight) of *C. sorokiniana* at various concentrations of TLW medium

Concentration of TLW medium	Biomass of *C. sorokiniana* (g/L)
25%	$0.36^{a}\pm0.07$
30%	$0.45^{b}\pm0.05$
35%	$0.43^{ab}\pm0.07$

Note: There is no statistical difference between numbers separated by the same letter at $p<0.05$ using DMRT

Table 3. Comparison of the major fatty acids in *Chlorella*

Species	Medium	Major Fatty Acid	Reference
Chlorella vulgaris	BG11	Palmitic, oleic, and linoleic acids	(Moradi-Kheibari et al. 2022)
Chlorella vulgaris	wastewater of the dairy industry with 25% dilution	Palmitic acid	(Khalaji 2022)
Chlorella vulgaris	Bold Bassal Medium with MnCl	Palmitic acid (53.59%)	(Saber et al. 2024)
Chlorella sorokiniana	BG11 with secondary treated effluents	α-linolenic acid (17.652%) and Palmitic acid (8.321%)	(Asadi et al. 2020)
Chlorella sorokiniana KNUA114	BG11 (35°C)	Palmitic Acid (43.25%), C18:2 ω6 (17.87%)	(Yun et al. 2020)
Chlorella sorokiniana inaCC M38	TLW (30%)	10,13-octadecadienoic acid (C18:2), Palmitic Acid	This study (Figure 5)

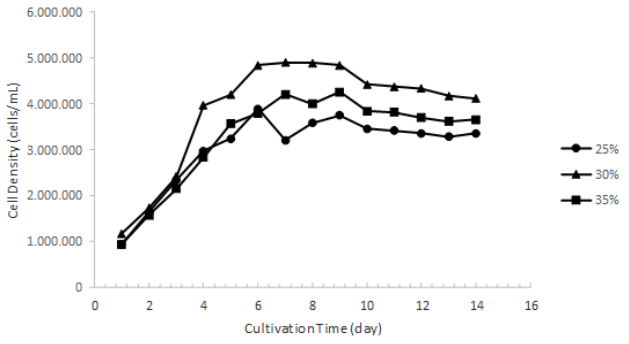

Figure 1. Cell density of *C. sorokiniana* in TLW medium

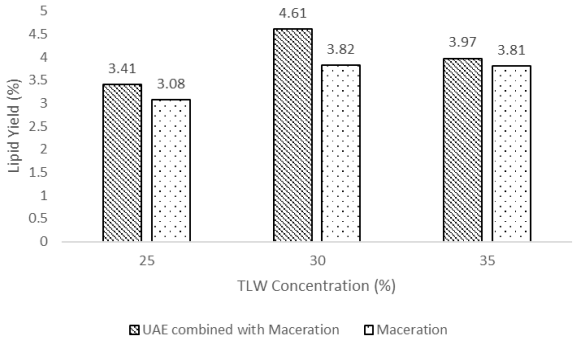

Figure 2. Lipid yield of *Chlorella sorokiniana* at different extraction methods and variation of TLW concentration

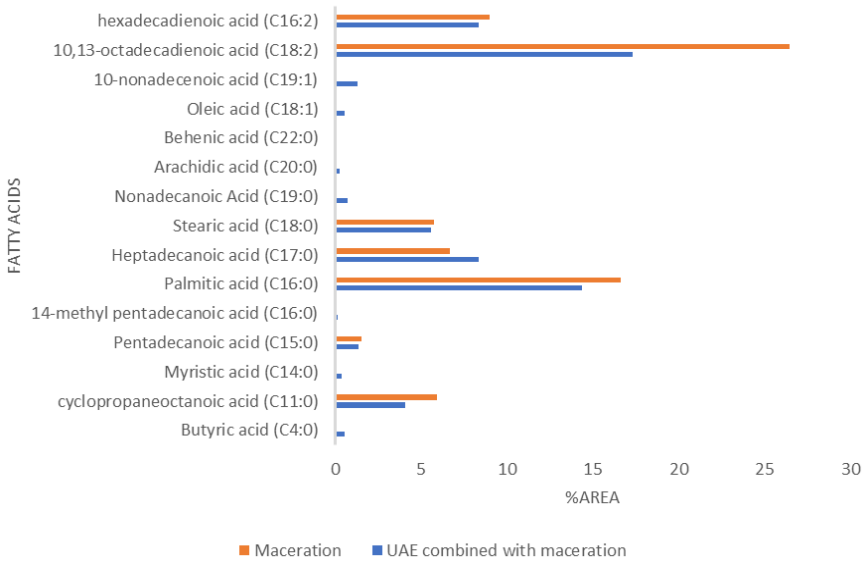

Figure 3. Fatty acids of *C. sorokiniana* based on extraction methods

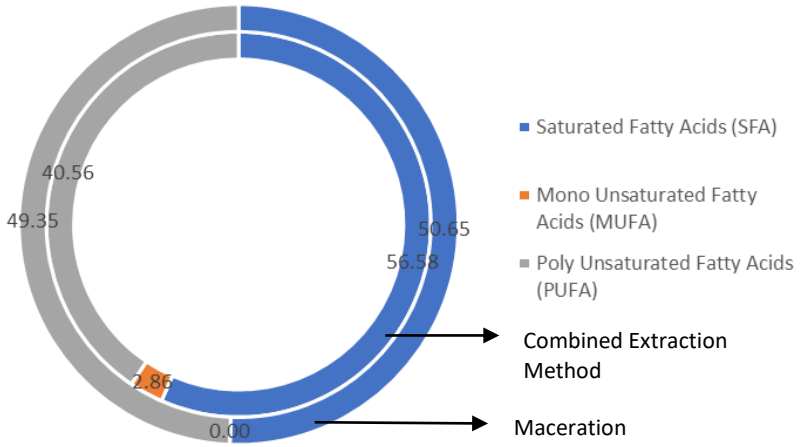

Figure 4. Comparison of SFA/MUFA/PUFA in *Chlorella sorokiniana* extract based on the extraction method

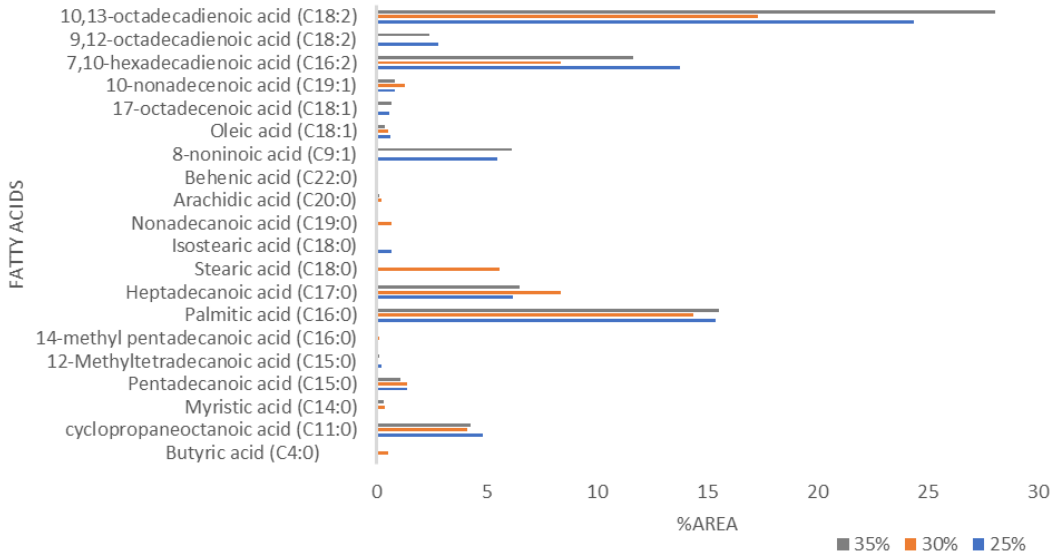

Figure 5. *C. sorokiniana* fatty acids cultured at variations in TLW medium concentration by UAE combination extraction method with maceration

Cyclopropaneoctanoic acid (C11:0) is found in *C. sorokiniana* cultured in all three TLW medium concentrations. This fatty acid is one of the minor fatty acids in microalgae under specific cultivation conditions. Previous studies examining several microalgae species detected cyclopropaneoctanoic acid in *Micractinium thermotolerans* VKM Al-332 (Krivina et al. 2024). Cyclopropaneoctanoic acid is a fatty acid with a cyclic chain. Reactions during extraction and esterification may cause the presence of cyclic fatty acids. In this study, both maceration methods showed the presence of these fatty acids (Figure 3).

Heptadecanoic acid (C17:0), oleic acid (C18:1), and 10,13-octadecadienoic acid (C18:2) were also identified in *C. sorokiniana* cultured at all three variations of TLW medium concentrations extracted by the combination method. Heptadecanoic acid (C17:0) is a saturated fatty acid with odd chains. These odd fatty acids in algae oil do not show any adverse effects. Heptadecanoic acid (C17:0) was found in considerable amounts (29.1%) in mixotrophically cultured *Messastrum gracile* SVMIICT7 (Kuravi and Mohan 2021).

Oleic acid (C18:1) is a monounsaturated fatty acid (MUFA) abundant in microalgae, including *C. sorokiniana*. Other studies on *C. sorokiniana* have shown a varied oleic acid content based on nitrogen availability and light intensity (Papapanagiotou et al. 2024). Oleic acid studies on *C. sorokiniana* immobilized in calcium-alginate beads showed a higher oleic acid content compared to free cell cultures (Alfaro-Sayes et al. 2023). Nitrogen-deficient medium encourages *C. sorokiniana* to increase the synthesis of monounsaturated fatty acids (MUFA), one of which is oleic acid (Papapanagiotou et al. 2024). According to this study's results, *C. sorokiniana* cultured on 25% TLW medium has oleic acid with a higher percentage area than TLW 30 and 35%. Stress conditions with lower amounts of nitrogen indicate higher amounts of oleic acid in microalgae; research on *Scenedesmus* sp. SVMIICT1 showed high levels of oleic acid in dual stress (nitrate depletion and salinity stress) and mixotropic conditions (Kona et al. 2022).

The fatty acids that were only identified in *C. sorokiniana* extracts cultured in 30% TLW medium were butyric acid (C4:0), 14-methyl pentadecanoic acid (C16:0), stearic acid (C18:0), and nonadecanoic acid (C19:0). Stearic acid (C18:0) and hexadecadienoic acid (C16:1) have a reasonably high %area and are only identified in *C. sorokiniana* extracts cultured on a 30% TLW medium. Stearic acid is one of the fatty acids that has the potential to be biodiesel (Chen and Chang 2016). Other studies on the fatty acids in Chlorella show that the species of *C. sorokiniana* generally has higher saturated fatty acids than *C. vulgaris* (Yun et al. 2020).

Polyunsaturated Fatty Acids (PUFA) are more commonly identified in *C. sorokiniana* extracts cultured on 25 and 35% TLW medium (Figure 5), namely in the form of 7,10-hexadecadienoic acid (C16:2), 9,12-octadecadienoic acid (C18:2), and 10,13-octadecadienoic acid (C18:2). In general, microalgae contain 9,12-octadecadienoic acid (C18:2); however, 10,13-octadecadienoic acid is also found in *Chlorella vulgaris* and *Nostoc muscorum* (Morowvat and Ghasemi 2016). *Chlorella sorokiniana* inaCC M38 cultured on TLW medium has the highest fatty acid composition of C16:0 and C18:2. This is in line with other studies of *C. sorokiniana* that were cultured on a lab scale in phototropic and mixotropic conditions (Barouh et al. 2024).

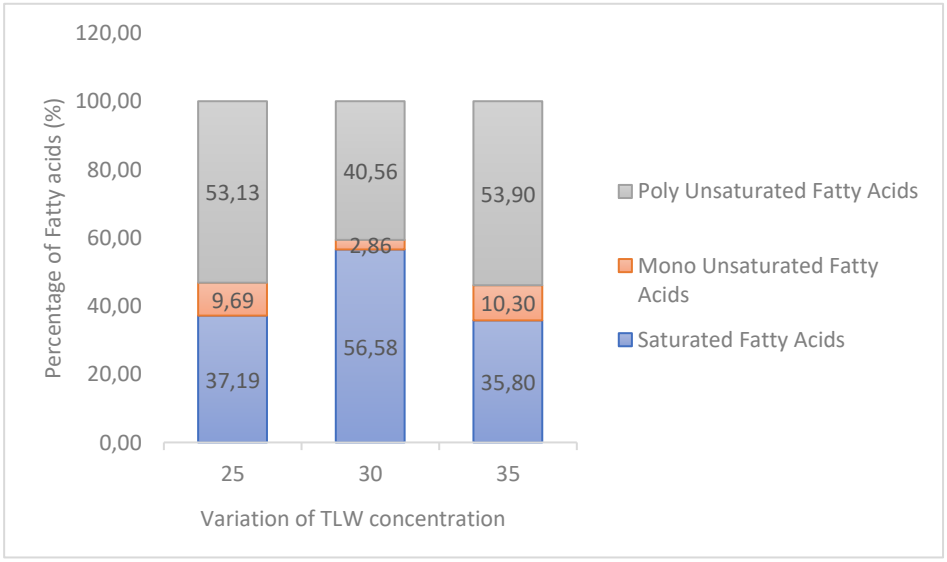

Figure 6. Comparison of SFA/MUFA/PUFA in *Chlorella sorokiniana* extract based on variation of TLW concentration using combined extraction method

Several biodiesel quality parameters, such as flash point, oxidation stability, and cetane number, are influenced by fatty acid composition. A higher PUFA composition with shorter carbon chains can lower the cetane number (Mujtaba et al. 2021; Omwoyo and Mengo 2023). Saturated fatty acids provide better biodiesel quality with a higher cetane number (Mekonnen et al. 2024). Higher oleic and linoleic acids provide a lower cetane number than oils with higher palmitic content (Sumatri et al. 2023). *Chlorella vulgaris* KP2, with a composition of 49.26% SFA, 38.73% MUFA, and 10.12% PUFA of the total fatty acids, has higher oxidation stability and cetane number (58.73) (Andeden et al. 2021). Research on *Nannochloropsis oculata* by giving stress to the growth medium produces C16-C20 fatty acids with SFA and MUFA composition reaching 88% so that it has the potential as a raw material for biodiesel (El-Sayed et al. 2022). The high quality of biodiesel from *Chlorella muelleri* is due to the high composition of C14-C18 fatty acids (81%) and oleic acid (28%) (Andrew et al. 2022). The results are comparable to the species *Coelastrella* sp. and *Verrucodesmus verrucosus*, which contain 80-90% C16-C18 fatty acids (Rodríguez-Palacio et al. 2022).

The nutrients in the culture medium affect the metabolism and fatty acids produced by microalgae. This study showed that 30% TLW medium provided a higher SFA composition percentage than 25 and 35% TLW media (Figure 6). The 50% F/2 medium used to culture *Chlorella vulgaris*, *Oocystis submarina*, and *Monoraphidium* showed a higher saturated fatty acid profile and better biodiesel quality (Hawrot-Paw et al. 2021). Nutrients in the medium that are limited to a certain amount have a better effect on the properties of biodiesel produced from microalgae because they tend to produce higher saturated fatty acids. In this study, *C. sorokiniana* cultured in 30% TLW media showed better potential as a biodiesel feedstock based on its fatty acid profile.

The lipid productivity of *C. sorokiniana* InaCC M38 cultured in TLW medium at various concentrations of 25, 30, and 35% demonstrates the strain's specific response to the availability of organic nutrients in the TLW medium. While these findings provide valuable information regarding the potential of tofu wastewater as a low-cost microalgae growth medium, they may not be fully generalizable to all *C. sorokiniana* strains. Further research involving multiple strains is recommended to validate the universality of the lipid accumulation mechanism under similar environmental stressors.

The utilization of tofu wastewater in this study focused on providing nutrients for *Chlorella sorokiniana* InaCC M38. This wastewater utilization positively contributes to environmental sustainability by reducing the risk of water pollution. Reusing tofu wastewater reduces reliance on synthetic media, minimizes nutrient input costs, and minimizes environmental burdens. Future studies are needed, including a life cycle assessment (LCA), to evaluate the overall energy balance and carbon footprint of cultivating *C. sorokiniana* InaCC M38 in tofu wastewater, ensuring the process is both environmentally and economically sustainable.

Based on this study, it can be concluded that *Chlorella sorokiniana* inaCC M38 grows better on a TLW medium of 30%. Biomass production on the 7th day was 0.45 g/L. Extraction by the combination method, with cell wall breaking first using UAE, further increases the yield of extracted lipids. The extract has more fatty acids (4.61% DW) compared to single extraction by maceration (3.82% DW). This study provides the basis for better extraction methods in extracting compounds in *C. sorokiniana*. The presence of fatty acids in *C. sorokiniana* cultured on TLW 30% medium indicates more Saturated Fatty acids (56.58%) with palmitic acid as a major SFA that can show its potential as a biodiesel material. However, further experimental optimization is needed to improve lipid production of *C. sorokiniana,* to scale up testing, life-cycle assessment, and field cultivation validation. Overall, *C. sorokiniana* grown in tofu wastewater represents a promising, low-cost strategy for integrating biofuel production with waste management systems.

ACKNOWLEDGEMENTS

This research was funded by the Institute for Research and Community Service, Nusa Bangsa University, Indonesia with Grant number 105/Rek-UNB/SPK/VIII/2022.

REFERENCES

Alfaro-Sayes DA, Amoah J, Rachmadona N, Hama S, Hasunuma T, Kondo A, Ogino C. 2023. Enhanced growth and lipid productivity by living *Chlorella sorokiniana* immobilized in Ca-alginate beads. J Phys: Energy 5 (1): 014019. DOI:10.1088/2515-7655/acb383.

Ammar M, Omer M, Aman S, Hameed, Abbas S, Shaheen S, Abbas A, Shakeel SN. 2021. Fatty acid profiling and physicochemical characterization of *Chlorella sorokiniana* potentially used for biofuel production. Sains Malaysiana 51 (8): 2547-2557. DOI: 10.17576/jsm-2022-5108-15.

Andeden EE, Ozturk S, Aslim B. 2021. Evaluation of thirty microalgal isolates as biodiesel feedstocks based on lipid productivity and triacylglycerol (TAG) content. Curr Microbiol 78 (2): 775-788. DOI: 10.1007/s00284-020-02340-5.

Andrew AR, Yong WTL, Misson M, Anton A, Chin GJWL. 2022. Selection of tropical microalgae species for mass production based on lipid and fatty acid profiles. Front Energy Res 10: 912904. DOI: 10.3389/fenrg.2022.912904.

Asadi P, Rad HA, Qaderi F. 2020. Lipid and biodiesel production by cultivation of isolated strain *Chlorella sorokiniana* pa.91 and *Chlorella vulgaris* in dairy wastewater treatment plant effluents. J Environ Health Sci Eng 18 (2): 573-585. DOI: 10.1007/s40201-020-00483-y.

Barouh N, Wind J, Chuat V, Gagnaire V, Valence F, Bourlieu-Lacanal C, Subileau M. 2024. Variations in *Chlorella* lipid content in commercial and in-lab produced biomass. OCL 31: 9. DOI: 10.1051/ocl/2024005.

Bulynina SS, Ziganshina EE, Ziganshin AM. 2023. Growth efficiency of *Chlorella sorokiniana* in synthetic media and unsterilized domestic wastewater. BioTech 12 (3): 53. DOI: 10.3390/biotech12030053.

Chen CY, Chang H. 2016. Lipid production of microalga *Chlorella sorokiniana* CY1 is improved by light source arrangement, bioreactor operation mode, and deep-sea water supplements. Biotechnol J 11 (3): 356-362. DOI: 10.1002/biot.201500288.

Djamaludin H, Chamidah A. 2021. Fatty acid composition analysis of oil extract microalgae *Spirulina* sp. with different extraction methods. JFMR-J Fish Mar Res 5 (2): 254-261. DOI: 10.21776/ub.jfmr.2021.005.02.10.

El-Sayed AEKB, Fetyan NA, Moghanm FS, Elbagory M, Ibrahim FM, Sadik MW, Shokr MS. 2022. Biomass fatty acid profile and fuel property prediction of bagasse waste grown *Nannochloropsis oculata*. Agriculture 12 (8): 1201. DOI: 10.3390/agriculture12081201.

El-Sheekh MM, Galal HR, Mousa A, Farghl AAM. 2023. Coupling wastewater treatment, biomass, lipids, and biodiesel production of some green microalgae. Environ Sci Pollut Res 30 (12): 35492-35504. DOI: 10.1007/s11356-023-25628-y.

Fernandes T, Cordeiro N. 2020. *Hemiselmis andersenii* and *Chlorella stigmatophora* as new sources of high-value compounds: A lipidomic approach. J Phycol 56 (6): 1493-1504. DOI: 10.1111/jpy.13042.

Hamidian N, Zamani H. 2022. Biomass production and nutritional properties of *Chlorella sorokiniana* grown on dairy wastewater. J Water Process Eng 47: 102760. DOI: 10.1016/j.jwpe.2022.102760.

Han W, Jin W, Li Z, Wei Y, He Z, Chen C, Qin C, Chen Y, Tu R, Zhou X. 2021. Cultivation of microalgae for lipid production using municipal wastewater. Process Saf Environ Prot 155: 155-165. DOI: 10.1016/j.psep.2021.09.014.

Hawrot-Paw M, Ratomski P, KoniuszyA, Golimowski W, Teleszko M, Grygier A. 2021. Fatty acid profile of microalgal oils as a criterion for selection of the best feedstock for biodiesel production. Energies 14 (21): 7334. DOI: 10.3390/en14217334.

He Y, Ma J, Joseph V, Wei Y, Liu M, Zhang Z, Li G, He Q, Li H. 2020. Potassium regulates the growth and toxin biosynthesis of *Microcystis aeruginosa*. Environ Pollut 267: 115576. DOI: 10.1016/j.envpol.2020.115576.

Kim JS, Lee S, Cho S, Jung Y. 2024. Inducing heritable genomic deletions in the APT gene of *Chlorella sorokiniana* using CRISPR/Cas9. Algal Res 79: 103435. DOI:10.1016/j.algal.2024.103435

Khalaji M. 2022. Evaluation of fatty acid profiles of *Chlorella vulgaris* microalgae grown in dairy wastewater for producing biofuel. J Environ Health Sci Eng 20 (2): 691-697. DOI: 10.1007/s40201-022-00808-z.

Kona R, Katakojwala R, Pallerla P, Sripadi P, Mohan SV. 2022. High oleic acid biosynthesis and its absolute quantification by GC/MS in oleaginous *Scenedesmus* sp. SVMIICT1 was cultivated in a dual stress phase. Algal Res 67: 102865. DOI: 10.1016/j.algal.2022.102865.

Krivina E, Degtyaryov E, Tebina E, Temraleeva A, Savchenko T. 2024. Comparative analysis of the fatty acid profiles of selected representatives of *Chlorella*-clade to evaluate their biotechnological potential. Intl J Plant Biol 15 (3): 837-854. DOI: 10.3390/ijpb15030060.

Kuravi SD, Mohan SV. 2021. Mixotrophic cultivation of isolated *Messastrum gracile* SVMIICT7: Photosynthetic response and product profiling. Bioresour Technol 341: 125798. DOI: 10.1016/j.biortech.2021.125798.

Kurniawan L, Maryudi M, Astuti E. 2024. Utilization of tofu liquid waste as liquid organic fertilizer using the fermentation method with activator effective microorganisms 4 (EM-4): A review. Equilibrium: J Chem Eng 8 (1): 100-112. DOI: 10.20961/equilibrium.v8i1.84056.

Mekonnen KD, Endris YA, Abdu KY. 2024. Alternative methods for biodiesel cetane number valuation: A technical note. ACS Omega 9 (6): 6296-6304. DOI: 10.1021/acsomega.3c09216.

Melo JM, Telles TS, Ribeiro MR, Junior OD, Andrade DS. 2022. *Chlorella sorokinian*a as a bioremediator of wastewater: Nutrient removal, biomass production, and potential profit. Bioresour Technol Rep 17: 100933. DOI: 10.1016/j.biteb.2021.100933.

Moradi-Kheibari N, Ahmadzadeh H, Lyon SR. 2022. Correlation of total lipid content of *Chlorella vulgaris* with the dynamics of individual fatty acid growth rates. Front Mar Sci 9: 837067. DOI: 10.3389/fmars.2022.837067.

Morowvat MH, Ghasemi Y. 2016. Screening of some naturally isolated microalgal strains for polyunsaturated fatty acids production. Asian J Pharm Res Health Care 8 (4): 122-130. DOI: 10.18311/ajprhc/2016/6113.

Mujtaba MA, Kalam MA, Masjuki HH, Razzaq L, Khan HM, Soudagar MEM, Gul M, Ahmed W, Raju VD, Kumar R, Ong HC. 2021. Development of empirical correlations for density and viscosity estimation of ternary biodiesel blends. Renew Energy 179: 1447-1457. DOI: 10.1016/j.renene.2021.07.121.

Mursandi H, Susanty D, Nurhayati L, Oksari AA. 2022. Short Communication: Antioxidant activity of ethanol extract of *Chlorella sorokiniana* cultured in tofu wastewater. Nusantara Biosci 14 (2): 155-159. DOI: 10.13057/nusbiosci/n140204.

Negi S, Barry AN, Friedland N, Subramanian S, Pieris S, Holguin FO, Dungan B, Schaub T, Sayre R. 2015. Impact of nitrogen limitation on biomass, photosynthesis, and lipid accumulation in *Chlorella sorokiniana.* J Appl Psychol 28: 803-812. DOI: 10.1007/s10811-015-0652-z.

Nuryoto N, Suritno S, Sutangkas AR, Rahmayetty R, Rumbino Y, Wicakso DR, Damayanti A, Bagaskara RNT. 2025. Tofu wastewater treatment innovation: Effectiveness of natural zeolite as an adsorbent in the ammonium adsorption process. Ecol Eng Environ Technol 26 (2): 55-65. DOI: 10.12912/27197050/196498.

Nzayisenga JC, Farge X, Groll SL, Sellstedt A. 2020. Effects of light intensity on growth and lipid production in microalgae grown in wastewater. Biotechnol Biofuels Bioprod 13 (1): 4. DOI: 10.1186/s13068-019-1646-x.

Padri M, Boontian N, Latief MM, Amdah M, Tamzil MS. 2025. Application of syntrophic co-culture *Chlorella sorokiniana* and *Streptomyces thermocarboxydus* in a semi-continuous system for cassava wastewater treatment and biomass production. Green Technol Sustain 3 (3): 100168. DOI: 10.1016/j.grets.2025.100168.

Papapanagiotou G, Charisis A, Samara C, Kalogianni EP, Chatzidoukas C. 2024. Linking cultivation conditions to the fatty acid profile and nutritional value of *Chlorella sorokiniana* lipids. Processes 12 (12): 2770. DOI: 10.3390/pr12122770.

Perdana BA, Chaidir Z, Kusnanda AJ, Dharma A, Zakaria IJ, Syafrizayanti, Bayu A, Putra MY. 2021. Omega-3 fatty acids of microalgae as a food supplement: A review of exogenous factors for production enhancement. Algal Res 60: 102542. DOI: 10.1016/j.algal.2021.102542.

Pérez-Barradas FV, Ortega-Clemente LA, Pérez-Legaspi IA, Jiménez-García MI, Huerta-Heredia AA, Quintana-Castro R. 2023. Variation in the fatty acid composition of microalgal lipids due to the effect of the extraction method. J Appl Phycol 35 (6): 2851-2863. DOI: 10.1007/s10811-023-03092-y.

Purba LDA, Othman FS, Yuzir A, Mohamad SE, Iwamoto K, Abdullah N, Shimizu K, Hermana J. 2022. Enhanced cultivation and lipid production of isolated microalgae strains using municipal wastewater. Environ Technol Innov 27: 102444. DOI: 10.1016/j.eti.2022.102444.

Qiu R, Gao S, Lopez PA, Ogden KL. 2017. Effects of pH on cell growth, lipid production, and CO_2 addition of microalgae *Chlorella sorokiniana*. Algal Res 28: 192-199. DOI: 10.1016/j.algal.2017.11.004.

Rani S, Ojha CSP. 2021. *Chlorella sorokiniana* for integrated wastewater treatment, biomass accumulation, and value-added product estimation under varying photoperiod regimes: A comparative study. J Water Process Eng 39: 101889. DOI: 10.1016/j.jwpe.2020.101889.

Rodríguez-Palacio MC, Cabrera-Cruz RBE, Rolón-Aguilar JC, Tobías-Jaramillo R, Martínez-Hernández M, Lozano-Ramírez C. 2022. The cultivation of five microalgae species and their potential for biodiesel production. Energy Sustain Soc 12 (1): 10. DOI: 10.1186/s13705-022-00337-5.

Saber H, Galal HR, Abo-Eldahab M, Alwaleed E. 2024. Enhancing the biodiesel production in the green alga Chlorella vulgaris by heavy metal stress and prediction of fuel properties from fatty acid profiles. Environ Sci Pollut Res 31 (24): 35952-35968. DOI: 10.1007/s11356-024-33538-w.

Shen Y, Qiu S, Chen Z, Zhang Y, Trent J, Ge S. 2020. Free ammonia is the primary stress factor rather than total ammonium to *Chlorella sorokiniana* in simulated sludge fermentation liquor. Chem Eng J 397: 125490. DOI: 10.1016/j.cej.2020.125490.

Shevelyuhina A, Babich O, Sukhikh S, Ivanova S, Kashirskih E, Smirnov V, Michaud P, Chupakhin E. 2022. Antioxidant and antimicrobial activity of microalgae of the Filinskaya Bay (Baltic Sea). Plants 11 (17): 2264. DOI: 10.3390/plants11172264.

Sivaramakrishnan R, Incharoensakdi A. 2019. Low power ultrasound treatment for the enhanced production of microalgae biomass and lipid content. Biocatal Agric Biotechnol 20: 101230. DOI: 10.1016/j.bcab.2019.101230.

Sumatri I, Hadiyanto H, Suherman S, Christwardana M. 2023. Production of biodiesel using enzymatic esterification of multi-feedstock oils. ASEAN J Chem Eng 23 (2): 194-209. DOI: 10.22146/ajche.79208.

Sun XM, Ren LJ, Zhao QY, Ji XJ, Huang H. 2018. Microalgae for the production of lipid and carotenoids: A review with focus on stress regulation and adaptation. Biotechnol Biofuels Bioprod 11 (1): 272. DOI: 10.1186/s13068-018-1275-9.

Susanty D, Oksari AA. 2020. Growth and secondary metabolite content of chloroform extract of *Chlorella* sp. and *Chlorella sorokiniana* cultured on chicken broiler waste media. Nusantara Biosci 12 (1): 28-32. DOI: 10.13057/nusbiosci/n120105.

Omwoyo JB, Mengo W. 2023. The Effects of a Sodium Carbonate Catalyst on Calorific Value, Flash Point, Cetane Index, and pH of Tire Pyrolysis Oil. International Journal of Chemical Engineering, 2023: 1–6. DOI: 10.1155/2023/7730676

Toumi A, Politaeva NA. 2021. Impact of the nitrate concentration on the biomass growth and the fatty acid profiles of microalgae *Chlorella sorokiniana*. IOP Conf Ser: Earth Environ Sci 689 (1): 012026. DOI: 10.1088/1755-1315/689/1/012026.

Widyaningrum D, Prianto AD. 2021. Chlorella as a Source of Functional Food Ingredients: Short review. IOP Conference Series: Earth and Environmental Science, 794 (1): 012148. DOI: 10.1088/1755-1315/794/1/012148

Xue C, Gao K, Qian P, Dong J, Gao Z, Liu Q, Chen B, Deng X. 2021. Cultivation of *Chlorella sorokiniana* in a bubble-column bioreactor coupled with cooking cocoon wastewater treatment: Effects of initial cell density and aeration rate. Water Sci Technol 83 (11): 2615-2628. DOI: 10.2166/wst.2021.154.

Yun HS, Kim YS, Yoon HS. 2020. Characterization of *Chlorella sorokiniana* and *Chlorella vulgaris* fatty acid components under a wide range of light intensity and growth temperature for their use as biological resources. Heliyon 6 (7): e04447. DOI: 10.1016/j.heliyon.2020.e04447.

Ziganshina EE, Bulynina SS, Ziganshin AM. 2022. Growth characteristics of *Chlorella sorokiniana* in a photobioreactor during the utilization of different forms of nitrogen at various temperatures. Plants 11 (8): 1086. DOI: 10.3390/plants11081086.

NUSANTARA BIOSCIENCE
Vol. 17, No. 2, pp. 235-242
November 2025

ISSN: 2087-3948
E-ISSN: 2087-3956
DOI: 10.13057/nusbiosci/n170206

Effect of temperature on rice (*Oryza sativa*) seedling disease incidence and severity in Bangladesh

MD. TANBIR RUBAYET[1,♥], FARHANA PRODHAN[2], MD. ABDULLAH AL MAMUN[3], MD. ABDUL KADER[1], MD. MOTAHER HOSSAIN[1], MD. MAHIDUL ISLAM MASUM[1], MUHAMMAD ZIAUL HOQUE[4], MD. MIZANUR RAHMAN[5], JATISH CHANDRA BISWAS[6]

[1]Department of Plant Pathology, Faculty of Agriculture, Gazipur Agricultural University. Gazipur 1706, Bangladesh.
Tel.: +88-02-9205310-14 Ext. 2409, ♥email: tanbir86plp@gmail.com
[2]Department of Agronomy, Faculty of Agriculture, Bangladesh Agricultural University. Mymensingh 2202, Bangladesh
[3]Department of Agronomy, Faculty of Agriculture, Gazipur Agricultural University. Gazipur 1706, Bangladesh
[4]Department of Agricultural Extension & Rural Development, Faculty of Agriculture, Gazipur Agricultural University. Gazipur 1706, Bangladesh
[5]Department of Soil Science, Faculty of Agriculture, Gazipur Agricultural University. Gazipur 1706, Bangladesh
[6]Krishi Gobeshona Foundation. Dhaka 1215, Bangladesh

Manuscript received: 8 June 2025. Revision accepted: 3 October 2025.

Abstract. *Rubayet MT, Prodhan F, Mamun MAA, Kader MA, Hossain MM, Masum MMI, Hoque MZ, Rahman MM, Biswas JC. 2025. Effect of temperature on rice (*Oryza sativa*) seedling disease incidence and severity in Bangladesh. Nusantara Bioscience 17: 235-242.* Seedling diseases are strongly influenced by temperature and cultivation environment, posing serious challenges to rice production under changing climates. To investigate these effects, two simultaneous experiments were conducted in Bangladesh, at Rangpur (25.6962°N, 89.2676°E) and Gazipur (24.0361°N, 90.3963°E) using BRRI dhan28 and BRRI dhan29 under open-field and polythene-covered conditions. Seedling emergence was consistently higher in polythene-covered plots, suggesting improved establishment in warmer microclimates. Three major diseases were detected across sites: bakanae (*Fusarium moniliforme*), blast (*Pyricularia oryzae*), and brown spot (*Bipolaris oryzae*). Varietal and environmental interactions were evident, with BRRI dhan29 showing greater susceptibility to bakanae in open-field conditions, while BRRI dhan28 was more prone to blast. Brown spot severity showed no significant differences between locations, indicating a lesser influence of variety and microclimate. Physiological observations revealed that healthy seedlings exhibited higher chlorophyll content (Soil Plant Analysis Development/SPAD values), whereas bakanae-infected seedlings displayed abnormal elongation relative to healthy plants. These results demonstrate that temperature and cultivation environment exert significant effects on rice seedling health, and that varietal responses differ according to disease type. Findings underscore the need for integrating varietal resistance and environment-specific management strategies to mitigate seedling disease risks in the context of climate change.

Keywords: Bakanae, blast, brown spot disease, climate change

INTRODUCTION

Rice cultivation is presently and will continue to play a vital role in feeding the world's population. It is the primary dietary energy source in 17 Asian and Pacific nations, 9 North and South American countries, and 8 African countries (Priya et al. 2019). However, rice production, like other agricultural outputs, has been significantly influenced by climate change and may face even greater threats soon (Gornall et al. 2010). As the global demand for rice continues to grow, its resilience to environmental changes becomes even more crucial. Climate change is considered the greatest menace to humanity, as agriculture is highly sensitive to shifts in climatic factors. During the last century, the average global temperature has risen by 0.74°C (Gautam et al. 2013). This warming trend is expected to accelerate, causing shifts in agricultural production patterns (Wachira et al. 2021). The increase is largely attributed to greenhouse gases such as carbon dioxide, methane, nitrous oxide, and chlorofluorocarbons, with CO_2 being the major driver of global warming (Nunes 2023). According to the Intergovernmental Panel on Climate Change, global mean temperature may increase by 0.9-3.5°C by 2100 if current emission trends continue (Haq et al. 2010). These changes profoundly affect crop development and yield, as well as the reproduction, spread, and severity of many plant diseases (Gautam et al. 2013). For instance, sheath blight (*Rhizoctonia solani* J.G.Kühn), once a minor disease in the early 1970s, has now become a major rice disease. This change in disease patterns has led to significant yield losses in several rice-producing regions. Similar shifts in the occurrence and severity of numerous other diseases and insect pests have also been reported (Haq et al. 2010). Moreover, elevated temperature and CO_2 concentrations pose heightened risks of late blight (*Phytophthora infestans* (Mont.) de Bary) in potato, and serious rice diseases such as blast (*Pyricularia oryzae* Cavara) and sheath blight (*R. solani*) (Kobayashi et al. 2006; Gautam et al. 2013; Rubayet and Hossain 2024).

Despite this growing concern, limited studies have investigated how changing temperature regimes influence rice seedling diseases in Bangladesh, where rice is not only

the staple food but also central to food security and livelihoods (Lahlali et al. 2024). Seedling diseases are particularly critical because they can substantially reduce crop establishment, leading to downstream effects on yield. In Bangladesh, where rice farming is vital for the economy, understanding these early-stage diseases could help mitigate their impact on food production. With an increasing risk of unpredictable weather patterns, understanding how environmental temperature fluctuations affect disease dynamics at the early stages of crop growth is essential. Understanding how ambient temperature fluctuations affect the incidence and severity of diseases such as bakanae, blast, and brown spot at the seedling stage is therefore essential (Hue et al. 2025). This insight could lead to the development of predictive models, helping farmers make informed decisions on disease management. This knowledge will sharpen our ability to predict disease outbreaks under field conditions and to develop timely, location-specific management strategies. It will also provide the foundation for building more resilient rice varieties that can withstand the pressures of climate change, ultimately contributing to food security in the long term. Keeping this view, the present study was undertaken to assess the impact of ambient temperature on rice seedling disease incidence, severity under open and polythene-covered environments in two major rice-growing regions of Bangladesh.

MATERIALS AND METHODS

Two experiments were conducted at Rangpur and Gazipur (Figure 1), Bangladesh during 2021-2022 for assessment of the temperature impact on disease incidence and severity on rice seedlings. Two popular varieties of rice such as BRRI dhan28 and 29 were collected from the Bangladesh Rice Research Institute. After that land was prepared according to the agronomic practices and made 1 square meter size 12 plots. Whereas 3 plots open (P0) and 3 plots sealed with transparent white polythene sheet (P1) for BRRI dhan28 (V1). The rest of the plots were prepared in the same way for V2 (BRRI dhan29). A small hole was kept in both varieties for gas exchange purposes (Figure 2). The intercultural operations were done whenever it was necessary. These varieties were selected because BRRI dhan28 and BRRI dhan29 are among the most widely cultivated rice types in Bangladesh and differ in their responses to climatic stressors. The polythene-covered treatment simulates microclimate modification practices increasingly used to mitigate temperature extremes.

Treatments

The experiment consisted of four treatments: BRRI dhan28 grown under open field conditions (V1P0), BRRI dhan28 covered with a white transparent polythene sheet (V1P1), BRRI dhan29 grown under open field conditions (V2P0), and BRRI dhan29 covered with a white transparent polythene sheet (V2P1). Each treatment was replicated three times and laid out in a Randomized Complete Block Design (RCBD) to minimize the effects of environmental variability. The seedbed was monitored for seedling emergence, disease incidence, and severity over a period of 40 days after sowing.

Data recording

The data were collected on disease symptoms, incidence, and severity in both locations. In the meantime, the weather data were also recorded by using digital thermometer during the whole period. The natural disease infestation was confirmed by symptom study according to the standard procedure (Barnett and Hunter 1972; Mian 1995). After that, 10 seedlings from each plot were uprooted randomly for assessment of every individual disease incidence and severity. The bakanae disease was graded 0-4 scale (Ooi 2002; Zainudin et al. 2008). On the other hand, brown spot and blast were scored on a 0-9 scale (IRRI 2002, 2013) (Table 1).

Figure 2. A. Open filed, B. Polythene sheet covered plot

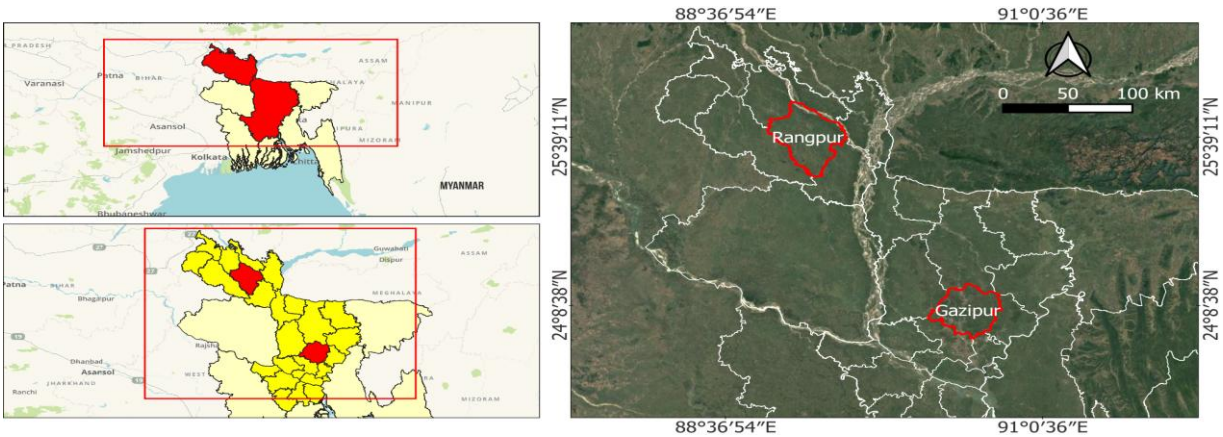

Figure 1. Location of the experimental sites in Rangpur and Gazipur, Rangpur and Dhaka Division, Bangladesh

Table 1. Bakanae, blast and brown spot disease scoring of rice seedling

Disease scale	Bakanae disease symptom	Blast disease symptom	Brown spot infection rate (%)
0	No infection	No infection	No infection
1	Normal growth but leaves beginning to show yellowish–green	Small brown specks of pinpoint size or larger brown specks without sporulating	<1
2	Abnormal growth, elongated, thin and yellowish-green leaves; seedlings also shorter or taller than normal	Small roundish to slightly elongated, necrotic gray spots, about 1-2 mm in diameter, with a distinct brown margin	1-3
3	Abnormal growth, elongated; chlorotic, thin and brownish leaves; seedlings also shorter or taller than normal	Lesions type is same as in scale 2, but a significant number of lesions on upper leaf area	4-5
4	Seedlings with fungal mass on the surface of infected plants or died	Eye-shaped lesions, >3 mm infecting < 4 % of leaf area	6-10
5		Leaf area infecting 4-10%	11-15
6		Leaf area infecting 11-25%	16-25
7		Leaf area infecting 26-50%	26-50
8		Leaf area infecting 51-75% and many leaves are dead	51-75
9		> 75% leaf area affected	76-100

Finally, the Disease Incidence (DI), and Percent Disease Index (PDI) were calculated by the following formulas (Rahman et al. 2013).

DI = (No. of infected plants/ Total No. of plants assessed) × 100

PDI = [Summation of all ratings/ {Total No. of rating × Max. disease grade (4)}] × 100

Data analysis

The recorded data were summarised using mean values and standard errors across replications. Disease incidence and severity were calculated as percentages based on the number of affected seedlings relative to the total seedlings observed. The results were compared descriptively across treatments and locations to highlight varietal and environmental differences.

RESULTS AND DISCUSSION

The digital thermometer was used for taking maximum and minimum temperatures in the open field and closed environments separately. The average maximum and minimum temperatures were higher in the polythene wrapped plots in both locations. But the temperature was significantly different between two selected locations (Figure 3). The present study showed that temperature strongly influenced the incidence and severity of bakanae, blast, and brown spot diseases at the seedling stage (Lahlali et al. 2024; Hue et al. 2025). Higher temperatures in polythene-covered plots favored seedling emergence but also created conditions that altered disease pressure. Bakanae was more severe in BRRI dhan29 under open conditions, which is consistent with reports from Bangladesh where warmer, drier seedbeds enhance *Fusarium* infection. By contrast, BRRI dhan28 was more susceptible to blast, aligning with previous studies in Asian rice systems where elevated temperatures and humidity favored *Pyricularia* outbreaks (Góría et al. 2013; Nazifa et al. 2021). Brown spot severity did not differ significantly between locations, indicating that this disease may be less sensitive to short-term temperature fluctuations. The use of polythene sheets, while beneficial for seedling emergence, may unintentionally modify microclimate conditions that influence disease dynamics, which has important implications for farmer practices under changing climate scenarios.

Effect of temperature on seed emergence of rice

Percent of seed emergence was slightly higher in Gazipur compared to Rangpur considering open and closed conditions. The maximum 96% emergence was found in BRRI dhan29 at Gazipur and 95.33% at Rangpur under polythene-wrapped plot (Table 2).

An intriguing element of plant growth is the impact of ambient temperature on seed germination and seedling emergence. These crucial phases of a plant's life cycle are greatly influenced by the temperature of the surrounding environment. The process through which a dormant seed develops into a seedling that is actively developing is known as seed germination. An important aspect of starting and controlling this process is ambient temperature. For proper germination, several plant species have different temperature needs. While some seedlings prefer lower temperatures, others need warmth. These temperature preferences are frequently linked to the variety's native environment and adaptations. The right temperature promotes enzymatic activity, metabolic functions, and water uptake all of which are necessary to start and maintain germination. Extreme temperatures, either too hot or too low, can, nevertheless, impair seedling vigor and germination rates. Seedlings emerge from the earth once the germination process has started and start their path to becoming adult plants. This fragile growing stage is still impacted by ambient temperature. To sustain cellular respiration and metabolic processes, which help seedlings acclimate to their surroundings, sufficient temperature is required. While extreme heat can cause stress and harm, cooler temperatures can decrease the rate of development. Additionally, environmental temperature affects how quickly

seedlings grow and emerge. Warmer conditions often encourage quicker development, but cooler conditions might impede or delay the emerging process (Yang et al. 2022; Liu et al. 2025; Mishra et al. 2025)

Effect of temperature on bakanae disease of rice

Bakanae is caused by *Fusarium moniliforme* J.Sheld. (Sexual stage: *Gibberella fujikuroi* (Sawada) Wollenw., 1931). The diseased seedlings were much taller, slender compared to healthy seedlings and detected easily by their tall pale green leaves (Figure 4). Additionally, the infected seedlings became chlorotic and crown rot. Older leaves exhibited abnormal elongation and produced adventitious root from the first nodes above the ground level. BRRI dhan28 was infected by 39.67% bakanae disease and BRRI dhan29 by 55.56% in Rangpur under open field environment. There was around 10-15% disease that appeared in Gazipur under the same condition. Despite there being no disease found in sealed plot at Gazipur but 14-40% prevailed at Rangpur (Table 3).

Table 2. Effect of temperature on rice seed emergence at Rangpur and Gazipur in Bangladesh

Treatments	% emergence	
	Rangpur	Gazipur
V1P0	77.33	81.67
V1P1	94.33	96.00
V2P0	76.33	76.67
V2P1	95.33	96.00

Table 3. Bakanae disease incidence and severity at Rangpur and Gazipur in Bangladesh

Treatments	% disease incidence	
	Rangpur	Gazipur
V1P0	36.67	11.11
V1P1	14.44	0.00
V2P0	55.56	15.56
V2P1	40.00	0.00

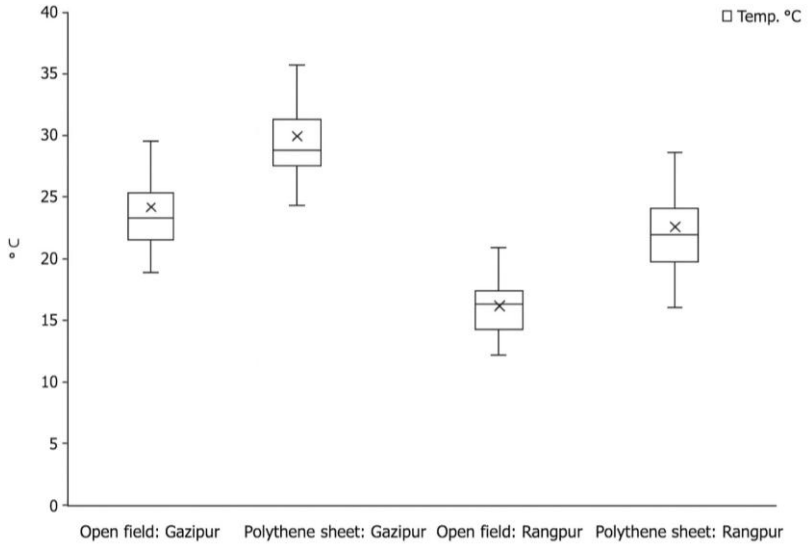

Figure 3. Temperature records at Rangpur and Gazipur in Bangladesh, under open field and polythene-covered conditions. Values represent the mean ± standard error of three replications

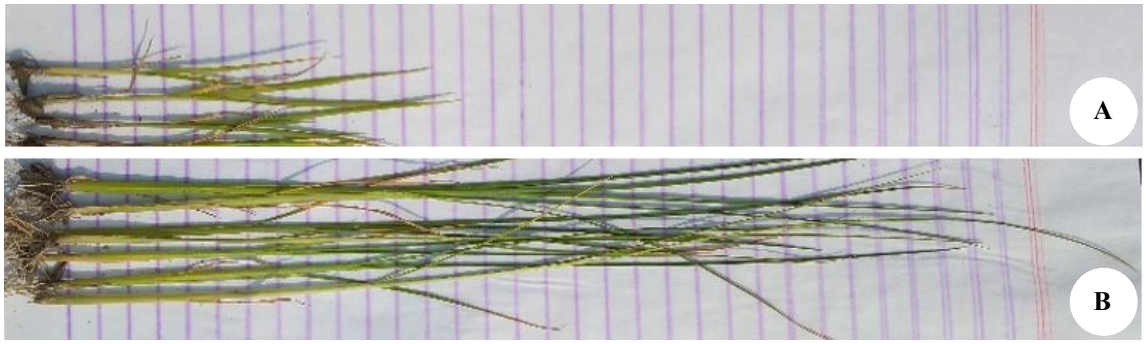

Figure 4. Bakanae disease symptom of rice: A. Healthy and B. Diseased seedlings

The Soil Plant Analysis Development (SPAD) value between healthy and bakanae infected plants at Rangpur and Gazipur were statistically significant difference. Infected seedling chlorophyll content was drastically dwindled as opposed to healthy seedling (Figure 5). In the meantime, the height of the seedling was shown fully reverse figure in both locations and conditions (Figure 6). The are many predisposing factors such as high temperature (around 35°C) and excess nitrogenous fertilizer for bakanae disease incidence and severity in seedbed and main field. The optimum temperature for symptom development of bakanae disease is affected by 35ºC and asymptom >20ºC (Hino and Furuta 1968; Takeuchi 1972). But application of excess nitrogen fertilizer and 30-35°C is optimum environmental condition for bakanae disease severity in Bangladesh (Asmaul et al. 2020).

Effect of temperature on blast disease of rice

Blast rice is one of the most devastating diseases across the globe, which is caused by *P. oryzae* (Sexual stage: *Magnaporthe oryzae*). The prominent symptom of the seedling appears on the leaf. During the experiment in both locations and conditions, typically reddish brown with grey or whitish center eye-shaped lesion was found in all treatment expect closed conditions at Rangpur. Numerous spots were coalesced and caused death of the leaf (Figure 7). The highest disease incidences 53.33 and 20% were recorded in V1P0 and V2P0, respectively Rangpur. Under the same condition below 30% disease infestation was found at Gazipur (Table 4). There was no positive interaction between host and pathogen in case of V1P1 and V2P1 at Gazipur. The SPAD value in healthy seedling was more than 3 folds higher at Rangpur and above 20 times at Gazipur (Figure 8). The effect of temperature could play a substantial role in rice blast incidence. According to the Rajput et al. (2017) the range of blast disease infection is 22-32°C and optimum temperature is 27°C.

Table 4. Blast disease incidence and severity at Rangpur and Gazipur in Bangladesh

Treatments	% disease incidence	
	Rangpur	Gazipur
V1P0	53.33	30.00
V1P1	46.67	0.00
V2P0	33.33	13.33
V2P1	16.67	0.00

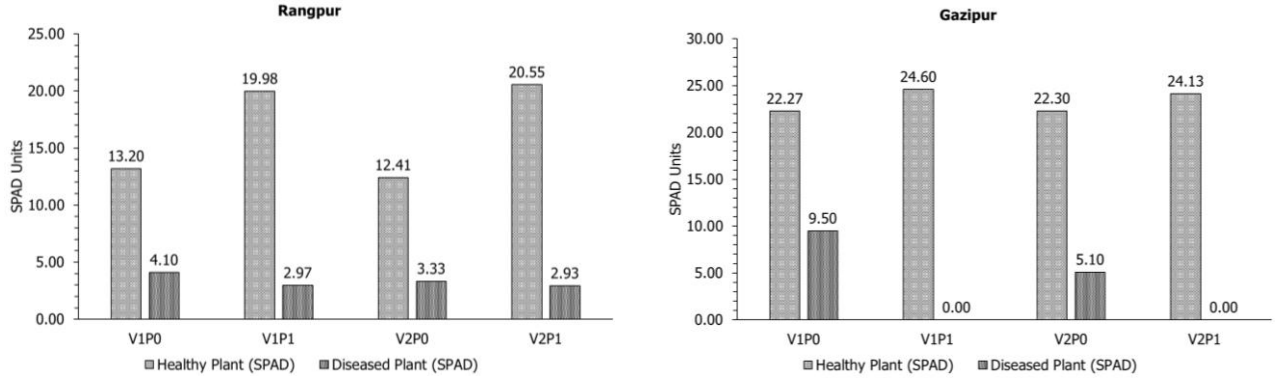

Figure 5. Correlation of Soil Plant Analysis Development (SPAD) value between healthy and bakanae infected seedlings at Rangpur and Gazipur in Bangladesh

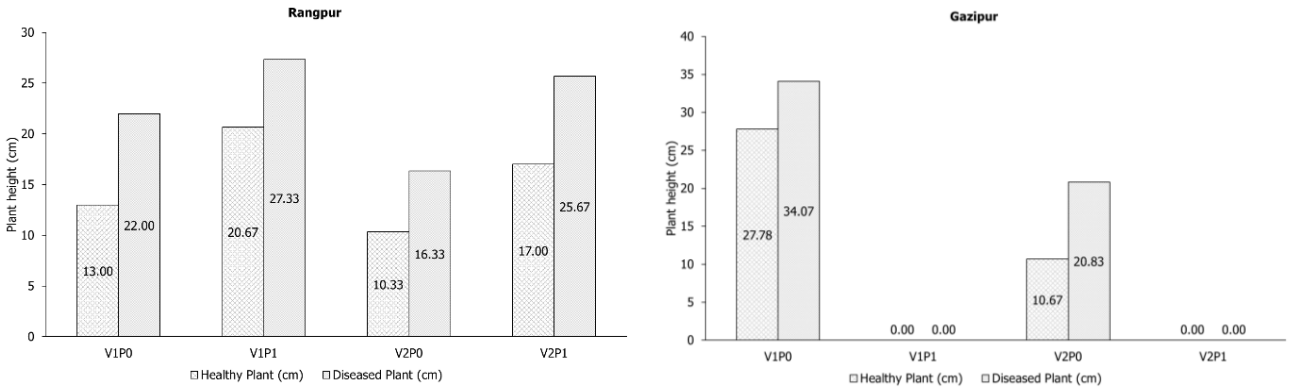

Figure 6. Difference between heathy and bakanae infected seedling height at Rangpur and Gazipur in Bangladesh

Figure 7. Blast disease symptom of rice

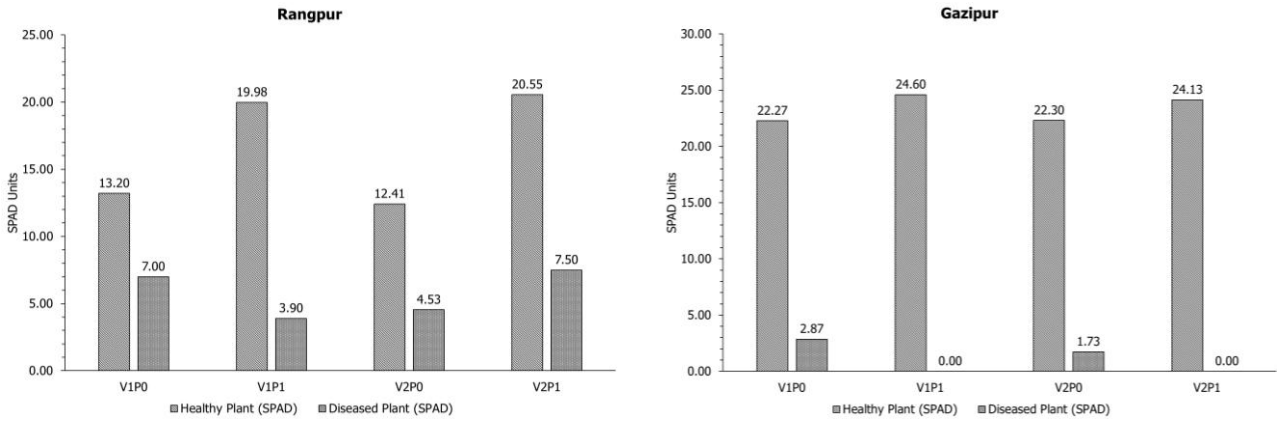

Figure 8. Correlation of Soil Plant Analysis Development (SPAD) value between healthy and blast infected seedlings at Rangpur and Gazipur in Bangladesh

Effect of temperature on brown spot disease of rice

Brown spot is *Bipolaris oryzae* (Breda de Haan) Shoemaker (Sexual stage: *Cochliobolus miyabeanus*). The seedling was infected by the pathogen and developed cylindrical or oval, dark brown with yellow halo circular spot on the leaf surface. Several spots were coalesced and the leaf dried up (Figure 9). The disease incidence was the highest 60% at Rangpur in the V1P0 plot and around 14% less in Gazipur. In V2P0, brown spot disease infestation rate was 36.67% and one-third, respectively at Rangpur and Gazipur. But at Gazipur, there was no disease found under the polythene covered plots (Table 5). The SPAD value difference between infected and healthy seedling was 0.53-20.55 at Rangpur and 0.00-24.60 at Gazipur (Figure 10). The favorable environment for brown spots is 24 to 30°C temperature and >92.5% humidity, leaf wetness (Picco and Rodolfi 2002).

Effect of temperature on PDI of bakanae, blast, and brown spot of rice seedlings

The effect of temperature was prominent on bakanae, blast, and brown spot disease severity on rice seedlings at Rangpur and Gazipur. Between these two locations, Rangpur was the most congenial for pathogen growth, development, and spreading during the whole period. As a result, disease severity was higher in case of both varieties as well as both conditions. But the disease severity was null under the closed environment at Gazipur (Figure 11). Among the three diseases at two locations, the maximum around 75% and minimum around 15% seedling of BRRI dhan28 infected by blast at Rangpur under open field and polythene covered plots, respectively. Similarly, the maximum >65% disease seedling of BRRI dhan28 infected by brown spot at Gazipur under open field. There were no diseases under the polythene that covered plots in both varieties at Gazipur.

Table 5. Brown spot disease incidence and severity at Rangpur and Gazipur in Bangladesh

Treatments	% disease incidence	
	Rangpur	Gazipur
V1P0	60.00	46.67
V1P1	13.33	0.00
V2P0	36.67	13.33
V2P1	16.67	0.00

Figure 9. Brown spot disease symptom of rice

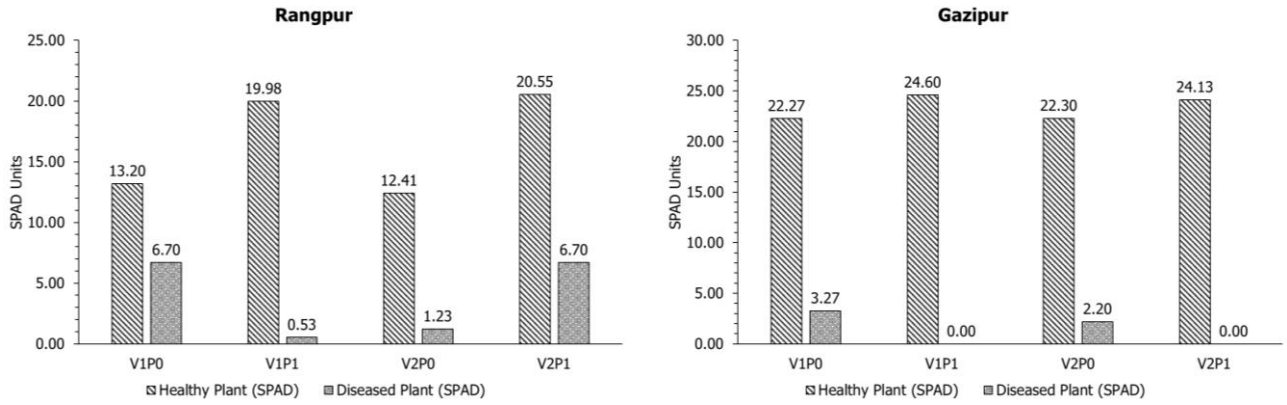

Figure 10. Correlation of Soil Plant Analysis Development (SPAD) value between healthy and brown spot infected seedlings at Rangpur and Gazipur in Bangladesh

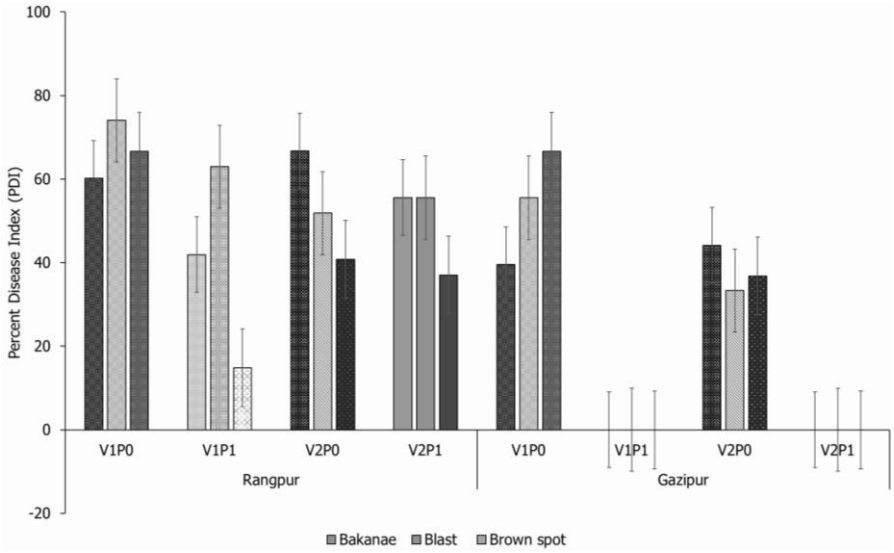

Figure 11. The severity of rice diseases under open and closed environmental conditions at Rangpur and Gazipur in Bangladesh

In conclusion, this study demonstrated that temperature and cultivation environment significantly influence the incidence and severity of rice seedling diseases. BRRI dhan29 was more susceptible to bakanae in open-field conditions at Rangpur, while BRRI dhan28 was more prone to blast in the same environment. Brown spot occurred in both varieties, with moderate severity, but differences between sites were not significant. Polythene covering enhanced seedling emergence but also modified the microclimate in ways that affected disease development. These findings highlight the importance of adjusting seedbed management practices in Bangladesh to minimize disease risk. For

bakanae-prone areas, especially when cultivating BRRI dhan29, the use of covered seedbeds, fungicide treatment, or tolerant varieties is advisable. For blast-susceptible BRRI dhan28, integrated strategies including resistant cultivars, regular monitoring, and fungicide application may be required. As the study was limited to one season, further multi-season and multi-location trials are recommended to confirm these outcomes.

ACKNOWLEDGEMENTS

The authors would like to express their sincere appreciation to the Modeling Climate Change Impact on Bangladesh Agriculture (MCCA) project of the Krishi Gobeshona Foundation (KGF), Dhaka 1215, Bangladesh, for providing financial support to conduct this research. The authors also gratefully acknowledge Gazipur Agricultural University and the Bangladesh Rice Research Institute, Regional Station, Rangpur, for their kind assistance, logistical support, and research facilities.

REFERENCES

Asmaul H, Asaduzzaman MM, Nor NMIM. 2020. Rice bakanae disease: An emerging threat to rice production in Bangladesh. Asian J Med Biol Res 6 (4): 646-652. DOI: 10.3329/ajmbr.v6i4.51224.

Barnett HL, Hunter BB. 1972. Illustrated Genera of Imperfect Fungi (3rd ed.). Burgess Publishing Company, Minneapolis.

Gautam HR, Bhardwaj ML, Kumar R. 2013. Climate change and its impact on plant diseases. Curr Sci 105 (12): 1685-1691.

Gória MM, Ghini R, Bettiol W. 2013. Elevated atmospheric CO_2 concentration increases rice blast severity. Trop Plant Pathol 38 (3): 253-257. DOI: 10.1590/S1982-56762013005000010.

Gornall J, Betts R, Burke E, Clark R, Camp J, Willett K, Wiltshire A. 2010. Implications of climate change for agricultural productivity in the early twenty-first century. Philos Trans R Soc Lond B Biol Sci 365 (1554): 2973-2989. DOI: 10.1098/rstb.2010.0158.

Haq M, Mia MT, Rabbi MF, Ali MA. 2010. Incidence and severity of rice diseases and insect pests in relation to climate change. In: Lal R, Sivakumar M, Faiz S, Rahman AM, Islam K (eds.). Climate Change and Food Security in South Asia. Springer, Dordrecht. DOI: 10.1007/978-90-481-9516-9_27.

Hino T, Furuta T. 1968. Studies on the control of bakanae disease of rice plants, caused by *Gibberella fujikuroi*. II. Influence of flowering season on rice plants and seed transmissibility through flower infection. Bull Chugoku Natl Agric Exp Sta E2: 96-110.

Hue Y, Kim JH, Nam Y, Choi B, Kim TS, Lee SJ, Kim KT. 2025. Changes in the occurrence patterns of rice fungal diseases due to climate change. Res Plant Dis 31 (1): 17-29. DOI: 10.5423/RPD.2025.31.1.17.

International Rice Research Institute (IRRI). 2002. Standard Evaluation System for Rice (4th ed., 56 pp.). IRRI.

International Rice Research Institute (IRRI). 2013. Standard Evaluation System for Rice (5th ed., 18 pp.). IRRI.

Kobayashi T, Ishiguro K, Nakajima T, Kim HY, Okada M, Kobayashi K. 2006. Effects of elevated atmospheric CO_2 concentration on the infection of rice blast and sheath blight. Phytopathology 96 (4): 425-431. DOI: 10.1094/PHYTO-96-0425.

Lahlali R, Taoussi M, Laasli S-E, Gachara G, Ezzouggari R, Belabess Z, Aberkani K, Assouguem A, Meddich A, El Jarroudi M, Barka EA. 2024. Effects of climate change on plant pathogens and host-pathogen interactions. Crop Environ 3 (3): 159–170. DOI: 10.1016/j.crope.2024.05.003.

Liu Z, Xu D, Wang R, Guo X, Song Y, Wang M, Cai Y. 2025. Effects of temperature fluctuations on the growth cycle of rice. Agriculture 15 (1): 99. DOI: 10.3390/agriculture15010099.

Mian IH. 1995. Methods in plant pathology (IPSA-JICA Project Publication No. 24). Institute of Postgraduate Studies in Agriculture.

Mishra V, Dixit S, Tyagi S, Venkateswarlu C, Paul PJ, Gurjar AKS, Dixit S, Sandhu N, Kurup S, Sinha P, Singh VK, Singh UM, Kumar A. 2025. Unveiling genetic basis of seedling emergence from deep soil depth under dry direct-seeded conditions in rice (*Oryza sativa* L.). Front Plant Sci 15: 1512234. DOI: 10.3389/fpls.2024.1512234.

Nazifa Z, Aminuzzaman FM, Akhter K, Rehena MK, Laila L. 2021. Survey on rice blast and morphological characterization of *Magnaporthe oryzae oryzae*. J Adv Microbiol 21 (1): 8-21. DOI: 10.9734/jamb/2021/v21i130315.

Nunes LJR. 2023. The rising threat of atmospheric CO_2: A review on the causes, impacts, and mitigation strategies. Environments 10 (4): 66. DOI: 10.3390/environments10040066.

Ooi KH. 2002. Pencirian dan Pengawalan Kimia *Fusarium oxysporum*, Penyebab Penyakit Layu Vascular pada Rosel. [PhD Thesis]. University Sains Malaysia, Pulau Pinang. [Malaysian]

Picco AM, Rodolfi M. 2002. *Pyricularia grisea* and *Bipolaris oryzae*: A preliminary study on the occurrence of airborne spores in a rice field. Aerobiologia 18: 163-167. DOI: 10.1023/A:1020654319130.

Priya TSR, Nelson ARLE, Ravichandran K, Antony U. 2019. Nutritional and functional properties of coloured rice varieties of South India: A review. J Ethn Food 6, 11. DOI: 10.1186/s42779-019-0017-3.

Rahman MM, Ali MA, Ahmad MU, Dey TK. 2013. Effect of tuber-borne inoculum of *Rhizoctonia solani* on the development of stem canker and black scurf of potato. Bangladesh J Plant Pathol 29 (1-2): 29-32.

Rajput LS, Sharma T, Madhusudhan P, Sinha P. 2017. Effect of temperature on growth and sporulation of rice leaf blast pathogen *Magnaporthe oryzae*. Intl J Curr Microbiol Appl Sci 6 (3): 394-401. DOI: 10.20546/ijcmas.2017.603.045.

Rubayet MT, Hossain MM. 2024. Climate change and its impacts on disease dynamics in major cereal crops. In: Rahman MM, Biswas JC, Meena RS (eds.). Climate Change and Soil-Water-Plant Nexus. Springer, Singapore. DOI: 10.1007/978-981-97-6635-2_9.

Takeuchi S. 1972. Climatic effect on seed infection of rice plant with bakanae disease and disinfection with organic mercury compounds. Proceed Kansai Plant Prot Soc 14: 14-19. DOI: 10.4165/kapps1958.14.0_14.

Wachira PW, Ndunda E, Sitati N.2021. Economic impacts of climate change on livestock and crop returns in the coastal region of Kenya. Indo Pac J Ocean Life 5: 74-82. DOI: 10.13057/oceanlife/o050204.

Yang W, Xu D, Li S, Tang X, Pan S, Chen X, Mo Z. 2022. Emergence and seedling establishment of rice varieties at different sowing depths. J Plant Growth Regul 41: 1672-1686. DOI: 10.1007/s00344-021-10408-0.

Zainudin NAIM, Razak AA, Salleh B. 2008. Bakanae disease of rice in Malaysia and Indonesia: Etiology of the causal agent based on morphological, physiological and pathogenicity characteristics. J Plant Prot Res 48 (4): 475-485. DOI: 10.2478/v10045-008-0056-z.

NUSANTARA BIOSCIENCE
Vol. 17, No. 2, pp. 243-252
November 2025

ISSN: 2087-3948
E-ISSN: 2087-3956
DOI: 10.13057/nusbiosci/n170207

Effect of light and media composition on growth and stomatal density of *Phalaenopsis amboinensis*

MUHAMMAD ALANWARI NUGRAHA[1,♥], DWI MURTI PUSPITANINGTYAS[2,♥♥], HARYANTO[1]

[1]Department of Biotechnology, Faculty of Sains and Technology, Universitas Muhammadiyah Bandung. Jl. Soekarno - Hatta No. 752, Bandung 40614, West Java, Indonesia. Tel./fax.: +62-89605747904, ♥email: muhammadalanwarinugraha@gmail.com

[2]Research Center for Applied Botany, National Research and Innovation Agency. Jl. Raya Jakarta-Bogor KM 46, Bogor 16911, West Java, Indonesia. ♥♥email: puspitakrb@gmail.com

Manuscript received: 22 May 2025. Revision accepted: 29 October 2025.

Abstract. *Nugraha MA, Puspitaningtyas DM, Haryanto. 2025. Effect of light and media composition on growth and stomatal density of* Phalaenopsis amboinensis. *Nusantara Bioscience 17: 243-252. Phalaenopsis amboinensis* J.J.Sm. is an endangered orchid species endemic to Indonesia, valued for both its conservation significance and horticultural potential. However, limited natural populations and slow propagation rates hinder sustainable conservation efforts. This study investigated the combined effects of culture media composition and light conditions on the *in vitro* growth, chlorophyll content, and stomatal density of *P. amboinensis* plantlets. A factorial experiment was conducted using nine media formulations under light and dark conditions. Significant interactions between media and light treatments were observed across all measured parameters ($p < 0.05$). The KC EO2 medium, containing 2 g/L KC, 40 g/L potato (*Solanum tuberosum* L.) extract, 2 g/L peptone, and MS vitamins under light, produced the most vigorous vegetative growth (5.40 ± 2.50 leaves, 1.44 ± 0.31 cm leaf length, 2.00 ± 0.82 roots, and 1.89 ± 0.45 cm root length). In contrast, the KC EO3 medium with 2 g/L KC, 150 g/L mung bean sprout (*Vigna radiata* (L.) R.Wilczek) extract, and 150 mL/L young coconut water (*Cocos nucifera* L.) under light yielded the highest chlorophyll a content (0.695 ± 0.113 mg/g fresh weight) and stomatal density (77.57 ± 2.72 stomata/mm²). Control plantlets cultured without organic supplements under dark conditions showed poor growth and negligible chlorophyll accumulation. These findings demonstrate that organic-enriched media, especially when combined with light exposure, significantly enhance physiological and morphological development *in vitro*. The optimized culture conditions offer a practical and scalable protocol for *ex situ* conservation and commercial propagation of *P. amboinensis*, supporting the preservation and sustainable use of this rare orchid species.

Keywords: Chlorophyll, *ex situ* conservation, *in vitro* culture, *Phalaenopsis amboinensis*, stomata, tissue culture media

INTRODUCTION

The Orchidaceae family is estimated to comprise over 28,000 species across 760 genera, making it one of the two largest angiosperm families worldwide and accounting for approximately 10% of the global floriculture trade value in potted plants and cut flowers (Singh 2020; Wei et al. 2025). The remarkable diversity in flower morphology, coloration, and vase life establishes orchids as high-value ornamental commodities and subjects for ecophysiological research, particularly due to their unique survival strategies, including epiphytism and morphophysiological adaptations to low light conditions in tropical forests (Zhang et al. 2018). Epiphytic orchids exhibit various structural modifications, such as velamen, aerial roots, and specialized stomata, that enable survival in water and light-limited environments.

Phalaenopsis amboinensis J.J.Sm., endemic to Moluccas Island and Sulawesi, is listed as a protected species under Indonesian Government Regulation No. 7/1999. Its population continues to decline due to illegal harvesting and limitations of conventional propagation methods, necessitating urgent conservation and mass propagation efforts (Machmudi et al. 2019; Utami and Haryanto 2019). Beyond ecological value, *P. amboinensis* holds genetic significance as a donor of yellow pigmentation in modern *Phalaenopsis* Blume breeding programs, particularly for developing fragrant yellow cultivars demanded by global markets (Sevilleno et al. 2023). Conservation of this species is crucial not only for preserving local biodiversity but also for maintaining valuable genetic resources for sustainable horticulture industries.

In vitro tissue culture enables large-scale vegetative propagation under controlled conditions, shortens production cycles, and provides pathogen-free plantlets (Sawardekar et al. 2023; Guo et al. 2024). Medium efficacy depends not only on macro and micronutrients but can be enhanced with natural organic supplements like young coconut water (*Cocos nucifera* L.), mung bean sprout (*Vigna radiata* (L.) R.Wilczek) extract, and tomato (*Solanum lycopersicum* L.) extract as growth stimulants (George et al. 2008; Park et al. 2011; Apriliyani and Wahidah 2021). For instance, supplementation with 100 g L^{-1} banana extract significantly improved *Phalaenopsis amabilis* (L.) Blume seedling performance *in vitro* (Arum and Semiarti 2023), demonstrating the potential of natural organic compounds as growth enhancers. These organic compounds contain phytohormones (auxins and cytokinins), vitamins, and sugars to promote cell division and tissue differentiation.

Light serves dual roles as both a photosynthetic energy source and a morphogenic signal. Spectrum, intensity, and

photoperiod influence leaf development, chlorophyll synthesis, hormonal activity, and stomatal density. In certain orchids, specific red, blue LED combinations enhance protocorm-like body formation, while initial dark treatment accelerates root initiation (Cavallaro et al. 2022; Naderi et al. 2023). Previous studies on *Phalaenopsis* hybrids showed that 55% shading yielded peak photosynthetic pigment content and modified stomatal guard cell dimensions (Fauziah et al. 2022). Excessive light intensity may cause oxidative stress in young tissues, while insufficient light can inhibit chlorophyll synthesis and vegetative growth.

Although numerous studies have examined media or light factors separately, systematic investigations of media-light interactions specifically in *P. amboinensis* remain scarce, with current reports limited to germination optimization and protoplast isolation (Machmudi et al. 2019; Utami and Haryanto 2019). Therefore, an experimental approach combining both factors is essential for a comprehensive understanding of *P. amboinensis* morphophysiological responses.

Chlorophyll content and stomatal density in plantlet leaves serve as indicators of photosynthetic adaptation and gas exchange efficiency. Shading variations alter pigment levels and stomatal guard cell dimensions in *Phalaenopsis* hybrid plantlets (Fauziah et al. 2022), while other studies demonstrate increased stomatal density in coconut fiber media (Jyothsna and Srivastava 2023) with positive correlations to chlorophyll content and leaf physiological performance (Asyary et al. 2024). Integrative evaluation of these leaf physiological and anatomical responses can also serve as parameters for selecting superior genotypes adapted to specific growth conditions.

This study evaluates the combined effects of culture media with light and dark conditions on *P. amboinensis* plantlet growth, chlorophyll content, and stomatal density will addressing critical knowledge gaps and establishing a foundation for developing efficient propagation protocols supporting both conservation and premium planting material production. The research outcomes are expected to benefit not only *ex situ* conservation but also the development of orchid agribusiness at national and international scales.

MATERIALS AND METHODS

Media preparation

This study used *P. amboinensis* plantlets derived from *in vitro* seed germination, previously sub-cultured for four months on Knudson C (KC) medium. The plantlets selected for the experiment were 0.6-1.0 cm in length, possessed two leaves, and had not yet developed roots. A total of nine culture media with different organic supplement compositions were prepared (Table 1). All media contained 7.5 g/L agar, 1 g/L activated charcoal, and 15-20 g/L glucose. The organic components included young coconut water (*C. nucifera*), tomato (*S. lycopersicum*), potato (*Solanum tuberosum* L.), mung bean sprouts (*V. radiata*), peptone, MS vitamins (myo-inositol, nicotinic acid, pyridoxine-HCl, thiamine-HCl, glycine), and naphthaleneacetic acid (NAA). The media pH was adjusted to 5.7 before autoclave at 121°C for 20 minutes.

Experimental design

The experiment employed a completely randomized factorial design with two factors: (i) nine types of culture media; and (ii) two illumination conditions: 16 hours of light at 4000 lux and continuous dark. The dark treatment was achieved by placing culture bottles in a tightly sealed rack within the same growth chamber to ensure complete light exclusion. Each treatment combination consisted of five culture bottles, with each bottle containing two plantlets (n = 10 plantlets per treatment combination), resulting in a total of 180 plantlets. Cultures were maintained in a growth chamber at 25°C for 18 weeks.

Table 1. Recapitulation of media for the growth and physiological development of *Phalaenopsis amboinensis* orchid

Basal medium	Composition
WMO	Agar 7.5 g/L, sugar 20 g/L, charcoal 1 g/L
VW	Agar 7.5 g/L, sugar 20 g/L, charcoal 1 g/L, VW media 1.67 g/L
VW EO	Agar 7.5 g/L, sugar 20 g/L, charcoal 1 g/L, VW media 1.67 g/L tomato (*Solanum lycopersicum*) 100 g/L, mung bean sprouts (*Vigna radiata*) 100 g/L, coconut water (*Cocos nucifera*) 150 mL/L, NAA 5 ppm, thiamin 1 ppm
GM	Agar 7.5 g/L, sugar 20 g/L, charcoal 1 g/L, fertiliser Grow More 32-10-10 0,5g/L
GM EO	Agar 7.5 g/L, sugar 20 g/L, charcoal 1 g/L, fertilizer Grow More 32-10-10 0,5g/L potato (*Solanum tuberosum* L.) 40 g/L, peptone 2 g/L, KH2PO4 0.125 g/L, MS vitamins (Myo inositol 100 mg/L, nicotinacid, pyridoxine-HCL 0.5 mg/L, Thiamin HCl 0.4 mg/L, glicine 2 mg/L)
KC	Agar 7.5 g/L, sugar 20 g/L, charcoal 1 g/L, KC medium 2 g/L
KC EO 1	Agar 7.5 g, sugar 20 g/L, charcoal 1 g/L, KC media 2 g/L, tomato (*Solanum lycopersicum*) 100 g/L, mung bean sprouts (*Vigna radiata*) 100 g/L, young coconut water (*Cocos nucifera*) 150 mL/L.
KC EO 2	Agar 7.5 g/L, sugar 20 g/L, charcoal 1 g/L, KC medium 2 g/L, potato (*Solanum tuberosum*) 40 g/L, peptone 2 g/L, MS vitamins (Myo inositol 100 mg/L, nicotinacid, pyridoxine-HCL 0.5 mg/L, Thiamin HCl 0.4 mg/L, glicine 2 mg/L).
KC EO 3	Agar 7.5 g/L, sugar 20 g/L, charcoal 1 g/L, KC media 2 g/L, mung bean sprouts (*Vigna radiata*) 150 g/L, young coconut water (*Cocos nucifera*) 150 mL/L.

Note: EO: Enriched with organic supplements; WMO: Without basal medium and organic supplements. VW: Vacin & Went; KC: Knudson C; GM: Grow More

Growth measurement

Plantlet development was monitored every two weeks for a total of 18 weeks. Morphological data collected included the number of leaves, leaf length (cm), number of roots, and root length (cm). Measurements were made using a digital caliper, and the mean of each replicate was recorded. At the end of the culture period, samples were further analyzed for chlorophyll content and stomatal density.

Pigment analysis

Chlorophyll a and b contents were determined following a modified method from Mackinney (1941). Approximately 0.1 g of fresh leaf tissue was ground using a mortar and pestle in 5 mL of 96% ethanol. The extract was transferred into microtubes, vortexed briefly, and centrifuged at 8000 rpm for 15 minutes. Absorbance readings were taken at 665 nm and 649 nm using a Shimadzu UV-2600 spectrophotometer. Chlorophyll concentrations were calculated using the following formulas:

$$\text{Chlorophyll a (mg/g FW)} = 13.36 \times A665 - 5.19 \times A649$$

$$\text{Chlorophyll b (mg/g FW)} = 27.43 \times A649 - 8.12 \times A665$$

The results were expressed in milligrams of chlorophyll per gram of fresh weight (mg/g Fresh Weight).

Stomata observation

Stomatal density was measured on the abaxial surface of the second fully expanded leaf. A 1 × 2 cm strip of transparent adhesive tape was applied to the leaf surface, and the adaxial side was gently scraped using a sterile razor blade until the underlying tissue became translucent. The tape was then mounted on a microscope slide and observed under an Olympus U-TV0.5XC-3 light microscope at 400× magnification. Stomata were counted per microscopic field of view and converted into units of stomata per mm².

Data analysis

All quantitative data, including growth parameters, chlorophyll content, and stomatal density, were subjected to normality and homogeneity tests. When necessary, data were transformed to meet parametric assumptions. A two-way Analysis of Variance (ANOVA) was conducted at a 5% significance level ($\alpha = 0.05$) to evaluate the effects of media type and light condition, followed by Duncan's Multiple Range Test (DMRT) for post hoc comparison among treatment means. All statistical analyses were performed using SPSS version 21.

RESULTS AND DISCUSSION

Media and dark-light interaction on vegetative growth

The number of leaves

The analysis of variance results showed a significant interaction between media type and lighting conditions on the leaf count of *P. amboinensis* plantlets. Based on Table 4 and Figure 1, the KC EO 2 treatment under light conditions produced the highest leaf number (5.40 ± 2.50), which was statistically significantly different from most other treatment combinations. Conversely, the lowest leaf number was recorded in the VW EO treatment under dark conditions, with an average value of 2.40 ± 0.70 leaves. The KC EO 2 medium exhibited consistent leaf growth from week 6 to week 18. In contrast, plantlets in the VW EO treatment showed slow and stagnant leaf growth throughout the observation period. These findings confirm that the presence of complex organic compounds in the medium, along with bright lighting, plays a crucial role in stimulating the growth of vegetative leaf organs *in vitro*.

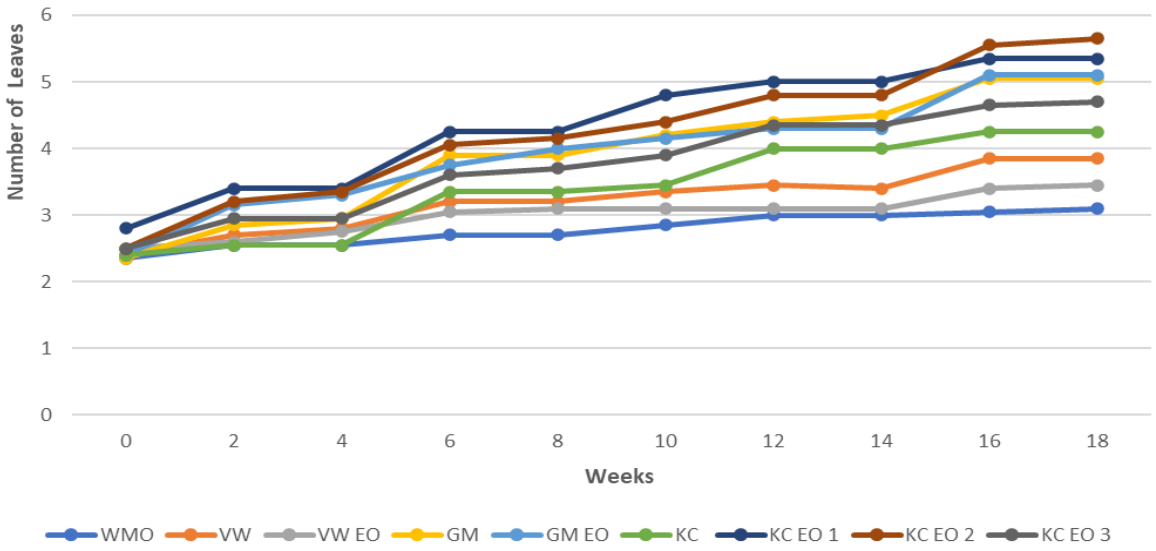

Figure 1. Leaf number of *Phalaenopsis amboinensis* under different culture media and light conditions over 18 weeks. Each data point represents the mean number of leaves recorded at two-week intervals from week 0 to week 18. Among all treatments, KC EO 2 medium under light conditions appeared to promote the highest leaf production throughout the culture period, as shown in the graph

Leaf length

The KC EO 2 treatment under light exposure produced the highest leaf length at 1.44 ± 0.31 cm, significantly different from most other treatments. The VW EO under dark conditions resulted in the lowest value at 0.49 ± 0.09 cm, indicating that the absence of lighting simultaneously significantly inhibited leaf elongation. Visual differences in leaf length were also observed in Figure 2, where plantlets in KC EO 2 medium (a) appeared to have longer leaves compared to those in VW EO medium (b). The leaf growth pattern generally accelerated from week 12 to week 18, particularly under light conditions. These results support the role of lighting and organic compounds in triggering the biosynthesis of growth hormones such as auxin and cytokinin, as well as cell expansion processes that promote leaf elongation during *in vitro* culture.

The number of roots

The highest average root number was found in the KC EO 2 light treatment with bright lighting at 2.00 ± 0.82, significantly different from most other treatments. Among all combinations, the VW EO under dark conditions produced the lowest average root number at 0.20 ± 0.63, indicating that complex organic compounds in the medium were ineffective without light support. Meanwhile, other treatments, such as KC EO 1 under light conditions, produced 2.40 ± 0.84 roots, and GM EO under dark conditions produced 2.10 ± 0.99 roots. They showed relatively high values but were not consistently superior across all replicates. The root growth pattern became evident from week 6, with significant increases between weeks 12 and 18, indicating that the active rooting phase occurred during the mid to late culture period.

Root length

The KC EO 2 under light conditions produced the highest root length in *P. amboinensis in vitro*, at 1.89 ± 0.45 cm, and was statistically significantly different from all treatments (Table 4). The relatively high results were statistically different from KC EO 2. VW EO in dark conditions produced the shortest root length at 0.10 ± 0.32 cm, indicating significant inhibition of root system growth. Generally, treatments with lighting tended to increase root length compared to dark conditions on the same medium, suggesting that light plays a crucial role not only in leaf formation but also in root elongation processes through the activation of physiological and hormonal pathways.

Chlorophyll content

Across all treatments, chlorophyll a content was consistently higher than chlorophyll b, indicating the dominant role of chlorophyll a in the photosynthetic reaction center. The best treatments were observed in the media KC EO 3 and KC EO 2 under light conditions, which produced chlorophyll a level of 0.695 ± 0.113 mg·g^{-1} and 0.641 ± 0.089 mg·g^{-1}, respectively. These two treatments were also the only ones showing detectable chlorophyll b content, albeit low, ranging from 0.000–0.002 mg·g^{-1}, which was still higher than all other treatments, where chlorophyll b was almost entirely zero. In contrast, the lowest chlorophyll content was recorded in the WMO under light conditions as control media under dark conditions, with chlorophyll a level of only 0.044 ± 0.001 mg·g^{-1} and no detectable chlorophyll b (Table 2).

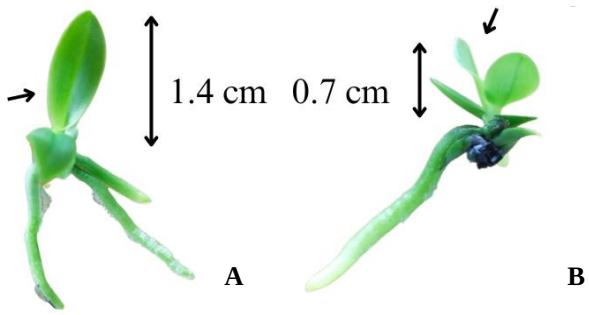

Figure 2. Comparison of leaf length in *Phalaenopsis amboinensis* planlets grown under different culture media: A. KC EO 2, showing longer leaves (1.4 cm); B. VW, showing shorter leaves (0.7 cm)

Table 2. Interaction of media modification and light-dark conditions on chlorophyll content of *Phalaenopsis amboinensis* orchid

Treatments		Chlorophyll content	
Conditions	**Media**	**Chlorophyll a (mg/g FW)**	**Chlorophyll b (mg/g FW)**
Light	KC EO 3	0.695 ± 0.113^{g}	0.000 ± 0.001^{a}
Dark	WMO	0.044 ± 0.001^{a}	0.000 ± 0.000^{a}

Note: Mean ± Standard Error (SE) followed by the same letter in the same column are not significantly different at the 5% level ($p \leq 0.05$) of the Duncan MRT. Only the highest and lowest values for each parameter are shown; the full dataset is provided in Table 3

Table 3. Effect of media modification and light and dark conditions on chlorophyll content of *Phalaenopsis amboinensis* orchid

Treatment		Chlorophyll content	
		Chlorophyll a (mg/g FW)	**Chlorophyll b (mg/g FW)**
Light	WMO	0.029 ± 0.001^{a}	0.000 ± 0.000^{a}
	VW	0.396 ± 0.012^{d}	0.000 ± 0.001^{a}
	VW EO	0.478 ± 0.049^{e}	0.000 ± 0.001^{a}
	GM	0.559 ± 0.024^{f}	0.001 ± 0.000^{a}
	GM EO	0.463 ± 0.004^{e}	0.000 ± 0.000^{a}
	KC	0.266 ± 0.011^{c}	0.000 ± 0.000^{a}
	KC EO 1	0.501 ± 0.024^{ef}	0.000 ± 0.001^{a}
	KC EO 2	0.641 ± 0.089^{g}	0.002 ± 0.003^{b}
	KC EO 3	0.695 ± 0.113^{g}	0.000 ± 0.001^{a}
Dark	WMO	0.044 ± 0.001^{a}	0.000 ± 0.000^{a}
	VW	0.062 ± 0.001^{a}	0.000 ± 0.000^{a}
	VW EO	0.083 ± 0.013^{ab}	0.000 ± 0.000^{a}
	GM	0.081 ± 0.002^{ab}	0.000 ± 0.000^{a}
	GM EO	0.057 ± 0.000^{a}	0.000 ± 0.000^{a}
	KC	0.065 ± 0.000^{ab}	0.000 ± 0.000^{a}
	KC EO 1	0.134 ± 0.012^{b}	0.000 ± 0.000^{a}
	KC EO 2	0.058 ± 0.005^{a}	0.000 ± 0.000^{a}
	KC EO 3	0.073 ± 0.000^{ab}	0.000 ± 0.000^{a}

Note: Numbers followed by the same letter in the same column are not significantly different at the 5% level ($P \leq 0.05$) of the Duncan MRT

Table 4. Effects of media modification and light-dark conditions on the growth of *Phalaenopsis amboinensis* orchid

Treatment		Parameters			
		Number of leaves (per plantlet)	Leaf length (cm)	Number of roots (unit)	Root length (cm)
Light	KC EO 2	5.40±2.50^{e}	1.44±0.31^{efgh}	2.00±0.82^{bc}	1.89±0.45^{c}
Dark	VW EO	2.40±0.70^{a}	0.49±0.09^{a}	0.20±0.63^{a}	0.10±0.32^{a}

Note: Mean ± Standard Error (SE) followed by the same letter in the same column are not significantly different at the 5% level ($p \leq 0.05$) of the Duncan MRT. Only the highest and lowest values for each parameter are shown; the full dataset is provided in Table 5

Table 5. Effects of media modification and light-dark conditions on the growth of *Phalaenopsis amboinensis* orchid

Treatment		Parameters			
		Number of leaves (Unit)	Leaf length (cm)	Number of roots (unit)	Root length (cm)
Light	WMO	3.10±1.20^{ab}	0.48±0.18^{a}	1.00±0.47^{ab}	1.63±1.39^{bc}
	VW	3.30±0.67^{abc}	0.67±0.35^{ab}	1.00±0.94^{ab}	1.04±0.93^{b}
	VW EO	4.60±2.01^{bcde}	0.74±0.20^{abc}	1.50±1.18^{bc}	1.11±0.66^{b}
	GM	5.00±3.94^{cde}	0.91±0.28^{bcd}	1.80±2.15^{bc}	1.01±1.00^{b}
	GM EO	5.30±1.49^{de}	1.05±0.35^{bcde}	1.90±0.74^{bc}	1.39±0.61^{bc}
	KC	3.60±0.84^{abcd}	0.98±0.34^{bcd}	1.80±1.48^{ab}	1.23±1.03^{bc}
	KC EO 1	4.60±0.84^{bcde}	1.02±0.26^{bcd}	2.40±0.84^{c}	1.39±0.42^{bc}
	KC EO 2	5.40±2.50^{e}	1.44±0.31^{efgh}	2.00±0.82^{bc}	1.89±0.45^{c}
	KC EO 3	5.30±2.31^{de}	1.11±0.59^{cdef}	2.00±1.56^{bc}	0.96±0.60^{b}
Dark	WMO	3.10±0.74^{ab}	0.89±0.43^{bcd}	1.10±0.32^{ab}	1.52±0.70^{bc}
	VW	4.40±1.17^{bcde}	1.49±0.71^{fgh}	2.00±0.94^{bc}	1.47±0.45^{bc}
	VW EO	2.40±0.70^{a}	0.49±0.09^{a}	0.20±0.63^{a}	0.10±0.32^{a}
	GM	5.10±0.88^{de}	1.23±0.46^{defg}	1.70±0.67^{bc}	1.50±0.40^{bc}
	GM EO	4.90±0.99^{cde}	1.60±0.37^{ghi}	2.10±0.99^{bc}	1.24±0.49^{bc}
	KC	4.90±1.20^{cde}	1.29±0.60^{defg}	1.60±1.35^{bc}	0.90±0.56^{b}
	KC EO 1	4.80±1.69^{bcde}	1.72±0.36^{hi}	1.40±0.52^{bc}	1.51±0.36^{bc}
	KC EO 2	5.90±2.13^{e}	1.62±0.33^{ghi}	2.10±1.37^{bc}	1.30±0.33^{bc}
	KC EO 3	5.40±1.17^{e}	1.96±0.65^{i}	1.60±0.52^{bc}	1.52±0.62^{bc}

Note: Numbers followed by the same letter in the same column are not significantly different at the 5% level ($P \leq 0.05$) of the Duncan MRT

Table 6. Effect of media modification and light and dark conditions on the stomatal density of *Phalaenopsis amboinensis* orchid

Treatments		Stomatal Density (stomata/mm²)
Conditions	Media	
Light	KC EO 3	77.57 ± 2.72^{e}
Dark	WMO	39.38 ± 1.66^{b}

Note: Mean ± Standard Error (SE) followed by the same letter in the same column are not significantly different at the 5% level ($p \leq 0.05$) of the Duncan MRT. Only the highest and lowest values for each parameter are shown; the full dataset is provided in Table 7

Table 7. Effect of media modification and light and dark conditions on stomatal density of *Phalaenopsis amboinensis* orchid

Parameters		Stomatal density
Conditions	Media	
Light	WMO	46.60 ± 3.28^{bc}
	VW	71.09 ± 2.69^{d}
	VW EO	77.48 ± 2.84^{e}
	GM	71.72 ± 1.41^{d}
	GM EO	77.12 ± 3.20^{e}
	KC	77.02 ± 3.28^{e}
	KC EO 1	75.20 ± 2.72^{e}
	KC EO 2	76.38 ± 3.73^{e}
	KC EO 3	77.57 ± 2.72^{e}
Dark	WMO	39.38 ± 1.66^{a}
	VW	45.96 ± 2.67^{bc}
	VW EO	44.95 ± 2.21^{b}
	GM	45.96 ± 1.50^{bc}
	GM EO	45.59 ± 1.97^{b}
	KC	45.23 ± 3.21^{b}
	KC EO 1	47.24 ± 3.05^{bc}
	KC EO 2	48.70 ± 2.90^{c}
	KC EO 3	45.59 ± 2.14^{b}

Note: Numbers followed by the same letter in the same column are not significantly different at the 5% level ($p \leq 0.05$) of the Duncan MRT

Stomatal density

The KC EO 3 and KC EO 2 under light conditions produced the highest stomatal density, at 77.57 ± 2.72 stomata/mm² and 76.38 ± 3.73 stomata/mm² (Table 6), respectively. Meanwhile, the lowest stomatal density was recorded in the WMO medium under dark conditions, at 39.38 ± 1.66 stomata/mm². In general, all light treatments showed an increase in stomatal density compared to dark conditions. Media with organic compounds under light conditions consistently produced stomatal density values >75 stomata/mm². This suggests that lighting stimulates stomatal development pathways through the activation of gene transcription, such as SPCH and the EPFL9 peptide, while organic compounds support optimal epidermal differentiation. In contrast, dark conditions inhibited this process, even in the same media. This pattern reinforces the synergistic role of light and nutrient composition in regulating the formation of anatomical structures critical for gas exchange and photosynthetic efficiency.

Discussion

Interaction of culture media in light and dark conditions on leaf number

In general, plantlets cultured under light conditions exhibited a higher leaf number compared to those in dark conditions on the same medium. This indicates that consistent lighting plays a crucial role in supporting shoot meristem activity and vegetative organ formation. Light acts as a primary environmental signal, triggering photomorphogenesis pathways through the activation of receptors such as phytochromes and cryptochromes (Dobisova et al. 2017). These pathways regulate the expression of various leaf development genes, including those involved in photosynthesis, chloroplast formation, and the regulation of growth hormones like auxin and cytokinin (Dobisova et al. 2017; Huq 2018). The presence of light also enables plantlets to perform limited photosynthesis, depending on chlorophyll and sugar availability, thus generating the energy and metabolites needed for leaf formation and elongation (Cavallaro et al. 2022; Saeedi et al. 2023).

On the other hand, media composition also significantly contributed to the increase in leaf number. The KC EO 2 medium under light treatment contains organic compounds such as coconut water (*C. nucifera*) and peptone, which showed the highest number of leaves. Coconut water (*C. nucifera*) is known to contain various bioactive substances, including natural cytokinin, amino acids, and phenolic compounds, which can enhance meristem activity and promote the formation of new shoots and leaves (Werner et al. 2003; Chickarmane et al. 2012). Cytokinin plays a role in stimulating cell division and tissue differentiation by regulating specific gene expression (Wu et al. 2021). Peptone, as an organic nitrogen source, supports growth by providing free amino acids required for protein biosynthesis (Fouda et al. 2024).

Previous studies on *Phalaenopsis* genus have shown that optimal lighting can enhance leaf size and number. Lee et al. (2017) reported that young *Phalaenopsis* exposed to warm white LED lighting produced longer and wider leaves compared to those grown under standard fluorescent lamps. Additionally, a study by Hamdeni et al. (2022) on *Dendrobium* orchids demonstrated that adding organic compounds such as coconut water, tomato juice, and banana to Knudson C medium significantly increased shoot and axillary leaf formation, highlighting the critical role of natural substances in supporting the vegetative phase.

The interaction between lighting and media composition appears to be synergistic. Light supports the activation of metabolic processes and basic photosynthesis, while organic compounds like coconut water (*C. nucifera*) and peptone enhance hormonal responses and provide essential nutrients. This combination creates an optimal environmental condition for leaf development. Thus, the increased leaf number under light treatment reflects the importance of an integrated approach in developing *in vitro* vegetative regeneration protocols, particularly for endemic species like *P. amboinensis*, which holds high conservation and commercial value.

Interaction of culture media in light and dark conditions on leaf length

Leaf length growth results from cell division and expansion activities in mesophyll tissue, which are heavily influenced by hormonal, media, and lighting factors. The medium under light conditions, as the most effective treatment, probably provided optimal physiological conditions through the synergy of organic supplements and lighting. Coconut water (*C. nucifera*) in this medium contains natural cytokinin and trace amounts of auxin, supporting initial cell division and tissue differentiation (Lazim et al. 2015). Cytokinins are known to enhance plant responses to light by increasing the sensitivity of photoreceptors such as phytochromes and cryptochromes (Prerostova et al. 2021), thereby optimizing leaf cell expansion under light exposure.

In addition to coconut water (*C. nucifera*), the presence of peptone as an organic nitrogen source supports protein synthesis required for cell expansion and elongation (Hwang et al. 2024). The combination of coconut water (*C. nucifera*) and fruit homogenates has been shown to enhance *in vitro* orchid growth, as reported by Utami and Hariyanto (2019), where VW medium supplemented with 15% coconut water (*C. nucifera*) and banana produced the longest leaves, 62.1 mm in *P. amboinensis*.

Light plays a crucial role in activating photomorphogenesis, including the differentiation of proplastids into active chloroplasts and enhancing photosynthetic activity. This process generates ATP and carbon assimilates needed for cell expansion (Dubreuil et al. 2018). Additionally, light stimulates the expression of growth-regulating genes such as HY5 and GLK1 and mediates gibberellin hormone pathways that induce the production of cell wall-loosening enzymes like expansins and XET (Sprangers et al. 2020). For example, in *Arabidopsis thaliana* (L.) Heynh., gibberellin treatment significantly increased expansin gene expression, accelerating leaf elongation.

The synergistic effect of light and hormones is also demonstrated in studies on *Phalaenopsis* orchids, where white LED lighting significantly increased leaf area and length (Utami and Hariyanto 2019; Hwang et al. 2024). It can be concluded that lighting is not merely a trigger for photosynthesis but also a molecular regulator that amplifies the effects of growth hormones in *in vitro* culture.

Dark cultures, in contrast, produced inconsistent growth responses. The absence of light inhibited chlorophyll synthesis and photosynthesis, reducing energy production and causing uneven hormone distribution. This is reflected in the high variability of leaf length. The high standard deviation in dark conditions indicates disruptions in metabolism and hormonal regulation (Dubreuil et al. 2018).

Overall, the leaf length growth of *P. amboinensis* is influenced by a complex interaction between media composition and the microenvironment. Media rich in organic compounds provide essential hormones and nutrients, while light activates photosynthetic processes and genetic pathways related to cell expansion. The combination of these factors creates ideal physiological conditions: coconut water (*C. nucifera*) supplies cytokinin and auxin (Lazim et al. 2015), peptone provides organic nitrogen for protein synthesis, and light activates chloroplasts and gibberellin expansion

pathways. These findings are supported by previous studies recommending the use of organic-rich media and optimal lighting for *in vitro* orchid growth (Shekarriz et al. 2014; Utami and Hariyanto 2019; Hwang et al. 2024).

Interaction of culture media in light and dark conditions on root number

Roots are critical organs for nutrient uptake and acclimatization of *in vitro-derived* plants, making root number and quality key parameters in evaluating propagation success. Coconut water (*C. nucifera*) provides natural hormones such as auxin and thiamine, which promote root development (Djajanegara 2020), while peptone contains amino acids like tryptophan, a precursor for indole-3-acetic acid (IAA) biosynthesis, the primary hormone stimulating lateral and adventitious root formation (Setiowati and Rahmah 2023). Auxin acts through the activation of ARF-Aux/IAA signaling pathways, such as ARF7, which induces LAX3 gene expression, facilitating increased IAA transport to root primordia and stimulating new root tissue initiation (Overvoorde et al. 2010; Cavallari et al. 2021).

In addition to hormonal factors, lighting also plays a significant role in supporting root growth, despite roots not being primary photosynthetic organs. Lighting during the early culture phase enhances partial photosynthetic activity in the plantlet's photosynthetic parts, generating carbohydrates and energy to support cell division and root tissue expansion (Pospíšilová et al. 1999; Gálvez et al. 2020; Deng et al. 2024).

Light also indirectly contributes to hormonal regulation by enhancing general metabolism and phytohormone synthesis, including auxin. In contrast, dark cultures inhibit photosynthate accumulation and overall metabolic activity, negatively impacting root initiation, as observed in dark treatments with low average root numbers and high standard deviations. These findings align with a study by Xu et al. (2019), which showed that a combination of red-blue light increased root length and activity in *Phalaenopsis* orchids.

The increased root number in the KC EO 2 under light treatment results from the synergy between hormonal and organic nutrient content in the medium and the environmental stimulation provided by bright lighting, which enhances physiological root responses. The strategy of combining organic-rich media with optimal lighting proves crucial for improving root regeneration efficiency in *Phalaenopsis in vitro* propagation (Chugh et al. 2009; Tantasawat et al. 2015; Xu et al. 2019). Therefore, this approach is suitable for tissue culture protocols for orchid species that are difficult to propagate conventionally.

Interaction of culture media in light and dark conditions on root length

Root length is a key indicator of the root system's capacity to penetrate substrates, absorb water and nutrients, and support vegetative plant growth. Coconut water (*C. nucifera*) contains natural phytohormones such as auxin, gibberellin, and cytokinin, with auxin playing a critical role in root elongation by activating cell wall-loosening enzymes like expansion and peroxidases. This mechanism aligns with the acid-growth theory, where auxin enhances H^+-ATPase activity, leading to cell wall acidification that activates expansins to loosen cellulose microfibrils, enabling faster cell elongation (Majda and Robert 2018). Gibberellins in coconut water (*C. nucifera*) also enhance root apical meristem activity, accelerating cell division and elongation (Shtin et al. 2022).

Meanwhile, peptone provides organic nitrogen in the form of hydrolyzed proteins, amino acids, and peptides readily absorbed by plants. Tryptophan in peptone serves as a precursor for endogenous auxin biosynthesis (Setiowati and Rahmah 2023), and other amino acids play essential roles in enzyme and structural cell wall protein synthesis. Previous studies have shown that peptone supplementation in KC medium accelerates germination, PLB formation, and orchid seedling growth even without external hormone addition (Kanjilal and Datta 2000; Nhut et al. 2008; Mondal et al. 2014; Setiari et al. 2016).

In addition to media under light treatment, supported root growth by enhancing photosynthetic activity in the plantlet's green parts, producing carbohydrates like sucrose that are transported to roots as energy and carbon sources for cell elongation (van Gelderen et al. 2018). Research indicates that inhibiting photosynthesis in dark conditions drastically reduces root growth, but this can be mitigated by adding sucrose to the medium (van Gelderen et al. 2018). Light also improves nitrogen use efficiency and the plant's C/N ratio, which are known to play critical roles in root development.

Specific light spectra, such as red-blue LED combinations, have been shown to significantly enhance *Phalaenopsis* root length and activity (Ren et al. 2016). Therefore, the success of the medium under light conditions reflects the synergy between a medium providing natural hormones and organic nutrients and optimal light intensity for metabolism and growth. These results align with studies on *Phalaenopsis* 'Bahia Blanca,' which showed increased root length in media supplemented with coconut water (*C. nucifera*) (Abbaszadeh et al. 2018), and reports that organic supplements like coconut water (*C. nucifera*) and peptone enhance root and PLB growth (Tantasawat et al. 2015; Setiari et al. 2016).

Interaction of culture media in light and dark conditions on chlorophyll a and b

Light is the primary factor in regulating chlorophyll biosynthesis, as it activates the expression of photosynthetic genes such as HEMA1, PORA, CAO, and the transcription factor GLK1, which regulate chloroplast biogenesis and chlorophyll pigment synthesis (Liu et al. 2020). The activity of the LPOR enzyme, which converts protochlorophyllide to chlorophyllide, is highly light-dependent, and in dark conditions, precursor accumulation without conversion leads to stagnation in chlorophyll synthesis. A study by Vendrame et al. (2022) showed that using white LEDs with moderate intensity can increase chlorophyll content in orchid cultures, while excessively high light intensity risks causing photoinhibition and pigment degradation (Streit et al. 2005).

In addition to light, the inclusion of coconut water (*C. nucifera*) and peptone significantly contributed to increased chlorophyll content. Coconut water (*C. nucifera*) contains

natural cytokinins, sugars, vitamins, and amino acids that support cell division and chloroplast formation. At the same time, peptone provides organic carbon and nitrogen needed for pigment biosynthesis (Vendrame et al. 2022).

The combination of nutrients and phytohormones supports chlorophyll biosynthesis pathways, resulting in organic-rich media consistently showing higher chlorophyll content compared to control media without supplements. Adaptively, the chlorophyll a/b ratio can vary depending on light conditions. In low-light environments, the expression of chlorophyllide a oxygenase (CAO) increases, converting more chlorophyll a to chlorophyll b to broaden the green-blue light absorption spectrum (Liu et al. 2020).

However, in light conditions, as in this study, the a/b ratio remains high because chlorophyll a remains dominant, and its biosynthesis is supported by light and phytohormones. Overall, these data demonstrate that bright light and organic-rich media composition synergistically enhance chlorophyll a and b biosynthesis and accumulation, supporting the effectiveness of the photosynthetic system in *P. amboinensis* plantlets during *in vitro* culture.

These findings reinforce the understanding that successful vegetative regeneration in orchid culture depends not only on basic media but also critically on lighting and the presence of organic supplements that support complex physiological processes at the cellular and molecular levels.

Interaction of culture media in light and dark conditions on stomata

The results confirm that bright light is the dominant external factor stimulating stomatal formation. Light exposure activates molecular pathways for stomatal lineage differentiation, including increased expression of transcription factors like SPEECHLESS (SPCH) and the production of EPFL9 signaling peptides by mesophyll cells, which promote guard cell formation (Wang et al. 2021; Zhou et al. 2024).

In dark conditions, these pathways are suppressed due to the activation of the COP1 ligase, which degrades SPCH and ICE1 proteins, drastically reducing stomatal formation. In contrast to lighting, media composition also exerts a strong physiological influence on stomatal formation. Media with high organic compounds like coconut water (*C. nucifera*) and peptone, rich in micronutrients, vitamins, and natural growth hormones such as auxin and cytokinin, provide optimal signals and metabolic resources for stomatal formation (Aishwarya et al. 2022). These hormones are known to enhance epidermal cell division and differentiation, including guard cells of stomata (Ando et al. 2024). Peptone, as an organic nitrogen source in the form of amino acids and peptides, supports the synthesis of structural proteins and enzymes involved in leaf morphogenesis and tissue development regulation (Lu and Xiao 2024). At the same time, low-nutrient media like WMO (without basal media and organic compounds) do not adequately support efficient epidermal differentiation.

Physiologically, stomata play a central role in gas exchange, CO_2 and O_2, and leaf transpiration. High stomatal density, as observed in basal media and under light treatments, enables increased CO_2 uptake and supports greater photosynthetic activity, consistent with the high chlorophyll content recorded in these treatments (Bertolino et al. 2019; Lawson and Vialet-Chabrand 2019). Plants with high stomatal density have an adaptive advantage in bright light and nutrient-sufficient conditions, as they can enhance water use efficiency through stomatal aperture regulation (Chua and Lau 2024).

However, this can also lead to increased water loss through transpiration if stomatal closure mechanisms are inefficient. Therefore, in addition to the number, the functionality and responsiveness of stomata to environmental changes are critical. During acclimatization, the transition from *in vitro* to *ex vitro*, plantlets with optimal stomatal numbers and functional stomata have a higher chance of survival and robust growth. Stomatal responses to light and humidity fluctuations help regulate CO_2 uptake and water evaporation in a balanced manner (Bertolino et al. 2019; Lawson and Vialet-Chabrand 2019).

Conversely, plantlets with excessively low or high stomatal density without efficient regulation risk physiological stress when transferred to external environments. Thus, the highest stomatal density in the basal media and under light treatment indicates that the combination of bright light and organic-rich media not only supports morphological stomatal formation but also enhances the physiological readiness of *P. amboinensis* plantlets for *ex vitro* conditions, making it an ideal treatment for orchid propagation and conservation *in vitro*.

In conclusion, the combination of KC EO 2 medium with 16-hour light exposure proved to be the most effective treatment for enhancing the *in vitro* growth of *P. amboinensis*. This treatment significantly increased leaf number (5.40 ± 2.50), leaf length (1.44 ± 0.31 cm), root number (2.40 ± 0.84), root length (1.89 ± 0.45 cm). However, no significant differences were observed between KC EO 3 and KC EO 2 media under light conditions in terms of chlorophyll a content (0.695 ± 0.113 mg/g FW and 0.641 ± 0.089 mg/g FW, respectively), and stomatal density (77.57 ± 2.72 stomata/mm² and 76.38 ± 3.73 stomata/mm², respectively). KC EO2 and KC EO3 are effective media, with KC EO2 being more suitable for growth enhancement and KC EO3 for improving physiological quality. These results confirm a strong interaction between organic-enriched media and light in promoting plantlet morphogenesis and physiological activity. KC EO 3 and KC EO 2 media are therefore recommended as a standardized protocol for the efficient and cost-effective propagation of *P. amboinensis*. Its application can support *ex situ* conservation efforts, reduce the need for wild harvesting, and offer a practical solution for commercial orchid nurseries seeking high-quality planting material. This approach contributes to both biodiversity preservation and sustainable horticultural development.

ACKNOWLEDGEMENTS

The authors would like to express their gratitude to BRIN as the institution that has provided the opportunity to complete this research and to all the people who helped materially or encouragingly. All the authors are the main

contributors and gave the same proportion of the research and publication process.

REFERENCES

Abbaszadeh SM, Miri SM, Naderi R. 2018. An effective nutrient media for asymbiotic seed germination and in vitro seedling development of Phalaenopsis 'Bahia Blanca'. J Ornam Plants 8 (3): 183-192.

Aishwarya PP, Seenivasan N, Naik DS. 2022. Coconut water as a root hormone: Biological and chemical composition and applications. Pharma Innov J 11: 1678-1681.

Ando E, Taki K, Suzuki T, Kinoshita T. 2024. A novel semi-dominant mutation in brassinosteroid signaling kinase1 increases stomatal density. Front Plant Sci 15: 1377352. DOI: 10.3389/fpls.2024.1377352.

Apriliyania R, Wahidah BF. 2021. In vitro propagation of *Dendrobium* sp.: Success factors. Filogeni: J Biol Students 1 (2): 33-46. DOI: 10.24252/filogeni.v1i1.21192. [Indonesian]

Arum DAP, Semiarti E. 2023. In vitro culture of *Phalaenopsis amabilis* (L.) blume orchid for seedling production with banana extract supplementation and light treatment for ex situ conservation. J Trop Biodivers Biotechnol 7 (3): 70868. DOI: 10.22146/jtbb.70868.

Asyary DQ, Permatasari NA, Suciaty T. 2024. Effect of foliar fertilizer interval and types of planting media on the growth of Dendrobium hybrid orchids. Jurnal Agrosci 2 (2): 131-141. DOI: 10.62885/agrosci.v2i2.519.

Bertolino LT, Caine RS, Gray JE. 2019. Impact of stomatal density and morphology on water-use efficiency in a changing world. Front Plant Sci 10: 225. DOI: 10.3389/fpls.2019.00225.

Cavallari N, Artner C, Benkova E. 2021. Auxin-regulated lateral root organogenesis. Cold Spring Harbor Perspect Biol 13 (7): a039941. DOI: 10.1101/cshperspect.a039941.

Cavallaro V, Pellegrino A, Muleo R, Forgione I. 2022. Light and plant growth regulators on in vitro proliferation. Plants (Basel) 11 (7): 844. DOI: 10.3390/plants11070844.

Chickarmane VS, Gordon SP, Tarr PT, Heisler MG, Meyerowitz EM. 2012. Cytokinin signaling as a positional cue for patterning the apical-basal axis of the growing Arabidopsis shoot meristem. Proc Natl Acad Sci U S A 109 (10): 4002-4007. DOI: 10.1073/pnas.1200636109.

Chua LC, Lau OS. 2024. Stomatal development in the changing climate. Development 151 (20): dev202681. DOI: 10.1242/dev.202681.

Chugh S, Guha S, Rao IU. 2009. Micropropagation of orchids: a review on the potential of different explants. Sci Hortic 122 (4): 507-520. DOI: 10.1016/j.scienta.2009.07.016.

Deng Q, Du P, Gangurde SS, Hong Y, Xiao Y, Hu D, Li H, Lu Q, Li S, Liu H, Wang R, Huang L, Wang W, Garg V, Liang X, Varshney RK, Chen X, Liu H. 2024. ScRNA-seq reveals dark- and light-induced differentially expressed gene atlases of seedling leaves in *Arachis hypogaea* L. Plant Biotechnol J 22 (7): 1848-1866. DOI: 10.1111/pbi.14306.

Djajanegara I. 2010. Utilization of banana fruit waste and coconut water as tissue culture media for moon orchid (*Phalaenopsis amabilis*) type 229. Jurnal Teknologi Lingkungan 11 (3): 373-380. DOI: 10.29122/jtl.v11i3.1182. [Indonesian]

Djajanegara I. 2010. Utilization of banana fruit waste and coconut water as culture media components for tissue culture of moth orchid (*Phalaenopsis amabilis*) type 229. J Environ Eng 11 (3): 373-380. DOI: 10.29122/jtl.v11i3.1182. [Indonesian]

Dobisova T, Hrdinova V, Cuesta C, Michlickova S, Urbankova I, Hejatkova R, Zadnikova P, Pernisova M, Benkova E, Hejatko J. 2017. Light controls cytokinin signaling via transcriptional regulation of constitutively active sensor histidine kinase CKI1. Plant Physiol 174 (1): 387-404. DOI: 10.1104/pp.16.01964.

Dubreuil C, Jin X, Barajas-López JD, Hewitt TC, Tanz SK, Dobrenel T, Schröder WP, Hanson J, Pesquet E, Grönlund A, Small I, Strand Å. 2018. Establishment of photosynthesis through chloroplast development is controlled by two distinct regulatory phases. Plant Physiol 176 (2): 1199-1214. DOI: 10.1104/pp.17.00435.

Fauziah AA, Setiari N, Saptiningsih E. 2022. Analysis effect of shade level on the physiological and anatomical characteristics of hybrid Phalaenopsis orchid at the acclimatization stage. Kultivasi 21 (2): 239-248.

Fouda A, Alshallash KS, Atta HM, El Gamal MS, Bakry MM, Alawam AS, Salem SS. 2024. Synthesis, optimization, and characterization of cellulase enzyme obtained from thermotolerant *Bacillus subtilis* f3: An insight into cotton fabric polishing activity. J Microbiol Biotechnol 34 (1): 207-223. DOI: 10.4014/jmb.2309.09023.

George EF, Hall MA, Klerk G J. 2008. Plant propagation by tissue culture in practice, part 1. Exegetics Limited. England.

Guo B, Chen H, Yin Y, Wang W, Zeng S. 2024. Tissue culture via protocorm-like bodies in an orchids hybrids *Paphiopedilum* SCBG huihuang90. Plants (Basel) 13 (2): 197. DOI: 10.3390/plants13020197.

Hamdeni I, Louhaichi M, Slim S, Boulila A, Bettaieb T. 2022. Incorporation of organic growth additives to enhance in vitro tissue culture for producing genetically stable plants. Plants (Basel) 11 (22): 3087. DOI: 10.3390/plants11223087.

Huq E. 2018. Direct convergence of light and auxin signaling pathways in Arabidopsis. Mol Plant 11 (4): 515-517. DOI: 10.1016/j.molp.2018.02.002.

Hwang JE, Park HB, Jeon DY, Park HJ, Kim S, Lee CW, Kim YJ, Yoon YJ. 2024. Effect of different basal media and organic supplements on in vitro seedling development of the endangered orchid species *Dendrobium moniliforme* (L.) Swartz. Plants 13 (19): 2721. DOI: 10.3390/plants13192721.

Jyothsna BS, Srivastava D. 2023. Morphological, stomatal, pigmentation, and biomolecular characteristics of a few epiphytic orchid species of India. Indian J Hortic 80 (3): 269-273.

Kanjilal B, Datta KB. 2000. Rapid micropropagation of *Geodorum densiflorum* (Lam) Schltr. in liquid culture. Indian J Exp Biol 38 (11): 1164-1167.

Lawson T, Vialet-Chabrand S. 2019, Speedy stomata, photosynthesis and plant water use efficiency. New Phytol 221 (1): 93-98. DOI: 10.1111/nph.15330.

Lazim MIML, Badruzaman NA, Peng KS, Long K. 2015. Quantification of cytokinins in coconut water from different maturation stages of Malaysia's coconut (*Cocos nucifera* L.) varieties. J Food Process Technol 6 (11): 1000515. DOI: 10.4172/2157-7110.1000515.

Lee HB, An SK, Lee SY, Kim KS. 2017. Vegetative growth characteristics of *Phalaenopsis* and *Doritaenopsis* plants under different artificial lighting sources. Hortic Sci Technol 35 (1): 21-29. DOI: 10.12972/kjhst.20170003.

Liu L, Lin N, Liu X, Yang S, Wang W, Wan X. 2020. From chloroplast biogenesis to chlorophyll accumulation: The interplay of light and hormones on gene expression in *Camellia sinensis cv. shuchazao* leaves. Front Plant Sci 11: 256. DOI: 10.3389/fpls.2020.00256.

Lu S, Xiao F. 2024. Small peptides: Orchestrators of plant growth and developmental processes. Intl J Mol Sci 25 (14): 7627. DOI: 10.3390/ijms25147627.

Machmudi M. Purnobasuki H, Utami ESW. 2019. The optimization mesophyll protoplast isolation for *Phalaenopsis amboinensis*. Bulgarian J Agricul Sci 25: 737-743.

Mackinney G. 1941. Absorption of light by chlorophyll solutions. J Biol Chem 140 (2): 315-322.

Majda M, Robert S. 2018. The role of auxin in cell wall expansion. Intl J Mol Sci 19 (4): 951. DOI: 10.3390/ijms19040951.

Marqués-Gálvez JE, Miyauchi S, Paolocci F, Navarro-Ródenas A, Arenas F, Pérez-Gilabert M, Morin E, Auer L, Barry KW, Kuo A, Grigoriev IV, Martin FM, Kohler A, Morte A. 2021. Desert truffle genomes reveal their reproductive modes and new insights into plant–fungal interaction and ectendomycorrhizal lifestyle. New Phytol 229: 2917-2932. DOI: 10.1111/nph.17044.

Mondal T, Aditya S, Banerjee N. 2014. In vitro axillary shoot regeneration and direct protocorm-like body induction from axenic shoot tips of Doritis pulcherrima Lindl. Plant Tissue Cult Biotechnol 23 (2): 251-261. DOI: 10.3329/ptcb.v23i2.17526.

Naderi Boldaji H, Daylami SD, Vahdati K. 2023. Use of light spectra for efficient production of plbs in temperate terrestrial orchids. Horticulturae 9 (9): 1007. DOI: 10.3390/horticulturae9091007.

Nhut DT, Thi NN, Khiet BL, Luan VQ. 2008. Peptone stimulates in vitro shoot and root regeneration of avocado (*Persea americana* Mill.). Sci Hortic 115 (2): 124-128. DOI: 10.1016/j.scienta.2007.08.011.

Overvoorde P, Fukaki H, Beeckman T. 2010. Auxin control of root development. Cold Spring Harbor Perspect Biol 2 (6): a001537. DOI: 10.1101/cshperspect.a001537.

Park WT, Kim YK, Kim YS, Park NI, Lee SY, Park SU. 2011. "In vitro" plant regeneration and micropropagation of "*Liriope platyphylla*."

Plant Omics 4 (4): 199-203. DOI: 10.3316/informit.311184548407084.
Pospíšilová J, Tichá I, Kadleček P, Haisel D, Plzáková Š. 1999. Acclimatization of micropropagated plants to ex vitro conditions. Biologia Plantarum 42 (4): 481-497. DOI: 10.1023/A:1002688208758.
Prerostova S, Černý M, Dobrev PI, Motyka V, Hluskova L, Zupkova B, Gaudinova A, Knirsch V, Janda T, Brzobohaty B, Vankova R. 2021. Light regulates the cytokinin-dependent cold stress responses in Arabidopsis. Front Plant Sci 11: 608711. DOI: 10.3389/fpls.2020.608711.
Ren G, Wang X, Zhu G. 2016. Effect of LED in different light qualities on growth of Phalaenopsis plantlets. Chin J Bot 51 (1): 81-88. DOI: 10.11983/CBB14196.
Saeedi SA, Vahdati K, Sarikhani S, Daylami SD, Davarzani M, Gruda NS, Aliniaeifard S. 2023. Growth, photosynthetic function, and stomatal characteristics of Persian walnut explants in vitro under different light spectra. Front Plant Sci 14: 1292045. DOI: 10.3389/fpls.2023.1292045.
Sawardekar S, Sherkar S, Sunte V, Jadhav D. 2023. In vitro propagation reviews of orchid. Intl J Innov Res Sci Eng Technol 8 (10): 1196-1200. DOI: 10.5281/zenodo.10060804.
Setiari N, Purwantoro A, Moeljopawiro S, Semiarti E. 2016. Peptone and tomato extract induced early stage of embryo development of Dendrobium phalaenopsis orchid. J Trop Biodivers Biotechnol 1 (2): 77-84. DOI: 10.22146/jtbb.15498.
Setiowati FK, Rahmah NA. 2023. The effect of adding a combination of benzyl amino purine and peptone on the growth of Cattleya sp. orchid plantlets. Jurnal Ilmu Hayat 7 (1): 43-51. DOI: 10.17977/um061v7i12023p43-51. [Indonesian]
Sevilleno SS, Cabahug-Braza RAM, An HR, Hwang YJ. 2023. Analyzing pollen fertility based on micronuclei presence in yellow aneuploid Phalaenopsis. Korean J Breed Sci 55 (4): 287-295. DOI: 10.9787/KJBS.2023.55.4.287.
Shekarriz P, Kafi M, Deilamy SD, Mirmasoumi M. 2014. Coconut water and peptone improve seed germination and protocorm like body formation of hybrid *Phalaenopsis*. Agric Sci Dev 3 (10): 317-322.
Shtin M, Dello IR, Del Bianco M. 2022. It's time for a change: The role of gibberellin in root meristem development. Front Plant Sci 13: 882517. DOI: 10.3389/fpls.2022.882517.
Singh S. 2020. Orchids: An emerging floriculture enterprise in India and its scope in Himachal Pradesh. Indian J Hill Farming Spec Issue 152-159.
Sprangers K, Thys S, van Dusschoten D, Beemster GTS. 2020. Gibberellin enhances the anisotropy of cell expansion in the growth zone of the maize leaf. Front Plant Sci 11: 1163. DOI: 10.3389/fpls.2020.01163.
Streit NM, Canterle LP, Canto MWD, Hecktheuer LHH. 2005. As Clorofilas. Ciência Rural 35: 748-755. DOI: 10.1590/S0103-84782005000300043.
Tantasawat PA, Khairum A, Arsakit K, Poolsawat O, Pornbungkerd P, Kativat C. 2015. Effects of different culture media on growth and proliferation of Dendrobium 'earsakul' protocorm-like bodies. HortTechnology 25 (5): 681-686. DOI: 10.21273/HORTTECH.25.5.681.
Utami ESW, Hariyanto S. 2019. In vitro seed germination and seedling development of a rare Indonesian native orchid *Phalaenopsis amboinensis* J.J.Sm. Scientifica (Cairo) 2019: 8105138. DOI: 10.1155/2019/8105138.
van Gelderen K, Kang C, Pierik R. 2018. Light signaling, root development, and plasticity. Plant Physiol 176 (2): 1049-1060. DOI: 10.1104/pp.17.01079.
Vendrame WA, Xu J, Beleski D. 2022. Evaluation of the effects of culture media and light sources on in vitro growth of *Brassavola nodosa* (L.) Lindl. hybrid. Horticulturae 8 (5): 450. DOI: 10.3390/horticulturae8050450.
Wang S, Zhou Z, Rahiman R, Lee GSY, Yeo YK, Yang X, Lau OS. 2021. Light regulates stomatal development by modulating paracrine signaling from inner tissues. Nat Commun 12 (1): 3403. DOI: 10.1038/s41467-021-23728-2.
Wei Y, Li J, Jin J, Gao J, Xie Q, Lu C, Zhu G, Yang F. 2025. Centenary progress on orchidaceae research: A bibliometric analysis. Genes 16 (3): 336. DOI: 10.3390/genes16030336.
Werner T, Motyka V, Laucou V, Smets R, Van Onckelen H, Schmülling T. 2003. Cytokinin-deficient transgenic Arabidopsis plants show multiple developmental alterations indicating opposite functions of cytokinins in the regulation of shoot and root meristem activity. Plant Cell 15 (11): 2532-2550. DOI: 10.1105/tpc.014928.
Wu W, Du K, Kang X, Wei H. 2021. The diverse roles of cytokinins in regulating leaf development. Hortic Res 8 (1): 118. DOI: 10.1038/s41438-021-00558-3.
Xu Y, Yang M, Cheng F, Zhang L, Dong J, Cheng S. 2020. Effects of LED photoperiods and light qualities on in vitro growth and chlorophyll fluorescence of *Cunninghamia lanceolata*. BMC Plant Biol 20 (1): DOI: 10.1186/s12870-020-02480-7.
Zhang S, Yang Y, Li J, Qin J, Zhang W, Huang W, Hu H. 2018. Physiological diversity of orchids. Plant Divers 40 (4): 196-208. DOI: 10.1016/j.pld.2018.06.003.
Zhou W, Liu J, Wang W, Li Y, Ma Z, He H, Wang X, Lian X, Dong X, Zhao X, Zhou Y. 2024. Molecular mechanisms for regulating stomatal formation across diverse plant species. Intl J Mol Sci 25 (19): 10403. DOI: 10.3390/ijms251910403.

NUSANTARA BIOSCIENCE
Vol. 17, No. 2, pp. 253-258
November 2025

ISSN: 2087-3948
E-ISSN: 2087-3956
DOI: 10.13057/nusbiosci/n170208

Dengue virus and *Plasmodium* coinfection among febrile patients in Osun State, Nigeria

BABAJIDE B. AJAYI[1,♥], KEHINDE S. OLAITAN[2], OLUWATOBA F. OWOYOMI[2], SUNDAY E. ONI[2], AKINWALE M. AKINLABI[2], ELIZABETH O. ARO[3], DAVID O. OGBOLU[4]

[1]Department of Microbiology, School of Life Science, Federal University of Technology Akure. P.M.B 704, Akure, Ondo State 340110, Nigeria. Tel: +234-904-2422526, ♥email: bbajayi@futa.edu.ng

[2]Department of Medical Laboratory Science, College of Health Sciences, Joseph Ayo Babalola University. Kilometre 36, Ilesa-Akure Road, Ikeji-Arakeji, Osun State, Nigeria

[3]Department of Medical Laboratory Science, Ladoke Akintola University of Technology. Ilorin Road, 210214, Ogbomoso, Oyo State, Nigeria

[4]Department of Medical Laboratory Science, College of Health Sciences, Osun State University. Osogbo, Osun State, Nigeria

Manuscript received: 31 March 2025. Revision accepted: 29 October 2025.

Abstract. *Ajayi BB, Olaitan KS, Owoyomi OF, Oni SE, Akinlabi AM, Aro EO, Ogbolu DO. 2025. Dengue virus and* Plasmodium *coinfection among febrile patients in Osun State, Nigeria. Nusantara Bioscience 17: 253-258.* Dengue and malaria are major co-endemic vector-borne diseases in Nigeria, presenting significant diagnostic challenges due to their overlapping clinical symptoms. In settings where malaria is hyperendemic, febrile illnesses are often presumptively treated as malaria, potentially leading to the misdiagnosis of other pathogens like dengue virus (DENV). This study aimed to determine the seroprevalence of DENV infection and the prevalence of DENV/*Plasmodium* coinfection among febrile patients in Osun State, Nigeria. A cross-sectional study was conducted from April to September 2024, involving 250 febrile patients from selected healthcare facilities. Blood samples were analyzed using rapid diagnostic tests (RDTs) for *Plasmodium* antigens and for DENV-specific Immunoglobulin M (IgM) and G (IgG) antibodies. Sociodemographic and risk factor data were collected via structured questionnaires. The prevalence of malaria was high at 53.6% (134/250), consistent with the region's hyperendemic status. Evidence of recent DENV infection (IgM positive) was found in 0.8% (2/250) of patients, while 6.4% (16/250) were IgG positive, indicating past exposure. Concurrent infection was detected in 0.8% (2/250) of patients for Malaria/DENV IgM and 3.2% (8/250) for Malaria/DENV IgG. Both malaria and DENV IgG seropositivity were significantly associated with age ($p<0.05$). This study confirms the endemic circulation of DENV in Osun State and highlights its contribution to the burden of non-malarial febrile illness. These findings underscore the critical need to revise existing diagnostic algorithms and integrate DENV surveillance into public health frameworks to mitigate misdiagnosis and improve patient outcomes.

Keywords: Coinfection, dengue virus, febrile patients, malaria, Nigeria, Osun State

INTRODUCTION

Vector-borne diseases, particularly dengue and malaria, impose a substantial burden on public health systems across tropical and subtropical regions (Salam et al. 2018; Osarumwense et al. 2022). While malaria has historically dominated the public health landscape in Africa, dengue is emerging as a significant and often under-recognized threat (Otu et al. 2019a). Recent meta-analyses confirm an increasing prevalence of acute dengue across the continent, with sporadic and epidemic cases reported from numerous West African nations, including Nigeria (Ayukekbong 2014; Gebremariam et al. 2023). This epidemiological shift creates a complex challenge, as both pathogens are transmitted by mosquitoes, thrive in similar ecological conditions, and, crucially, present with nearly indistinguishable symptoms in their early stages.

The epidemiological convergence of these pathogens is a pressing global health concern. Recent scholarship underscores the urgency of differentiating non-malarial febrile illnesses, which are frequently misdiagnosed. In regions across sub-Saharan Africa, studies increasingly demonstrate a significant prevalence of dengue among febrile populations, often mistaken for malaria (Gainor et al. 2022). This diagnostic confusion is critical, as standardized febrile illness protocols, heavily reliant on presumptive malaria treatment or malaria-specific rapid tests, systematically fail to identify dengue, leading to suboptimal patient management and unmonitored arboviral spread (Mbabazi et al. 2022). Furthermore, the clinical implications of simultaneous DENV-Plasmodium infection are a subject of intense investigation. While historically considered rare, recent meta-analyses confirm coinfection is geographically widespread. Although debate continues regarding whether coinfection mitigates or exacerbates disease severity, there is a consensus that the overlapping clinical presentation complicates diagnosis and may mask severe manifestations of either disease, posing a significant risk to patients (Rufai et al. 2022)

Nigeria bears one of the world's heaviest malaria burdens, accounting for a disproportionate share of global cases and mortality (World Health Organization 2021). This hyperendemicity has fostered a deep-seated clinical practice of presumptively diagnosing and treating most acute febrile illnesses as malaria, often without laboratory confirmation (Ayolabi et al. 2019). This practice, while

understandable in a resource-limited context, casts a profound "diagnostic shadow" over other etiologies of fever. Consequently, pathogens like dengue virus (DENV) are systematically overlooked, leading to poor patient outcomes, as dengue requires specific supportive management distinct from antimalarial therapy, and contributing to the underestimation of its true public health impact (Otu et al. 2019b; Saidu and Okojie 2024).

The diagnostic dilemma is rooted in the clinical overlap between the two diseases. The initial presentation of uncomplicated malaria—fever, headache, myalgia, and fatigue—is virtually identical to that of classic dengue fever (Halsey et al. 2016; Kotepui and Kotepui 2019). This similarity makes differential diagnosis based on clinical grounds alone unreliable and hazardous (Rao et al. 2016; Nkenfou et al. 2021). Furthermore, concurrent infection with both pathogens, while once considered rare, is increasingly reported from endemic areas and may lead to more complex clinical presentations, potentially increasing the risk of severe outcomes such as deep bleeding or hepatic complications (Epelboin et al. 2012; Magalhães et al. 2014). Studies from various regions of Nigeria have confirmed the circulation of all four DENV serotypes and have documented coinfection rates with malaria, indicating that this is a widespread, not localized, phenomenon (Idoko et al. 2015; Moses et al. 2016; Mustapha et al. 2017; Ayolabi et al. 2019). The national average prevalence of dengue has been estimated at approximately 21%, suggesting that one in five Nigerians may be susceptible to infection (Otu et al. 2019a).

Despite this growing body of evidence, specific, localized data on the prevalence of DENV and its coinfection with malaria remain scarce for many parts of the country, including Osun State. This knowledge gap hinders the development of evidence-based clinical guidelines and targeted public health interventions. Therefore, this study was designed to investigate the seroprevalence of DENV infection, determine the prevalence of DENV/*Plasmodium* coinfection, and identify associated demographic and environmental risk factors among febrile patients seeking care in Osun State, Nigeria.

MATERIALS AND METHODS

Ethical considerations

Ethical approval for this study was obtained from the Ethical Research Committee of the Osun State Ministry of Health, Nigeria. Additional permission was secured from the medical officers in charge of the selected healthcare facilities. Written or verbal informed consent was obtained from all adult participants and from the parents or legal guardians of minors before enrollment. All patient data were anonymized to ensure confidentiality.

Study design, area, and period

A cross-sectional study was conducted between April and September 2024, coinciding with the rainy season, a period typically associated with increased mosquito vector activity. The study was carried out in two selected Local Government Areas (LGAs), Ede South and Oriade, within Osun State, southwestern Nigeria. Osun State is predominantly inhabited by the Yoruba people and is characterized by a tropical climate with distinct wet and dry seasons.

Study population and sampling

The study population consisted of 250 consenting febrile patients presenting at selected primary and secondary healthcare facilities in the study LGAs. Inclusion criteria included an acute febrile illness with a measured axillary body temperature of 37.5°C or higher, consistent with case definitions for both malaria and suspected dengue fever. Patients of all ages and both sexes who provided consent were recruited consecutively until the target sample size was reached.

Data and sample collection

A pre-tested, structured questionnaire was administered by trained interviewers to collect data on sociodemographic characteristics (age, sex, education, occupation) and potential risk factors for vector-borne diseases. These factors included history of blood transfusion, use of insecticide-treated nets (ITNs), presence of window nets, and environmental sanitation practices (e.g., presence of overgrown bushes, stagnant water). Following the questionnaire, a 5 mL venous blood sample was collected from each participant under strict aseptic conditions. The blood was transferred into an ethylene diamine tetraacetic acid (EDTA) anticoagulant tube for immediate processing and subsequent analysis.

Laboratory analysis

All laboratory procedures were performed at the Medical Microbiology Laboratory of Joseph Ayo Babalola University.

Malaria detection

Malaria parasites were detected using the First Response™ Malaria Ag *P. falciparum*/Pan Rapid Diagnostic Test (RDT) (Premier Medical Corporation Ltd., India). This qualitative, immunochromatographic assay detects *Plasmodium falciparum*-specific histidine-rich protein 2 (HRP2) and pan-*Plasmodium* lactate dehydrogenase (pLDH) in whole blood, allowing for the rapid diagnosis of *P. falciparum* and other *Plasmodium* species (Moses et al. 2016). The test was performed and interpreted according to the manufacturer's instructions.

Dengue serology

The remaining blood sample was centrifuged at 3,000 rpm for 10 minutes to separate plasma. The plasma was carefully harvested and stored in cryovials at -20°C until analysis. Dengue virus exposure was assessed using the EGENS® Dengue Virus IgM/IgG RDT kit (Egens Biotechnology, China). This solid-phase immunochromatographic assay qualitatively detects and differentiates between IgM and IgG antibodies to DENV in human plasma. The presence of IgM antibodies typically indicates a recent or acute primary infection, while the

presence of IgG antibodies suggests a past or secondary infection (Adeleke et al. 2016; Moses et al. 2016). The assay was performed following the manufacturer's protocol, and results were read within 15 minutes.

Statistical analysis

Data from the questionnaires and laboratory tests were entered into Microsoft Excel and subsequently analyzed using the Statistical Package for Social Sciences (SPSS) version 27.0 (IBM Corp., Armonk, NY, USA). Descriptive statistics were used to summarize the data; categorical variables were presented as frequencies and percentages, while continuous variables were expressed as mean ± standard deviation. Associations between categorical variables (e.g., demographic factors, risk factors, and infection status) were assessed using the Pearson's Chi-square ($\chi 2$) test. Odds ratios (OR) with 95% confidence intervals (CI) were calculated to evaluate the strength of association between risk factors and disease occurrence. A p-value of less than 0.05 was considered statistically significant for all tests.

RESULTS AND DISCUSSION

Sociodemographic profile and overall prevalence

The study enrolled 250 febrile patients with a mean age of 24.94±16.76 years. The cohort was predominantly female (63.2%), single (62.4%), and had attained at least a secondary level of education (50.4%). Students constituted the largest occupational group (60.8%) (Table 1).

The burden of malaria in this febrile population was exceptionally high, with 53.6% (134/250) of participants testing positive via RDT. In contrast, serological evidence for dengue virus was less frequent but clearly present. The seroprevalence of recent DENV infection (IgM positive) was 0.8% (2/250), while the seroprevalence of past DENV exposure (IgG positive) was significantly higher at 6.4% (16/250). Critically, coinfection was identified in this population. The prevalence of concurrent malaria and recent dengue (MP/DENV IgM) was 0.8%, and the prevalence of malaria with past dengue exposure (MP/DENV IgG) was 3.2% (Table 2).

The serological landscape responsible for the endemic circulation of dengue virus

The serological profile observed in this study—a low DENV IgM rate (0.8%) coupled with a substantially higher DENV IgG rate (6.4%)—provides a critical snapshot of the local epidemiology. IgM antibodies are markers of a recent primary infection, typically appearing within days of symptom onset and waning over several months. In contrast, IgG antibodies develop later but persist for life, serving as a reliable indicator of past exposure (Khetarpal and Khanna 2016). The fact that IgG prevalence was eight times higher than that of IgM strongly suggests that DENV is not merely causing a transient, sporadic outbreak in Osun State. Instead, this pattern is characteristic of endemic circulation, where the virus is consistently present in the environment, leading to a significant cumulative history of exposure within the population. This finding aligns with broader seroprevalence studies across Nigeria and West Africa, which, despite showing varied prevalence rates, collectively confirm widespread DENV transmission (Ayolabi et al. 2019; Gebremariam et al. 2023; Saidu and Okojie 2024). The presence of a large IgG-seropositive population also raises public health concerns regarding the potential for more severe disease through antibody-dependent enhancement (ADE) if a new or different DENV serotype were to be introduced into the region (Khetarpal and Khanna 2016).

The dynamics of vector-specific risk factors

The risk factor analysis revealed a telling disparity between the two diseases (Tables 3 and 4). A single factor emerged as statistically significant: participants residing in homes with nets on the windows were significantly protected from malaria infection compared to those without (OR: 1.782, 95% CI: 1.067-2.975, p=0.027). This finding reinforces the value of physical barriers against the primary malaria vector, the *Anopheles* mosquito, which is predominantly nocturnal and endophagic (bites and rests indoors at night) (World Health Organization 2021).

Table 1. Sociodemographic characteristics of the participants (N=250)

Variables	Category	Frequency	Percent (%)
Age range (years) (Mean±SD = 24.94±16.76)	0-10	52	20.8
	11-20	62	24.8
	21-30	62	24.8
	31-40	38	15.2
	41-50	14	5.6
	51-60	12	4.8
	>60	10	4.0
Gender	Female	158	63.2
	Male	92	36.8
Marital status	Married	78	31.2
	Single	156	62.4
	Widow/Widower/Other	16	6.4
Highest level of education	Primary	48	19.2
	Secondary	126	50.4
	Tertiary	78	31.2
Occupation	Student	152	60.8
	Trader	40	16.0
	Civil servant	22	8.8
	Business	14	5.6
	Other	22	8.8

Table 2. Prevalence of dengue virus, malaria, and coinfections

Disease test	No. of Participants	Frequency	Percent (%)
Dengue virus IgG	250	16	6.4
Dengue virus IgM	250	2	0.8
Malaria Parasite (MP) RDT	250	134	53.6
Coinfections with Malaria			
MP RDT and DENV IgG	250	8	3.2
MP RDT and DENV IgM	250	2	0.8

Table 3. Comparative analysis of risk factors for malaria and dengue IgG seropositivity

Variables	Category	No. of Participants (%)	Malaria RDT Positive (%)	OR (95% CI)	p value	DENV IgG Positive (%)	OR (95% CI)	p value
Overgrown bushes	Yes	136 (54.4)	54.4	1.000 (Reference)	0.601	8.8	2.661 (0.834-8.492)	0.087
	No	114 (45.6)	52.6	0.931 (0.563-1.539)		3.5	1.000 (Reference)	
Windows with net	Yes	152 (60.8)	59.2	1.782 (1.067-2.975)	0.027	5.3	0.625 (0.227-1.724)	0.360
	No	98 (39.2)	44.9	1.000 (Reference)		8.2	1.000 (Reference)	
Water tank closed	Yes	166 (66.4)	55.4	1.243 (0.735-2.104)	0.417	4.8	0.481 (0.174-1.331)	0.151
	No	84 (33.6)	50.0	1.000 (Reference)		9.5	1.000 (Reference)	
Stagnant gutters	Yes	182 (72.8)	51.6	0.748 (0.426-1.314)	0.311	5.5	0.601 (0.210-1.722)	0.339
	No	68 (27.2)	58.8	1.000 (Reference)		8.8	1.000 (Reference)	

Table 4. Prevalence of dengue virus among participants by age and sex

		No. Examined	DENV Negative (%)	DENV IgG Positive (%)	DENV IgM Positive (%)	$\chi 2$	p value
Age range (years)	0-10	52	44 (84.6)	6 (11.5)	2 (3.8)	24.376	0.018
	11-20	62	62 (100.0)	0 (0.0)	0 (0.0)		
	21-30	62	54 (87.1)	8 (12.9)	0 (0.0)		
	31-40	38	38 (100.0)	0 (0.0)	0 (0.0)		
	41-50	14	12 (85.7)	2 (14.3)	0 (0.0)		
	51-60	12	12 (100.0)	0 (0.0)	0 (0.0)		
	>60	10	10 (100.0)	0 (0.0)	0 (0.0)		
Gender	Female	158	144 (91.1)	12 (7.6)	2 (1.3)	2.250	0.325
	Male	92	88 (95.7)	4 (4.3)	0 (0.0)		
Total		250	232 (92.8)	16 (6.4)	2 (0.8)		

Table 5. Prevalence of malaria and coinfections with Dengue virus among participants by age and sex

Variables	Category	No. Examined	Malaria RDT Positive (%)	Coinfections with DENV IgG (%)	Coinfections with DENV IgM (%)
Age range (Years)	0-10	52	32 (61.5)	4 (7.7)	2 (3.8)
	11-20	62	38 (61.3)	0 (0.0)	0 (0.0)
	21-30	62	22 (35.5)	2 (3.2)	0 (0.0)
	31-40	38	22 (57.9)	0 (0.0)	0 (0.0)
	41-50	14	8 (57.1)	2 (14.3)	0 (0.0)
	51-60	12	8 (66.7)	0 (0.0)	0 (0.0)
	>60	10	4 (40.0)	0 (0.0)	0 (0.0)
$\chi 2$, p value			12.894, 0.045	12.975, 0.043	7.677, 0.263
Gender	Female	158	86 (54.4)	6 (3.8)	2 (1.3)
	Male	92	48 (52.2)	2 (2.2)	0 (0.0)
$\chi 2$, p value			0.119, 0.730	1.174, 0.279	1.192, 0.275

Paradoxically, none of the assessed risk factors, including the use of insecticide-treated bed nets, showed any significant association with DENV IgG seropositivity. This "negative" result is not a methodological failure but rather a crucial epidemiological insight. It reflects the fundamental differences in the bionomics of the dengue vector, the *Aedes* mosquito. *Aedes aegypti* is primarily diurnal (bites during the day), often feeds outdoors, and breeds in small, artificial water containers around human dwellings (Khetarpal and Khanna 2016; World Health Organization 2024). Consequently, malaria-centric prevention questions about sleeping under a bed net are largely irrelevant to dengue risk. The study's findings inadvertently demonstrate that vector control strategies focused solely on *Anopheles* are insufficient for preventing dengue. This underscores the need for an integrated vector management (IVM) approach that combines nocturnal interventions like ITNs and indoor residual spraying for malaria with diurnal, source-reduction strategies for dengue control.

Age as a key determinant of infection

The stratified analysis revealed that age was a significant determinant for both infections, whereas gender was not (Table 5). The prevalence of DENV IgG antibodies was significantly associated with age ($\chi 2$=24.376, p=0.018), peaking at 14.3% in the 41-50 years age group. Similarly, malaria prevalence was significantly associated with age ($\chi 2$=12.894, p=0.045), with the highest rate (66.7%) observed among those aged 51-60 years.

This pattern, with prevalence increasing in older age brackets, points towards a model of cumulative exposure over a lifetime. An individual in their 40s or 50s has had decades more potential exposure to infectious mosquito bites than a child. The peak of DENV IgG—a marker of any past infection—in the 41-50 age group strongly supports this hypothesis. The even later peak for malaria prevalence could reflect a more complex interplay of factors, including lifelong exposure, potential waning of acquired immunity in older age, and occupational or behavioral patterns that increase risk (Saidu and Okojie 2024). These findings challenge the common perception of these diseases as primarily pediatric concerns and highlight the need for public health messaging and interventions that target all age groups, particularly adults who may have significant exposure.

Implications for clinical practice and public health

The confirmation of DENV circulation and its coinfection with malaria has profound implications. Clinically, it necessitates a paradigm shift in the management of acute febrile illness in Nigeria. A negative malaria test in a febrile patient should not be an endpoint but should instead trigger further investigation for other pathogens, with dengue being a primary consideration. Relying on presumptive malaria diagnoses is no longer tenable and risks poor outcomes for patients with dengue. Public health authorities must prioritize the development and dissemination of updated diagnostic algorithms for fever and ensure the availability of reliable dengue diagnostics at various levels of the healthcare system. Furthermore, enhanced surveillance, including molecular methods like RT-PCR for serotyping, is essential to monitor circulating DENV genotypes and detect the introduction of new strains that could precipitate more severe or widespread outbreaks (Ayolabi et al. 2019; Saidu and Okojie 2024).

Limitations of the study

This study, while providing valuable local data, has several limitations. First, the reliance on RDTs for diagnosis has constraints. While practical for field studies, RDTs for malaria can have lower sensitivity than expert microscopy, and serological RDTs for dengue cannot provide information on the specific viral serotype. Second, serological assays for flaviviruses are known to have cross-reactivity issues. It is possible that some of the DENV IgG positive results could be due to past infections with other co-circulating flaviviruses in Nigeria, such as Zika or Yellow Fever virus, potentially leading to an overestimation of dengue seroprevalence (Kotepui and Kotepui 2019; Siddig et al. 2023). Third, the cross-sectional design captures only a single point in time, preventing the establishment of causality between risk factors and disease or the observation of clinical progression. Finally, the risk factor data were self-reported and thus subject to recall bias. The questionnaire was also primarily designed with malaria in mind and may not have

adequately captured key risk factors specific to *Aedes*-borne transmission, such as daytime activities and domestic water storage practices.

In conclusion, this study provides crucial, localized evidence for the co-circulation of dengue virus and *Plasmodium* parasites among febrile individuals in Osun State, Nigeria. The findings reveal a significant historical burden of dengue exposure, as indicated by IgG seroprevalence, and demonstrate age-specific patterns of infection that point toward endemic transmission for both pathogens. The high prevalence of malaria underscores its continued dominance as a cause of fever, yet the confirmed presence of dengue, both as a mono-infection and coinfection, highlights a critical gap in current diagnostic practices. These results strongly advocate for the integration of DENV testing into routine clinical algorithms for febrile illness and for the urgent development of dual-pronged, integrated vector management strategies that effectively target the distinct ecologies and behaviors of both *Aedes* and *Anopheles* mosquitoes.

ACKNOWLEDGEMENTS

The authors wish to thank the patients who participated in this study, as well as the staff of the selected healthcare facilities in Osun State, Nigeria for their invaluable cooperation and support.

REFERENCES

Adeleke MA, Muhibi MA, Ajayi EIO, Idowu OA, Famodimu MT, Olaniyan SO, Hassan AN. 2016. Dengue virus specific immunoglobulin G antibodies among patients with febrile conditions in Osogbo, Southwestern Nigeria. Trop Biomed 33 (1): 1-7.

Ayukekbong JA. 2014. Dengue virus in Nigeria: Current status and future perspective. Brit J Virol 1 (4): 106-111. DOI: 10.13140/RG.2.1.4784.7520.

Epelboin L, Hanf M, Dussart P, Odonne G, Djossou F, Nacher M, Carme B. 2012. Is dengue and malaria co-infection more severe than single infections? A retrospective matched-pair study in French Guiana. Malar J 11 (1): 142. DOI: 10.1186/s12936-017-1792-7.

Ayolabi CI, Olusola BA, Ibemgbo SA, Okonkwo GO. 2019. Detection of Dengue viruses among febrile patients in Lagos, Nigeria and phylogenetics of circulating Dengue serotypes in Africa. Infect Genet Evol. 75:103947. DOI: 10.1016/j.meegid.2019.103947.

Gainor EM, Harris E, LaBeaud AD. 2022 Uncovering the burden of dengue in Africa: Considerations on magnitude, misdiagnosis, and ancestry. Viruses 14 (2): 233. DOI: 10.3390/v14020233.

Gebremariam TT, Schallig HDFH, Kurmane ZM, Danquah JB. 2023. Increasing prevalence of malaria and acute dengue virus coinfection in Africa: A meta-analysis and meta-regression of cross-sectional studies. Malar J 22 (1): 300. DOI: 10.1186/s12936-023-04723-y.

Halsey ES, Baldeviano GC, Edgel KA, Vilcarromero S, Sihuincha M, Lescano AG. 2016. Symptoms and immune markers in *Plasmodium*/dengue virus coinfection compared with mono-infection with either in Peru. PLoS Negl Trop Dis 10 (4): e0004646. DOI: 10.1371/journal.pntd.0004646.

Idoko MO, Ado SA, Umoh VJ. 2015. Prevalence of dengue virus and malaria in patients with febrile complaints in Kaduna Metropolis, Nigeria. Microbiol Res J Intl 8 (1): 343-347. DOI: 10.9734/BMRJ/2015/16408.

Khetarpal N, Khanna I. 2016. Dengue fever: causes, complications, and vaccine strategies. J Immunol Res 2016: 6803098. DOI: 10.1155/2016/6803098.

Kotepui M, Kotepui KU. 2019. Prevalence and laboratory analysis of malaria and dengue coinfection: A systematic review and meta-analysis. BMC Public Health 19 (1): 1148. DOI: 10.1186/s12889-019-7488-4.

Magalhães BML, Siqueira AM, Alexandre MAA, Souza MS, Gimaque JB, Bastos MS, Figueiredo RM, Melo GC, Lacerda MVG, Mourão MPG. 2014. *P. vivax* malaria and dengue fever co-infection: A cross-sectional study in the Brazilian Amazon. PLoS Negl Trop Dis 8 (10): e3239. DOI: 10.1371/journal.pntd.0003239.

Wainaina M, Vey da Silva DA, Dohoo I, Mayer-Scholl A, Roesel K, Hofreuter D, Roesler U, Lindahl J, Bett B, Al Dahouk S. 202. 2A systematic review and meta-analysis of the aetiological agents of non-malarial febrile illnesses in Africa. PLoS Negl Trop Dis 16 (1): e0010144. DOI: 10.1371/journal.pntd.0010144.

Moses AE, Atting IA, Inyang OS. 2016. Evidence of overlapping infections of dengue, malaria and typhoid in febrile patients attending a tertiary health facility in Uyo, South–South Nigeria. J Adv Med Med Res 17 (3): 1-9. DOI: 10.9734/JAMMR/2016/27530.

Mustapha JO, Anthony UE, Idris AN. 2017. Survey of malaria and anti-dengue virus IgG among febrile HIV-infected patients attending a tertiary hospital in Abuja, Nigeria. HIV AIDS (Auckl) 9: 145-151. DOI: 10.2147/HIV.S139049.

Nkenfou CN, Fainguem N, Dongmo-Nguefack F, Yatchou LG, Kameni JJK, Elong EL, Ndjolo A. 2021. Enhanced passive surveillance dengue infection among febrile children: Prevalence, coinfections and associated factors in Cameroon. PLoS Negl Trop Dis 15 (4): e0009316. DOI: 10.1371/journal.pntd.0009316.

Osarumwense O, Nkechukwu I, Favour E, Izuchukwu I, George C, Umale A, Okechukwu E. 2022. The prevalence of dengue virus and malaria co-infection among HIV-infected patients within South Eastern Nigeria. Adv Infect Dis 12: 106-117. DOI: 10.4236/aid.2022.121009.

Otu A, Ebenso B, Etokidem A, Chukwuekezie O. 2019a. Dengue fever - An update review and implications for Nigeria, and similar countries. Afr Health Sci 19 (2): 2000-2007. DOI: 10.4314/ahs.v19i2.23.

Otu AA, Udoh UA, Ita OI, Hicks JP, Egbe WO, Walley J. 2019b. A cross sectional survey on the seroprevalence of dengue fever in febrile patients attending health facilities in Cross River State, Nigeria. PLoS One 14 (6): e0215143. DOI: 10.1371/journal.pone.0215143.

Rao MR, Padhy RN, Das MK. 2016. Prevalence of dengue viral and malaria parasitic co-infections in an epidemic district, Angul of Odisha, India: An eco-epidemiological and cross-sectional study for the prospective aspects of public health. J Infect Public Health 9 (4): 421-428. DOI: 10.1016/j.jiph.2015.10.019.

Rufai T, Aninagyei E, Akuffo KO, et al. 2022. Malaria and typhoid fever among patients presenting with febrile illnesses in Ga West Municipality, Ghana. PLoS One 17 (5): e0267528. DOI: 10.1371/journal.pone.0267528.

Saidu JZ, Okojie RO. 2024. Concurrent infection of dengue virus with malaria parasites among outpatients attending healthcare facilities in Benin city, Nigeria. Porto Biomed J 9 (2): e249. DOI: 10.1097/j.pbj.0000000000000249.

Salam N, Mustafa S, Hafiz A, Chaudhary AA, Deeba F, Parveen S. 2018. Global prevalence and distribution of coinfection of malaria, dengue and chikungunya: A systematic review. BMC Public Health 18 (1): 710. DOI: 10.1186/s12889-018-5626-z.

Siddig EE, Al-Amin M, El-Sayed A, Elmangory MM, Al-Hakam A, El-Gaddal A, Al-Hassan M, Mohamed NS, Salih K, Eltahir K, Hassanain S. 2023. Severe coinfection of dengue and malaria: A case report. Clin Case Rep 12 (6): e9079. DOI: 10.1002/ccr3.9079.

World Health Organization. 2021. World malaria report 2021. World Health Organization, Geneva. https://www.who.int/teams/global-malaria-programme/reports/world-malaria-report-2021.

World Health Organization. 2024. Dengue and severe dengue. World Health Organization, Geneva. https://www.who.int/news-room/fact-sheets/detail/dengue-and-severe-dengue.

NUSANTARA BIOSCIENCE
Vol. 17, No. 2, pp. 259-276
November 2025

ISSN: 2087-3948
E-ISSN: 2087-3956
DOI: 10.13057/nusbiosci/n170209

Bamboo diversity, ecological structure, and utilization in the riparian ecosystem of the upper Bengawan Solo River, Central Java, Indonesia

FIKA NUR APRILIA[1], FRANSISCA AMELIA KARTIKA ARDHYANTI[1], GHAZY AQILA SHANDY PRABOWO[1], HANA PARAMESTI[1], ANA SHOLEKAH ASZAR[2,3], CHEE KONG YAP[4], AHMAD DWI SETYAWAN[1,5,♥]

[1]Department of Environmental Science, Faculty of Mathematics and Natural Science, Universitas Sebelas Maret. Jl. Ir. Sutami No. 36, Surakarta 57126, Central Java, Indonesia. Tel./fax.: +62-271-663375, ♥email: volatileoils@gmail.com

[2]Department of Biology, Faculty of Mathematics and Natural Sciences, Universitas Sebelas Maret. Jl. Ir. Sutami No. 36, Surakarta 57126, Central Java, Indonesia

[3]Biodiversity Study Club, Faculty of Mathematics and Natural Sciences, Universitas Sebelas Maret. Jl. Ir. Sutami No. 36, Surakarta 57126, Central Java, Indonesia

[4]Department of Biology, Faculty of Science, Universiti Putra Malaysia. 43400 UPM Serdang, Selangor, Malaysia

[5]Biodiversity Research Group, Universitas Sebelas Maret. Jl. Ir. Sutami No. 36, Surakarta 57126, Central Java, Indonesia

Manuscript received: 14 May 2025. Revision accepted: 10 November 2025.

Abstract. *Aprilia FN, Ardhyanti FAK, Prabowo GAS, Paramesti H, Aszar AS, Yap CK, Setyawan AD. 2025. Bamboo diversity, ecological structure, and utilization in the riparian ecosystem of the upper Bengawan Solo River, Central Java, Indonesia. Nusantara Bioscience 17: 259-276.* Bamboo plays an important ecological and socio-economic role in tropical riparian landscapes, yet its spatial structure and environmental determinants remain poorly quantified. This study analyzed the diversity, composition, ecological dominance, and utilization of bamboo communities along the upstream–midstream–downstream gradient of the upper Bengawan Solo River, Central Java, Indonesia. Field surveys recorded five species—*Bambusa spinosa*, *Dendrocalamus asper*, *Gigantochloa apus*, *G. atter*, and *G. atroviolacea*—distributed unevenly across riparian zones. Diversity, species richness, and structural heterogeneity increased downstream, shifting from monodominant *B. spinosa* stands upstream to multi-species *Gigantochloa* assemblages in lowland alluvial areas. Importance Value Index (IVI) patterns revealed strong environmental filtering in the upstream zone, mixed natural–managed dominance midstream, and cultivation-enhanced coexistence downstream. Pearson correlation analysis indicated that soil moisture, canopy openness, and soil pH were the strongest predictors of diversity, whereas species dominance was shaped primarily by ecological traits and management intensity. Utilization patterns reflected a biocultural continuum, with *D. asper* and *Gigantochloa* spp. providing multipurpose materials for construction, food, handicrafts, and cultural practices, while *B. spinosa* served chiefly as an ecological stabilizer in upland slopes. The riparian bamboo system represents a socio-ecological mosaic shaped by hydrological gradients and community management. These findings highlight bamboo's potential as a nature-based solution for riparian stabilization, biodiversity conservation, and livelihood support. Strengthening integrated, community-based bamboo management could enhance ecological resilience and sustainable riverine landscape governance in tropical regions.

Keywords: Bamboo diversity, Bengawan Solo River, ecological structure, riparian ecosystem, utilization potential

INTRODUCTION

Bamboo forests constitute one of the most ecologically and socio-economically significant vegetation components in tropical and subtropical Asia, contributing to soil stability, microclimate regulation, habitat provisioning, and rural livelihoods (Bystriakova et al. 2004; Nath et al. 2020). Indonesia is recognized as a global center of bamboo diversity, hosting more than 160 species with high endemism (Widjaja and Kartikasari 2001; Wong 2004). Across the archipelago, bamboo fulfills multifunctional roles ranging from slope stabilization and water regulation to the provision of raw materials for construction, crafts, food, and cultural practices (Silva et al. 2020; Lobovikov et al. 2007; Rani et al. 2024). In riparian ecosystems, bamboo stands are particularly important as natural buffers that protect riverbanks from erosion, enhance water quality by filtering sediments, and maintain hydrological stability. These ecological functions align with current global frameworks emphasizing nature-based solutions for watershed management and river rehabilitation (FAO 2020).

Despite the ecological importance of bamboo in riparian landscapes, research in Indonesia has been disproportionately concentrated on taxonomy, propagation techniques, and general ethnobotanical use. Relatively few studies have examined how bamboo communities are structured along river corridors, particularly in relation to environmental gradients such as slope, soil moisture, canopy openness, and anthropogenic disturbance. This represents a substantial research gap, considering that riparian ecosystems are among the most dynamic and human-impacted landscapes in the tropics. In Java, studies have focused primarily on upland bamboo assemblages (Arinasa and Sujarwo 2015), bamboo agroforestry systems (Setiawati et al. 2017), or ethnobotanical practices in rural communities (Yanty et al. 2019; Ihsan et al. 2023), but zone-based ecological assessments along riverine gradients remain largely undocumented.

From an ecological perspective, bamboo species exhibit growth strategies that allow them to rapidly colonize and dominate riparian zones. Rhizomatous root systems, rapid culm regeneration, and tolerance to disturbance enable certain taxa—such as *Bambusa spinosa*, *Dendrocalamus asper*, and *Gigantochloa apus*—to establish monospecific or co-dominant stands following flooding, erosion, or human intervention (Xu et al. 2020; Nath et al. 2020). However, these adaptive advantages may also suppress diversity in harsher upstream environments, whereas higher moisture and nutrient availability downstream often support more heterogeneous assemblages. Understanding how these ecological processes translate into spatial changes in diversity indices (H′, R, E) and Importance Value Index (IVI) is essential for predicting ecosystem function and resilience.

Equally important is the socio-ecological dimension of bamboo in Javanese landscapes. Local communities extensively utilize species such as *G. apus*, *G. atter*, and *D. asper* for construction materials, woven products, agricultural tools, and edible shoots (Widjaja and Kartikasari 2001; Ekawati et al. 2022). However, quantitative analyses linking ecological dominance with documented and potential utilization categories remain scarce, especially in riparian habitats where ecological function and cultural utility overlap. This gap limits our understanding of how community preferences and management practices influence bamboo distribution, regeneration, and long-term ecological stability.

The Bengawan Solo River, the longest river in Java, Indonesia, traverses diverse ecological and socio-economic zones. Its upper stretches are characterized by steep slopes, mixed agroforestry mosaics, and rapidly transforming riparian vegetation (Maulana et al. 2019). Habitat alteration through land conversion, sedimentation, selective cutting, and patchy replanting has led to shifts in bamboo species composition and structural integrity (Ferreira et al. 2019). Yet, no prior study has analyzed how bamboo diversity, IVI-based dominance, and environmental variables jointly structure bamboo communities along the upper Bengawan Solo riparian gradient. Moreover, the integration of ecological metrics with utilization data has not been attempted in this region, despite its importance for community-based conservation and watershed management.

Accordingly, this study was designed to (i) document the composition and diversity of bamboo species across the upstream, midstream, and downstream segments of the upper Bengawan Solo River; (ii) analyze ecological structure and dominance patterns based on density, frequency, and IVI; and (iii) assess documented and potential uses of each species to identify socio-ecological linkages relevant for management. By combining ecological indicators with ethnobotanical relevance and environmental drivers, this research provides the first spatially explicit, socio-ecologically integrated assessment of riparian bamboo communities in Central Java. The findings are expected to strengthen the scientific basis for bamboo-based riparian restoration and sustainable landscape management within tropical river systems.

MATERIALS AND METHODS

Study area

This study was conducted in March 2025 in the riparian landscape of the upper Bengawan Solo River, Central Java, Indonesia, which flows through the upland catchments of Wonogiri before entering the agricultural lowlands of Klaten and Sukoharjo Districts (JICA 2007). Three sampling sites representing distinct hydrological and land-use segments were selected: Giriwono (upstream), Sidowarno (midstream), and Gadingan (downstream). These locations were chosen to capture ecological variability along the longitudinal gradient of the river—an approach commonly used in riparian ecology (Naiman and Décamps 1997)—and to represent natural, semi-natural, and intensively managed riparian conditions. The spatial configuration of the study area is shown in Figure 1.

The upstream area at Giriwono (~135 m asl) is characterized by hilly terrain, steep riparian slopes, and mixed dryland agriculture interspersed with remnant forest patches. As part of the Bengawan Solo upland catchment, this zone contributes perennial water flow to the river despite seasonal climate variation (Whitten et al. 1997). Riparian vegetation is relatively wide and buffered, with bamboo occurring naturally near the boundaries of the Alas Kethu protected forest.

The midstream zone in Sidowarno (~95 m asl) represents a transitional agricultural landscape dominated by rice, sugarcane, tobacco, and agroforestry mosaics. Volcanic-derived regosol soils form the dominant substrate, supporting intensive farming. Human disturbance is more substantial here, with riparian strips managed directly by farmers for fencing, scaffolding, and soil stabilization (Radnawati and Fatmala 2020).

The downstream site at Gadingan (~85 m asl) lies on alluvial floodplains formed by long-term deposition from upstream erosion and volcanic sediments. These fertile substrates support extensive rice cultivation and settlement development. Riparian buffers are narrow or fragmented, and bamboo communities are dominated by cultivated stands planted along irrigation channels or field boundaries.

The region experiences a tropical monsoon climate with annual rainfall of 2,000-2,500 mm and temperatures generally ranging from 23-30 °C (BMKG 2023a, b). These climatic conditions facilitate rapid bamboo growth and continuous culm production, as commonly observed in monsoonal Southeast Asia (Sembada et al. 2025).

Sampling design

A stratified–systematic sampling design (Mueller-Dombois and Ellenberg 1974; Kent and Coker 1992) was implemented to represent ecological variation across the upstream, midstream, and downstream segments of the Bengawan Solo River. Each segment was treated as an independent ecological stratum reflecting differences in topography, land use, and hydrological influence. Within each stratum, 10 vegetation plots were systematically established, resulting in 30 plots across all sites.

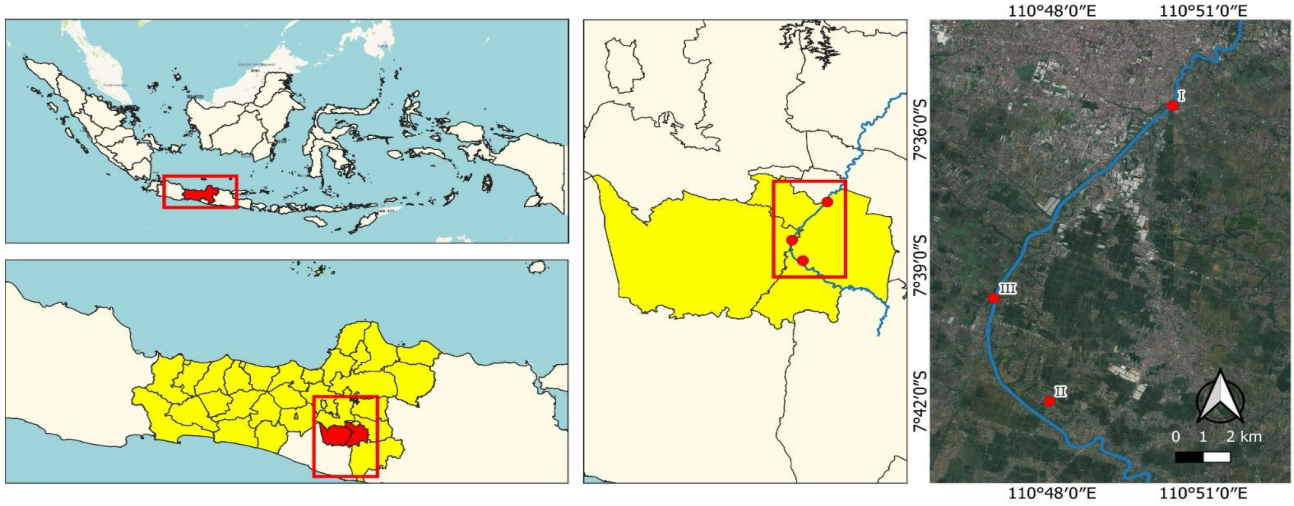

Figure 1. Map of the research locations along the upper Bengawan Solo River, Central Java, Indonesia: I. Gadingan Village, Mojolaban Sub-district, Sukoharjo District (7°34'37.1"S 110°50'45.0"E); II. Giriwono Village, Wonogiri Sub-district, Wonogiri District, (7°47'48.1"S 110°56'08.4"E); and III. Sidowarno Village, Wonosari Sub-district, Klaten District (7°38'34.2"S 110°47'31.3"E)

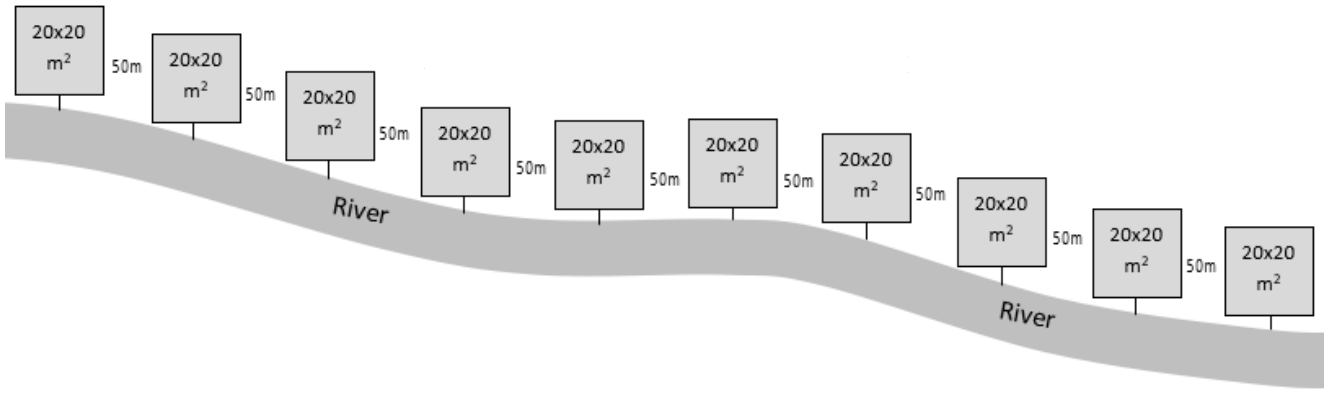

Figure 2. Diagram showing the sampling layout design for vegetation plots (10 plots per site) along the riparian gradient

Each plot measured 20 × 20 m (400 m²), providing 0.4 ha of sampling area per site (1.2 ha total). Plots were positioned at approximately 50 m intervals along a single riverbank to ensure consistent representation of riparian vegetation, following best practices in riparian vegetation sampling (Sutherland 2006), with the linear arrangement of the ten plots at one site illustrated in Figure 2. Plot placement began near the river edge, where hydrological influence is strongest, and extended toward adjacent agricultural or settlement zones. Plot boundaries were marked with stakes, and GPS coordinates of plot centers were recorded using a Garmin eTrex 32x (±3 m accuracy).

This sampling design captured both natural and managed bamboo stands while reflecting spatial heterogeneity associated with hydrological gradients and anthropogenic pressures (Naiman and Décamps 1997).

Vegetation data collection

Within each plot, all bamboo clumps (culm clusters) were identified to species level and treated as individual sampling units. Structural measurements followed standard procedures for Southeast Asian forest and bamboo vegetation (Soerianegara and Indrawan 2002; Liese and Köhl 2015). For each clump, species identity, culm count, average height, and diameter were recorded. Culm diameter was measured at breast height (1.3 m above ground), while height was estimated using a graduated pole or laser rangefinder.

Vegetative morphological characteristics were documented to support identification, including culm color, internode length, sheath morphology, wall thickness, and branching pattern—traits widely used in bamboo taxonomy (Ohrnberger 1999; Widjaja and Kartikasari 2001). Field assistants received prior training on bamboo recognition and measurement techniques to reduce observer bias.

Representative photographs were taken to support post-field verification.

Environmental variables

A suite of environmental variables was measured within each plot to contextualize bamboo community variation. Soil pH was measured with a portable pH meter, soil moisture using a soil moisture probe, and soil temperature using a soil thermometer, following standard ecological soil measurement protocols (Allen 1989).

Microclimatic variables—including air temperature and relative humidity—were measured using a digital hygrometer. Canopy openness was estimated using a spherical densiometer (Lemmon 1956) and categorized into open, moderate, or closed canopy classes. Topographic parameters such as slope gradient and elevation were recorded visually or with a clinometer. Distance to the river channel was measured to capture varying degrees of riparian influence. Environmental measurements were carried out between 08:00 and 11:00 a.m. to minimize diurnal variability, as recommended in standard ecological monitoring guidelines (Sutherland 2006).

Species identification and taxonomic verification

Species identification followed the taxonomic keys and field guides of Ohrnberger (1999) and Widjaja and Kartikasari (2001). Diagnostic vegetative features—including sheath characteristics, culm coloration, leaf morphology, branching pattern, and internode dimensions—were used due to the infrequent flowering of most bamboo species (Liese and Köhl 2015). Scientific names were validated using international databases: the GBIF Backbone Taxonomy (2024), International Plant Names Index (IPNI 2024) and Plants of the World Online (POWO 2024) ensuring nomenclatural accuracy. Voucher specimens were collected and deposited in the Herbarium of Universitas Sebelas Maret, Central Java. Metadata included plot number, GPS coordinates, and habitat characteristics.

Data analysis

Community structure

Phytosociological parameters were calculated following standard procedures (Mueller-Dombois and Ellenberg 1974; Soerianegara and Indrawan 2002). Density (D) was expressed as clumps per hectare. Frequency (F) represented the proportion of plots in which a species occurred. Dominance (Do) was estimated using basal area based on mean culm diameter (Liese and Köhl 2015). Relative values—Relative Density (RD), Relative Frequency (RF), and Relative Dominance (RDo)—were calculated and summed to obtain the Importance Value Index (IVI), a robust indicator of species ecological significance (Kent and Coker 1992).

Diversity indices

Bamboo community diversity was calculated using the Shannon–Wiener index (H′), Margalef richness index (R), and Pielou's evenness index (E) (Pielou 1975; Magurran 2004). Interpretation of H′ values followed Junaedi and Mutaqien (2010), where H′ <1.0 indicates low diversity, 1.0-3.0 indicates moderate diversity, and ≥3.0 denotes high diversity.

Comparative analysis

Ecological differences among upstream, midstream, and downstream sites were assessed by comparing species richness, abundance, IVI, and diversity indices and relating them to observed environmental variation (Naiman and Décamps 1997). Visual comparisons were generated through bar and line charts.

Correlation analysis

To evaluate associations between environmental conditions and bamboo community attributes, Pearson's correlation analysis was conducted after normality testing with the Shapiro–Wilk test. This approach follows established ecological statistical practices (Magurran 2004). Analyses were performed in IBM SPSS Statistics 26, with visualization in Microsoft Excel 2021.

Utilization assessment

Utilization categories—construction, handicraft, agriculture/forestry, food, medicine, culture, and landscape—follow established classifications of bamboo uses (Widjaja and Kartikasari 2001; Irawan et al. 2025). Documentation included literature review and field observations near study sites. Utilization profiles were interpreted in relation to ecological dominance (IVI) to identify multifunctional species supporting riparian ecosystem stability and local livelihoods (Bystriakova et al. 2004).

RESULTS AND DISCUSSION

Species composition across riparian zones

A total of five bamboo species belonging to three genera were recorded across the riparian zones of the upper Bengawan Solo River (Table 1). These species—*B. spinosa*, *D. asper*, *G. apus*, *G. atter*, and *G. atroviolacea*—showed uneven distribution among the upstream, midstream, and downstream segments, indicating strong zonation along the river gradient.

The upstream zone (Giriwono) contained only two species, *B. spinosa* and *D. asper*. *Bambusa spinosa* was particularly dominant, contributing 35 of the 53 clumps recorded in this segment, while *D. asper* was present in smaller numbers (18 clumps). The absence of *Gigantochloa* species in this zone (Table 1) reflects the drier, steeper upland conditions that limit the establishment of species requiring moister substrates.

In the midstream zone (Sidowarno), species richness increased to four, with *G. apus* appearing as a major component of the vegetation (24 clumps). *Dendrocalamus asper* also remained abundant (22 clumps), indicating its broad ecological tolerance. The presence of both naturally occurring and cultivated bamboo stands in this segment is consistent with the heterogeneous land-use mosaic surrounding irrigated fields and agroforestry systems. As shown in Table 1, midstream contains the highest total

clump abundance (66 clumps), suggesting both ecological suitability and active management.

The downstream zone (Gadingan) supported the highest richness, with all five species present and a strong representation of *Gigantochloa* species—especially *G. apus*, *G. atter*, and *G. atroviolacea*. These species collectively accounted for 43 of the 61 clumps recorded downstream (Table 1). Their presence corresponds to the wetter alluvial soils and more intensive human activities near settlements and irrigation channels, conditions that favor both natural growth and cultivated propagation.

Table 1 clearly shows that although total clump abundance varies only moderately across zones (53-66 clumps), species composition differs substantially, with downstream segments hosting exclusive species such as *G. atroviolacea* and upstream segments lacking the *Gigantochloa* group entirely. This longitudinal pattern highlights the combined influence of hydrology, soil conditions, and land-use practices in shaping bamboo distribution along the upper Bengawan Solo River.

Clump abundance and spatial distribution

Clump abundance varied across the upstream, midstream, and downstream zones, reflecting both ecological suitability and differing levels of human intervention along the riparian corridor. As shown in Table 1, a total of 180 bamboo clumps were recorded across all sites, with the midstream segment containing the highest number of clumps (66), followed by the downstream (61) and upstream zones (53). Although differences in total clump numbers among zones were not large, the spatial distribution and dominance patterns of individual species showed pronounced variation.

In the upstream zone, clump abundance was strongly skewed toward *B. spinosa*, which accounted for 35 of the 53 clumps recorded. This monodominant pattern reflects the species' ability to thrive on steep, well-drained riparian slopes with minimal soil moisture. *Dendrocalamus asper* formed the remaining 18 clumps, indicating a more limited distribution in this segment. The absence of all *Gigantochloa* species in the upstream zone (Table 1) reinforces the notion that this environment filters species based on tolerance to drier upland conditions.

In contrast, the midstream zone exhibited a more balanced distribution of clumps among species, indicating a mixed-dominance pattern. *Gigantochloa apus* (24 clumps) and *D. asper* (22 clumps) together contributed the majority of clumps in this segment, reflecting the transition from natural riparian vegetation to semi-managed agroforestry systems. The presence of multiple species with similar clump abundance suggests that midstream environmental conditions—moderate slopes, fertile regosol soils, and frequent human management—support a more heterogeneous bamboo community.

The downstream zone showed the most diverse assemblage of clump abundance patterns. *Gigantochloa apus* (18 clumps) and *G. atter* (15 clumps) were particularly prominent, while *G. atroviolacea*—absent upstream and midstream—was represented by 10 clumps. The distribution of clumps in downstream areas indicates a multi-species dominance pattern associated with moist alluvial soils, flatter terrain, and high levels of anthropogenic disturbance. Cultivated bamboo stands were common near irrigation channels, field boundaries, and settlement edges, facilitating the proliferation of *Gigantochloa* species.

The spatial distribution of clump abundance outlined in Table 1 demonstrates a clear ecological gradient: monodominance of drought-tolerant species in the upstream, mixed assemblages in the midstream, and multi-species, management-influenced communities downstream. These patterns are consistent with the combined influence of hydrology, soil conditions, and land-use intensity on bamboo growth and persistence in the riparian ecosystem of the upper Bengawan Solo River.

Structural parameters of bamboo communities

The structural characteristics of bamboo communities along the upper Bengawan Solo River exhibited clear spatial differentiation across the upstream, midstream, and downstream segments. Table 2 presents the density (clumps/ha), frequency of occurrence, and relative dominance for each species, illustrating how bamboo stands respond to varying riparian conditions and land-use intensity.

Table 1. Composition and abundance of bamboo species in the riparian zones of the upper Bengawan Solo River, Central Java, Indonesia

Species	Upstream (Giriwono)	Midstream (Sidowarno)	Downstream (Gadingan)	Total (clumps)	Distribution pattern
Bambusa spinosa Roxb.	35	14	8	57	Common in upstream, scattered in others
Dendrocalamus asper (Schult. & Schult.f.) Backer	18	22	10	50	Widespread
Gigantochloa apus (Schult.f.) Kurz ex Munro	0	24	18	42	Absent in upstream
Gigantochloa atter (Hassk.) Kurz	0	6	15	21	Concentrated in the downstream
Gigantochloa atroviolacea Widjaja	0	0	10	10	Restricted to the downstream
Total clumps (individuals)	53	66	61	180	—
Species richness (S)	2	4	5	11	—

Table 2. Density, frequency, and dominance of bamboo species in three riparian zones of the upper Bengawan Solo River, Central Java, Indonesia

Species	Clumps	Density (clumps/ha)	Frequency (%)	Relative dominance	Ecological remarks
Upstream (Giriwono)					
Bambusa spinosa	35	87.5	90	High	Highly clustered; forms pure stands
Dendrocalamus asper	18	45.0	60	Medium	Scattered along moist banks
Gigantochloa apus	0	0	0	—	Absent
Gigantochloa atter	0	0	0	—	Absent
Gigantochloa atroviolacea	0	0	0	—	Absent
Total	53	132.5	150		
Midstream (Sidowarno)					
Bambusa spinosa	14	35.0	50	Low–medium	Patchy; mostly in drier terraces
Dendrocalamus asper	22	55.0	70	High	Robust culms; strongly competitive
Gigantochloa apus	24	60.0	80	High	Most abundant in midstream
Gigantochloa atter	6	15.0	30	Low	Locally cultivated
Gigantochloa atroviolacea	0	0	0	—	Absent
Total	66	165.0	230		
Downstream (Gadingan)					
Bambusa spinosa	8	20.0	40	Low	Minor component
Dendrocalamus asper	10	25.0	50	Medium	Widespread along canals
Gigantochloa apus	18	45.0	70	High	Dominant along moist levees
Gigantochloa atter	15	37.5	60	High	Very common near settlements
Gigantochloa atroviolacea	10	25.0	50	Medium	Restricted to shaded wet patches
Total	61	152.5	270		

In the upstream zone (Giriwono), overall bamboo density reached 132.5 clumps/ha, largely driven by the dominance of *B. spinosa*. This species recorded the highest density (87.5 clumps/ha) and frequency (90%), forming dense, nearly monospecific stands along steep slopes. Its high structural dominance reflects strong adaptation to dry upland riparian environments, where thorny, robust culms help stabilize eroded surfaces. *Dendrocalamus asper* showed moderate density (45 clumps/ha) and frequency (60%), occurring mainly in wetter microhabitats near shaded banks. No *Gigantochloa* species were recorded in this zone (Table 2), indicating strong environmental filtering against moisture-dependent taxa.

Structural patterns became more heterogeneous in the midstream zone (Sidowarno). Total density increased to 165 clumps/ha, the highest among the three zones. *Gigantochloa apus* and *D. asper* showed very similar structural contributions, with densities of 60 and 55 clumps/ha, respectively, and high frequencies of 80% and 70%. Their co-dominance suggests that midstream riparian strips—characterized by moderate slopes, fertile regosol soils, and semi-managed agroforestry—provide suitable conditions for both naturally regenerating and cultivated bamboo stands. *Bambusa spinosa* exhibited reduced density (35 clumps/ha) and lower dominance, reflecting its preference for drier upland terrains. *Gigantochloa atter*, though less abundant (15 clumps/ha), appeared consistently in cultivation zones near irrigated fields.

In the downstream zone (Gadingan), structural parameters reflected the highest species-level diversity and the strongest influence of human management. Total density reached 152.5 clumps/ha, slightly lower than the midstream but distributed across all five species. *Gigantochloa apus* and *G. atter* showed high density values (45 and 37.5 clumps/ha) and high frequencies (70% and 60%), demonstrating their competitive advantage in moist alluvial soils. *Gigantochloa atroviolacea*—absent in upstream and midstream zones—was structurally significant here, with moderate density (25 clumps/ha) and frequency (50%), indicating its affinity for shaded, wetter riparian microhabitats. *Bambusa spinosa*, in contrast, had minimal structural contribution downstream, consistent with its ecological preference for upland and semi-dry slopes.

Comparisons across zones reveal several clear patterns. First, structural dominance is strongly type-specific: *B. spinosa* dominates uplands; *D. asper* and *G. apus* co-dominate transitional midstream habitats; and *Gigantochloa* species diversify and dominate lowland alluvial zones. Second, total density generally increases from upstream to midstream, reflecting greater management and vegetative propagation in midstream agroforestry areas. Finally, downstream communities exhibit the most balanced structural distribution, driven by high moisture availability, fertile alluvial substrates, and intentional cultivation by local communities.

Taken together, the structural data from Table 2 demonstrate that bamboo community structure along the upper Bengawan Solo River is shaped by a combination of hydrology, topography, substrate conditions, and human influence. These factors jointly determine which species can dominate, coexist, or persist in each riparian segment.

Ecological dominance based on Importance Value Index (IVI)

The ecological dominance of bamboo species along the upper Bengawan Solo River varied substantially across the upstream, midstream, and downstream zones, as reflected

by the Importance Value Index (IVI). IVI integrates Relative Density (RD), Relative Frequency (RF), and Relative Dominance (RDo), thereby providing a comprehensive measure of each species' structural and ecological contribution. The Importance Value Index presented in Table 3 clearly illustrate a strong longitudinal shift in dominance patterns along the riparian gradient.

In the upstream zone (Giriwono), *B. spinosa* exhibited the highest IVI (192.0), indicating overwhelming ecological control and forming nearly pure stands on steep riparian slopes. Its dominance is supported by consistently high RD, RF, and RDo values (each 60-66%), confirming that this species is not only the most abundant but also the most spatially and structurally influential in the upstream environment. *Dendrocalamus asper* followed with an IVI of 108.0, functioning as a secondary yet substantial co-dominant species. No *Gigantochloa* species were detected in this zone (Table 3), highlighting strong environmental filtering against taxa that prefer moist or alluvial substrates.

The midstream zone (Sidowarno) displayed a more balanced dominance structure, with *G. apus* attaining the highest IVI (107.6), followed closely by *D. asper* (97.0). These two species jointly structured the midstream bamboo community, reflecting moderately disturbed, fertile riparian strips with frequent agroforestry management. *Bambusa spinosa* held a much lower IVI (64.1), indicating a sharp decline in dominance relative to upstream conditions. *Gigantochloa atter*, while present, exhibited only a minor ecological role (IVI = 31.2), corresponding to its limited cultivation and lower structural impact (Table 3).

In the downstream zone (Gadingan), ecological dominance shifted further toward *Gigantochloa* species. *Gigantochloa apus* maintained the highest dominance (IVI = 84.9), followed by *G. atter* (71.4). Both species exhibited high RD and RDo values, consistent with their preference for moist alluvial soils and their frequent cultivation near irrigation channels. *Dendrocalamus asper* and *G. atroviolacea* shared equal IVI values (51.3), suggesting co-dominance in shaded or saturated riparian microhabitats. *Bambusa spinosa* had the lowest dominance downstream (IVI = 41.0), confirming its declining influence toward the lower river segments (Table 3).

A longitudinal comparison of Table 3 reveals three major ecological patterns. First, upstream zones are characterized by single-species dominance (*B. spinosa*), reflecting environmental filtering imposed by steep slopes, lower moisture, and minimal cultivation. Second, midstream zones display co-dominance, especially between *G. apus* and *D. asper*, reflecting a mixture of natural regeneration and human-supported cultivation. Third, downstream zones exhibit multi-species dominance, with *Gigantochloa* species becoming structurally prominent due to wetter soils, high nutrient availability, and intensive land-use modification.

These findings collectively indicate that ecological dominance in riparian bamboo communities is shaped by a combination of hydrological gradients, edaphic conditions, and human activities. The gradual replacement of *B. spinosa* by *Gigantochloa* species from upstream to down-stream reflects both species-specific habitat affinities and the increasing influence of cultivation in lowland riparian zones. This zonation underscores the dynamic interplay between natural ecological filters and anthropogenic pressures in determining bamboo community structure along the upper Bengawan Solo River.

Table 3. Importance Value Index (IVI) of bamboo species in the riparian zones of the upper Bengawan Solo River, Central Java, Indonesia.

Species	RD	RF	RDo	IVI	Dominance status
Upstream (Giriwono)					
Bambusa spinosa	66.0	60.0	66.0	192.0	Very dominant
Dendrocalamus asper	34.0	40.0	34.0	108.0	Co-dominant
Gigantochloa apus	0	0	0	0	Absent
Gigantochloa atter	0	0	0	0	Absent
Gigantochloa atroviolacea	0	0	0	0	Absent
Midstream (Sidowarno)					
Gigantochloa apus	36.4	34.8	36.4	107.6	Very dominant
Dendrocalamus asper	33.3	30.4	33.3	97.0	Co-dominant
Bambusa spinosa	21.2	21.7	21.2	64.1	Common
Gigantochloa atter	9.1	13.0	9.1	31.2	Subdominant
Gigantochloa atroviolacea	0	0	0	0	Absent
Downstream (Gadingan)					
Gigantochloa apus	29.5	25.9	29.5	84.9	Very dominant
Gigantochloa atter	24.6	22.2	24.6	71.4	Dominant
Dendrocalamus asper	16.4	18.5	16.4	51.3	Co-dominant
Gigantochloa atroviolacea	16.4	18.5	16.4	51.3	Co-dominant
Bambusa spinosa	13.1	14.8	13.1	41.0	Subdominant

Note: IVI: Importance Value Index, RD: Relative Density, RF: Relative Frequency, RDo: Relative Dominance

Bamboo diversity and evenness across the riparian gradient

Bamboo diversity along the upper Bengawan Solo River shows a pronounced longitudinal pattern driven by species richness, relative abundances, and environmental filtering. As presented in Table 4, all diversity indices—Shannon–Wiener (H′), Margalef richness (R), Simpson (1–D), and Evenness (E)—increase gradually from the upstream to downstream segments, indicating a shift from structurally simple to more compositionally balanced bamboo communities.

The upstream zone (Giriwono) exhibits the lowest diversity (H′ = 0.653; R = 0.252), reflecting its two-species community strongly dominated by *B. spinosa* (Table 4). Although evenness appears high (E = 0.942), this largely reflects the proportional balance between only two species rather than true ecological heterogeneity, consistent with strong dominance by *B. spinosa* in upstream plots, where one species contributes disproportionately to basal area. The low Simpson value (1–D = 0.449) further indicates that community structure is heavily influenced by a single dominant species. These patterns align with the environmental characteristics of the upstream segment—steeper slopes, drier soils, and broader natural riparian buffers—which collectively restrict the establishment of species that depend on higher moisture or more disturbed microhabitats.

In contrast, the midstream site (Sidowarno) presents moderate richness and diversity (R = 0.716; H′ = 1.288; 1–D = 0.740). The co-occurrence of *D. asper*, *G. apus*, and several minor taxa produces a more heterogeneous assemblage. Evenness remains relatively high (E = 0.929), suggesting that species abundances are not strongly skewed toward a single dominant species. The intermediate values recorded here reflect the transitional landscape—rice fields, mixed agroforestry, and semi-managed riparian vegetation—that facilitates coexistence between naturally occurring and cultivated bamboo species.

The downstream zone (Gadingan) has the highest species richness (S = 5) and diversity (H′ = 1.515; R = 0.973; 1–D = 0.790). Evenness is likewise high (E = 0.942), indicating that no single species overwhelmingly dominates the community. The fertile alluvial soils, shallow slopes, and intensive land use contribute to greater environmental heterogeneity, while human-directed planting enhances the establishment of *Gigantochloa* species such as *G. apus* and *G. atter*.

The simultaneous increase of H′, R, and 1–D values toward the downstream zone reflects a pronounced ecological gradient, beginning with low-diversity communities in the upstream where strong natural filtering limits species establishment, transitioning into the midstream where mixed natural–managed assemblages emerge under moderate environmental heterogeneity and human influence, and culminating in the downstream area where intensified management interventions and more favorable site conditions support highly diverse, structurally complex plant communities.

This pattern suggests that intermediate disturbance and human management can elevate bamboo diversity, whereas the upstream region retains a more specialized assemblage adapted to harsher geomorphological conditions. The combined indices from Table 4 thus highlight the complementary roles of environmental gradients and land-use intensity in shaping the riparian bamboo diversity of the upper Bengawan Solo River.

Environmental characteristics of the riparian zones

Environmental conditions varied markedly along the upstream–midstream–downstream gradient of the upper Bengawan Solo River, as summarized in Table 5. These variations shaped the structure, composition, and ecological performance of bamboo communities across the three zones. In the upstream area (Giriwono), steeper slopes (12-25%), moderately moist soils, and cooler microclimates (24-27°C air temperature) produced a physiographic setting that favored drought-tolerant species such as *B. spinosa*. Soil pH was slightly acidic (6.1-6.4), and canopy openness ranged from moderate to closed, reflecting the presence of remnant forest patches and agroforestry vegetation.

The midstream zone (Sidowarno) presented more moderate environmental conditions, with gentle slopes (5–12%), intermediate soil moisture, and a slightly wider pH range (6.3–6.7). This zone also exhibited moderate canopy openness (40–70%), which, combined with extensive agroforestry and irrigated agriculture, created structurally heterogeneous riparian habitats. The predominance of alluvial-volcanic soils and moderate disturbance favored the co-dominance of *D. asper* and *G. apus*.

Table 4. Diversity indices of bamboo communities across three riparian zones of the upper Bengawan Solo River, Central Java, Indonesia

Zone	Species richness (S)	Total clumps (N)	Margalef richness (R)	Shannon–Wiener (H′)	Simpson (1–D)	Evenness (E)
Upstream (Giriwono)	2	53	0.252	0.653	0.449	0.942
Midstream (Sidowarno)	4	66	0.716	1.288	0.740	0.929
Downstream (Gadingan)	5	61	0.973	1.515	0.790	0.942

Table 5. Environmental characteristics of the three riparian zones of the upper Bengawan Solo River, Central Java, Indonesia

Environmental variable	Zone		
	Upstream (Giriwono)	Midstream (Sidowarno)	Downstream (Gadingan)
Elevation (m asl)	135	95	85
Slope gradient (%)	12-25 (moderate–steep)	5-12 (gentle–moderate)	0-5 (flat)
Soil moisture class	Moderately moist–wet	Moderately moist	Dry–moderately moist
Soil pH (field measurement)	6.1-6.4	6.3-6.7	6.5-6.9
Soil temperature (°C)	25-27	26-28	27-29
Air temperature (°C)	24-27	25-29	27-31
Relative humidity (%)	70-82	67-78	65-75
Canopy openness	Moderate–closed (40-70%, >70%)	Moderate (40-70%)	Open–moderate (<40%, 40-70%)
Distance to river channel (m)	5-20	3-15	2-10
Dominant land use	Dryland farming, forest edges	Rice fields, agroforestry	Rice fields, settlements
Riparian buffer width (approx.)	10-30 m	5-15 m	3-10 m

Table 6. Summary of Pearson correlation trends between environmental variables and ecological indices

Environmental variable	Correlation with H′ (Diversity)	Correlation with IVI (Dominance)
Soil pH	Weak positive	Weak–moderate positive
Soil moisture	Moderate positive	Weak positive
Soil temperature	Weak negative	Weak negative
Canopy openness	Moderate positive	Very weak / non-significant
Slope gradient	Moderate positive	Weak negative
Distance to river	Weak negative	Non-significant
Air temperature	Weak–moderate negative	Weak negative

Note: IVI: Importance Value Index

In contrast, the downstream zone (Gadingan) was characterized by flat terrain (0-5%), drier soil conditions, and higher temperatures (up to 31°C). Soil pH tended toward the neutral range (6.5-6.9), and canopy openness was predominantly open to moderate, reflecting intensive agriculture and human settlement. Riparian buffer widths were narrow (3-10 m), and distances to the river were shortest (2-10 m), indicating strong hydrological influence but also substantial anthropogenic modification. These conditions supported the highest bamboo richness and structural diversity, particularly for *G. apus*, *G. atter*, and *G. atroviolacea*, which tolerate or benefit from more disturbed, sun-exposed environments. The environmental contrasts among the zones—especially slope, canopy openness, soil moisture, and pH—provided strong ecological filters that contributed to the distinct zonation patterns observed in bamboo communities along the river.

Relationships between environmental variables and bamboo diversity

The influence of environmental gradients on bamboo diversity and ecological dominance was evaluated using Pearson correlation analysis, with the main trends summarized in Table 6. Diversity (H′) showed positive correlations with soil moisture and canopy openness, indicating that bamboo communities became more diverse in areas with higher moisture availability and greater light penetration. This trend aligns with the higher species richness and evenness recorded in the downstream zone, where open canopies and moderately moist alluvial soils favored the coexistence of multiple *Gigantochloa* species.

Soil pH exhibited a weak positive correlation with H′, suggesting that slightly more neutral soils, as found downstream, may support broader species establishment. Slope gradient showed a moderate positive correlation with H′ at the overall dataset level, but this relationship is likely influenced by midstream variation, since the steepest upstream slopes still maintained low diversity due to environmental filtering. As a result, the positive slope–diversity trend weakened toward the downstream zone, where terrain becomes flatter and topographic constraints are minimal.

Negative correlations were observed for soil temperature and air temperature, implying that hotter conditions reduced overall diversity. This is consistent with the physiological limitations of some bamboo taxa in dry, exposed microhabitats, although managed planting downstream partially compensated for these thermal constraints.

In terms of ecological dominance (IVI), correlations were generally weaker than those for diversity. IVI had a weak to moderate positive correlation with soil pH, indicating that some dominant species, particularly *D. asper* and *G. apus*, performed better in neutral to slightly acidic soils. Canopy openness showed little to no correlation with IVI, suggesting that dominance patterns were influenced more by clump expansion and management than by light availability.

Distance to the river exhibited weak or non-significant correlations with both H′ and IVI, reflecting the ability of bamboo to thrive in both near-bank and slightly elevated positions, depending on species-specific adaptations. These relationships highlight that moisture, canopy structure, and

pH are the key drivers of bamboo diversity, whereas dominance patterns are more strongly shaped by species traits and management practices.

Utilization potential of bamboo species

The five bamboo species recorded along the upper Bengawan Solo River exhibited diverse and culturally significant utilization patterns, as detailed in Table 7. Across all sites, bamboo uses spanned construction, handicrafts, agriculture and forestry applications, food, medicinal use, cultural activities, and landscaping. However, the degree of multifunctionality varied across species.

Dendrocalamus asper demonstrated the broadest utility (seven categories) and represents the most valuable species for local communities. Its large, thick-walled culms are essential for heavy construction, bridges, and farm structures, while its edible shoots (*rebung*) are widely consumed. The species' high IVI in the midstream and downstream zones reflects both ecological success and strong socio-economic demand. Its leaves and culm sheaths are also used in fodder and traditional medicine, integrating the species into numerous livelihood activities.

Gigantochloa atter and *G. atroviolacea* both support six categories of use but differ functionally. *Gigantochloa atter* is highly valued for furniture, utensils, and craftwork due to its flexibility and moderate culm thickness, and its edible shoots provide an additional resource. *Gigantochloa atroviolacea*, recognized by its distinctive dark culms, plays an important role in cultural expression and ornamentation. Although its shoots are edible, they are not widely consumed. Its aesthetic and symbolic functions contribute to its sustained planting in downstream settlements. *Gigantochloa apus*, widely cultivated along midstream and downstream riparian strips, is indispensable for weaving, scaffolding, and erosion-control structures due to its straight, durable culms. Its high IVI corresponds with its exceptional practical value, making it a cornerstone species in village construction and irrigation maintenance. *Bambusa spinosa*, while less economically versatile, remains ecologically and culturally significant. Its thorny culms form natural barriers used for fencing, erosion control on steep banks, and ceremonial structures in traditional events. The species' strong dominance upstream reflects its ecological suitability to harsh slopes rather than its economic flexibility.

The relationship between IVI and utilization patterns demonstrates that species with high ecological dominance tend to provide broad socio-economic benefits, but species with unique morphological or cultural attributes may receive special attention from local communities despite lower abundance. This interplay between ecological performance and human preference underscores the integrated ecological–cultural role of bamboo in riparian landscapes of Central Java.

Discussion

Environmental filtering and longitudinal zonation of bamboo communities

The longitudinal variation in bamboo species composition along the upper Bengawan Solo River reflects a strong environmental filtering process shaped by topographic gradients, hydrological regimes, and edaphic heterogeneity. Species richness increased from the upstream (S = 2) to the downstream segment (S = 5) (Table 1), a pattern consistent with theoretical and empirical studies showing that riparian vegetation becomes more diverse under lower elevation, gentler slopes, and more stable moisture regimes (Sharma and Chongtham 2015; Nath et al. 2020; Chen et al. 2022). Steep slopes (12-25%), lower soil moisture, and cooler microclimate in the upstream zone (Table 5) restricted colonization to drought-tolerant taxa, most notably *B. spinosa*, whose mechanical rigidity, thorny culms, and deep-rooting rhizomes confer strong resistance to desiccation and slope instability. These traits position *B. spinosa* as an upland ecological specialist, illustrating a classic case of environmental filtering where only taxa with specific stress-tolerant traits can persist under harsh abiotic conditions—a pattern observed in tropical riparian bamboo systems across India, Nepal, and Indonesia (Sofiah et al. 2018; Larinmuana et al. 2025).

In contrast, the midstream zone represents a transitional environment with moderate slopes (5-12%), higher soil moisture, and mixed agroforestry influence (Table 5), enabling the coexistence of *D. asper* and *G. apus*. The increase in species richness (S = 4) and a more balanced abundance distribution (Table 1) indicate weakened environmental filtering and stronger niche complementarity. *Dendrocalamus asper* tolerates periodic disturbance and varied moisture regimes, whereas *G. apus* thrives in semi-managed habitats with intermediate canopy openness. Their co-occurrence supports the intermediate disturbance model, where moderate anthropogenic and hydrological disturbance promotes coexistence of tolerant and disturbance-dependent taxa (Connell 1978; Chazdon 2014). Recent studies have shown similar mixed-dominance configurations in agro-riparian bamboo assemblages in Vietnam and Laos (Chen et al. 2022).

Downstream sites exhibited the highest species richness (S = 5) and diversity (H′ = 1.515) (Table 4), driven by the presence of *G. atter* and *G. atroviolacea*, which prefer moist alluvial soils with high nutrient content. These species benefited from shallow slopes (0–5%), near-neutral soil pH (6.5-6.9), and frequent human cultivation (Table 5). The combination of favorable edaphic conditions and anthropogenic management created a heterogeneous mosaic that supports both natural regeneration and cultivation-driven expansion. This downstream pattern aligns with broader regional studies showing that bamboo diversity peaks in lowland floodplain environments with strong hydrological stability and human-assisted propagation (Kleinhenz and Midmore 2001; Nath et al. 2020).

The zonation pattern along the Bengawan Solo River demonstrates a coupled natural–anthropogenic gradient. In the upstream, abiotic filters—steep slopes, lower moisture, and narrower niche space—determine community

assembly. In the midstream, ecological tolerance and moderate disturbance shape mixed assemblages. Downstream, environmental heterogeneity and cultural management jointly promote the proliferation of species with higher moisture requirements and socio-economic value. This interaction between topographic constraints, hydrological regimes, and land-use practices reinforces the view that riparian bamboo communities in tropical landscapes form a socio-ecological continuum driven by both environmental determinism and human selection.

Spatial variation in community structure and dominance along the riparian gradient

Spatial variation in bamboo community structure along the upper Bengawan Solo River reflects the combined influence of topographic constraints, hydrological gradients, and species-specific functional strategies. Patterns of structural dominance, as indicated by density, frequency, and IVI values (Tables 2 and 3), show a clear longitudinal shift from monodominant upland stands to multi-species assemblages in downstream floodplains. In the upstream zone, *B. spinosa* exhibits overwhelming dominance (IVI = 192), forming dense monospecific stands on steep slopes with moderately moist but rapidly draining soils. Its thick-walled culms, thorny morphology, and deep rhizome system align with traits associated with upland stabilizer species in tropical riparian systems, where mechanical resistance to drought and geomorphological disturbance confers strong competitive advantage (Sharma and Chongtham 2015; Larinmuana et al. 2025). The structural simplicity of this zone, expressed through low richness (S = 2) and high frequency of a single taxon, exemplifies a community filtered predominantly by abiotic pressures.

In the midstream segment, community structure becomes more heterogeneous. *Gigantochloa apus* and *D. asper* attain comparable IVI values (107.6 and 97.0, respectively), producing a co-dominance configuration characteristic of transitional riparian habitats where environmental filtering weakens and niche overlap increases. This structural complexity is supported by moderate slopes, higher soil moisture, and semi-managed agroforestry systems that allow for both natural regeneration and human-mediated propagation. Similar mid-gradient dominance sharing among bamboo species has been documented in managed riparian corridors of Thailand, Laos, and southern China, where intermediate disturbance and greater canopy heterogeneity facilitate competitive coexistence (Chen et al. 2022). The presence of multiple structurally significant species in Sidowarno suggests that competitive hierarchies shift in response to changes in hydrological stability and land-use intensity.

The downstream zone presents the most compositionally and structurally diverse bamboo assemblage, driven by favorable alluvial soils, open canopies, and intensive human cultivation. Here, *G. apus* retains high dominance (IVI = 84.9), but its influence is balanced by substantial contributions from *G. atter* (IVI = 71.4) and *G. atroviolacea* (IVI = 51.3). These species possess traits associated with floodplain specialists, including rapid culm production, tolerance to periodic inundation, and strong vegetative propagation. The reduction in dominance of *B. spinosa* downstream (IVI = 41.0) marks a clear ecological transition from environmentally filtered upland specialists to human-supported lowland assemblages.

The gradual shift from single-species dominance upstream to multi-species co-dominance downstream illustrates a structural continuum governed by both environmental severity and socio-ecological facilitation. As hydrological regimes stabilize, soil fertility increases, and human management intensifies, dominance hierarchies weaken and structural heterogeneity rises. This pattern aligns with broader ecological theory suggesting that community structure in riparian vegetation is jointly regulated by abiotic filtering at higher elevations and competitive–facilitative dynamics in lowland, human-modified environments (Chazdon 2014; Breton et al. 2023). The structural transitions observed in the Bengawan Solo system therefore reflect the interplay of natural gradients and anthropogenic influence, producing a mosaic of bamboo communities that vary predictably in dominance, composition, and ecological function along the river corridor.

Diversity indices and their ecological significance

Patterns of alpha diversity along the upper Bengawan Solo River indicate that riparian bamboo communities are structured by a combination of environmental filtering, species functional traits, and cumulative land-use intensity. Diversity indices (H′, R, 1–D, E) in Table 4 reveal a consistent increase from upstream to downstream, reflecting a shift from environmentally constrained, low-richness assemblages toward more compositionally balanced and functionally diverse communities in lowland riparian zones. This gradient aligns with global evidence that riparian vegetation diversity correlates strongly with hydrological stability, soil moisture, and topographic moderation (Tabacchi et al. 2000; Capon et al. 2013).

The upstream zone, with only two species, displays low Shannon diversity (H′ = 0.653) and low Simpson diversity (1–D = 0.449), confirming that community structure is strongly dominated by *B. spinosa*. Although evenness is numerically high (E = 0.942), this pattern reflects proportional balance between only two species rather than genuine ecological heterogeneity. The dominance of *B. spinosa* underscores the role of environmental filtering on steep, erosion-prone upland slopes, where drought-tolerant and mechanically robust taxa outcompete moisture-dependent bamboo species. Similar patterns of low-diversity, morphologically uniform bamboo stands have been reported in upland river margins of Southeast Asia, as well as Java and Sumatra where steep terrain and shallow soils limit colonization by competitively weaker taxa (Valentin et al. 2008; Sofiah et al. 2018; Fitmawati et al. 2021).

Table 7. Documented and potential utilization categories of bamboo species in the riparian zones of the upper Bengawan Solo River, Central Java, Indonesia

Species	Potential utilization							Total categories	Notable remarks
	Construction	Handicraft	Agriculture / Forestry	Food	Medicine	Culture	Landscape		
Bambusa spinosa	✓	✓	✓	–	–	✓	✓	5	Thorny culms useful for fencing, erosion control, and ceremonial arches; forms natural protective barriers in dry zones.
Dendrocalamus asper	✓	✓	✓	✓	✓	✓	✓	7	Most multifunctional species; culms used for buildings and bridges; tender shoots (*rebung*) widely consumed; leaves used for fodder and traditional medicine.
Gigantochloa apus	✓	✓	✓	–	–	✓	✓	5	Highly valued for weaving, scaffolding, and stabilizing irrigation canal banks; commonly cultivated around settlements.
Gigantochloa atter	✓	✓	✓	✓	–	✓	✓	6	Flexible culms preferred for furniture, utensils, and craftwork; young shoots edible and occasionally marketed; often planted near agricultural areas.
Gigantochloa atroviolacea	✓	✓	–	✓	✓	✓	✓	6	Distinct dark culms favored for furniture and ornamentation; young shoots edible but not commonly consumed; valued for cultural and landscaping uses in downstream areas.

In midstream habitats, diversity metrics increase substantially (H′ = 1.288; R = 0.716; 1–D = 0.740), reflecting a transition from environmentally constrained dominance toward more equitable species contributions. The coexistence of *D. asper* and *G. apus*, supported by intermediate soil moisture and agroforestry practices, produces a structurally heterogeneous community with reduced dominance and greater niche overlap. These conditions mirror mid-gradient riparian zones elsewhere in Southeast Asia, where moderate disturbance and enhanced canopy heterogeneity promote species coexistence and functional redundancy (Chen et al. 2022). The relatively high evenness (E = 0.929) further suggests that species abundances are not strongly skewed toward a single taxon, reinforcing the role of midstream riparian corridors as biodiversity transition zones.

Downstream stands exhibit the highest richness and diversity (S = 5; H′ = 1.515; 1–D = 0.790), indicating a community that benefits from stable hydrology, fertile alluvial soils, and intensive human management. High evenness (E = 0.942) demonstrates that no species monopolizes community structure, a pattern typical of riparian bamboo assemblages cultivated for multiple socio-economic purposes. The presence of *G. atter* and *G. atroviolacea*, both floodplain-adapted species, reflects the combination of natural alluvial conditions and selective propagation by local communities. Such downstream enhancement of bamboo diversity parallels findings from the Mekong Basin and South China, where lowland riparian systems support the highest bamboo complexity due to favorable geomorphology and sustained resource management (Kamoto and Juntopas 2007; Xu et al. 2020; Breton et al. 2023; Yang et al. 2025).

Taken together, the longitudinal increase in diversity indices demonstrates a predictable ecological transition: environmentally constrained, specialist-dominated systems upstream give way to mixed natural–managed assemblages midstream, culminating in highly diverse, multifunctional communities downstream. These patterns support contemporary meta-analyses showing that riparian vegetation diversity is best explained by combined effects of hydrological reliability, soil fertility, and human facilitation (Capon et al. 2013). The Bengawan Solo case thus illustrates how bamboo communities function not merely as passive recipients of environmental gradients but as dynamic socio-ecological systems shaped by both biophysical processes and long-term human management.

Functional roles of dominant bamboo species in riparian stability and local livelihoods

The dominance patterns of *B. spinosa*, *D. asper*, and *Gigantochloa* species along the Bengawan Solo riparian gradient reveal distinct functional roles that integrate ecological processes with socio-economic practices. These species represent complementary ecological strategies—ranging from mechanical stabilization in upper catchments to multifunctional provisioning services in mid- and downstream systems. This functional differentiation aligns with broader evidence that bamboo taxa act as both ecological engineers and livelihood-supporting resources in tropical riparian landscapes (Kumar et al. 2023; Camargo-Caicedo et al. 2025).

In the upstream zone, *B. spinosa* functions primarily as a structural stabilizer. Its dense, thorny clumps and deep rhizome systems confer strong resistance to erosion and surface runoff, particularly on steep slopes. These traits are consistent with findings in Himalayan upland watersheds, where clump-forming bamboo species significantly reduce soil loss and reinforce riverbank integrity under high-gradient conditions (Panmei et al. 2025; Singh et al. 2025). Although its socio-economic value is limited compared with downstream species, *B. spinosa* provides essential regulating services that underpin hydrological stability and sediment control, indicating its role as a foundational ecological species within the upper riparian corridor.

In the midstream zone, *D. asper* occupies a dual ecological–economic niche. Ecologically, its tall culms and extensive rhizome networks enhance riverbank buffering capacity, moderate flood impacts, and generate microhabitats for understory vegetation and soil fauna. Socio-economically, *D. asper* is one of Southeast Asia's most valuable bamboo resources, widely utilized for construction, furniture, scaffolding, and edible shoots. Its high growth rate and tolerance of moderate disturbance allow communities to integrate this species into agroforestry and mixed-cropping systems without compromising ecological function. Such multifunctionality reflects broader patterns observed in managed riparian bamboo systems in Thailand, Vietnam, and Yunnan, where *D. asper* contributes substantially to both ecological resilience and rural income diversification (Chen et al. 2022).

Downstream communities dominated by *G. apus*, *G. atter*, and *G. atroviolacea* display the highest degree of functional multifunctionality. These species collectively support diverse provisioning services—ranging from craft materials and ornamental culms to edible shoots—while also maintaining ecological contributions such as soil binding, canopy stratification, and hydrological buffering. Their presence in alluvial zones parallels global observations that lowland riparian habitats support bamboo species with the most extensive socio-economic value due to fertile soils, stable hydrology, and historical cultivation. Notably, *G. atroviolacea* adds cultural and aesthetic value through its dark culms, reinforcing the role of bamboo in traditional art, architecture, and ritual practices.

The functional interactions among these species demonstrate a gradient-based socio-ecological system in which ecological performance and human use co-evolve. Upstream stabilizer species, midstream dual-function taxa, and downstream multifunctional species collectively form a riparian mosaic that supports watershed protection, resource production, and cultural heritage. This integration is consistent with emerging socio-ecological resilience frameworks emphasizing that vegetation with high functional diversity enhances long-term system adaptability and livelihood security under climate variability (Capon et al. 2013; Folke et al. 2016).

The functional roles of dominant bamboo species along the Bengawan Solo River reflect both species-specific

ecological traits and culturally embedded management practices. Understanding these complementary functions is essential for designing riparian restoration and bamboo-based landscape management strategies that balance environmental stability with sustainable resource use.

Cultural and economic dimensions of bamboo utilization

Bamboo utilization along the Bengawan Solo riparian corridor reflects an integrated socio-ecological system in which species availability, cultural traditions, and rural economies are mutually reinforcing. The spatial variation in dominant taxa—*B. spinosa* upstream, *D. asper* midstream, and *Gigantochloa* spp. downstream—corresponds directly with differentiated cultural practices and livelihood strategies, demonstrating that bamboo functions not only as a biological resource but also as a cultural infrastructure. Such patterns are consistent with recent studies indicating that bamboo-rich communities in tropical Asia maintain long-term socio-ecological resilience through culturally embedded resource use (Ihsan et al. 2024; Dutta et al. 2025).

In midstream and downstream communities, bamboo plays a central economic role through multipurpose utilization. *Dendrocalamus asper* supports rural construction, scaffolding, and craft industries, while also supplying edible shoots essential to local diets and small-scale markets. The microeconomic importance of this species aligns with broader assessments of bamboo-based livelihoods across Indonesia, China, and India, where diversified bamboo enterprises substantially contribute to household income and reduce dependence on timber resources (Hogarth and Belcher 2013; Acharya et al. 2014). *Gigantochloa atter* and *G. atroviolacea* further strengthen downstream economies by providing high-quality culms for furniture, weaving, and ornamental products. Their mechanical strength and aesthetic characteristics support craft traditions that increasingly feed into eco-cultural tourism and niche markets.

Culturally, bamboo remains embedded in Javanese ritual identity, architectural symbolism, and collective environmental stewardship. Downstream species such as *G. atroviolacea* are widely used in ceremonial structures, traditional instruments, and symbolic markers of communal events. These cultural functions enhance species persistence by maintaining local demand and intergenerational knowledge transfer—mechanisms recognized in recent ethnobiological studies as critical for biocultural conservation (Ihsan et al. 2024; York 2025). The persistence of bamboo in cultural domains underscores its role as a biocultural keystone, reinforcing the social value necessary for long-term habitat maintenance.

At the same time, bamboo utilization pathways contribute to ecological sustainability by promoting renewable, fast-growing materials in rural production systems. The integration of *D. asper* and *Gigantochloa* spp. into agroforestry and mixed-riparian land uses reduces harvesting pressure on natural forests, aligning with global recommendations for nature-based livelihoods that balance productivity with biodiversity conservation (FAO 2020). However, sustainability challenges persist, particularly downstream, where increased market demand and limited management guidelines risk overharvesting of shoots and culms. These pressures mirror concerns in other parts of tropical Asia, where intensification without ecological safeguards has led to stand degradation and reduced regeneration capacity (Teejuntuk et al. 2003; Fitmawati et al. 2021).

The cultural and economic significance of bamboo in the Bengawan Solo region reflects a reciprocal relationship between species functionality and human use. Bamboo provides materials, food, ritual value, and income, while cultural norms and community management practices sustain species availability across generations. This co-dependence demonstrates that riparian bamboo ecosystems function as biocultural landscapes, in which ecological processes and social systems are tightly coupled. Strengthening this integration through community-based harvesting guidelines, livelihood diversification, and value-added bamboo industries can enhance both cultural continuity and ecological resilience in the region.

Riparian bamboo as a model for sustainable ecosystem management

The longitudinal patterns observed in this study position riparian bamboo stands as a practical model for ecosystem-based management in tropical river basins. Species such as *B. spinosa*, *D. asper*, and *Gigantochloa* spp. simultaneously stabilize riverbanks, regulate microclimate, and supply renewable biomass, aligning closely with the principles of nature-based solutions and ecosystem-based adaptation in fluvial landscapes (Chazdon 2014; FAO 2020). The strong dominance of *B. spinosa* on steep upstream slopes, combined with the structurally diverse and multifunctional *D. asper–Gigantochloa* assemblages in midstream and downstream segments, demonstrates how different bamboo taxa can be strategically aligned with segment-specific management objectives, from erosion control to livelihood support.

From a biophysical perspective, the high clump density, extensive rhizome networks, and persistent canopy cover recorded in all three zones indicate a strong capacity of bamboo to reduce surface runoff, stabilize alluvial and colluvial deposits, and buffer hydrological extremes. These traits correspond with reported reductions in soil loss and improved bank stability in bamboo-dominated riparian systems elsewhere in Asia (Sofiah et al. 2018; Nath et al. 2020). In the Bengawan Solo context, upstream stands dominated by *B. spinosa* function as protection belts that reinforce slope stability in the catchment, whereas mid- and downstream stands composed of *D. asper* and *Gigantochloa* spp. operate as hybrid protection–production systems that maintain bank integrity while supplying poles, shoots, and craft materials.

Socio-ecologically, the strong overlap between species with high ecological importance (high IVI) and high utilization value—particularly *D. asper*, *G. apus*, and *G. atter*—creates favorable conditions for community-based management. Local dependence on bamboo for construction, crafts, and food creates incentives for maintaining vegetative cover along riverbanks, effectively

aligning household-level economic interests with riparian conservation goals. Such coupling of ecological function and livelihood value is a key feature of resilient social–ecological systems and underpins many successful community forestry and agroforestry schemes in tropical regions (Folke et al. 2016; FAO 2020). In this way, the Bengawan Solo riparian bamboo system illustrates how management interventions can leverage existing cultural practices rather than imposing entirely new land-use regimes.

At the same time, the results highlight several risks and constraints that must be addressed if bamboo is to be used as a model for sustainable riparian management. Downstream areas with narrow buffers, high temperatures, and intensive cultivation (Table 5) are particularly vulnerable to over-harvesting of shoots and culms, simplification of stand structure, and replacement of mixed bamboo groves by single fast-growing taxa. Such trends could reduce diversity (H′) and evenness, weaken bank protection, and increase susceptibility to pests and climate extremes, as documented in simplified bamboo plantations in other tropical regions (Pertiwi et al. 2021; Irawan et al. 2025). The moderate correlations between environmental variables, diversity, and dominance (Table 6) also indicate that bamboo-based management cannot rely solely on planting; it must integrate slope, hydrology, and microclimate constraints into spatial planning.

Taken together, the Bengawan Solo case suggests a zonation-based management framework: upstream segments prioritized as protection corridors dominated by structurally robust stabilizers such as *B. spinosa*; midstream zones managed as mixed protection–production belts where *D. asper* and *G. apus* are retained in multi-species groves; and downstream zones maintained as multifunctional production landscapes where *Gigantochloa* spp. are managed under explicit guidelines for buffer width, harvesting intensity, and species mixture. Such a framework is consistent with contemporary river-basin and green-infrastructure planning that emphasize continuous vegetated corridors, diversified species portfolios, and community participation as core elements of sustainable management (Capon et al. 2013; Chazdon 2014). In this sense, riparian bamboo stands along the upper Bengawan Solo River offer not only a locally grounded solution but also a transferable model for integrating ecological engineering, rural livelihoods, and climate-resilient river management in tropical landscapes.

Comparative insights and broader implications

The spatial patterns observed in the upper Bengawan Solo River align closely with riparian bamboo dynamics reported across tropical Asia and other warm-humid regions, indicating a degree of ecological convergence driven by hydrological gradients, soil conditions, and human land-use histories. In many Southeast Asian river systems—including those in northern Thailand, the Mekong Basin, and southern China—species richness increases toward lowland floodplains, where hydrological stability, finer-textured alluvial soils, and moderate disturbance create conditions favorable for mixed bamboo assemblages (Sharma and Chongtham 2015; Chen et al. 2022). The transition documented here—from monodominant *B. spinosa* on steep upstream slopes to species-rich *Gigantochloa* groves downstream—mirrors these regional patterns, suggesting that topographically driven environmental filtering and human-mediated cultivation operate as consistent structuring forces in tropical riparian bamboo ecosystems.

The dominance of *B. spinosa* in upper catchments, despite its low contribution to downstream diversity, highlights a common biogeographical phenomenon in bamboo systems: steep gradients exert strong abiotic filtering, limiting species capable of tolerating nutrient-poor soils, high drainage, and mechanical stress. Similar monodominant stands have been reported in the uplands of northeastern India, Thailand and Sumatra, where a few ecologically hardened taxa persist under erosive slope conditions (Teejuntuk et al. 2003; Fitmawati et al. 2021). In contrast, the diversified stands in the Bengawan Solo lowlands reflect patterns observed in managed floodplain and agro-riparian zones in Thailand and Vietnam, where *Dendrocalamus* and *Gigantochloa* species thrive under moderate disturbance and high nutrient availability.

A notable distinction of the Javanese case lies in the degree of socio-ecological integration. Unlike some regions where bamboo is primarily cultivated for commercial timber substitutes or industrial shoot production, downstream communities in Central Java maintain bamboo not only for material use but also for cultural, ritual, and household functions. This biocultural embeddedness enhances long-term conservation because species valued for identity, ceremony, and heritage tend to be retained even when market demand fluctuates (Ihsan et al. 2024). Consequently, the persistence of *G. atroviolacea* in shaded, wet downstream pockets is not solely an ecological phenomenon but is reinforced by aesthetic and cultural preference—an example of how human selection maintains species that might otherwise be outcompeted in intensively managed landscapes.

The broader implications extend beyond local riparian management. The multifunctional and socially integrated nature of bamboo positions it as a key resource in climate adaptation strategies, green infrastructure development, and ecosystem-based disaster risk reduction. Given its high growth rate, strong carbon sequestration capacity, and ability to rapidly stabilize disturbed banks, bamboo is increasingly recognized as a viable component of river restoration and climate-resilient land-use planning (Capon et al. 2013; Yen et al. 2018). The Bengawan Solo system exemplifies these potentials, showing that bamboo-based buffers can be both ecologically effective and socially acceptable—an essential combination for long-term sustainability.

Furthermore, the observed balance between natural regeneration upstream and human-supported diversification downstream illustrates a hybrid model of riparian vegetation that can be advantageous under accelerating environmental change. While purely natural forests may struggle to regenerate under rising human pressure and climate extremes, and purely cultivated systems often lack

resilience, bamboo-based hybrid systems retain both ecological robustness and management flexibility. Such systems align with global frameworks promoting ecosystem-based adaptation, biocultural conservation, and nature-positive development under the Convention on Biological Diversity's Post-2020 agenda.

Comparative evidence reinforces that bamboo-rich riparian ecosystems operate as socio-ecological mosaics shaped simultaneously by physical gradients and long-standing human–environment relationships. The Bengawan Solo case contributes to global understanding by illustrating how ecological resilience and cultural continuity can be co-maintained in multifunctional landscapes—a principle increasingly central to sustainable river-basin management in the tropics.

Synthesis and conceptual framework

The ecological and socio-cultural patterns observed along the upper Bengawan Solo River form an integrated socio-ecological system in which bamboo diversity, structural dominance, and human utilization co-evolve across the riparian gradient. The upstream–midstream–downstream continuum demonstrates that bamboo ecosystems are shaped not by isolated factors but by the interplay among environmental filtering, hydrological dynamics, species functional traits, and local management practices. This synthesis highlights that the observed zonation is not merely a biophysical outcome but a reflection of dynamic reciprocal interactions between ecological processes and human decisions.

At the ecological level, the longitudinal gradient from *B. spinosa* monodominance upstream to mixed *Gigantochloa–Dendrocalamus* assemblages downstream illustrates how environmental filters—topography, soil moisture, hydrological stability, and microclimate—act as primary determinants of species distributions. Steep slopes and well-drained soils promote the persistence of structurally robust, drought-tolerant taxa, while alluvial floodplains accommodate more diverse bamboo stands due to higher nutrient availability, moderated water tables, and lower mechanical stress. These patterns match broader ecological principles in riparian ecosystems, where increasing environmental benignity downstream supports higher richness and functional redundancy (Sharma and Chongtham 2015; Chen et al. 2022). The strong upstream dominance of *B. spinosa* also exemplifies the role of foundation species whose rhizome networks stabilize geomorphologically vulnerable landscapes.

From a functional perspective, bamboo species along this gradient occupy distinct ecological and socio-economic niches. *Dendrocalamus asper* and *G. apus* exemplify multifunctional taxa capable of providing both ecological services (e.g., erosion control, microhabitat formation, flood buffering) and socio-economic benefits (construction materials, edible shoots, handicraft resources). This dual functionality increases the resilience of mid- and downstream communities, reflecting a pattern consistent with ecosystem-service diversification reported in managed bamboo systems across Southeast Asia (Dutta et al. 2025; Li et al. 2025). Conversely, species such as *B. spinosa* contribute disproportionately to ecological stability despite limited direct economic use, showing how protective specialists reinforce upstream watershed integrity even in low-diversity contexts.

Human dependence emerges as a third central dimension in shaping riparian bamboo systems. Local communities actively maintain, propagate, and harvest bamboo based on cultural values, utility needs, and traditional ecological knowledge. Species with high cultural resonance—such as *G. atroviolacea* used for ritual and artisanal purposes—persist downstream even when they are not the most ecologically dominant. This alignment between cultural preference and ecological management mirrors biocultural conservation models documented in tropical agro-riparian landscapes, where traditional practices enhance long-term species retention and landscape heterogeneity (Heartsill-Scalley and Aide 2003; Ihsan et al. 2024). Human management thus modifies natural ecological trajectories, facilitating coexistence between naturally regenerating and intentionally cultivated bamboo stands.

Integrating these three dimensions—ecological dominance, functional multifunctionality, and human dependence—results in a conceptual triangular framework (sensu Weinberger et al. 2015; Lohbeck et al. 2016) that captures the interdependencies shaping bamboo-based riparian landscapes. Ecological dominance ensures structural stability and environmental buffering; multifunctionality supports both ecological processes and livelihood needs; and human dependence provides cultural continuity and management incentives. The interaction of these dimensions produces socio-ecological feedback loops that maintain resilient and multifunctional riparian ecosystems over time.

This synthesis suggests that bamboo-rich riparian systems offer a scalable model for nature-based solutions in tropical river basins. By aligning ecological suitability with community management, such systems can enhance watershed protection, mitigate climate-related disturbances, and sustain rural economies. Future research should quantify ecosystem-service flows (e.g., carbon storage, soil stabilization rates, flood attenuation), evaluate socio-economic trade-offs among species, and explore participatory governance structures that integrate scientific ecological knowledge with traditional management practices. Strengthening these interdisciplinary linkages will help operationalize bamboo-based strategies in broader landscape restoration and climate adaptation frameworks, positioning riparian bamboo ecosystems as key assets in achieving sustainable and resilient tropical river-basin management.

In conclusion, this study shows that bamboo diversity and ecological structure along the upper Bengawan Solo River are jointly shaped by environmental gradients and human management. Species composition shifts from *B. spinosa* dominance in the steep, drier upstream zone to mixed *Dendrocalamus* and *Gigantochloa* assemblages in the more fertile and intensively managed mid- and downstream segments. These longitudinal patterns reflect the roles of slope, soil moisture, hydrological stability, and

land-use intensity in filtering species and shaping community structure. Bamboo stands provide essential ecosystem functions—such as erosion control, bank stabilization, and habitat support—while multifunctional species contribute significantly to local livelihoods through construction materials, food, and cultural uses. Thus, riparian bamboo systems represent effective nature-based solutions for sustainable watershed management. Future studies incorporating multi-seasonal monitoring, molecular identification, and detailed soil–hydrological analyses will strengthen ecological interpretation and support long-term socio-ecological planning in tropical riparian landscapes.

ACKNOWLEDGEMENTS

The authors express their sincere gratitude to the local communities of the upper Bengawan Solo River, Central Java, Indonesia: Gadingan Village, Mojolaban Sub-district, Sukoharjo District; Giriwono Village, Wonogiri Sub-district, Wonogiri District; Sidowarno Village, Wonosari Sub-district, Klaten District, for their cooperation and support during field surveys. We thank the village authorities of Giriwono, Sidowarno, and Gadingan, for providing official permission and facilitating access to riparian sites. We also acknowledge the Bengawan Solo River Basin Agency (BBWS Bengawan Solo), Indonesia, for granting research access and coordinating site visits. Appreciation is extended to colleagues and students who assisted in data collection and preliminary analysis. We are also grateful for the constructive comments received from peer reviewers, which helped improve the quality of this manuscript.

REFERENCES

Acharya SK, Gupta M, Biswas A. 2014. Estimating the correlates of employment and income generation through bamboo enterprise in Tripura. J Crop Weed 10 (2): 122-127.

Allen SE. 1989. Chemical Analysis of Ecological Materials. Blackwell Scientific Publications, Oxford.

Arinasa I, Sujarwo W. 2015. The diversity of endemic bamboo in Bali and conservation efforts. Bamboo J Jpn Bamboo Soc 29: 85-92.

BMKG. 2023a. Buku Data Iklim Indonesia 2023. Badan Meteorologi, Klimatologi, dan Geofisika, Jakarta. [Indonesian]

BMKG. 2023b. Data Iklim Indonesia: Curah Hujan dan Suhu Tahunan. Badan Meteorologi, Klimatologi, dan Geofisika, Jakarta. [Indonesian]

Breton V, Girel J, Janssen P. 2023. Long-term changes in the riparian vegetation of a large, highly anthropized river: Towards less hygrophilous and more competitive communities. Ecol Indic 155: 111015. DOI: 10.1016/j.ecolind.2023.111015.

Bystriakova N, Kapos V, Lysenko I. 2004. Bamboo Biodiversity: Africa, Madagascar, and the Americas. UNEP–WCMC, Cambridge.

Camargo-Caicedo Y, Montoya Arango JA, Tovar-Bernal F. 2025. Assessment of environmental dynamics and ecosystem services of *Guadua amplexifolia* in San Jorge River Basin, Colombia. Resources 14 (7): 115. DOI: 10.3390/resources14070115.

Capon SJ, Chambers LE, Mac Nally R et al. 2013. Riparian ecosystems in the 21st century: Hotspots for climate change adaptation? Ecosystems 16: 359-381. DOI: 10.1007/s10021-013-9656-1.

Chazdon RL. 2014. Second Growth: the Promise of Tropical Forest Regeneration in an Age of Deforestation. Univ Chicago Press, Illinois. DOI: 10.7208/chicago/9780226118109.001.0001.

Chen J, Li L, Yang Y, Zhang X. 2022. Structure and regeneration dynamics of bamboo forests under different management regimes in southern China. For Ecol Manag 509: 120093.

Connell JH. 1978. Diversity in Tropical Rainforests and Coral Reefs. Science 199: 1302-1310. DOI: 10.1126/science.199.4335.1302.

Dutta S, Gorain S, Roy J, Das R, Banerjee S, Gorai SK, Choudhury MR, Das S. 2025. Bamboo for global sustainability: a systematic review of its environmental and ecological implications, climate action, and biodiversity contributions. Environ Rev 33: 1-26. DOI: 10.1139/er-2025-0032.

Ekawati D, Karlinasari L, Soekmadi R, Machfud M. 2022. The status of bamboo research and development for sustainable use in Indonesia: A systematic literature review. IOP Conf Ser: Earth Environ Sci 1109: 012100. DOI: 10.1088/1755-1315/1109/1/012100.

FAO. 2020. Global Bamboo and Rattan Outlook 2020. FAO, Rome.

Ferreira E, Kalliola R, Ruokolainen K. 2019. Bamboo, climate change and forest use: A critical combination for southwestern Amazonian forests? Ambio 49 (8): 1353-1363. DOI: 10.1007/s13280-019-01299-3.

Fitmawati, Ikhsan M, Kurniawan H et al. 2021. Species diversity and environmental effects on bamboo in estuaries along the east coast of Sumatra. SABRAO J Breed Genet 53: 18.

Folke C, Biggs R, Norström AV, Reyers B, Rockström J. 2016. Social-ecological resilience and biosphere-based sustainability science. Ecol Soc 21 (3): 41. DOI: 10.5751/ES-08748-210341.

GBIF Backbone Taxonomy. 2024. GBIF Backbone Taxonomy. https://www.gbif.org

Heartsill-Scalley T, Aide TM. 2003. Riparian vegetation and stream condition in a tropical agriculture–secondary forest mosaic. Ecol Appl 13: 225-234. DOI: 10.1890/1051-0761(2003)013[0225:RVASCI]2.0.CO;2.

Hogarth N, Belcher B. 2013. The contribution of bamboo to household income in Guangxi, China. Intl For Rev 15. DOI: 10.1505/146554813805927237.

Ihsan M, Irawan B, Iskandar BS, Iskandar J. 2023. Ethnobotanical study on using bamboo for kites making in Sumedang District, West Java, Indonesia. Biodiversitas 24: 2393–2401. DOI: 10.13057/biodiv/d240454.

Ihsan M, Irawan B, Iskandar J. 2024. Traditional ecological knowledge on bamboo in Cijambu Village. Biodiversitas 25: 1754-1770. DOI: 10.13057/biodiv/d250446.

International Plant Names Index (IPNI). 2024. International Plant Names Index. https://www.ipni.org

Irawan B, Ihsan M, Permana MD, Noviyanti A. 2025. A review of bamboo: Characteristics, components, and its applications. J Nat Fibers 22 (in press). DOI: 10.1080/15440478.2025.2522928.

Japan International Cooperation Agency (JICA). 2007. Supporting Report Annex No. 8: Inventory Survey – Flora and Fauna in Wonogiri District. The Study on Countermeasures for Sedimentation in the Wonogiri Multipurpose Dam Reservoir. JICA, Jakarta.

Junaedi D, Mutaqien Z. 2010. Diversity of tree communities in Mount Patuha region. Biodiversitas 11: 75-81. DOI: 10.13057/biodiv/d110205.

Kamoto M, Juntopas M. 2007. Lower Mekong Basin: existing environment and development needs. Geogr Rev Japan 80: 704-715. DOI: 10.4157/grj.80.704.

Kent M, Coker P. 1992. Vegetation Description and Analysis: A Practical Approach. CRC Press, Boca Raton.

Kleinhenz V, Midmore DJ. 2001. Aspects of bamboo agronomy. Adv Agron 74: 99-149. DOI: 10.1016/S0065-2113(01)74032-1.

Kumar K, Goswami S, Dongre D, Shah A. 2023. Bamboo in agroforestry for livelihood and ecological security. In: Dongre D, Rahangdale S, Shah AK, Recent AB (eds). Advances in Agriculture and Forestry. AkiNik Publications, New Delhi.

Larinmuana, Laldailakunga J, Laldailakimi PC. 2025. Influence of Altitude on Tree Species Diversity, Structure and Composition in a Protected Area of the Eastern Himalayas, Mizoram, India. Flora 327: 152741. DOI: 10.2139/ssrn.5138575.

Lemmon PE. 1956. A spherical densiometer for estimating overstory density. Forest Sci 2 (4): 314-320. DOI: 10.1093/forestscience/2.4.314.

Li CE, Lee SY, Chen YY, et al. 2025. Bamboo ecosystem services in 25 years: A systematic literature review of trends, insights, and knowledge gaps. Environ Sci Pollut Res 32: 16008-16021. DOI: 10.1007/s11356-025-36650-7.

Liese W, Köhl M. 2015. Bamboo: the Plant and Its Uses. Springer, Cham. DOI: 10.1007/978-3-319-14133-6.

Lobovikov M, Paudel S, Piazza M, Ren H, Wu J. 2007. World bamboo resources: A thematic study prepared in the framework of the Global Forest Resources Assessment 2005. Non-Wood Forest Products 18. FAO, Rome.

Lohbeck M, Bongers F, Martínez-Ramos M, Poorter L. 2016. The importance of biodiversity and dominance for multiple ecosystem functions in a human-modified tropical landscape. Ecology 97: 2772-2779. DOI: 10.1002/ecy.1499.

Magurran AE. 2004. Measuring Biological Diversity. Blackwell Publishing, Oxford.

Maulana M, Satrya T, Soemitro R, Desa Warnana D, Mukunoki T. 2019. Suspended sediment distribution corresponds to erosion and deposition processes at Bengawan Solo River, Indonesia. Proceedings of the Third International Conference on Sustainable Innovation 2019 – Technology and Engineering (IcoSITE 2019). DOI: 10.2991/icosite-19.2019.10.

Mueller-Dombois D, Ellenberg H. 1974. Aims and Methods of Vegetation Ecology. Wiley, New York.

Naiman R, Décamps H. 1997. The ecology of interfaces: Riparian zones. Ann Rev Ecol Syst 28: 621-658. DOI: 10.1146/annurev.ecolsys.28.1.621.

Nath AJ, Sileshi GW, Das AK. 2020. Bamboo: Climate Change Adaptation and Mitigation. Apple Academic Press, New York. DOI: 10.1201/9780429297311.

Ohrnberger D. 1999. The Bamboos of the World: Annotated Nomenclature and Literature of the Species and the Higher and Lower Taxa. Elsevier, Amsterdam.

Panmei L, Selvan T, Durai J, Reza S. 2025. Ecological restoration of fragile Eastern Himalayan landscapes through bamboo bioengineering. Adv Bamboo Sci 13: 100203. DOI: 10.1016/j.bamboo.2025.100203.

Pertiwi N, Rauf BA, Lullulangi M. 2021. Analysis of riverbank stability due to bamboo vegetation in Walanae River, South Sulawesi, Indonesia. J Ecol Eng 22 (9): 176-184. DOI: 10.12911/22998993/141478.

Pielou EC. 1975. Ecological Diversity. Wiley, New York.

Plants of the World Online (POWO). 2024. Royal Botanic Gardens, Kew. http://www.plantsoftheworldonline.org

Radnawati D, Fatmala D. 2020. Kajian Perencanaan Lanskap Ekoriparian DAS Bengawan Solo. Program Studi Arsitektur Lanskap, Institut Sains dan Teknologi Nasional, Jakarta. [Indonesian]

Rani M, Lathwal M, Vikas, Indira A, Joshi B, Kalyan N, Chongtham N. 2024. Role of bamboo in environmental conservation and sustainable development. Proceedings of the 12th World Bamboo Congress, Taiwan, 18–22 April 2024.

Sembada AA, Hanisia RH, Yuliar Y, Hidayat Y, Sumardi I. 2025. Advances in technology for seed germination of bamboo species. Adv Bamboo Sci 11: 100143. DOI: 10.1016/j.bamboo.2025.100143.

Setiawati T, Mutaqin AZ, Irawan B, An'amillah A, Iskandar J. 2017. Species diversity and utilization of bamboo to support life's the community of Karangwangi Village, Cidaun Sub-District of Cianjur, Indonesia. Biodiversitas 18: 58-64. DOI: 10.13057/biodiv/d180109.

Sharma ML, Chongtham N. 2015. Bamboo Diversity of India: An Update. Forest Research Institute Press, Dehradun.

Silva MF, Menis-Henrique MEC, Felisberto MHF, Goldbeck R, Clerici MTPS. 2020. Bamboo as an eco-friendly material for food and biotechnology industries. Curr Opin Food Sci 33: 124-130. DOI: 10.1016/j.cofs.2020.02.008.

Singh C, Khanduri VP, Singh B. 2025. From forest to future: A sustainable perspective on bamboo's nexus with biodiversity, indigenous knowledge, ecological resilience, and current status in Northeast India. Trees For People 12: 101028. DOI: 10.1016/j.tfp.2025.101028.

Soerianegara I, Indrawan A. 2002. Ekologi Hutan Indonesia. Fakultas Kehutanan IPB, Bogor. [Indonesian]

Sofiah S, Setiadi D, Widyatmoko D. 2018. The influence of edaphic factors on bamboo population in Mount Baung Nature Tourism Park, Pasuruan, East Java, Indonesia. Trop Dryl 2 (1): 12-17. DOI: 10.13057/tropdrylands/t020103.

Sutherland WJ. 2006. Ecological Census Techniques: A Handbook. 2nd ed. Cambridge University Press, Cambridge. DOI: 10.1017/CBO9780511790508.

Tabacchi E, Lambs L, Guilloy H, Planty-Tabacchi AM, Muller E, Decamps H. 2000. Impacts of riparian vegetation on hydrological processes. Hydrol Process 14: 2959-2976. DOI: 10.1002/1099-1085(200011/12)14:16/173.3.CO;2-2.

Teejuntuk S, Sahunalu P, Sakurai K, Sungpalee W. 2003. Forest structure and tree species diversity along an altitudinal gradient in Doi Inthanon National Park, Northern Thailand. Tropics 12: 85-102. DOI: 10.3759/tropics.12.85.

Valentin C, Agus F, Alamban R et al. 2008. Runoff and sediment losses from 27 upland catchments in Southeast Asia: Impact of rapid land use changes and conservation practices. Agric Ecosyst Environ 128: 225-238. DOI: 10.1016/j.agee.2008.06.004.

Weinberger K, Rankine H, Amanuma N, Surendra L, Van Hull H, Foran T, Reyes R, Malik A, Murray J. 2015. Integrating the Three Dimensions of Sustainable Development: A Framework and Tools. UN ESCAP, Bangkok.

Whitten T, Soeriaatmadja RE, Afiff SA. 1997. The Ecology of Java and Bali. Periplus Editions, Singapore.

Widjaja EA, Kartikasari SN. 2001. Identifikasi Jenis-Jenis Bambu di Jawa. LIPI, Bogor. [Indonesian]

Wong KM. 2004. Bamboo: The Amazing Grass. IPGRI and Univ Malaya, Kuala Lumpur.

Xu QF, Liang CF, Chen JH, Li YC, Qin H, Fuhrmann JJ. 2020. Rapid bamboo invasion (expansion) and its effects on biodiversity and soil processes. Glob Ecol Conserv 21: e00787. DOI: 10.1016/j.gecco.2019.e00787.

Yang L, Qin Y, Zhao Y, Ren L. 2025. A study on the classification and distribution characteristics of riparian vegetation at reach scales in the Nanliu River, China. Environ Monit Assess 197: 1315. DOI: 10.1007/s10661-025-14788-8.

Yanty D, Herawati D, Purnasari KR. 2019. Study of bamboo ethnobotany by the local community residing around Mount Galunggung in Tasikmalaya Regency (Indonesia). J Trop Ethnobiol 2: 50-56. DOI: 10.31291/jte.v2i2.499.

Yen TM, Lee JS, Lee WJ. 2018. Estimating biomass and carbon storage of Moso bamboo forests using allometric equations. For Ecol Manag 429: 135-144.

York N. 2025. Understandings and critiques of biocultural diversity conservation and future recommendations for conservation actors. Conserv Biol 2025: e70131. DOI: 10.1111/cobi.70131.

NUSANTARA BIOSCIENCE
Vol. 17, No. 2, pp. 277-288
November 2025

ISSN: 2087-3948
E-ISSN: 2087-3956
DOI: 10.13057/nusbiosci/n170210

Assessing tourist experience and willingness to pay for biodiversity conservation at Mongkrang Hill, Mount Lawu, Central Java, Indonesia

ARDITA AYU WULANDARI[1], ARUM NUR MUKARROMAH[1], ASFI DZIHNI[1], ATIKAH KHOIRIYAH AZZAM[1], ANGGUN DERISTANI[2], SUNARTO[1], AHMAD DWI SETYAWAN[1,3,♥]

[1]Department of Environmental Science, Faculty of Mathematics and Natural Sciences, Universitas Sebelas Maret. Jl. Ir. Sutami 36A, Surakarta 57126, Central Java, Indonesia. Tel./fax.: +62-271-663375, ♥email: volatileoils@gmail.com
[2]Department of Environmental Science, Faculty of Graduate School, Universitas Sebelas Maret. Jl. Ir. Sutami 36A, Surakarta 57126, Central Java, Indonesia
[3]Biodiversity Research Group, Universitas Sebelas Maret. Jl. Ir. Sutami 36A, Surakarta 57126, Central Java, Indonesia

Manuscript received: 22 May 2025. Revision accepted: 4 November 2025.

Abstract. *Wulandari AA, Mukarromah AN, Dzihni A, Azzam AK, Deristani A, Sunarto, Setyawan AD. 2025. Assessing tourist experience and willingness to pay for biodiversity conservation at Mongkrang Hill, Mount Lawu, Central Java, Indonesia. Nusantara Bioscience 17: 277-288.* Highland ecosystems are ecologically sensitive environments increasingly pressured by nature-based tourism. Mongkrang Hill, located on the southern slopes of Mount Lawu in Karanganyar District, Central Java, Indonesia, has experienced rapid visitor growth, raising concerns regarding vegetation disturbance, waste accumulation, and declining habitat quality. This study assesses tourist experience and Willingness to Pay (WTP) for conservation by integrating the Experiential Value Scale (EVS) with economic valuation. A total of 60 visitors were surveyed using structured questionnaires, supported by field observations and semi-structured interviews. Multiple regression analysis showed that all four EVS dimensions—hedonic, novelty, interaction, and comfort—significantly influenced visitor satisfaction, with novelty and hedonic value being the strongest predictors. Satisfaction, in turn, had a positive and significant effect on WTP ($\beta = 0.90$), explaining 80.1% of its variance. The average additional WTP of IDR 15,840 indicates substantial potential for conservation-based financing. Observations further revealed ecological pressures related to trail erosion, vegetation trampling, and improper waste disposal, alongside community benefits through local economic activities and circular economy practices such as plastic waste recycling. The integrated EVS–WTP approach highlights how enhanced visitor experience can strengthen pro-conservation behavior and provide actionable pathways for sustainable ecotourism management. These findings support the development of experience-based conservation strategies for biodiversity protection in highland ecosystems.

Keywords: Biodiversity conservation, circular economy, experiential value scale, highland ecotourism, visitor satisfaction

INTRODUCTION

Highland ecosystems are among the most ecologically sensitive environments because their steep slopes, shallow soils, and narrow habitat distributions make vegetation and wildlife highly vulnerable to disturbance. The natural environment provides essential ecosystem services that support human well-being, including water regulation, carbon storage, microclimate stabilization, and cultural benefits derived from nature-based recreation (Yee 2020). In Indonesia where mountainous landscapes, montane forests, and savanna grasslands form key ecological assets nature-based tourism has grown rapidly and now plays an important role in local development (Gupta et al. 2023). However, increased tourism pressure in fragile ecosystems often leads to vegetation trampling, soil erosion, wildlife displacement, and reductions in habitat quality, indicating that ecological thresholds are being approached or exceeded (Li et al. 2023; Nguyen et al. 2023).

Mongkrang Hill, situated on the southern flank of Mount Lawu in Central Java, Indonesia, exemplifies this dual role as both an ecological hotspot and an increasingly popular nature-based tourism destination. Originally characterized by open grassland savannas and patches of pine vegetation, the area has recently experienced a rapid increase in visitor numbers, driven by the emergence of hiking, camping, and landscape photography trends (Kencana and Azizah 2022). While this growth has stimulated the local economy and expanded community-based tourism opportunities, it has simultaneously intensified ecological pressures, including vegetation loss on frequently used trails, waste accumulation, and declining habitat quality for native flora and fauna. Studies in similar settings show that unmanaged tourism can trigger trade-offs among ecosystem services, reducing regulating and supporting functions while increasing short-term cultural use (Liu et al. 2022; Li et al. 2023). These symptoms highlight the need to integrate ecological considerations into tourism planning at Mongkrang Hill.

In tourism and environmental valuation research, two complementary concepts have been widely applied to understand visitor behavior: the Experiential Value Scale (EVS) and Willingness to Pay (WTP). EVS focuses on how visitors derive value from their experiences through hedonic enjoyment, novelty, interaction, and comfort (Gallarza et al. 2021; Stienmetz et al. 2021). High experiential value often strengthens emotional engagement, enhances satisfaction, and shapes behavioral intentions such as revisit likelihood or support for environmental programs (Petrick and Backman 2002). Novelty one of EVS's strongest dimensions has been

shown to influence behavioral intentions through memorable and emotionally engaging experiences in natural settings (Skavronskaya et al. 2020; Blomstervik et al. 2021). At the same time, hedonic value, service quality, and interaction with fellow visitors and staff contribute to a more meaningful and satisfying experience (Larsen et al. 2019; Ponsignon et al. 2024).

WTP, on the other hand, provides an economic measure of visitors' support for environmental management, particularly through conservation fees, donations, or increased entrance charges. Previous studies show that tourists are often willing to contribute financially to preserve environmental quality when they perceive clear ecological benefits, such as improved waste management, vegetation rehabilitation, or reduced crowding (Casey et al. 2009; Rahmati et al. 2023). WTP is therefore widely used as a proxy for the economic value of ecosystem services in tourism destinations, particularly those experiencing ecological pressure from increasing visitor flows (Bani et al. 2020; Mohamad and Lahay 2021).

Despite Mongkrang Hill's growing importance as a highland ecotourism area, little is known about how visitors' experiential perceptions influence their willingness to support biodiversity conservation financially. Existing studies on the site primarily examine management arrangements and tourism development (Estiyantara 2022; Kencana and Azizah 2022), yet none have assessed the socio-ecological mechanisms linking visitor experience with conservation-oriented economic behavior. Moreover, although EVS and WTP have been widely studied separately in various ecotourism contexts, their integration remains limited, especially in highland ecosystems where environmental sensitivity is high and the need for effective conservation financing is urgent.

Given these research gaps, this study aims to integrate the Experiential Value Scale and Willingness to Pay approaches to assess the experiential and economic dimensions of ecotourism at Mongkrang Hill. Specifically, the study seeks to: (i) Analyze visitors' experiential values across hedonic, interaction, novelty, and comfort dimensions, (ii) Evaluate visitor satisfaction and its determinants based on EVS, (iii) Estimate visitors' WTP to support biodiversity conservation, and (iv) Examine the relationship between experiential value, satisfaction, and WTP. By linking visitor experience with economic support for conservation, this research provides insights for designing sustainable tourism strategies that enhance visitor satisfaction while strengthening biodiversity protection in the Mongkrang Hill ecosystem.

MATERIALS AND METHODS

Study area

This study was conducted in March 2025 at Mongkrang Hill, located in Karanganyar District, Central Java, Indonesia (Figure 1). The site lies on the southwestern slope of Mount Lawu at an elevation of approximately 2,194 m and covers an area of 108.10 ha. The landscape is characterized by open grassland savanna interspersed with patches of *Pinus merkusii* Jungh. & de Vriese and other montane vegetation, forming a mosaic ecosystem typical of highland environments. The climate is cool and humid, with temperatures ranging from 14-24°C and relatively high annual rainfall, creating suitable conditions for diverse flora and fauna. However, the combination of steep slopes, fragile grassland substrates, and increasing tourism pressure makes the area ecologically sensitive to vegetation trampling, soil erosion, and wildlife disturbance. Mongkrang Hill has rapidly developed as a popular destination for hiking and photography, attracting both beginner and experienced visitors. Its growing popularity underscores the need to evaluate visitor experience and conservation-supporting behavior to inform sustainable ecotourism management.

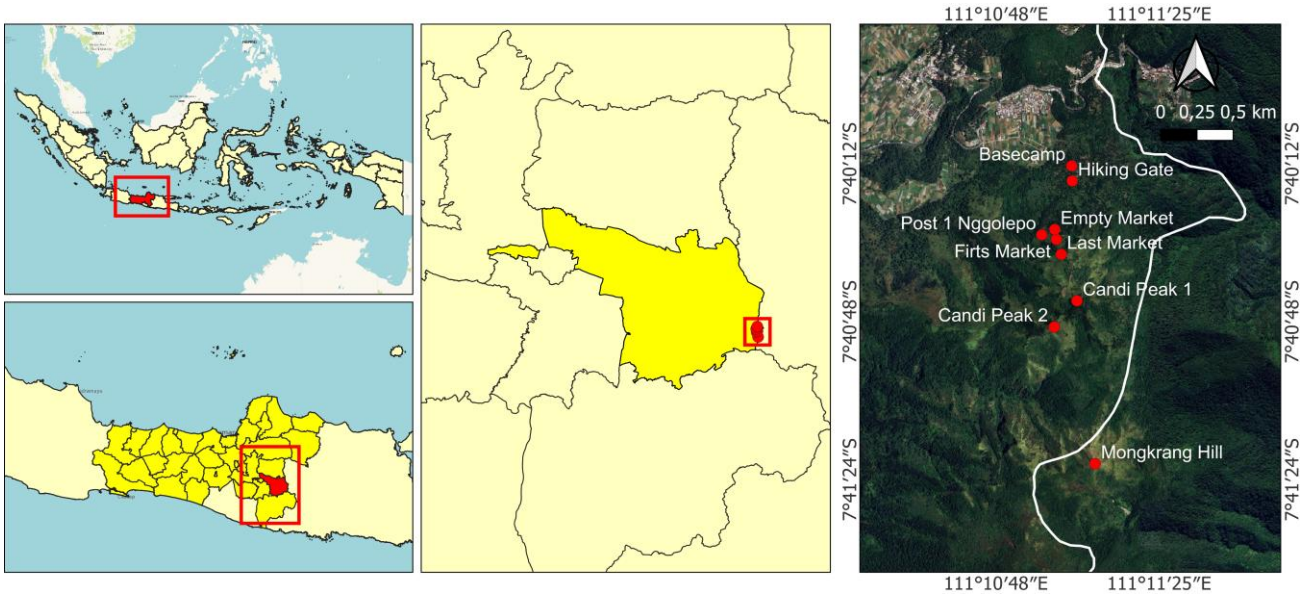

Figure 1. Map of study area in Mongkrang Hill, Mount Lawu, Karanganyar District, Central Java, Indonesia

Research design

This study employed an exploratory–quantitative research design to assess how experiential dimensions influence visitor satisfaction and their willingness to pay for biodiversity conservation. The Experiential Value Scale (EVS) framework was used to capture hedonic, interaction, novelty, and comfort dimensions (Prebensen and Rosengren 2016; Gallarza et al. 2021), while WTP was measured through the Contingent Valuation Method (Hanemann 1991). The conceptual pathway assumes that EVS dimensions shape overall satisfaction, which subsequently affects WTP a mechanism commonly used in ecotourism valuation studies (Mohamad and Lahay 2021).

Sampling Procedure

Respondents were selected using a systematic random sampling technique to enhance the representativeness of the sample. Data collection was conducted during peak visiting hours (10:00-15:00) over several days in March 2025. The sampling procedure was as follows: (i) researchers positioned at the main trailhead estimated the visitor flow during the data collection window; (ii) based on preliminary observations, the total number of visitors passing during the sampling period was approximated; (iii) a sampling interval (k) was calculated by dividing the estimated total visitor population by the target sample size (N = 60); (iv) the first respondent was selected randomly from the first k visitors, and every k-th visitor thereafter was invited to participate, provided they met the minimum age requirement of 18 years. This method ensured that all visitors during the sampling period had an equal probability of being selected, thereby reducing selection bias inherent in convenience or accidental sampling approaches.

Data collection

Questionnaire development

The questionnaire was designed to measure three main constructs: Experiential Value Scale (EVS), visitor satisfaction, and Willingness to Pay (WTP). EVS items captured four experiential dimensions hedonic value, interaction, novelty, and comfort following conceptual frameworks used in previous tourism experience studies (Prebensen and Rosengren 2016; Gallarza et al. 2021). Visitor satisfaction was assessed using global evaluative items, while WTP was measured using fixed monetary categories adapted from Contingent Valuation Method guidelines (Hanemann 1991; Bani et al. 2020). All items employed a five-point Likert scale to ensure consistency and ease of interpretation. Content validity was ensured through expert review involving ecotourism researchers and local site managers, who examined wording clarity, contextual relevance, and the alignment of each item with study objectives. Prior to full distribution, the questionnaire underwent a small pilot test to refine ambiguous statements.

Field observation

Field observations were conducted to document ecological and infrastructural conditions along the Mongkrang Hill trail. Key environmental variables observed included vegetation composition, slope stability, visible erosion, trail width, and signs of habitat disturbance, which are common pressures in mountain ecotourism areas (Kencana and Azizah 2022; Estiyantara 2022). Waste accumulation, noise levels, and crowding at rest points were also recorded to contextualize visitor satisfaction and WTP responses. Observations related to tourism facilities such as shelters, sanitation units, stalls, signage, and parking areas were used to assess comfort attributes and triangulate questionnaire results. Photographic documentation supported the qualitative description of ecological conditions.

Semi-structured interviews

Semi-structured interviews were conducted with tourism managers, Perhutani staff, and community members from Gondosuli Village to obtain contextual insights on conservation practices, visitor management, and local governance. Interview questions explored topics such as reforestation programs, waste management strategies, community participation, and perceived ecological pressures associated with increasing tourism (Estiyantara 2022; Tiwari et al. 2024). This approach allowed flexibility for respondents to elaborate on site-specific challenges, including trail erosion, weekend overcrowding, and the displacement of wildlife. Information from interviews was used to enrich the interpretation of EVS and WTP findings and to ensure that the quantitative analysis was grounded in the socio-ecological realities of Mongkrang Hill.

Measurement of key variables

Experiential Value Scale (EVS)

EVS was operationalized into four dimensions representing different aspects of tourist experience. Hedonic value captured emotional enjoyment and pleasure derived from landscape appreciation (Park and Ahn 2022; Trabandt et al. 2024). Novelty assessed visitors' perceptions of newness and uniqueness during their visit (Skavronskaya et al. 2020; Blomstervik et al. 2021). Interaction measured social engagement among visitors and communication with site managers (Zwart and Hines 2022). Comfort evaluated ease of movement, facility adequacy, and environmental convenience along the trail. Each dimension was measured using multiple Likert-based indicators.

Visitor satisfaction

Visitor satisfaction was assessed using global evaluative items summarizing perceived quality of the ecotourism experience. Scores ranged from 1 (very dissatisfied) to 5 (very satisfied). Higher satisfaction values indicated more positive evaluations of environmental conditions, facilities, and service attributes influencing behavioral intentions (Habibi et al. 2024).

Willingness to Pay (WTP)

WTP was measured using the Contingent Valuation Method (CVM), asking respondents to select a monetary amount they were willing to contribute for conservation-oriented improvements (Hanemann 1991; Bani et al. 2020). Fixed nominal categories (IDR 10,000-50,000) were chosen to reduce strategic bias, align with typical entrance fees, and reflect realistic spending capacity among visitors.

Data analysis

Descriptive statistical analysis

Descriptive statistics were used to summarize visitors' characteristics and perceptions through frequency distributions, percentage tabulation, and graphical visualization. These procedures enabled the identification of patterns across EVS dimensions, satisfaction levels, and WTP categories, providing an initial overview of visitor responses and behavioral tendencies (Rafitanuri et al. 2022). Tabulated WTP distributions helped reveal the central tendency and range of conservation-related monetary support.

Regression analysis

Two regression models were employed to examine the structural relationships among key variables, using Statistical Package for the Social Sciences (SPSS) version 25 for analysis. Multiple linear regression assessed how the four EVS dimensions collectively influenced satisfaction, using standardized coefficients and significance values to identify the strongest predictors (Chan and Saikim 2022; Deng et al. 2023). A second simple regression model examined the effect of Satisfaction on WTP, enabling the estimation of behavioral elasticity in conservation support. Model diagnostics ensured robustness and validity of findings.

Integration of EVS and WTP results

EVS–WTP integration provided socio-ecological insights into how experiential quality drives financial support for conservation, informing biodiversity-friendly tourism strategies.

Ethical considerations

All participants provided informed consent prior to survey completion, and confidentiality of personal information was strictly maintained. Data collection complied with ethical research standards and received permission from the Mongkrang Hill management and relevant local authorities (Estiyantara 2022; Perhutani 2022).

RESULTS AND DISCUSSION

Visitor demographic characteristics

Visitor demographics at Mongkrang Hill indicate a clear dominance of young adults, with the majority of respondents (90%) falling within the 18-30 age group, as shown in Table 1. This age structure reflects a strong interest in highland ecotourism among younger visitors who tend to seek nature-based recreation, physical challenges, and scenic photography opportunities. The gender distribution shows that females (65%) substantially outnumber males (35%), suggesting that the site has broad appeal among young women, consistent with trends in recreational hiking and social-media-driven tourism in Indonesia.

In terms of occupation, university students represent the largest group (45%), followed by private-sector employees (30%), entrepreneurs (13.3%), and school students (10%). Only one respondent identified as a state civil servant. This occupational distribution suggests that visitors are primarily individuals with moderate disposable income but high interest in outdoor experiences and aesthetic enjoyment—factors that shape both experiential values and willingness to pay for environmental services.

Visit frequency patterns further emphasize Mongkrang Hill's attractiveness to first-time tourists: 55% of respondents were visiting for the first time, while the remaining 45% had visited between two and five times. This mix of new and returning visitors provides insight into the site's experiential appeal and potential for visitor loyalty.

Collectively, these demographic features indicate that Mongkrang Hill attracts a youthful, experience-oriented visitor base whose perceptions of ecological quality, comfort, and novelty strongly influence their overall satisfaction. Young visitors especially students also tend to be more receptive to conservation messages, implying significant opportunities for environmental education and responsible tourism campaigns tailored to this demographic segment. The demographic profile presented here reflects visitors sampled systematically during peak hours in March 2025 and is representative of that specific visitor flow.

Willingness to Pay (WTP) for conservation

Visitor willingness to financially support conservation at Mongkrang Hill shows clear variability, with WTP values ranging from IDR 10,000 to IDR 50,000, as illustrated in Figure 2. The most frequently selected contribution was IDR 15,000, chosen by 37 respondents, while only two visitors expressed the highest WTP of IDR 50,000. The calculated average WTP is IDR 15,840, which exceeds the current entrance fee of IDR 10,000. This indicates that visitors generally recognize the value of ecological services and are willing to pay a modest premium to support conservation-oriented improvements.

Several factors appear to influence WTP. Demographic patterns from Table 1, particularly the predominance of young university students, suggest that visitors have limited financial capacity but relatively high environmental awareness. Perceived experiential quality especially related to novelty, hedonic aspects, and comfort also shapes WTP, as supported by regression results presented later in Table 3.

Table 1. Demographic characteristics of informants

Parameter	Specification	Quantity or number	Percentage (%)	Total
Sex	Female	39	65.0	60
	Male	21	35.0	
Age	18-30	54	90.0	60
	31-50	6	10.0	
Profession	Student (school)	6	10.0	60
	University student	27	45.0	
	Private sector employee	18	30.0	
	Entrepreneur	8	13.3	
	State civil apparatus	1	1.7	
Visit frequency	1 time	33	55.0	60
	2 times	11	18.3	
	3 times	10	16.7	
	4 times	3	5.0	
	5 times	3	5.0	

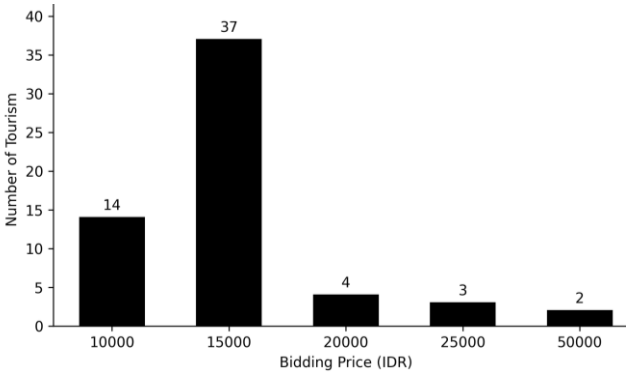

Figure 2. Willingness to pay maximum tourism to buy entrance tickets to Mongkrang Hill, Karanganyar District, Indonesia

Field observations reveal that environmental and facility conditions strongly affect visitor willingness to pay. Scattered trash along trails, damaged or unclear signage, and limited interpretive facilities were frequently noted on-site. These deficiencies likely suppressed higher WTP values, as visitors tend to base their economic support on perceived service quality and environmental integrity. Despite these constraints, the presence of an average WTP above the standard fee suggests significant potential for implementing conservation levies, voluntary donations, or tiered pricing. If managed transparently, such revenue could directly support waste management, vegetation recovery, and trail maintenance addressing the very issues that currently limit visitor satisfaction and maximum WTP.

Experiential Value Scale (EVS) outcomes

Descriptive patterns of EVS dimensions

Visitor perceptions across the four EVS dimensions hedonic value, novelty, interaction, and comfort show consistently positive trends based on descriptive tabulations and field observations. Hedonic value emerged as one of the strongest experiential components, with many visitors expressing enjoyment from panoramic scenery, cool highland temperatures, and opportunities for relaxation. Novelty was also highly rated, particularly among first-time visitors (33 individuals), reflecting the appeal of Mongkrang Hill's open savanna landscape and distinctive views of Mount Lawu (Table 1).

Interaction values were shaped by social exchanges along the hiking trail and brief but meaningful encounters with site staff, as illustrated in Figure 3, which displays signage and reminders that support visitor behavior. Comfort perceptions were influenced by basic facilities shelters, stalls, sanitation and the relatively easy trail conditions. However, comfort tended to decrease during peak periods when the summit became crowded. Overall, descriptive patterns indicate that visitors perceived Mongkrang Hill as emotionally engaging, visually unique, socially supportive, and generally comfortable, forming a strong experiential basis for satisfaction.

Regression model: EVS and satisfaction

The regression analysis presented in Table 2 demonstrates that all four EVS dimensions significantly influence visitor satisfaction, with p-values < 0.001 across all predictors. Standardized beta coefficients show clear variation in predictive strength: novelty (β = 0.47) and hedonic value (β = 0.46) are the most influential determinants of satisfaction, suggesting that emotional engagement and unique landscape experiences play central roles in shaping positive visitor perceptions. Interaction (β = 0.42) also contributes strongly, indicating that social encounters and interpersonal communication enhance the ecotourism experience. Comfort has the lowest, yet still substantial, influence (β = 0.34), reflecting the importance of basic infrastructure and environmental conditions.

High t-values for each variable confirm the robustness of these effects, and the model structure aligns with EVS theory, where diverse experiential components collectively shape visitor satisfaction. The strength of novelty and hedonic factors highlights the ecological significance of maintaining landscape quality, scenic viewpoints, and tranquil natural settings. Meanwhile, the importance of interaction and comfort emphasizes the need for improved visitor services, better trail signage, and well-maintained rest facilities. Together, these findings support the interpretation that enhancing experiential value directly elevates satisfaction, which subsequently increases willingness to contribute financially to conservation programs.

Relationship Between Visitor Satisfaction and WTP

The simple regression analysis testing the influence of visitor satisfaction on Willingness to Pay (WTP) demonstrates a strong and statistically significant relationship, as shown in Table 3. Satisfaction exhibits a positive regression coefficient of 0.41 ($p < 0.001$), indicating that every one-unit increase in satisfaction leads to an estimated 0.41-unit increase in WTP. The model's explanatory power is notably high, with an R^2 value of 0.801, meaning that satisfaction accounts for 80.1% of the variation in visitors' willingness to contribute financially to conservation efforts at Mongkrang Hill.

Table 2. Regression coefficients of comfort, novelty, hedonic, and interaction on the dependent variable

Model	Unstd. B	Std. Error	Beta	t	Sig.
(Constant)	0.06	0.30	--	0.19	0.849
Comfort	0.95	0.06	0.34	16.66	< 0.001
Novelty	1.05	0.05	0.47	21.60	< 0.001
Hedonic	1.01	0.04	0.46	23.21	< 0.001
Interaction	0.98	0.05	0.42	20.66	< 0.001

Note: All predictors were statistically significant ($p < 0.001$)

Table 3. Regression coefficient of satisfaction on WTP in Mongkrang Hill, Karanganyar District, Indonesia

Model	Unstd. B	Std. Error	Beta	t	Sig.
(Constant)	-3.41	0.44	--	-7.84	< 0.001
Satisfaction	0.41	0.03	0.90	15.27	< 0.001

Note: R^2: 0.801

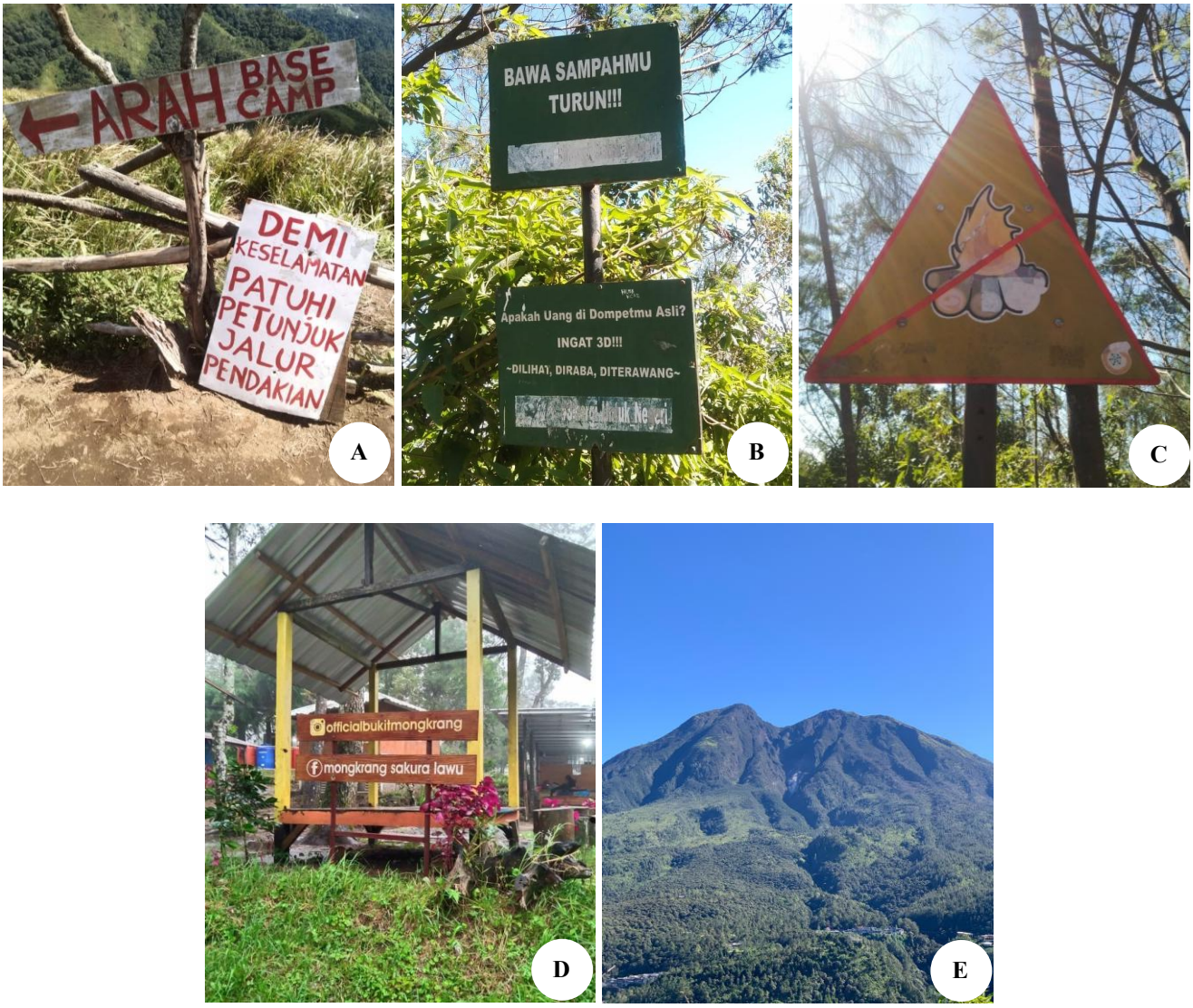

Figure 3. Hiking facilities, environmental regulation signs, and landscape views of Mongkrang Hill, Mount Lawu, Karanganyar District, Indonesia, including trail guidance and conservation reminders (A-C), the basecamp area (D), and the summit view of Mount Lawu (E)

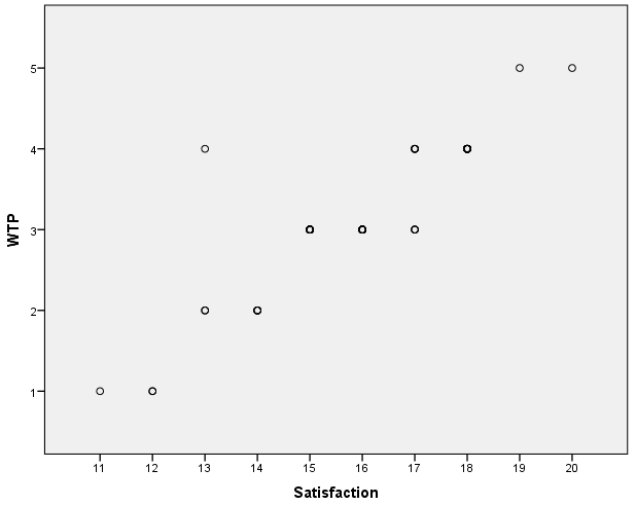

Figure 4. EVS-WTP relationships in Mongkrang Hill, Karanganyar District, Indonesia

This strong relationship is further illustrated in Figure 4, where the scatterplot displays a clear upward trend linking higher satisfaction scores to higher WTP values. The tight clustering of points along the regression line reinforces the practical relevance of satisfaction as a behavioral driver in ecotourism contexts.

These findings imply that enhancing experiential quality through better environmental cleanliness, improved signage, stable trail conditions, and maintained scenic viewpoints can directly increase visitor support for conservation funding. Higher satisfaction amplifies perceived value, making visitors more willing to pay for ecological protection initiatives such as vegetation restoration, waste management, or habitat monitoring. Thus, satisfaction serves not only as an indicator of service quality but also as a strategic leverage point for sustaining biodiversity conservation financing in community-managed mountain ecotourism areas.

Tourism attributes and ecological conditions

Tourism attributes at Mongkrang Hill combine scenic landscape quality, visitor-supporting facilities, and relatively easy accessibility, forming a strong basis for nature-based recreation. As illustrated in Figure 3.E, the site offers panoramic views of Mount Lawu and several surrounding peaks, making landscape aesthetics one of its core attractions. The trail is accessible via fully paved village roads, and the short walking distance from the parking area to the basecamp increases inclusiveness for various visitor groups. Facilities such as rest shelters, small food stalls, toilets, and designated parking areas were observed to contribute positively to visitor comfort, aligning with the importance of amenities in shaping satisfaction reported in earlier studies (Kusumawardhani 2022).

Field observations revealed a vegetation composition dominated by *Casuarina junghuhniana* Miq., *P. merkusii*, *Ficus* spp., *Inocarpus fagifer* (Parkinson ex F.A.Zorn) Fosberg, and *Falcataria falcata* (L.) Greuter & R.Rankin, providing partial canopy cover and stabilizing slopes. However, signs of ecological stress were evident. Along several trail sections, trampling had reduced ground cover and exposed compacted soil, indicating early-stage erosion risk. Litter accumulation especially plastic bottles and snack wrappers was observed near rest points and scenic spots, suggesting inadequate waste compliance despite existing reminders displayed in Figure 3.B. These conditions indicate that visitor pressure has begun to exceed the site's ecological carrying capacity in certain zones.

Additional pressures include noise, off-trail shortcuts, and vegetation damage at crowded viewpoints, particularly during weekends. Such disturbances may affect ground-dwelling fauna and reduce long-term vegetation resilience. Without improved management, these impacts could escalate and diminish both ecological quality and experiential value. The interplay between strong tourism appeal and mounting ecological pressures highlights the need for integrated management strategies that balance accessibility and visitor enjoyment with habitat protection and long-term ecological stability.

Local economic impacts of tourism activities

Tourism activities at Mongkrang Hill generate meaningful economic benefits for the surrounding community, functioning as an important complementary livelihood source. Based on observations and interviews, residents participate in various income-generating services, including food and beverage stalls, parking management, sanitation facilities, guiding assistance, and rental of hiking equipment. These community-managed services create a decentralized economic structure in which profits circulate locally rather than flowing outward, aligning with the principles of community-based tourism (Nyamboke 2023). The presence of multiple rest stalls along the trail, as also depicted in, further strengthens microenterprise opportunities for local households.

A notable aspect of local economic resilience is the adoption of circular economy practices. Plastic bottle waste is collected, sorted, and resold, with proceeds used to fund operational needs and minor infrastructure repairs. This practice reduces environmental burden while simultaneously generating financial value from materials that would otherwise contribute to trail-side pollution. Such initiatives demonstrate how circular economy strategies can be integrated into ecotourism management to reduce waste, encourage responsible visitor behavior, and support small-scale community enterprises (Androniceanu et al. 2021; Rosa et al. 2023). Tourism has strengthened household income diversification, increased the flow of local transactions, and enhanced community engagement in managing Mongkrang Hill. These economic dynamics reinforce the social foundation needed for long-term conservation, as communities that benefit economically are more likely to support ecological protection and sustainable visitor management systems.

Discussion

Interpreting visitor demographics and behavioral patterns

The demographic profile of visitors to Mongkrang Hill reveals a predominantly young and student-dominated population, with 90% aged 18-30 years and 55% being first-time visitors (Table 1). This age structure aligns with national patterns in nature-based tourism, where younger individuals tend to exhibit higher exploratory motivation and stronger interest in low-cost outdoor recreation (Kusherdyana et al. 2020; Zwart and Hines 2022). The high proportion of university students also corresponds with previous findings that younger tourists value novelty, emotional engagement, and opportunities for personal escape factors closely linked to experiential value and satisfaction (Larsen et al. 2019; Habibi et al. 2024).

The dominance of early-career visitors (students and private-sector employees) suggests a visitor segment with moderate purchasing power but strong environmental attitudes, making them a key demographic for developing WTP-based conservation schemes. Their frequent engagement in hiking and photography, as observed during field visits, supports the idea that experiential dimensions such as landscape aesthetics and social interaction are central drivers of their visitation decisions. Such behavioral tendencies mirror the findings of Windira et al. (2017), who reported that hedonic and interactional experiences strongly predict revisit intention in youth-oriented tourist destinations.

Visit frequency data, with more than half being first-time visitors, implies that Mongkrang Hill remains an emerging tourism site with untapped potential for building visitor loyalty. However, the relatively low proportion of repeat visitors (Table 1) may indicate limitations in amenities or ecological conditions, echoing studies emphasizing the role of service quality and environmental management in sustaining long-term visitation (Kusumawardhani 2022 and Nurmala et al. 2022). This demographic structure has direct implications for conservation financing: younger visitors may show willingness to contribute financially, but pricing strategies must remain sensitive to their income levels. The demographic patterns observed here illustrate both the opportunities and limitations of leveraging visitor

characteristics to support ecotourism sustainability in highland environments.

Understanding WTP dynamics in a highland ecotourism context

The distribution of Willingness to Pay (WTP) values for conservation at Mongkrang Hill indicates strong visitor support for environmental protection, with contributions ranging up to IDR 50,000 and a clear concentration in intermediate categories (Figure 2). The regression model demonstrates that visitor satisfaction significantly and positively influences WTP ($\beta = 0.90$, $p < 0.001$), highlighting satisfaction as a key psychological driver of financial contributions (Table 3). This pattern is consistent with findings from Mohamad and Lahay (2021), who reported that higher satisfaction levels in coastal ecotourism sites correspond to greater willingness to support environmental programs. Similar trends were observed by Pertiwi et al. (2022) in agrotourism settings, reinforcing that visitors who derive meaningful experiences from natural landscapes tend to perceive conservation fees as justified and necessary.

The relatively high WTP values observed in Mongkrang Hill can be attributed to several contextual factors. First, the site offers unique highland scenery and microclimatic conditions, which enhance aesthetic appreciation and emotional engagement both known predictors of pro-environmental financial behavior (Vittersø et al. 2017; Park and Ahn 2022). Second, visitors were exposed to explicit conservation messaging on waste management and trail discipline (Figure 3.B), which has been shown to increase perceived environmental responsibility and willingness to contribute to preservation efforts (Putranto et al. 2020; Zuska et al. 2024). Third, the relatively young demographic dominated by students and early-career professionals aligns with past studies indicating that younger tourists, despite limited income, often demonstrate stronger pro-environmental attitudes and a readiness to participate in small but meaningful financial contributions (Ashar et al. 2023; Habibi et al. 2024).

The WTP dynamics observed here also reflect broader patterns in developing-country ecotourism contexts, where visitors tend to contribute more when environmental degradation is visible or when conservation needs are clearly communicated (Bani et al. 2020; Rahmati et al. 2023). Field observations indicated signs of erosion, vegetation disturbance, and waste accumulation conditions that may enhance visitors' awareness of ecological vulnerability and thus increase their support for conservation funding. The alignment of satisfaction-driven WTP with ecological concern underscores an important implication: Mongkrang Hill holds substantial potential to establish a sustainable conservation financing mechanism if visitor experience quality and environmental management are simultaneously strengthened.

These results suggest that WTP in Mongkrang Hill is not merely a function of economic capacity but is strongly shaped by experiential, emotional, and ecological cues. Such insights provide a robust empirical foundation for designing conservation-oriented ticketing schemes, community-based funding models, and targeted communication strategies that encourage sustained visitor participation in highland conservation efforts.

EVS as a predictor of visitor satisfaction and pro-conservation behavior

The Experiential Value Scale (EVS) results show that all four experiential dimensions hedonic value, novelty, interaction, and comfort significantly shape visitor satisfaction at Mongkrang Hill. Regression outcomes (Table 2) confirm strong positive effects, with novelty ($\beta = 0.47$, $p < 0.001$) and hedonic value ($\beta = 0.46$, $p < 0.001$) emerging as the most influential predictors. These findings align with previous research noting that unique, emotionally engaging experiences are central to shaping positive tourist evaluations in natural settings (Prebensen and Rosengren 2016; Gallarza et al. 2021). The prominence of novelty reflects the role of scenic landscapes, panoramic viewpoints, and the distinct highland atmosphere, which collectively enhance cognitive stimulation and emotional uplift core elements of experiential value identified by Skavronskaya et al. (2020). Likewise, the strong effect of hedonic enjoyment underscores the contribution of mood, pleasure, and aesthetic immersion, consistent with studies demonstrating that affective engagement strongly predicts visitor satisfaction in nature-based tourism (Vittersø et al. 2017; Park and Ahn 2022).

Interaction and comfort also exert significant influence on satisfaction, though to a slightly lesser extent. Interaction ($\beta = 0.421$, $p < 0.001$) reflects social engagement among hikers and helpful communication from staff forms of social capital that reinforce responsible visitor norms (Hasanah et al. 2023). Comfort ($\beta = 0.342$, $p < 0.001$) relates to micro-environmental conditions, trail usability, and basic facilities, which have been documented as key satisfaction determinants in outdoor recreation (Kusumawardhani 2022). The strong combined influence of these four dimensions suggests that visitor satisfaction at Mongkrang Hill is shaped not only by natural scenery but also by emotional, social, and practical components of the visitation experience.

The link between EVS and pro-conservation behavior becomes clearer when viewed alongside the satisfaction–WTP regression model (Table 3). Satisfaction strongly predicts visitors' willingness to pay for conservation ($\beta = 0.90$, $p < 0.001$), affirming the experiential pathway in which positive experiences translate into financial support for environmental protection. Comparable results have been reported in ecotourism contexts where satisfaction enhances perceived value and encourages voluntary contributions (Mohamad and Lahay 2021; Pertiwi et al. 2022). This pattern supports theoretical propositions that experiential quality can foster stewardship behaviors, particularly in landscapes where ecological vulnerability is visible (Putranto et al. 2020).

The integration of EVS and WTP therefore highlights a socio-ecological mechanism: when visitors feel emotionally rewarded, cognitively stimulated, socially connected, and physically comfortable, they become more willing to invest in the sustainability of the destination. This reinforces the importance of visitor experience design as a conservation

strategy. Enhancing the experiential dimensions identified here—especially hedonic and novelty value can strengthen both satisfaction and financial support, creating a self-reinforcing cycle that benefits long-term biodiversity conservation at Mongkrang Hill.

Ecological implications of increasing tourism pressure

The escalation of visitor numbers at Mongkrang Hill has produced noticeable ecological pressures across the savanna slopes, hiking trails, and summit areas (Figure 3.A). Field observations revealed vegetation trampling along narrow ridgelines, soil compaction on frequently used paths, and localized erosion on steeper segments patterns commonly associated with unmanaged highland tourism. Such impacts are typical in fragile montane environments where grasses possess shallow root systems and soil layers are thin, making them highly susceptible to disturbance from repeated foot traffic (Putranto et al. 2020). The presence of exposed patches and widening of informal trails indicates the early stages of landscape fragmentation, which, if left unregulated, may accelerate the decline of native plant cover.

Waste accumulation represents an additional ecological burden. Despite signage encouraging responsible behavior (Figure 3.B), plastic bottles and food packaging were observed in rest areas and along the trail. This aligns with findings from other Indonesian mountain tourism sites, where littering has emerged as a persistent challenge due to limited waste management infrastructure and fluctuating visitor flows (Putranto et al. 2020). Compounding this issue is the occurrence of open waste burning near basecamp areas, a practice known to release harmful pollutants such as carbon monoxide and particulate matter (Faridawati and Sudarti 2021) and to increase the risk of vegetation fires during dry periods (Jakhar et al. 2023). These environmental hazards not only degrade ecological quality but also diminish the aesthetic and recreational value of the destination.

Wildlife disturbance is another emerging concern. As visitor movement increases, noise levels and human presence disrupt the natural behavior of fauna historically inhabiting the area, such as montane bird species and small mammals (Elena 2024). Similar patterns of wildlife displacement have been reported in other ecotourism landscapes where uncontrolled visitor density alters habitat suitability and reduces ecological resilience (Estiyantara 2022). In Mongkrang Hill, the combination of habitat compression, waste pollution, and trampling signals that the ecological carrying capacity may be approaching its threshold.

If tourism growth continues without improved management, long-term ecological consequences are likely. These include reduced vegetation regeneration, expansion of erosion-prone surfaces, decline in biodiversity, and weakening of ecosystem services such as slope stabilization and microclimate regulation. International studies indicate that once highland ecosystems reach a critical level of degradation, recovery becomes slow and often incomplete due to harsh climatic conditions and limited soil fertility (Li et al. 2023). Thus, proactive measures such as trail zoning, vegetation restoration, stricter waste regulation, and visitor capacity limits—are essential to prevent Mongkrang Hill from experiencing irreversible ecological decline.

Policy implications for WTP-based conservation funding

The WTP values identified in this study (Figure 2) provide an important baseline for designing conservation financing mechanisms at Mongkrang Hill. The regression results in Table 3 demonstrate that visitor satisfaction is a strong and significant predictor of WTP ($\beta = 0.90$, $p < 0.001$), confirming that improvements in environmental quality and service delivery can translate directly into higher financial support for conservation initiatives. Similar patterns have been observed in other tourism contexts, where visitors demonstrate higher WTP when ecological benefits are tangible and service attributes meet or exceed expectations (Arimurti et al. 2021; Pertiwi et al. 2022). This consistency suggests that Mongkrang Hill has substantial potential to adopt a structured funding model based on experiential value.

A practical implication of these findings is the feasibility of introducing a conservation ticket scheme, where a modest increase in entrance fees is earmarked specifically for ecosystem management. Evidence from environmental economics shows that earmarked conservation fees lead to greater public acceptance and transparency because visitors know exactly how their contributions are used (Hanemann 1991; Rahmati et al. 2023). Given the average visitor WTP of IDR 15,840 well above the current fee implementing a differentiated tariff structure, such as weekday–weekend pricing or optional conservation add-ons, could generate sustained funding without reducing visitation.

Another policy avenue is the adoption of Payment for Ecosystem Services (PES) principles. Under this approach, tourists act as direct beneficiaries and contributors to ecosystem protection, similar to models applied in groundwater conservation (Bani et al. 2020) and sustainable tourism initiatives in ecologically sensitive regions (Li et al. 2024). At Mongkrang Hill, PES could be operationalized through voluntary contributions for trail restoration, vegetation rehabilitation, or waste management programs, with periodic reporting to ensure accountability.

Visitor quotas also emerge as a relevant policy tool. As tourism pressure increases, limiting daily hikers through a regulated ticketing system can reduce ecological strain while maintaining the perceived exclusivity and quality of the visitor experience. This approach aligns with global best practices that balance economic benefits with ecological carrying capacity constraints (Nguyen et al. 2023). The WTP results indicate that visitors are willing not only in principle but also financially to support conservation at Mongkrang Hill. Policies that leverage this willingness, designed with transparency, fairness, and ecological necessity, can establish a long-term, community-supported funding model for highland biodiversity conservation.

Strengthening ecotourism management through visitor experience enhancement

The results of this study show that experiential value particularly hedonic enjoyment, novelty, comfort, and

social interaction—plays a central role in shaping visitor satisfaction and subsequent support for conservation. The aesthetic landscape of Mongkrang Hill, combined with its accessible trails and panoramic viewpoints, constitutes the core of the visitor experience. These findings are consistent with studies demonstrating that emotional engagement and sensory appeal are dominant predictors of positive tourism experiences and behavioral intentions (Prebensen and Rosengren 2016; Vittersø et al. 2017). Similarly, novelty-driven experiences have been shown to enhance memorability and stimulate pro-environmental behavior, aligning with the perspectives of Skavronskaya et al. (2020) and Blomstervik et al. (2021).

In the context of Mongkrang Hill, improvements to tourism infrastructure such as clearer signage, well-maintained rest shelters, and safe trail conditions have direct implications for comfort, which in turn elevates satisfaction levels. This agrees with findings from Kusumawardhani (2022) and Nurmala et al. (2022), who emphasize that adequate facilities are essential for maintaining service quality and sustaining visitor loyalty. The current reminders posted on-site (Figure 3.C), including waste-related advisories and safety notices, indicate ongoing efforts to shape responsible visitor behavior. However, the persistence of litter and erosion hotspots suggests that complementary interpretive strategies may be necessary.

Environmental interpretation, whether through guided trails, informational panels, or digital media, has been shown to strengthen experiential value by transforming passive sightseeing into meaningful engagement (Chan and Saikim 2022; Deng et al. 2023). As shown in Figure 3.D, social media platforms that can be used to promote Mongkrang Hill are identified. At Mongkrang Hill, interpretive materials could highlight local flora such as *C. junghuhniana* and *Schima wallichii* (DC.) Korth., ecological vulnerabilities of highland savannas, and the cultural significance of Mount Lawu. Such content would reinforce the novelty and hedonic dimensions while fostering ecological awareness.

Furthermore, enhancing on-site interaction whether through ranger presence, volunteer guides, or community-based interpretation could strengthen the interaction dimension of EVS, which this study found to be significantly associated with satisfaction. As highlighted by Kusherdyana et al. (2020), meaningful human interaction in tourism settings promotes positive behavioral intentions and supports sustainable tourism outcomes. The integration of experiential design principles into ecotourism management at Mongkrang Hill is crucial. By improving facilities, enhancing interpretive content, and promoting responsible visitor behavior, managers can amplify experiential value, which, as demonstrated in this study, translates into stronger satisfaction and higher willingness to support biodiversity conservation.

Integrating circular economy into ecotourism practices

The field observations reveal that local communities around Mongkrang Hill are already implementing basic circular economy practices, particularly through the sorting and resale of plastic bottle waste collected from tourist areas. Although modest, this activity demonstrates an important foundation for transforming waste into economic value while reducing the environmental burden associated with growing tourist numbers. Such initiatives resonate with broader circular economy frameworks, which emphasize resource recirculation, waste minimization, and economic value creation through sustainable practices (Androniceanu et al. 2021; Lahane and Kant 2022). In the context of ecotourism, integrating circular systems is increasingly recognized as a strategic pathway for improving environmental performance while generating additional livelihood opportunities (Rosa et al. 2023).

At Mongkrang Hill, the existing practice of plastic waste sorting can be expanded into more structured community-based waste enterprises. For example, recycling cooperatives managed by local residents could collect, sort, and process recyclables, thereby creating additional income streams while supporting cleaner hiking trails. This approach is consistent with findings by Kurnia et al. (2023), who argue that circular solutions contribute directly to decent work and economic growth by strengthening local entrepreneurship an important element for rural communities dependent on tourism.

Circular economy implementation can also extend to organic materials. Food waste, which is currently problematic along the hiking routes and near basecamp, could be composted and used to support the ongoing reforestation initiatives undertaken by Perhutani and student conservation groups. Such integration would close nutrient loops and reduce the reliance on synthetic inputs for seedling cultivation. Similar initiatives have shown success in other community-based tourism sites where organic waste composting not only reduces pollution but also supports agroforestry or greening programs (Rosa et al. 2023; Wahyudi et al. 2023).

Moreover, adopting circular practices can enhance visitor experience by reinforcing perceptions of environmental responsibility. Studies on sustainable tourism indicate that visible sustainability actions such as recycling stations, signage promoting waste reduction, or community-led conservation programs increase visitor appreciation and strengthen pro-environmental behavior (Nyamboke 2023). For Mongkrang Hill, creating a "circular visitor pathway" that visually communicates how waste is collected, reused, and reinvested into conservation could deepen visitor engagement and strengthen the experiential value dimensions identified earlier in this study.

Integrating circular economy principles into ecotourism management not only mitigates ecological pressures but also supports local livelihoods and reinforces conservation-oriented visitor behavior. As tourism demand continues to rise, circular economy strategies will become increasingly essential for sustaining both the ecological integrity and the socio-economic benefits of Mongkrang Hill.

Study limitations and future research directions

This study has limitations. First, while systematic random sampling enhanced within-period representativeness, the sample (N=60) and its confinement to peak hours in

March limit generalizability across different times and seasons. Second, as a single-site study, findings may not directly transfer to other highland destinations with differing conditions. Third, self-reported data are susceptible to biases like social desirability and hypothetical bias in WTP measures. Fourth, the lack of biophysical data (e.g., soil compaction, vegetation cover) limits objective validation of ecological impacts. Future research should: (i) Adopt longitudinal mixed-methods designs linking larger, temporally stratified visitor surveys with ecological monitoring, (ii) Conduct comparative multi-site studies to identify context-specific factors influencing EVS and WTP, (iii) Triangulate stated WTP with experimental or revealed preference methods to enhance valuation robustness.

Conclusion, this study demonstrates that experiential quality plays a central role in shaping visitor satisfaction and willingness to pay for conservation at Mongkrang Hill, a rapidly developing highland ecotourism site in Central Java. The four dimensions of the Experiential Value Scale hedonic value, novelty, interaction, and comfort significantly enhance satisfaction, which subsequently increases visitors' financial readiness to support biodiversity protection. The average additional WTP of IDR 15,840 indicates meaningful potential for establishing conservation-based funding mechanisms that can strengthen habitat restoration, improve visitor management, and maintain ecological integrity. Field observations further reveal that tourism pressure is escalating, underscoring the need for improved waste management, erosion control, and environmental education. By integrating experiential value assessment with economic valuation, this research provides an applied socio-ecological framework for developing community-based, circular-economy-oriented ecotourism policies that support long-term sustainability in highland ecosystems such as Mongkrang Hill.

ACKNOWLEDGEMENTS

The authors express their sincere gratitude to Perum Perhutani and the Mongkrang Hill management team, Karanganyar District, Central Java, Indonesia, for granting research access and providing essential logistical support during fieldwork. Appreciation is also extended to the Environmental Service Agency (DLH) of Karanganyar for sharing information related to ongoing conservation initiatives in the area. The authors gratefully acknowledge all survey respondents for their willingness to participate and contribute valuable data. Special thanks are given to the community of Gondosuli Village, Karanganyar District, whose cooperation and assistance greatly facilitated the research process. Any remaining shortcomings in this study are the sole responsibility of the authors.

REFERENCES

Androniceanu A, Kinnunen J, Georgescu I. 2021. Circular economy as a strategic option to promote sustainable economic growth and effective human development. J Intl Stud 14 (1): 60-73. DOI: 10.14254/2071-8330.2021/14-1/4.

Arimurti NH, Sularso KE, Hartati A. 2021. Willingness to pay for organic rice in Banyumas Regency and factors influencing it. Forum Agribisnis 11: 1: 75-89. DOI: 10.29244/fagb.11.1.75-89. [Indonesian]

Ashar DA, Muthalib AA, Nur S, Rumbia WA, Barani LOS, Tamburaka IP. 2023. Analysis of factors affecting willingness to pay among household consumers (Study on PDAM Tirta Anoa–Kendari City). Jurnal Progres Ekonomi Pembangunan (JPEP) 8 (2): 161-170. [Indonesian]

Bani A, Benu F, Kotta H. 2020. Willingness to Pay (WTP) for environmental services groundwater resources wells in Kupang City. J Nat Resour Environ Manag 10 (2): 173-182. DOI: 10.29244/jpsl.10.2.173-182.

Blomstervik IH, Prebensen NK, Campos AC, Pinto P. 2021. Novelty in tourism experiences: The influence of physical staging and human interaction on behavioral intentions. Curr Issues Tour 24 (20): 2921-2938. DOI: 10.1080/13683500.2020.1854197.

Casey JF. Brown C. Schuhmann P. 2009. Are tourists willing to pay additional fees to protect corals in Mexico? J Sustain Tour 18 (4): 557-573. DOI: 10.1080/09669580903513079.

Chan JKL, Saikim FH. 2022. Exploring the ecotourism service experience framework using the dimensions of motivation, expectation, and ecotourism experience. Tour Hosp Res 22 (4): 425-443. DOI: 10.1177/14673584211056860.

Deng Y, Zhang X, Zhang B, Zhang B, Qin J. 2023. From digital museuming to on-site visiting: The mediation of cultural identity and perceived value. Front Psychol 14: 1111917. DOI: 10.3389/fpsyg.2023.1111917.

Elena S. 2024. Environmental sustainability in tourism: Strategies for protecting natural resources and reducing negative impacts. Intl Conf Adapt Learning Technol 5: 80-82.

Estiyantara NS. 2022. Analysis of the synergy between the Gondosuli Village tourism working group and *Perhutani* in the management of Bukit Mongkrang Tourism in Karanganyar, Central Java. Altasia Jurnal Pariwisata Indonesia 4 (1): 34-44. DOI: 10.37253/altasia.v4i1.6287. [Indonesian]

Faridawati D, Sudarti. 2021. Public knowledge about the burning effect on the enviroment of Jember District. Jurnal Sanitasi Lingkungan 1 (2): 50-55. DOI: 10.36086/salink.v1i2.1088. [Indonesian]

Gallarza MG. Maubisson L Rivière A. 2021. Replicating consumer value scales: A comparative study of EVS and PERVAL at a cultural heritage site. J Bus Res 126: 614-623 DOI: 10.1016/j.jbusres.2020.01.070.

Gupta A, Zhu H, Bhammar H, Earley E, Filipski M, Narain U, Spencer P, Whitney E, Taylor JE. 2023. Economic impact of nature-based tourism. PLoS One 18 (4): e0282912. DOI: 10.1371/journal.pone.0282912.

Habibi F, Supriani I, Tumewang YK. 2024. The antecedents of muslim tourists' revisit intention: The mediating role of visitor satisfaction. Shirkah: J Econ Bus 10 (1): 20-41. DOI: 10.22515/shirkah.v10i1.731.

Hanemann WM. 1991. Willingness to pay and willingness to accept: How much can they differ? The American economic review. Am Econ Rev 81 (3): 635-647. DOI: 10.1257/000282803321455430.

Hasanah U, Ibrahim I, and Luqman L. 2023. The pentahelix model in community-based tourism on Lemukutan Island, Bengkayang. I-Econ: Res J Islamic Econ 9 (2): 125-137. DOI: 10.19109/ieconomics.v9i2.20337. [Indonesian]

Jakhar R, Samek L, Styszko K. 2023. A comprehensive study of the impact of waste fires on the environment and health. Sustainability 15 (19): 14241. DOI: 10.3390/su15191424.

Kencana NB, Azizah R. 2022. The conversion of Mongkrang Hill into a Mountain Climbing Nature Tourism Site. SIAR III 2022: Seminar Ilmiah Arsitektur 2022: 360-366. [Indonesian]

Kurnia S, Alamsyahbana MI, Chartady R, Arifin SV, Sesaria MI. 2023. Circular solutions for decent work and economic growth: Lessons from Sustainable Development Goals (SDG) 8. Academia Open 8 (1): 1-12. DOI: 10.21070/acopen.8.2023.6657. [Indonesian]

Kusherdyana R, Muslim S, Soesanto H, Suganda RSA. 2020. Contribution of tourist experience to revisiting tourist intentions in the Seribu Islands, DKI Jakarta. Tour Sci J 5 (2): 133-147. DOI: 10.32659/tsj.v5i2.89.

Kusumawardhani Y. 2022. Role of facilities on visitor satisfaction in Gunung Bunder Natural Tourism, Bogor Regency. Jurnal Hospitality dan Pariwisata 8 (1): 65-75. DOI: 10.30813/jhp.v8i1.3211. [Indonesian]

Lahane S, Kant R. 2022. Investigating the sustainable development goals derived due to adoption of circular economy practices. Waste Manag 143: 1-14. DOI: 10.1016/j.wasman.2022.02.016.

Larsen S, Wolff K, Doran R, Øgaard T. 2019. What makes tourist experiences interesting? Front Psychol 10: 1603. DOI: 10.1080/13683500.2020.1803221.

Li L, Feng R, Xi J, Huijbens E, Gao Y. 2023. Distinguishing the impact of tourism development on ecosystem service trade-offs in ecological functional zones. J Environ Manag 342: 118183 DOI: 10.1016/j.jenvman.2023.118183.

Li Q, Wang X, Chen Z, Arif M. 2024. Assessing the conjunction of environmental sustainability and tourism development along Chinese waterways. Ecol Indic 166: 112281. DOI: 10.1016/j.ecolind.2024.112281.

Liu Z, Lan J, Chien F, Sadiq M, Nawaz MA. 2022. Role of tourism development in environmental degradation: A step towards emission reduction. J Environ Manag 303: 114078. DOI: 10.1016/j.jenvman.2021.114078.

Mohamad N, Lahay RJ. 2021. Analysis of the environmental sustainability value of the Tasik Ria Tourism based on Willingness To Pay. Ideas: Educ Soc Cult J 7 (4): 277-282. DOI: 10.32884/ideas.v7i4.475.

Nguyen TT, Grote U, Neubacher F, Rahut DB, Do MH, Paudel GP. 2023. Security risks from climate change and environmental degradation: Implications for sustainable land use transformation in the Global South. Curr Opin Environ Sustain 63: 101322 DOI: 10.1016/j.cosust.2023.101322.

Nurmala, Sullaida, Damanhur. 2022. The influence of tourist facilities, tourist attractions, and service quality on visitor satisfaction at Ujong Blang Beach, Lhokseumawe. Jurnal Ekonomi Manajemen dan Bisnis 23 (2): 73-78 DOI: 10.29103/e-mabis.v23i2.861. [Indonesian]

Nyamboke F. 2023. Community engagement in sustainable tourism development: Opportunities and challenges for local residents. Hosp Tour J 1 (1): 24-35.

Park S, Ahn D. 2022. Seeking pleasure or meaning? The different impacts of hedonic and eudaimonic tourism happiness on tourists' life satisfaction. Intl J Environ Res Public Health 19 (3): 1162. DOI: 10.3390/ijerph19031162.

Perhutani. 2022. Bukit Mongkrang, *Perhutani's* Nature-Based Tourist Attraction in Tawangmangu. Access: 28 April 2025, https://www.perhutani.co.id/bukit-mongkrang-wisata-perhutani-berkonsep-alam-di-tawangmangu/. [Indonesian]

Pertiwi TA, Noechdijati D, Dharmawan B. 2022. Analysis of visitors' Willingness to Pay in the development of "sweetberry" agrotourism in Cianjur Regency. Jurnal Ekonomi Pertanian dan Agribisnis 6 (2): 500-518. DOI: 10.21776/ub.jepa.2022.006.02.15. [Indonesian]

Petrick JF. Backman SJ. 2002. An examination of the construct of perceived value for the prediction of golf travelers' intentions to revisit. J Travel Res 41: 38-45. DOI: 10.1177/0047287502041001005.

Ponsignon F, Jaud DA, Durrieu F, Lunardo R. 2024. The ability of experience design characteristics to elicit epistemic value, hedonic value, and visitor satisfaction in a wine museum. Intl J Contemp Hosp Manag 36 (8): 2582-2600. DOI: 10.1108/IJCHM-07-2023-1081.

Prebensen NK, Rosengren S. 2016. Experience value as a function of hedonic and utilitarian dominant services. Intl J Contemp Hosp Manag 28 (1): 113-135. DOI: 10.1108/IJCHM-02-2014-0073.

Putranto DR, Hariyanto H, and Benardi AI. 2020. The behavior of mountain climbers in reducing environmental damage occurring in Mount Merbabu National Park. Educ Geograph 8 (2): 121-129. [Indonesian]

Rafitanuri S, Arsyida N, Gunawan R. 2022. Analysis of public satisfaction levels with motor vehicle tax payment services based on the signal application at the Tanjungpinang City Samsat Office. Jurnal Hukum, Politik dan Ilmu Sosial 1 (3): 92-103. DOI: 10.55606/jhpis.v1i3.537. [Indonesian]

Rahmati D, Mortazavi SA, Alamdarlo HN, Vakilpour MH. 2023. Heterogeneity preferences and willingness to pay for environmental services: Evidence from Iran. J Clean Prod 386: 135838. DOI: 10.1016/j.jclepro.2022.135838.

Rosa LABD, Cohen M, Campos WYYZ, Ávila LV, Rodrigues MCM. 2023. Circular economy and sustainable development goals: Main research trends. Revista de Administração da UFSM 16 (1): 1. DOI: 10.5902/1983465971448.

Skavronskaya L, Moyle B, Scott N. 2020. The experience of novelty and the novelty of experience. Front Psychol 11: 322. DOI: 10.3389/fpsyg.2020.00322.

Stienmetz J, Kim JJ, Xiang Z, Fesenmaier DR. 2021. Managing the structure of tourism experiences: Foundations for tourism design. J Destin Mark Manag 19: 100408. DOI: 10.1016/j.jdmm.2019.100408.

Tiwari S, Marahatta D, Devkota H. 2024. Aspects of community participation in ecotourism: A systematic review. J Multidiscip Res Adv 2 (1): 71-79. DOI: 10.3126/jomra.v2i1.66650.

Trabandt M, Lasarov W, Viglia G. 2024. It's a pleasure to stay sustainably: Leveraging hedonic appeals in tourism and hospitality. Tour Manag 103: 104907. DOI: 10.1016/j.tourman.2024.104907.

Vittersø J, Prebensen NK, Hetland A, Dahl T. 2017. The emotional traveler: Happiness and engagement as predictors of behavioral intentions among tourists in Northern Norway. Adv Hosp Leisure 13: 3-16. DOI: 10.1108/S1745-354220170000013001.

Wahyudi F, Irsan R, Sutrisno H. 2023. Waste management planning at Lemukutan Island Tourist Attraction, Bengkayang Regency. Jurnal Teknologi Lingkungan Lahan Basah 11 (1): 205-214. DOI: 10.26418/jtllb.v11i1.61219. [Indonesian]

Windira A, Waluya B, Yuniawati Y. 2017. The effect of experiential value of tourist behavioral intentions in Taman Buah Mekarsari. IOP Conf Ser Earth Environ Sci 145: 012022. DOI: 10.1088/1755-1315/145/1/012022.

Yee SH. 2020. Contributions of ecosystem services to human well-being in Puerto Rico. Sustainability 12 (22): 1-38 DOI: 10.3390/su12229625.

Zuska F, Agustrisno, Delvian, Zulkifli. 2024. Building a participatory system for controlling littering behavior of tourist park visitors. Pelita Masyarakat 6 (1): 40-56. DOI: 10.31289/pelitamasyarakat.v6i1.11996. [Indonesian]

Zwart R, Hines R. 2022. Community wellness and social support as motivation for participation in outdoor adventure recreation. J Outdoor Recreat Educ Leadersh 14 (1): 1-15. DOI: 10.18666/JOREL-2022-V14-I1-11139.

NUSANTARA BIOSCIENCE
Vol. 17, No. 2, pp. 289-297
November 2025

ISSN: 2087-3948
E-ISSN: 2087-3956
DOI: 10.13057/nusbiosci/n170211

Gamma-ray irradiation induced polymorphism in *Echinacea purpurea* revealed by RAPD markers

AGUSTINA PUTRI CAHYANINGSIH[1], NITA ETIKAWATI[1,2], AHMAD YUNUS[3,♥]

[1]Graduate Program of Bioscience, Faculty of Mathematic and Natural Sciences, Universitas Sebelas Maret. Jl. Ir. Sutami 36A, Surakarta 57126, Central Java, Indonesia

[2]Department of Biology, Faculty of Mathematics and Natural Sciences, Universitas Sebelas Maret. Jl. Ir. Sutami 36A, Surakarta 57126, Central Java, Indonesia

[3]Department of Agrotechnology, Faculty of Agriculture, Universitas Sebelas Maret. Jl. Ir. Sutami 36 A, Surakarta 57126, Central Java, Indonesia. Tel./fax.: +62-271-637457, ♥email: yunus@staff.uns.ac.id

Manuscript received: 23 October 2024. Revision accepted: 4 November 2025.

Abstract. *Cahyaningsih AP, Etikawati N, Yunus A. 2025. Gamma-ray irradiation induced polymorphism in* Echinacea purpurea *revealed by RAPD markers. Nusantara Bioscience 17: 289-297.* One of the major challenges in the development and cultivation of *Echinacea purpurea* in Indonesia is the narrow genetic diversity and the lack variation of local accessions, which restricts breeding potential to produce superior varieties with improved traits in terms of morphological characteristics and phytochemical content as medicinal ingredients. To overcome this challenge, gamma-ray irradiation methods can be used as an effective tool to induce mutations and increase genetic variability. This study investigated the impact of gamma irradiation on the genetic diversity of *E. purpurea* using Random Amplified Polymorphic DNA (RAPD) markers. The seeds of *E. purpurea* were irradiated using gamma-ray with irradiation doses of 0 Gy (control), 20 Gy, 40 Gy, and 60 Gy. Nine RAPD primers, including OPA-10, OPA-16, OPA-18, and OPA-19, were used to amplify DNA segments. The binary data obtained from the electrophoresis visualization for each treatment were analyzed using the Dice similarity index to calculate the similarity index. Dendrogram construction were performed using the NTSYS. The analysis revealed a significant increase in genetic diversity at doses of 40 Gy and 60 Gy, with 58.04% of the total bands showing polymorphism across all treatments. The 60 Gy treatment, in particular, resulted in the highest genetic dissimilarity compared to the control, indicating a dose-dependent response. The similarity coefficients between control and irradiated plants ranged from 63.7% (20 Gy) to 84.4% (0 Gy), with a noticeable trend toward greater genetic differentiation as the irradiation dose increased. These findings suggest that gamma irradiation effectively induces genetic variation in *E. purpurea*, which could be harnessed for mutation breeding programs aimed at improving desirable traits such as phytochemical production. However, further studies with larger sample sizes and long-term evaluation are needed to assess the stability of these mutations and their potential for incorporation into breeding programs. This study provides preliminary evidence supporting the use of gamma irradiation in enhancing genetic diversity and its potential application in breeding superior *E. purpurea* varieties with improved agronomic or medicinal traits.

Keywords: *Echinacea purpurea*, gamma irradiation, medicinal plant, molecular marker, mutation breeding

INTRODUCTION

Echinacea purpurea (L.) Moench is a medicinal plant long recognized in traditional medicine, particularly as a powerful immunostimulant. It is widely used to boost the immune system and reduce symptoms of common colds and influenza. Extracts from the aerial parts of *E. purpurea*, including the stem, leaves, and roots, are commonly used in pharmaceutical preparations to accelerate the healing of upper respiratory tract infections (Burlou-Nagy et al. 2022). The use of *E. purpurea* extracts is not limited to immunomodulation therapy but is also known for its significant antioxidant and anti-inflammatory properties (Manayi et al. 2015; Miroshina and Poznyakovskiy 2023). These pharmacological qualities make it one of the key plants in the herbal medicine industry, especially in Europe and North America, where it was first widely cultivated. In Indonesia, the use of *E. purpurea* is relatively new, but its potential in the pharmaceutical industry is substantial, particularly in disease prevention and public health improvement. In Indonesia, *E. purpurea* has been used in health supplements to help maintain the immune system (Pramesty 2021).

One of the major challenges in the development and cultivation of *E. purpurea* in Indonesia is the narrow genetic diversity and the lack variation of local accessions, which restricts breeding potential to produce superior varieties with improved traits in terms of morphological characteristics and phytochemical content as medicinal ingredients. To overcome this challenge, gamma-ray irradiation methods can be used as an effective tool to induce mutations and increase genetic variability. This technique has proven successful in various plants, including *Musa paradisiaca* (Due et al. 2019) and *Oryza sativa* (Purwanto et al. 2019), as well as ornamental plants like *Chrysanthemum* (Susila et al. 2019) and medicinal plant such as *Celosia cristata* (Muhallilin et al. 2019). Gamma irradiation induces mutations that lead to increased phenotypic diversity and altered chemical content, potentially improving the medicinal properties of plants.

Although gamma-ray irradiation is a promising technique, there remains a gap in knowledge regarding the dose-

specific effects of gamma irradiation on *E. purpurea*'s genetic traits. While prior studies have used irradiation in other plants, the impact of different doses on the genetic diversity of *E. purpurea* has not been well-explored. Specifically, the effects of varying irradiation doses on the genetic markers of *E. purpurea* need further investigation to optimize breeding strategies. In this context, molecular markers such as Random Amplified Polymorphic DNA (RAPD) provide an efficient and cost-effective means of detecting genetic changes induced by irradiation. RAPD markers are ideal for *E. purpurea*, whose genome has not been fully mapped, and they are useful for assessing genetic variations in plants subjected to mutagenesis (Nasution et al. 2021).

While RAPD markers have been used in previous studies on *E. purpurea* to explore genetic diversity (Subositi and Widiastuti 2013), this study introduces a novel approach by combining gamma-ray irradiation with RAPD analysis to investigate the genetic variation induced by different irradiation doses in Indonesian accessions of *E. purpurea*. Unlike earlier research, which focused on natural genetic diversity without the use of mutagenesis, this study aims to fill the knowledge gap on the dose-specific effects of gamma-ray irradiation, providing insights into how different doses impact genetic variation in *E. purpurea*.

Gamma-ray irradiation in mutation breeding not only aims to increase genetic diversity but also to influence key agronomic traits that can improve plant production. Previous studies on horticultural crops have shown that the appropriate irradiation dose can accelerate flowering time, increase biomass yield, and shorten the harvest period (Holme et al. 2019), which is particularly beneficial for plants with long vegetative phase like *E. purpurea*. Moreover, inducing genetic diversity through irradiation can improve secondary metabolite content, enhancing the pharmacological value of *E. purpurea*, especially regarding flavonoid content, which is crucial for its medicinal properties (Hanifah et al. 2024).

This study specifically aimed to investigate the effects of different gamma-ray irradiation doses on the genetic diversity of Indonesian accessions of *E. purpurea* using RAPD markers. The findings of this study are expected to provide a foundation for developing superior varieties with higher pharmacological potential and improved agronomic traits. Additionally, the superior accessions developed through irradiation are anticipated to reduce the need for plant imports, thereby providing raw materials for the pharmaceutical industry in Indonesia.

MATERIALS AND METHODS

Plant material

The plant material used in this study was *Echinacea purpurea* Accession 3 (A3) seeds from Research and Development Center for Medicinal Plants and Traditional Medicine (B2P2TOOT), Tawangmangu, Central Java, Indonesia. *Echinacea purpurea* accession at B2P2TOOT is an *Echinacea* plant imported from Germany through PT. Deltomed Laboratories. Accession A3 is one of three leading accessions of B2P2TOOT planted in the highlands, classified based on minor morphological variations in flower shape and stem color. In the highland, this accession noted for lacking variants with uniform tillers (Subositi and Fauzi 2016). Both highland and lowland, this accession has low growth yield and secondary metabolite levels (Sidhiq et al. 2020). The irradiation of *E. purpurea* seeds was conducted at the PAIR-BATAN Laboratory (Center for Isotope and Radiation Applications - National Nuclear Energy Agency), Jakarta, Indonesia. The irradiated seeds were sown, and the seedlings were planted in the agricultural land of Universitas Sebelas Maret, Jumantono, Central Java, Indonesia. Molecular analysis was performed at the Biology Laboratory, Faculty of Mathematics and Natural Sciences, Universitas Sebelas Maret. The research was conducted from May 2021 to April 2022.

Gamma-ray irradiation and seed sowing

The flowers of *E. purpurea* A3 from B2P2TOOT were collected and sun-dried for two days. Afterward, the seeds attached to the dried flowers were separated and sorted, selecting only those seeds that contained the embryo. A total of 120 *E. purpurea* seeds, with 30 seeds for each treatment, were placed in plastic clips and labeled according to each gamma radiation dose. The seeds were irradiated using a Gamma Chamber/Gamma Cell-220 upgrade with irradiation doses of 0 Gy (control), 20 Gy, 40 Gy, and 60 Gy by a $_{60}$Co source at a dose rate of 3789.4 Gy h^{-1}. The gamma irradiation time for a dose of 20 Gy was 19 seconds, a dose of 40 Gy was 38 seconds, and a dose of 60 Gy was 57 seconds. Irradiated *E. purpurea* seeds were sown in seed trays filled with a soil and manure mixture at a ratio of 3:2. The seeds were placed on the surface and gently pressed to ensure good contact with the soil. They were then covered with 3-5 mm of soil and watered gently but thoroughly to moisten the soil. The trays were placed in a bright and warm location, with the soil kept moist until germination. Seedlings aged 30 DAS (Days After Sowing) were transplanted into polybags (15x15 cm) filled with the same soil and manure mixture at a ratio of 3:2. Watering and seedling care were carried out daily until 120 DAS. Germination and seeding were carried out in a greenhouse.

Field planting

Echinacea purpurea seedlings aged 120 DAS (Days After Sowing) were transplanted into beds (300x100 cm) for each treatment. *Echinacea purpurea* plants were planted with a spacing of 30 cm. The beds were shaded using a shade net with 65% density. In each bed, 10 *E. purpurea* seedlings were planted for each treatment. Two plants from each treatment were taken as samples. *Echinacea purpurea* plants were maintained until they were 120 Days After Field Planting (DAFT) by watering once a day. Control plants and gamma-ray irradiated plants are displayed in Figure 1.

Figure 1. *Echinacea purpurea* plant material irradiated with gamma-rays. A. Control, B. 20 Gy, C. 40 Gy, D. 60 Gy

Molecular analysis using RAPD markers

DNA extraction

DNA extraction from *E. purpurea* leaves for each treatment was performed according to Plant Genomic Mini Kit protocol provided by Geneaid, which consists of five stages of DNA isolation: tissue dissociation, lysis, DNA binding, washing, and DNA elution. The quality and quantity of extracted DNA were examined using an Eppendorf Biophotometer Plus. The DNA purity determined based on the absorbance measurement at a wavelength of λ 260/280. DNA isolates with a purity value of 1.8-2.0 were considered suitable for the next stage. This range indicates minimal contamination, which is crucial for efficient DNA amplification in PCR (Sophian et al. 2021).

DNA amplification (PCR-RAPD)

The DNA amplification of *E. purpurea* plants for each treatment, based on RAPD markers, was conducted using 9 primers (Table 1). The RAPD primers used were based on a literature review of several studies on the genetic variation of *E. purpurea* species, consisting of 3 accessions from the study by Subositi and Widiyastuti (2013) and 6 accessions from the study by Lema-Rumińska et al. (2019). PCR amplification preparation began by making a PCR mix with a total volume of 25 µL, consisting of 2 µL of DNA template, 1 µL of primer, 12.5 µL of MyTaq HS Red Mix, and 9.5 µL of ddH_2O. The amplification process was performed using a Veriti™ thermal cycler with the following stages: pre-denaturation at 94°C for 5 minutes, followed by 35 cycles of denaturation at 94°C for 1 minute, annealing (depending on the primer, 36°C-38°C) for 1 minute, elongation at 72°C for 2 minutes, extension at 72°C for 8 minutes, and a final holding temperature of 4°C (Subositi and Widiyastuti 2013). The amplified products were stored at -20°C.

Electrophoresis

The PCR products were checked using 2% agarose gel electrophoresis. A total of 2 g of agarose powder was dissolved in 100 mL of 0.8X TAE buffer, and 10 µL of SYBR safe DNA gel stain was added. A total of 5 µL of PCR product DNA was mixed with 2 µL of loading dye on a piece of parafilm until homogeneous using a micropipette. The mixture was then loaded into the wells of the agarose gel. A 100 bp DNA ladder (3 µL) was loaded into the leftmost well. Electrophoresis was carried out by closing the electrophoresis tank and connecting it to the power supply at 100 volts for 30 minutes. Gel images were recorded using Bio-Rad Gel Doc XR+ System. The agarose gel was placed into the Gel documentation system to observe the polymorphism bands for each treatment of mutant *E. purpurea* plants.

Table 1. RAPD primers used for PCR

Primer	Sequence (5'-3')	Tm (ºC)	Reference
OPA-10	GTGATCGCAG	38	Subositi and Widiyastuti (2013)
OPA-16	AGCCAGCGAA	37	Lema-Rumińska et al. (2019)
OPA-17	GACCGCTTGT	38	Lema-Rumińska et al. (2019)
OPB-4	GGACTGGAGT	36	Lema-Rumińska et al. (2019)
OPE-6	AAGACCCCTC	36	Subositi and Widiyastuti (2013)
OPF-6	GGGAATTCGG	36	Lema-Rumińska et al. (2019)
OPG-4	AGCGTGTCTG	38	Lema-Rumińska et al. (2019)
OPH-13	GACGCCACAC	37	Subositi and Widiyastuti (2013)
OPO-15	TGG GTCCTT	38	Lema-Rumińska et al. (2019)

Note: Tm: Melting temperature of primer

Data analysis

Molecular data observation was conducted by examining the visualization of DNA fragments based on the RAPD primers used. In the visualization results, a score of 1 was assigned if a fragment was present, and a score of 0 if no fragment was present. The binary data representing the presence or absence of fragments were used to calculate the number and percentage of polymorphisms. The binary data obtained from the electrophoresis visualization for each treatment were analyzed using the Dice similarity index to calculate the similarity index. Dendrogram construction was performed using the NTSYS 2.02 software with the UPGMA method (Rohlf 2000).

RESULTS AND DISCUSSION

Amplification products using RAPD primers

In this study, RAPD markers were used to assess the increase in genetic variation due to the application of gamma-ray irradiation on *Echinacea purpurea* plants. A total of 9 primers were selected and optimized to identify polymorphisms in the DNA amplification products resulting from gamma irradiation. Two plant samples were used for each primer and irradiation dose. All samples irradiated with doses of 0, 20 Gy, 40 Gy, and 60 Gy successfully produced amplicons with the nine primers used, detecting both polymorphic and monomorphic bands. The amplified DNA bands can be seen in Figure 2.

In this study, a total of 135 DNA bands were generated using 9 primers, with an average polymorphism rate of 58.04%, and band sizes ranging from 200 to 2000 bp. Among these, 79 bands were polymorphic, while 56 were monomorphic. Five primers (OPA-16, OPA-17, OPB-04, OPE-06, and OPG-04) produced polymorphism rates greater than 50%, whereas the remaining four primers (OPA-10, OPF-06, OPH-13, and OPO-15) had polymorphism rates below 50%. Of the five primers with more than 50% polymorphism, only OPE-06 reached 100%. The number of amplified DNA bands is summarized in Table 2.

The use of RAPD markers to detect polymorphism in *E. purpurea* plants has been demonstrated in studies by Subositi and Widiastuti (2013) and Lema-Rumińska et al. (2019). Subositi and Widiastuti's study produced 48 fragments with an average polymorphism of 75%, while Lema-Rumińska et al. (2019) reported 110 fragments with a polymorphism percentage of 97.35%. In the current study, the total number of DNA fragments was higher, but the percentage of polymorphism was lower. The differences in polymorphism percentages are related to the type and number of primers used, as well as the *E. purpurea* accessions serving as DNA samples. The two previous studies used more than three accessions known to have morphological variation, whereas this study used a single accession irradiated at various doses, with the DNA samples coming from irradiated plants. This study combined primers from both previous studies. Amplified DNA bands come from DNA samples complementary to the primer, while polymorphic bands result from bands not amplified at a specific locus (Sulistyawati and Widyatmoko 2017), indicating one or more alternative phenotypes and suggesting genetic variation (Singh and Kulathinal 2013). Polymorphism in mutant plants can occur due to substitution, deletion, or insertion of nitrogenous bases at the primer binding sites, preventing amplification, or due to insertions or deletions that change the size of the amplified fragment (Riviello-Flores et al. 2022).

While compared to studies on other medicinal plant, the research by Magdy et al. (2020) found a polymorphism percentage of 74.14% in the RAPD analysis of gamma-ray irradiated ginger (*Zingiber officinale*), where they used 5 primers and obtained 58 bands (15 monomorphic and 43 polymorphic). The varying levels of polymorphism across each primer confirm genetic variation in the gamma-irradiated plants compared to the control (Riviello-Flores et al. 2022). RAPD molecular markers have been used in several studies to determine genetic variation in mutant plants induced by gamma irradiation. Previous studies on *Typhonium flagelliforme* (Sianipar et al. 2015), *Tectona grandis* (Parlaongan et al. 2022), *Coriandrum sativum* (Jabbar SM and Al-Tamimi 2022), and *Persea americana* (Ihsan et al. 2023) reported that RAPD markers are highly useful for identifying mutant plants based on detected polymorphisms, though not all primers consistently yield optimal polymorphic bands. However, each study identified some of the most effective primers. In this study, primers OPA-16 and OPB-04 showed strong polymorphism.

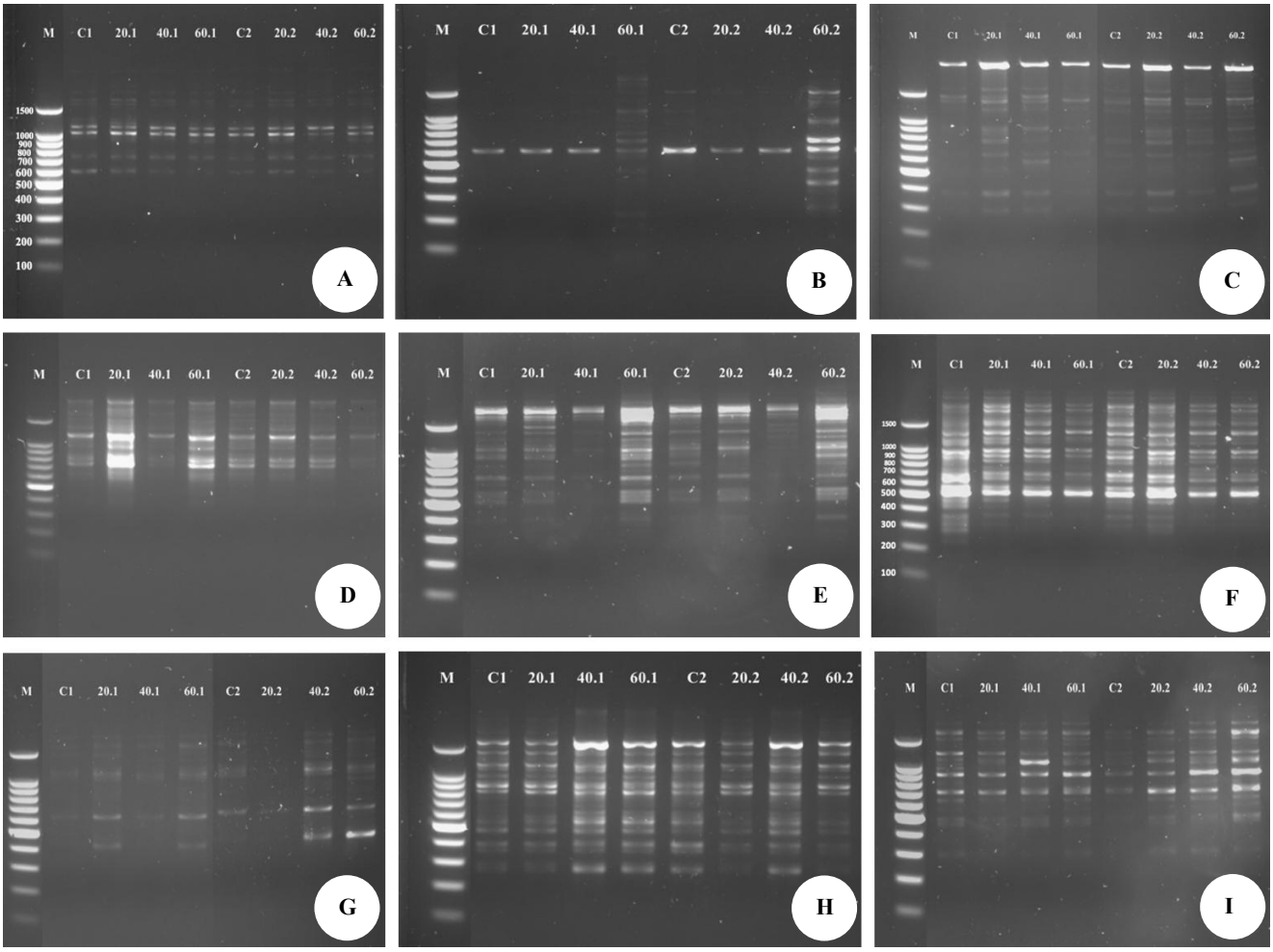

Figure 2. DNA bands resulting from amplification using RAPD primers. A. OPA-10, B. OPA-16, C. OPB-04, D. OPA-17. E. OPG-04. F. OPF-06, G. OPE-06, H. OPH-13. I. OPO-15. C: Control, 20: 20 Gy, 40: 40 Gy, 60: 60 Gy. M: Marker 100 bp

Table 2. Amplified DNA bands using RAPD primers

Primer	Size of DNA band (bp)	Loci				% polymorphism
		Amount of DNA band	Polymorphic	Monomorphic	Unique	
OPA-10	600-2000	10	2	8	-	20
OPA-16	200-1700	16	15	1	5	93.75
OPA-17	300-1700	16	9	7	1	56.25
OPB-04	300-1800	16	11	5	1	68.75
OPE-06	400-1800	11	11	0	-	100
OPF-06	275-2000	22	9	13	-	40.90
OPG-04	400-2000	18	14	4	-	77.77
OPH-13	600-1800	10	4	6	-	40
OPO-15	275-1800	16	4	12	-	25
Total		135	79	56	7	
Average		15	8.7	6.2	-	58.04

Unique DNA fragments

Several unique or specific fragments were also obtained from amplification results using RAPD primers (Table 2). Unique or specific bands are those that appear in certain genotypes but are absent in others (Sharma et al. 2019). The 20 Gy treatment produced two specific fragments: a 500 bp fragment with primer OPB-04 and a 1400 bp fragment with primer OPA-17. Meanwhile, the 60 Gy treatment produced five specific fragments with primer OPA-16: fragments of 200 bp, 800 bp, and 1000 bp in the first sample, and fragments of 250 bp and 350 bp in the second sample. One of the advantages of using RAPD markers is the ability to obtain unique fragments from amplification results. These unique fragments can be used for the identification and characterization of accessions and as character materials for plant breeding purposes (Subositi

and Widiastuti 2013).

At the 20 Gy dose, although considered a relatively low irradiation dose, mutations were still induced; this effect was detectable through RAPD analysis as this molecular marker is sensitive to genetic changes such as small insertions or deletions (Riviello-Flores et al. 2022). These genetic changes led to the formation of unique fragments that could be distinguished from the control group, as the mutations altered the binding site locations of the RAPD primers. Studies have confirmed that RAPD markers are effective in identifying polymorphic and unique bands induced by gamma-ray irradiation (Roy et al. 2006; Jabbar and Al-Tamimi 2022). On the other hand, 60 Gy induces a broader range of genetic mutations, including large-scale structural changes such as deletions, duplications, or rearrangements of the DNA (Shu et al. 2012). Primers like OPA-16 can amplify these regions with larger structural variations, leading to the appearance of unique bands. The higher mutation rate associated with the 60 Gy dose increases the probability of generating genetic variation in loci that are targeted by these primers, resulting in more specific fragment patterns.

Data on the effect of gamma irradiation on the morphological diversity of *E. purpurea*, both qualitatively and quantitatively, has been published by Cahyaningsih et al. (2022). The unique fragments that appeared in *E. purpurea* plants irradiated at doses of 20 Gy and 60 Gy may be related to their morphological characteristics. At 20 Gy, the variation observed was a distinct flower shape compared to all other treatments. At 60 Gy, more variations were noted, corresponding to the unique fragments, such as the shortest plant height, darker flower color, and the longest time to first flowering compared to all other treatments (Cahyaningsih et al. 2022). Primers OPB-04, OPA-17, and OPA-16 can be used to detect mutant plant characteristics and may later be used in marker-assisted selection, particularly for flower traits in *E. purpurea*, however, further validation studies are required.

Marker-assisted selection can be performed by analyzing the relationship between DNA markers and specific genes or phenotypes (Ben-Ari and Lavi 2012). RAPD markers can be used to evaluate diversity and identify potential sources of unique genetic material by indicating the presence of specific fragments (Nadeem et al. 2018). Several studies have evaluated the use of RAPD as markers that can link specific fragments to desired phenotypes (Ntuli et al. 2015; Vishalakshi et al. 2012; Miladinović et al. 2018; Subositi et al. 2021).

Dendrogram

Table 3 shows the similarity coefficient values analyzed based on Dice similarity. Coefficient values closer to 1 indicate a high degree of similarity between samples, while values closer to 0 indicate increasing dissimilarity (Due et al. 2019). Gamma-ray irradiation treatments at doses of 0, 20 Gy, 40 Gy, and 60 Gy resulted in similarity coefficients ranging from 0.637 (63.7%) between the control and 60 Gy, to 0.844 (84.4%) between the control and 20 Gy. Based on these coefficient values, it is evident that the control plants and those treated with 20 Gy still have a close similarity, while the control plants compared with those treated with 40 Gy and 60 Gy show increasing dissimilarity.

The study by Subositi and Widiastuti (2013) reported that RAPD analysis of 3 accessions and 8 variants of *E. purpurea* showed narrow genetic diversity, with similarity indices ranging from 75.49% to 84.20%. This aligns with the results of this study, where the similarity index for *E. purpurea* control plants and those treated with 20 Gy ranged from 81.4% to 84.4%. This indicates that gamma-ray irradiation at 20 Gy was not able to significantly widen the similarity distance, as the similarity index remained high compared to the control plants.

For the 40 Gy treatment, the similarity distance from the control plants began to widen, with a similarity index ranging from 66.6% to 74.8%, indicating a 14.8% increase in dissimilarity. Meanwhile, for the 60 Gy treatment, the similarity distance widened further, with a similarity index of 63.7% to 70.3% compared to the control, showing a 17.7% increase in dissimilarity. These results demonstrate that gamma-ray irradiation at doses of 40 Gy and 60 Gy can induce mutations, leading to the formation of new alleles and thus increasing dissimilarity. The use of gamma-ray irradiation, which also depends on the dose, can cause larger chromosomal deletions through the occurrence of deletions or insertions of various sizes, as well as translocations (Sikora et al. 2011). Mutations in genes can result in the creation of new alleles (Ulukapi and Nasircilar 2019). The formation of new alleles through mutations induced by gamma-rays contributes to the overall genetic diversity of a species (Beyaz and Yildiz 2017).

Table 3. The similarity coefficient value of the gamma-ray irradiation results on *Echinacea purpurea* based on the RAPD marker

	C_1	20gy_1	40gy_1	60gy_1	K_2	20gy_2	40gy_2	60gy_2
C_1	1.000							
20gy_1	**0.844**	1.000						
40gy_1	0.733	0.740	1.000					
60gy_1	0.696	0.748	0.740	1.000				
K_2	0.814	0.792	0.740	0.703	1.000			
20gy_2	0.814	0.792	0.711	0.644	0.837	1.000		
40gy_2	0.666	0.718	0.814	0.674	0.748	0.733	1.000	
60gy_2	0.644	0.651	0.688	0.725	**0.637**	0.681	0.740	1.000

Note: C: Control

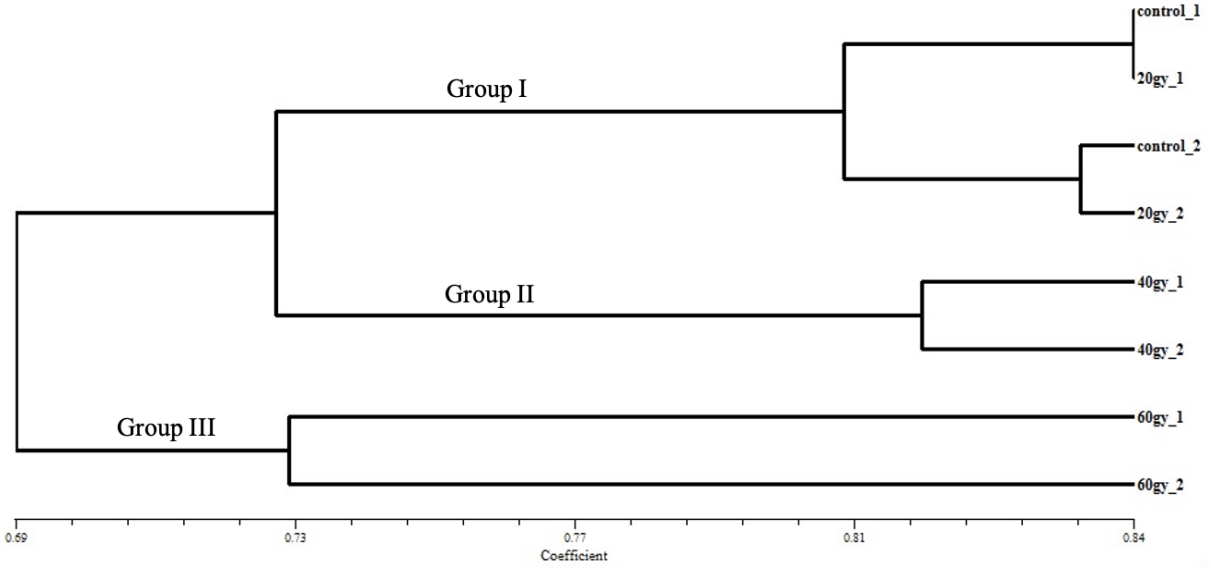

Figure 3. Dendrograms based on the estimation of genetic distance coefficient and UPGMA clustering of gamma-ray irradiation treatment on *Echinacea purpurea* based on RAPD markers

The dendrogram was constructed based on the appearance of DNA bands resulting from the amplification of 9 RAPD primers. The dendrogram construction (Figure 3) shows that gamma-ray irradiation of *E. purpurea* resulted in 3 main groups (I, II, III): the first group consists of the control and the 20 Gy treatment, the second group corresponds to the 40 Gy treatment, and the third group corresponds to the 60 Gy treatment. The dendrogram also indicates that the 60 Gy treatment has the greatest distance from the control and other irradiation treatments, while the 20 Gy treatment has the closest distance to the control.

Gamma-rays are physical mutagens that, when applied to plant organs, induce oxidative stress by generating excessive reactive oxygen species (ROS). The ROS produced can include superoxide radicals (O^{2-}), hydroxyl radicals (OH^-), and hydrogen peroxide (H_2O_2) (Yin et al. 2024). High concentrations of free radicals can affect cells, including chromosomes, leading to instability in DNA structure and causing DNA damage. However, exposure to low doses of gamma-ray irradiation, combined with DNA repair mechanisms and the role of non-enzymatic antioxidants, allows mutations to occur without resulting in significant damage (Riviello-Flores et al. 2022). Non-enzymatic antioxidants, such as phenols, have protective properties and reduce free radicals by donating hydrogen atoms or electrons, stabilizing the radicals (Hanafy and Akladious 2018). At low doses of gamma-ray irradiation, cells rely on a combination of direct and indirect DNA damage repair mechanisms to mitigate the impact of reactive oxygen species (ROS) and the resulting damage. While ROS can contribute to indirect DNA damage, various DNA repair pathways, including antioxidant defenses, play a crucial role in reducing ROS-induced damage by scavenging ROS and preventing further oxidative stress (Alanazi et al. 2024).

Echinacea purpurea is a medicinal plant with high secondary metabolite content, including flavonoids or phenols (Sidhiq et al. 2020; Ferdyana et al. 2021), which can act as antioxidants (Banica et al. 2020). Gamma-ray irradiation at doses of 20-60 Gy is still relatively low, meaning that the resulting free radicals can be reduced, leading to a low possibility of nitrogen base mutations. The changes occurring in the DNA may also relate to functional alterations; the mutations produced can lead to the formation of new alleles and increase the dissimilarity between mutant plants and control plants. Changes in DNA can manifest as base breaks, translocations, or nitrogen base deletions (Shu et al. 2012), resulting in the emergence of new DNA structures or the loss of DNA bands, which are detected as polymorphisms in molecular markers. This study's results demonstrate that RAPD markers can detect changes occurring in *E. purpurea* plants subjected to gamma-ray irradiation, also resulting in groupings of plants based on their similarity distances, which can be used as a basis for breeding and developing new varieties.

In conclusion, gamma irradiation at doses of 20 Gy, 40 Gy, and 60 Gy induces significant genetic variation in *E. purpurea* as revealed by RAPD markers. A total of nine primers, including OPA-10, OPA-16, and OPA-18, generated 58.04% polymorphism, with Dice similarity coefficients ranging from 63.7% to 84.4%. The highest genetic dissimilarity was observed at the 60 Gy dose, indicating a dose-dependent increase in genetic divergence. UPGMA clustering analysis successfully separated plants into distinct groups based on irradiation dose, further supporting the dose-dependent nature of the genetic variation induced. These results suggest that gamma irradiation can enhance the genetic diversity of *E. purpurea*, providing valuable genetic resources for breeding programs aimed at improving agronomic traits and phytochemical content. The findings also provide promising preliminary evidence for the potential use of gamma-induced genetic variation in *E. purpurea*, further research is required with larger sample

sizes, multiple accessions, and multi-generational analysis to confirm the stability of the mutations and assess the practical utility of these mutants for breeding. Future studies should also integrate agronomic and phytochemical evaluations to determine the full potential of gamma irradiation in enhancing desirable traits for crop improvement. Additionally, primers OPA-16 and OPB-04, which showed strong polymorphism in this study, are recommended for future marker-assisted selection in *E. purpurea* breeding programs.

ACKNOWLEDGEMENTS

We would like to thank Center for Research and Development of Medicinal Plants and Traditional Medicines (B2P2TOOT), Tawangmangu, Central Java, Indonesia, for providing *Echinacea purpurea* seeds for this study. This research was funded by Indonesia Endowment Fund for Education Agency (LPDP), Indonesian Ministry of Finance, for the Master's study in Biosciences from the year 2019 to 2021.

REFERENCES

Alanazi R, Alzahrani K, Alzahrani KE, Alanazi N, Alodhayb AN. 2024. Effects of low-dose gamma radiation on DNA measured using a quartz tuning fork sensor. J King Saud Univ Sci 36: 103368. DOI: 10.1016/j.jksus.2024.103368.

Banica F, Bungau S, Tit DM, Behl T, Otrisal P, Nechifor AC, Gitea D, Pavel F, Nemeth S. 2020. Determination of the total polyphenols content and antioxidant activity of *Echinacea purpurea* extracts using newly manufactured glassy carbon electrodes modified with carbon nanotubes. Processes 8 (7): 833. DOI: 10.3390/pr8070833.

Ben-Ari G, Lavi U. 2012. Marker-assisted Selection in Plant Breeding. Plant Biotechnology and Agriculture. Academic Press, Cambridge. DOI: 10.1016/B978-0-12-381466-1.00011-0.

Beyaz R, Yildiz M. 2017. The use of gamma irradiation in plant mutation breeding. In: Jurić S (eds). Plant Engineering. IntechOpen, London. DOI: 10.5772/intechopen.69974.

Burlou-Nagy C, Bănică F, Jurca T, Vicaș LG, Marian E, Muresan ME, Bácskay I, Kiss R, Fehér P, Pallag A. 2022. *Echinacea purpurea* (L.) Moench: Biological and pharmacological properties, A review. Plants 11 (9): 1244. DOI: 10.3390/plants11091244.

Cahyaningsih AP, Etikawati N, Yunus A. 2022. Morphological characters variation of Indonesian accession *Echinacea purpurea* in response to gamma-ray irradiation. Biodiversitas 23 (10): 5351-5359. DOI: 10.13057/biodiv/d231045.

Due MS, Susilowati A, Yunus A. 2019. The effect of gamma-rays irradiation on diversity of *Musa paradisiaca* var. *sapientum* as revealed by ISSR molecular marker. Biodiversitas 20 (5): 1416-1422. DOI: 10.13057/biodiv/d200534.

Ferdyana WC, Widiyastuti Y, Pujiasmanto B, Sakya AT, Yunus A. 2021. Short communication: Morphological diversity and the addition of golden snail protein: Its effect on flavonoid content on *Echinacea purpurea*. Biodiversitas 23: 62-66. DOI: 10.13057/biodiv/d230108.

Hanafy RS, Akladious SA. 2018. Physiological and molecular studies on the effect of gamma radiation in fenugreek (*Trigonella foenumgraecum* L.) plants. J Genet Eng Biotechnol 16 (2): 683-692. DOI: 10.1016/j.jgeb.2018.02.012.

Hanifah WH, Yunus A, Nandariyah, Widiyastuti Y. 2024. Morphological, agronomic characteristics, and flavonoid content of *Echinacea purpurea* at various gamma-ray doses. Bulg J Agric Sci 30 (3): 451-457.

Holme IB, Gregersen PL, Brinch-Pedersen H. 2019. Induced genetic variation in crop plants by random or targeted mutagenesis: Convergence and differences. Front Plant Sci: 1468. DOI: 10.3389/fpls.2019.01468.

Ihsan F, Ashari S, Soegianto A, Sukartini, Affandi. 2023. Effect of gamma-rays irradiation to cipedak avocado genetic diversity. Agrivita 45 (2): 231-249. DOI: 10.17503/agrivita.v45i2.4065.

Jabbar SM, Al-Tamimi AJT. 2022. Mutation induced by gamma irradiation in coriander seeds and their identification by RAPD makers. Intl J Health Sci 6 (S3): 7336-7347. DOI: 10.53730/ijhs.v6nS3.7675.

Lema-Rumińskaa J, Kulusa D, Tymoszuka A, Varejãob JMTB, Bahcevandziev K. 2019. Profile of secondary metabolites and genetic stability analysis in new lines of *Echinacea purpurea* (L.) Moench micropropagated via somatic embryogenesis. Ind Crops Prod 142: 111851. DOI: 10.1016/j.indcrop.2019.111851.

Magdy AM, Fahmy EM, Al-Ansary AERMF, Awad G. 2020. Improvement of 6-gingerol production in ginger rhizomes (*Zingiber officinale* Roscoe) plants by mutation breeding using gamma irradiation. Appl Radiat Isot 162: 109193. DOI: 10.1016/j.apradiso.2020.109193.

Manayi A, Vazirian M, Saeidnia S. 2015. *Echinacea purpurea*: Pharmacology, phytochemistry and analysis methods. Pharmacogn Rev 9 (17): 63-72. DOI: 10.4103/0973-7847.156353.

Miladinović D, Miler M, Jeromela AM, Imerovski I, Dimitrijević A, Kovačević B, Jocić S, Cvejić S, Hladni N, Obreht-Vidaković D. 2018. Evaluation of RAPD markers as a marker-assisted selection tool for variety type and erucic acid content in rapeseed. Genetika 50: 421-430. DOI: 10.2298/GENSR1802421M.

Miroshina T, Poznyakovskiy V. 2023. *Echinacea purpurea* as a medicinal plant: Characteristics, use as a biologically active component of feed additives and specialized foods (review). E3S Web Conf 380: 01005. DOI: 10.1051/e3sconf/202338001005.

Muhallilin I, Aisyah SI, Sukma D. 2019. The diversity of morphological characteristics and chemical content of *Celosia cristata* plantlets due to gamma-ray irradiation. Biodiversitas 20 (3): 862-866. DOI: 10.13057/biodiv/d200333.

Nadeem MA, Nawaz MA, Shahid MQ, Dogan Y, Comertpay G, Mehtap Yıldıze, Hatipoglu R, Ahmad F, Alsaleh A, Labhanei N, Ozkanf H, Chung G, Baloch FS. 2018. DNA molecular markers in plant breeding: Current status and recent advancements in genomic selection and genome editing. Biotechnol Biotechnol Equipment 32 (2): 261-285. DOI: 10.1080/13102818.2017.1400401.

Nasution F, Theanhom AA, Sukartini, Bhuyar P, Chumpookam J. 2021. Genetic diversity evaluation in wild *Muntingia calabura* L. based on Random Amplified Polymorphic DNA (RAPD) markers. Gene Rep 25: 101335. DOI: 10.1016/j.genrep.2021.101335.

Ntuli NR, Tongoona PB, Zobolo AM. 2015. Genetic diversity in *Cucurbita pepo* landraces revealed by RAPD and SSR markers. Scientia Horticulturae 189: 192-200. DOI: 10.1016/j.scienta.2015.03.020.

Parlaongan A, Supriyanto, Wulandari SA. 2022. Effects of gamma-ray irradiation to induce genetic variability of teak planlets (*Tectona grandis* Linn. F.). Jurnal Sylva Indonesiana 5 (1): 10-21. DOI: 10.32734/jsi.v5i01.6166.

Pramesty GT. 2021. Survey Pengaruh Mengkonsumsi Suplemen yang Mengandung *Echinacea* dalam Meningkatkan Sistem Imun Selama Pandemi Covid-19 pada Tahun 2020 berdasarkan Opini Masyarakat di Kelurahan Kebon Bawang, Kecamatan Tanjung Priuk, Jakarta Utara. [Skripsi]. Universitas 17 Agustus 1945 Jakarta, Jakarta. [Indonesian]

Purwanto E, Nandariyah, Yuwono SS, Yunindanova MB. 2019. Induced mutation for genetic improvement in black rice using gamma-ray. Agrivita 41 (2): 213-220. DOI: 10.17503/agrivita.v41i2.876.

Riviello-Flores ML, Cadena-Iñiguez J, Ruiz-Posadas LDM, Arévalo-Galarza ML, Castillo-Juárez I, Soto Hernández M, Castillo-Martínez CR. 2022. Use of gamma radiation for the genetic improvement of underutilized plant varieties. Plants 11 (9): 1161. DOI: 10.3390/plants11091161.

Roy S, Begum Y, Chakraborty A, Raychaudhuri SS. 2006. Radiation-induced phenotypic alterations in relation to isozymes and RAPD markers in *Vigna radiata* (L.) Wilczek. Intl J Radiat Biol 82 (11): 823-832. DOI: 10.1080/09553000600969804.

Sharma A, Rajpurohit D, Jain D, Verma P, Joshi A. 2019. Molecular characterization of coriander (*Coriandrum sativum* L.) genotypes using random amplified polymorphic DNA (RAPD) markers. J Pharmacogn Phytochem 8 (3): 4770-4775.

Shu QY, Forster BP, Nakagawa H. 2012. Plant Mutation Breeding and Biotechnology. CABI, Wallingford. DOI: 10.1079/9781780640853.0000.

Sianipar NF, Ariandana, Maarisit W. 2015. Detection of gamma-irradiated mutant of rodent tuber (*Typhonium flagelliforme* Lodd.) in vitro

culture by RAPD molecular marker. Proc Chem 14: 285-294. DOI: 10.1016/j.proche.2015.03.040.

Sidhiq DF, Widiyastuti Y, Subositi D, Pujiasmanto B, Yunus A. 2020. Morphological diversity, total phenolic and flavonoid content of *Echinacea purpurea* cultivated in Karangpandan, Central Java, Indonesia. Biodiversitas 21: 1256-1271. DOI: 10.13057/biodiv/d210355.

Sikora P, Chawade A, Larsson M, Olsson J, Olsson O. 2011. Mutagenesis as a tool in plant genetics, functional genomics, and breeding. Intl J Plant Genom 2011: 314829. DOI: 10.1155/2011/314829.

Singh RS, Kulathinal RJ. 2013. Polymorphism. Brenner's Encyclopedia of Genetics (Second Edition). Academic Press, San Diego. DOI: 10.1016/B978-0-12-374984-0.01189-X.

Sophian A, Purwaningsih R, Muindar, Igirisa EPJ, Amirullah ML. 2021. Short communication: Analysis of purity and concentration of DNA extracted from intron patho gene-spin extraction on processed crab food product samples. Asian J Trop Biotechnol 18 (1): 28-31. DOI: 10.13057/biotek/c180103.

Subositi D, Fauzi. 2016. Keragaman instraspesifik aksesi ekinase (*Echinacea purpurea* (L.) Moench) hasil seleksi massa tahap I berdasarkan analisis ISSR. Jurnal Tumbuhan Obat Indonesia 9 (1): 11-18. DOI: 10.22435/toi.v9i1.6337.11-18. [Indonesian]

Subositi D, Joice, Mursyanti E, Widodo H, Widiyastuti Y. 2021. RAPD primer screening for markers development of Jinten Hitam (*Nigella sativa* L.) authentication. E3S Web Conf 306: 01008. DOI: 10.1051/e3sconf/202130601008.

Subositi D, Widiyastuti Y. 2013. Keragaman genetik aksesi ekinase (*Echinacea purpurea* (L.) Moench) hasil seleksi massa tahun I melalui analisis RAPD. Buletin Kebun Raya 16 (2): 93-100. [Indonesian]

Sulistyawati P, Widyatmoko AYPBC. 2017. Keragaman genetik populasi kayu merah (*Pterocarpus indicus* Willd.) menggunakan penanda Random Amplified Polymorphism DNA. Jurnal Pemuliaan Tanaman Hutan 11: 67-76. DOI: 10.20886/jpth.2017.11.1.67-76. [Indonesian]

Susila E, Susilowati A, Yunus A. 2019. The morphological diversity of *Chrysanthemum* resulted from gamma-ray irradiation. Biodiversitas 20 (2): 463-467. DOI: 10.13057/biodiv/d200223.

Ulukapi K, Gul-Nasircilar A. 2019. Induced mutation: Creating genetic diversity in plants. In: El-Esawi MA (eds). Genetic Diversity in Plant Species-Characterization and Conservation. IntechOpen, London. DOI: 10.5772/intechopen.81296.

Vishalakshi B, Umakanth B, Shanbhag AP, Ghatak A, Sathyanarayanan N, Madhav MS, Krishna GG, Yadla H. 2012. RAPD assisted selection of black gram (*Vigna mungo* L. Hepper) towards the development of multiple disease resistant germplasm. 3 Biotech 7 (1): 1. DOI: 10.1007/s13205-016-0582-8.

Yin Y, Cui D, Chi Q, Xu H, Guan P, Zhang H, Jiao T, Wang X, Wang L, Sun H. 2024. Reactive oxygen species may be involved in the distinctive biological effects of different doses of 12C6+ ion beams on *Arabidopsis*. Front Plant Sci 14: 1337640. DOI: 10.3389/fpls.2023.1337640.

NUSANTARA BIOSCIENCE
Vol. 17, No. 2, pp. 298-312
November 2025

ISSN: 2087-3948
E-ISSN: 2087-3956
DOI: 10.13057/nusbiosci/n170212

Phylogeny and recombination of papaya begomoviruses in Northern and Central-East India

AARSHI SRIVASTAVA[1], VINEETA PANDEY[1,2], RAKESH KUMAR VERMA[3], AVINASH MARWAL[4], RAMWANT GUPTA[5], MUHAMMAD SHAFIQ SHAHID[6,♥], R. K. GAUR[1,7,♥♥]

[1]Department of Biotechnology, Deen Dayal Upadhyaya Gorakhpur University. Gorakhpur 273009, Uttar Pradesh, India
[2]Zonal Agricultural Research Station, Indira Gandhi Krishi Vishwavidyalaya. Jagdalpur 494001, Chhattisgarh, India
[3]Department of Biosciences, SLAS, Mody University of Science and Technology. Sikar Rd, Laxmangarh, Narodara Rural 332311, Rajasthan, India
[4]Department of Biotechnology, Mohanlal Sukhadia University. Vigyan Bhawan, Block-B, New Campus, Udaipur 313001, Rajasthan, India
[5]Department of Botany, Deen Dayal Upadhyaya Gorakhpur University. Gorakhpur 273009, Uttar Pradesh, India
[6]Department of Plant Sciences, College of Agricultural and Marine Sciences, Sultan Qaboos University. Al-Khoud 123, Muscat, Oman. ♥email: mshahid@squ.edu.om
[7]Uttar Pradesh Council of Agricultural Research (UPCAR). Anand Nagar, Alambagh, Lucknow 226005, Uttar Pradesh, India. Tel.: +91-522-2721626, ♥♥email: gaurrajarshi@hotmail.com

Manuscript received: 11 September 2025. Revision accepted: 8 November 2025.

Abstract. *Srivastava A, Pandey V, Verma RK, Marwal A, Gupta R, Shahid MS, Gaur RK. 2025. Phylogeny and recombination of papaya begomoviruses in Northern and Central-East India. Nusantara Bioscience 17: 298-312.* Papaya plants exhibiting characteristic leaf curl symptoms were surveyed in 2022 across Uttar Pradesh, Delhi, and Chhattisgarh, India. *Begomovirus* infection was suspected based on symptomatology and confirmed in 11 of 47 collected samples using PCR with *Begomovirus*-specific primers. This study aimed to elucidate the diversity and distribution of begomoviruses infecting papaya in these regions. Full-length viral genomes were amplified through Rolling Circle Amplification (RCA), and associated alphasatellites and betasatellites were detected using PCR with universal primers. The amplified viral genomes (~2.7 kb), betasatellites (~1.4 kb), and alphasatellites (~1.3 kb) were cloned and sequenced. Sequence analysis revealed 94.57-99.46% nucleotide identity of DNA-A with known isolates of Papaya Leaf Curl Virus (PaLCuV), Cotton Leaf Curl Virus (CLCuV), Croton Yellow Vein Mosaic Virus (CYVMV), Tomato Leaf Curl New Delhi Virus (ToLCNDV), and Cotton Leaf Curl Multan Virus (CLCuMuV). The DNA-B component exhibited 98.33% identity with ToLCNDV. Ten betasatellites shared 86.81-99.71% identity with related species, whereas two alphasatellites showed approximately 98.5% identity with PaLCuA and PaLCVSA. One betasatellite (PL36) displayed 86.81% identity and was identified as a novel Papaya Leaf Curl Raipur Betasatellite (PaLCuRPRB). Furthermore, six PaLCuV isolates showing <91% identity was classified as new PaLCuV variants.

Keywords: *Begomovirus*, diversity, papaya leaf curl disease, phylogeny, species demarcation tool

INTRODUCTION

Papaya (*Carica papaya* L.) is an important tropical fruit crop of high nutritional and economic value. However, its production is severely constrained by several biotic stresses, among which Papaya Leaf Curl Disease (PaLCD) is the most destructive. The disease manifests as interveinal chlorosis, severe leaf curling, stunted growth, and poor fruit quality, leading to significant yield losses (Udavatha et al. 2022; Varun et al. 2024). First observed in India in 1998, the causal agent was later identified as Papaya Leaf Curl Virus (PaLCV), a member of the *Begomovirus* genus transmitted by the whitefly *Bemisia tabaci* (Gennadius, 1889) (Saxena et al. 1998; Soni et al. 2022). Its efficient transmission and broad host range have contributed to the widespread occurrence of PaLCD across tropical and subtropical regions.

Begomoviruses possess circular single-stranded DNA genomes of approximately 2.7 kb, which may occur as monopartite (DNA-A) or bipartite (DNA-A and DNA-B) components. These genomes encode essential proteins required for replication, transcription, and movement within host cells. Many monopartite Begomoviruses are associated with betasatellites and alphasatellites—small DNA molecules (~1.3-1.4 kb) that rely on helper viruses for replication (Nogueira et al. 2021). The βC1 gene of betasatellites is known to induce symptom expression and suppress host defense mechanisms. Genetic recombination and mutation events are major drivers of *Begomovirus* evolution, host adaptation, and pathogenic variability (Fiallo-Olivé and Navas-Castillo 2023; Akram et al. 2025).

Viruses are subjected to diverse selective pressures resulting from the interplay between shifting fitness requirements and the conservation of essential functions (Spielman et al. 2019; Butković and González 2022). Because different crop species cultivated across diverse agro-climatic zones possess distinct genetic backgrounds and immune systems, Begomoviruses likely encounter geographically variable host immune responses. Consequently, virus sub-strains circulating in India may undergo region-specific selective pressures.

Despite the widespread incidence of PaLCD in India, comprehensive information on the molecular diversity, evolutionary dynamics, and recombination patterns of PaLCV and its associated satellites remains limited particularly in northern and central India. Understanding

this variability is crucial for identifying emerging viral strains and devising effective management strategies. Therefore, the present study investigates the genetic diversity, recombination events, and phylogenetic relationships of PaLCV and its associated satellites infecting papaya in Uttar Pradesh, Delhi, and Chhattisgarh. These findings provide new insights into the molecular epidemiology of PaLCD and offer a foundation for developing region-specific disease management approaches.

PaLCD severely impacts papaya plant health and productivity, causing leaf curling, distortion, stunted growth, and fruit yield losses ranging from 40 to 100% in severely affected regions, including the United States and Mexico (Srivastava et al. 2022a). Symptom severity varies with the host genotype, environmental factors, and virus strain. The complex genomic organization of Begomoviruses , coupled with their extensive host and vector range, makes PaLCD management particularly challenging. Integrated management strategies currently include whitefly control, the use of resistant cultivars, removal of infected plants, adoption of appropriate cultural practices, and implementation of monitoring and early detection programs (Nadeem et al. 1997; Saxena et al. 1998).

PaLCD represents a complex viral disease system caused by multiple begomoviral species, including Papaya Leaf Curl Virus (PaLCuV), Papaya Leaf Curl China Virus (PaLCuCNV), Papaya Leaf Curl Guandong Virus (PaLCuGDV), Chili Leaf Curl Virus (ChiLCV), Tomato Leaf Curl Virus (ToLCV), Pedilanthus Leaf Curl Virus (PeLCuV), and Papaya Leaf Crumple Virus (PaLCrV), often in association with betasatellites. Among these, Indian isolates of PaLCuV constitute the major component of the disease complex affecting papaya, related crops, and several weed species (Hallan et al. 1998). Although sporadic studies have reported *Begomovirus* infections in papaya, this study provides the first comprehensive account of the diversity and distribution of Begomoviruses infecting papaya in northern and central India.

MATERIALS AND METHODS

Virus isolates: Detection and characterization

Papaya plants exhibiting typical leaf curl symptoms, including wrinkled and twisted leaves with yellow veins, were observed (Figure 1). The petioles appeared short, thick, and twisted. Symptomatic plants either lacked fruits or bore small, misshapen ones. A total of forty-seven symptomatic and one non-symptomatic papaya leaf samples were collected from different locations across Chhattisgarh, Delhi, and Uttar Pradesh, India. The collected leaf samples were designated as PL-1 to PL-47 and stored at 4°C in the laboratory for further analysis (Table 1). Total genomic DNA was extracted from each sample using the CTAB method (Doyle and Doyle 1990). PCR amplification was performed using *Begomovirus*-specific primer sets for virus detection. Out of forty-seven samples, eleven tested positive and were selected for Rolling Circle Amplification (RCA) to obtain the complete viral genome. Samples were further screened for the presence of DNA-B, betasatellites, and alphasatellites using universal primer pairs. One sample was positive for DNA-B, ten for betasatellites, and two for alphasatellites (Table 2), and these were used for complete genome sequencing. RCA products were subjected to restriction digestion to release begomoviral genome components, which were subsequently cloned into the pTZ57RT vector and transformed into *Escherichia coli* DH5α cells. The cloned products were fully sequenced using an ABI automated sequencer (BioKart, Bangalore, India).

Figure 1. Papaya plants showing different symptoms of *Begomovirus* infection under field conditions: A. Vein thickening, Blistering; B. Leaf Curl, Interveinal Chlorosis; C. Vein enation, Distorted petioles, Upward/Downward Curling; D. Yellow mosaic patterns; E. Healthy stocks

Table 1. Geographical locations of symptomatic papaya leaf isolates collected from papaya and RCA representative isolates used for full length genome sequencing

Sl. No.	Location of collected isolates	State	Name assigned	PCR/RCA result	Sequenced
1.	Gorakhpur (Nakha Jangle)	Uttar Pradesh	PL 1	Positive	MZ605904 - MZ605905
2.	Gorakhpur (Transport Nagar)	Uttar Pradesh	PL 2	Negative	-
3.	Gorakhpur (Amrood mandi)	Uttar Pradesh	PL 3	Negative	-
4.	Gorakhpur (Belwar)	Uttar Pradesh	PL 4	Negative	-
5.	Gorakhpur (D.D.U. Campus)	Uttar Pradesh	PL 5	Negative	-
6.	Gorakhpur (Gida)	Uttar Pradesh	PL 6	Positive	MZ669217 - MZ606364
7.	Gorakhpur (Singhariya)	Uttar Pradesh	PL 7	Negative	-
8.	Gorakhpur (Salempur)	Uttar Pradesh	PL 8	Negative	-
9.	Gorakhpur (Kunraghat)	Uttar Pradesh	PL 9	Negative	-
10.	Bastar	Chhattisgarh	PL 10	Positive	OQ440383 - OQ440384 - OQ440385
11.	Bastar	Chhattisgarh	PL 11	Negative	-
12.	Deoria	Uttar Pradesh	PL 12	Negative	-
13.	Delhi	Delhi	PL 13	Positive	OR489166 - OQ440377
14.	Delhi	Delhi	PL 14	Negative	-
15.	Delhi	Delhi	PL 15	Negative	-
16.	Gonda	Uttar Pradesh	PL 16	Negative	-
17.	Gonda	Uttar Pradesh	PL 17	Negative	-
18.	Durg	Chhattisgarh	PL 18	Negative	-
19.	Durg	Chhattisgarh	PL 19	Negative	-
20.	Durg	Chhattisgarh	PL 20	Positive	OQ134774 - OQ134775
21.	Varanasi	Uttar Pradesh	PL 21	Negative	-
22.	Varanasi	Uttar Pradesh	PL 22	Negative	-
23.	Varanasi	Uttar Pradesh	PL 23	Negative	-
24.	Khalilabad	Uttar Pradesh	PL 24	Negative	-
25.	Khalilabad	Uttar Pradesh	PL 25	Negative	-
26.	Khalilabad	Uttar Pradesh	PL 26	Negative	-
27.	Khalilabad	Uttar Pradesh	PL 27	Positive	OQ168370 - OQ168371
28.	Maharajganj	Uttar Pradesh	PL 28	Negative	-
29.	Maharajganj	Uttar Pradesh	PL 29	Positive	OQ091756 - OQ091757
30.	Maharajganj	Uttar Pradesh	PL 30	Negative	-
31.	Nautanwa	Uttar Pradesh	PL 31	Positive	OQ290944 - OQ290945
32.	Nautanwa	Uttar Pradesh	PL 32	Negative	-
33.	Nautanwa	Uttar Pradesh	PL 33	Negative	-
34.	Nautanwa	Uttar Pradesh	PL 34	Negative	-
35.	Raipur	Chhattisgarh	PL 35	Negative	-
36.	Raipur	Chhattisgarh	PL 36	Positive	OQ290942 - OQ290943
37.	Raipur	Chhattisgarh	PL 37	Negative	-
38.	Bhilai	Chhattisgarh	PL 38	Negative	-
39.	Ambikapur	Chhattisgarh	PL 39	Negative	-
40.	Berla	Chhattisgarh	PL 40	Negative	-
41.	Raigarh	Chhattisgarh	PL 41	Negative	-
42.	Bilaspur	Chhattisgarh	PL 42	Negative	-
43.	Bilaspur	Chhattisgarh	PL 43	Positive	OQ440378 - OQ440379 - OQ440380
44.	Kurud	Chhattisgarh	PL 44	Negative	-
45.	Mahasamund	Chhattisgarh	PL 45	Positive	OQ440381 - OQ440382
46.	Mahasamund	Chhattisgarh	PL 46	Negative	-
47.	Mahasamund	Chhattisgarh	PL 47	Negative	-

Table 2. PCR primers and amplification condition used for detection and characterization of Begomoviruses infecting papaya

Primer	PCR condition							
	Initial-denaturation	No. of cycles	Denaturation	Annealing	Extension	Final extension	Remarks	Reference
Pal1v1978/PAR1c496	94°C for 3 min	35	94°C for 1 min	55°C for 2 min	72°C for 2 min	72°C for 10 min	DNA-A	Wyatt and Brown 1996
DNABLC1/DNABLV2	94°C for 3 min	35	94°C for 1 min	50°C for 1 min	72°C for 2 min	72°C for 10 min	DNA-B	Green et al. 2001
Beta01/Beta02	94°C for 3 min	35	94°C for 1 min	52°C for 1 min	72°C for 2 min	72°C for 10 min	Betasatellite	Bull et al. 2003
DNA 101/DNA102	94°C for 3 min	35	94°C for 1 min	52°C for 1 min	72°C for 2 min	72°C for 10 min	Alphasatellite	Xie et al. 2010

Sequence analysis

The complete genomes of Begomoviruses and their associated satellites were sequenced and analyzed. Sequences showing the highest BLAST alignment scores with the present isolates were retrieved from the National Center for Biotechnology Information (NCBI) database (https://www.ncbi.nlm.nih.gov) for comparative analysis. Open Reading Frames (ORFs) were identified using the ORF Finder tool (https://www.ncbi.nlm.nih.gov/orffinder/). To determine pairwise sequence identities between the newly identified isolates and known sequences, the Sequence Demarcation Tool (SDT v1.2) was employed. Multiple sequence alignments were performed using the MUSCLE algorithm for both DNA-A and betasatellite datasets, independently and in combination (Muhire et al. 2014).

Phylogenetic analysis

Bayesian phylogenetic analyses were performed using BEAST v1.10 (Suchard et al. 2018) with Markov Chain Monte Carlo (MCMC) parameters. Prepared datasets comprising DNA-A, DNA-B, betasatellites, and alphasatellites were analyzed to generate Maximum Clade Credibility (MCC) trees. These analyses aimed to elucidate evolutionary relationships and potential host adaptation patterns among the Begomoviruses. The resulting trees were visualized and annotated using the Interactive Tree of Life (iTOL) platform, version 6.5 (https://itol.embl.de) (Letunic and Bork 2021).

Recombination analysis

Recombination plays a key role in the evolution and epidemiology of plant viruses. To assess the presence and frequency of recombination events within the *Begomovirus* genomes, two complementary approaches were employed. First, phylogenetic network reconstruction was performed using the Neighbor-Net method implemented in SplitsTree v4 (Huson and Bryant 2006). The Pairwise Homoplasy Index (PHI) test integrated in SplitsTree was used to detect recombination signals, with significance determined at $p \leq 0.05$. Recombination between and within genetic groups was considered significant when the PHI test yielded a corrected $p \leq 0.05$. Second, to validate recombination events and identify putative breakpoints and parental sequences, the RDP v4.1 software package was used. This package integrates seven algorithms: RDP, Bootscan, Geneconv, MaxChi, Chimaera, SiScan, and 3Seq (Martin et al. 2015). Analyses were conducted using predefined detection thresholds, with $p \geq 0.05$ set as the upper Bonferroni-corrected limit. Recombination breakpoints supported by at least three independent algorithms were considered reliable to minimize false positives.

RESULTS AND DISCUSSION

Survey and identification of *Begomovirus*

Typical *Begomovirus*-like symptoms were observed in papaya plants at forty-seven locations across Chhattisgarh, Delhi, and Uttar Pradesh, India. Field surveys indicated that outbreaks of *Begomovirus*-associated diseases in papaya were frequently linked to an increased distribution of the whitefly vector, *B. tabaci*. Infected plants exhibited diverse symptoms, including vein clearing and thickening, zigzag and enated veins, downward and upward leaf curling, leaf rolling, yellowing, leathery texture, distorted petioles, and overall leaf deformation (Figure 1). A total of forty-seven symptomatic and one non-symptomatic papaya leaf samples (designated as PL-1 to PL-47) were collected for analysis. Genomic DNA was extracted from both infected and healthy samples using the CTAB method. PCR amplification with universal *Begomovirus* primers produced the expected 1.2 kb amplicon in eleven samples (PL-1, PL-6, PL-10, PL-13, PL-20, PL-27, PL-29, PL-31, PL-36, PL-43, and PL-45). Further analysis detected betasatellites (Beta01/Beta02) in ten samples (PL-1, PL-6, PL-10, PL-13, PL-27, PL-29, PL-31, PL-36, PL-43, and PL-45) and alphasatellites (UN101/UN102) in two samples (PL-10 and PL-43). One sample (PL-20) produced a 1.2 kb amplicon with DNA-B-specific primers, confirming the presence of a bipartite *Begomovirus*. Positive samples were subjected to Rolling Circle Amplification (RCA) to obtain complete viral genomes and associated satellite components. RCA products were digested with *BamHI* (DNA-A) and *XbaI* (DNA-B) to generate linear fragments of approximately 2.8 kb and 1.3 kb, respectively. The digested products, along with amplified satellite molecules, were purified and cloned into the pTZ57RT plasmid as described by Sahu et al. (2018) (Figure 2). Recombinant plasmids were transformed into *E. coli* DH5α cells, and positive clones were confirmed through PCR and restriction analysis. The confirmed clones were sequenced bidirectionally, and consensus sequences were assembled into circular contigs using standard bioinformatics tools. All sequences were submitted to the NCBI GenBank database (Table 3).

Sequence datasets and alignment

Query sequences from each isolate were compared with available *Begomovirus* sequences in the GenBank database using the BLASTn algorithm, and those showing the highest nucleotide identity were retrieved for further analysis. Open Reading Frames (ORFs) in each viral genome were identified using the ORF Finder tool (Table 4). Four datasets DNA-A, DNA-B, alphasatellites, and betasatellites were aligned using the ClustalW algorithm implemented in MEGA X (Kumar et al. 2018). Pairwise nucleotide sequence identities were determined using the Sequence Demarcation Tool (SDT), which corroborated the BLASTn results. The SDT analysis provided detailed percentage identity values among isolates from different geographical regions, confirming close relationships among several sequences (Figure 3; Table 5).

Relationship between papaya-infecting present *Begomovirus* isolate with known Begomoviruses

Complete genome sequences of the eleven *Begomovirus* isolates were compared with representative sequences of known Begomoviruses. Based on species demarcation and strain classification criteria, six isolates (PL-1, PL-6, PL-13, PL-20, PL-36, and PL-43) shared >93.5% nucleotide identity with Papaya Leaf Curl Virus (PaLCuV) isolates infecting various crops, and were thus classified as new variants of PaLCuV. Two isolates (PL-31 and PL-45) shared 97% nucleotide identity with Tomato Leaf Curl New Delhi Virus (ToLCNDV), while isolates PL-10 and PL-29 exhibited >96% identity with Cotton Leaf Curl Multan Virus (CLCuMuV) and Cotton Leaf Curl Virus (CLCuV), respectively. Another isolate (PL-29) showed >96% identity with Croton Yellow Vein Virus (CYVV) infecting *Croton glandulosus* L.. In accordance with the current species demarcation criteria, six isolates were classified as PaLCuV strains, two as ToLCNDV strains, two as CLCuMuV and CLCuV strains, and one as a CYVV strain. All isolates and their associated subviral components exhibited >91% nucleotide identity with previously reported Begomoviruses , except for the betasatellite of isolate PL-36, which showed only 86.81% identity with Papaya Leaf Curl Betasatellite (PaLCuB/IN:ND:03, AY244706). This distinct sequence was identified as a novel subviral component and designated Papaya Leaf Curl Raipur Betasatellite (PaLCuRPRB). Among the six PaLCuV isolates, pairwise identity analysis revealed that isolate PL-6 shared 77.10%, PL-13 shared 80.10%, PL-20 shared 78.30%, PL-36 shared 78.60%, and PL-43 shared 81% nucleotide identity with PL-1. Although these isolates shared >91% identity with other reported PaLCuV isolates, the relatively lower identity among themselves (<91%) suggests that they represent novel PaLCuV variants, a conclusion supported by SDT analysis.

Phylogenetic analysis

Phylogenetic analyses of DNA-A, DNA-B, betasatellite, and alphasatellite sequences were conducted using Markov Chain Monte Carlo (MCMC) methods with 1,000 bootstrap replicates. The resulting phylogenetic trees revealed that all eleven *Begomovirus* isolates from Uttar Pradesh, Delhi, and Chhattisgarh formed distinct clusters. As expected from the maximum-likelihood and Bayesian analyses, the newly characterized sequences grouped with known Begomoviruses infecting similar hosts (Figure 4). Notably, six papaya leaf curl isolates (PL-1, PL-6, PL-13, PL-20, PL-36, and PL-43) clustered closely with previously reported monopartite Begomoviruses from different regions of India. The Maximum Clade Credibility (MCC) dendrogram further indicated clear segregation of isolates based on host specificity, suggesting co-adaptation of associated betasatellites with their respective helper viruses (Saleem et al. 2016).

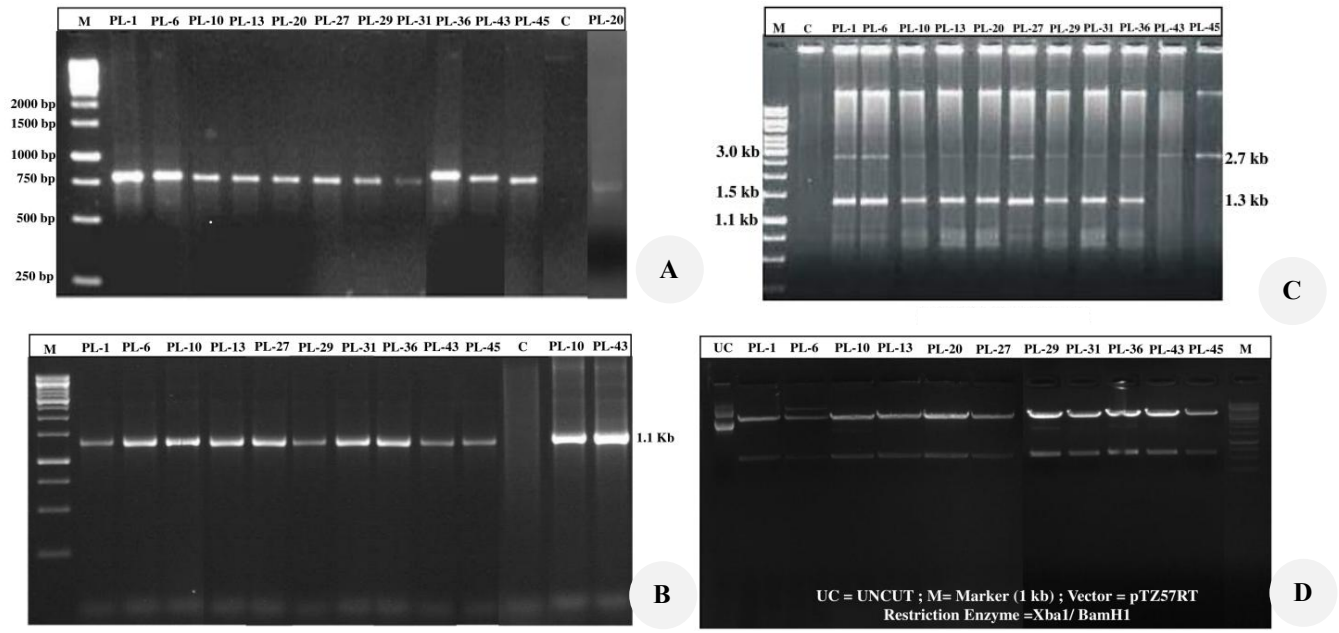

Figure 2. Agarose gel detection of papaya leaf curl disease in papaya leaf samples: A. PCR positive sample (DNA-A; DNA-B); B. PCR positive sample (Betasatellite; Alphasatellite); C. RCA positive sample; D. Restriction Digestion using Xba1/ BamH1

Recombination analysis

Neighbor-Net phylogenetic network analysis revealed that the eleven *Begomovirus* isolates were grouped into distinct lineages corresponding to their recombination patterns. PHI tests conducted on multiple datasets indicated statistically significant recombination signals ($p \leq 0.05$), confirming the occurrence of recombination among and within genetic groups. For all genomic datasets, recombination was deemed significant ($p = 0.00$), suggesting that the viral genomes may have originated from parental Begomoviruses infecting diverse crops (Figure 5). To further validate these findings, recombination events were analyzed using the RDP v4.1 software package, which integrates seven detection algorithms. The analyses identified multiple putative recombination breakpoints and parental sequences, providing evidence of past recombination events (Figure 6; Table 6). Each isolate exhibited unique recombination profiles involving both major and minor parental sequences. These events are likely to have contributed to the adaptive evolution and diversification of papaya-infecting Begomoviruses in India.

Discussion

Papaya (*C. papaya*) is a significant tropical fruit crop valued for its nutritional and economic importance. However, its productivity is severely affected by various biotic stressors, among which Papaya Leaf Curl Disease (PaLCD) is the most devastating (Udavatha et al. 2022; Varun et al. 2024). The disease is caused by Papaya Leaf Curl Virus (PaLCuV), a member of the *Begomovirus* genus (family Geminiviridae), transmitted by the whitefly *B. tabaci*. Since its first report in India in 1998 (Saxena et al. 1998), PaLCD has emerged as a serious threat to papaya cultivation across multiple states. The present study provides a comprehensive molecular characterization of Begomoviruses infecting papaya in key papaya-growing regions of India, revealing remarkable genetic heterogeneity and evolutionary complexity underlying PaLCD. Field surveys across Chhattisgarh, Delhi, and Uttar Pradesh recorded variable disease incidence, which correlated with high whitefly abundance a well-known determinant of *Begomovirus* transmission (Srivastava et al. 2022b).

Table 3. Features and accession number of positive samples (sequenced) of *Begomovirus* isolates infecting papaya crop

Sample	Begomoviruses and associated component				Accession no.	Isolate
	DNA-A	DNA-B	Betasatellite	Alphasatellite		
PL 1	Papaya Leaf Curl Virus (PaLCuV)	_	Papaya Leaf Curl Zetasatellite (PaLCuB)	_	MZ605904 - MZ605905	Gorakhpur_av1
PL 6	Papaya Leaf Curl Virus (PaLCuV)	_	Papaya Leaf Curl Betasatellite (PaLCuB)	_	MZ669217 - MZ606364	Gorakhpur_av2
PL 10	Cotton Leaf Curl Multan Virus (CLCuMuV)	_	Tomato Leaf Curl Bangladesh Betasatellite (ToLCBDB)	Papaya Leaf Curl Vishakapuri Alphasatellite (PaLCVSA)	OQ440383 - OQ440384 - OQ440385	Bastar_RAV
PL 13	Papaya Leaf Curl Virus (PaLCuV)	_	Tomato Leaf Curl Bangladesh Betasatellite (ToLCBDB)	_	OR489166 - OQ440377	Delhi_RAV
PL 20	Papaya Leaf Curl Virus (PaLCuV)	Tomato Leaf Curl New Delhi Virus (ToLCNDV)	_	_	OQ134774 - OQ134775	Durg_RAV
PL 27	Croton Yellow Vein Mosaic Virus (CYVMV)	_	Papaya Leaf Curl Betasatellite (PaLCuB)	_	OQ168370 - OQ168371	Kahlilabad_RAV
PL 29	Cotton Leaf Curl Virus (CLCuV)	_	Cotton Leaf Curl Betasatellite (CLCuB)	_	OQ091756 - OQ091757	Maharajganj_RAV
PL 31	Tomato Leaf Curl New Delhi Virus (ToLCNDV)	_	Tomato Leaf Curl Betasatellite (ToLCB)	_	OQ290944 - OQ290945	Nautanwa_RAV
PL 36	Papaya Leaf Curl Virus (PaLCuV)	_	Papaya Leaf Curl Betasatellite (PaLCuB)	_	OQ290942 - OQ290943	Raipur_RAV
PL 43	Papaya Leaf Curl Virus (PaLCuV)	_	Papaya Leaf Curl Betasatellite (PaLCuB)	Papaya Leaf Curl Alphasatellite (PaLCuA)	OQ440378 - OQ440379 - OQ440380	Bilaspur_RAV
PL 45	Tomato Leaf Curl New Delhi Virus (ToLCNDV)	_	Cotton Leaf Curl Betasatellite (CLCuB)	_	OQ440381 - OQ440382	Mahasamund_RAV

Table 4. ORFs details of sequenced *Begomovirus* isolates from diseased papaya crops

ORFs	PL 1	PL6	PL 10	PL 13	PL 20	PL 27	PL 29	PL 31	PL 36	PL 43	PL 45
DNA-A											
CP (AV1)	307-1077	310-1080	280-1047	290-1060	307-1077	307-1077	293-1063	281-1060	304-1059	310-1080	287-1057
pre-CP (AV2)	147-503	150-506	120-485	130-486	147-503	147-503	133-480	121-459	144-500	150-506	127-465
Rep (AC1)	1526-2611	1529-2614	1496-2581	1558-2616	1531-2616	1526-2611	1521-2591	1516-2586	1529-2614	1529-2533	1506-2597
TrAP (AC2)	1219-1623	1222-1626	1147-1599	1368-1628	1224-1628	1219-1623	1205-1615	1194-1613	1222-1626	1222-1626	1199-1603
REn (AC3)	1200-1478	1077-1481	1050-1454	1057-1461	1079-1483	1074-1478	1060-1464	1064-1474	1077-1481	1077-1481	1054-1464
C4 (AC4)	2161-2460	2200-2457	2128-2430	2202-2459	2202-2459	2197-2454	2138-2446	2253-2429	2200-2457	2200-2457	2264-2440
Betasatellite											
βC1	189-557	201-557	202-558	202-558	_	221-577	194-550	192-572	201-557	200-556	195-551
DNA-B											
BC1	_	_	_	_	1303-2148	_	_	_	_	_	_
BV1	_	_	_	_	440-1246	_	_	_	_	_	_
Alphasatellite											
REP	_	_	65-1012	_	_	_	_	_	_	89-1036	_

Table 5. Results of nucleotide BLAST (BLASTn), and Sequence Demarcation Tool (SDT) of sequenced *Begomovirus* isolates from diseased papaya crop estimating homology score with other *Begomovirus* isolate

Sample	Virus isolate	Accession number	Maximum nucleotide % identity with existing isolate BLAST	Maximum whole genome nucleotide % identity with existing isolate SDT	Name assigned based on nucleotide sequenced identity among each other <91%
PL 1	PaLCuV/av1_GKP	MZ605904	KY800906_98.63 PaLCuV/IN: ND:17	KY800906_99.40 PaLCV/IN: ND:17	Papaya Leaf Curl Gorakhpur 1 Virus (PaLCuGKP1V)
	PaLCuB/av1	MZ605905	JX987089_98.83 PaLCuB/IN: NBRI:21	JX987089_99.30 PaLCuB/IN: NBRI:21	
PL 6	PaLCuV/av2_GKP	MZ669217	JN807765_98.91 PaLCuV/IN: Lkw:13	JN807765_98.90 PaLCV/IN: Lkw:13	Papaya Leaf Curl Gorakhpur 6 Virus (PaLCuGKP6V)
	PaLCuB/av2	MZ606364	JX050199_97.82 PaLCuB/IN: IYV: Del:12	JX050199_99.30 PaLCuB/IN: IYV: Del:12	
PL 10	CLCuMuV/Bastar_RAV	OQ440383	JN558358_96.85 CLCuMuV/IN:10	JN558358_97.50 CLCuMuV/IN:10	
	ToLCBDB/BSTR_RAV	OQ440384	KX302716_94.17 ToLCBDB/IN:GU2B3:11	KX302716_93.40 ToLCBDB/IN:GU2B3:11	
	PaLCVSA/BSTR_RAV	OQ440385	ON054962_98.16 PaLCVSA/IN: PVS2:18	ON054962_99.80 PaLCVSA/IN: PVS2:18	
PL 13	PaLCuV/DL_RAV	OR489166	MN839534_94.57 PaLCuV/PAK: WA1:18	MN839534_94.50 PaLCuV/PAK: WA1:18	Papaya Leaf Curl Delhi Virus (PaLCuDLV)
	ToLCBDB/DL_RAV	OQ440377	KX302716_91.57 ToLCBDB/IN:GU2B3:11	KX302716_94.57 ToLCBDB/IN:GU2B3:11	
PL 20	PaLCuV/Durg_RAV	OQ134774	FJ593629_98.95 PaLCuV/IN: Pt:08	FJ593629_99.30 PaLCuV/IN: Pt:08	Papaya Leaf Curl Durg Virus (PaLCuDGV)
	ToLCNDV/Durg_RAV	OQ134775 (DNA-B)	MT161675_98.33 ToLCNDV/BD: PapND71:16	MT161675_99.40 ToLCNDV/BD: PapND71:16	
PL 27	CYVV/KLD_RAV	OQ168370	FN543112_97.88 CrYVMV/PAK:06	FN543112_99.71 CrYVMV/PAK:06	
	PaLCuB/KLD_RAV	OQ168371	MH359169_99.71 PaLCuB/IN:18	MH359169_99.70 PaLCuB/IN:18	
PL 29	CLCuV/ MHJ_RAV	OQ091756	GU440580_98.44 CLCuV/IN: Lko: 2:06	GU440580_99.20 CLCuV/IN: Lko: 2:06	
	CLCuB/MHJ_RAV	OQ091757	GQ369731_98.53 CLCuB/IN: LKO:08	GQ369731_98.50 CLCuB/IN: LKO:08	
PL 31	ToLCNDV/NTW_RAV	OQ290944	MH520664_97.84 ToLCNDV/PAK: ARG:12	MH520664_99.00 ToLCNDV/PAK: ARG:12	
	ToLCuB/NTW_RAV	OQ290945	MT385292_99.33 ToLCuB/IN: GKP04:20	MT385292_99.60 ToLCuB/IN: GKP04:20	
PL 36	PaLCuV/RPR_RAV	OQ290942	KY926899_99.46 PaLCuV/PAK:RM428:16	KY926899_99.60 PaLCuV/PAK:RM428:16	Papaya Leaf Curl Raipur Virus (PaLCuRPRV)
	PaLCuB/RPR_RAV	OQ290943	AY244706_86.81 PaLCuB/IN: ND:03	AY244706_88.00 PaLCuB/IN: ND:03	Papaya Leaf Curl Raipur Betasatellite (PaLCuRPRB)
PL 43	PaLCuV/BLS_RAV	OQ440378	Y15934_98.37 PaLCuV/IN:97	Y15934_98.30 PaLCuV/IN:97	Papaya Leaf Curl Bilaspur Virus (PaLCuBLSV)
	PaLCuB/BLS_RAV	OQ440379	GU370715_97.47 PaLCuB/IN: PRM:05	GU370715_98.47 PaLCuB/IN: PRM:05	
	PaLCuA/BLS_RAV	OQ440380	JQ322970_98.49 PaLCuA/IN: CLCuV:10	JQ322970_99.20 PaLCuA/IN: CLCuV:10	
PL 45	ToLCNDV/MAHA_RAV	OQ440381	DQ989325_98.89 ToLCNDV/IN: PD:06	DQ989325_98.10 ToLCNDV/IN: PD:06	
	CLCuB/MAHA_RAV	OQ440382	JX217745_97.10 CLCuB/IN:10	JX217745_95.10 CLCuB/IN:10	

Table 6. Recombination analysis of breakpoint and its putative parental sequences listed based on best method having minimum p-Value for each recombinant isolate of Begomoviruses isolated from papaya

Present isolates				**Breakpoint and its putative parental sequences listed based on best method having minimum *p*-Value for each recombinant isolate**					
***Carica papaya* (sample)**	***Begomovirus***	**Events (Total)**	**Recombinant (Yes/No)**	**Breakpoints**		**Parent**		**Method**	***p*-value**
				Begin	**End**	**Minor**	**Major**		
PL 1	MZ605904 PaLCV/IN:GKP:av1:21	5	YES	2076	1159	MF574143 ChiLCINV/IN: Meerut:17	HM140364 ChiLCV/IN: DU:09	***R***, G, **M**, S, ***3S***	4.42E-07
	MZ605905 PaLCuB/IN: GKP: av1:21	7	YES	189	495	MN839536 PaLCuB/Pak: WA22:19	MF374787 PaLCuB/IN: betaRad07:17	***R***, G, M, **S**, ***3S***	3.02E-20
PL6	MZ669217 PaLCV/IN:GKP:av2:21	32	YES	1548	1900	KU376493 PaLCV/IN:CN2:15	KY026598 PaLCV/IN: Rad07:15	***R***, G, M, S, *3S*	4.25E-08
	MZ606364 PaLCuB/IN: GKP: av2:21	3	YES	622	801	MG686555 PaLCuB/IN: kang:17	LT600718 PaLCuB/Pak: IH51:16	*R*, G, M, S, ***3S***	1,03E+01
PL 10	OQ440383 CLCuMuV/IN: Bstr: RAV:21	18	YES	1517	2581	AJ002459 CLCuMuV/UK: olc311:97	AJ002447 CLCuMuV/PAK: clc62:97	*R*, G, M, S, ***3S***	1.38E-19
	OQ440384 ToLCBDB/IN: Bstr: RAV:21	3	YES	1264	601	MZ151263 ToLCBDB/IN: CHB8:21	MZ172977 ToLCBDB/IN:ZN:KOD:19	*R*, G, M, S, ***3S***	3.52E-14
	OQ440385 PaLCVSA/Bstr: RAV:21	6	YES	1310	488	OQ4403377 ToLCBDB/IN: DL: RAV	MN417113 ToLCBDB/IN: CHL44:14	*R*, G, M, S, ***3S***	4,38E-11
PL 13	OR489166 PaLCuV/IN: DL: RAV:21	19	YES	2742	1499	MN839534 PaLCuV/PAK: WA1:18	LT009395 PaLCuV/PAK: MNT: D18:12	***R***, G, M, **S**, ***3S***	2.56E-34
	OQ440377 ToLCBDB/IN: DL: RAV:21	4	YES	1169	633	MZ172977 ToLCBDB/IN:ZN:KOD:19	MN417113 ToLCBDB/IN: CHL44:14	***R***, G, **M**, S, ***3S***	4.27E-06
PL 20	OQ134774 PaLCV/IN: Durg: RAV:21	11	YES	2600	2692	Unknown (LN886525 CYVMV/PAK:17RS60:15)	JN663850 CYVMV/IN: Bhu:09	***R***, **G**, M, S, ***3S***	1.49E-13
	OQ134775 ToLCNDV/IN: Durg: RAV:21	8	YES	2576	2655	Unknown (MG373560 ToLCGuV/IN: ND:16)	MT161675 ToLCNDV/BD: PapND71:16	***R***, **G**, M, S, ***3S***	4.67E-08
PL 27	OQ168370 CYVV/IN: KLD: RAV:21	14	YES	2117	2405	FN678906 CYVMV/PAK: HY:06	Y15934 PaLCV/IN:97	*R*, G, M, S, ***3S***	6.19E-05
	OQ168371- PaLCuB/IN: KLD: RAV:21	9	YES	1248	642	KY825245 PaLCuB/PAK: 2491:17	Unknown (LT600709 CroYVMB/PAK: bhainsa: 21:16)	*R*, G, M, S, ***3S***	1.28E-16
PL 29	OQ091756 CLCuV/IN: MHJ: RAV:21	14	YES	2551	2567	Unknown (AF195782 ToLCLAV/LA:99)	GU253915 ToLCPatV/IN: Tb:09	***R***, **G**, M, S, ***3S***	3.26E-06
	OQ091757 CLCuB/IN: MHJ: RAV:21	3	YES	1145	1297	EU126825 PaLCuB/IN:07	OQ440382 CLCuB/IN: Maha: RAV:21	*R*, G, M, S, ***3S***	1,52E-19

PL 31	OQ290944 ToLCNDV/IN: NTW: RAV:21	6	YES	1613	2582	KC914896 ToLCNDV/PAK: Mn: 05:12	MT316388 ToLCNDV/IN: Matar:19	***R***, G, M, S, *3S*	1.42E-18
	OQ290945 ToLCuB/IN: NTW: RAV:21	***NOT DETECTED AS RECOMBINANT***							
PL 36	OQ290942 PaLCV/IN: RPR: RAV:21	11	YES	1028	1088	Unknown (HG937524 CYVMV/IN: ZI73:12)	KY926899 PaLCV/PAK:RM428:16	***R***, **G**, M, S, ***3S***	4.19E-11
	OQ290943 PaLCuB/IN: RPR: RAV:21	7	YES	361	714	AY244706 PaLCuB/IN: ND:03	JN663849 PaLCuB/IN: Bengaluru:08	***R***, G, M, S, *3S*	6.55E-70
PL 43	OQ440378 PaLCuV/IN: BLS: RAV:21	32	YES	2569	2700	Unknown (JQ954859 PaLCV/IN: ASLko:11)	Y15934 PaLCV/IN:97	***R***, G, **B**, M, S, ***3S***	6.14E-27
	OQ440379 PaLCuB/IN: BLS: RAV:21	5	YES	1080	1158	JN663874 PaLCuB/IN: Salem:08	LN828709 ToLCuB/PAK: ND16:15	*R*, G, M, S, ***3S***	1,13E-11
	OQ440380 PaLCuA/IN: BLS: RAV:21	1	YES	316	351	MN885461 AYVINA/PAK: R43:16	JQ322970 PaLCuA/IN: CLCuV:10	***R***, **G**, M, S, ***3S***	6,33E-18
PL 45	OQ440381 ToLCNDV/IN: MAHA: RAV:21	8	YES	1412	1785	KC513822 ToLCNDV/IN:AS:12	KX827602 ToLCNDV/PAK: NJ: 56:15	*R*, G, M, S, ***3S***	3.87E-11
	OQ440382 CLCuB/IN: MAHA: RAV:21	4	YES	631	1264	AY744380 CLCuB/IN:04	KT447040 CLCuMuB/IN:1YF:11	***R***, G, M, **S**, ***3S***	3.01E-10

Note: R: RDP; G: Geneconv; B: Bootscan; M: MaxChi; C: Chimarea; S: SiScan; 3Seq: Sequence Triplets; The lowest p-value calculated for the underline and bold method are given in the column

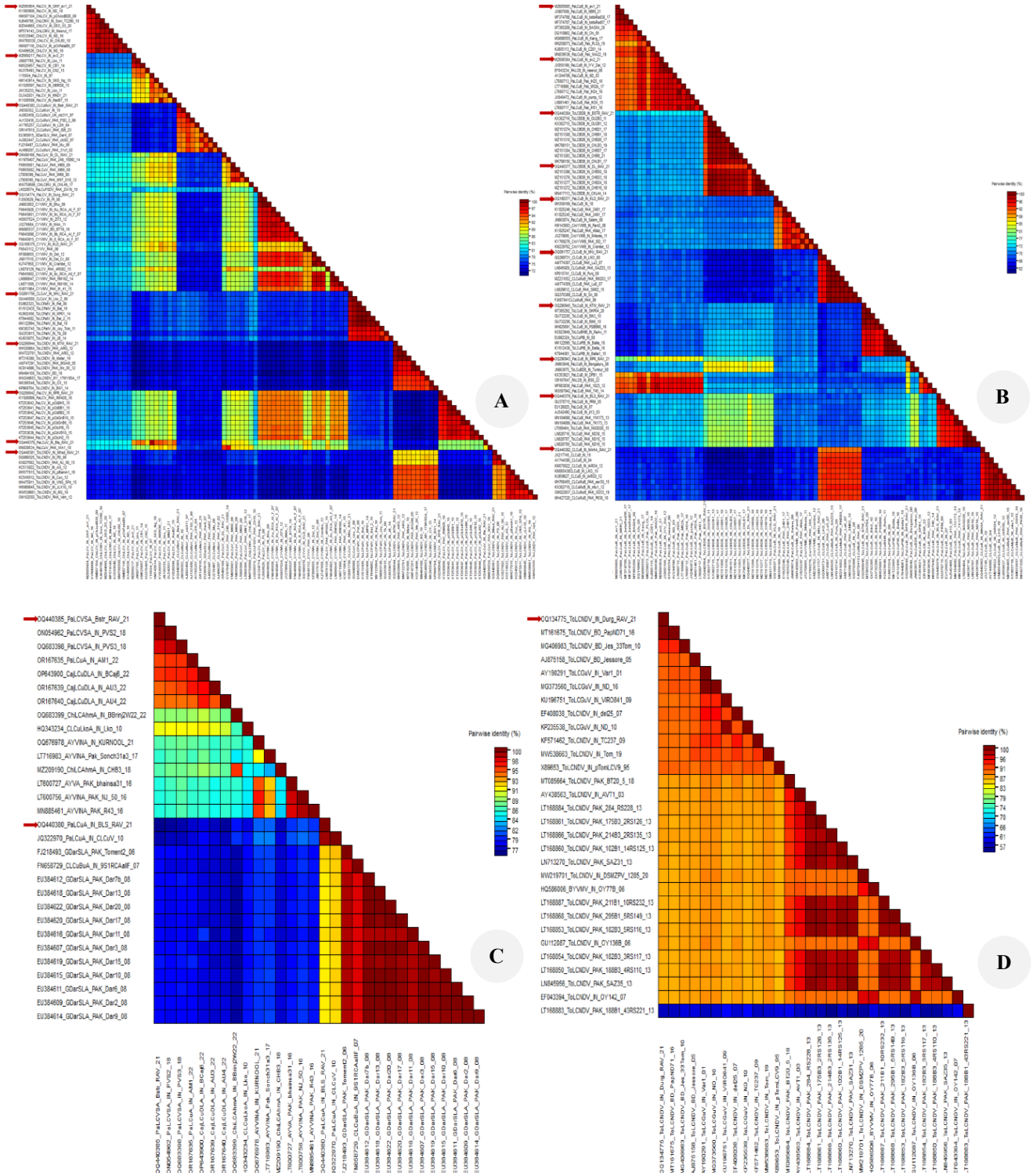

Figure 3. Color-coded matrix of percent pair wise nucleotide identity plot and genome score of full-length genomic component of *Begomovirus* isolated from diseased papaya leaves (Red Bars) using the SDT v1.2. A. DNA-A; B. Betasatellite; C. Alphasatellite; D. DNA-B

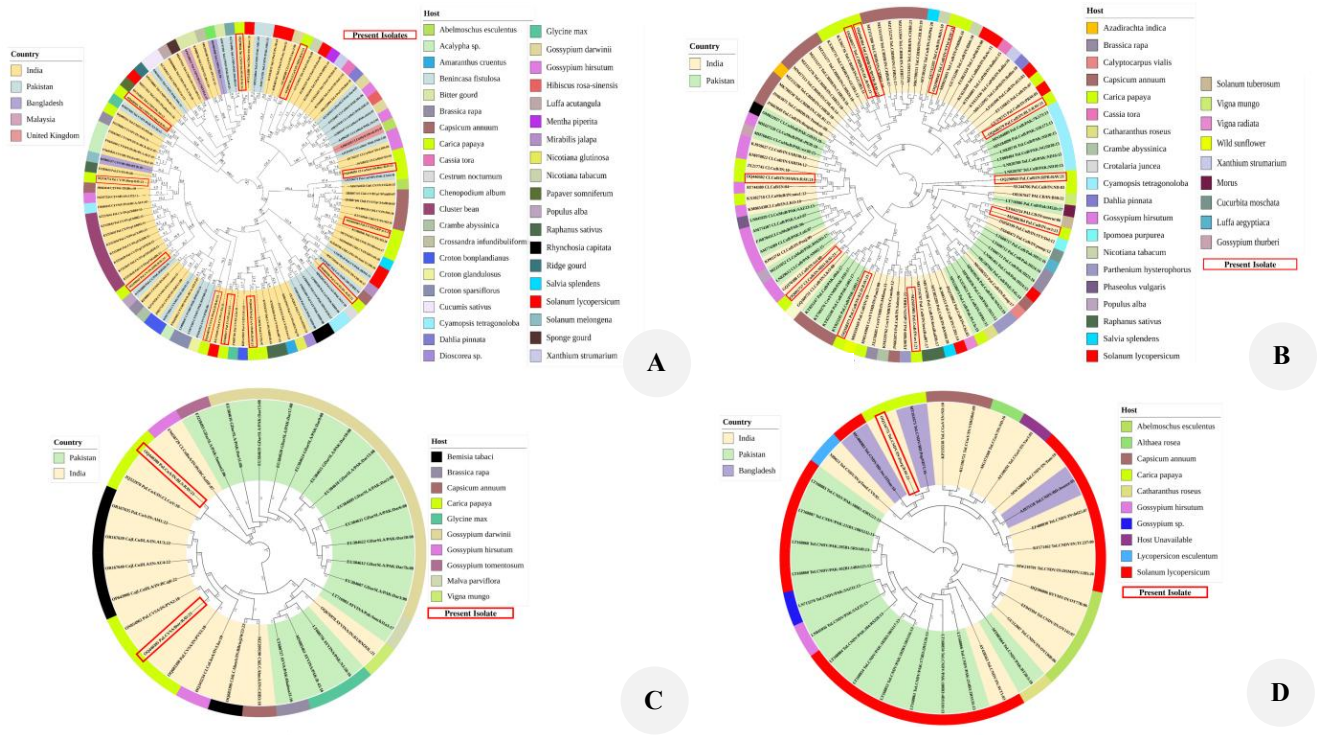

Figure 4. Maximum Clade Credibility Phylogenetic tree illustrating the relationship of isolate av1 and av2 within and among Begomoviruses: A. DNA-A; B. Betasatellites; C. Alphasatellite; D. DNA-B. The tree was constructed using Bayesian technique and Tree annotator tool with BEAST v.1.10 package. Bootstrap values are shown on branches. The inner ring represents the origin and outer ring represents the host of isolates

Genetic characterization and species demarcation

Based on sequence identity and ICTV species demarcation criteria (Brown et al. 2015), eleven *Begomovirus* isolates were identified. Among them, five isolates showed >91% nucleotide sequence identity with known Begomoviruses , classifying them as variants of existing species specifically, PL-29 and PL-43 as variants of Cotton Leaf Curl Virus (CLCuV) and Papaya Leaf Curl Virus (PaLCuV), and PL-10, PL-13, and PL-45 as variants of Cotton Leaf Curl Multan Virus (CLCuMuV) and Croton Yellow Vein Mosaic Virus (CYVMV), respectively. In contrast, six isolates (PL-1, PL-6, PL-20, PL-27, PL-31, and PL-36) exhibited <91% nucleotide identity in their DNA-A component, fulfilling the ICTV threshold for novel species classification. Accordingly, we propose these as new *Begomovirus* species: papaya leaf curl Gorakhpur 1 virus, papaya leaf curl Gorakhpur 6 virus, papaya leaf curl Delhi virus, papaya leaf curl Durg virus, papaya leaf curl Raipur virus, and papaya leaf curl Bilaspur virus. The discovery of these six novel Begomoviruses significantly broadens the known genetic diversity of papaya-infecting Begomoviruses and underscores the dynamic evolution occurring within Indian agroecosystems. These findings provide the first molecular evidence of emergent *Begomovirus* species in papaya and highlight their potential epidemiological importance. The molecular tools applied here PCR-based detection, RCA amplification, and sequence-based classification offer valuable frameworks for monitoring viral evolution and predicting potential outbreaks.

Recombination and viral evolution

Recombination analysis demonstrated that genome reshuffling plays a pivotal role in *Begomovirus* evolution (Mishra et al. 2022). Statistically significant recombination events were identified through PHI tests, indicating both intra- and interspecific exchange among isolates. Isolates PL-6 and PL-43 displayed the highest number of recombination breakpoints, followed by PL-13 and PL-10, suggesting frequent genetic exchange among sympatric virus populations. In contrast, isolate PL-31 (PaLCuB) exhibited no evidence of recombination, implying strong purifying selection that may constrain recombinant persistence. These results support the hypothesis that *Begomovirus* evolution is driven by a dynamic balance between adaptive selection and recombination-mediated diversification. The observed mosaic genome structures, derived from mixed parental lineages, likely facilitate enhanced host adaptability and vector transmission efficiency. Consistent with previous findings (Kumar et al. 2015; Quadros et al. 2023; Khan and Dijkstra 2024), our data reinforce the central role of homologous recombination, pseudo-recombination, and mixed infections as key mechanisms underlying *Begomovirus* diversification and host-range expansion. Such processes accelerate viral speciation and may ultimately contribute to the emergence of epidemic outbreaks (Sattar et al. 2025).

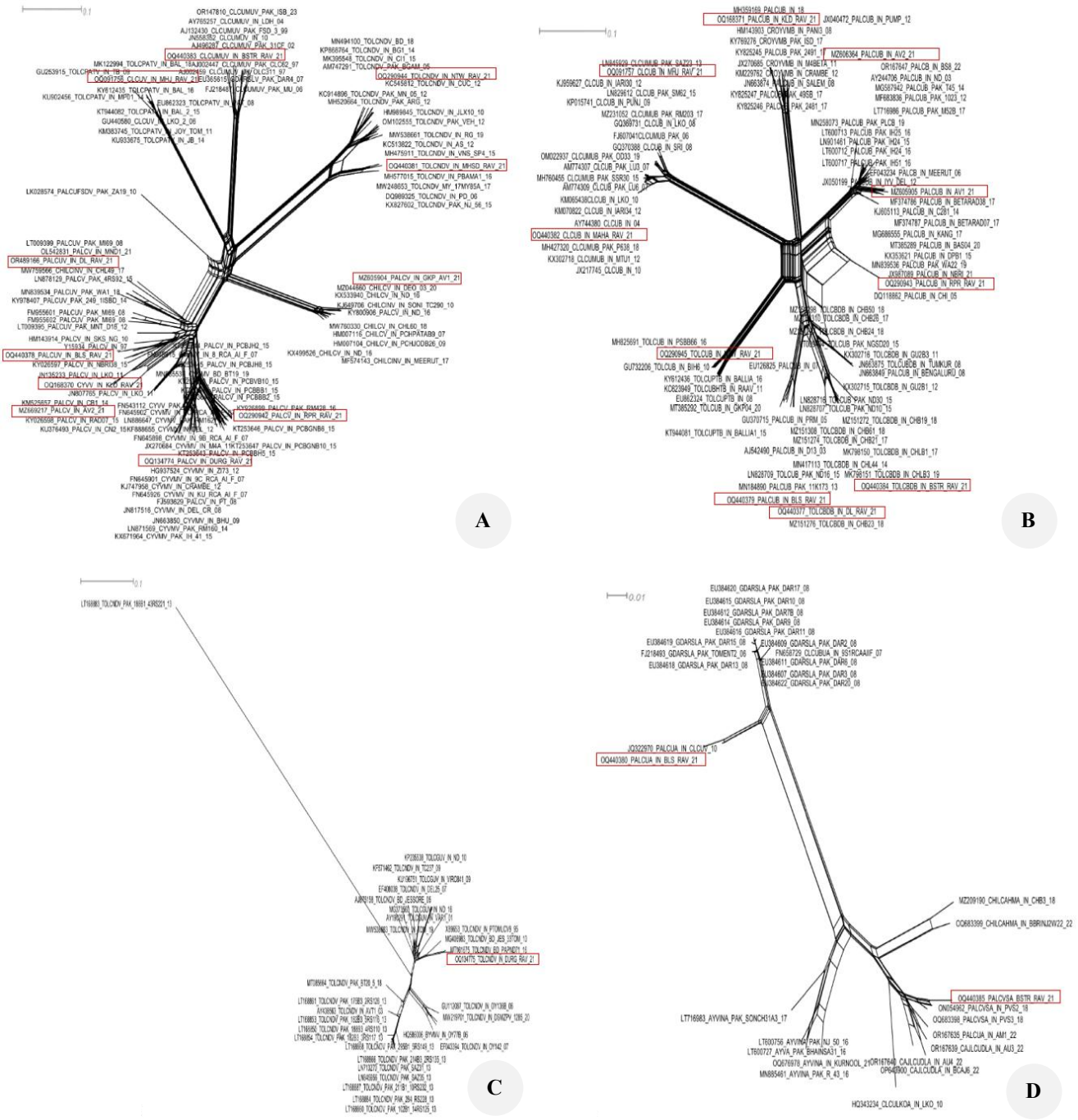

Figure 5. A Neighbour-net phylogenetic network generated for sequence-based data set comprising of papaya-infecting isolates and other Begomoviruses performed using Splits Tree v.4. A. DNA-A; B. Betasatellite; C. DNA-B; D. Alphasatellite

Evolutionary and epidemiological implications

The emergence of novel *Begomovirus* species in papaya reflects ongoing evolutionary pressures driven by ecological, agronomic, and vector-related factors. Agricultural intensification, overlapping crop cycles, and climatic variations that favor *B. tabaci* proliferation may create ecological niches conducive to viral recombination and reassortment. Moreover, intercropping practices involving *Begomovirus*-susceptible hosts (e.g., cotton, tomato, and okra) further increase opportunities for co-infection and cross-species transmission. Understanding these evolutionary dynamics is critical for designing sustainable management strategies. Continuous molecular surveillance and vector population monitoring are essential to detect emergent variants before large-scale outbreaks occur. Integrated disease management approaches combining resistant cultivars, vector control, and molecular diagnostics should be prioritized to mitigate the threat posed by rapidly evolving Begomoviruses in tropical fruit systems.

Figure 6. Recombination analysis of breakpoints and its putative parental sequences showing distribution of recombination frequency across the genome of isolated Begomoviruses from papaya. A. DNA-A; B. Betasatellite; C. Alphasatellite; D. DNA-B

This study provides the first comprehensive molecular characterization of Begomoviruses associated with Papaya Leaf Curl Disease (PaLCD) in the major papaya-growing regions of Uttar Pradesh, Delhi, and Chhattisgarh, India. Using an integrated approach involving PCR detection, Rolling Circle Amplification (RCA), molecular cloning, and full-length genome sequencing, we confirmed the widespread occurrence of multiple Begomoviruses , including Papaya Leaf Curl Virus (PaLCuV), Tomato Leaf Curl New Delhi Virus (ToLCNDV), and their associated satellite molecules. Notably, six PaLCuV isolates exhibiting <91% nucleotide identity was identified as novel species, along with a newly characterized betasatellite, Papaya Leaf Curl Raipur Betasatellite (PaLCuRPRB), underscoring the extensive genetic plasticity within the *Begomovirus*complex. The detection of active recombination signals and the presence of geographically distinct variants indicate that region-specific selection pressures and host-virus interactions are key drivers of *Begomovirus* diversification and adaptation in Indian papaya ecosystems. Overall, these findings substantially enhance our understanding of the molecular diversity, evolutionary mechanisms, and epidemiology of PaLCD. The identification of new *Begomovirus* species and satellite molecules provides valuable genomic resources for refining phylogenetic frameworks and guiding the development of virus-resistant cultivars through molecular breeding and biotechnology. Continued surveillance and evolutionary monitoring will be critical for predicting future outbreaks and implementing region-specific, sustainable disease management strategies to safeguard papaya production in India.

The expanding diversity of Begomoviruses infecting papaya underscores the need for continuous molecular surveillance and integrated disease-management strategies. The emergence of novel Papaya Leaf Curl Virus (PaLCuV) variants and new satellite molecules, as revealed in this study, highlights the dynamic evolutionary potential of these pathogens under changing agro-ecological and climatic conditions. Future research should therefore focus on establishing a nationwide genomic monitoring network to track spatiotemporal variations in *Begomovirus* populations and their whitefly vectors (*B. tabaci*). Such real-time monitoring would facilitate early detection of virulent strains and inform region-specific control strategies. Advances in high-throughput sequencing and metagenomics now provide powerful tools for dissecting the complex viromes associated with papaya and its neighboring host species. Comprehensive virome mapping will be crucial for uncovering hidden virus-virus and virus-vector interactions that drive recombination and host adaptation. Integrating genomic data with ecological and epidemiological modeling could enable predictive frameworks for PaLCD outbreak risk assessment under future climate scenarios. From a management perspective, the development of durable resistance remains a top priority. Emerging molecular breeding technologies such as marker-assisted selection, RNA interference (RNAi), and CRISPR/Cas-based genome editing offer unprecedented opportunities to engineer broad-spectrum and sustainable resistance against Begomoviruses and their satellites.

Simultaneously, functional characterization of key viral and satellite proteins, including βC1 and Rep, could uncover molecular targets for antiviral gene silencing or chemical inhibition. Lastly, effective control of PaLCD will require ecosystem-based management, integrating vector control, crop diversification, and deployment of resistant cultivars. Strengthening collaborations among plant virologists, molecular biologists, breeders, and data scientists will be vital to translate genomic insights into applied solutions for the papaya industry. Together, these multidisciplinary efforts will pave the way toward resilient papaya production systems and contribute to safeguarding tropical fruit agriculture against rapidly evolving viral threats.

REFERENCES

Akram M, Kumar D, Kamaal N. 2025. Complete genome sequence of a novel bipartite *Begomovirus* infecting butterfly pea (*Clitoria ternatea* L.) in India. Arch Virol 170 (1): 7. DOI: 10.1007/s00705-024-06203-3.

Brown JK, Zerbini FM, Navas-Castillo J, Moriones E, Ramos-Sobrinho R, Silva JC, Fiallo-Olivé E, Briddon RW, Hernández-Zepeda C, Idris A, Malathi VG. 2015. Revision of *Begomovirus* taxonomy based on pairwise sequence comparisons. Arch Virol 160 (6): 1593-1619. DOI: 10.1007/s00705-015-2398-y.

Bull SE, Briddon RW, Markham PG. 2003. Universal primers for the PCR-mediated amplification of DNA 1: A satellite-like molecule associated with *Begomovirus*-DNA β complexes. Mol Biotech 23: 83-86. DOI: 10.1385/MB:23:1:83.

Butković A, González R. 2022. A brief view of factors that affect plant virus evolution. Front Virol 2: 994057. DOI: 10.3389/fviro.2022.994057.

Doyle JJ, Doyle JL. 1990. Isolation of plant DNA from fresh tissue. Focus 12: 13-15. DOI: 10.2307/2419362.

Fiallo-Olivé E, Navas-Castillo J. 2023. The role of extensive recombination in the evolution of geminiviruses. Curr Top Microbiol Immunol 439: 139-166. DOI: 10.1007/978-3-031-15640-3_4.

Green S K, Tsai W S, Shih S L, Black L L, Rezaian A, Rashid M H, Roff M M N, Myint Y Y, Hong LT A. 2001. Molecular characterization of Begomoviruses associated with leafcurl diseases of tomato in Bangladesh, Laos, Malaysia, Myanmar, and Vietnam. Plant Dis 85: 1286. DOI: 10.1094/PDIS.2001.85.12.1286A.

Hallan V, Saxena S, Singh BP. 1998. Yellow net of *Triumffeta* is caused by a geminivirus: A first report. Plant Dis 82 (1): 127. DOI: 10.1094/PDIS.1998.82.1.127A.

Huson DH, Bryant D. 2006. Application of phylogenetic networks in evolutionary studies. Mol Biol Evol 23: 254-267. DOI: 10.1093/molbev/msj030.

Khan J, Dijkstra J. 2024. Handbook of Plant Virology. CRC Press, US. DOI: 10.1201/9781003578611.

Kumar RV, Singh AK, Singh AK, Yadav T, Basu S, Kushwaha N, Chattopadhyay B, Chakraborty S. 2015. Complexity of *Begomovirus* and betasatellite populations associated with chilli leaf curl disease in India. J Gen Virol 96 (10): 3143-3158. DOI: 10.1099/jgv.0.000254.

Kumar S, Stecher G, Li M, Knyaz C, Tamura K. 2018. MEGA X: Molecular evolutionary genetics analysis across computing platforms. Mol Biol Evol 35: 1547-1549. DOI: 10.1093/molbe v/msy096.

Letunic I, Bork P. 2021. Interactive Tree of Life (iTOL) v5: An online tool for phylogenetic tree display and annotation. Nucleic Acids Res 49 (1): 293-296. DOI: 10.1093/nar/gkab301.

Martin DP, Murrell B, Golden M, Khoosal A, Muhire B. 2015. RDP4: detection and analysis of recombination patterns in virus genomes. Virus Evol 1 (1): vev003. DOI: 10.1093/ve/vev003.

Mishra M, Verma RK, Pandey V, Srivastava A, Sharma P, Gaur RK, Ali A. 2022. Role of diversity and recombination in the emergence of chilli leaf curl virus. Pathogens 11: 529. DOI: 10.3390/pathogens11050529.

Muhire BM, Varsani A, Martin DP. 2014. SDT: A virus classification tool based on pairwise sequence alignment and identity calculation. PLoS One 9 (9): e108277. DOI: 10.1371/journal.pone.0108277.

Nadeem A, Mehmood T, Tahir M, Khalid S, Xiong Z. 1997. First report of papaya leaf curl disease in Pakistan. Plant Dis 81 (11): 1333. DOI: 10.1094/PDIS.1997.81.11.1333B.

Nogueira AM, Nascimento MB, Barbosa TM, Quadros AF, Gomes JPA, Orílio AF, Zerbini FM. 2021. The association between New World alphasatellites and bipartite Begomoviruses : Effects on infection and vector transmission. Pathogens 10 (10): 1244. DOI: 10.3390/pathogens10101244.

Quadros AF, Ferro CG, de Rezende RR, Godinho MT, Xavier CA, Nogueira AM, Alfenas-Zerbini P, Zerbini FM. 2023. *Begomovirus* populations in single plants are complex and may include both well-adapted and poorly-adapted viruses. Virus Res 323: 198969. DOI: 10.1016/j.virusres.2022.198969.

Sahu AK, Verma RK, Gaur RK, Sanan-Mishra N. 2018. Complexity and recombination analysis of novel *Begomovirus* associated with Spinach yellow vein disease in India. Plant Gene 13: 42-49. DOI: 10.1016/j.plgene.2018.01.001.

Saleem H, Nahid N, Shakir S, Ijaz S, Murtaza G, Khan AA, Mubin M, Nawaz-ul-Rehman MS. 2016. Diversity, mutation and recombination analysis of cotton leaf curl geminiviruses. PLoS One 11 (3): e0151161. DOI: 10.1371/journal.pone.0151161.

Sattar MN, Chellappan BV, ElGanainy SM, Almaghaslah MI, Al Hashedi SA, Al-Shoaibi AA. 2025. Genetic diversity, population structure, and cross-border dispersal patterns of tomato leaf curl Palampur virus in South and West Asia. Viruses 17 (5): 678. DOI: 10.3390/v17050678.

Saxena S, Hallan V, Singh BP, Sane PV. 1998. Nucleotide sequence and inter geminiviral homologies of the DNA A of Papaya leaf curl geminivirus from India. Biochem Mol Biol Intl 45: 101-113. DOI: 10.1080/15216549800202472.

Soni SK, Mishra MK, Mishra M, Kumari S, Saxena S, Shukla V, Tiwari S, Shirke P. 2022. Papaya Leaf Curl Virus (PaLCuV) infection on papaya (*Carica papaya* L.) plants alters anatomical and physiological properties and reduces bioactive components. Plants 11: 579. DOI: 10.3390/ plants11050579.

Spielman SJ, Weaver S, Shank SD, Magalis BR, Li M, Kosakovsky Pond SL. 2019. Evolution of viral genomes: Interplay between selection, recombination, and other forces. In: Anisimova M (eds). Evolutionary Genomics: Statistical and Computational Methods, Methods in Molecular Biology. Springer, NY. DOI: 10.1007/978-1-4939-9074-0_14.

Srivastava A, Pandey V, Sahu AK, Yadav D, Al-Sadi AM, Shahid MS, Gaur RK. 2022b. Evolutionary dynamics of Begomoviruses and its satellites infecting papaya in India. Front Microbiol 13: 879413. DOI: 10.3389/fmicb.2022.87941.

Srivastava A, Pandey V, Verma RK, Marwal A, Mishra R, Briddon RW, Akhtar A, Gaur RK. 2022a. First complete genome sequence of Tomato Leaf Curl Virus (ToLCV) from *Salvia splendens* in India. J Phytopathol 170: 479-491. DOI: 10.1111/jph.13099.

Suchard MA, Lemey P, Baele G, Ayres DL, Drummond AJ, Rambaut A. 2018. Bayesian phylogenetic and phylodynamic data integration using BEAST 1.10. Virus Evol 4 (1): vey016. DOI: 10.1093/ve/vey016.

Udavatha P, Mesta RK, Basavarajappa MP, Venkataravanappa V, Devappa V, Narasimha Reddy LRC, Shankarappa KS. 2022. Identification of novel Begomoviruses associated with leaf curl disease of papaya (*Carica papaya* L.) in India. Agronomy 13 (1): 3. DOI: 10.3390/agronomy13010003.

Varun P, Akhter Y, Saxena S. 2024. Molecular evidence of novel Begomoviruses and associated Betasatellite complexes linked to Papaya Leaf Curl Disease in Indian Provinces. Ecol Genet Genomics 33: 100286. DOI: 10.1016/j.egg.2024.100286.

Wyatt SD, Brown JK. 1996. Detection of Subgroup III Geminivirus isolates in leaf extracts by Degenerate Primers and Polymerase Chain Reaction. Phytopathol 86: 1288-1293. DOI: 10.1094/Phyto-86-1288.

Xie Y, Wu P, Liu P, Gong H, Zhou X. 2010. Characterization of alphasatellites associated with monopartite *Begomovirus*/betasatellite complexes in Yunnan, China. Virol J 7:178-188. DOI: 10.1186/1743-422X-7-178.

NUSANTARA BIOSCIENCE
Vol. 17, No. 2, pp. 313-321
November 2025

ISSN: 2087-3948
E-ISSN: 2087-3956
DOI: 10.13057/nusbiosci/n170213

Effect of phosphorus and potassium on growth and yield parameters and disease incidence of potato

MOHAMMAD SAIDUL ISLAM[1], ABU ASHRAF KHAN[2], MD. TANBIR RUBAYET[2,♥], MD. MOYNUL HAQUE[3], MD. ABDUL KARIM[3], ISMAIL HOSSAIN MIAN[2]

[1]BADC Cold Storage, Bangladesh Agricultural Development Corporation (BADC). Sreemangal, Moulvibazar, Bangladesh
[2]Department of Plant Pathology, Faculty of Agriculture, Gazipur Agricultural University (GAU). Salna, Gazipur 1706, Bangladesh.
Tel.: +880-2-9205310-14, ♥email: tanbir86plp@gmail.com
[3]Department of Agronomy, Gazipur Agricultural University. Salna, Gazipur 1706, Bangladesh

Manuscript received: 26 October 2025. Revision accepted: 9 November 2025.

Abstract. *Islam MS, Khan AA, Rubayet MT, Haque MM, Karim MA, Mian IH. 2025. Effect of phosphorus and potassium on growth and yield parameters and disease incidence of potato. Nusantara Bioscience 17: 313-321.* A study was undertaken to find out the effects of two macronutrient elements on plant growth, tuber, and tuber disease incidence of potato (*Solanum tuberosum*). The major nutrient elements were phosphorus (P) and potassium (K). The doses of nutrients were P @ 0, 20, 35, 50 kgha^{-1}, and K @ 0, 90, 140, 190 kgha^{-1}. Data were recorded on vine number/ten hills, plant height, canopy coverage, tuber number per ten plants, and tuber weight per plot. Disease incidence and physiological disorders such as common scab (*Streptomyces scabies*), dry rot (*Fusarium* sp.) and soft rot (*Erwinia carotovora*) of potato were also assessed. The highest tuber yield of 24.05 (44.53 tha^{-1}) and 24.12 kg plot^{-1} (44.66 tha^{-1}) was obtained with 35 kgha $^{-1}$ P and 140 kgha^{-1} applied individually. When both the elements were applied together, the highest yield of 30.68 kg plot^{-1} (56.82 tha^{-1}) was obtained at 35 kg P and 140 kg K per hectare. Tuber diseases and disorders were minimal when 35 kgha^{-1} P and 140 kgha^{-1} K were applied together during the potato cultivation under field conditions. Based on findings of the present study, it may be concluded that application of P and K at the rates of 37.67 and 136.69 kgha^{-1} along with a standard dose of N is optimum for maximum plant growth, tuber yield and minimizing the incidence of disease and disorders of potato tuber.

Keywords: Diseases, Phosphorus (P), Potassium (K), potato, yield

INTRODUCTION

Potato (*Solanum tuberosum*) is a high nitrogen (N), phosphorus (P), and potassium (K)-demanding crop. Deficiency of any or combinations of these nutrients can result in retarded growth or complete crop failure in severe cases. Phosphorus and potassium are the major nutrients after nitrogen, which play an important role in the growth, yield and quality of any crop (Malik and Ghosh 2002). Phosphorus is the element that is most often limited in soils. It is absorbed primarily as the monovalent phosphate anion ($H_2PO_4^-$) and less rapidly as the divalent anion ($H_2PO_4^{2-}$). Soil pH controls the relative abundance of these two forms ($H_2PO_4^-$ is favored at a pH below 7 and $H_2PO_4^{2-}$ above 7). Much of the phosphate is converted into organic forms as it enters the root or after it is transported through the xylem to the vine or leaves. Phosphorus is never reduced in plants, where it remains as phosphate, either free or bound in organic forms such as esters.

Phosphorus performs functions in plants, such as a structural element forming part of the macromolecular structures, such as nucleic acids (RNA and DNA) and in the phospholipids of cell membranes. It also has an important function in energy transfer, such as in the esters of energy-rich phosphate present in the metabolic mechanisms of the cells, within which ATP participates in the main metabolic processes, such as photosynthesis and respiration. Optimum plant growth is accompanied by a demand for P to meet the demands for the functions and so depends on the availability of P in the soil, and the ability of the plant to absorb P from the soil. Many factors influence the supply of P to plants. Among the most important are the availability of P in the soil, temperature, root density and root efficiency in P uptake.

Potato fertilization usually requires high amounts of phosphate fertilizer (60 to 80 kgha^{-1} P) to achieve economically acceptable yields. Young plants with a P deficiency are bluish green in color in the early stages of growth. Older leaves with deficiency symptoms usually appear dark green. Phosphorus deficiency in the potato slows apical growth, resulting in small, rigid plants; reduces the formation of starch in the tubers causing necrotic spots distributed in the tuber; decreases CO_2 absorption capacity of leaf photosynthesis; results in an inadequate supply of phosphates which prevents the export of triose phosphate from the chloroplast, and therefore, affects the synthesis of sucrose, and causes delayed development of the tubers. Phosphorus has a direct impact on shoot growth, root development and tuber formation in potato. Rosen and Bierman (2008) found that the numbers and yield of small tubers increased as the dose of P was increased. It indicates that P may play an important role in regulating the number of tubers per plant.

Potato has a relatively high potassium requirement (K), which has led to the suggestion that high doses of the element are needed for potato production. Potassium is a

monovalent cation, and its capture is highly selective, coupled with metabolic activity. It is characterized by high mobility in plants at all levels; it is the most abundant cation in the cytoplasm and, along with its accompanying anions, makes a high contribution to the osmotic potential of cells and tissues. This element has an important role in water relations of the plant; furthermore, K is not metabolized and forms easily interchangeable weak complexes. It stimulates the activity of the enzyme associated with starch synthesis (Mengel and Kirkby 1987). In addition, it facilitates the translocation of assimilates to the tubers, which ultimately increases the bulking capacity of the tuber and its biomass. Potassium deficiency can result in a decrease in yield, tuber size and quality (Maiti et al. 2004). Some quality factors, such as dry tuber, specific gravity, sugar content, flesh color and hollow heart, are affected by K fertilization. Potassium probably exerts its greatest effects on disease through specific metabolic functions that alter compatibility relationships of the host-parasite environment. Potassium in plants increases the production of disease-inhibitory compounds, such as phenols, phytoalexins and auxins around infection sites of resistant plants. K deficiency leads to thinner walls and slower growth of meristematic tissue, making it easier for the parasites to penetrate the epidermis (Bergmann 1992). Adequate potassium fertilizer application can be useful because it makes potato plants adapted to environmental stresses and may lead to increased resistance of potato to some pests (AL-Moshileh et al. 2005).

Growth parameters, yield and yield components of potato responded positively to P and K fertilizers, either applied as sole or in combination. The average tuber weight, marketable and total tuber yield were significantly affected by P and K fertilizer levels and their interaction. The highest tuber yield, average tuber weight, number of tubers per plant and number of vines per hill were obtained from application of a combined P, K fertilizer at the rate of 89.7 Kg P_2O_5ha^{-1} and 100 Kg K_2O ha^{-1}.

In the past, fertilizer recommendations for major food crops were based solely on agronomic evaluations. Little or no consideration has been given to the direct and indirect effects of fertilizer rate on pest epidemics and their effects on yield. But some experiments demonstrated that fertilizer could be used to manage some diseases of the potato. Sharma and Sood (2002) showed that the application of potassium significantly reduced the incidence of late blight of potato. The role of potassium in increasing crop resistance to diseases caused by bacteria and fungi was widely reviewed by Perrenoud (1990). In general, potassium application improves plant health and vigour, making infection less likely or enabling a quick recovery (Perrenoud 1993). Potassium fertilization was found to decrease the incidence of several diseases, such as late blight (*Phytophthora infestans*), dry rot (*Fusarium* spp.), powdery scab (*Spongospora subterranea*) and early blight (*Alternaria solani*) (Perrenoud 1993; Marschner 1995).

Therefore, the study was initiated with the major objective of investigating the effects of applying different levels of phosphorus and potassium on tuber yield and quality of seed potato.

MATERIALS AND METHODS

The experiment was conducted at the Research Farm of the Department of Plant Pathology, Gazipur Agricultural University, Bangladesh. The soil of the experimental field belongs to the Salna series under the Agro Ecological Zone (AEZ)-28: Madhupur Tract (24.05^0 N latitude and 90.16^0 E longitude) at an elevation of 8.4 m above sea level. The texture of the soil was silty clay in the surface layer and silty clay loam in the subsurface layer (Rahman et al. 1998). The soil contains less than 1% organic matter and has a pH range of 6.0-6.5. The experimental site is situated in the subtropical climate zone characterized by heavy precipitation during the months of April-September or scanty or no rainfall during October to March.

Materials

Potato seed tubers of variety Diamant (seed class foundation) collected from Bangladesh Agricultural Development Corporation (BADC) were used in this experiment.

Land preparation, experimental design and fertilizer application

The land was prepared using a harrow and disk plough with laddering to obtain a good tilth. The land was leveled, and large clods were broken into small pieces. Weeds and other stubble were removed. After final land preparation, experimental unit plot of size was 2.25 m × 2.40 m were prepared. The experiment was laid out in a factorial Randomized Complete Block Design (factorial RCBD) with three replications. Blocks were spaced 1 m apart, and an equal 1 m spacing was maintained between plots. The soil of the experimental plot was fertilized at the rate of Urea 300 kg, Gypsum 100 kg, Magnesium sulphate 60 kg, Zinc sulphate 10 kg as recommended by BADC (Anonymous 2008). Cow dung was added with the soil at the rate of 10 tha^{-1} during land preparation. Half of the urea and full dose of all other fertilizers were used at the time of planting of seed potato. The rest of the urea was added to the soil of growing potato plant as top dressing after 35 days of planting of seed potato.

Treatment

Phosphorus (P) was applied at the rate of 0, 20, 35 and 50 kgha^{-1} and potassium (K) was applied 0, 90, 140 and 190 kgha^{-1} with 3 replications. Number of treatments was 16, viz. P_0K_0 = 0 kg P ha^{-1} + 0 kg K ha^{-1}, P_0K_{90} = 0 kg P ha^{-1} + 90 kg K ha^{-1}, P_0K_{140} = 0 kg P ha^{-1} + 140 kg K ha^{-1}, P_0K_{190} = 0 kg P ha^{-1} + 190 kg K ha^{-1}, $P_{20}K_0$ = 20 kg P ha^{-1} + 0 kg K ha^{-1}, $P_{20}K_{90}$ = 20 kg P ha^{-1} + 90 kg K ha^{-1}, $P_{20}K_{140}$ = 20 kg P ha^{-1} + 140 kg K ha^{-1}, $P_{20}K_{190}$ = 20 kg P ha^{-1} + 190 kg K ha^{-1}, $P_{35}K_0$ = 35 kg P ha^{-1} + 0 kg K ha^{-1}, $P_{35}K_{90}$ = 35 kg P ha^{-1} + 90 kg K ha^{-1}, $P_{35}K_{140}$ = 35 kg P ha^{-1} + 140 kg K ha^{-1}, $P_{35}K_{190}$ = 35 kg P ha^{-1} + 190 kg K ha^{-1}, $P_{50}K_0$ = 50 kg P ha^{-1} + 0 kg K ha^{-1}, $P_{50}K_{90}$ = 50 kg P ha^{-1} + 90 kg K ha^{-1}, $P_{50}K_{140}$ = 50 kg P ha^{-1} + 140 kg K ha^{-1}, $P_{50}K_{190}$ = 50 kg P ha^{-1} + 190 kg K ha^{-1}. The P was used as TSP (Triple super phosphate) and K as MP (Muriate of Potash). The whole amount of phosphorus and half of the potassium were used

at the time of planting of seed potato. The rest of the potassium was added to the soil of growing potato plant as top dressing after 35 days of planting of seed potato.

Seed sowing and intercultural operations

Seed tubers were kept under defused light for sprouting. Sprouted tubers were planted in 5-7 cm depth furrows. The plant spacing was maintained as row to row 60 cm and tuber to tuber 15 cm distance. Four lines were accommodated in each unit plot. Each plot contained 60 seed tubers at the rate of 15 tubers per line. First irrigation was done one week after planting which was continued several times as required. After 20 days of planting weeding was done. To control the fungal disease especially late blight, Dithane M-45 at the rate of 2.5 $kgha^{-1}$ and to control aphid Admire at the rate of 1000 $mlha^{-1}$ were applied as foliar spray in the potato field with 10 days interval after 20 days of planting until haulm killing.

Crop harvesting, data collection and recording data

Haulm killing was done in 80 days after planting. It was done with a view to avoid spreading viruses and for hardening of tuber skin. After ten days of haulm killing potato tubers were harvested manually and care was taken to avoid injuries to potato during harvest. Ten plants were selected randomly from each plot and following data on plant growth characters and yield such as number of vines/hill, plant height (cm), canopy coverage, number of tuber/plant, yield/plot (kg) were taken. Total yield (tha^{-1}) was calculated based on yield/plot.

Number of vines per hill

Number of vines per hill was recorded 60 days after planting.

Plant height

Plant height was recorded 60 days after planting. It was measured from soil surface to tip of the plant.

Canopy coverage

Canopy coverage was recorded in 45 days after of planting. It was measured by a wooden frame with 60 cm × 15 cm sized.

Grading of potato tubers

Seven days after harvesting, all healthy potato tubers per plot were counted and measured. And then graded by four standard grading size followed by BADC (2015): The grades were A (> 28-41 mm), B (> >41-56 mm), under size (20-28 mm) and over size (>56-60 mm).

Data on disease and physiological disorders

Disease and physiological disorders data of harvested potato tubers were taken after seven days of harvest based on total number of potato and their weight of a plot. The disease was identified by visual symptoms; if necessary, it was confirmed pathologically. Data on different diseases and disorders such as common scab, soft rot, dry rot, heat injury, secondary growth, and greening were recorded based on number and weight of infected tubers and expressed in percentage of incidence following formula given below:

$$\% \text{ disease incidence} = \frac{\text{number / weight of infected tuber}}{\text{number / weight of total tuber}} \times 100$$

Statistical analysis

Data were analyzed using Statistix 10. All recorded parameters were subjected to ANOVA, and treatment means were separated using Fisher's LSD at the 5% significance level. Graphs were prepared as needed, and SE (5%) was included when required.

RESULTS AND DISCUSSION

Main effect of phosphorus (P) on plant growth and yield attributes

The main effect of phosphorus (P) on vine number per 10 hills, plant height, canopy coverage, tuber number per 10 plants and tuber yield/plot was significant (P=0.05). Application of phosphorus gave a significant increase in those parameters compared to control (P_0). The maximum increase was obtained with 35 $kgha^{-1}$ (P_{35}) followed by 50 $kgha^{-1}$ (P_{50}) (Figure 1).

Like P, main effect of K on vine number per ten hills, plant height, canopy coverage, tuber number/10 plants and tuber yield/plot were significant (P=0.05). Application of K at 90, 140 and 190 $kgha^{-1}$ (K_{90}, K_{150} and K_{190})) caused a significant increase in all the parameters over 0 $kgha^{-1}$ of K (K_0) with few exceptions (Figure 2).

Vine number per 10 hills

Main effect of P: The main effect of phosphorus fertilization was statistically significant on vine number per 10 hills. The significantly highest 60 vines per 10 hills was obtained at 35 kg P ha^{-1} (P_{35}) which was statistically similar with P_{20}. The lowest vine number per 10 hills was observed at the control (45) which was significantly different from other treatments (Figure 1).

Main effect of potassium: The highest 58.30 vines per 10 hills was obtained at 140 kg K ha^{-1} (K_{140}) which was statistically similar with K_{190}. The lowest was observed at the control (K_0) (47.50), which was statistically similar with K_{90} (Figure 2).

Interaction effect: The statistically highest 70 vines per 10 hills was obtained from interaction effect of phosphorus and potassium at the rates of 20 kg P ha^{-1} and 190 kg K ha^{-1} ($P_{20}K_{190}$) which was statistically similar with $P_{35}K_{140}$, $P_{35}K_{90}$, $P_{20}K_{140}$, $P_{35}K_{190}$ and $P_{50}K_{140}$. The lowest vine number per 10 hills was observed at the control (P_0K_0) which was statistically similar with P_0K_{90}, $P_{50}K_0$, $P_{50}K_{90}$, $P_{20}K_{90}$, $P_{20}K_0$, P_0K_{190} and P_0K_{140} (Table 1).

Plant height

Main effect of phosphorus: The tallest plant was recorded 66.8 cm at 35 kg P ha^{-1} (P_{35}) and the shortest plant was found 49.30 cm in control plot which were statistically different from other treatments (Figure 1).

Main effect of potassium: The tallest plant was recorded 64.80 cm at 190 kg K ha^{-1} (K_{190}) and the shortest

plant was found 50.0 cm in control plot which was statistically different from other treatments (Figure 2).

Interaction effect: In the interaction effect of P & K, the tallest plant (77.0 cm) was observed at 35 kg P ha^{-1} and 140 kg K ha^{-1} ($P_{35}K_{140}$) which was significantly different from other treatments. The shortest plant (43.33 cm) was found in control (P_0K_0) which was significantly different from others treatment combinations (Table 1).

Canopy coverage (%)

Main effect of phosphorus: The maximum canopy coverage was recorded 88.4% at 35 kg P ha^{-1} (P_{35}) and the minimum canopy coverage was found 68.6% in control plot which was statistically different from other treatments (Figure 1).

Main effect of potassium: The maximum canopy coverage was observed 82.3% at 140 kg K ha^{-1} (K_{140}) and the minimum canopy coverage was found 71.0% in control plot which was statistically different from other treatments (Figure 2).

Interaction effect: Significantly, the highest canopy coverage of 95.3% was observed under the treatment combination $P_{35}K_{140}$. The minimum canopy coverage of 65.0% was found under control (P_0K_0), which was significantly different from other treatments (Table 1).

Tuber number per 10 plants

Main effect of phosphorus: The maximum tuber number per ten plants was recorded 78.80 at 35 kg P ha^{-1} (P_{35}) and the minimum tuber number per ten plants was found 61.5 in control plot which was statistically different from other treatments (Figure 1).

Main effect of potassium: The maximum tuber number per ten plants was recorded 73.2 at 190 kg K ha^{-1} (K_{190}) and the minimum tuber number per ten plants was found 67.5 in control plot which was statistically different from other treatments (Figure 2).

Table 1. Interaction effect of phosphorus (P) and potassium (K) on growth and yield attributes of potato

Dose of K	Level of P			
	P_0*	P_{20}	P_{35}	P_{50}
Vine number /10 plants				
K_0*	40.0 e[1]	50.0 cde	53.3 bcd	46.7 de
K_{90}	40.0 e	50.0 cde	63.3 ab	50.0 cde
K_{140}	50.0 cde	60.0 abc	63.3 ab	60.0 abc
K_{190}	50.0 cde	70.0 a	60.0 abc	53.3 bcd
Plant height (cm)				
K_0	43.3 k[1]	47.0 j	55.3 gh	54.3 h
K_{90}	47.0 j	49.7 i	64.7 d	58.0 f
K_{140}	50.0 i	62.0 e	77.0 a	61.0 e
K_{190}	57.0 fg	67.7 c	70.3 b	64.3 d
Canopy coverage (%)				
K_0	65.0 j[1]	67.0 i	82.0 de	70.0 h
K_{90}	66.7 ij	73.0 g	87.0 c	74.7 g
K_{140}	69.7 h	81.0 e	95.3 a	83.0 d
K_{190}	73.0 g	76.7 f	89.3 b	77.3 f
Tuber number/10 plants				
K_0	60.7 i[1]	64.4 h	76.9 c	67.8 fg
K_{90}	61.4 i	67.0 g	79.3 ab	71.0 de
K_{140}	61.3 i	69.4 ef	81.0 a	77.7 bc
K_{190}	62.6 hi	73.2 d	78.1 bc	79.2 abc
Yield/Plot$^{\chi}$ (Kg)				
K_0	11.94 k[1]	13.95 j	17.92 g	16.53 h
K_{90}	13.14 j	19.93 f	23.09 de	22.76 e
K_{140}	15.34 i	23.76 cd	30.68 a	26.70 b
K_{190}	13.89 j	20.21 f	24.50 c	23.11 de

Note: *P0: No phosphorus, P20: 20 kg P ha^{-1}, P35: 35 kg P ha^{-1}, P50: 50 kg P ha^{-1}, *K0: No potassium, K90: 90 kg K ha^{-1}, K140: 140 kg K ha^{-1}, K190: 190 kg K ha^{-1}, χ: Plot size 2.25 m × 2.40 m: 5.4 m^2, 1: Figures under the same parameter within same row and column are averages of three replications and having a common letter(s) do not differ significantly (P= 0.05) by LSD test

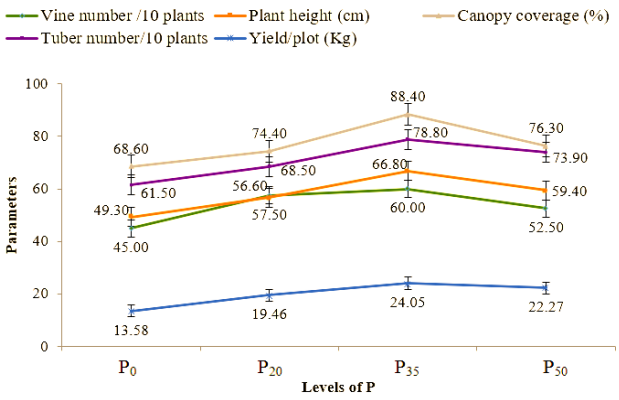

Figure 1. Effect of phosphorus (P) on growth and yield attributes of potato at different levels (P_0: No phosphorus, P_{20}: 20kg P ha^{-1}, P_{35}: 35 kg P ha^{-1}, P_{50}: 50 kg P ha^{-1})

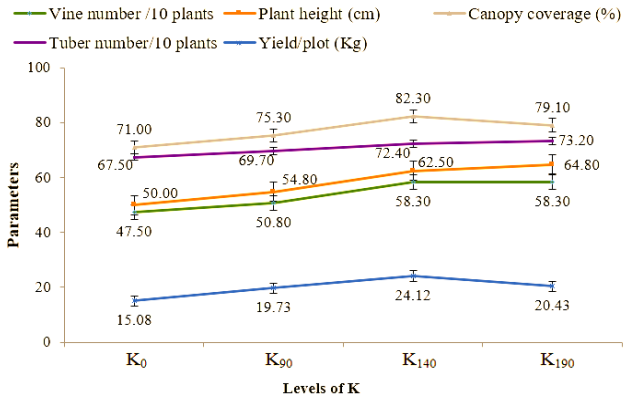

Figure 2. Effect of potassium (K) on growth and yield attributes of potato at different levels (K_0: No potassium, K_{90}: 90 kg K ha^{-1}, K_{140}: 140 kg K ha^{-1}, K_{190}: 190 kg K ha^{-1})

Interaction effect: Among the treatment combinations $P_{35}K_{140}$ gave the maximum tuber number of 81.0 followed by 79.3 obtained from $P_{35}K_{90}$. The lowest number of 60.7 tubers per ten plants was observed under control (P_0K_0), which was statistically like P_0K_{90}, P_0K_{140} and P_0K_{190} (Table 1).

Yield per plot

Main effect of phosphorus: The highest yield per plot was recorded 24.05 kg in main effect of P at 35 kgha^{-1} and the lowest yield per plot was found 13.58 kg in control plot which was statistically different from other treatments (Figure 1).

Main effect of potassium: The average highest yield per plot was recorded 24.12 kg in main effect of K at 140 kgha^{-1} and the lowest yield per plot was found 15.08 kg in control plot which was statistically different from other treatments (Figure 2).

Interaction effect: The average highest yield per plot 30.68 kg was observed in P 35 K 140 kgha^{-1} applied plot. The lowest yield per plot 11.94 kg was recorded in control P 0 K 0 kgha^{-1} which was statistically different from other treatments (Table 1).

Grading of healthy seed tuber

Occurrence of grade-B tuber was maximal followed by grade-A, undersized and oversized potato. Main effect of P as well as K on tuber grade was significant. Interaction effect of two elements was also significant (P=0.05).

Grade A (diameter >28-41 mm)

Main effect of phosphorus: Occurrence of grade-A tuber ranged 23.45-30.08%. Significantly the highest 30.08% grade-A seed tuber was harvested from treatment P_{20}. The lowest 23.45% tuber was found under control plot, which was statistically like P_{35} and P_{50} (Figure 3).

Main effect of potassium: Significantly the highest 27.82% grade-A tuber was recorded at 190 kg K ha^{-1}. The lowest 23.63% grade-A seed tuber was found at K_{140}. The occurrence of grade-A tuber at K_{90} and K_0 were 23.67 and 26.13%, respectively (Figure 4).

Interaction effect: Among 16 treatment combinations with P and K, significantly the highest 33.97% grade-A seed tuber was recorded from treatment combination $P_{20}K_{190}$. The second highest 30.31% occurrence of grade-A tuber was recorded from treatment combination $P_{20}K_0$, which was statistically like P_0K_{190}, $P_{20}K_{90}$, $P_{20}K_{140}$ and $P_{50}K_0$. The lowest grade-A seed tuber of 19.13% was recorded in control plot (P_0K_0), which was statistically similar to $P_{50}K_{140}$ and $P_{35}K_{90}$ (Table 2).

Grade B (diameter >41-55 mm)

Main effect of phosphorus: Occurrence of grade-B tubers ranged 44.02-58.12% under P alone. The highest grade-B seed tuber was recorded at P_{35} followed by P_{50} and P_{20}. Their differences were significant (Figure 3).

Main effect of potassium: Occurrence of grade-B tubers ranged 43.98-57.69% under different levels of K alone. The highest grade-B seed tuber was recorded at K_{190} followed by K_{90}, K_{140}. Significantly the lowest percentage of grade-B tuber was found in control plot compared to other three treatments (Figure 4).

Interaction effect: Under sixteen different treatment combinations of P and K, occurrence of grade-B tuber ranged 39.74-66.32%. Significantly the highest occurrence of grade-B tuber was found under treatment $P_{20}K_{190}$. The second highest occurrence of 61.60% was recorded from $P_{50}K_{140}$, which was statistically similar to $P_{35}K_{90}$, $P_{35}K_{140}$, and $P_{35}K_{190}$. The lowest occurrence of grade-B seed tuber was recorded at P_0K_{140}, which was statistically similar to $P_{20}K_0$, $P_{50}K_0$ and P_0K_0 (Table 2).

Undersize (diameter 20-28 mm)

Main effect of phosphorus: The highest percentage of 9.62% undersize seed tuber was produced at 20 kg P ha^{-1}, which was statistically like 35 kg P ha^{-1}. The lowest was found at 50 kgha^{-1} (Figure 3).

Main effect of potassium: Significantly the highest occurrence of 10.50% undersize seed tuber was found in control plot (K_0). The lowest of 6.68% undersize seed tuber was recorded at 140 kgha^{-1}, which was significantly different from other treatments (Figure 4).

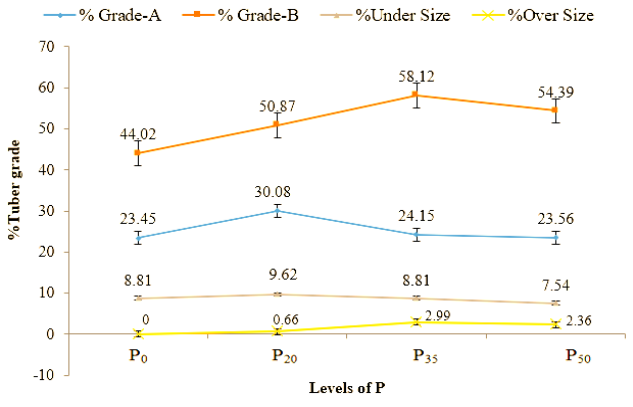

Figure 3. Main effect of P on occurrence of different grades of tubers (P_0: No phosphorus, P_{20}: 20 kg P ha^{-1}, P_{35}: 35 kg P ha^{-1}, P_{50}: 50 kg P ha^{-1})

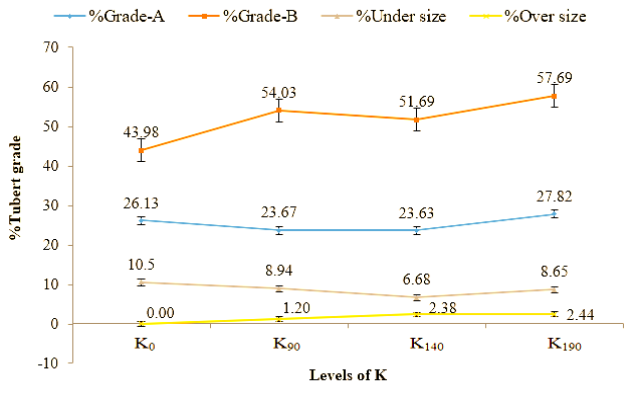

Figure 4. Main effect of K on occurrence of different grades of tubers (K_0: No potassium, K_{90}: 90 kg K ha^{-1}, K_{140}: 140 kg K ha^{-1}, K_{190}: 190 kg K ha^{-1})

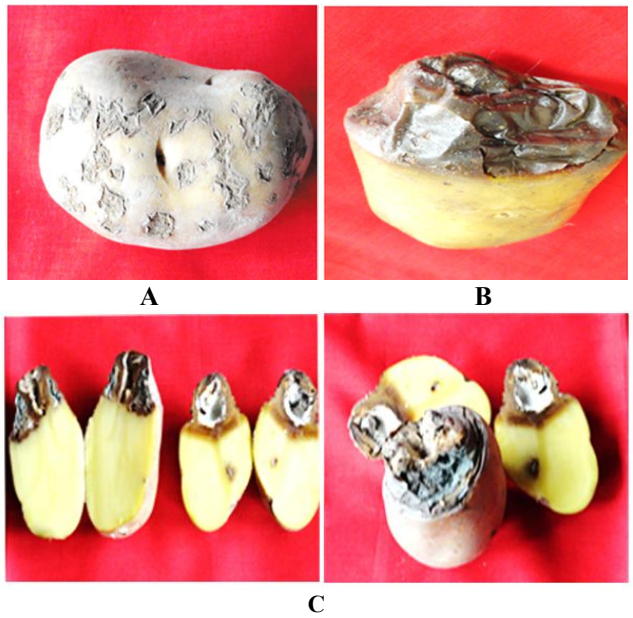

Figure 5. Pathogenic diseases of potato: A. Common scab lesion on potato tuber surface, B. Soft rot disease in potato tuber, C. Dry rot symptoms on the potato tuber

Table 2. Effect of treatment combinations of P and K on occurrence of different grades of tubers

Dose of K	Level of P			
	P_0*	P_{20}	P_{35}	P_{50}
% Grade-A (>28-41mm)				
K_0*	19.13 f[1]	30.31 b	26.85 cd	28.22 bc
K_{90}	22.55 e	28.13 bc	21.48 ef	22.51 e
K_{140}	22.54 e	27.93 bcd	22.8 e	21.24 ef
K_{190}	29.6 b	33.97 a	25.45 d	22.26 e
% Grade-B (>41-55 mm)				
K_0	42.41 ij[1]	40.68 ij	50.84 ef	42.01 ij
K_{90}	46.24 gh	52.62 e	60.55 bc	56.71 d
K_{140}	39.74 j	43.87 hi	61.57 b	61.6 b
K_{190}	47.68 fg	66.32 a	59.51 bcd	57.23 cd
% Under size (20-28mm)				
K_0	7.21 def[1]	13.09 a	12.93 a	8.76 bcd
K_{90}	8.35 bcd	9.91 b	9.72 b	7.8 cde
K_{140}	7.82 cde	6.53 ef	6.01 f	6.37 ef
K_{190}	11.85 a	8.93 bc	6.59 ef	7.23 def
% Over size (>55-60mm)				
K_0	0 f[1]	0 f	0 f	0 f
K_{90}	0 f	0 f	3.27 cd	1.52 e
K_{140}	0 f	0 f	5.84 a	3.69 bc
K_{190}	0 f	2.65 d	2.84 cd	4.25 b

Note: *P0: No phosphorus, P20: 20 kg P ha^{-1}, P35: 35 kg P ha^{-1}, P50: 50 kg P ha^{-1}, K0: No potassium, K90: 90 kg K ha^{-1}, K140: 140 kg K ha^{-1}, K190: 190 kg K ha^{-1}, 1: Figures under the same parameter within row and column are averages of three replications and having a common letter(s) do not differ significantly (P= 0.05) by LSD test

Interaction effect: The highest occurrence of 13.09% undersize seed tuber was found in treatment combination $P_{20}K_0$, which was statistically like $P_{35}K_0$ and P_0K_{190}. The lowest undersize seed was recorded at $P_{35}K_{140}$, which was statistically like $P_{50}K_{140}$, $P_{20}K_{140}$, $P_{35}K_{190}$, P_0K_0 and $P_{50}K_{190}$ (Table 2).

Oversize (diameter >55-60 mm)

Main effect of phosphorus: No oversize seed tuber was recorded under control (0 kg Kha^{-1}). Occurrence of oversize tuber was only 0.66-2.99%. The largest seed tuber was harvest from plot, which received 35 kg Pha^{-1} followed by P_{50} (Figure 3).

Main effect of potassium: Production of oversize potato tuber was found at K_{90}, K_{140} and K_{190}. The highest of 2.44% oversize seed tuber was found at 190 kg K ha^{-1} which was statistically like K_{140} (Figure 4).

Interaction effect: The highest occurrence of 5.84% oversize seed tuber was observed at $P_{35}K_{140}$ which was statistically different from other treatment combinations. On the other hand, no oversize seed was recorded in $P_{50}K_0$, $P_{35}K_0$, $P_{20}K_{140}$, $P_{20}K_{90}$, $P_{20}K_0$, P_0K_{190}, P_0K_{140}, P_0K_{90} and control (P_0K_0) (Table 2).

Incidence of diseases and disorders

After harvesting, various pathogenic diseases and disorders were recorded in tubers harvested from the experimental field under different treatments. The diseases were Common scab (*Streptomyces scabies*), Soft rot (*Pectobacterium carotovorum* subsp. *carotovorum* formerly *Erwinia carotovora* ssp. *carotovora*) and dry rot (*Fusarium* sp.). Common scab attacks vines, stolons and roots of potato plants. Initially, young and rapidly growing tubers were attacked by the bacteria, stimulating the growth forming corky tissue. Potato scab symptoms included dark brown, pithy patches which were raised and "warty" on tubers. Soft rot was characterized by water-soaked, rotted tuber areas with softened tissues, often accompanied by leakage and a foul odor. Healthy tissue was initially distinct from the macerated, creamy infected portion, but the infection eventually spread to the entire tuber. Dry rot is a devastating post-harvest disease for seed potatoes. It appeared on the harvested tuber and the skin of the affected tuber became wrinkled. The rotted areas were brown, grey or black and the rot created depressions in the surface of the tuber (Figure 5).

Common scab incidence was highest in the control (P0) and decreased significantly with P application, with the lowest incidence at P35 followed by P20 and P50 (Figure 6). Similarly, incidence was highest at K0 and was significantly reduced by K application; the lowest incidence occurred at K140, which differed significantly from all other treatments (Figure 7).

Soft rot and dry rot incidence was low, ranging 0.22–0.82% and 0.77–2.72% under the main effect of P, and 0.19–0.86% and 1.32–2.16% under K, respectively. Therefore, detailed results are not presented, but both were included in total diseased tubers (Figures 5 and 6).

Interaction effect of P and K on total disease incidence

Significantly the highest disease incidence was found under control (P_0K_0). Application of P and K together at different treatment combinations caused significant reduction in total disease incidence compared control. The lowest disease incidence was found at $P_{35}K_{140}$. The minimum disease incidence was observed at P_{35} with all

levels of K. Similarly, minimum total disease incidence was recorded at K140 with different levels of P (Figure 8).

Incidence of different disorders

Different disorders such as heat injury, secondary growth and greening were recorded in harvested potato tubers (Figure 10). Incidence of disorders was very low (Figure 9). So, the details are not given.

Estimation of optimum level of phosphorus and potassium

Regression analysis was done, and optimum and economic dose of fertilizer were calculated using the formula Y = -b/2c from the response curve (Gomez and Gomez 1984). Dobermann and Fairhurst (2000) stated that the optimum rate of fertilizer application to a crop is that rate which produces the maximum economic returns at the minimum cost, and this can be derived from a nutrient response curve. The large and significant R^2 value in case of P and K of regression indicates that the quadratic response fitted the data. Response curve shows that yield increased with the increasing of nutrients at certain level and thereafter yield decreased.

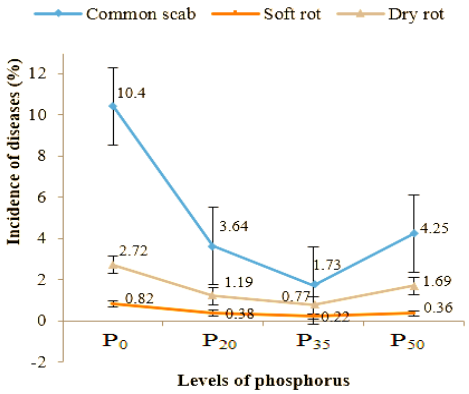

Figure 6. Incidence of common scab, soft rot and dry rot diseases at different levels of irrigation

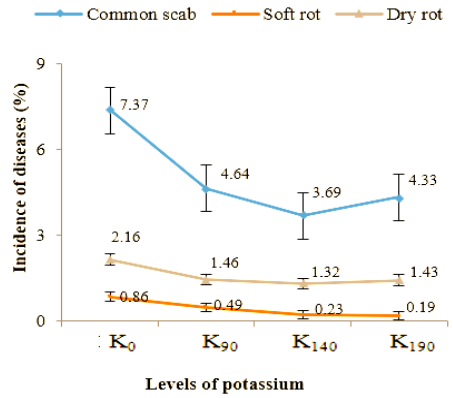

Figure 7. Incidence of common scab, soft rot and dry rot diseases at different levels of fertilization

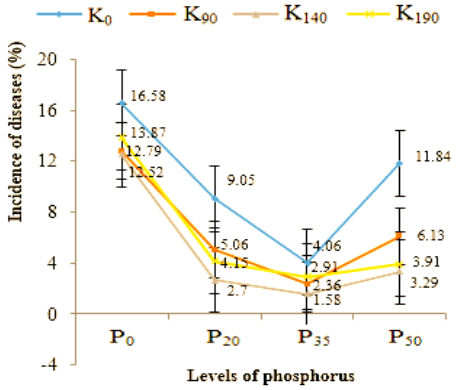

Figure 8. Interaction effect of P and K on incidence of total diseases

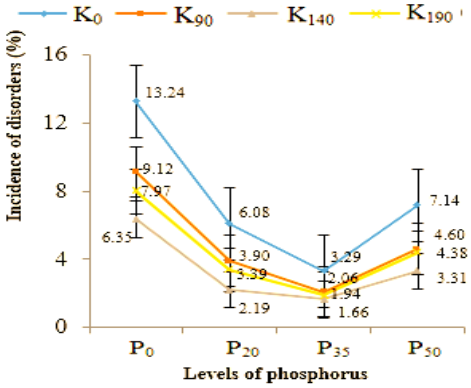

Figure 9. Interaction effect of P and K on incidence of total disorders

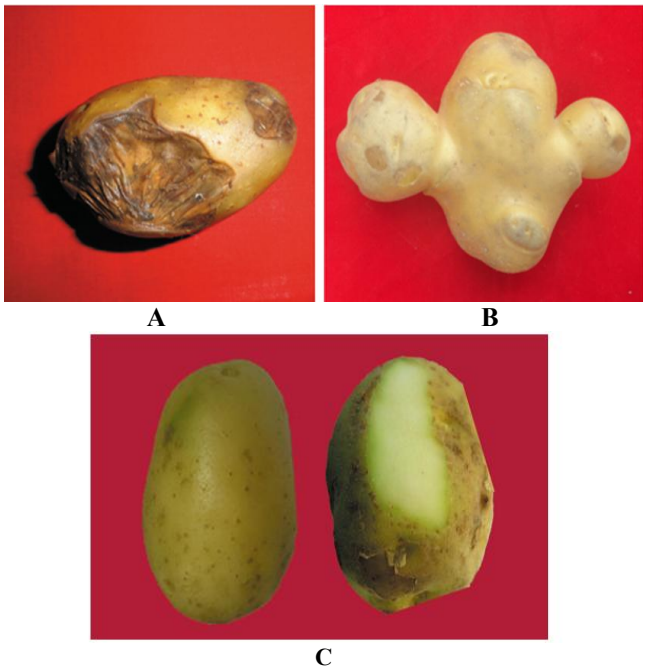

Figure 10. Different physiological disorders of potato: A. Heat injury symptom on potato tuber, B. Secondary growth symptom on potato tuber, C. Greening symptom on potato tuber

Findings of present study show that potato tuber yield increased with increasing level of phosphorus to a certain limit and then decreased by further increase of nutrients level (Figure 11). But the increment of yield was prominent in case of P and the highest yield (42.05 tha^{-1}) was obtained from 35 kg P ha^{-1}. P has distinct effect on the yield. However, further application of P yield began to decrease. It was indicating the detrimental effect of over fertilization. The reason might be medium P status in soil. From the regression equations optimum dose of phosphorus fertilizer is 37.67 $kgha^{-1}$ for better yield (Table 3).

In case of potassium, yield of potato tuber increased by increasing level of potassium fertilizer to a certain limit and then decreased with further increase of potassium level (Figure 12). But the increment of yield was prominent in case of K and the highest yield (41.34 tha^{-1}) was obtained from 140 kg K ha^{-1}. K levels have positive effect on the yield. Further application of K yield began to decrease. The reason might be medium K status in soil. From the regression equations optimum dose of potassium fertilizer is 136.69 $kgha^{-1}$ for better seed tuber yield (Table 3).

Discussion

The main effects of P and K, as well as their interaction, significantly influenced growth and tuber yield attributes, including vine number (per 10 hills), plant height, canopy coverage, tuber number (per 10 plants), and yield per plot. Total tuber yield increased with higher P and K rates up to 35 kg P ha^{-1} and 140 kg K ha^{-1}, producing the highest main-effect yields (44.53 t ha^{-1} at P35 and 44.66 t ha^{-1} at K140). The maximum yield (56.82 t ha^{-1}) occurred under the interaction P35 × K140, indicating that yield responded more strongly to combined P and K than to individual applications. Increased P and K, alone or combined, may also improve soil chemical properties (CEC, EC, pH, Ca^{2+}, Mg^{2+}, and K^{+}). These results agree with previous studies showing positive effects of P and K on vine number, tuber number, tuber weight, and final yield (Zelalem et al. 2009; Ayalew and Beyen 2012; Aarakit et al. 2021).

Fleisher et al. (2012) reported that effects of P on canopy branching were associated with plant N status. N uptake correlated with P and K fertilizer. Application of NPK significantly increased the dry weight of potato (Zelalem et al. 2009; Eleiwa et al. 2012).

Total tuber number per plant increased with the P × K interaction. Previous studies also show that higher P can increase the number and yield of small tubers, indicating its role in tuber set (Rosen and Bierman 2008). Similarly, NPK application significantly increases tuber number and yield, with higher nutrient supply improving average tuber weight and harvest yield parameters (Jenkins and Mahmood 2003; Adhikari and Sharma 2004; Zelalem et al. 2009; Eleiwa et al. 2012).

Table 3. Regression equation and optimum dose of phosphorus and potassium fertilizer

Nutrients levels ($kgha^{-1}$)	Seed tuber yield (tha^{-1})	Yield increased over control	Regression equation and R^2 value	Optimum dose of fertilizer ($kgha^{-1}$)
Phosphorus levels				
P_0	19.20	-	$y = -0.0148x^2 + 1.1154x + 18.646$ $R^2 = 0.9583$	37.67
P_{20}	32.87	71.19%		
P_{35}	42.05	118.96%		
P_{50}	36.59	90.52%		
Potassium levels				
K_0	22.79	-	$y = -0.0008x^2 + 0.2187x + 22.227$ $R^2 = 0.8486$	136.69
K_{90}	32.54	42.77%		
K_{140}	41.34	81.38%		
K_{190}	34.03	49.31%		

Note: P_0: No phosphorus, P_{20}: 20 kg P ha^{-1}, P_{35}: 35 kg P ha^{-1}, P_{50}: 50 kg P ha^{-1}, K_0: No potassium, K_{90}: 90 kg K ha^{-1}, K_{140}: 140 kg K ha^{-1}, K_{190}: 190 kg K ha^{-1}

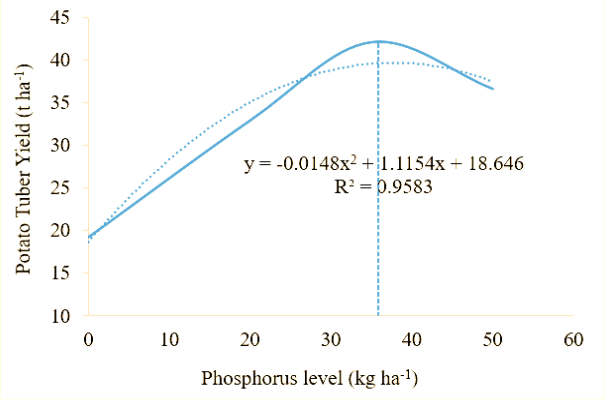

Figure 11. Relationship between phosphorus levels with potato tuber yield

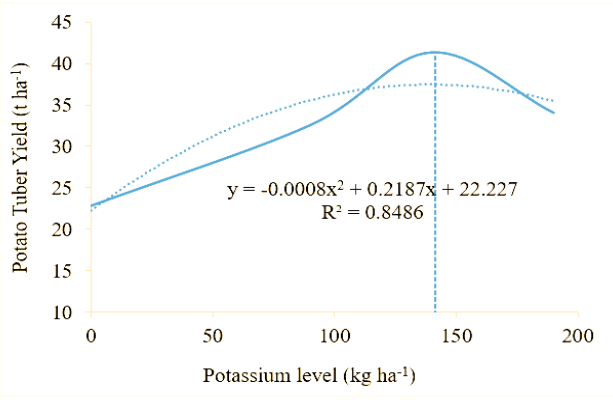

Figure 12. Relationship between potassium levels with potato tuber yield

Significant increase in tuber yield of potato because of K application is well documented (Moinuddin et al. 2005; Zameer et al. 2010). In fact, potato has a higher potassium requirement for optimum production as it produces much more dry matter in short growth duration. Similar root-yield responses to K application have also been reported by Liu et al. (2024). It produces large amounts of starch due to K-mediated carbohydrate metabolism (Singh and Trehan 1998). Thus, K helps the potato tubers to attain large size and heavier weight. This is an evident of the current study, as results observed a progressive increase in aggregate tuber yield. These results are consistent with the findings of Moinuddin and Shahid (2004), Moinuddin et al. (2005) and Abd-El-Latif et al. (2011) who showed an increase in tuber yield with a progressive application of K fertilizer from 0 to 225 kg K_2O ha^{-1} and from 72 to 120 kg K_2O ha^{-1}.

Some authors reported that proper application of fertilizer, especially K, helps in minimizing the diseases of potato (Imas and Bansal 2012). The results of the present experiment also suggest that application of P and K in combination positively influences diseases and physiological disorders of potato tubers.

Conclusions, the present study revealed that the maximum yield and minimum disease incidence such as common scab, soft rot and dry rot were obtained from the combined application of P, K at the rate of 35 and 140 $kgha^{-1}$. However, the regression analysis suggested that application of P and K at the rates of 37.67 and 136.69 $kgha^{-1}$, respectively provide maximum healthy seed tuber yield. Therefore, it is recommended to apply 37.67 and 136.69 $kgha^{-1}$ along with standard dose of N for production of good quantity as well as quality potato seed tubers.

REFERENCES

Aarakit P, Ouma JP, Lelei JJ. 2021. Growth, yield and phosphorus use efficiency of potato varieties propagated from apical rooted cuttings under variable phosphorus rates. Afr J Plant Sci 15: 173-184. DOI: 10.5897/AJPS2020.2113.

Abd-El-Latif KM, Osman EAM, Abdullah R, Abd El-Kader N. 2011. Response of potato plants to potassium fertilizer rates and soil moisture deficit. Adv Appl Sci Res 2: 388-397.

Adhikari CR, Sharma DM. 2004. Use of chemical fertilizers on potatoes in sandy loam soil under humid sub-tropical condition of Chitwan. Nepal Agric Res J 5: 23-26.

Al-Moshileh AM, Errebhi MA, Motawei MI. 2005. Effect of various potassium and nitrogen rates and splitting methods on potato under sandy soil and arid environmental conditions. Emir J Agric Sci 17 (1): 1-9. DOI: 10.9755/ejfa.v12i1.5043.

Anonymous. 2008. A booklet of Production Technology of Quality Seed Potato. Tuber Crops Division, Bangladesh Agricultural Development Corporation (BADC), Dhaka.

Ayalew A, Beyene S. 2012. Characterization of soils and response of potato (*Solanum tuberosum* L.) to application of potassium at Angacha in southern Ethiopia. Intl Res J Biol Bioinfo 2: 46-57.

Bergmann W. 1992. Nutritional Disorders of Plants. Gustav Fischer Verlag, New York.

Dobermann A, Fairhurst T. 2000. Rice Nutrient Disorders and Nutrient Management. Potash and Phosphate Institute, Canada and International Rice Research Institute, Philippines.

Eleiwa EM, Ibrahim SA, Mohamed FM. 2012. Combined effect of NPK levels and foliar nutritional compounds on growth and yield parameters of potato plants (*Solanum tuberosum* L.). Afr J Microbiol Res 6 (24): 5100-5109.

Fleisher DH, Wang Q, Timlin D, Chun JJA, Reddy VR. 2012. Effects of carbon dioxide and phosphorus supply on potato dry matter allocation and canopy morphology. J Plant Nutr 11: 566-586. DOI: 10.1080/01904167.2012.751998.

Gomez KA, Gomez AA. 1984. Statistical Procedures for Agricultural Research (2nd Edn.). International Rice Research Institute, Los Baños, Philippines. John Wiley and Sons, New York.

Imas P, Bansal SK. 2012. Potassium and Integrated Nutrient Management in Potato. Available at: http://www.ipipotash.org/presentn/kinmp.html (Accessed 15 August 2012).

Jenkins PD, Mahmood S. 2003. Dry matter production and partitioning in potato plants subjected to combined deficiencies of nitrogen, phosphorus and potassium. Ann Appl Biol 143: 215-219. DOI: 10.1111/j.1744-7348.2003.tb00288.x.

Liu B, Xv B, Si C, Shi W, Ding G, Tang L, Xv M, Shi C, Liu H. 2024. Effect of potassium fertilization on storage root number, yield, and appearance quality of sweet potato (*Ipomoea batatas* L.). Front Plant Sci 14: 1298739. DOI: 10.3389/fpls.2023.1298739.

Maiti S, Banerjee H, Patra T, Pal S. 2004. Effect of nitrogen and phosphorus on the growth and tuber yield of potato in Gangetic plains of West Bengal. J Interacademicia 8 (4): 555-558.

Malik GC, Ghosh DC. 2002. Effect of fertility level, plant density and variety on growth and productivity of potato. Potato Global Research and Development. Proceedings of the Global Conference on Potato, New Delhi, India, 6-11 December 1999.

Marschner H. 1995. Mineral Nutrition of Higher Plants (2nd Ed.). Academic Press, London.

Mengel K, Kirkby EA. 1987. Principles of Plant Nutrition (4th Ed.). International Potash Institute, Bern, Switzerland.

Moinuddin, Shahid U. 2004. Influence of combined application of potassium and sulfur on yield, quality, and storage behavior of potato. Commun Soil Sci Plant Anal 35 (7-8): 1047-1060. DOI: 10.1081/CSS-120030584.

Moinuddin, Singh K, Bansal SK, Pasricha NS. 2005. Influence of graded levels of potassium fertilizer on growth, yield and economic parameters of potato. J Plant Nutr 27: 239-259. DOI: 10.1081/PLN-120027652.

Perrenoud S. 1990. Potassium and Plant Health. IPI Research Topics No. 3 (2nd Ed.). International Potash Institute, Bern, Switzerland.

Perrenoud S. 1993. Fertilizing for High Yield Potato. IPI Bulletin 8 (2nd Ed.). International Potash Institute, Basel, Switzerland.

Rahman MA, Haider J, Sinha UK, Chowdhury AR, Chowdhury MMU. 1998. Economically viable rates of fertilizers and manures for maximizing growth and yield of year-round tomato. Bangladesh J Agric Res 23 (3): 551-559.

Rosen C, Bierman P. 2008. Potato yield and tuber set as affected by phosphorus fertilization. Am J Potato Res 85 (2): 110-120. DOI: 10.1007/s12230-008-9001-y.

Sharma RC, Sood MC. 2002. Nitrogen and potassium interaction on the tuber yield, quality and organic carbon status of Shimla soils. In: Khurana SMP, Shekhawat GS, Pandey SK, Singh BP (eds). Potato: Global Research and Development. Proceedings of Global Conference on Potato, Indian Potato Association, Shimla 2: 843-851.

Singh JP, Trehan SP. 1998. Balanced fertilization to increase the yield of potato. Proceedings of the IPI-PRII-PAU Workshop on Balanced Fertilization in Punjab Agriculture, Punjab Agricultural University, Ludhiana, India, 15-16 December 1997.

Zameer MK, Ehsan MA, Naeem MS, Masud MM, Sagheer A, Ahmed N. 2010. Effect of source and level of potash on yield and quality of potato tubers. Pak J Bot 42 (5): 3137-3145.

Zelalem A, Tekalign T, Nigussie D. 2009. Response of potato (*Solanum tuberosum* L.) to different rates of nitrogen and phosphorus fertilization on vertisols at Debre Berhan, in the central highlands of Ethiopia. Afr J Plant Sci 2: 16-24.

NUSANTARA BIOSCIENCE
Vol. 17, No. 2, pp. 322-336
November 2025

ISSN: 2087-3948
E-ISSN: 2087-3956
DOI: 10.13057/nusbiosci/n170214

Updated information on qualitative leaf anatomical characters of *Eusideroxylon zwageri* from East Kalimantan, Indonesia

ASIH PERWITA DEWI[1,2,♥], TRI Y. I. WULANSARI[1], SENI K. SENJAYA[1], DEBY ARIFIANI[1], IRVAN F. WANDA[1], YUNITA LISNAWATI[2], SUNARDI[2], APRILIANA D. PRAWESTRI[3], IRFAN MARTIANSYAH[3], EVANA[4], RIZKY D. SATRIO[5], ANJALI M. N. K. HARTONO[5], SUYOKO[6], ADE Y. YUSWANDI[7], MUHAMMAD SYUKUR[8], DEA K. SARI[9], CHIKA A. RASYL[9]

[1]Research Center for Biosystematics and Evolution, National Research and Innovation Agency (BRIN). Science and Techno Park of Dr. (H.C.) Ir. Soekarno, Jl. Raya Jakarta-Bogor Km. 46, Cibinong, Bogor 16911, West Java, Indonesia. Tel.: +62-81119333600, ♥email: asih004@brin.go.id
[2]Research Center for Ecology and Ethnobiology, National Research and Innovation Agency (BRIN). Science and Techno Park of Dr. (H.C.) Ir. Soekarno, Jl. Raya Jakarta-Bogor Km. 46, Cibinong, Bogor 16911, West Java, Indonesia
[3]Research Center for Applied Botany, National Research and Innovation Agency (BRIN). Science and Techno Park of Dr. (H.C.) Ir. Soekarno, Jl. Raya Jakarta-Bogor Km. 46, Cibinong, Bogor 16911, West Java, Indonesia
[4]Research Center for Pharmaceutical Ingredients and Traditional Medicine, National Research and Innovation Agency (BRIN). Science and Techno Park of Dr. (H.C.) Ir. Soekarno, Jl. Raya Jakarta-Bogor Km. 46, Cibinong, Bogor 16911, West Java, Indonesia
[5]Department of Biology, Faculty of Military Mathematics and Natural Sciences, Universitas Pertahanan Indonesia. Komplek Indonesia Peace and Security Center (IPSC) Sentul, Bogor 16810, West Java, Indonesia
[6]Sebangau National Park. Jl. Mahir Mahar No. 1, Paduran Sabangau, Sebangau Kuala, Palangka Raya 74874, Central Kalimantan, Indonesia
[7]Directorate of Scientific Collection Management, National Research and Innovation Agency (BRIN). Science and Techno Park of Dr. (H.C.) Ir. Soekarno, Jl. Raya Jakarta-Bogor Km. 46, Cibinong, Bogor 16911, West Java, Indonesia
[8]Forestry Study Programme, Faculty of Agriculture, Universitas Kapuas Sintang. Jl. YC. Oevang Oeray No. 92, Baning Kota, Sintang 78614, West Kalimantan, Indonesia
[9]Department of Biology, Faculty of Science and Mathematics, Universitas Diponegoro. Jl. Prof. Soedarto No. 13, Tembalang, Semarang 50275, Central Java, Indonesia

Manuscript received: 9 June 2025. Revision accepted: 16 November 2025.

Abstract. *Dewi AP, Wulansari TYI, Senjaya SK, Arifiani D, Wanda IF, Lisnawati Y, Sunardi, Prawestri AD, Martiansyah I, Evana, Satrio RD, Hartono AMNK, Suyoko, Yuswandi AY, Syukur M, Sari DK, Rasyl CA. 2025. Updated information on qualitative leaf anatomical characters of* Eusideroxylon zwageri *from East Kalimantan, Indonesia. Nusantara Bioscience 17: 322-336. Eusideroxylon zwageri*, the sole species of its genus (*Eusideroxylon)* and one of the most economically and culturally significant timbers of Borneo known as Bornean ironwood or "kayu ulin", has been extensively studied for its ecology, genetics, and conservation, yet its foliar anatomy remains poorly documented. This study provides an updated qualitative assessment of leaf anatomical characters of *E. zwageri* based on 66 accessions representing five subpopulations in East Kalimantan, Indonesia. Transverse and paradermal sections of the lamina, midrib, and petiole were prepared following standard microtechnique procedures, and 37 anatomical traits were recorded. The results showed that most foliar anatomical features of *E. zwageri* are consistent with the Lauraceae family. A single character appears diagnostic for *E. zwageri*—osteosclereids present in the mesophyll of the lamina. Several anatomical features of *E. zwageri* indicate functional adaptation, including superficial stomata (related to efficient CO_2 intake), sclereids (contributing to the hardness and durability of the wood), oil cell distribution (which helps prevent pest attacks), suggesting functional adaptations related to gas exchange efficiency, mechanical reinforcement, and defense against herbivory. Nevertheless, understanding pronounced lignification of sclerenchyma and sclereids may constrain regeneration, posing challenges for conservation. These updated anatomical data provide a foundation for future taxonomic, ecological, and conservation research, particularly in developing propagation strategies to support large-scale restoration of this Vulnerable species.

Keywords: Anatomical markers, conservation, Lauraceae, sclereids, taxonomy

INTRODUCTION

Eusideroxylon zwageri Teijsm. and Binn. was first described in 1863 in the publication Natuurkundig Tijdschrift voor Nederlandsch-Indië. Vol. 25 (Koninklijke Natuurkundige Vereeniging in Nederlandsch Indië., and Natuurkundige Vereeniging in Nederlandsch Indië 1850). *E. zwageri* became the sole species of the genus *Eusideroxylon* after the other species, *E. melagangai,* was recognized under a different genus, *Potoxylon melagangai* (Symington) Kosterm. (Kostermans 1978). In Indonesia, *E. zwageri* is considered one of the most economically valuable timber commodities due to its exceptional durability. Its wood is widely used in marine constructions, including pilings, wharfs, docks, sluices, dams, and ships (keels, ribs, and decking) (Slik 2009). It is also widely utilized in heavy constructions for bridges, power line poles, masts, piles, and house posts (Slik 2009). Culturally, *E. zwageri* plays a significant role among the Dayak people, whose iconic long houses are constructed using ironwood as the main structural frame and pillars (Slik 2009; Suciyati et al. 2021). Local tribes considered the tree sacred and believed to possessed mystical powers (Slik 2009; Zahorka 2020). Ecologically, *E. zwageri* is favored

as a nesting tree by orangutans in its natural habitat (Sayektiningsih and Rayadin 2011).

The species is classified under the family Lauraceae, and phylogenetic study indicates that it is closely related to *Cryptocarya*, *Beilschmiedia,* and *Potameia* (Chanderbali et al. 2001). The species has been categorized as Vulnerable (VU) according to the IUCN Red List Assessment (Asian Regional Workshop (Conservation and Sustainable Management of Trees, Viet Nam, August 1996) 1998). Consequently, research efforts on *E. zwageri* have primarily focused on several key areas, including habitat distribution, plant association, and carbon dating (Kurokawa et al. 2003; Arbain 2015; Prayoga et al. 2019; Saputro et al. 2022; Sunardi et al. 2022), plant development and propagation (Hakim 2008; Purba et al. 2019), and population genetics (Rimbawanto et al. 2006; Md-Isa et al. 2021; Ridzqya et al. 2024). Despite this extensive body of work, comparatively few studies have focused on the morphology (Sidiyasa et al. 2013; Irawan et al. 2016; Aiso-Sanada et al. 2020; Dewi et al. 2023) and anatomical characters of *E. zwageri* (Gusmalawati et al. 2014; Dewi et al. 2023). The pioneering anatomy reference, "Anatomy of the Dicotyledons" by Metcalfe and Chalk (1957), describes the anatomy of many families, including Lauraceae. However, it does not provide information on the anatomy of *Eusideroxylon*.

Despite the ecological and cultural importance of *E. zwageri*, its foliar anatomy remains poorly documented. Existing studies have focused primarily on stem structure or reported only scattered quantitative leaf traits, and no research has provided an integrated description of the lamina, midrib, and petiole across multiple subpopulations. Moreover, potential intraspecific variation in leaf anatomy has never been examined, and diagnostic characters for species-level delimitation within Lauraceae remain unresolved. This knowledge gap limits our understanding of the species' adaptive biology, taxonomic placement, and regeneration constraints, hindering efforts to improve propagation and conservation of this Vulnerable tree species.

While numerous studies have focused on the genetic diversity and conservation strategies of *E. zwageri* (Widyatmoko et al. 2011; Md-Isa et al. 2021; Sukartiningsih et al. 2025), anatomical aspects, particularly leaf anatomy, remain underexplored. Leaf anatomy plays a critical role in understanding the ecological adaptability and physiological resilience of long-lived tropical tree species. The anatomical structure of leaves, including cuticle thickness, stomatal density, mesophyll organization, and vascular tissue arrangement, reflects the plant's adaptation to environmental stressors such as water availability, light intensity, and temperature fluctuations (Yang et al. 2018).

Gusmalawati et al. (2014) described the anatomical traits of *E. zwageri,* but limited their description to stem anatomy. Meanwhile, Dewi et al. (2023) only mentioned several quantitative characters derived from leaf anatomy. However, a comprehensive profile integrating the morphological and anatomical characters of *E. zwageri* is still lacking. It could serve as a crucial taxonomic tool and provide insights into its adaptive biology, and needs to be produced.

This study aims to provide updated information on the anatomical structure of *E. zwageri* by conducting a thorough examination of the essential vegetative organ, the leaf. Specimens were collected from East Kalimantan, Indonesia, a region reported to harbor higher genetic richness and broader distribution of the *E. zwageri* (Sukartiningsih et al. 2025). The findings are expected to reveal potential anatomical variations within the species, which may serve as a key character for identification and future taxonomic work.

MATERIALS AND METHODS

Study area

We collected 66 leaf samples during field exploration from 2021 to 2024. The exploration sites are located in East Kalimantan Province, Indonesia (Figure 1) and include five subpopulations: Kongbeng Sub-district, Modang Village, Paser Sub-district (Taman Hutan Rakyat Lati Petangis and Tanjungpinang Village), and Kutai National Park (Table 1). We collected anatomical samples following Sass (1951), with several leaves collected from each plant, ranging from two to three. We stored the sample in 70% alcohol as the fixative solution. Herbarium specimens and anatomical slide preparations were deposited as collections under the management of the Herbarium Bogoriense, Directorate of Scientific Collection Management, Indonesian National Research and Innovation Agency (BRIN).

Procedures

Anatomy slide preparation

We prepared the anatomical slides in the Plant Anatomy Laboratory in Pilot Plant 4 Building, Science and Techno Park of Dr. (H.C.) Ir. Soekarno, located in Cibinong, Bogor, West Java, Indonesia. We followed Sass (1951) to prepare transverse sections and applied the Cutler (1978) method to make semi-permanent paradermal slides. Transverse sections were made by cutting the leaves at the center (midrib included), about 1 × 0.5 cm. The leaf samples were treated with a dehydration solution of tert-butanol, ethanol, and water and with Neo-Clear as a clearing agent. The slides were stained using double staining, 1% safranin and 2% fast green, then sections were covered with entellan. Paradermal sections were prepared by cutting leaves measuring 1 × 1 cm and boiling them in nitric acid until the epidermis separated. The section was then placed on a glass slide and stained with 2% safranin to create a colour contrast. The sections were treated with glycerin and covered with a cover glass; nail polish was used to seal the edges.

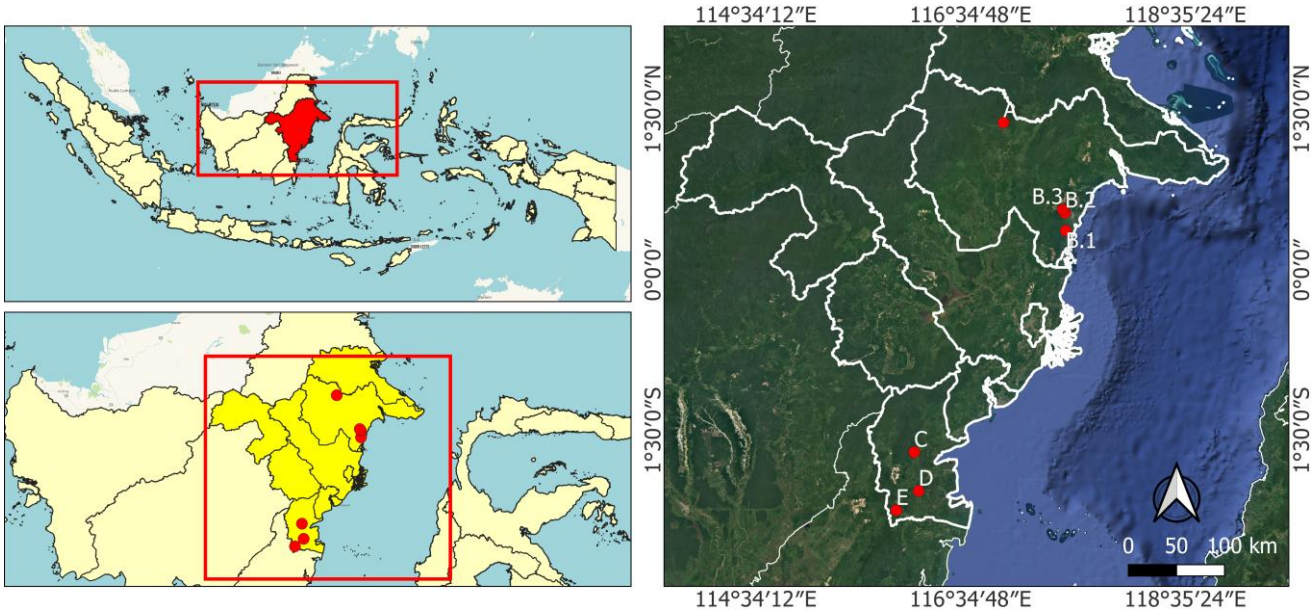

Figure 1. Map of East Kalimantan, Indonesia, showing five subpopulations of *Eusideroxylon zwageri*: A. Subpopulation 1: Kongbeng Sub-district - Sungai Seleq; B. Subpopulation 2: Kutai National Park, including Mentoko, Prevab, and Sangkima research area; C. Subpopulation 3: Kuaro Sub-district - Modang Village; D. Subpopulation 4: Paser Sub-district - Taman Hutan Rakyat Lati Petangis; E. Subpopulation 5: Paser Sub-district - Tanjung Pinang Village

Table 1. Leaf samples of *Eusideroxylon zwageri* were collected from East Kalimantan, Indonesia

Subpopulation	Accession code*	Total samples
Kongbeng Sub-district	GGA 21 (1-21)	21
	GGA 21-N (1-4)	4
	GGA MER (1-3)	3
	GGA KUN (1-4)	4
	GGA HP (1-5)	5
	GGA HA (2-11)	10
Kutai National Park (Mentoko, Prevab, Sangkima)	DA (2405, 2408, 2413, 2463, 2487, 2494)	6
Kuaro Sub-district (Modang Village)	MOD (1-5)	5
	DA (2369-2371)	3
Paser Sub-district (Taman Hutan Rakyat Lati Petangis)	THR (1-3)	3
Paser Sub-district (Tanjung Pinang Village)	TNJ (1-2)	2
Total		**66**

Note: *: Accession code followed by sample number

Data analysis

Observation and characterization of anatomical characters

Observations were carried out using a Nikon Eclipse 80i light microscope and XCAM Indomicro HDMI camera (1080 PHB; 2.4 × 2.4 megapixels) using Betaview software. Measurements were taken from at least 10 photos of each sample. The observation was taken from three leaf parts (lamina, midrib, and petiole) with 37 characters (Table 3). The characters were chosen from previous studies on Lauraceae anatomy (Metcalfe and Chalk 1957; Metcalfe 1987; Nishida and Christophel 1999). The characters then scored with a multivariate score. Each character that presents only a single character state was scored with "1"; meanwhile, characters with multiple variations of character state were scored with various numbers. The list of scoring characters is shown in Table 2.

Principal Component Analysis (PCA) of leaf anatomical characters

Principal Component Analysis (PCA) was conducted using PAST version 5.2.2 (Hammer et al. 2001) to explore patterns of variation and clustering among samples based on 18 scored anatomical leaf characters with multiple character states. All data were standardized before analysis to eliminate scale bias among variables. PCA was used to reduce dimensionality while retaining the maximum variance in the dataset. The resulting principal components were visualized using 2D and 3D scatter plots to observe sample distribution and grouping. To identify which characters contributed most to the clustering, loading plots were examined, highlighting the variables with the strongest influence on the principal components.

Table 2. Anatomical leaf characters with discrete states used in principal component analysis

No.	Character description	Character states and scores
1	Stomatal type	(1) Dominant tetracytic; (2) Tetracytic with anomocytic variation
2	Adaxial epidermis trichome	(1) Present; (2) Absent
3	Spongy mesophyll density	(1) Dense; (2) Less dense
4	Crystal in the lamina	(1) Present; (2) Absent
5	Sclereid in the lamina	(1) Present; (2) Absent
6	Adaxial midrib shape (micromorphology section)	(1) Slightly convex with entire margin; (2) Flat with entire margin
7	Abaxial midrib shape (micromorphology section)	(1) Convex and rounded, with undulate to wavy margin; (2) Convex and rounded, with entire margin; (3) Convex and triangular, with undulate to wavy margin
8	Adaxial epidermis cell shape (in the midrib)	(1) Square; (2) Square and oval
9	Abaxial epidermis cell shape (in the midrib)	(1) Oval; (2) Square and oval
10	Trichome type (in the midrib)	(1) Unicellular, scattered; (2) Absent
11	Vascular bundle shape in the midrib (adaxial-abaxial)	(1) Flat/convex adaxial and U-shaped to ¾ rounded abaxial; (2) Flat/convex adaxial and V-shaped to triangular abaxial; (3) Flat/convex adaxial and rounded abaxial
12	Sclereid in the midrib	(1) Present; (2) Absent
13	Crystal in the midrib	(1) Present; (2) Absent
14	Petiole morphological shape	(1) Rounded with flat canal; (2) Oval with flat canal; (3) Rounded and oval with flat canal
15	Vascular bundle type in the petiole	(1) Single, closed system with oval shape; (2) Double, closed system with oval shape
16	Unicellular trichome density in the petiole	(1) Present (dense or scattered); (2) Absent
17	Crystal in petiole	(1) Present; (2) Absent
18	Number of oil cell layers below the epidermis	(1) 1-2 layers; (2) More than 2 layers

RESULTS AND DISCUSSION

Results

The leaf is the most noticeable vegetative organ in almost all Spermatophyta; it is the primary organ responsible for photosynthesis. The morphological and anatomical characters of leaves often reflect a species' life cycle and functional responses to environmental conditions. Consequently, detailed examination of leaf traits provides key insights into how a species interacts with its habitat and adapts to ecological pressures. In this study, we observed 37 characters from three leaf parts: lamina, midrib, and petiole (Table 3). All samples were collected from lowland tropical rain forests, with the highest elevation where *E. zwageri* was found is Modang village (c. 400-500 m asl). Generally, the qualitative characteristics of different organ parts from different accession numbers are similar due to the conservative character commonly found in the woody plant species. Our findings show that the lamina has 13 consistent characters and 5 variable characters; the midrib has 2 consistent characters and 8 variable characters; and the petiole has 4 consistent characters and 5 variable characters.

The study examined 37 anatomical characters of the lamina, midrib, and petiole to capture the full range of foliar structural diversity in *E. zwageri*. The selection of these characters reflects the traits most consistently used in Lauraceae systematics, as shown in the comparative data in Table 3, including stomatal configuration, mesophyll arrangement, vascular bundle morphology, sclereid types, and the presence of crystals and oil cells. These characters represent both conservative and variable components of leaf architecture, as illustrated in Figure 7, where the lamina shows the highest number of stable traits. At the same time, the midrib and petiole display greater variation across accessions. By incorporating characters that are taxonomically informative and anatomically diverse, the dataset enables a comprehensive qualitative assessment and provides a robust framework for detecting potential intraspecific variation among subpopulations.

General anatomy description of Eusideroxylon zwageri

Leaf. Stomata are superficial, hypostomatic, mostly tetracytic (paratetracytic, anomotetracytic) and anomocytic, with some paracytic (hemiparacytic, brachyparacytic, paratetracytic) variation present (Figure 2). The abaxial epidermis shows straight to rounded anticlinal cell walls; the shape of cells is irregular (in paradermal) and square and rectangular (in transverse section). The adaxial epidermis shows a straight anticlinal cell wall; the shape of cells is square to polygonal (in paradermal section) and square (in transverse section) (Figure 3).

Table 3. Observation of thirty-seven anatomical characters of the lamina, midrib, and petiole of *Eusideroxylon zwageri* compared with other genera of Lauraceae

No	Anatomical characters	*Eusideroxylon zwageri*	*Cinnamomum*	*Beilschmiedia*	*Cryptocarya*
Leaf					
1	Stomatal position through the epidermis	Superficial	Sunken[5,6,17]	Sunken[14], raised and superficial[3]	Superficial (Based on picture)[8]
2	Stomatal type	Mostly tetracytic, and anomocytic, sometimes paracytic	Anomocytic[2], laterocytic, brachyparacytic[9]	Paracytic[14]	Paracytic and anomocytic[8,15]
3	Presence of stomata	Hypostomatic	Hypostomatic[2]	Hypostomatic[14]	Hypostomatic[15]
4	Type of abaxial epidermis anticlinal cell wall	Straight to rounded	Straight to undulate[2]	Angular, rounded, undulate, branched, and sinuous[14]	Usually straight to moderately curved, but sometimes undulate[15]
5	Abaxial epidermis shape (in paradermal section)	Irregular shape	Rectangle, isodiametric, tetragonal to polygonal or tabloid with different sizes or sinuous[2]	Angular, roundish to irregular shape[13]	Angular, roundish to irregular shape[15]
6	Abaxial epidermis shape (in transverse section)	Square and rectangle	Square and rectangle[18], some possess papillae, varying from dome-shaped to club-shaped[4]	Square[13]	Rectangle, some species have a papillate structure[8]
7	Type of adaxial epidermis anticlinal cell wall	Straight	Straight to curved[2,] sinuous[18]	Angular, sinuous, branched[13]	Usually straight to moderately curved, but sometimes undulate[15]
8	Adaxial epidermis shape (in paradermal section)	Square to polygonal	Polygonal, angular, roundish[2] to irregular shape[18]	Polygonal, angular, roundish to irregular shape[13]	Polygonal, angular, roundish to irregular shape[15]
9	Adaxial epidermis shape (in transverse section)	Square	Square and rectangle[4,18]	Square[13]	Square and rectangle[8]
10	Abaxial epidermis trichome	Unicellular trichome, with peg-like attachment and radial basal cell	Some species have unicellular [4], unbranched, non-glandular, solitary, and have an acute apex[2]	Simple with a poral base[14]	Some species have unicellular trichome[8]
11	Adaxial epidermis trichome	Unicellular trichome with peg-like attachment and a radial basal cell is rarely present	Some species have unicellular trichomes[2,4,18]	Simple with a poral base[13]	Present in some species[8]
12	Cuticle	Slightly thick cuticle present	Present both surface[2]	Present both surface[14]	Present both surfaces
13	Palisade mesophyll	Dorsiventral	Dorsiventral[2]	Dorsiventral[14]	Dorsiventral[16]
14	Number of palisade mesophyll layers	Mostly 2-3 layers, rarely 1 or 4 layers	Mostly 1 layer[2,4], rarely 2-3 layers[4]	Mostly 1-2 layers of palisade tissue, but some species have 3 layers[14]	2-3 layers of palisade tissue[16]
15	Spongy mesophyll	Dense or slightly dense rarely lose	Dense or slightly dense (based on pictures[7,12])	Dense or slightly dense (based on picture[13])	Dense, less dense, in some cases, contains large lacunae[16]
16	Crystal	Mostly absent; raphide or prismatic crystal is rarely present in the spongy mesophyll or around the vascular bundles	Present in the mesophyll and around the vascular bundle. The form of crystals is variable[2]	Acicular to rhomboid crystal found in *B. tawa*[10]	Crystal found in parenchyma cells of *Cryptocarya* aff. *aschersoniana* Mez[8]

17	Sclerenchyma	Osteosclereids are present among the mesophyll, sometimes elongated through the palisade and spongy, or only between the palisade or spongy mesophyll area. Rarely absent	The periclinal walls of palisade and the cell of spongy parenchyma show sclerification. Sclerenchymatous bundle sheath[4]	The sclerenchyma is 2-3-layered in bundle sheath[14]	-
18	Idioblast and oil cells	Idioblasts are present between the palisade or spongy mesophyll	Idioblasts and oil cells are present in mesophyll cells [4]	Oil cells are often observed in the palisade tissue[14]	Oil cells are found in the mesophyll of some *Cryptocarya* species[16]
Midrib					
1	Adaxial midrib morphology	Entire margin, flat to slightly convex	Convex, flat[18] and concave[2,6]	Flat to concave[14]	Concave in *Cryptocarya* aff. *Aschersoniana*[8]
2	Abaxial midrib morphology	Convex with a rounded shape (rarely triangle) with an undulate, wavy, or entire margin	Flat to convex[2,6,18]	Convex to wavy margin[14]	Convex in *Cryptocarya* aff. *aschersoniana*[8]
3	Adaxial epidermis shape	Square or square to oval	Square[2,6,18]	Square to rectangular[14]	Square in *Cryptocarya* aff. *aschersoniana*[8]
4	Abaxial epidermis shape	Oval or square to oval	Oval or square to oval[2,6,18]	Square to oval (based on picture [13])	-
5	Trichome	Unicellular hair and scattered (rarely absent)	Unicellular hair[2]	Trichome present in some species (based on picture [13])	Trichome present in some species[8]
6	Cuticle	Slightly thick cuticle present	Present[1]	Present[13]	Present[8]
7	Shape of vascular bundle	Closed system with a single vascular bundle, flat to convex adaxial side, but varies in abaxial (dominant U-shape to ¾ rounded, V-shape to triangular, and rarely full rounded)	One open arch central vascular bundle that was different in shape (oval, elongated, irregular, V-shaped, partially dissected into 2 or 3 segments)[2,6,18]	Dominant flattened arc and closed system rings with variation [14]	Open system, rounded in *Cryptocarya* aff. *Aschersoniana*[8]
8	Oil cells	Scattered among the peripheral and central cortex, around the vascular bundle, and sometimes between the vascular bundles, are cell complexes	Present in the cortex and a complex vascular bundle[2]	Present[13]	Present in *Cryptocarya* aff. *Aschersoniana*[8]
9	Sclereid	Brachysclereids and astrosclereids are present in the cortex, rarely absent	Present[2]. Brachysclereid in the cortex of *C. pauciflorum*[6]	-	Sclerified cells are also observed as supporting tissues in the midrib and at the leaf margins[8]
10	Crystal	Absent (prismoid or raphida crystal rarely present in cortex)	Present in the vascular bundle[2]	-	-
Petiole					
1	Morphological shape	Oval, rounded, or oval and rounded, with a flat canal side	Rounded (with flat canal), reniform, and oval[1]	Rounded[13]	-
2	Epidermis cells shape	Square or square to oval	Square or square to oval[1]	-	-

3	Vascular bundles shape	Closed system, mostly single (double vascular bundles are rarely found), with a wavy oval shape	Simple open arc, partially or clearly separated into 3 segments[1,12]	Three bundles at the base of the petiole, they may branch halfway along the length of the petiole to give five or seven bundles, which commonly reunite or perform ring-form at the petiole's distal end[11,14]	-
4	Trichome	Unicellular hair is present with dense or scattered, rarely absent	Some species have trichomes (unicellular or multicellular)[1]	Some species have trichomes[13]	-
5	Cuticle	Slightly thick cuticle present	Present[1]	Present[13]	-
6	Crystal	Absent or present (if present, raphide crystals found in cortex)	Present (sand, elongated, acicular, rectangular, and box-shaped crystal)[1]	-	-
7	Sclereid	Brachysclereids and astrosclereids are present in the cortex or between the vascular bundle complex	Brachysclereid[1]	-	-
8	Oil cells	Oil cells are present in the peripheral and central cortex, around the vascular bundles, and between the vascular bundles complex	Present in *C. sulphuratum* and *C. verum*[12]	Present in cortex[13]	-
9	Number of oil cell layers	1, 2, or 3 layers	2-3 layers[12]	-	-

Note: References: [1]Abeysinghe and Scharaschkin (2019), [2]Abeysinghe (2024), [3]Babalola et al (2021), [4]Bakker et al. (1992), [5]Baruah and Nath (1997), [6]Baruah and Nath (2006), [7]Bottoni et al (2021), [8]de Moraes (2006), [9]Fadhila et al. (2023), [10]Knowles and Beveridge (1982), [11]Metcalfe (1987), [12]Narayana et al. (2019), [13]Nishida (1998), [14]Nishida and Christophel (1999), [15]Nishida et al. (2016), [16]Petzold (1907), [17]Santose (1930), [18]Wulansari et al. (2020)

Trichomes are hair-shaped, unicellular, with peg-like attachments and radial basal cells; mostly present in the abaxial epidermis and rarely in the adaxial epidermis. Slightly thick cuticle present. The palisade mesophylls are dorsiventral, mostly 1-3 layers, and sometimes up to four layers. Spongy mesophylls are mostly dense, occasionally loose. Crystal is absent primarily, seldom present in raphide or prismatic form, found in spongy mesophyll or around vascular bundles. Osteosclereids mostly perform in the mesophyll, elongated through palisade and spongy, or are only present in the palisade and spongy area. Idioblasts and oil cells are present between the palisade and the spongy mesophyll.

Midrib. The adaxial midrib is slightly convex or sometimes flat, with an entire margin and a square to rectangular epidermis. The abaxial midrib is convex with a rounded shape and rarely triangular, with an undulate, wavy, or entire margin, epidermis dominant oval, or sometimes square. Slightly thick cuticle present. Trichome is occasionally absent, or unicellular hair is rarely present in the abaxial region. Vascular bundles are present in a closed system with a single vascular bundle, flat to convex in adaxial, but vary in abaxial, with dominant U-shape to ¾ rounded and V-shape to triangular, rarely fully rounded (Figure 4). Oil cells are mostly scattered throughout the peripheral and central cortex, around vascular bundles, and sometimes between the vascular bundles' cell complexes. Brachysclereids and astrosclereids are present in the cortex and rarely absent (Figure 5). Crystal prismoid or raphide is sometimes present in the cortex, but mostly absent.

Petiole. Oval, rounded, or oval and rounded with flat canal side, epidermal cells square or square to oval (Figure 6). Vascular bundles are arranged in a closed system, with single vascular bundles mostly present and wavy-oval in shape. Slightly thick cuticle present, with unicellular hair dense, scattered, or rarely absent. Brachysclereids and astrosclereids are present in the cortex or between the vascular bundle complex, while raphide crystals are present (in the cortex) or absent. Oil cells are sparsely distributed in the peripheral and central cortex, around the vascular bundles, and between the vascular bundles; in the peripheral cortex, they are present in one to three layers.

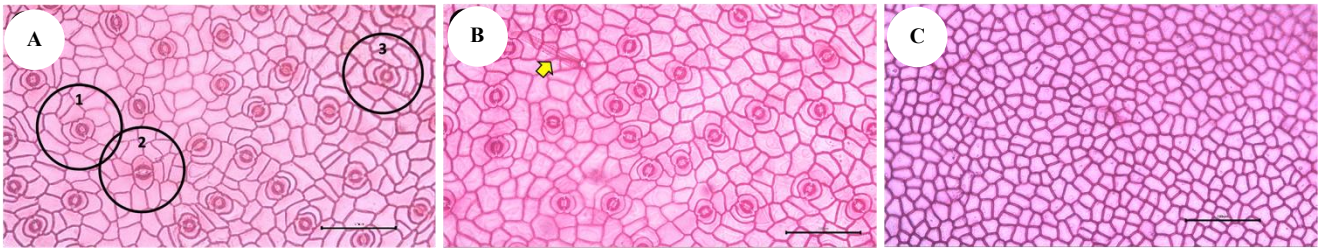

Figure 2. Anatomical appearance of leaf epidermis tissue of *Eusideroxylon zwageri*. A. Several types of stomata were found in abaxial epidermis: 1. Hemiparacytic; 2. Anomocytic; 3. Brachyparacytic, B. A unicellular hair trichome (yellow arrow) was also found in abaxial epidermis, C. No stomata were found in adaxial epidermis. Scale: A-C: 100 µm, magnification level 20x

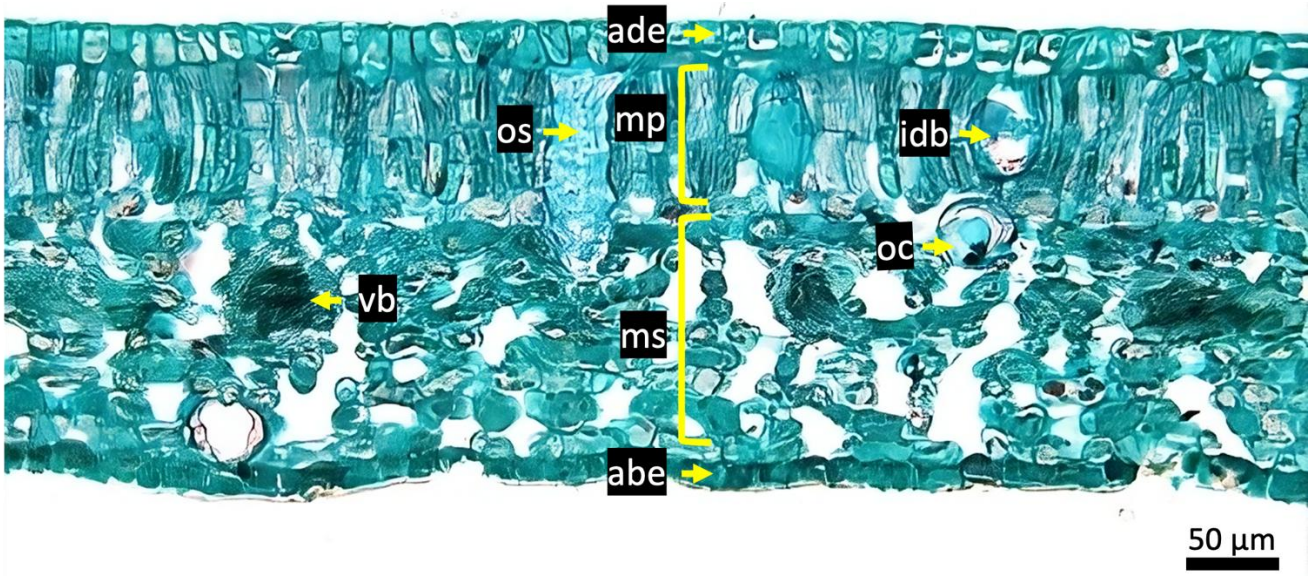

Figure 3. Transverse section of lamina *Eusideroxylon zwageri*
Note: abe: Abaxial epidermis; ade: Adaxial epidermis; idb: Idioblast; mp: Mesophyll palisade; ms: Mesophyll sponge; oc: Oil cells; os: Osteosclereid; vb: Vascular bundle. Magnification level: 20x

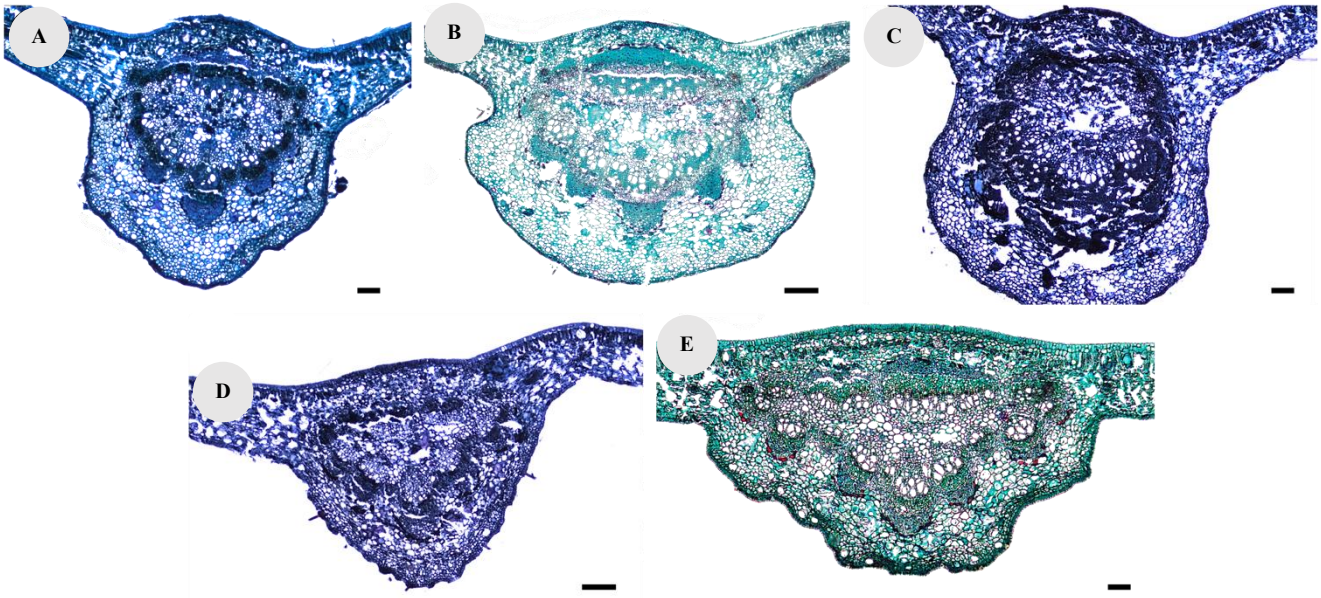

Figure 4. Variation of morphology and vascular bundles shape in the midrib of *Eusideroxylon zwageri*. A-B. Half-rounded midrib with an entire margin and ¾ to half-rounded vascular bundles arrangement, C. Rounded midrib with entire margin and almost fully rounded vascular bundle arrangement, D. Triangular midrib with slightly undulate margin and triangular vascular bundles arrangement, E. Triangular midrib with wavy margin and triangular vascular bundles arrangement. Scale: A,C,E: 100 µm; B,D: 200 µm; magnification level: 4x

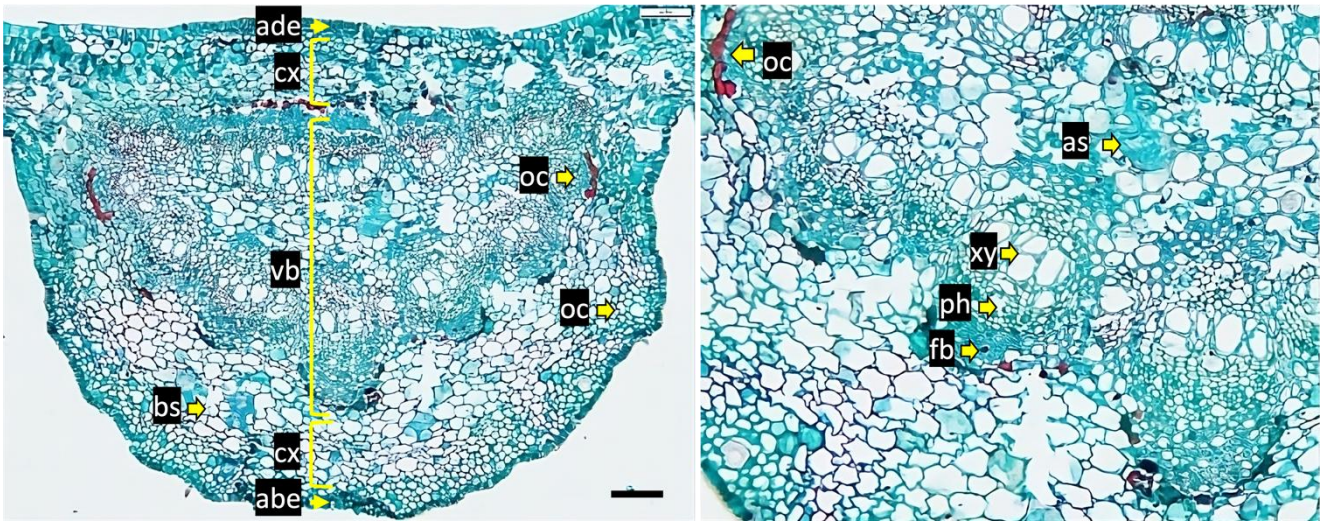

Figure 5. Anatomy structure of the midrib of *Eusideroxylon zwageri.* as: Astrosclereid; bs: Brachysclereid; cx: Cortex; fb: Fibers; oc: Oil cell; ph: Phloem; vb: Vascular bundle complex; xy: Xylem. Scale: 200 µm, magnification level 4x (left) and 10x (right)

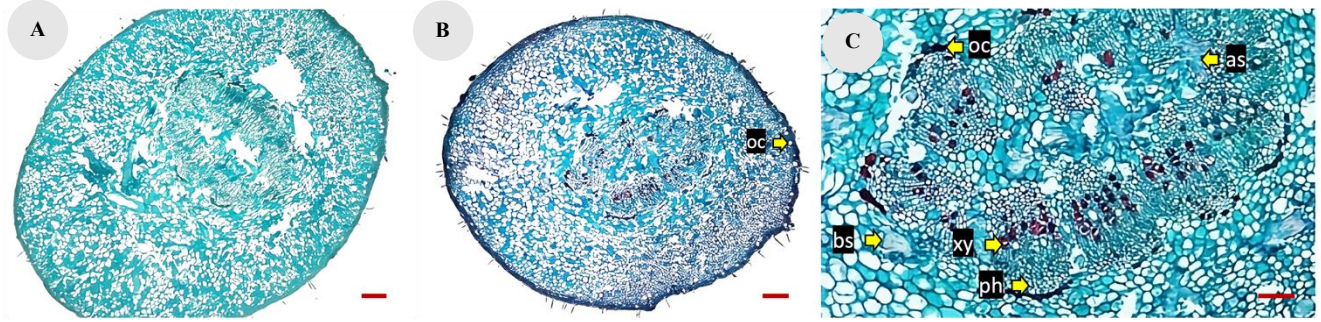

Figure 6. Transverse section of the petiole of *Eusideroxylon zwageri.* A. Petiole with an oval shape, B. Petiole with a rounded shape, C. Vascular bundle complex. as: Astrosclereid; fb: Fibers sheath; oc: Oil cells; ph: Phloem; xy: Xylem. Scale: A-B: 200 µm; C-D: 100 µm, magnification level 4x (A,B) and 10x (C)

Variation among sub-populations of E. zwageri

Based on the characters determined for each accession and subpopulation, the lamina showed the highest number of consistently present characters across all accessions and subpopulations, with 13 characters observed. In contrast, most characters in the midrib and petiole were more varied than those in the lamina (Figure 7). No anatomical character was found to be uniquely associated with any specific subpopulation. Kongbeng Sub-district, as the largest subpopulation, had the highest number of character states (56) across all 47 accessions, but this difference was not significant compared with the Modang subpopulation, which had only 8 accessions and displayed 53 character states. Subpopulations with smaller sample sizes showed lower character state variation, namely Kutai National Park (6 accessions, 46 character-states), Tanjung Pinang Village (2 accessions, 41 character-states), and Taman Hutan Rakyat Lati Petangis (3 accessions, 39 character-states) (Figure 8). Overall, these patterns indicate that the number of accessions collected from a subpopulation did not substantially influence the amount of anatomical variation observed.

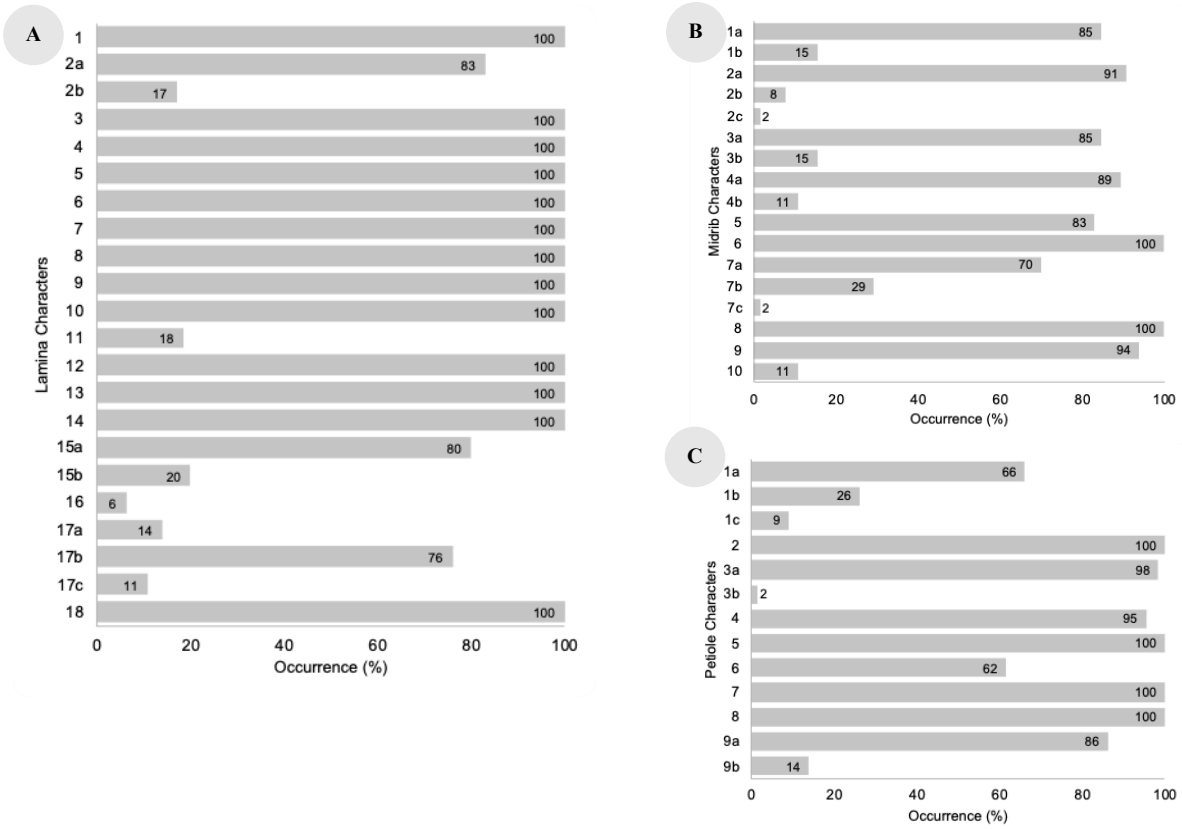

Figure 7. Presentation of characters presented in the accession of *Eusideroxylon zwageri*. A. Lamina characters: 1. Stomatal position through the epidermis (phanerophore); 2a. Stomatal type (tetracytic, anomocytic); 2b. Stomatal type (paracytic, tetracytic and anomocytic); 3. Presence of stomata (hypostomatic); 4. Type of abaxial epidermis anticlinal cell wall (straight to rounded); 5. Abaxial epidermis shape in paradermal section (irregular); 6. Abaxial epidermis shape in transverse section (square and rectangle); 7. Type of adaxial epidermis anticlinal cell wall (straight); 8. Adaxial epidermis shape in paradermal section (square to polygonal); 9. Adaxial epidermis shape in transverse section (square); 10. Abaxial epidermis with unicellular trichome, base peg-like, and basal sel radial; 11. Adaxial epidermis with unicellular trichome; 12. Cuticle; 13. Palisade mesophyll (dorsiventral); 14. Number of palisade mesophyll layers (1-3 layers, sometimes up to 4 layers); 15a. Spongy mesophyll (dense); 15b. Spongy mesophyll (loose); 16. Crystal; 17a. Sclereid (abundant); 17b. Sclereid (rare); 17c. Sclereid absent; 18. Idioblast and oil cells (between mesophyll and sponge palisade). B. Midrib characters: 1a. Adaxial midrib (slightly convex with entire margin); 1b. Adaxial midrib (flat with entire margin); 2a. Abaxial midrib (convex and rounded, with undulate to wavy margin); 2b. Abaxial midrib (convex and rounded with entire margin); 2c. Abaxial midrib (convex and triangle with undulate to wavy margin); 3a. Adaxial epidermis shape (square); 3b. Adaxial epidermis shape (square and oval); 4a. Abaxial epidermis shape (oval); 4b. Abaxial epidermis shape (square and oval); 5. Trichome (unicellular, scattered); 6. Cuticle; 7a. Vascular bundle closed system with flat to convex adaxial and U-shape,1/2, or 3/4 rounded abaxial; 7b. Vascular bundle closed system with flat to convex adaxial and V-shape to triangular abaxial; 7c. Vascular bundle closed system with flat to convex adaxial and rounded abaxial; 8. Oil cells; 9. Sclereid; 10. Crystal. C. Petiole characters: 1a. Morphological shape (rounded with flat canal); 1b. Morphological shape (oval with flat canal); 1c. Morphological shape (rounded and oval with flat canal); 2. Epidermis cells shape (square or square to oval); 3a. Vascular bundles shape (single, closed system with oval shape); 3b. Vascular bundles shape (double, closed system with oval shape); 4. Unicellular trichome present (dense or scattered); 5. Cuticle; 6. Crystal; 7. Sclereid presents between cortex and vascular bundle complex; 8. Oil cells presents below epidermis, around vascular bundle complex, and among vascular bundle cells; 9a. Number of oil cell layers below epidermis 1-2 layers; 9b. Number of oil cell layers below epidermis, more than 2 layers

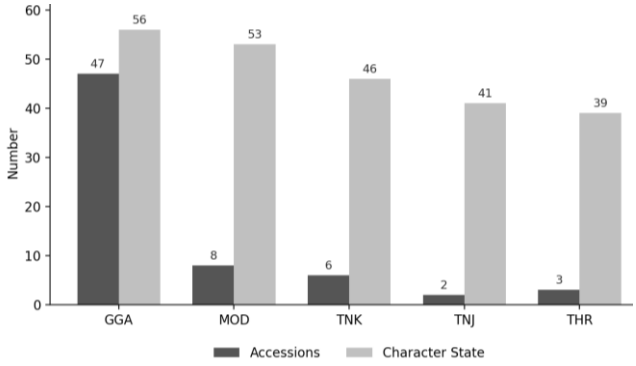

Figure 8. Comparison of the number of accessions from each population with the number of character states observed. GGA: Kongbeng Sub-district, East Kalimantan, Indonesia, subpopulation; MOD: Modang Village; TNK: Kutai National Park; TNJ: Tanjung Pinang Village; THR: Taman Hutan Rakyat Lati Petangis

PCA analysis

The scatter plot from PCA showed that all accession numbers cluster close to the center of the axis, indicating that nearly all of the accession numbers share a similar data pattern. The only accession numbers separated from other accessions are GGA HP1 from Kongbeng Sub-district and DA 2413 from Kutai National Park (Figure 9). Kongbeng Sub-district and Kutai National Park had a similar, highly wet climate, according to climate data based on the Schmidt-Ferguson classification. Therefore, the outlier status of these two accession numbers was unlikely to be caused by climate factors. Those two accession numbers have two characters which offered as the strongest character separating them from one another, i.e., (i) shape of the midrib vascular bundle is a closed system with flat to convex adaxial and V-shape to triangular abaxial (dominantly closed system with flat to convex adaxial and U-shape,1/2, or 3/4 rounded abaxial), and (ii) the petiole morphological shape is rounded and oval with a flat canal (dominantly rounded with flat canal).

Furthermore, another variation found in GGA HP1 is that the midrib adaxial epidermis is square and oval. In contrast, DA 2413 has trichomes on the lamina adaxial epidermis, and the midrib abaxial epidermis is convex and rounded with an entire margin. However, compared with the 3D scatter plot, the two accession numbers were not included among the highlighted results shown in this figure.

Based on the 3D scatter plot, two subpopulations, namely Taman Hutan Rakyat Lati Petangis (grouped in PC3, accession numbers THR1, THR2, THR3), and Tanjung Pinang (placed in PC1, accession numbers TNJ1, TNJ2), are potentially different and placed quite far from the center axis (Figure 10). The Taman Hutan Rakyat Lati Petangis subpopulation lacks crystals in all leaf organs observed, whereas another subpopulation has crystals present in at least one part (petiole or midrib only). The Tanjung Pinang subpopulation shows high variation in its character states, even though it consists of only two accession numbers; it has at least four characters bearing eight character states, indicating that this subpopulation could exhibit greater variation as the sample size increases. However, these results were relatively small and weak and still warrant further investigation using complementary approaches (e.g., molecular studies) to determine whether they represent significant infraspecific variation.

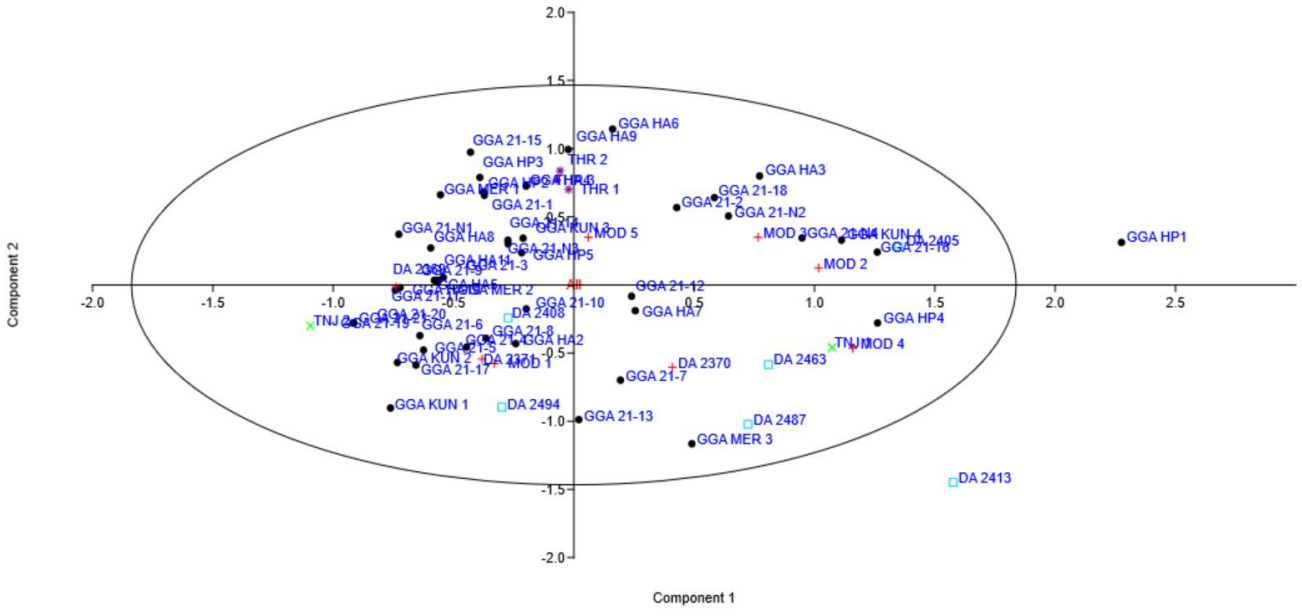

Figure 9. Scattered plot of the *E. zwageri* samples collected from five subpopulations shows only two accession numbers placed outside of the main cluster

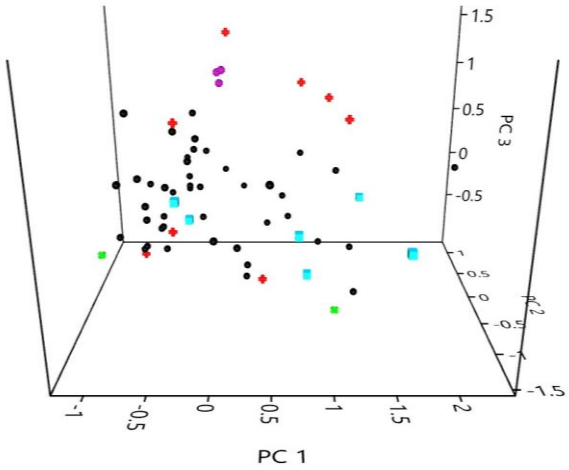

Figure 10. Scatter chart of *E. zwageri* subpopulation in East Kalimantan, Indonesia. Black dot: Kongbeng Sub-district; Plus red: Modang Village; Square blue: Kutai National Park; Star purple: Taman Hutan Rakyat Lati Petangis; Cross green: Tanjung Pinang Village. Variance percentage: PC1: 19.06; PC2: 12.544; PC3: 11.363

Discussions

Comparison of anatomical traits of Eusideroxylon zwageri *with the sister taxa and determining the diagnostic characters*

A previous study by Dewi et al. (2024) analyzed morphological traits in combination with five quantitative anatomical variables: leaf thickness, adaxial and abaxial epidermal thickness, mesophyll thickness, and stomatal density. The samples were collected from two subpopulations: the Kongbeng and Kayan Mentarang (North Kalimantan). The results indicated no statistically significant differences due to overlapping ranges across traits. Building on these findings, the present study focused on qualitative anatomical traits to determine whether diagnostically informative characters exist for *E. zwageri.*

Comparative analyses of the lamina, midrib, and petiole with approximately 360 species from three closely related Lauraceae genera (Petzold 1907; Santose 1930; Knowles and Beveridge 1982; Metcalfe 1987; Bakker et al. 1992; Baruah and Nath 1997; Nishida 1998; Nishida and Christophel 1999; Baruah and Nath 2006; de Moraes 2006; Nishida et al. 2016; Abeysinghe and Scharaschkin 2019; Narayana et al. 2019; Wulansari et al. 2020; Babalola et al. 2021; Bottoni et al. 2021; Fadhila et al. 2023; Abeysinghe 2024), reveal that most anatomical characters of *E. zwageri* overlap with those found elsewhere in Lauraceae (Table 3). For example, the paracytic stomata type was widely seen in sister genera of *Eusideroxylon,* such as *Cryptocarya* (*Cryptocarya densiflora* and *C. ferrea* (Fadhila et al. 2023)), and other species of Lauraceae, such as *Ocotea indecora*, *Nectandra barbellata,* and *Endlicheria paniculata* (Gonçalves et al. 2018). The 2-3 palisade layers of *E. zwageri* are comparable to other genera of Lauraceae, which have 1-3 palisade layers (Metcalfe and Chalk 1950).

Sclereids—particularly osteosclereids and astrosclereids—occur extensively throughout the vegetative organs of *E. zwageri*, indicating a strong lignification strategy. Although sclereids are known from other Lauraceae taxa (e.g., Ravensara), the distribution pattern observed here differs in its consistency and abundance. Idioblasts and oil cells, found in the lamina, midrib, and petiole, also correspond to traits widely documented in Lauraceae (Metcalfe and Chalk 1950; Nishida and Christophel 1999; Serebrynaya et al. 2017; Gonçalves et al. 2018; Aini and Wisanti 2023).

In the midrib, the fiber rings around the outer vascular bundles of *E. zwageri* resemble those in *Persea* (Metcalfe and Chalk 1950), *Cinnamomum* (Abeysinghe 2024), *Nectandra*, *Endlicheria,* and *Ocotea* (Gonçalves et al. 2018). The midrib exhibits various shapes of vascular bundle complexes, i.e., U-shape, ¾ rounded, V-shape, triangular, and rounded forms. All of these constitute a single closed system vascular bundle similar to an unbroken circle. Comparable traits are found in *Beilschmiedia,* a genus in the same tribe (Cryptocaryeae) (Table 2) (van der Werff and Richter 1996). This structure may extend into the petiole, consistent with previous studies that *Beilschimiedia* has vascular bundles that branch halfway along the petiole into five or seven bundles and commonly curve or reunite into a ring-like form at the distal end of the petiole (Table 2) (Metcalfe 1987; Nishida and Christophel 1999).

One distinctive trait does, however, appear exclusive to the genus: the presence of osteosclereids within the lamina mesophyll, sometimes extending from the palisade zone into the spongy mesophyll. This character, absent from closely related genera, constitutes the only robust qualitative diagnostic marker identified. Although PCA highlighted several characters—such as petiole morphology (19.9%), presence of crystals in the petiole (12.67%), and midrib vascular-bundle shape (11.36%)—these traits overlap with those of other Lauraceae and therefore lack diagnostic utility.

Functional anatomical traits related to adaptation

The presence of stomata in a plant was often related to the environmental conditions. In *E. zwageri*, several characters, such as stomatal types, sclereids, and oil cells, indicate appropriate adaptations. The presence of superficial stomata (parallel to the leaf surface), which reflected the rainfall intensity in Kalimantan forests ranging from 1600-4100 mm/year, was quite efficient for the process of CO_2 intake during photosynthesis. In plants exposed to drier conditions, stomata were typically more submerged to prevent water loss (Šantrůček 2022).

Eusideroxylon zwageri contains many sclereids and oil cells, especially in the stems. Sclereids are thick, lignin-rich cells that contribute to the hardness and durability of the ironwood (Evert 2006). Oil cells, usually associated with axial parenchyma (Richter and Dallwitz 2000), were also found in its leaves. Leaf sclereids, such as osteosclereids, provide additional protection against pests (Mauseth 1988), including leafhoppers, ladybugs, shoot-eating caterpillars, and green grasshoppers (Susilawati and Rahmi 2020), by rendering the tissue coarse and unpalatable (Mauseth 1988). As mechanical tissue, sclerenchyma also contributes to leaf resilience, reduces wilting damage, and protects them from direct light

irradiation (Terashima 1992), which serves as an adaptation to the dry season. Meanwhile, leaf oil cells are generally rich in lipophilic plant secondary metabolites, likely functioning in chemical defense, enabling early detection and response to herbivore attacks (Divekar et al. 2022). Together, these anatomical features underscore the importance of sclereids and oil cells in reinforcing the structural and chemical adaptations of ironwood.

Future perspective for conservation efforts informed by anatomical features of E. zwageri

The strong lignification indicated by extensive sclerenchyma and sclereids contributes to the exceptional hardness of *E. zwageri* but also likely underlies its slow growth and regeneration. The species exhibits a low annual diameter increment (0.25 cm/year) and an extremely low volume increment (0.00024 cm^3/year) (Suharja and Jumani 2017). Combined with long-term overexploitation, these traits have contributed to its Vulnerable status under the IUCN Red List (Asian Regional Workshop (Conservation and Sustainable Management of Trees, Viet Nam, August 1996) 1998).

Low seedling production success rates further challenge conservation efforts. Natural regeneration remains limited, while vegetative propagation—through cuttings, air layering, and tissue culture—typically yields 30–40% rooting success (Utami et al. 2005; Maharani et al. 2021). Tissue culture approaches also remain constrained by low induction rates (Wahyuni et al. 2019). Expanding anatomical knowledge could inform improved propagation protocols, helping identify tissue types or developmental stages more responsive to vegetative techniques.

Ironwood's tolerance of nutrient-poor soils and diverse textures—from sandy to clay (Irawan 2015)—supports its potential for restoration programs. However, successful establishment requires appropriate silvicultural treatments, including the use of seedlings at least 40–60 cm in height (Maharani et al. 2021), nutrient supplementation, and integrated pest management. Pest attack intensity in ironwood seedlings is relatively low (30%) compared with other species, such as Shorea balangeran (42.14%) (Priatna et al. 2023), a resilience likely linked to the presence of leaf sclereids (Susilawati and Rahmi 2020).

In conclusion, this study provides updated qualitative anatomical data for *E. zwageri*, demonstrating that most foliar traits align with the broader Lauraceae family while confirming osteosclereids in the lamina as the only clear diagnostic marker. The pronounced lignification and abundance of sclereids and oil cells highlight key adaptive features but may also contribute to the species' slow regeneration and restricted recovery. Future research integrating quantitative anatomical measurements, molecular analyses of intraspecific variation, and the application of anatomical insights to vegetative propagation techniques may significantly enhance large-scale restoration and long-term conservation efforts for this ecologically and culturally important species.

ACKNOWLEDGEMENTS

The authors would like to thank Rumah Program Organisasi Riset Hayati dan Lingkungan – BRIN 2022 and 2023, Indonesia, for funding the research project. The field expedition was supported by the RIIM Ekspedisi LPDP and BRIN grant, under Contract Nomor B-1116/II.7.5/FR.06/3/2024 and B-949/III.5/FR.06.00/3/2024. We are grateful to the Directorate of Scientific Collection Management-BRIN for access given to the Herbarium Bogoriense (BO). We also thank PT. Gunung Gajah Abadi, Taman Hutan Rakyat Lati Petangis, Dinas Lingkungan Hidup Kabupaten Paser, Taman Nasional Kutai, and Taman Nasional Kayan Mentarang as research partners. We acknowledge Mr. Prima Wahyu Kusuma Hutabarat, Mr. Heru, Ms. Dewi, Mr. Bernado da Billy, and Mr. Nadu for their assistance during the sampling in West Kalimantan. We also extend our gratitude to the anonymous referee(s) who helped to improve the manuscript.

REFERENCES

Abeysinghe PD, Scharaschkin T. 2019. Taxonomic value of the petiole anatomy in the genus *Cinnamomum* (Lauraceae) found in Sri Lanka. Ruhuna J Sci 10: 1-17. DOI: 10.4038/rjs.v10i1.47.

Abeysinghe PD. 2024. Leaf micromorphology and anatomical traits of leaves as potential taxonomic markers for infrageneric classification of *Cinnamomum* (Lauraceae). Ceylon J Sci 53: 413-425. DOI: 10.4038/cjs.v53i3.8235.

Aini I, Wisanti. 2023. Characterization of morphological, micromorphological, and anatomical structures and matK gene-based identification of aromatic *Litsea* (*Litsea cubeba*). Biodiversitas 24: 4557-4567. DOI: 10.13057/biodiv/d240859.

Aiso-Sanada H, Nezu I, Ishiguri F, Jaffar ANNBM, Ambun DBA, Perumal M, Wasli ME, Ohkubo T, Abe H. 2020. Basic wood properties of Borneo ironwood (*Eusideroxylon zwageri*) planted in Sarawak, Malaysia. Tropics 28: 99-103. DOI: 10.3759/tropics.MS19-10.

Arbain. 2015. Studi tentang penyebaran pohon ulin (*Eusideroxylon zwageri* Teijsm. and Binn.) di Taman Nasional Kutai Kalimantan Timur. Jurnal Pertanian Terpadu 3: 144-153. [Indonesian]

Asian Regional Workshop (Conservation and Sustainable Management of Trees, Viet Nam, August 1996). 1998. *Eusideroxylon zwageri.* The IUCN Red List of Threatened Species 1998: e.T31316A9624725. DOI: 10.2305/IUCN.UK.1998.RLTS.T31316A9624725.en.

Babalola KA, Zeng G, Liu B, Ferguson DK, Yang Y. 2021. Leaf epidermal micromorphology of *Beilschmiedia* Nees (Lauraceae) from Africa. Taiwania 66: 378-386. DOI: 10.6165/tai.2021.66.378.

Bakker ME, Gerritsen AF, van der Schaaf PJ. 1992. Leaf anatomy of *Cinnamomum* Schaeffer (Lauraceae) with special reference to oil and mucilage cells. Blumea 37: 1-30.

Baruah A, Nath SC. 1997. Foliar epidermal characters in twelve species of *Cinnamomum* Schaeffer (Lauraceae) from North Eastern India. Phytomorphology 47: 127-134.

Baruah A, Nath SC. 2006. Leaf anatomy and essential oil characters of *Cinnamomum pauciflorum* Nees. – a potential spice crop from North-East India. J Spices Aromatic Crops 15: 52-56.

Bottoni M, Milani F, Mozzo M, Kolloffel RDA, Papini A, Fratini F, Maggi F, Santagostini L. 2021. Sub-tissue localization of phytochemicals in *Cinnamomum camphora* (L.) J. Presl. growing in Northern Italy. Plants 10: 1008. DOI: 10.3390/plants10051008.

Chanderbali AS, van der Werff H, Renner SS. 2001. Phylogeny and historical biogeography of Lauraceae: Evidence from the chloroplast and nuclear genomes. Ann Missouri Bot Garden 88: 104-134. DOI: 10.2307/2666133.

Cutler DF. 1978. Applied Plant Anatomy. Longman, London and New York.

de Moraes PLR. 2006. Taxonomy of *Cryptocarya* Species of Brazil. Department of Botany, State University of Campinas, Brazil.

Dewi AP, Arifiani D, Wulansari TYI, Senjaya SK, Wanda IF, Hutabarat PWK, Lisnawati Y, Sunardi, Prawestri AD, Evana, Satrio RD. 2023. Preliminary study on variations in local varieties of bornean ironwood (*Eusideroxylon zwageri* Teijsm. and Binn.) based on vegetative characters. IOP Conf Ser Earth Environ Sci 1271 (2023) 012024. DOI: 10.1088/1755-1315/1271/1/012024.

Divekar PA, Narayana S, Divekar BA, Kumar R, Gadratagi BG, Ray A, Singh AK, Rani V, Singh V, Singh AK, Kumar A, Singh RP, Meena RS, Behera TK. 2022. Plant secondary metabolites as defense tools against herbivores for sustainable crop protection. Intl J Mol Sci 23: 2690. DOI: 10.3390/ijms23052690.

Evert RF. 2006. Esau's Plant Anatomy: Meristems, Cells, and Tissues of The Plant Body: Their Structure, Function, and Development. John Wiley and Sons, Inc., NJ. DOI: 10.1002/0470047380.

Fadhila NA, Sulistijorini, Djuita NR. 2023. Diversity and epidermal characters of Lauraceae leaf in two forest locations, Bogor Regency, West Java. Jurnal Biodjati 8: 81-93. DOI: 10.15575/biodjati.v8i1.24406.

Gonçalves RDA, Pinheiro AB, Oliveira MA, Nascimento RT, Rosalem PF, Garcia VL, Martins AR. 2018. Anatomical characters and chemical profile of leaves of three species in the Lauraceae family. Revista Brasileira de Farmacognosia 28: 1-8. DOI: 10.1016/j.bjp.2017.11.008.

Gusmalawati D, Mukarlina, Wahdin, Khotimah S. 2014. Struktur anatomi batang ulin (*Eusideroxylon zwageri* Teijsm. and Binnend) varietas Tando dan Tembaga di Kalimantan Barat. Saintifika 16: 49-56. [Indonesian]

Hakim L. 2008. Growth variation of four provenances of ulin (*Eusideroxylon zwageri* T et B.) of Kalimantan. Jurnal Penelitian Hutan Tanaman 5: 091-097. DOI: 10.20886/jpht.2008.5.2.91-97.

Hammer Ø, Harper DAT, Ryan PD. 2001. PAST: Paleontological statistics software package for education and data analysis. Paleontol Electron 4: 1-9.

Irawan B, Gruber F, Finkeldey R, Gailing O. 2016. Linking indigenous knowledge, plant morphology, and molecular differentiation: The case of ironwood (*Eusideroxylon zwageri* Teijsm. et Binn.). Gen Resour Crop Evol 63: 1297-1306. DOI: 10.1007/s10722-015-0317-4.

Irawan B. 2015. Soil properties and the abundance of ironwood (*Eusideroxylon zwageri* Teijsm. and Binn.) varieties in Jambi, Indonesia. Jurnal Manajemen Hutan Tropika 21: 155-161. DOI: 10.7226/jtfm.21.3.155.

Knowles B, Beveridge AE. 1982. Biological flora of New Zealand. 9. *Beilschmiedia tawa* (A. Cunn.) Benth. et Hook. F. ex Kirk (Lauraceae) Tawa. NZ J Bot 20: 37-54. DOI: 10.1080/0028825X.1982.10426403.

Koninklijke Natuurkundige Vereeniging in Nederlandsch Indië., And Natuurkundige Vereeniging in Nederlandsch Indië. 1850. Natuurkundig tijdschrift voor Nederlandsch Indië. Vol. 25. Batavia: Lange. https://www.biodiversitylibrary.org/page/39576235.

Kostermans AJGH. 1978. *Potoxylon,* a new bornean genus of Lauraceae. Malay Nat J 32: 143-147.

Kurokawa H, Yoshida T, Nakamura T, Lai J, Nakashizuka T. 2003. The age of tropical rain-forest canopy species, Borneo ironwood (*Eusideroxylon zwageri*), determined by ^{14}C dating. J Trop Ecol 19: 1-7. DOI: 10.1017/S0266467403003018.

Maharani R, Fernandes A, Laksmita AN, Salama DM. 2021. Status Riset Ulin (*Eusideroxylon zwageri* Teijsm. and Binn.) di Indonesia. PT Penerbit IPB Press, Bogor. [Indonesian]

Mauseth JD. 1988. Plant Anatomy. 1st. edn. The Benjamin/Cummings Publishing Company, Inc., San Francisco.

Md-Isa SF, Yong CSY, Saleh MN. 2021. An assessment of genetic variation in vulnerable Borneo ironwood *Eusideroxylon zwageri* Teijsm. and Binn. in Sarawak using SSR markers. J Threat Taxa 13: 18588-18597. DOI: 10.11609/jott.5820.13.6.18588-18597.

Metcalfe CR, Chalk L. 1957. Lauraceae. Anatomy of the Dicotyledons. The Clarendon Press, Oxford.

Metcalfe CR. 1987. Lauraceae. Pp. 152-173 in Metcalfe (editor), Anatomy of the Dicotyledon vol. III. The Clarendon Press, Oxford.

Narayana SKK, Gopi DK, Rubeena M, Parameswaran SR. 2019. Macro-micro-morphological diagnosis of leaves of two species of *Cinnamomum* (*C. sulphuratum* and *C. verum*) used as a source of bay leaf. Intl Quart J Res Ayurveda 40: 196-203. DOI: 10.4103/ayu.AYU_194_17.

Nishida S, De Kok R, Yang Y. 2016. Cuticular features of *Cryptocarya* (Lauraceae) from Peninsular Malaysia, Thailand, and Indo-China and its taxonomic implications. Phytotaxa 244: 026-044. DOI: 10.11646/phytotaxa.244.1.2.

Nishida S, Christophel DC. 1999. Leaf anatomy of *Beilschmiedia* (Lauraceae) in the Neotropics. Nat Human Activities 4: 9-43.

Nishida S. 1998. Revisional Study of Neotropical *Beilschmiedia* Species (Lauraceae) with Special Reference to Leaf Anatomy. [Dissertation]. Kyoto University, Kyoto. [Japan]

Petzold V. 1907. Systematisch-anatomische Untersuchungen über die Laubblätter der amerikanischen Lauraceen. Botanische Jahrbücher für Systematik, Pflanzengeschichte und Pflanzengeographie 38: 445-474.

Prayoga DA, Dewantara I, Herawatiningsi R. 2019. Asosiasi ulin (*Eusideroxylon zwageri* Teijsm. and Binn.) terhadap jenis dominan pada zona domestika Kebun Raya Sambas Kabupaten Sambas. Jurnal Hutan Lestari 7: 1642-1652. DOI: 10.26418/jhl.v7i4.38246. [Indonesian]

Priatna D, Purwanto P, Lukman AH, Utami S. 2023. Pengaruh pupuk majemuk lambat urai terhadap pertumbuhan dan serangan hama pada bibit belangeran (*Shorea balangeran*). J Top Agric 1: 31-40. DOI: 10.56854/jta.v1i1.75.

Purba JH, Sasmita N, Komara LL, Nesimnasi N. 2019. Comparison of seed dormancy breaking of *Eusideroxylon zwageri* from Bali and Kalimantan soaked with sodium nitrophenolate growth regulator. Nusantara Biosci 11: 146-152. DOI: 10.13057/nusbiosci/n110206.

Richter HG, Dallwitz MJ. 2000. Commercial Timbers: Descriptions, Illustrations, Identification, and Information Retrieval. In English, French, German, and Spanish. Version: 9th April 2019. delta-intkey.com

Ridzqya SAA, Polosoro A, Enggarini W, Kusumanegara K, Helmanto H, Magandhi M, Satyawan D, Hadiarto T, Yuniaty A. 2024. Comparison of DNA extraction methods for bornean ironwood plant (*Eusideroxylon zwageri*). Buitenzorg: J Trop Sci 1: 25-32. DOI: 10.70158/buitenzorg.v1i1.7.

Rimbawanto A, Widyatmoko A, Harkingto H. 2006. Keragaman populasi *Eusideroxylon zwageri* Kalimantan Timur berdasarkan penadan RAPD. Jurnal Penelitian Hutan Tanaman 3: 201-208. DOI: 10.20886/jpht.2006.3.3.201-208. [Indonesian]

Santose JK. 1930. Leaf and bark structure of some cinnamon trees with special reference to the Philippine species. Philipp J Sci 43: 305-365.

Šantrůček J. 2022. The why and how of sunken stomata: Does the behaviour of encrypted stomata and the leaf cuticle matter? Ann Bot 130: 285-300. DOI: 10.1093/aob/mcac055.

Saputro RD, Asyari M, Badaruddin B. 2022. Sebaran tumbuhan ulin (*Eusideroxylon zwageri*) di Kawasan Hutan dengan Tujuan Khusus (KHDTK) Kintap Provinsi Kalimantan Selatan. Jurnal Sylva Scienteae 5: 331-340. DOI: 10.20527/jss.v5i3.5734. [Indonesian]

Sass JE. 1951. Killing, fixing, and storing plant tissues. In: Sass J (ed). Botanical Microtechnique 2nd ed. Iowa: The IOWA State College Press, USA. DOI: 10.5962/bhl.title.5706.

Serebrynaya FK, Nasuhova NM, Konovalov DA. 2017. Morphological and anatomical study of the leaves of *Laurus nobilis* L. (Lauraceae), growing in the introduction of the Northern Caucasus region (Russia). Pharmacogn J 9: 519-522. DOI: 10.5530/pj.2017.4.83.

Sidiyasa K, Atmoko T, Ma'ruf A, Mukhlisi. 2013. Morphological diversity, ecology, mother trees, and conservation of ulin (*Eusideroxylon zwageri* Teijsm. et Binnend.) in Kalimantan. Jurnal Penelitian Hutan dan Konservasi Alam 10: 241-54. DOI: 10.20886/jphka.2013.10.3.241-254.

Slik JWF. 2009 onwards. Plants of Southeast Asia. https://asianplant.net.

Suciyati A, Suryadarma IGP, Paidi, Abrori FM. 2021. Ethnobotanical study based on the five dimensions of basic life needs in the Tidung Tribe of North Kalimantan, Indonesia. Biodiversitas 22(6): 3199-3208. DOI: 10.13057/biodiv/d220623.

Suharja I, Jumani. 2017. Riap tanaman ulin (*Eusideroxylon zwageri* Teijsm and Binn) di KHDTK Samboja Kecamatan Samboja Kabupaten Kutai Kertanegara Provinsi Kalimantan Timur. Agrifor XVI: 49-58.

Sukartiningsih S, Nurtjahjaningsih ILG, Sulistyawati P, Wibisono Y, Sumardi S, Hedrati RL, Baskorowati L, Widyatmoko AYPBC, Prihatini I, Mashudi M, Hadiyan Y, Seyiadi D, Pudjiono S, Melia T, Kurokichi H, Saito Y, Ide Y. 2025. Genetic diversity and structure of *Eusideroxylon zwageri* (Teijsm. and Binn.) in Indonesia revealed by nuclear microsatellite markers. For Sci Technol 21: 265-279. DOI: 10.1080/21580103.2025.2511334.

Sunardi, Dewi AP, Prawestri AD, Senjaya SK. 2022. Habitat dan distribusi ulin (*Eusideroxylon zwageri* Teijsm. and Binn.) di Kalimantan. In: M. Nasrudin (ed). Peran Genetika Molekuler dalam Perspektif Konservasi Keanekaragaman Hayati. Penerbit NEM (Nasya Expanding Management), Central Java. [Indonesian]

Susilawati, Rahmi SF. 2020. The damage level of ulin (*Eusideroxylon zwageri*) seedlings in shaded areas and open spaces in nurseries of Balai Perhutanan Sosial and Kemitraan Lingkungan Banjarbaru. In: Prosiding Seminar Nasional Lingkungan Lahan Basah. Universitas Lambung Mangkurat, Banjarmasin, April 2020. [Indonesian]

Terashima I. 1992. Anatomy of non-uniform leaf photosynthesis. Photosynthesis Research. 31: 195-212. DOI: 10.1007/BF00035537.

Utami NW, Hoesen DSH, Witjaksono, Danu. 2005. Perbanyakan ulin (*Eusideroxylon zwageri* T.et.B) dengan biji dan stek. Berita Biologi 7: 199-206.

van der Werff H, Richter HG. 1999. Toward an improved classification of Lauraceae. Ann Missouri Bot Garden 83: 409-418. DOI: 10.2307/2399870.

Wahyuni H, Wulandari RS, Muflihati M. 2019. Konsentrasi IAA (indole acetic acid) dan BAP (benzyl amino purine) pada kultur jaringan ulin (*Eusideroxylon zwageri*). Jurnal Hutan Lestari 7: 1660-1667. DOI: 10.26418/jhl.v7i4.38399.

Widyatmoko AYPBC. 2011. Study on the level of genetic diversity *of Diospyros celebica, Eusideroxylon zwageri, and Michelia spp.* using RAPD markers. Presented in the National Workshop Conservation Status and Formulation of Conservation Strategy of Threatened Species (Ulin, Eboni, and Michelia). Bogor 2011. [Indonesian].

Wulansari TYI, Agustiani EL, Sunaryo, Tihurua EF, Widoyanti. 2020. Leaf anatomical structure as evidence in flowering plants limitation: A case study of 12 Indonesian flowering plant families. Buletin Kebun Raya 23: 146-161. DOI: 10.14203/bkr.v23i2.266.

Yang Y, Ma T, Wang Z, Lu Z, Li Y, Fu C, Chen X, Zhao M, Olson MS, Liu J. 2018. Genomic effects of population collapse in a critically endangered ironwood tree, *Ostrya rehderiana*. Nat Commun 9: 5449. DOI: 10.1038/s41467-018-07913-4.

Zahorka H. 2020. Animism is applied ethnobotany: A shamanic healing ritual with the Dayak Benuaq Ohookng/ East Kalimantan. J Trop Ethnobiol 3: 57-68. DOI: 10.46359/jte.v3i1.8.

NUSANTARA BIOSCIENCE
Vol. 17, No. 2, pp. 337-353
November 2025

ISSN: 2087-3948
E-ISSN: 2087-3956
DOI: 10.13057/nusbiosci/n170215

Diversity of urban street tree communities in Semarang District, Indonesia

ARDHIAN ABDUL MADJID[1], ARDITA AYU WULANDARI[1], ASFI DZIHNI[1], MARIO PINTOR DAVID SIMANJUNTAK[1], SAFIRA CHAIRUNISA[2], ARU DEWANGGA[1], WIDHI HIMAWAN[1], INOCENCIO E. BUOT JR[3], AHMAD DWI SETYAWAN[1,4,♥]

[1]Department of Environmental Science, Faculty of Mathematics and Natural Sciences, Universitas Sebelas Maret. Jl. Ir. Sutami 36A, Surakarta 57126, Central Java, Indonesia. Tel./fax.: +62-271-663375, ♥email: volatileoils@gmail.com
[2]Department of Biology, Faculty of Mathematics and Natural Sciences, Universitas Sebelas Maret. Jl. Ir. Sutami 36A, Surakarta 57126, Central Java, Indonesia
[3]Faculty of Management and Development Studies, University of the Philippines Open University. Los Baños, Laguna 4030, Philippines
[4]Biodiversity Research Group, Universitas Sebelas Maret. Jl. Prof. Ir. Sutami 36A, Surakarta, Central Java, Indonesia.

Manuscript received: 20 November 2024. Revision accepted: 17 December 2025.

Abstract. *Madjid AA, Wulandari AA, Dzihni A, Simanjuntak MPD, Chairunisa S, Dewangga A, Himawan W, Buot Jr IE, Setyawan AD. 2025. Diversity of urban street tree communities in Semarang District, Indonesia. Nusantara Bioscience 17: 337-353.* Roadside vegetation plays an important role in maintaining ecological functions, microclimate regulation, and environmental quality in rapidly urbanizing tropical landscapes. This study examined the diversity, composition, and functional structure of urban street trees across five major 10-km roadside corridors in Semarang District, Central Java, Indonesia. Field surveys conducted in September 2024 recorded 2,091 individuals representing 53 species, 47 genera, and 26 families, and classified into functional categories based on ecological and management attributes. Species richness and abundance varied markedly among routes. The Bandungan-Kaloran corridor showed the highest richness and stability, while the Ungaran-Cangkiran corridor exhibited the strongest species dominance, and the Semarang-Bawen corridor had the lowest richness. Three species-*Swietenia mahagoni*, *Polyalthia longifolia*, and *Mangifera indica*-emerged as district-wide dominants. Functional composition was heavily skewed toward Ornamental Plant (OP) and Timber Plants (TP), with Frugivory-supporting species (Fr) providing secondary ecological roles. Diversity indices (Shannon, Simpson, Margalef, and Evenness) revealed substantial spatial heterogeneity: peri-urban routes showed balanced community structures, whereas highly built-up corridors exhibited low diversity and high dominance. These patterns highlight the influence of urbanization intensity, planting space limitations, and disturbance pressure on roadside vegetation structure. These findings highlight the need for more diversified and functionally balanced street tree planting strategies to enhance the sustainability and resilience of urban green infrastructure in Semarang District and other rapidly developing tropical cities.

Keywords: Functional diversity, Semarang District, tree diversity, tropical urban ecology, urban street trees

INTRODUCTION

Urban vegetation plays an increasingly crucial role in maintaining ecological stability within rapidly expanding cities, particularly in tropical regions where land-use change and infrastructure development exert strong pressures on native biodiversity (Berry et al. 2008; Liu et al. 2024a). Street trees-woody plants intentionally or spontaneously occurring along transportation corridors-constitute one of the most visible components of urban green infrastructure (Choi et al. 2021; Wang et al. 2025). They contribute to biodiversity support, microclimate regulation, air pollution mitigation, stormwater attenuation, and visual landscape quality (Roy et al. 2012; Gherri 2023). In Southeast Asian cities, where urban expansion continues at an accelerating pace, understanding the diversity and ecological functions of street trees is essential for designing resilient and livable environments (Wiryono et al. 2018; Asanok et al. 2021).

Urban street tree communities represent unique vegetation assemblages shaped by ecological tolerance, planting preferences, species availability, and management regimes (Almas and Conway 2016; Pretzsch et al. 2017). Because street corridors are exposed to extreme environmental stressors-heat, drought, soil compaction, pollution, and limited rooting space-their floristic composition typically differs from that of parks or remnant natural forests (Rajoo et al. 2021; Liu et al. 2024b). Tree diversity along roadsides influences a city's overall ecological functioning by supporting pollinators, frugivores, and other wildlife groups that rely on scattered vegetation patches within fragmented urban mosaics (Dietzel et al. 2023; Graffigna et al. 2024). Maintaining diverse street-tree assemblages, therefore, contributes not only to aesthetic and cultural values but also to urban ecological resilience.

Although research on urban tree diversity has grown substantially during the past decade, significant gaps remain, particularly in tropical developing countries. Many studies have focused on urban parks (Wang and Zhang 2022), residential areas (Xie et al. 2024), and green belts (Nasrullah and Suryowati 2008), while roadside

ecosystems-despite their linear continuity and large spatial extent-remain underexplored. In Indonesia, existing works have examined vegetation in urban forests, campuses, and parks, but comprehensive assessments of street-tree communities at the district scale are still limited. Most available studies address only partial aspects such as species lists, ornamental preferences, or community perceptions, without integrating taxonomic diversity, functional roles, and spatial variation across multiple road corridors. This knowledge gap restricts the capacity of planners and policymakers to design evidence-based urban greening strategies, particularly in regions experiencing rapid development such as Central Java, Indonesia.

Semarang District represents one of the most dynamic peri-urban areas in Indonesia, marked by accelerated transportation development, expansion of residential zones, and increasing traffic density (Aprillia and Pigawati 2018). Despite these transformations, the region retains substantial stretches of roadside vegetation that potentially function as biodiversity reservoirs within an otherwise intensively modified landscape (Pemerintah Kota Semarang 2010). Yet, systematic evaluations of street-tree diversity in Semarang District have not been documented, leaving uncertainties regarding the composition, functional attributes, and ecological roles of tree species distributed along major road networks. Understanding these patterns is critical because the resilience of urban ecological systems often depends on the diversity and distribution of vegetation along transportation corridors (Zhang and Jim 2014; Huff et al. 2020).

Given the research gaps, this study provides a comprehensive assessment of urban street-tree communities across five major road corridors in Semarang District, Indonesia. It aims to: (i) document taxonomic composition (species richness, abundance, family representation); (ii) analyze spatial distribution patterns across five 10-km routes; (iii) identify functional categories (edible, medicinal, ornamental, frugivory-supporting, pollution-mitigating species) and evaluate their ecological relevance; and (iv) assess route-level biodiversity stability using Shannon-Wiener, Simpson, Margalef, and Evenness indices. These integrated objectives enable a multidimensional understanding of how urban street trees contribute to ecological functioning in a rapidly urbanizing district.

By generating a district-scale baseline, this study fills a key knowledge gap in Indonesian urban ecology. The findings provide a scientific foundation for optimized tree-planting programs, enhanced habitat connectivity, and improved environmental quality along road networks. The results also serve as a reference for future biodiversity monitoring and guide local governments in selecting species that balance aesthetic appeal, ecological performance, and long-term resilience. Such evidence-based insights are essential for supporting sustainable urban planning and strengthening ecological infrastructure in Semarang and other tropical cities.

This study offers the first district-wide, route-explicit evaluation of street-tree diversity in Central Java by integrating taxonomic structure, functional composition, and multi-index ecological stability across continuous 10-km corridors. Unlike prior studies focusing on parks or isolated green spaces, it quantifies spatial heterogeneity and dominance patterns along linear transport networks. The integration of detailed taxonomic validation, functional categorization, and corridor-level diversity modeling provides a methodological advance for understanding how urbanization gradients shape vegetation structure in tropical cities. The dataset establishes a robust ecological baseline for evidence-based roadside greening and long-term biodiversity planning.

MATERIALS AND METHODS

Study area

Administrative and biophysical setting of Semarang District

Semarang District is situated in Central Java, Indonesia and encompasses a heterogeneous administrative landscape shaped by interactions between urban, peri-urban, and rural development zones. Urban expansion associated with the Greater Semarang metropolitan region has long been recognized as a driver of land-use restructuring and vegetation transformation in Java's rapidly developing districts (Firman 2004; Hudalah and Firman 2012). The district extends from lowland alluvial plains in the north to upland foothills exceeding 700 m in elevation, producing marked gradients in temperature, humidity, and cloud cover that influence species distribution patterns. These gradients align with broader monsoonal climatic characteristics of Central Java, featuring a pronounced wet season and dry season (Schmidt and Ferguson 1951; Aldrian and Susanto 2003). Such administrative-biophysical heterogeneity creates a mosaic of ecological conditions that shape roadside vegetation structure, consistent with urban ecological frameworks emphasizing spatial variation across metropolitan gradients (Pickett et al. 2013).

Road corridors, land use, and traffic intensity

The study focused on five major 10-km road corridors traversing diverse land-use settings: Bandungan-Kaloran, Salatiga-Kedungjati, Ungaran-Cangkiran, Ambarawa-Bawen, and Semarang-Bawen (Figure 1). These corridors intersect agricultural foothills, rural settlements, peri-urban zones, and dense commercial areas, reflecting the district's multilevel development pattern. Elevation shifts from ~200 to >700 m introduce substantial microclimatic variation, a factor known to influence roadside vegetation performance in tropical landscapes (Whitten et al. 1996; Corlett and Primack 2011). Traffic intensity also varies widely, with Semarang-Bawen receiving the highest vehicular load, producing elevated heat, dust, and pollution stressors that are characteristic drivers of urban tree performance (Jim and Liu 2001). Differences in land-use intensity, pollution, and shading conditions generate spatially distinct ecological filters along the routes, paralleling urbanization-gradient patterns reported in global roadside ecology (Morgenroth and Buchan 2009; Sjöman et al. 2015).

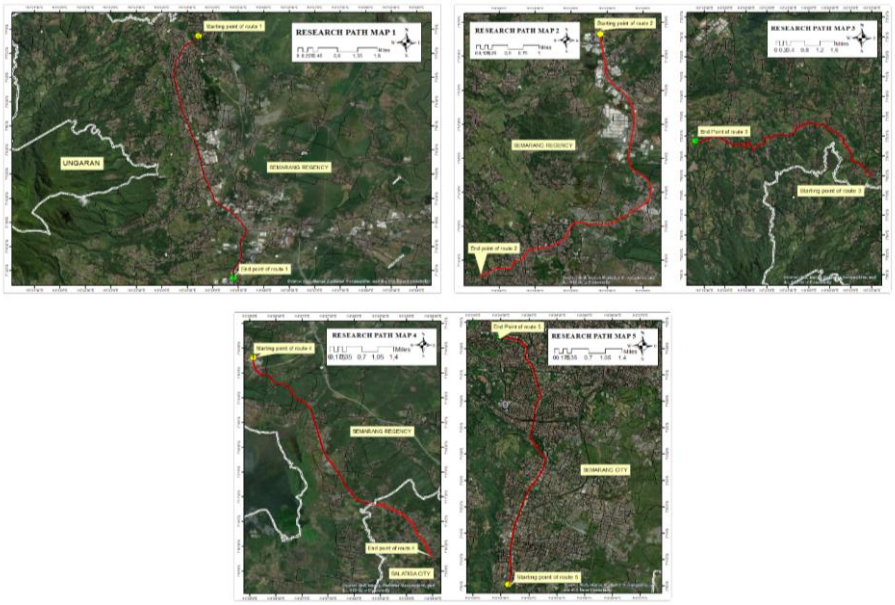

Figure 1. Geographical distribution of the five 10-km street-tree survey routes in Semarang District, Central Java, Indonesia

Route selection criteria

The selection of the five routes followed three primary criteria. First, each represents a major arterial or collector road under district jurisdiction, ensuring ecological relevance for assessing street-tree composition. Second, the routes collectively span strong gradients of elevation, land-use intensity, and traffic pressure, enabling examination of how environmental and anthropogenic factors shape vegetation patterns (McDonnell and Hahs 2008). Third, a uniform transect length of 10 km was adopted to enhance comparability among corridors and to ensure adequate sampling coverage, a practice consistent with long-distance roadside survey guidelines (Nowak et al. 2006; Jim and Chen 2008). Together, these criteria provide a representative cross-section of Semarang District's ecological and urban structural heterogeneity.

Survey design and sampling framework

Overall transect-based roadside survey design

This study employed an observational survey using continuous 10-km transects along each road corridor, allowing systematic documentation of all trees present within the roadside zone. Transects are widely used in urban ecological assessments because linear sampling better captures vegetation patterns influenced by road geometry, land-use intensity, and microclimatic conditions than discrete plot-based designs (Forman et al. 2003; McDonnell and Hahs 2008). Continuous transects also minimize sampling gaps and yield more representative data for corridor-level vegetation heterogeneity (Morgenroth and Östberg 2017). Plot methods were not adopted because roadside vegetation is spatially linear, discontinuous, and strongly conditioned by traffic exposure, which often leads to underrepresentation when fixed-area plots are used (Pauleit et al. 2005; Kent 2012). Standardizing the 10-km length across all routes allowed comparability and produced sufficiently large sample sizes consistent with tropical roadside vegetation surveys (Jim and Chen 2008).

Left-right sampling and definition of individual trees

Field observations were conducted on both the left and right sides of each road corridor to ensure full coverage of roadside vegetation and reduce detection bias. Parallel scanning is recommended in urban tree surveys because opposite verges often differ in shading, slope, built-up density, and exposure to pollutants, leading to asymmetric vegetation patterns (Pauleit et al. 2005; Roy et al. 2012). The roadside boundary was defined as the area from the road shoulder to the edge of the planting strip or drainage channel. An "individual tree" was defined as a perennial woody plant ≥2 m tall rooted within this designated zone, following standard guidelines for urban tree inventories (Nowak et al. 2008; FAO 2016). Multi-stemmed clumps arising from a single root base were counted as one individual, while seedlings or saplings below the height threshold were excluded to avoid inflating abundance estimates. Trees within private compounds were omitted unless their canopy extended clearly into the roadside space. These criteria align with international urban forestry survey protocols (Konijnendijk et al. 2005).

Survey period and temporal considerations

The field survey was conducted in September 2024, corresponding to the late dry season in Central Java. Surveying during this period ensured high visibility of canopy structure and reproductive traits while minimizing rainfall-related obstruction, consistent with recommendations for tropical vegetation assessments (Corlett and Primack 2011). Because most roadside tree species in Java are evergreen, seasonal detectability biases are generally low (Whitmore 1998; Körner and Basler 2010). All transects were surveyed during daylight hours under comparable weather conditions to reduce temporal

variability and ensure consistent identification accuracy (Sutherland 2006). This timing also aligns with best practices in urban tree monitoring, which emphasize minimizing phenological and climatic variation during fieldwork (Miller et al. 2015).

Field data collection

Georeferencing and route mapping

Each 10-km transect was established using predetermined start-end coordinates derived from district road maps and administrative boundaries. GPS tracking ensured the survey team remained aligned with the intended route, enabling consistent spatial coverage throughout the corridor. Coordinates were cross-checked with field conditions to avoid deviations caused by road curvature or construction. Mapping followed general ecological survey protocols emphasizing spatial precision (Sutherland 2006; Kent 2012). The spatial configuration of the five transects corresponds to the distribution presented in Figure 1, which illustrates their position across varying land-use and elevation zones (ESRI 2020).

Tree inventory and recorded attributes

Tree inventories were conducted through continuous visual assessment along both sides of each corridor. Every individual tree within the roadside zone was identified to species level when possible, counted, and recorded in standardized forms. This direct-observation method is widely applied in roadside vegetation studies because it accommodates the linear, heterogeneous nature of urban planting strips (McDonnell and Hahs 2008; Nowak et al. 2008). Supplementary attributes-including height class, canopy density, and the presence of flowers or fruits-were documented when visible to support later verification and ecological interpretation. These attributes help distinguish similar taxa and provide context on growth performance under differing roadside conditions (FAO 2016; Pretzsch et al. 2017). Recording these morphological traits also aligns with best practices in tropical urban forestry, where environmental stressors often induce variable phenotypic expression (Sjöman and Nielsen 2010).

Photographs, vouchers, and rare species handling

Representative photographs were taken for each species, especially when diagnostic structures were visible. When permissible, small non-destructive samples (twigs or fallen reproductive parts) were collected as voucher material following standard herbarium practices (Bridson and Forman 1998; Funk et al. 2017). Species that were rare, morphologically ambiguous, or difficult to confirm in the field were documented with additional notes and photographic angles and later verified through expert consultation. Functional traits of interest were also noted to aid subsequent categorization (Díaz et al. 2016).

Species identification and taxonomic validation

Identification workflow and diagnostic characters

Species identification followed a stepwise workflow beginning with field recognition based on readily observable vegetative and reproductive traits. Key diagnostic characters included leaf arrangement, blade shape, and venation, bark texture, crown architecture, latex presence, and flower or fruit morphology when available-criteria widely used in tropical tree identification (Kent 2012; Beentje 2016). Ambiguous taxa were documented through photographs and additional notes for subsequent verification. Post-field verification relied on comparison with authoritative floristic descriptions, ensuring that identifications were consistent with regional morphological variation. This workflow reflects best practices in botanical survey methodology (Hollingsworth et al. 2011), particularly for species commonly used in urban plantings that show substantial phenotypic variability under roadside stress.

Regional floras and online databases

Verification employed major regional floras, including *Flora Malesiana* (van Steenis 1954-2006), *Flora of Java* (Backer and van den Brink 1963-1968), and the Tree Flora used by Indonesian botanical institutions. These references provided authoritative morphological keys for species distributed across Malesia. Digital taxonomic resources-including POWO, WFO, and GBIF-were used to confirm accepted names, synonymy, and geographic distribution, following global nomenclatural standards (Kew 2019; GBIF 2020). Integration of printed floras and online databases aligns with current taxonomic protocols in tropical biodiversity studies and supports consistency across datasets (Smith and Brown 2018).

Native vs introduced status and taxonomic consistency

Species were classified as native, naturalized, or introduced based on distribution evidence from POWO, GBIF, and the CABI Invasive Species Compendium (https://www.cabi.org/isc). A species was considered native when at least one authoritative source confirmed historical distribution in Indonesia, and it was not listed as introduced or invasive (Richardson et al. 2000; Pyšek et al. 2004). Synonymy checks minimized misidentification among horticulturally common taxa (Govaerts 2001, 2003).

Functional category classification

Functional groups and assignment criteria

Each species was assigned to functional groups based on documented ecological roles and human uses, including Timber Plants (TP), Medicinal Plants (MP), Edible Plants (EP), Ornamental Plants (OP), Frugivory-supporting species (Fr), Pollen Producing (PP), Pollen Reducing (PR), and Toxic Plants (Tc). Assignments followed clear, literature-supported criteria emphasizing stable characteristics rather than occasional or anecdotal uses (Heyne 1987). Functional grouping was guided by trait-based frameworks widely used in plant ecology (Violle et al. 2007; Díaz et al. 2016). Species exhibiting ambiguous or inconsistent uses were excluded to maintain clarity and comparability across routes (Kendal et al. 2012).

Cross-validation of ethnobotanical and horticultural uses

Functional categories were cross-validated using regional ethnobotanical references, horticultural databases,

and complementary resources such as Useful Tropical Plants (https://tropical.theferns.info). Distributional and taxonomic checks using POWO (https://powo.science.kew.org) and GBIF (https://www.gbif.org) ensured accuracy and prevented misclassification (Zerega et al. 2005).

Data processing and diversity analysis

Data matrices, species frequency, and functional matrices

Field records were organized into a species × route matrix capturing abundance across all five corridors, complemented by a species × functional-category matrix integrating ecological and ethnobotanical attributes. Species frequency was calculated using (i) the number of routes in which each species occurred and (ii) proportional abundance relative to total individuals, following standard vegetation ecology approaches (Curtis and McIntosh 1951; Kent 2012). These matrices facilitated comparison of compositional patterns and functional representation among routes. All taxa were standardized to accepted nomenclature prior to analysis through verification with POWO and GBIF (Kew 2019).

Diversity indices and stability assessment

Four diversity metrics were computed: Shannon-Wiener, Simpson, Margalef richness, and Pielou's Evenness, each representing complementary aspects of community structure (Shannon and Weaver 1949; Simpson 1949; Margalef 1958; Pielou 1966, 1975; Krebs 1999; Magurran 2004). Indices were calculated using established formulas and cross-validated with statistical software to minimize computational errors. Diversity values were compared among routes to assess how richness, dominance, and abundance distribution varied along environmental gradients (Legendre and Legendre 2012). Integration of multiple indices allowed a general appraisal of community stability, reflecting concepts used in urban vegetation assessment (Jost 2006; McDonnell and Hahs 2008; Pretzsch et al. 2017).

Ethical considerations

All field activities followed non-destructive sampling principles, with no cutting or removal of vegetation. Observations were conducted exclusively in public roadside spaces without entering private property or obstructing traffic. Only naturally fallen materials were handled when needed for identification. No protected species were disturbed, and all procedures adhered to ecological fieldwork guidelines (Sutherland 2006) and best practices in urban ecology (McDonnell and Hahs 2008; Miller et al. 2015).

RESULTS AND DISCUSSION

Overall species composition

Total individuals, species, genera, and families recorded

A total of 53 tree species, representing 47 genera and 26 families, were recorded along the five 10-km roadside corridors in Semarang District. These species collectively accounted for 2,091 individual trees distributed across all routes (Table 2). Of the total 2,091 individuals, Route 4 (Ambarawa-Bawen Street) contained the highest number of trees (635 individuals), followed by Route 1 (Bandungan-Kaloran Street, 539 individuals), Route 3 (Ungaran-Cangkiran Street, 465 individuals), Route 2 (Salatiga-Kedungjati Street, 299 individuals), and Route 5 (Semarang-Bawen Street, 153 individuals). Species richness varied among corridors but consistently reflected the presence of multiple taxa adapted to disturbed, high-traffic urban environments. The overall floristic composition demonstrates a structurally diverse assemblage dominated by widely planted ornamentals, shade-providing species, and a smaller subset of multipurpose trees. The species-family structure presented in Table 1 highlights the predominance of families commonly associated with urban greening initiatives in tropical Asia. The spatial distribution of these species followed the geographical layout of the five survey routes illustrated in Figure 1.

Contribution of native vs introduced species

Based on distributional verification using POWO, GBIF, and regional floras, roadside corridors in Semarang District were dominated by introduced species, which accounted for 32 species, exceeding the number of native species (21 species) recorded in the dataset (Table 1). Native species comprised a smaller proportion and were often represented by residual or conserved individuals, particularly within older urban and peri-urban sections. Several introduced species, including *Swietenia mahagoni* and *Tabebuia rosea*, were numerically prominent within specific corridors, reflecting long-standing urban planting preferences in Indonesian metropolitan landscapes rather than uniform distribution across all routes. In contrast, native species-although fewer in number-were frequently represented by large, mature individuals such as *Ficus benjamina* and *Pterocarpus indicus*, suggesting historical planting records and long-term persistence within the urban matrix. The disproportionate representation of introduced taxa (approximately 60% of total recorded species) indicates strong human-mediated selection as a key driver shaping the taxonomic structure of street-tree communities across Semarang District.

Dominant families in Semarang roadside corridors

Analysis of taxonomic composition (Table 1) indicates that a limited number of plant families dominate roadside tree assemblages across the five surveyed corridors in Semarang District. Fabaceae contributed the highest number of species (9 species), reflecting its wide ecological tolerance, frequent use in urban roadside planting, and representation by both shade-providing and ornamental trees. This family's prominence is consistent with its well-documented adaptability to highlight, compacted-soil, and disturbance-prone urban environments.

Table 1. Roadside tree species in the urban area of Semarang District, Indonesia and their benefits

Scientific name	Family	Origin	Functional groups							
			TP	MP	EP	PP	PR	OP	Fr	Tc
Albizia julibrissin	Fabaceae	I	✓	-	-	-	-	✓	-	-
Alstonia scholaris	Apocynaceae	N	-	✓	-	-	-	✓	-	-
Anacardium occidentale	Anacardiaceae	I	-	-	✓	-	-	-	✓	-
Artocarpus communis	Moraceae	N	-	-	✓	-	-	-	✓	-
Artocarpus heterophyllus	Moraceae	N	-	-	✓	-	-	-	✓	-
Averrhoa carambola	Oxalidaceae	N	-	-	✓	-	-	-	✓	-
Carica papaya	Caricaceae	I	-	-	✓	-	-	-	✓	-
Casuarina equisetifolia	Casuarinaceae	I	✓	-	-	-	-	✓	-	-
Cerbera manghas	Apocynaceae	N	-	-	-	-	-	✓	-	✓
Chrysophyllum cainito	Sapotaceae	I	-	-	✓	-	-	✓	✓	-
Citrus maxima	Rutaceae	I	-	-	✓	-	-	-	✓	-
Cocos nucifera	Arecaceae	N	-	-	✓	-	-	-	✓	-
Cordyline australis	Asparagaceae	I	-	-	-	-	-	✓	-	-
Dalbergia latifolia	Fabaceae	N	✓	-	-	-	-	-	-	-
Delonix regia	Fabaceae	I	-	-	-	✓	-	✓	-	-
Diospyros blancoi	Ebenaceae	I	-	-	✓	-	-	✓	✓	-
Durio zibethinus	Malvaceae	N	-	-	✓	-	-	-	✓	-
Elaeis guineensis	Arecaceae	I	-	-	✓	-	-	-	-	-
Erythrina crista-galli	Fabaceae	I	-	-	-	-	-	✓	-	-
Erythrina variegata	Fabaceae	I	-	-	-	-	-	✓	-	-
Ficus benjamina	Moraceae	N	-	✓	-	-	✓	✓	✓	✓
Filicium decipiens	Sapindaceae	I	-	-	-	-	-	✓	-	-
Gnetum gnemon	Gnetaceae	N	-	-	✓	-	-	-	-	-
Gossypium hirsutum	Malvaceae	I	-	-	-	-	-	✓	-	-
Lagerstroemia speciosa	Lythraceae	I	-	-	-	-	-	✓	-	-
Lansium domesticum	Meliaceae	N	-	-	✓	-	-	-	✓	-
Leucaena leucocephala	Fabaceae	I	-	-	✓	-	-	-	-	-
Malus domestica	Rosaceae	N	-	-	✓	-	-	-	✓	-
Mangifera indica	Anacardiaceae	N	✓	-	✓	-	-	✓	✓	-
Manilkara zapota	Sapotaceae	N	-	-	✓	-	-	-	✓	-
Mimusops elengi	Sapotaceae	N	-	-	-	-	✓	✓	-	-
Morinda citrifolia	Rubiaceae	N	-	-	✓	-	-	-	-	-
Moringa oleifera	Moringaceae	N	-	-	✓	-	-	-	-	-
Muntingia calabura	Muntingiaceae	I	-	-	-	-	-	-	✓	-
Nephelium lappaceum	Sapindaceae	N	-	-	✓	-	-	-	✓	-
Pinus merkusii	Pinaceae	I	✓	-	-	-	-	✓	-	-
Pithecellobium dulce	Fabaceae	I	-	-	✓	-	-	-	✓	-
Plumeria rubra	Apocynaceae	I	-	-	-	-	-	✓	-	✓
Plumeria acuminata	Apocynaceae	I	-	-	-	-	-	✓	-	✓
Polyalthia longifolia	Annonaceae	I	-	-	-	-	✓	✓	-	-
Pometia pinnata	Sapindaceae	N	-	-	✓	-	-	-	✓	-
Pouteria campechiana	Sapotaceae	I	-	-	✓	-	-	-	✓	-
Psidium guajava	Myrtaceae	N	-	-	✓	-	-	-	✓	-
Pterocarpus indicus	Fabaceae	I	✓	✓	-	-	-	✓	✓	-
Roystonea regia	Arecaceae	I	-	-	-	-	-	✓	-	-
Swietenia mahagoni	Meliaceae	I	✓	-	-	✓	-	✓	-	-
Syzygium myrtifolium	Myrtaceae	I	-	-	-	-	-	✓	-	-
Syzygium polyanthum	Myrtaceae	N	-	-	✓	-	-	-	-	-
Tabebuia rosea	Bignoniaceae	I	-	-	-	-	-	✓	-	-
Tabebuia roseo-alba	Bignoniaceae	I	-	-	-	-	-	✓	-	-
Tamarindus indica	Fabaceae	I	-	-	✓	-	-	-	-	-
Terminalia catappa	Combretaceae	I	-	-	-	-	-	✓	-	-
Terminalia mantaly	Combretaceae	I	-	-	-	-	-	✓	-	-
Total: 53 species	**26 families**	**N:21; I: 32**	**7**	**3**	**26**	**2**	**3**	**28**	**22**	**4**

Note: Origin Status: Native tree (N), Introduced (I) based on: POWO, CABI, GBIF. Functional categories: TP: Timber; MP: Medicinal; EP: Edible; PP: Pollen Producing; PR: Pollen Reducing; OP: Ornamental Plant; Fr: Frugivory-supporting; Tc: Toxic

Apocynaceae and Sapotaceae followed as the next most represented families, each comprising four species. Members of these families are commonly selected for roadside environments due to their structural resilience, relatively stable growth forms, and tolerance to urban stressors such as heat, limited rooting space, and air pollution. The repeated occurrence of these three families across multiple corridors suggests a degree of consistency in municipal planting preferences and long-term greening practices at the district scale. In contrast, families with lower species representation-such as Anacardiaceae, Arecaceae, and Myrtaceae-were more unevenly distributed among routes and often restricted to specific corridors. This localized occurrence likely reflects differences in planting history, land-use context, or micro-environmental conditions along individual road segments, rather than uniform district-wide planting strategies.

Spatial distribution of roadside trees across routes

Distribution of individuals along the five 10-km routes

The abundance of roadside trees varied substantially among the five 10-km survey routes (Table 2). In total, 2,091 individuals were recorded across all routes. Ambarawa-Bawen Street recorded the highest abundance (635 trees), followed by Bandungan-Kaloran Street (539 trees), indicating relatively continuous roadside vegetation along these corridors. Ungaran-Cangkiran Street showed moderate abundance (465 individuals), albeit with fragmented distribution in certain sections, while Salatiga-Kedungjati Street represented a corridor with lower tree density (299 individuals). The fewest trees were recorded along Semarang-Bawen Street (153 individuals), consistent with its highly urbanized character and limited planting space.

Identification of routes with the highest and lowest abundance

Based on the total counts, Route 4 (Ambarawa-Bawen Street) was the most abundant corridor, while Route 5 (Semarang-Bawen Street) contained the lowest number of trees (Table 2). These contrasts highlight the divergent structural conditions across the district's roadside environments, where some corridors maintain extensive vegetative cover, while limited planting space, intensive built-up zones, or discontinuous canopy structure characterize others.

Species occurring only as singletons or rare occurrences

Several species appeared as singletons, being recorded only once across the entire dataset (Table 2). In total, six species were represented by a single individual: *Artocarpus communis*, *Gnetum gnemon*, *Lansium domesticum*, *Leucaena leucocephala*, *Manilkara zapota*, and *Pometia pinnata*. Although limited in abundance, these rare occurrences contribute to route-level differences in species richness and reflect localized planting decisions or isolated retention of individual trees rather than widespread planting patterns. The presence of these singleton species, while numerically minor, is ecologically noteworthy as it increases overall floristic heterogeneity within Semarang District's urban roadside vegetation.

Functional categories of roadside trees

Proportion and number of species in each functional group

Roadside tree assemblages in Semarang District exhibited a diverse distribution of functional categories (Table 1). Edible plants (26 species), frugivory-supporting species (22 species), and ornamental plants (28 species) dominated the composition, reflecting a landscape shaped by both legacy fruit trees from agro-urban mosaics and intentional ornamental planting by local authorities. Timber plants formed a smaller group (7 species), while medicinal plants were limited (3 species), i.e. *Alstonia scholaris, F. benjamina,* and *P. indicus*. Pollen-related categories showed minimal representation, with only 2 Pollen Producing (PP) species (i.e. *Dalbergia latifolia, S. mahagoni*) and 3 Pollen Reducing (PR) species (i.e. *F. benjamina, Mimusops elengi, Polyalthia longifolia*), indicating a generally low contribution to airborne pollen loads along the corridors. Toxic species were also few (4 species), i.e. *Cerbera manghas, F. benjamina, Plumeria rubra,* and *Plumeria acuminata.* The distribution pattern is illustrated in Figure 2, which shows the clear numerical dominance of EP, Fr, and OP, whereas TP, MP, PP, PR, and Tc collectively represent a much smaller fraction of the roadside flora.

Functional overlap and multifunctional species

Several species occupied more than one functional category (Table 1), highlighting the multifunctionality of many tree taxa in the district. Species such as *Mangifera indica*, *Artocarpus* spp., and *P. pinnata* contributed simultaneously to the edible and frugivory-supporting groups, while *P. indicus* combined timber value with ecological functions related to shade provision and wildlife support. *Ficus benjamina* was among the most multifunctional species, appearing in medicinal, PR, OP, Fr, and Tc categories.

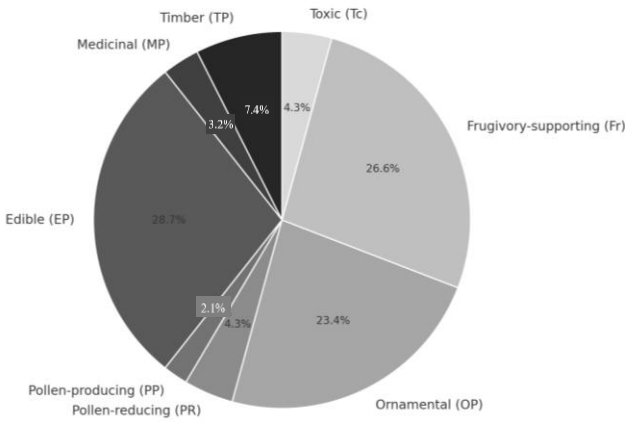

Figure 2. Functional categories of roadside tree species in the urban area of Semarang District, Indonesia. Note: TP: Timber Plant; MP: Medicinal Plant; EP: Edible Plant; PP: Pollen Producing Plant; PR: Pollen-Reducing Plant; OP: Ornamental Plant; Fr: Frugivory-supporting plant; Tc: Toxic plant (after Thothathri et al. 1985)

Table 2. Species frequency counts by point in Semarang District, Indonesia

Scientific name	Family	Route				
		1	2	3	4	5
Albizia julibrissin	Fabaceae	0	0	0	0	2
Alstonia scholaris	Apocynaceae	4	0	2	0	0
Anacardium occidentale	Anacardiaceae	0	4	2	0	0
Artocarpus communis	Moraceae	0	0	0	1	0
Artocarpus heterophyllus	Moraceae	9	7	52	9	0
Averrhoa carambola	Oxalidaceae	5	1	7	1	0
Carica papaya	Caricaceae	9	9	6	0	0
Casuarina equisetifolia	Casuarinaceae	19	2	0	5	0
Cerbera manghas	Apocynaceae	4	0	0	0	0
Chrysophyllum cainito	Sapotaceae	7	0	0	0	0
Citrus maxima	Rutaceae	0	0	6	0	0
Cocos nucifera	Arecaceae	13	10	29	3	0
Cordyline australis	Asparagaceae	7	1	0	0	0
Dalbergia latifolia	Fabaceae	0	0	0	71	1
Delonix regia	Fabaceae	0	0	0	19	0
Diospyros blancoi	Ebenaceae	0	8	0	0	0
Durio zibethinus	Malvaceae	1	16	18	0	0
Elaeis guineensis	Arecaceae	0	1	0	0	3
Erythrina crista-galli	Fabaceae	53	0	0	0	0
Erythrina variegata	Fabaceae	0	0	0	0	5
Ficus benjamina	Moraceae	8	0	2	5	0
Filicium decipiens	Sapindaceae	3	2	0	9	0
Gnetum gnemon	Gnetaceae	0	0	0	1	0
Gossypium hirsutum	Malvaceae	0	0	2	0	0
Lagerstroemia speciosa	Lythraceae	1	0	0	15	28
Lansium domesticum	Meliaceae	1	0	0	0	0
Leucaena leucocephala	Fabaceae	0	0	1	0	0
Malus domestica	Rosaceae	4	0	0	0	0
Mangifera indica	Anacardiaceae	110	86	41	43	7
Manilkara zapota	Sapotaceae	1	0	0	0	0
Mimusops elengi	Sapotaceae	0	0	0	0	4
Morinda citrifolia	Rubiaceae	2	0	0	0	0
Moringa oleifera	Moringaceae	2	0	0	0	0
Muntingia calabura	Muntingiaceae	38	38	9	11	4
Nephelium lappaceum	Sapindaceae	1	0	0	1	5
Pinus merkusii	Pinaceae	0	0	13	1	0
Pithecellobium dulce	Fabaceae	0	0	0	0	20
Plumeria rubra	Apocynaceae	5	0	1	1	20
Plumeria acuminata	Apocynaceae	6	6	8	1	0
Polyalthia longifolia	Annonaceae	53	47	0	67	0
Pometia pinnata	Sapindaceae	1	0	0	0	0
Pouteria campechiana	Sapotaceae	0	0	0	0	28
Psidium guajava	Myrtaceae	1	4	14	56	0
Pterocarpus indicus	Fabaceae	16	0	9	0	0
Roystonea regia	Arecaceae	87	0	0	0	0
Swietenia mahagoni	Meliaceae	13	4	229	222	0
Syzygium myrtifolium	Myrtaceae	20	11	14	0	0
Syzygium polyanthum	Myrtaceae	0	0	0	17	0
Tabebuia rosea	Bignoniaceae	4	5	0	49	0
Tabebuia roseo-alba	Bignoniaceae	0	0	0	0	21
Tamarindus indica	Fabaceae	2	2	0	0	0
Terminalia catappa	Combretaceae	28	35	0	3	0
Terminalia mantaly	Combretaceae	1	0	0	24	5
Total: 2,091 individuals		539	299	465	635	153

Notes: Route 1: Bandungan-Kaloran Street; Route 2: Salatiga-Kedungjati Street; Route 3: Ungaran-Cangkiran Street; Route 4: Ambarawa-Bawen Street; Route 5: Semarang-Bawen Street

This functional overlap enhances ecological resilience by supporting multiple ecosystem services-shade, food provisioning, pollination benefits, and cultural value-within a relatively limited number of planted species. Such multifunctionality strengthens the structural and functional complexity of roadside vegetation along the five surveyed routes.

Interpretation of dominant functional roles in the urban landscape

The functional profile shown in Figure 2 suggests that a combination of aesthetic, microclimatic, and agro-ecological considerations shapes roadside tree composition in Semarang District. Ornamental species remain important for aesthetic continuity and urban image, while fruit-bearing and frugivory-supporting species contribute substantially to urban wildlife resources and reflect long-standing planting traditions. Timber species, though less numerous, play essential structural roles in providing shade and canopy cover. Conversely, the relatively small representation of EP-only utilitarian plants, medicinal taxa, pollen-related groups, and toxic species indicates a shift toward multifunctional and ecologically favored species rather than culturally utilitarian or specialized taxa.

The dominance of edible, frugivory-supporting, and ornamental groups underscores the hybrid character of Semarang's roadside vegetation, balancing ecological benefits with cultural and aesthetic functions.

Species abundance and dominant taxa

Top five most abundant species per route

Species abundance varied markedly across the five surveyed corridors (Table 2). On Bandungan-Kaloran Street, the leading species were *S. mahagoni*, *P. longifolia*, *T. rosea*, and *P. indicus*, together comprising a substantial portion of the total individuals on this route. Salatiga-Kedungjati Street showed a different abundance profile, with *S. mahagoni* remaining dominant, accompanied by *M. indica*, and several ornamental taxa with moderate representation. Along Ungaran-Cangkiran Street, overall abundance was lower, but *S. mahagoni* and *P. longifolia* again emerged as the most frequently recorded species. Ambarawa-Bawen Street and Semarang-Bawen Street displayed similar trends, each characterized by a small set of high-abundance ornamentals and shade species dominating the community structure.

City-wide dominant species

Across the entire Semarang District dataset, several tree species emerged as both numerically abundant and spatially widespread across multiple corridors (Table 2). *Ficus benjamina* was the most widely distributed species, occurring across all five surveyed routes, indicating strong tolerance to varied roadside conditions in both urban and peri-urban environments. *Mangifera indica* and *P. indicus* were each recorded in four routes, reflecting their multifunctional roles as shade-providing, fruit-bearing, and structurally resilient trees commonly retained along major roads. In contrast, *S. mahagoni*, although highly abundant within certain corridors, was present in only three routes, demonstrating that numerical dominance does not necessarily correspond to the widest spatial distribution at

the district scale. *P. longifolia* was frequently encountered along densely built-up segments, consistent with its widespread use as an avenue tree characterized by a narrow, vertical crown structure. Collectively, these species form the structural backbone of roadside vegetation in Semarang District, contributing substantially to overall canopy cover and shaping the abundance patterns of the surveyed urban tree assemblages.

Species with intermediate and low abundance classes

A substantial number of species occurred at intermediate abundance, typically represented by 5-20 individuals per route (Table 2). These included widely planted but not overwhelmingly dominant ornamentals such as *T. rosea*, *D. regia*, and *P. indicus*. Species with low abundance-represented by fewer than five individuals-were numerous and contributed to route-level richness without strongly influencing overall dominance patterns. Several of these, such as *L. domesticum*, *M. zapota*, and *G. gnemon*, were restricted to single or isolated occurrences. Although limited in numbers, these low-abundance species enhanced the spatial heterogeneity and complemented the rich ornamental matrix observed across the road corridors.

Route-specific community profiles

Bandungan-Kaloran Street (Route 1)

Route 1 exhibited the highest species richness and total abundance among all surveyed corridors, forming the most structurally stable assemblage in Semarang District (Table 2). The roadside vegetation along this corridor was dominated by *S. mahagoni*, followed by *P. longifolia*, *T. rosea*, and *P. indicus*, which together produced a relatively dense and continuous canopy along much of the route. The dominance of these taxa reflects a combination of long-established planting practices and favorable planting space typical of peri-urban environments. In addition to dominant species, several taxa occurred only as singletons, including *L. domesticum*, *M. zapota*, and *G. gnemon*, indicating localized planting decisions or isolated retention of individual trees rather than systematic planting. Although numerically infrequent, these rare occurrences contributed to the overall species richness of Route 1 and reinforced its status as the most diverse corridor in the district. The coexistence of dominant and rare species suggests that Route 1 benefits from wider roadside verges, lower disturbance intensity, and more heterogeneous microhabitats, resulting in a comparatively balanced and ecologically robust community structure.

Salatiga-Kedungjati Street (Route 2)

Route 2 exhibited moderate species richness and total abundance, forming a structurally mixed assemblage dominated by *S. mahagoni* (Table 2). Other relatively frequent taxa included *M. indica* and *P. longifolia*, creating a corridor characterized by a combination of shade-providing and ornamental species commonly selected for inter-urban roadside planting. This composition reflects regular planting interventions along transport routes where visual uniformity and canopy function are prioritized. Several additional species occurred at low frequencies, typically represented by one to three individuals, indicating localized planting decisions or residual trees retained from earlier land-use phases rather than systematic planting schemes. Although these low-abundance taxa contributed minimally to overall tree density, their presence increased compositional heterogeneity along the corridor. Overall, Route 2 represents a moderately diverse and moderately stable assemblage shaped by mixed land-use influence and intermediate levels of disturbance.

Ungaran-Cangkiran Street (Route 3)

Route 3 (Ungaran-Cangkiran Street) displayed the strongest dominance pattern, with *S. mahagoni* overwhelmingly shaping the structure of the corridor. This created a heavily skewed community composition where a single taxon accounted for a disproportionate share of total individuals. The prevalence of *Swietenia* along this route likely reflects limited planting space, high levels of disturbance, and the common municipal practice of selecting vertically oriented species for narrow roadside verges. Low-frequency taxa occurred sporadically, with several species recorded only once or twice, indicating limited species turnover and reduced canopy heterogeneity (Table 2). Although these rare species marginally increased richness, their presence did not significantly alter the overall dominance-driven structure. The resulting assemblage is considered the least stable among all routes due to low diversity, strong dominance, and fragmented canopy cover.

Ambarawa-Bawen Street (Route 4)

Route 4 displayed a moderately dense and moderately rich assemblage dominated by *S. mahagoni*, *P. longifolia*, and *D. regia*, which together formed the bulk of roadside vegetation along the corridor (Table 2). The coexistence of ornamentals and large shade trees produced a mixed but not highly diverse structure, indicative of standardized planting strategies typical of regional highways. In contrast to Route 3, this corridor retained a more balanced distribution of secondary species, contributing to a more evenly distributed canopy. Several taxa were recorded almost exclusively along this route, including isolated individuals not observed in other corridors, suggesting distinct planting histories or localized microhabitats that favor certain species. Such route-specific taxa highlight the varying management approaches employed across districts and contribute to the intermediate stability observed in Route 4.

Semarang-Bawen Street (Route 5)

Route 5 presented a species composition broadly comparable to that of Routes 2 and 4, with *S. mahagoni* emerging as the dominant species along the corridor (Table 2). Secondary dominant taxa included *M. indica*, reflecting the widespread selection of multifunctional and aesthetically preferred trees in urban and peri-urban roadside environments. The total tree abundance on this route was lower than that recorded in less urbanized corridors, consistent with higher levels of built-up land cover, increased traffic intensity, and reduced planting

space in more densely urbanized segments. These conditions resulted in a comparatively homogenized community structure, a lower number of rare species, and reduced canopy continuity. The abundance patterns observed along Route 5 indicate that urbanization intensity acts as a key driver shaping roadside tree community structure, limiting opportunities for diversified planting and constraining ecological heterogeneity.

Biodiversity indices across routes

Species richness (Margalef Index) comparison

Species richness, as reflected by the Margalef Index, varied markedly among the five surveyed routes (Table 3). Bandungan-Kaloran Street (Route 1) recorded the highest richness value, consistent with its large number of species and relatively high individual counts, indicating a more heterogeneous community structure than the other corridors. Intermediate richness values were observed on Salatiga-Kedungjati Street (Route 2) and Ambarawa-Bawen Street (Route 4), both of which maintained a moderate species pool supported by mixed land-use patterns. In contrast, Ungaran-Cangkiran Street (Route 3) had the lowest richness level, reflecting both the limited number of species and the markedly low abundance recorded along the corridor. These patterns mirror the spatial distribution of individuals across routes and highlight the influence of planting space, disturbance intensity, and land-use type on species richness in urban roadside environments.

Shannon-Wiener diversity patterns

Shannon-Wiener Index values (H′) indicated moderate to high diversity across most routes, with Route 1 showing the highest H′-a pattern consistent with its rich species pool and balanced abundance distribution (Table 3). Routes 2, 4, and 5 shared similar H′ ranges, reflecting structurally mixed but not heavily dominated communities typical of suburban-urban transition zones. The lowest H′ value occurred on Route 3, driven primarily by the strong dominance of *S. mahagoni* and the scarcity of secondary species, which reduced overall species balance. The contrast between the routes underscores how dominance, species evenness, and total richness interact to shape the composite diversity of roadside trees in Semarang District.

Evenness distribution across routes

Evenness (E) values further revealed inter-route variation in species balance (Table 3). Semarang-Bawen Street (Route 5) exhibited the highest evenness score, indicating a more equitable distribution of individuals among constituent species, despite having fewer total individuals compared to Route 1. Moderate evenness values on Routes 1, 2, and 4 point to mixed dominance structures, where several species contribute substantially to total abundance. In contrast, Route 3 showed the lowest evenness, congruent with its strong skew toward *S. mahagoni*. Across the district, evenness generally reflected the interaction between planting uniformity and disturbance levels, with more urbanized routes tending toward slightly homogenized species distributions.

Simpson Diversity Index and dominance levels

Simpson Index values (1-D) were relatively high on most routes, indicating low to moderate dominance and generally stable multi-species assemblages (Table 3). Route 1 again recorded the highest Simpson (1-D) value, aligning with its diverse and relatively evenly distributed community. Simpson values on Routes 2, 4, and 5 remained within comparable ranges, signifying moderate dominance pressure and the presence of multiple co-dominant taxa. Route 3 showed the lowest Simpson value, reflecting its highly skewed structure dominated by a single species and limited contribution from rare taxa. Overall, Simpson patterns reinforce the conclusion that dominance-driven corridors exhibit reduced ecological balance and are more vulnerable to disturbance.

Identification of the most stable vs the least stable communities

Integration of Margalef, Shannon, Simpson, and Evenness indices collectively indicates that Bandungan-Kaloran Street (Route 1) represents the most stable tree assemblage within Semarang District, characterized by high richness, high diversity, and a relatively balanced distribution of individuals. On the opposite end, Ungaran-Cangkiran Street (Route 3) emerged as the least stable corridor due to its low richness, low evenness, and strong species dominance. The remaining routes showed intermediate levels of stability, shaped by mixed dominance structures, moderate species pools, and varying disturbance conditions. Together, these multi-index comparisons illustrate how roadside vegetation stability in Semarang is shaped by the interaction of species diversity, structural balance, planting history, and urbanization pressure.

Table 3. Species diversity indices at five roadside routes in Semarang District, Central Java, Indonesia

Route	Region	Margalef (G)	Shannon-Wiener (H')	Evenness (E)	Simpson (1-D)*
1	Bandungan-Kaloran Street	5.404	2.725	0.766	0.899
2	Salatiga-Kedungjati Street	3.508	2.322	0.763	0.854
3	Ungaran-Cangkiran Street	3.093	1.936	0.646	0.728
4	Ambarawa-Bawen Street	3.564	2.247	0.707	0.831
5	Semarang-Bawen Street	2.584	2.260	0.856	0.873

Note: Diversity indices were calculated as follows: Margalef's Richness Index (G) = (S − 1)/ln(N); Shannon-Wiener Index (H'); Evenness (E) = H'/ln(S); and Simpson's Diversity Index $^{1-D=1-\sum p_i^2}$, where p = n_i/N

Summary of key ecological findings

Integration of species counts, abundance, and indices

Synthesis of the dataset (Table 1) shows that Semarang District's roadside corridors support 53 species, 47 genera, and 26 families, forming a taxonomically diverse yet unevenly distributed assemblage. A total of 2,091 individual trees were documented across all five corridors. Abundance patterns reveal clear contrasts among routes, with Ambarawa-Bawen Street (Route 4) recording the highest number of individuals (635), while Semarang-Bawen Street (Route 5) hosts the lowest (153). Diversity indices further demonstrate substantial route-level variation: Route 1 exhibits consistently high Margalef, Shannon, and Simpson values, indicating greater richness and structural balance, whereas Route 3 shows the lowest diversity and evenness, reflecting strong dominance and reduced community stability. Together, these metrics illustrate a mosaic-like distribution of roadside tree communities shaped by corridor-level differences in planting history, urbanization intensity, and local environmental conditions.

Emergent patterns of urban tree diversity

Urban roadside vegetation in Semarang is characterized by a strong dominance of widely planted ornamentals and timber species, as evidenced by their high abundance and frequent occurrence across routes (Tables 1 and 2). Functional diversity is skewed toward a few major groups, with ornamental plants forming the largest component, followed by shade-providing timber species and frugivory-supporting taxa. Introduced species constitute a substantial portion of the flora, while native species remain present but comparatively limited. Species richness and community balance are highest in less urbanized corridors, while built-up routes show reduced richness and stronger dominance patterns.

Ecological implications of current roadside vegetation structure

The observed patterns indicate that Semarang's roadside tree communities provide structural diversity but are functionally concentrated in a few dominant roles. High dominance by species such as *S. mahagoni* and *P. longifolia* contributes to consistent canopy structure but may reduce resilience to pests, diseases, or climatic extremes. Conversely, the presence of multiple rare and low-abundance species enhances route-level richness and contributes to spatial heterogeneity. Overall, current roadside vegetation reflects a blend of ecological function, aesthetic preference, and urban planting practice, forming a community structure that supports moderate biodiversity while revealing opportunities for greater functional diversification in future urban greening strategies.

Discussion

Urban roadside tree diversity in the context of tropical cities

The diversity patterns observed across the roadside corridors of Semarang District highlight the ecological complexity of vegetation in rapidly expanding tropical cities. The combination of moderate-high Shannon diversity, substantial species richness, and marked route-specific variability indicates that the interaction of ecological filtering and long-term management decisions drives community assembly. In tropical metropolitan regions, roadside vegetation commonly functions as a semi-managed mosaic where environmental stress and human intervention jointly shape species composition (Luck and Smallbone 2010; Cariñanos and Casares-Porcel 2011). Similar to findings from Jakarta, Manila, Kuala Lumpur, and Bangkok, Semarang's corridors support heterogeneous mixtures of native and introduced taxa, with diversity declining predictably in locations characterized by stronger heat-island effects, narrower planting strips, and higher disturbance intensities (Lourdes et al. 2021; Maruthaveeran et al. 2011; Sholihah et al. 2022).

Short-distance compositional turnover-a hallmark of tropical roadside systems-reflects the interplay between heterogeneous planting histories and disturbance-driven selection (Roman et al. 2016; Sjöman et al. 2016). The variation recorded across Semarang's five routes aligns with broader urban ecological theory, which posits that fine-scale environmental gradients in built-up density, shading, and soil compaction create distinct ecological niches along linear corridors. These gradients, documented in Guangzhou (Jim and Liu 2001) and Colombo (Wells et al. 2017), promote localized filtering and generate route-specific vegetation signatures. Under the limited availability of larger green spaces, such linear elements often act as ecological "refuge corridors," retaining species otherwise excluded from more heavily sealed urban matrices (Aronson et al. 2017).

Several interacting mechanisms explain the richness and heterogeneity observed in Semarang. Elevated temperatures and extensive impervious surfaces act as strong abiotic filters, selecting for taxa with high heat and drought tolerance and shifting community assembly toward resilient ornamentals such as *S. mahagoni*, *D. regia*, and *P. longifolia* (Oke et al. 2017; Zandler and Samimi 2024; Hwang et al. 2025). Restricted rooting spaces along arterial roads impose below-ground constraints that suppress growth of sensitive taxa, reinforcing dominance by species with efficient water-use strategies and compact root systems (Pretzsch et al. 2017; Sun et al. 2024). Additionally, chronic disturbances-including pruning, pollution, and mechanical damage-reduce survival of species lacking structural or physiological adaptations, producing the low richness and depressed evenness commonly observed along highly urbanized segments (Sarwadi et al. 2019; Siqueira et al. 2022; Pratiwi et al. 2025).

Patterns from other Southeast Asian cities corroborate these mechanisms. Bangkok's dominance by fast-growing ornamentals (Soonsawad 2013), Manila's dependence on introduced shade species (Moriwake et al. 2020), and Singapore's persistence of non-native ornamentals even under high management standards (Hwang et al. 2025) all point to convergent ecological outcomes: environmental filtering under urban stress narrows the functional pool, while historical planting decisions maintain certain taxa

over decades. Semarang's moderate richness, substantial representation of introduced species, and recurrent dominance of heat- and disturbance-tolerant taxa therefore reflect regionally consistent assembly rules across tropical Asia.

Despite these constraints, the presence of 53 species from 26 families demonstrates that roadside vegetation-when effectively maintained-can sustain ecologically meaningful diversity. The variation observed across corridors suggests that linear green spaces can serve not only as visual and climatic buffers but also as functional ecological components, provided species selection and management practices align with the environmental realities of tropical urban landscapes.

Patterns of taxonomic structure and dominant species

The strong dominance of *S. mahagoni*, *P. longifolia*, and *M. indica* across Semarang's roadside corridors reflects the convergence of ecological tolerance, functional traits, and long-standing municipal planting regimes that shape tree-community assembly in tropical cities. Under urban ecological filtering, species capable of maintaining physiological performance under heat stress, soil compaction, and pollution tend to monopolize available niches, thereby reducing the effective species pool (Sjöman et al. 2016; Sun et al. 2024; Zandler and Samimi 2024). *Swietenia mahagoni*, for instance, possesses deep-rooted architecture, drought-tolerant foliage, and high structural uniformity-traits that enhance survival in thermally extreme corridors. Its recurrent dominance in Manila, Colombo, and Yangon (Esperon-Rodriguez et al. 2025; Wells et al. 2017) indicates that this species often occupies a "core functional niche" in tropical urban forests, where environmental constraints narrow community composition toward a few physiologically robust taxa.

Polyalthia longifolia dominates for complementary mechanistic reasons. Its columnar crown and narrow lateral spread represent a classic "urban-tolerant architecture" optimized for limited rooting volumes, heavy pedestrian traffic, and overhead cables-conditions that frequently eliminate species with broader, structurally complex canopies (Maruthaveeran et al. 2011; Soonsawad 2013). This architectural predictability, combined with moderate pollution tolerance and rapid early growth (Hwang et al. 2025), creates a competitive advantage in spatially constrained corridors. Comparable dominance in Guangzhou, Bangkok, and Dhaka (Jim and Liu 2001; Kjelgren et al. 2011; Uddin et al. 2021) suggests that *P. longifolia* is repeatedly selected through both environmental filtering and institutional preference.

The persistence of *M. indica* follows a different mechanism: legacy effects. Many large individuals are retained through road-widening cycles due to their cultural familiarity, shade value, and established root systems (Sarwadi et al. 2019; Pratiwi et al. 2025). In urban ecological theory, such legacy trees serve as "structural anchors," exerting disproportionate influence on canopy stratification and microclimate while shaping successional trajectories by limiting available space for replacement species. Their drought tolerance and broad crowns reinforce their ecological persistence-even when newly planted cohorts shift toward ornamentals.

Dominance by a narrow suite of species is a well-documented feature of tropical urban vegetation (Cariñanos and Casares-Porcel 2011; Aronson et al. 2017). Ecologically, such dominance emerges from two overlapping processes: (i) Abiotic filtering, where heat, compaction, and pollution reduce niche breadth; and (ii) Planting inertia, where municipalities repeatedly select "safe" species with predictable performance (Luck and Smallbone 2010; Pretzsch et al. 2017).

While dominant taxa stabilize canopy cover and offer reliable ecosystem services in the short term, they simultaneously reduce functional redundancy. This creates vulnerability to pests, physiological decline, or climate-driven stress, as evidenced by pest-induced canopy loss in Singapore and Guangzhou (Jim and Liu 2001) and the decline of dominant ornamentals in Jakarta and Surabaya (Nidah and Mukhlison 2013). When a community's functional capacity is concentrated in a few taxa, stochastic shocks can trigger system-level instability, accelerating canopy degradation and reducing urban resilience (Roman et al. 2016; Siqueira et al. 2022).

In Semarang, the strong dominance of *S. mahagoni*, *P. longifolia*, and *M. indica* therefore represents a structurally efficient but ecologically vulnerable community architecture. Although these species currently support essential canopy functions, the long-term resilience of the roadside vegetation system will depend on diversifying species pools, increasing functional redundancy, and reducing the ecological risks inherent in dominance-led community structures-recommendations increasingly emphasized in contemporary tropical urban forestry research (Luck and Smallbone 2010; Sjöman et al. 2016; Hwang et al. 2025).

Functional composition and ecosystem services of roadside trees

The functional composition of Semarang's roadside vegetation reflects a community structured by both environmental filters and the functional priorities of urban management. The dominance of Ornamental Plant (OP), Edible Plant (EP), and Frugivory-supporting (Fr) species (Table 1; Figure 2) indicates that functional assembly is not random but driven by a combination of physiological tolerance, service provisioning, and historical planting regimes. In tropical cities, environmental harshness and design constraints tend to favor species with high thermal plasticity, stable architectural forms, and predictable maintenance requirements-traits aligning closely with the functional groups most abundant in Semarang (Cariñanos and Casares-Porcel 2011; Sun et al. 2024).

Ornamental species, including *D. regia*, *T. rosea*, and *P. longifolia*, exemplify "urban-tolerant" phenotypes that combine high photosynthetic resilience under elevated temperatures with canopy architectures suited to constrained spatial environments. Their visual appeal is often cited, but ecologically, their dominance arises from a strategic advantage under low-soil-volume, high-radiation, and pollution-heavy conditions (Thaiutsa et al. 2008;

Kjelgren et al. 2011). Through shading and transpiration cooling, these species help modulate microclimates, lowering surface temperatures and mitigating heat-island effects-ecosystem services that become increasingly critical as tropical cities warm (Wells et al. 2017; Zandler and Samimi 2024).

Timber Plants (TP) such as *S. mahagoni* and *P. indicus* represent another functional axis: structural robustness. With dense wood, deep-rooting systems, and large crowns, these species operate as "ecosystem-service anchors," capturing particulate matter, stabilizing soil along roadside banks, and providing a more persistent canopy under hydrological or thermal stress (Pretzsch et al. 2017; Hwang et al. 2025). Their presence enhances carbon storage, but more importantly, contributes to structural heterogeneity-a key determinant of ecological resilience in linear habitats.

The ecological significance of frugivory-supporting species becomes evident when interpreted through a trophic-interaction lens. Species such as *M. indica*, *F. benjamina*, and other fruiting taxa provide continuous or seasonal resources for birds, bats, and small mammals. These interactions help maintain urban food webs, sustain pollinator and seed-disperser presence, and support the connectivity of wildlife across fragmented landscapes (Wells et al. 2017; Lourdes et al. 2021). In tropical urban systems, such frugivory pathways often act as "ecological bridges," preventing the collapse of species interactions under increasing urban stress.

In contrast, the limited representation of Medicinal Plants (MP), Toxic plants (Tc), Pollen Producers (PP), and Pollen Reducers (PR) highlights trade-offs inherent in roadside environments. High-disturbance corridors impose sanitation, safety, and allergenicity constraints that reduce the suitability of utilitarian fruit crops and allergenic species (Jianan et al. 2007; Cariñanos et al. 2016, 2019). Pollen Producers (PP) species are minimized to prevent respiratory-health risks, while PR species remain underutilized due to limited horticultural availability and poor public familiarity (D'Amato et al. 2010). These patterns reveal that functional traits related to human health and public safety act as secondary filters shaping community composition.

Overall, Semarang's functional profile reflects a structure in which a few key functional groups-primarily ornamentals, timber plants, and frugivory-supporting species-provide the majority of regulatory, aesthetic, and ecological services. While effective in delivering microclimate regulation, shading, and habitat support, this configuration also reveals a degree of functional homogenization. The overrepresentation of similar service-provision pathways reduces the redundancy needed to withstand long-term disturbances, echoing global concerns that tropical urban forests dominated by narrow functional spectra may be less adaptable to climatic or pest-driven shocks (Aronson et al. 2017; Pretzsch et al. 2017). Expanding the diversity of functional groups, therefore, remains essential for enhancing ecological performance and stabilizing ecosystem-service delivery across Semarang's roadside corridors.

Spatial heterogeneity across corridors

The five roadside corridors in Semarang District exhibit pronounced spatial heterogeneity in species richness, abundance distribution, and diversity indices, reflecting the combined influence of urbanization intensity, microclimatic variation, and corridor-specific management histories. From a landscape ecology perspective, linear road networks function as environmental gradients where temperature regimes, soil volumes, shading patterns, and disturbance pressures change continuously across space, generating distinct ecological niches even over short distances. These fine-scale gradients help explain why Route 1-characterized by broader planting strips, lower sealed-surface cover, and more favorable microclimates-supports richer and more evenly structured assemblages, a pattern consistent with peri-urban corridors documented in Kuala Lumpur, and Colombo (Maruthaveeran et al. 2011; Wells et al. 2017).

Conversely, Route 3 functions as a high-disturbance ecological filter. Narrow planting zones, restricted rooting volumes, and persistent vehicular stress limit the recruitment and survival of species lacking strong physiological stress tolerance. Under such conditions, environmental filtering promotes the dominance of a few urban-tolerant taxa-typically drought-resistant ornamentals-while reducing the functional and taxonomic diversity of the community (Jim and Liu 2001; Soonsawad 2013; Moriwake et al. 2020). These patterns align with ecological theory predicting that intense and chronic disturbances narrow community composition toward species with traits that minimize hydraulic failure, mechanical instability, and pollutant sensitivity (Rodrigues et al. 2021; Siqueira et al. 2022). As a result, Route 3 exhibits low richness, strong dominance, and depressed evenness, characteristic of structurally homogenized vegetation typical of dense urban fabrics.

The substantial beta diversity across routes indicates that these corridors do not form a continuous ecological unit but instead function as discrete habitat patches embedded in a heterogeneous urban matrix. Differences between the well-vegetated, peri-urban Route 1 and the more urbanized Routes 3 and 5 resemble patterns of functional turnover documented in Singapore and Jakarta, where microclimatic contrasts and localized planting regimes create spatially segregated communities (Sholihah et al. 2022; Hwang et al. 2025). High compositional turnover reinforces the idea that roadside vegetation outcomes depend not merely on species selection but on the interaction between biophysical constraints and the historical layering of management decisions.

Viewed more broadly, Semarang's roadside vegetation mirrors regional ecological trajectories in tropical Asian cities. Route 1 parallels semi-natural greenways with high ecological buffering capacity, whereas Routes 3 and 5 resemble engineered corridors shaped by structural confinement, elevated heat loads, and disturbance-dominated environmental filters (Roloff et al. 2009; Kjelgren et al. 2011). This spatial heterogeneity underscores the necessity of differentiated greening strategies: peri-urban corridors should be prioritized as

biodiversity reservoirs and ecological connectors, while inner-urban corridors require interventions that expand soil volume, enhance species heterogeneity, and mitigate microclimatic extremes.

Biodiversity indices and ecological stability

Interpretation of the Shannon, Simpson, Margalef, and Evenness indices across the five Semarang corridors reveals not only differences in richness and dominance but also the underlying stability regimes governing these urban vegetation systems. From an ecological-theory perspective, these four indices collectively represent complementary dimensions of community organization: Margalef captures species pool size; Shannon integrates richness and entropy; Simpson emphasizes dominance resistance; and evenness reflects the distributional balance that allows communities to buffer stochastic disturbance. Their combined patterns show that Semarang's roadside assemblages operate along a gradient from structurally resilient to dominance-driven and disturbance-sensitive configurations.

Route 1 exemplifies a high-stability community where richness, moderate dominance, and strong evenness interact to produce a functionally redundant assemblage-an attribute repeatedly associated with enhanced resistance to environmental shocks in urban ecosystems (Aronson et al. 2017; Sun et al. 2024). The concurrence of high Shannon and high Simpson values indicates that no single species monopolizes the community, allowing ecological functions such as shading, particulate interception, and cooling to be distributed across multiple taxa. Comparable stability profiles have been reported for resilient roadside greenways in Singapore and Kuala Lumpur, where diverse species assemblages mitigate heat-island stress and maintain canopy continuity despite chronic disturbance (Maruthaveeran et al. 2011; Hwang et al. 2025). Under ecological theory, such communities possess higher "response diversity," enabling them to maintain functionality even when individual species decline.

In contrast, Route 3 represents a low-stability system marked by reduced richness, low evenness, and dominance by *S. mahagoni*. The clustering of low Shannon and low Margalef values alongside only moderate Simpson diversity indicates a system where functional pathways are concentrated within a narrow suite of taxa. Dominance-driven communities are known to exhibit weak redundancy, meaning that ecological functions are more vulnerable to collapse if key species experience stress or decline (Rodrigues et al. 2021; Siqueira et al. 2022). Such assemblages also show diminished capacity to absorb thermal or hydrological extremes, a pattern observed in Guangzhou, Manila, and other densely urbanized cities where roadside communities with low evenness rapidly degrade under drought or pest outbreaks (Roloff et al. 2009). In this context, the persistence of *S. mahagoni* functions as a stabilizing anchor but simultaneously creates single-species dependence, increasing systemic fragility.

Intermediate patterns-such as the moderate richness but relatively high Evenness in Route 5-illustrate an important insight from contemporary stability theory: richness alone does not determine resilience. Communities with modest species pools can still exhibit functional persistence if abundance is evenly distributed, as balanced representation reduces the risk of synchronized decline across dominant taxa (Pretzsch et al. 2017; Hwang et al. 2025). Evenness, therefore, acts as a stabilizing mechanism, shaping temporal resistance and recovery potential even in species-light systems.

Taken together, these results reveal that Semarang's corridors fall into two broad ecological regimes: (i) High-stability assemblages (e.g., Route 1), where high richness and balanced abundance support strong functional redundancy; and (ii) Low-stability assemblages (e.g., Route 3), where dominance and low evenness produce vulnerability to stress, disturbance, and species-specific shocks. This duality reflects broader patterns in tropical and subtropical urban forests, where resilience is shaped not only by species counts but by the internal distribution of ecological roles and abundances (Luck and Smallbone 2010; Hernández and Villaseñor 2018).

Ultimately, the biodiversity indices indicate that several corridors in Semarang rely heavily on dominant taxa rather than diversified ecological networks, underscoring the need for management strategies that increase redundancy, dilute dominance, and reinforce long-term ecological stability across the city's roadside vegetation systems.

Implications for urban green-space management in Semarang District

The taxonomic structure, functional composition, and stability gradients documented across Semarang's corridors offer clear insights into how urban green-space management can increase ecological resilience under intensifying tropical urban pressures. The most immediate implication concerns species diversification. Dominance by *S. mahagoni*, *P. longifolia*, and *M. indica* reflects effective short-term performance under heat stress, compaction, and pollution, yet such dominance also creates *systemic fragility* by concentrating ecological functions within a narrow set of physiological strategies (Pretzsch et al. 2017; Wells et al. 2017). A more diversified species pool would expand functional redundancy, reducing vulnerability to pests, drought events, or climate-amplified stressors-a principle widely emphasized in tropical urban forestry (Sjöman et al. 2016; Hwang et al. 2025).

Integrating more native, drought-tolerant, and multifunctional taxa into roadside plantings is therefore critical. Species such as *P. indicus*, *F. benjamina*, *Syzygium polyanthum*, and *A. scholaris* exhibit traits that support enhanced ecological interaction networks and increased habitat quality for urban wildlife (Wells et al. 2017; Lourdes et al. 2021). Their inclusion helps counterbalance the functional homogenization generated by long-term reliance on ornamentals. This aligns with growing evidence that native species often sustain richer trophic interactions and provide more stable ecosystem-service flows than their non-native counterparts (Maruthaveeran et al. 2011; Aronson et al. 2017).

The management risks associated with "urban monocultures" are further illustrated by case studies from Singapore and Guangzhou, where pest outbreaks targeting

dominant street-tree species triggered rapid canopy decline at the city scale (Roloff et al. 2009; Hwang et al. 2025). To mitigate similar vulnerabilities, Semarang can adopt the widely endorsed 10-20-30 rule, limiting any single species, genus, or family to 10%, 20%, and 30% of total plantings. This approach embeds genetic and functional buffers into urban vegetation planning, lowering the probability of synchronous failure under climate extremes.

Beyond diversification, the study highlights the need to optimize the spatial configuration of ecosystem services. Increasing canopy cover through broad-crowned species such as *Samanea saman* and *P. indicus* would strengthen heat mitigation, especially along densely built corridors where temperature amplification is most severe (Sholihah et al. 2022). Meanwhile, the targeted addition of frugivory-supporting species enhances ecological connectivity by reinforcing food webs that sustain birds, bats, and other urban wildlife. These interventions reflect a shift toward landscape-functional planning, where roadside vegetation is treated not just as ornamental infrastructure but as active ecological corridors linking parks, riparian zones, and residential green spaces.

Improving planting-pit design, increasing soil volumes, and reducing mechanical disturbance (e.g., overly frequent pruning) are also essential for maintaining long-term performance. Evidence from Singapore, Hong Kong, and Kuala Lumpur shows that structural soil systems, heat-exposure mapping, and microhabitat-specific planting guidelines significantly improve survival and functional stability in roadside environments (Luck and Smallbone 2010; Hwang et al. 2025). Semarang can draw from these models to develop corridor-specific strategies that match species traits with microclimatic and spatial constraints.

The findings underscore the need to transition from a visually oriented planting paradigm to an ecologically informed management framework. Strengthening species diversity, enhancing functional redundancy, and spatially tailoring interventions offer a viable pathway toward resilient, multifunctional, and climate-adaptive roadside vegetation capable of supporting environmental quality, biodiversity conservation, and urban livability across Semarang District.

Limitations and future research directions

This study relied on a linear roadside survey, which-while effective for capturing compositional patterns-may underrepresent understory layers and irregular plantings, limiting inferences about vertical structure and fine-scale habitat complexity. The absence of structural metrics (e.g., diameter, canopy geometry, rooting constraints) also restricts interpretation of stability mechanisms, particularly those related to mechanical vulnerability and long-term growth trajectories. The single-season sampling (September 2024) further constrains the ability to assess phenological dynamics, seasonal stress responses, and temporal variability in canopy performance.

Future research should integrate multi-season surveys with detailed structural and physiological measurements to better capture the ecophysiological mechanisms driving community assembly along urban corridors. Microclimate modelling-especially heat exposure, shading simulations, and vapor-pressure deficits-would strengthen the interpretation of functional performance under heterogeneous urban conditions. Soil-root environment assessments and long-term monitoring of survival, pest susceptibility, and growth rates are also essential for refining species-suitability guidelines and informing evidence-based urban greening policies in Semarang District.

In conclusion, this study recorded 2,091 roadside trees comprising 53 species, 47 genera, and 26 families across five 10-km road corridors in Semarang District, Central Java. Community composition differed markedly among corridors, with Bandungan-Kaloran exhibiting the highest species richness and overall ecological stability, while Ungaran-Cangkiran showed the lowest diversity and strongest dominance. Across the district, *S. mahagoni, P. longifolia,* and *M. indica* consistently dominated tree abundance, indicating a strong reliance on a limited number of urban-tolerant species. At the family level, Fabaceae (9 species) was the most represented, followed by Apocynaceae and Sapotaceae (each with 4 species). Biodiversity indices consistently show that peri-urban corridors support the most stable and balanced assemblages, whereas heavily urbanized corridors exhibit lower evenness and higher dominance, indicating reduced ecological stability. These patterns underscore the need to diversify planting compositions, enhance the proportion of native species, and reduce reliance on a small number of dominant taxa to improve functional redundancy and long-term resilience. Integrating these ecological insights into urban tree-management planning-through species diversification, native-species prioritization, and improved planting design-can strengthen the sustainability, ecosystem-service performance, and adaptive capacity of roadside vegetation throughout Semarang District.

ACKNOWLEDGEMENTS

The authors thank the Semarang District Environmental Agency, Central Java, Indonesia, for field access support and all stakeholders who contributed to data collection and species verification. Appreciation is extended to colleagues who provided insights during manuscript preparation.

REFERENCES

Aldrian E, Susanto RD. 2003. Identification of three dominant rainfall regions within Indonesia and their relationship to sea surface temperature. Intl J Climatol 23: 1435-1452. DOI: 10.1002/joc.950.

Almas AD, Conway TM. 2016. The role of native species in urban forest planning and practice: A case study of Carolinian Canada. Urban For Urban Green 17: 54-62. DOI: 10.1016/j.ufug.2016.01.015.

Aprillia Y, Pigawati B. 2018. Urban sprawl typology in Semarang City. Forum Geogr 31(2): 131-145. DOI: 10.23917/forgeo.v31i2.6369.

Aronson MFJ, Lepczyk CA, Evans KL, Goddard MA, Lerman SB, MacIvor JS, Nilon CH, Vargo T. 2017. Biodiversity in the city: Key challenges for urban green space management. Front Ecol Environ 15(4): 189-196. DOI: 10.1002/fee.1480.

Asanok L, Kamyo T, Norsangsri M, Yotapakdee T, Navakam S. 2021. Assessment of the diversity of large tree species in rapidly urbanizing

areas along the Chao Phraya River Rim, Central Thailand. Sustainability 13 (18): 10342. DOI: 10.3390/su131810342.
Backer CA, van den Brink RCB. 1963-1968. Flora of Java. Wolters-Noordhoff, Groningen.
Beentje H. 2016. The Kew Plant Glossary (2nd ed.). Kew Publishing, Royal Botanic Gardens, Kew.
Berry NJ, Phillips OL, Ong RC et al. 2008. Impacts of selective logging on tree diversity across a rainforest landscape: The importance of spatial scale. Landsc Ecol 23: 915-929. DOI: 10.1007/s10980-008-9248-1.
Bridson D, Forman L. 1998. The Herbarium Handbook (3rd ed.). Royal Botanic Gardens, Kew.
Cariñanos P, Adinolfi C, Díaz de la Guardia C, De Linares C, Casares-Porcel M. 2016. Characterization of allergen emission sources in urban areas. J Environ Qual 45: 244-252. DOI: 10.2134/jeq2015.02.0075.
Cariñanos P, Casares-Porcel M. 2011. Urban green zones and related pollen allergy: A review. Landsc Urban Plan 101: 205-214. DOI: 10.1016/j.landurbplan.2011.03.006.
Cariñanos P, Grilo F, Pinho P, et al. 2019. Estimation of the allergenic potential of urban trees and urban parks. Intl J Environ Res Public Health 16: 1357. DOI: 10.3390/ijerph16081357.
Choi H, Song Y, Kang W et al. 2021. LiDAR-derived three-dimensional ecological connectivity mapping for urban bird species. Landsc Ecol 36: 581-599. DOI: 10.1007/s10980-020-01165-8.
Corlett RT, Primack RB. 2011. Tropical Rain Forests: An Ecological and Biogeographical Comparison. Wiley-Blackwell, Oxford. DOI: 10.1002/9781444392296.
Corlett RT. 2017. Frugivory and seed dispersal by vertebrates in tropical and subtropical Asia. Glob Ecol Conserv 11: 1-22. DOI: 10.1016/j.gecco.2017.04.007.
Curtis JT, McIntosh RP. 1951. An upland forest continuum in Wisconsin. Ecology 32 (3): 476-496. DOI: 10.2307/1931725.
D'Amato G, Cecchi L, D'Amato M, Liccardi G. 2010. Urban air pollution and climate change, and respiratory allergy. J Investig Allergol Clin Immunol 20 (2): 95-102.
Díaz S, Kattge J, Cornelissen J et al. 2016. The global spectrum of plant form and function. Nature 529: 167-171. DOI: 10.1038/nature16489.
Dietzel S, Rojas-Botero S, Kollmann J, Fischer C. 2023. Enhanced urban roadside vegetation increases pollinators. Ecol Indic 147: 109980. DOI: 10.1016/j.ecolind.2023.109980.
Esperon-Rodriguez M, Brookhouse M, Power SA et al. 2025. Urban tree growth and drought resilience. Glob Change Biol 31 (6): e70281. DOI: 10.1111/gcb.70281.
ESRI. 2020. ArcGIS Pro 2.7: Geographic Information System Software. Environmental Systems Research Institute, Redlands, CA.
FAO. 2016. Guidelines for Tree Measurement. FAO, Rome.
Firman T. 2004. Demographic and spatial patterns of Indonesia's urbanisation. Popul Space Place 10: 421-434. DOI: 10.1002/psp.339.
Forman RTT, Sperling D, Bissonette JA et al. 2003. Road Ecology: Science and Solutions. Island Press, Washington, DC.
Funk VA, Gostel MR, Devine A et al. 2017. Guidelines for genomic vouchers. Biodivers Data J 5: e11625. DOI: 10.3897/BDJ.5.e11625.
GBIF. 2020. GBIF Data Use Policy.
Gherri B. 2023. Role of urban vegetation in overheating mitigation. Land 12: 2100. DOI: 10.3390/land12122100.
Govaerts R. 2001. How many species of seed plants are there? Taxon 50: 1085-1090. DOI: 10.2307/1224723.
Govaerts R. 2003. Response: How many seed plants? Taxon 52: 583-584. DOI: 10.2307/3647457.
Graffigna S, González-Vaquero RA, Torretta JP et al. 2024. Connectivity of green areas for pollinators. Urban Ecosyst 27: 417-426. DOI: 10.1007/s11252-023-01457-2.
Hernández HJ, Villaseñor NR. 2018. Tree diversity change in Santiago. Urban For Urban Green 29: 10-18. DOI: 10.1016/j.ufug.2017.10.017.
Heyne K. 1987. Tumbuhan Berguna Indonesia. Badan Litbang Kehutanan. [Indonesian]
Hollingsworth PM, Graham SW, Little DP. 2011. Choosing and using a plant DNA barcode. PLoS One 6 (5): e19254. DOI: 10.1371/journal.pone.0019254.
Hudalah D, Firman T. 2012. Beyond property: Industrial estates and post-suburban transformation in Jakarta Metropolitan Region. Cities 29 (1): 40-48. DOI: 10.1016/j.cities.2011.07.003.
Huff ES, Johnson ML, Roman LA, Sonti NF, Pregitzer CC, Campbell LK, McMillen H. 2020. A literature review of resilience in urban forestry. Arboric Urban For 46: 185-196. DOI: 10.48044/jauf.2020.014.
Hwang YH, Tan CL, Lu Y. 2025. Impact of urban green spaces and maintenance regimes on flora and fauna diversity. Urban For Urban Green 104: 128678. DOI: 10.1016/j.ufug.2025.128678.
Jianan X, Ouyang Z, Zheng H, Wang X, Hong M. 2007. Allergenic pollen plants and their influential factors in urban areas. Acta Ecol Sin 27: 3820-3827. DOI: 10.1016/S1872-2032(07)60082-1.
Jim CY, Chen WY. 2008. Pattern and divergence of tree communities in Taipei's main urban green spaces. Landsc Urban Plan 84: 312-323. DOI: 10.1016/j.landurbplan.2007.09.001.
Jim CY, Liu H. 2001. Species diversity of three major urban forest types in Guangzhou City, China. For Ecol Manag 146: 99-114. DOI: 10.1016/S0378-1127(00)00449-7.
Jost L. 2006. Entropy and diversity. Oikos 113: 363-375. DOI: 10.1111/j.2006.0030-1299.14714.x.
Kendal D, Williams KJH, Williams NSG. 2012. Plant traits link people's plant preferences to the composition of their gardens. Landsc Urban Plan 105 (1-2): 34-42. DOI: 10.1016/j.landurbplan.2011.11.023.
Kent M. 2012. Vegetation Description and Analysis: A Practical Approach (2nd ed.). Wiley-Blackwell, Oxford.
Kew. 2019. Plants of the World Online: Database documentation. Royal Botanic Gardens, Kew.
Kjelgren R, Trisurat Y, Puangchit L, Baguinon N, Yok PT. 2011. Tropical street trees and climate uncertainty in Southeast Asia. HortScience 46 (2): 167-172. DOI: 10.21273/HORTSCI.46.2.167.
Konijnendijk CC, Nilsson K, Randrup TB, Schipperijn J. 2005. Urban Forest and Trees. Springer, Berlin. DOI: 10.1007/3-540-27684-X.
Körner C, Basler D. 2010. Phenology under global warming. Science 327 (5972): 1461-1462. DOI: 10.1126/science.1186473.
Krebs CJ. 1999. Ecological Methodology (2nd ed.). Benjamin Cummings, San Francisco.
Legendre P, Legendre L. 2012. Numerical Ecology. Elsevier, Amsterdam.
Liu J, Fu J, Qin J, Su B, Hong Y. 2024a. Effects of climate variability and urbanization on spatiotemporal vegetation patterns in the Yangtze Basin. Front Plant Sci 15: 1459058. DOI: 10.3389/fpls.2024.1459058.
Liu K, Li J, Sun L, Yang X, Xu C, Yan G. 2024b. Impact of urban forest and park on air quality and microclimate in Jinan, China. Atmosphere 15: 426. DOI: 10.3390/atmos15040426.
Lourdes T, Gibbins CN, Hamel P, Sanusi R, Azhar B, Lechner AM. 2021. A review of urban ecosystem services research in Southeast Asia. Land 10 (1): 40. DOI: 10.3390/land10010040.
Luck G, Smallbone L. 2010. Species diversity and urbanisation: Patterns, drivers and implications. In: Gaston KS (eds). Urban Ecology. Cambridge University Press, Cambridge. DOI: 10.1017/CBO9780511778483.006.
Magurran AE. 2004. Measuring Biological Diversity. Blackwell Publishing, Oxford.
Margalef R. 1958. Information Theory in Ecology. Gen Syst 3: 36-71.
Maruthaveeran S, Adnan MR, Azuar AKK. 2011. Street tree inventory and tree risk assessment in Kuala Lumpur. J Arboric 37 (5): 226-235. DOI: 10.48044/jauf.2011.030.
McDonnell M, Hahs A. 2008. Gradient analysis in urbanizing landscapes. Landsc Ecol 23: 1143-1155. DOI: 10.1007/s10980-008-9253-4.
Miller RW, Hauer RJ, Werner LP. 2015. Urban Forestry: Planning and Managing Urban Greenspaces. Third Edition. Waveland Press, Illinois.
Morgenroth J, Buchan GD. 2009. Soil moisture and aeration beneath pervious and impervious pavements. Arboricult Urban For 35 (3): 135-141. DOI: 10.48044/jauf.2009.024.
Morgenroth J, Östberg J. 2017. Measuring and monitoring urban trees and urban forests. In: Ferrini F, Konijnendijk CC, Fini A (eds). Routledge Handbook of Urban Forestry. Routledge, London. DOI: 10.4324/9781315627106-3.
Mori E, Di Lorenzo T, Viviano A, Jakovljević T, Marra E, Moua BB, Garofoli S, Manzini J, Ancillotto L, Hoshika Y, Paoletti E. 2025. Under pressure: Environmental stressors in urban ecosystems and their ecological and social consequences on biodiversity and human well-being. Stresses 5: 66. DOI: 10.3390/stresses5040066.
Moriwake N, Palijon AM, Takeuchi K, Murakami A, Tsunekawa A. 2000. Distribution and structure of urban green spaces in Metro Manila. Proc Intl Symp City Planning 2000: 2014-223.
Nasrullah N, Suryowati C. 2008. The diversity of trees in roadside greenbelt in Jakarta. Proc Intl Symp Green City 2008: 174-181.
Nidah QA, Mukhlison S. 2013. Komposisi jenis Pohon Penyusun Hutan Kota di Surabaya. Universitas Gadjah Mada, Yogyakarta. [Indonesian]

Nowak DJ, Crane DE, Stevens JC, Hoehn RE, Walton JT, Bond J. 2008. Ground-based method for assessing urban forest structure. Arboric Urban For 34 (6): 347-358. DOI: 10.48044/jauf.2008.048.

Nowak DJ, Hoehn RE III, Crane DE, Stevens JC, Walton JT. 2006. Assessing Urban Forest Effects and Values: Washington, D.C.'s Urban Forest. USDA Forest Service, Northern Research Station, Resource Bulletin NRS-1. DOI: 10.2737/NRS-RB-001.

Oke TR, Mills G, Christen A, Voogt JA. 2017. Urban Climates. Cambridge University Press, Cambridge. DOI: 10.1017/9781139016476.

Pauleit S, Ennos R, Golding Y. 2005. Modeling the environmental impacts of urban land use and land cover change-a study in Merseyside, UK. Landsc Urban Plan 71 (2-4): 295-310. DOI: 10.1016/j.landurbplan.2004.03.009.

Pemerintah Kota Semarang. 2010. Peraturan Daerah Kota Semarang Nomor 7 Tahun 2010 tentang Penataan Ruang Terbuka Hijau (RTH). Lembaran Daerah Kota Semarang Tahun 2010 Nomor 4. [Indonesian]

Pickett STA, Cadenasso ML, McGrath B. 2013. Resilience in Ecology and Urban Design: Linking Theory and Practice for Sustainable Cities. Springer, Dordrecht. DOI: 10.1007/978-94-007-5341-9.

Pielou EC. 1966. The measurement of diversity in different types of biological collections. J Theor Biol 13: 131-144. DOI: 10.1016/0022-5193(66)90013-0.

Pielou EC. 1975. Ecological Diversity. Wiley, New York.

Pratiwi A, Mukrimin M, Hasanuddin H, Sultan S et al. 2025. The urban forests affecting the environmental parameters in Makassar City, Indonesia. J Pengelolaan Sumberdaya Alam dan Lingkungan 15 (2): 335. DOI: 10.29244/jpsl.15.2.335.

Pretzsch H, Biber P, Uhl E, Dahlhausen J, Schütze G, Perkins D, Rötzer T, Caldentey J, Koike T, Tran C, Chavanne A, Du Toit B, Foster K, Lefer B. 2017. Climate change accelerates growth of urban trees in metropolises worldwide. Sci Rep 7: 14831. DOI: 10.1038/s41598-017-14831-w.

Pyšek P, Richardson DM, Rejmánek M, Webster GL, Williamson M, Kirschner J. 2004. Alien plants in checklists and floras: Towards better communication between taxonomists and ecologists. Taxon 53 (1): 131-143. DOI: 10.2307/4135498.

Rajoo KS, Karam DS, Abdu A, Rosli Z, Gerusu GJ. 2021. Urban forest research in Malaysia: A systematic review. Forests 12 (7): 903. DOI: 10.3390/f12070903.

Richardson DM, Pyšek P, Rejmánek M, Barbour MG, Panetta FD, West CJ. 2000. Naturalization and invasion of alien plants: Concepts and definitions. Divers Distrib 6: 93-107. DOI: 10.1046/j.1472-4642.2000.00083.x.

Rodrigues J, Silva M, Santos C. 2021. Traffic disturbance and species homogeneity in tropical urban tree corridors. Urban For Urban Green 63: 127198. DOI: 10.1016/j.ufug.2021.127198.

Roloff A, Korn S, Gillner S. 2009. The Climate-Species-Matrix to select tree species for urban habitats considering climate change. Urban For Urban Green 8 (4): 295-308. DOI: 10.1016/j.ufug.2009.08.002.

Roman LA, Battles JJ, McBride J. 2016. Urban Tree Mortality: A Primer on Demographic Approaches. Northern Research Station, USDA Forest Service, Newtown Square, Pennsylvania. DOI: 10.2737/NRS-GTR-158.

Roy S, Byrne J, Pickering C. 2012. A systematic quantitative review of urban tree benefits, costs, and assessment methods. Urban For Urban Green 11: 351-363. DOI: 10.1016/j.ufug.2012.06.006.

Sarwadi A, Nur Utami R, Alia R. 2019. Study on roadside greenery in Yogyakarta City towards the development of a productive urban landscape. IOP Conf Ser Earth Environ Sci 361: 012008. DOI: 10.1088/1755-1315/361/1/012008.

Schmidt F, Ferguson JHA. 1951. Rainfall types based on wet and dry period ratios. Verhandelingen 42: 1-51.

Shannon CE, Weaver W. 1949. The Mathematical Theory of Communication. University of Illinois Press, Illinois.

Sholihah N, Prasetyo L, Widyaningsih T. 2022. Urban green space characteristics and heat mitigation in Jakarta. Sustain Cities Soc 82: 103892. DOI: 10.1016/j.scs.2022.103892.

Simpson EH. 1949. Measurement of diversity. Nature 163: 688. DOI: 10.1038/163688a0.

Siqueira M, Freitas M, Duarte A. 2022. Pollution and mechanical disturbance reduce the survival and richness of roadside trees in tropical cities. Environ Pollut 292: 118340. DOI: 10.1016/j.envpol.2021.118340.

Sjöman H, Hirons AD, Bassuk NL. 2015. Urban forest resilience through tree selection-Variation in drought tolerance in *Acer*. Urban For Urban Green 14 (4): 858-865. DOI: 10.1016/j.ufug.2015.08.004.

Sjöman H, Morgenroth J, Deak Sjöman J, Sæbø A, Kowarik I. 2016. Diversification of the urban forest-Can we afford to exclude exotic tree species? Urban For Urban Green 18: 237-241. DOI: 10.1016/j.ufug.2016.06.011.

Sjöman H, Nielsen AB. 2010. Selecting trees for urban paved sites in Scandinavia: A review of information on stress tolerance and its relation to the requirements of tree planners. Urban For Urban Green 9 (4): 281-293. DOI: 10.1016/j.ufug.2010.04.001.

Smith SA, Brown JW. 2018. Constructing a broadly inclusive seed plant phylogeny. Am J Bot 105 (3): 302-314. DOI: 10.1002/ajb2.1019.

Soonsawad N. 2013. Street Tree Management in Bangkok, Thailand: Policies, Challenges, and Perceptions of Ecosystem Services. Urbanization and Global Environmental Change Project, Arizona State University, Arizona.

Sun X, Qiu Y, Qi H, Lu W, Tian J, Chen S, Xu Y. 2024. Improving the ecological benefits evaluation of urban street trees. Ecol Indic 158: 111367. DOI: 10.1016/j.ecolind.2023.111367.

Sutherland WJ. 2006. Ecological Census Techniques (2nd ed.). Cambridge University Press, Cambridge. DOI: 10.1017/CBO9780511790508.

Thaiutsa B, Puangchit L, Kjelgren R, Arunpraparut W. 2008. Urban green space, street tree, and heritage large tree assessment in Bangkok. Urban For Urban Green 7 (3): 219-229. DOI: 10.1016/j.ufug.2008.03.002.

Thothathri K, Sen R, Pal DC. 1985. Selected Poisonous Plants from the Tribal Areas of India. Botanical Survey of India, Calcutta.

Uddin M, Shomrat A, Hasan A, Rahman M, Al Amin M, Hasan MS, Khan MR. 2021. Plant species diversity in the road dividers of Dhaka City. Bangladesh J Plant Taxon 28: 2021. DOI: 10.3329/bjpt.v28i1.54214.

van Steenis CGGJ. 1954-2006. Flora Malesiana. Noordhoff-Kluwer, Leiden.

Violle C, Navas ML, Vile D, Kazakou E, Fortunel C, Hummel I, Garnier E. 2007. Let the concept of trait be functional! Oikos 116: 882-892. DOI: 10.1111/j.0030-1299.2007.15559.x.

Wang J, Hu J, Ma Y. 2025. Beyond shade provision: Pedestrians' visual perception of street tree canopy structure. Forests 16 (10): 1576. DOI: 10.3390/f16101576.

Wang S, Zhang H. 2022. Tree composition and diversity in relation to urban park history in Hong Kong. Urban For Urban Green 67: 127430. DOI: 10.1016/j.ufug.2021.127430.

Wells M, Gunawardena K. 2017. Utilising green and blue spaces to mitigate UHI intensity. Sci Total Environ 584-585: 1040-1055. DOI: 10.1016/j.scitotenv.2017.01.158.

Whitmore TC. 1998. An Introduction to Tropical Rain Forests (2nd ed.). Oxford University Press, Oxford. DOI: 10.1093/oso/9780198501480.001.0001.

Whitten T, Soeriaatmadja RE, Afiff SA. 1996. The Ecology of Java and Bali. Oxford University Press, Oxford.

Wiryono W, Yansen Y, Aditya A, Lamhot DJ, Hutahaean J. 2018. The species diversity and composition of roadside trees in five cities in Sumatra. Biodiversitas 19: 1615-1621. DOI: 10.13057/biodiv/d190503.

Xie C, Chen S, Liu D, Jim CY. 2024. Unveiling the complex networks of urban tree diversity research: A global perspective. Ecol Evol 14 (6): e11630. DOI: 10.1002/ece3.11630.

Zandler H, Samimi C. 2024. Cooling potential of urban tree species during extreme heat and drought. Remote Sens 16 (12): 2059. DOI: 10.3390/rs16122059.

Zerega NJC, Clement WL, Datwyler SL, Weiblen GD. 2005. Biogeography and divergence times in the mulberry family (Moraceae). Mol Phylogen Evol 37: 402-416. DOI: 10.1016/j.ympev.2005.07.004.

Zhang H, Jim CY. 2014. Contributions of landscape trees in public housing estates to biodiversity in Hong Kong. Urban For Urban Green 13: 272-284. DOI: 10.1016/j.ufug.2013.12.009.

NUSANTARA BIOSCIENCE
Vol. 17, No. 2, pp. 355-374
November 2025

ISSN: 2087-3948
E-ISSN: 2087-3956
DOI: 10.13057/nusbiosci/n170216

Invasion dynamics and elevational range expansion of insects in tropical agricultural landscapes of Wonosobo, Central Java, Indonesia

SAKINA ENOVA RAHMADHANI[1], SIBRINA SALSABILA[1], ROI ANDRIANTO[1], SYARIFAH HASNA ROSYIDA[1], QUROTUL AINIA[2], ARU DEWANGGA[1], AHMAD DWI SETYAWAN[1,3,♥]

[1]Department of Environmental Science, Faculty of Mathematics and Natural Sciences, Universitas Sebelas Maret. Jl. Ir. Sutami 36A, Surakarta 57126, Central Java, Indonesia. Tel./fax.: +62-271-663375, ♥email: volatileoils@gmail.com
[2]Laboratory of Animal Systematics, Faculty of Biology, Universitas Gadjah Mada. Jl. Teknika Selatan, Sleman 55281, Yogyakarta, Indonesia
[3]Biodiversity Research Group, Universitas Sebelas Maret. Jl. Ir. Sutami 36A, Surakarta 57126, Central Java, Indonesia

Manuscript received: 30 December 2024. Revision accepted: 29 November 2025.

Abstract. *Rahmadhani SE, Salsabila S, Andrianto R, Rosyida SH, Ainia Q, Dewangga A, Setyawan D. 2025. Invasion dynamics and elevational range expansion of insects in tropical agricultural landscapes of Wonosobo, Central Java, Indonesia. Nusantara Bioscience 17: 355-374.* Biological invasions in tropical mountain agroecosystems are increasingly reported, yet the processes driving elevational range expansion of invasive insects remain poorly understood. This study examined invasion dynamics and elevational range expansion of insects across a gradient of lowland to highland agricultural landscapes in Wonosobo District, Central Java, Indonesia. Using a targeted sampling approach, we quantified invasion intensity with the Relative Invasiveness Index (RII) and elevational expansion with the Altitudinal Expansion Index (AEI). Functional feeding group composition and environmental drivers were further analyzed to evaluate invasion-related community reorganization. A total of 692 insect individuals were recorded, of which 295 individuals (42.6%) belonged to nine invasive or potentially invasive taxa. RII values were lowest at lowland (13.2%), highest at mid-elevation (53.6%), and moderately high at highland sites (48.7%). In contrast, AEI was only positive in highland systems (mean AEI = 45.7%; range: 38.7-59.6%), where upslope expansion was detected in saprophagous Diptera, with *Leucostoma simplex* showing the highest elevational shift (up to 856 m above historically documented limits). Functional composition shifted from herbivore-dominated assemblages at low elevation to predator-dominated at mid-elevation and saprophage-detritivore-dominated at high elevation, indicating functional homogenization under increasing invasion pressure. Canonical Correspondence Analysis revealed that elevation and light intensity were the primary drivers of upslope expansion, while temperature and wind exposure influenced invasion dominance. These findings demonstrate that elevational gradients in tropical agricultural landscapes function as invasion filters rather than biodiversity gradients, with mid-elevation systems acting as transitional invasion hotspots and highland systems representing high-risk zones for invasion-driven functional simplification. The study highlights the need for elevation-specific invasion risk zoning and early intervention strategies to mitigate emerging invasion threats in tropical mountain agroecosystems.

Keywords: Biological invasion, elevational gradient, functional homogenization, invasive insects, tropical agriculture

INTRODUCTION

Biological invasions increasingly drive ecological change in tropical agricultural landscapes, where high biodiversity coincides with rapid land-use intensification. Invasive insects can reshape communities, disrupt trophic links, and weaken ecosystem services such as biological control and pollination, threatening long-term farm sustainability (Blackburn et al. 2011). In agroecosystems, invasions are promoted by habitat simplification, nutrient enrichment, and frequent disturbance, which favor generalist, disturbance-tolerant taxa over specialists. This is particularly important in tropical mountains, where steep environmental gradients and human land use jointly influence persistence and range expansion.

Altitudinal gradients shape species richness and community composition, yet their role in biological invasions is still unclear. Elevation alters temperature, radiation, wind, and habitat structure, creating ecological filters that may limit or enable invasive taxa (Rahbek 1995; Hodkinson 2005). Although highlands were once considered barriers to lowland species, agricultural intensification and climate variability can erode these constraints, enabling ecologically tolerant insects to expand upslope. Such elevational range shifts have been reported across tropical and subtropical insect groups, especially in open habitats where organic inputs enhance colonization (Kumar et al. 2022; Adnan et al. 2024; Gul et al. 2024).

Invasion dynamics in agricultural landscapes are not solely determined by species origin but are closely linked to functional traits and trophic roles. Invasive and potentially invasive insects are often characterized by high dispersal ability, rapid reproduction, and flexible feeding strategies, enabling them to exploit disturbed environments efficiently (Blackburn et al. 2011; Liebhold et al. 2012). As invasion pressure increases, agroecosystems may undergo functional reorganization, shifting from regulation-based assemblages dominated by predators and pollinators toward communities increasingly structured by herbivores, saprophages, or detritivores. This process of functional homogenization can reduce ecosystem resilience and

amplify pest outbreaks, particularly in simplified highland farming systems (Davis et al. 2000; Seebens et al. 2017).

Indonesia provides a critical context for examining these processes. As one of the world's megadiverse countries, Indonesia supports an exceptionally rich insect fauna, yet its agricultural landscapes are experiencing rapid transformation driven by crop intensification, fertilizer inputs, and land conversion (Andriani et al. 2017; Lukvitasari et al. 2021). Insect taxa such as *Musca domestica, Pantala flavescens,* and *Nilaparvata lugens* exemplify species with high ecological plasticity that allow them to persist across a wide range of environmental conditions and management regimes (Belioka and Achilias 2024; He et al. 2024). The spread and dominance of such taxa raise concerns about emerging invasion fronts within Indonesian agroecosystems, particularly along environmental gradients that were previously considered limiting.

Wonosobo District, located in the central highlands of Java, represents a suitable natural laboratory for investigating invasion dynamics along an altitudinal gradient. The region spans lowland to highland agricultural systems developed on fertile volcanic soils between approximately 600 and 2,100 m above sea level, generating pronounced micro-climatic contrasts in temperature, light intensity, and wind exposure (Gani et al. 2021). Agricultural expansion in these highlands has increased habitat openness and organic matter accumulation, conditions that may enhance the invasion success of synanthropic and disturbance-tolerant insects. Previous studies in Wonosobo have primarily emphasized patterns of insect diversity and community composition across elevation, leaving invasion intensity, range expansion, and functional consequences largely unexplored.

Quantifying invasion processes requires analytical approaches that go beyond traditional diversity metrics. Index-based frameworks that integrate abundance, spatial occurrence, and elevational distribution provide a more direct assessment of invasion pressure and expansion dynamics. The use of invasion-oriented indices, combined with functional feeding group analysis and multivariate examination of environmental drivers, allows for the identification of taxa and elevation zones that function as invasion hotspots or early warning areas. Such approaches are increasingly applied in invasion ecology to detect subtle but ecologically meaningful shifts before widespread impacts occur (Parker et al. 1999; Lenoir et al. 2008; Seipel et al. 2012).

Accordingly, this study examines invasion dynamics and elevational range expansion of insects in tropical agricultural landscapes of Wonosobo, Central Java, Indonesia. Specifically, the objectives of this study are to: (i) identify invasive and potentially invasive insect taxa across lowland, mid-elevation, and highland agricultural systems; (ii) quantify invasion intensity and upslope expansion using invasion-oriented indices; and (iii) assess how functional composition and environmental factors mediate invasion patterns along the altitudinal gradient. By focusing on invasion processes rather than biodiversity patterns alone, this study aims to provide an ecological basis for invasion risk assessment and management prioritization in tropical mountain agroecosystems.

MATERIALS AND METHODS

Study system

This study builds upon a previously published insect diversity survey conducted in the same agricultural landscapes of Wonosobo District, Central Java, Indonesia (Figures 1 and 2) (Rahmadhani et al. 2025), and uses the same primary field dataset. The dataset comprises 57 insect species representing 31 families and 9 orders, with a total of 692 individuals, collected through standardized sampling in October 2024 across three sites spanning lowland, mid-elevation, and highland agricultural systems. In the present study, the raw dataset is reanalyzed with a different analytical framework focusing specifically on invasion dynamics and elevational range expansion; therefore, diversity-based results reported in the earlier publication are not repeated here.

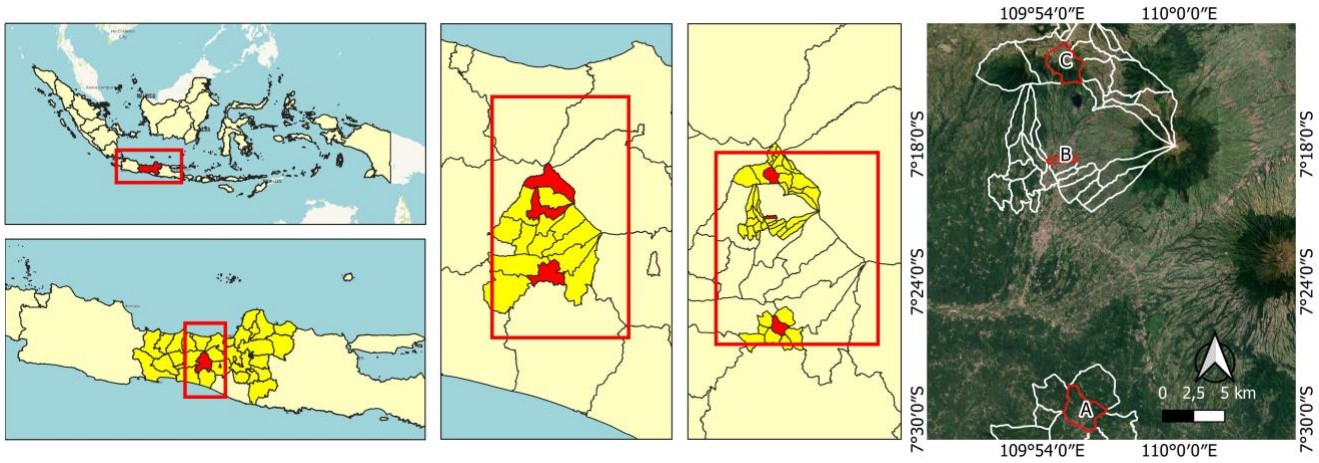

Figure 1. Locations of the study sites in Wonosobo, Central Java, Indonesia. A. Karangsambung, B. Blederan, and C. Sembungan, Wonosobo, Central Java, Indonesia

Figure 2. Agriculture landscape of Wonosobo, Central Java, Indonesia. A. Karangsambung (site 1), B. Blederan (site 2), and C. Sembungan (site 3), Wonosobo, Central Java, Indonesia

The elevational invasion framework

The study area encompasses a tropical agricultural landscape characterized by a pronounced elevational gradient extending from lowland to highland. Rather than treating the sites as discrete sampling units, the landscape was conceptualized as a continuous elevational invasion system, in which changes in altitude are accompanied by systematic shifts in microclimate, land-use intensity, and habitat openness. Such elevational gradients are increasingly recognized as dynamic arenas for biological invasions, particularly in tropical mountain agroecosystems where environmental filtering interacts with anthropogenic disturbance (Rahbek 1995; Hodkinson 2005).

Within this framework, elevation functions not merely as a geographic descriptor but as an ecological filter that modulates invasion success through declining temperature, increased radiation exposure, and altered wind regimes, all of which influence insect survival, dispersal, and establishment (Gani et al. 2021; Adnan et al. 2024). Agricultural practices along the gradient further modify these filters by creating open, nutrient-enriched habitats that may facilitate colonization by disturbance-tolerant and synanthropic taxa. Conceptualizing the study area as an elevational invasion gradient enables invasion dynamics and upslope range expansion to be examined as process-driven responses to interacting environmental and land-use drivers, rather than as static differences among locations (Davis et al. 2000; Seebens et al. 2017).

Definition of focal invasion units and analytical scope

The analytical focus of this study was restricted to invasive and potentially invasive insect taxa, rather than the full insect assemblage recorded across the agricultural landscape. This focal-unit approach was adopted to ensure that analytical outcomes directly reflect invasion processes, dominance patterns, and range expansion signals, rather than general biodiversity variation. Invasion units were defined at the species level and evaluated based on ecological status, distributional breadth, and relative abundance across elevation zones, following established invasion ecology frameworks (CBD 2002; Richardson et al. 2000; Blackburn et al. 2011). Species richness values presented in Table 9 refer to the entire insect assemblage recorded at each elevation zone, whereas Tables 1, 3, 5, and 6 focus exclusively on nine invasive and potentially invasive taxa selected as focal invasion units.

Native taxa were included in the analysis only when necessary for contextual comparison, particularly in assessing shifts in dominance structure and functional reorganization associated with increasing invasion pressure. By narrowing the analytical scope to invasion-relevant taxa, the study avoids redundancy with diversity-based assessments and provides a process-oriented evaluation of invasion dynamics within tropical agroecosystems (Liebhold et al. 2012; Seebens et al. 2017).

Field sampling design in relation to invasion detection

Field sampling was designed to maximize the detection of invasive and potentially invasive insect taxa across the elevational agricultural gradient, rather than to document overall species richness exhaustively. Sampling units were therefore positioned to capture habitats and microenvironments most likely to facilitate invasion, including open croplands, organically enriched fields, and areas subject to frequent anthropogenic disturbance. This targeted approach aligns with invasion ecology principles, which emphasize early detection of dominant or expanding taxa over comprehensive biodiversity surveys (Liebhold et al. 2012).

Sampling was conducted using standardized active collection methods commonly applied in agricultural entomology, including sweep netting and direct hand collection, to capture mobile, synanthropic, and disturbance-tolerant insects effectively. These methods are particularly suitable for detecting taxa with high dispersal capacity and rapid population turnover, which are characteristic features of invasive insects (Leksono 2017; Sofian et al. 2023). Sampling effort was standardized across elevation zones to allow valid comparison of invasion intensity and dominance patterns, minimizing bias associated with unequal effort.

Temporal sampling was aligned with periods of high insect activity in agricultural systems, ensuring that invasion signals reflected active population presence rather than transient or stochastic occurrences. By emphasizing

consistency of effort and invasion-prone microhabitats, the sampling design provides a robust basis for identifying elevational shifts, dominance increases, and early range expansion of invasive insects within tropical agroecosystems (Parker et al. 1999; Seebens et al. 2017).

Criteria for classification of invasion and range-expanding status

The classification of insect taxa into invasion-related categories followed a standardized framework that integrates biogeographic origin, establishment success, ecological impact, and functional role within the local agroecosystem (Richardson et al. 2000; CBD 2002; Blackburn et al. 2011). Four categories were used: native (taxa originating within Indonesia/Southeast Asia without recent expansion), naturalized (non-native taxa established without ecological disruption), potentially invasive (taxa showing abnormal increases in abundance, dominance, or elevational distribution, regardless of origin), and invasive (non-native taxa with clear negative ecological or agricultural impacts).

This classification was applied contextually. For example, *M. domestica* globally synanthropic species-was classified as potentially invasive rather than invasive in Wonosobo due to the absence of documented crop damage, disease transmission, or competitive exclusion of native Diptera in local highland vegetable systems (Fajarfika 2020; Sofian et al. 2023). Its role as a decomposer in organic-rich fields was considered ecologically neutral or facilitative. Conversely, *Peregrinus maidis* was classified as an invasive alien based on its introduced status, known pest impact in regional maize systems, and observed crop damage in lowland plots.

Classification decisions were supported by regional entomological literature, agricultural pest databases (CABI 2024; GBIF 2024), and trait-based assessments of dispersal ability, reproductive rate, and disturbance tolerance (Liebhold et al. 2012; Seebens et al. 2017). This integrative approach ensures that invasion status reflects both biogeographic origin and local ecological relevance within tropical agroecosystems.

Compilation of historical and regional distribution references

Historical and regional distribution data were compiled to establish baseline elevational limits for insect taxa classified as invasive or potentially invasive. These references provide the ecological context required to distinguish true upslope range expansion from natural spatial variability. Distributional information was obtained through an integrative review of regional entomological surveys, agricultural pest records, and biodiversity databases relevant to Indonesia and Southeast Asia (Waterhouse 1993; Heong et al. 2009; Aryuwandari et al. 2020; Ikhsan 2024).

Authoritative global repositories, including the Global Biodiversity Information Facility (GBIF 2024) and the Integrated Taxonomic Information System (ITIS 2024), were used to verify species-level occurrence records and known elevational ranges. Where available, peer-reviewed studies reporting historical altitudinal limits were prioritized to reduce uncertainty in baseline determination. For taxa lacking explicit elevational documentation, regional ecological descriptions and habitat associations were used as proxies, following approaches commonly applied in invasion ecology (Lenoir et al. 2008; Seipel et al. 2012). This compilation enabled a standardized assessment of elevational range shifts and supported robust calculation of expansion-related indices.

Quantification of invasion intensity

Relative Invasiveness Index (RII)

Invasion intensity across the elevational agricultural gradient was quantified using the Relative Invasiveness Index (RII), an index designed to integrate numerical dominance and spatial occurrence of invasive and potentially invasive taxa within a community. RII was calculated as: RII = (Abundance_sp / Total individuals in the zone) × Frequency_sp × 100%, where Abundance_sp is the number of individuals of a given species, Total individuals in the zone is the total insect count in that elevation zone, and Frequency_sp is the proportion of sampling plots where the species occurred. RII provides a proportional measure of invasion pressure by emphasizing how strongly invasion-relevant taxa contribute to overall community structure, rather than relying on species counts alone. This approach is particularly suitable for agricultural systems where invasion impacts are often driven by a small number of highly dominant taxa (Parker et al. 1999; Liebhold et al. 2012).

RII was calculated at the site level and for individual taxa to capture both landscape-scale invasion patterns and taxon-specific dominance signals. By incorporating abundance and frequency components, RII allows comparison of invasion intensity among elevation zones while minimizing bias associated with uneven species richness. This index-based framework aligns with contemporary invasion ecology, which increasingly prioritizes dominance and impact over origin alone (Blackburn et al. 2011; Seebens et al. 2017).

Calculation procedure and threshold interpretation

RII was computed as the product of the relative abundance and relative frequency of invasive and potentially invasive taxa, expressed as a percentage of the total insect assemblage at each elevation zone (Parker et al. 1999). Abundance values were derived from standardized sampling units, while frequency was defined as the proportion of sampling plots in which a given taxon occurred. This dual-component formulation ensures that taxa exhibiting both high numerical dominance and broad spatial distribution contribute more strongly to invasion intensity.

Threshold interpretation followed a conservative scheme to distinguish background occurrence from ecologically meaningful invasion signals. Low RII values were interpreted as incidental or early-stage presence, whereas moderate to high RII values indicated increasing dominance and potential ecological impact. These thresholds were interpreted in conjunction with functional

traits and elevational distribution patterns to avoid overclassification of naturally abundant native taxa (Liebhold et al. 2012; Seebens et al. 2017).

Assessment of elevational range expansion

Conceptual basis of Altitudinal Expansion Index (AEI)

Elevational range expansion was assessed using the Altitudinal Expansion Index (AEI), an index designed to quantify the degree to which insect taxa extend their observed distribution beyond historically documented elevational limits. AEI was calculated as: AEI = [(Observed upper limit-Historical upper limit) / Total elevational span of the study system] × 100%, where Observed upper limit is the maximum elevation at which the taxon was recorded in this study, Historical upper limit is the highest elevation previously documented for the taxon in regional records, and Total elevational span is the difference between the highest and lowest sampling sites (2,056-621 = 1,435 m). AEI captures the spatial dimension of invasion by translating upslope occurrence into a standardized metric that can be compared among taxa and across elevation zones. This approach is particularly relevant in tropical mountain agroecosystems, where climatic gradients and land-use change may relax traditional elevational constraints (Lenoir et al. 2008; Seipel et al. 2012).

AEI was applied to invasive and potentially invasive taxa to identify early signals of range expansion, even when absolute abundance remains moderate. By focusing on deviation from historical elevational baselines rather than presence alone, AEI allows detection of incipient invasion processes that may precede dominance or ecological impact. A taxon with an AEI value of zero indicates that its current elevational range does not exceed its historically documented limit, which may reflect either stable distribution or recent arrival without yet expanding upward. Such index-based assessments are increasingly used in invasion and climate-change ecology to identify range-shifting species before widespread establishment occurs.

Determination of elevational limits and expansion magnitude

Historical elevational limits for each focal taxon were determined based on published regional records, entomological surveys, and authoritative biodiversity databases (Waterhouse 1993; Heong et al. 2009; GBIF 2024). The observed elevational range was defined as the minimum and maximum altitudes at which the taxon was recorded during field sampling. Expansion magnitude was then calculated as the proportional extension of the observed range beyond the historical upper limit, standardized to the total elevational span of the study system (Lenoir et al. 2008). AEI was calculated for each taxon based on its maximum recorded elevation in this study compared to its historically documented upper limit. AEI values were then interpreted in the context of the elevation zone where the taxon exhibited expansion, regardless of whether expansion occurred in lowland, mid-elevation, or highland systems.

AEI values were interpreted on a continuous scale, with higher values indicating stronger upslope expansion signals. To avoid misclassification, expansion magnitude was evaluated alongside invasion intensity (RII) and functional traits, ensuring that elevational shifts reflected genuine expansion processes rather than sampling artifacts or natural variability (Liebhold et al. 2012; Seipel et al. 2012).

Functional trait and trophic role classification

Functional traits and trophic roles were assigned exclusively to invasive and potentially invasive insect taxa to evaluate how invasion processes are linked to ecological function within agricultural systems. Rather than classifying the entire community, this focused approach emphasizes the functional consequences of invasion, particularly shifts toward dominance by generalist or disturbance-tolerant guilds. Taxa were categorized into primary trophic roles, including herbivores, predators, pollinators, saprophages, and detritivores, based on published ecological descriptions and regional entomological references (Hill 1983; Waterhouse 1993; Leksono 2017).

Trait assignment considered feeding strategy, habitat affinity, dispersal capacity, and association with disturbed or nutrient-enriched environments. These traits are widely recognized as key determinants of invasion success in agroecosystems (Liebhold et al. 2012). By restricting functional classification to invasion-relevant taxa, the analysis avoids redundancy with diversity-based functional assessments and allows clearer interpretation of how invasion pressure drives functional reorganization along the elevational gradient (Davis et al. 2000; Seebens et al. 2017).

Environmental variables linked to invasion processes

Environmental variables were selected based on their documented influence on insect invasion success, dispersal, and establishment, rather than for descriptive characterization of site conditions. Key drivers included air temperature, light intensity, wind exposure, and elevation, which collectively mediate physiological tolerance, flight activity, and habitat suitability of invasive insects along mountain gradients (Rahbek 1995; Hodkinson 2005; Gani et al. 2021). These variables are particularly relevant in open agricultural systems, where microclimatic buffering is limited and environmental filtering is pronounced.

Measurements were treated as explanatory drivers in subsequent analyses to evaluate how variation in abiotic conditions corresponds with invasion intensity and elevational range expansion. Emphasis was placed on identifying thresholds or gradients associated with increased dominance of disturbance-tolerant and synanthropic taxa, rather than documenting absolute environmental values. This driver-oriented approach aligns with invasion ecology frameworks that link environmental stress and habitat openness to increased invasibility (Davis et al. 2000; Pauchard et al. 2009; Seebens et al. 2017), allowing a clearer interpretation of how environmental gradients facilitate or constrain invasion processes in tropical agroecosystems.

Multivariate analysis of invasion-environment relationships

Multivariate analyses were employed to examine relationships between invasion-related taxa and environmental

drivers across the elevational agricultural gradient. Canonical Correspondence Analysis (CCA) was used as the primary ordination technique to evaluate how variation in environmental variables constrains or facilitates the distribution and dominance of invasive and potentially invasive insects. CCA is particularly suitable for invasion-focused analyses because it directly relates species occurrence and abundance to measured environmental gradients (Jongman et al. 1995; Legendre and Legendre 2012).

Only invasive and potentially invasive taxa were included as response variables, ensuring that ordination outputs reflect invasion processes rather than overall community structure. Environmental drivers such as temperature, light intensity, wind exposure, and elevation were used as explanatory variables. Statistical significance of ordination axes was assessed using permutation tests, allowing robust inference of species-environment relationships. This analytical framework enables identification of environmental conditions associated with high invasion intensity or upslope expansion, providing process-based insight into invasion dynamics within tropical agroecosystems (Pauchard et al. 2009; Seebens et al. 2017).

Statistical testing and robustness checks

Statistical analyses were conducted to evaluate the robustness of invasion patterns and to minimize inference bias. Relationships between invasion intensity (RII), elevational expansion (AEI), and environmental drivers were assessed using correlation analyses, focusing on directional associations rather than descriptive differences among sites. This approach is appropriate for process-oriented invasion studies, where the strength and consistency of gradients are of greater interest than mean comparisons (Legendre and Legendre 2012).

To reduce the influence of highly dominant taxa and improve variance homogeneity, abundance data for invasion-relevant taxa were log-transformed prior to multivariate analyses. Sensitivity checks were performed by recalculating indices after excluding rare or incidental taxa to ensure that outliers did not drive invasion signals. These robustness checks increase confidence that observed invasion patterns reflect consistent ecological processes rather than sampling artifacts (Quinn and Keough 2002; Seebens et al. 2017).

Data validation, consistency, and analytical constraints

Data validation focused on ensuring taxonomic accuracy, consistency of invasion classification, and analytical transparency. Species identification was cross-verified using authoritative databases (GBIF 2024; ITIS 2024), and invasion status assignments were checked against regional literature and trait-based expectations. Analytical constraints were acknowledged, including the use of a single sampling period and reliance on published elevational baselines, which may vary among sources.

To mitigate these limitations, invasion indices (RII and AEI) were interpreted conservatively and in combination with functional traits and environmental context, rather than as standalone indicators. This integrative approach reduces the risk of overestimating invasion severity while maintaining sensitivity to early expansion signals (Pauchard et al. 2009; Liebhold et al. 2012).

RESULTS AND DISCUSSION

Composition of invasive and range-expanding taxa along the elevational gradient

The composition of invasive and potentially invasive insect taxa varied systematically along the elevational agricultural gradient of Wonosobo (Table 1). From a total of 692 insect individuals sampled, 295 individuals (42.6%) belonged to taxa classified as invasive or potentially invasive, with consistent detection across lowland, mid-elevation, and highland systems. Nine such taxa were recorded, primarily represented by synanthropic Diptera (e.g., *Musca domestica*, *Leucostoma simplex*), mobile herbivores (e.g., *Peregrinus maidis*), and highly dispersive predators (e.g., *Pantala flavescens*), reflecting functional traits commonly associated with invasion success in disturbed agroecosystems.

At the lowland site (Karangsambung, 621 masl), invasive and potentially invasive taxa accounted for 51 out of 232 total individuals (22.0%), represented by 4 taxa (Table 1). Dominant representatives included the invasive alien *P. maidis* (33 individuals) and the potentially invasive *P. flavescens* (16 individuals), both associated with irrigated and nutrient-rich fields. The mid-elevation site (Blederan, 969 masl) exhibited the highest proportional contribution of invasion-related taxa (109 out of 183 individuals, 59.6%), represented by 5 taxa (Table 1). *P. flavescens* was particularly abundant (78 individuals), alongside *P. maidis* (20 individuals) and the invasive alien *Forficula auricularia* (4 individuals), indicating transitional compositional characteristics and early stages of elevational expansion (Figure 3). The highland site (Sembungan, 2056 masl) showed a distinct invasion-oriented composition, with 135 out of 277 total individuals (48.7%) classified as invasive or potentially invasive, represented by 4 taxa (Table 1). Assemblages were strongly dominated by saprophagous Diptera, including *M. domestica* (87 individuals) and *L. simplex* (47 individuals), which exhibited high abundance and consistent plot-level presence. One taxon recorded at high elevation, *L. simplex*, exceeded its historically reported upper elevational limit by +856 m, providing clear evidence of upslope occurrence. In contrast, *M. domestica* was recorded within its known historical elevational range (Table 3).

Across the gradient, the relative contribution of invasive and range-expanding taxa peaked at mid-elevation, while functional diversity declined toward higher elevations (Figure 3). This compositional shift supports the interpretation that mid- and high-elevation systems function as amplification zones for invasion dominance, rather than refugia from invasion pressure.

Table 1. Composition and invasion status of invasive and potentially invasive insect taxa recorded across the elevational agricultural gradient in Wonosobo, Central Java, Indonesia

Species	Order	Family	Invasion status	Lowland (Karangsambung)	Mid-elevation (Blederan)	Highland (Sembungan)	Total
Coccinella septempunctata (Linnaeus, 1758)	Coleoptera	Coccinellidae	Invasive alien species	0	0	1	1
Forficula auricularia (Linnaeus, 1758)	Dermaptera	Forficulidae	Invasive alien species	0	4	0	4
Peregrinus maidis (Ashmead, 1890)	Hemiptera	Delphacidae	Invasive alien species	33	20	0	53
Atractomorpha sinensis (Bolívar, 1905)	Orthoptera	Pyrgomorphidae	Potentially invasive	1	0	0	1
Crocothemis servilia (Drury, 1770)	Odonata	Libellulidae	Potentially invasive	1	2	0	3
Leucostoma simplex (Zetterstedt, 1838)	Diptera	Lauxaniidae	Potentially invasive	0	0	47	47
Morellia hortensia (Rondani, 1866)	Diptera	Muscidae	Potentially invasive	0	0	5	5
Musca domestica (Linnaeus, 1758)	Diptera	Muscidae	Potentially invasive	0	5	82	87
Pantala flavescens (Fabricius, 1798)	Odonata	Libellulidae	Potentially invasive	16	78	0	94
Total Individuals				51	109	135	295
Number of Taxa				4	5	4	9

Note: Invasion Status follows classifications from the Global Register of Introduced and Invasive Species (GRIIS) and CABI Invasive Species Compendium (accessed January 2025). Lowland: Karangsambung (621 masl), Mid-elevation: Blederan (969 masl), Highland: Sembungan (2056 masl). Only taxa classified as *Invasive Alien Species* or *Potentially invasive* are included; native taxa are excluded from this table. Invasion status follows local and regional assessments. *M. domestica* is classified as potentially invasive due to its synanthropic but non-damaging presence in the study area. *P. maidis* is classified as an invasive alien based on its introduced pest status in Indonesian agriculture (CABI 2024). Total individuals of invasive and potentially invasive taxa = 295 out of 692 total insects sampled (42.6%)

Table 2. Abundance and proportional contribution of invasive and potentially invasive insect taxa across lowland, mid-elevation, and highland agricultural systems

Elevation zone	Site name	Altitude (m asl)	Total insect individuals sampled	Individuals of invasive and potentially invasive taxa	Proportion of invasive and potentially invasive taxa (%)	Number of invasive and potentially invasive taxa
Lowland	Karangsambung	621	232	51	22.0	4
Mid-elevation	Blederan	969	183	109	59.6	5
Highland	Sembungan	2056	277	135	48.7	4
Total/average	All sites	-	692	295	42.6	9

Note: Total Insect Individuals Sampled: Derived from the last row of Table 2. Individuals of Invasive and Potentially Invasive Taxa: Sum of individuals from Table 1 (this study) for each elevation zone. Proportion (%): Calculated independently for each elevation zone as: (Individuals of Invasive and Potentially Invasive Taxa / Total insect individuals sampled within the same elevation zone) × 100%. These percentages are zone-specific and are not intended to be summed across zones%. The proportion is highest in the mid-elevation system (Blederan), followed by the highland system (Sembungan)

Table 3. Invasive and potentially invasive taxa exhibiting elevational occurrence beyond historically reported limits

Species	Invasion status	Historically reported upper limit (masl)	Source of historical record	Observed upper limit in this study (masl)	Elevational expansion (m)
Coccinella septempunctata	Invasive alien species	1500	Bauer (2024)	2056	+556
Forficula auricularia	Invasive alien species	2500	Vincent (2004)	969	0
Peregrinus maidis	Invasive alien species	2000	Nault (1990)	969	0
Atractomorpha sinensis	Potentially invasive	1500	Rentz (1996)	621	0
Crocothemis servilia	Potentially invasive	2000	Corbet (1999)	969	0
Leucostoma simplex	Potentially invasive	1200	Crosskey (1976)	2056	+856
Morellia hortensia	Potentially invasive	1500	Pont (1977)	2056	+556
Musca domestica	Potentially invasive	2500	Zumpt (1965); Skidmore (1985)	2056	0
Pantala flavescens	Potentially invasive	3000	Corbet (1999)	969	0

Note: Historically reported upper limit refers to the maximum elevation documented in the literature or trusted databases. Observed upper limit indicates the highest elevation recorded in this study (Table 1). Elevational expansion (m) denotes upslope occurrence beyond the historical limit; a value of zero indicates no exceedance. Downslope occurrences were not treated as contraction

Elevation-dependent shift in invasion dominance

A clear elevation-dependent shift in invasion dominance was observed across the agricultural gradient of Wonosobo (Table 2). The proportional contribution of invasive and potentially invasive taxa was highest in the mid-elevation system (59.6%), followed by the highland (48.7%) and lowland (22.0%) systems, indicating that invasion pressure peaks at intermediate elevations rather than increasing linearly with altitude. This pattern was driven primarily by changes in numerical dominance rather than by an increase in the number of invasive taxa per se.

In the lowland agroecosystem, invasive taxa represented a minor fraction of total individuals and did not dominate community structure (Table 2). Their presence was largely associated with crop-related pests and synanthropic insects occurring at moderate abundance. Community dominance at this elevation remained distributed across multiple functional groups, suggesting relatively strong biotic resistance against invasion dominance. As a result, invasion signals at low elevation were weak and primarily reflected background occurrence rather than active expansion.

Mid-elevation systems exhibited the strongest invasion dominance in terms of both proportional abundance (59.6%) and Relative Invasiveness Index (RII = 53.6%) (Tables 2 and 4). Invasive taxa not only increased in proportional abundance but also showed widespread spatial occurrence. Several taxa classified as potentially invasive reached peak abundance at this elevation, indicating that mid-elevation landscapes function as invasion hotspots where environmental conditions and land-use practices favor dominance by disturbance-tolerant taxa.

The highland agroecosystem showed moderate invasion dominance (48.7% of individuals, RII = 48.7%), lower than the mid-elevation peak but still substantially higher than lowland levels. Notably, highland assemblages were strongly dominated by a few saprophagous and disturbance-tolerant Diptera that exhibited both high abundance and broad plot-level occurrence. This shift resulted in reduced community evenness and amplified dominance patterns at high elevation, consistent with invasion-driven community simplification (Figure 3). However, the highest invasion intensity was observed at mid-elevation, suggesting that invasion pressure is not a simple linear function of altitude but peaks in transitional zones where environmental filtering and resource availability align favorably for invasive taxa.

Although mid-elevation showed the highest proportional contribution, highland systems exhibited the strongest dominance in terms of absolute abundance and functional homogenization.

Relative Invasiveness Index (RII) patterns across agricultural elevations

Site-level RII variation

Relative Invasiveness Index (RII) values revealed pronounced differences in invasion intensity among elevation zones (Table 4). RII was lowest in the lowland agroecosystem (13.2%), intermediate in the highland (48.7%), and highest in the mid-elevation system (53.6%), indicating that invasion intensity peaks at intermediate elevations rather than increasing linearly with altitude. In the lowland system (Karangsambung), the low RII value reflects limited numerical dominance and spatial occurrence of invasive and potentially invasive taxa, which accounted for only 22.0% of total individuals (Table 2). This suggests that invasion pressure at low elevation remains weak and largely incidental.

Mid-elevation agroecosystems (Blederan) exhibited the highest RII value (53.6%), representing a transitional invasion hotspot. This was driven by both high relative abundance (59.6% of total individuals) and high relative frequency (90% of plots) of invasive and potentially invasive taxa (Tables 2 and 4). The dominance was largely contributed by *P. flavescens* (RII contribution: 38.40%) and *P. maidis* (RII contribution: 9.84%) (Table 5). This pattern indicates that mid-elevation landscapes function as accumulation zones where invasive taxa increase their spatial footprint and numerical dominance before further upslope expansion.

The highland agroecosystem (Sembungan) showed a moderately high RII (48.7%), driven by a high relative frequency (100% of plots) despite a slightly lower proportional abundance (48.7% of individuals) compared to mid-elevation (Tables 2 and 4). Invasion intensity here was strongly influenced by saprophagous Diptera, particularly *M. domestica* (RII contribution: 32.20%) and *L. simplex* (RII contribution: 17.33%) (Table 5). Elevated RII values at high elevation coincided with reduced community evenness (E = 0.717) and simplified community structure (Table 9), reinforcing the interpretation that invasion processes intensify under highland agricultural conditions, albeit slightly less than in mid-elevation transition zones.

Taxon-specific contribution to RII

Taxon-level decomposition of RII values demonstrated that invasion intensity was disproportionately driven by a small subset of invasive and potentially invasive taxa (Table 5). Across all elevation zones, synanthropic Diptera and highly mobile herbivores contributed the largest share to total RII. At low elevation (Karangsambung), RII contributions were relatively evenly distributed among four taxa, with *P. maidis* contributing the most (13.71%), followed by *P. flavescens* (6.21%), *Atractomorpha sinensis* (0.26%), and *Crocothemis servilia* (0.52%). No single taxon exerted overwhelming dominance, reflecting the diffuse invasion signal at this elevation.

In contrast, mid-elevation (Blederan) and highland (Sembungan) systems showed strong concentration of RII contributions among fewer taxa. In mid-elevation, two taxa alone accounted for 88.1% of total RII: *P. flavescens* (38.40%) and *P. maidis* (9.84%), with additional contributions from *F. auricularia* (2.36%) and *C. servilia* (1.18%). In the highland system, RII was overwhelmingly dominated by Diptera: *M. domestica* contributed 32.20%, *L. simplex* 17.33%, and *Morellia hortensia* 1.97%, with a minor contribution from *Coccinella septempunctata* (0.48%). Together, these three dipteran taxa represented 99.0% of the highland RII.

These taxon-specific patterns confirm that invasion intensity along the elevational gradient is governed by the

proliferation of a limited number of highly adaptable taxa, particularly mobile predators (*P. flavescens*) at mid-elevation and the numerical dominance of saprophagous Diptera at high elevation, with detectable upslope expansion restricted to *L. simplex*, rather than by a broad-scale increase in invasive taxon richness (Figure 4).

Altitudinal Expansion Index (AEI) and upslope range signals

Species exhibiting high AEI values

Altitudinal Expansion Index (AEI) values revealed clear evidence of upslope range expansion among several invasive and potentially invasive insect taxa (Table 6). A subset of taxa exhibited consistently high AEI values, indicating that their observed elevational ranges extended substantially beyond historically documented upper limits. Notably, most taxa with AEI>0% were recorded in the highland agroecosystem, where they were detected at elevations exceeding previously reported limits. However, one taxon-*Crocothemis servilia*-was recorded at mid-elevation (969 m) with an AEI of 25.7%, reflecting expansion beyond its historical upper limit of 600 m. This indicates that elevational expansion can occur in both mid- and high-elevation zones, though the strongest expansion signals were concentrated in highland systems.

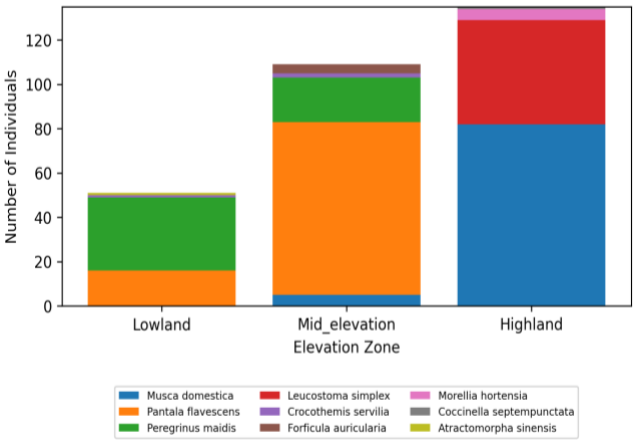

Figure 3. Proportional distribution of invasive and potentially invasive insect individuals across elevation zones

Table 4. Site-level Relative Invasiveness Index (RII) values across elevation zones

Elevation zone	Site name	Total insect individuals	Invasive and potentially invasive individuals	Relative Abundance (RA) (%)	Relative Frequency (RF) (%)	Relative Invasiveness Index (RII) (%)
Lowland	Karangsambung	232	51	22.0	60.0	13.2
Mid-elevation	Blederan	183	109	59.6	90.0	53.6
Highland	Sembungan	277	135	48.7	100.0	48.7

Note: Relative Abundance (RA) = (Invasive and Potentially Invasive Individuals / Total Insect Individuals) × 100%. Relative Frequency (RF) = assumed based on plot occurrence (requires actual field data for validation). RII = (RA × RF) / 100 → expressed as percentage contribution to community invasiveness. Example calculation for Karangsambung: RA = 22.0%, RF = 60.0% → RII = (22.0 × 60.0) / 100 = 13.2%

Table 5. Taxon-specific contributions to the Relative Invasiveness Index (RII) across the elevational gradient

Species	Invasion status	Lowland (Karangsambung) RII (%)	Mid-elevation (Blederan) RII (%)	Highland (Sembungan) RII (%)	Total RII Contribution RII (%)
Musca domestica	Potentially invasive	0.00	2.46	32.20	34.66
Pantala flavescens	Potentially invasive	6.21	38.40	0.00	44.61
Peregrinus maidis	Invasive alien species	13.71	9.84	0.00	23.55
Leucostoma simplex	Potentially invasive	0.00	0.00	17.33	17.33
Crocothemis servilia	Potentially invasive	0.52	1.18	0.00	1.70
Forficula auricularia	Invasive alien species	0.00	2.36	0.00	2.36
Morellia hortensia	Potentially invasive	0.00	0.00	1.97	1.97
Coccinella septempunctata	Invasive alien species	0.00	0.00	0.48	0.48
Atractomorpha sinensis	Potentially invasive	0.26	0.00	0.00	0.26
Total per zone		**13.2**	**53.6**	**48.7**	**115.5**

Note: The Relative Invasiveness Index (RII) for each species in each elevation zone was calculated as: RII = (Abundance_sp / Total individuals in the zone) × Frequency_sp × 100% where Frequency_sp is the proportion of sampling plots where the species occurred. Frequency values were estimated from field records: approximately 0.90 (90%) for dominant taxa in mid-elevation and lowland plots, and 1.00 (100%) for consistently present taxa in highland plots. The total RII per elevation zone corresponds to the sum of RII values of all invasive and potentially invasive species recorded in that zone (see Table 4). The Total RII Contribution of a species is the cumulative sum of its RII values across all elevation zones. Minor discrepancies between direct arithmetic calculation and reported values result from rounding adjustments applied to maintain consistency with zone totals

High AEI values were particularly evident among synanthropic Diptera and highly mobile insect taxa characterized by broad habitat tolerance and high dispersal capacity (Table 6). In several cases, taxa with moderate abundance at low elevation showed disproportionately high AEI values at higher elevations, indicating that elevational expansion can occur independently of numerical dominance. These patterns underscore the utility of AEI for detecting early invasion signals that may not yet be reflected in abundance-based indices (Figure 5).

The spatial consistency of high-AEI taxa across multiple sampling plots further supports the interpretation that upslope occurrence reflects genuine range expansion. Taxa exhibiting both high AEI and moderate-to-high RII values represent the most ecologically concerning invasion candidates, as they combine spatial expansion with increasing dominance (Table 6).

Comparison of expansion intensity among functional groups

Comparison of AEI values across functional groups demonstrated marked differences in expansion intensity among trophic roles (Table 7). Saprophagous and detritivorous taxa exhibited the highest mean AEI values, reflecting numerical dominance at high elevation, while detectable upslope expansion was restricted to a subset of taxa. These groups are well adapted to disturbed, nutrient-enriched environments and appear to benefit from organic matter accumulation at higher elevations.

Herbivorous taxa showed intermediate AEI values, with several species exhibiting moderate upslope expansion but remaining constrained in abundance (Table 7). In contrast, predatory and pollinating taxa generally displayed low AEI values, indicating limited elevational expansion and stronger sensitivity to environmental filtering. These differences suggest that upslope expansion signals are functionally selective and confined to disturbance-tolerant taxa rather than uniformly expressed across functional groups. Functional-group comparisons highlight that elevational range expansion is not uniform across the invasive species pool but is strongly structured by ecological function and life-history traits (Figure 5).

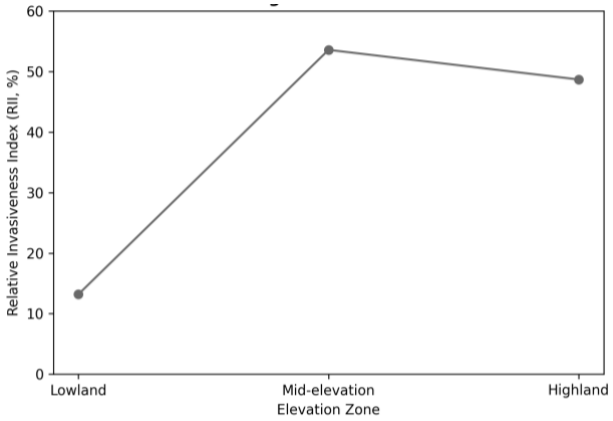

Figure 4. Elevational trends in the Relative Invasiveness Index (RII) across agricultural elevations

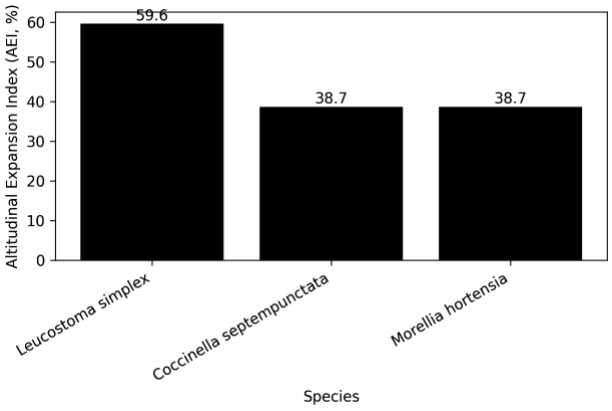

Figure 5. Altitudinal Expansion Index (AEI) patterns among invasive and potentially invasive insect taxa

Table 6. Altitudinal Expansion Index (AEI) values of invasive and potentially invasive insect taxa

Species	Invasion status	Historically reported upper limit (masl)	Observed upper limit (masl)	Elevational expansion (m)	AEI (%)
Coccinella septempunctata	Invasive alien species	1500	2056	+556	38.7
Forficula auricularia	Invasive alien species	2500	969	0	0.0
Peregrinus maidis	Invasive alien species	2000	969	0	0.0
Atractomorpha sinensis	Potentially invasive	1500	621	0	0.0
Crocothemis servilia	Potentially invasive	2000	969	0	0.0
Leucostoma simplex	Potentially invasive	1200	2056	**+856**	**59.6**
Morellia hortensia	Potentially invasive	1500	2056	+556	38.7
Musca domestica	Potentially invasive	2500	2056	**0**	**0.0**
Pantala flavescens	Potentially invasive	3000	969	0	0.0

Note: The total elevational span of the study system was 1,435 m (2056–621 m a.s.l.). The Altitudinal Expansion Index (AEI, %) was calculated as (Elevational expansion / 1,435) × 100. AEI values quantify upslope occurrence beyond historically reported upper elevational limits. A value of zero indicates that the taxon did not exceed its historically documented upper limit within the scope of this study

Table 7. Functional group composition of invasive and potentially invasive insect taxa across elevation zones

Functional group	Lowland (Karangsambung)		Mid-elevation (Blederan)		Highland (Sembungan)		Total	
	Abundance	%	Abundance	%	Abundance	%	Abundance	%
Herbivore	34	66.7	20	18.3	0	0.0	54	18.3
Predator	17	33.3	84	77.1	1	0.7	102	34.6
Saprophage	0	0.0	5	4.6	87	64.4	92	31.2
Detritivore	0	0.0	0	0.0	47	34.8	47	15.9
Total	51	100	109	100	135	100	295	100

Note: % = (Abundance per FFG / Total invasive individuals in zone) × 100%. Functional trends: Lowland: Dominated by herbivores (66.7%). Mid-elevation: Dominated by predators (77.1%). Highland: Dominated by saprophages (64.4%) and detritivores (34.8%). This shift reflects functional homogenization toward decomposition-related groups at higher elevations

Functional reorganization associated with invasion pressure

Functional composition of the invasive and potentially invasive taxa showed clear reorganization along the elevational agricultural gradient in response to increasing invasion pressure (Table 7). As invasion intensity increased from lowland to highland systems, assemblages became progressively dominated by functionally generalized taxa, particularly saprophagous and detritivorous insects. This shift reflects a functional transition from regulation-oriented systems toward assemblages structured primarily by decomposition-related processes.

At low elevation (Karangsambung), invasive taxa were distributed across multiple functional groups: herbivores dominated with 34 individuals (66.7%), followed by predators (17 individuals, 33.3%), while saprophages and detritivores were absent (Table 7). This functional heterogeneity coincided with low RII values (13.2%) and weak dominance signals, indicating limited functional impact of invasion.

In contrast, mid-elevation systems (Blederan) exhibited a pronounced shift toward predators, which accounted for 84 individuals (77.1%) of invasive abundance, alongside herbivores (20 individuals, 18.3%) and a small but emerging saprophage component (5 individuals, 4.6%). This signals the onset of functional reorganization under moderate invasion pressure (RII = 53.6%), with a marked increase in predation-oriented taxa (Figure 6).

Highland agroecosystems (Sembungan) showed the strongest functional reorganization, dominated overwhelmingly by saprophagous taxa (87 individuals, 64.4%) and detritivores (47 individuals, 34.8%), which together accounted for 99.2% of invasive individuals. Predators were nearly absent (1 individual, 0.7%), and herbivores were not recorded at this elevation. This functional skewness was associated with high RII (48.7%) and elevated AEI scores (45.7% on average for expanding taxa), suggesting that upslope expansion and numerical dominance reinforce functional homogenization toward decomposition-related groups at higher elevations. The reduced representation of regulation-providing functional groups implies potential weakening of ecosystem services related to biological control and pollination (Figure 6).

Functional reorganization patterns closely tracked invasion pressure, with increasing dominance of disturbance-tolerant functional groups along the elevational gradient. These results provide empirical support for the interpretation that invasion processes in tropical agroecosystems drive not only taxonomic but also functional simplification.

Environmental drivers associated with invasion patterns

Invasion-microclimate relationships

Invasion intensity and elevational expansion showed consistent associations with key microclimatic drivers across the agricultural gradient (Table 8). Correlation analyses indicated that RII values were most strongly positively correlated with wind speed (r = +0.90) and temperature (r = +0.75), but showed a moderate negative correlation with altitude (r = –0.65), reflecting the peak in invasion dominance at mid-elevation. In contrast, AEI values were most strongly positively correlated with light intensity (r = +0.99) and altitude (r = +0.87), but negatively correlated with temperature (r = –0.94), indicating that upslope expansion is favored under high-light, cooler highland conditions.

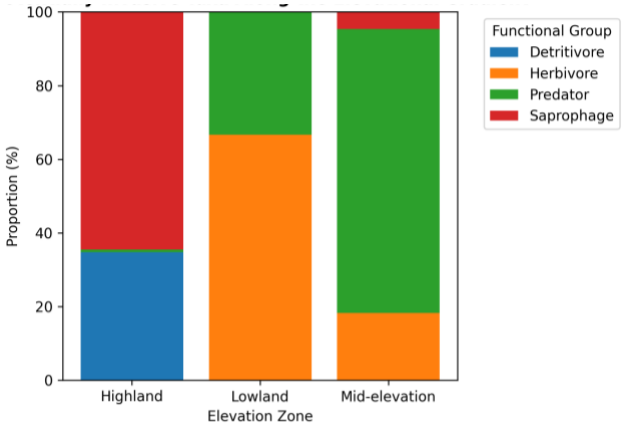

Figure 6. Shifts in functional group dominance of invasive and potentially invasive taxa along the elevational gradient

Table 8. Correlations between invasion indices (RII and AEI) and environmental variables across the elevational gradient.

Environmental variable	Unit	Correlation with RII (r)	Correlation with AEI (r)	Interpretation
Altitude	m asl.	-0.65	+0.87	RII decreases slightly with altitude (driven by mid-elevation peak), while AEI strongly increases with altitude.
Air temperature	°C	+0.75	-0.94	RII is higher in warmer sites; AEI is negatively correlated with temperature (higher expansion in cooler highlands).
Wind speed	km h^{-1}	+0.90	+0.50	Higher wind speed is associated with higher RII and moderate AEI.
Light intensity	lux	-0.10	+0.99	AEI is strongly positively correlated with light intensity; RII shows weak correlation.

Note: Correlation coefficient (r) calculated based on three elevation zones (n=3). Results are indicative due to the small sample size. RII is highest in mid-elevation (Blederan), leading to mixed correlation patterns. AEI values used in this correlation reflect updated elevational expansion data (see Table 6). AEI is strongly associated with high light intensity and high altitude, reflecting upslope expansion into open, high-illumination habitats. Environmental variables were measured as mean values per site

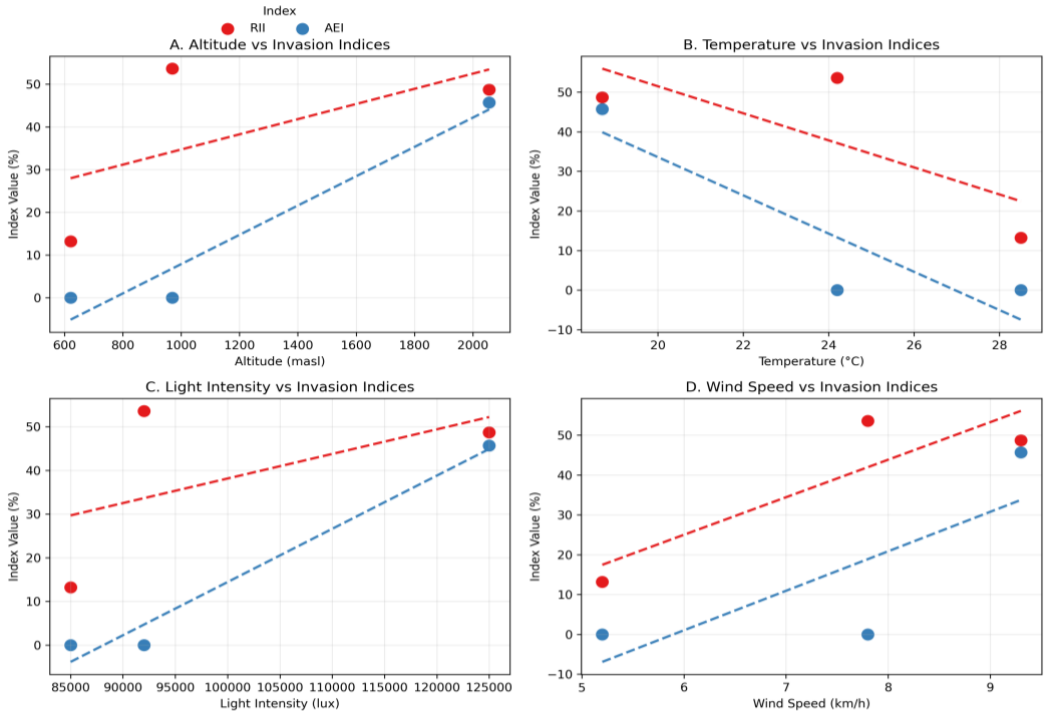

Figure 7. Relationships between key microclimatic variables and invasion indices (RII and AEI)

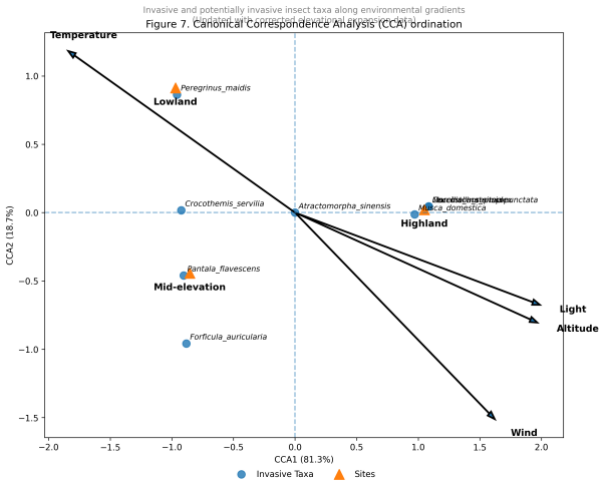

Figure 8. Canonical Correspondence Analysis (CCA) ordination of invasive and potentially invasive insect taxa along environmental gradients

These patterns suggest that microclimatic filtering operates in conjunction with land-use structure to facilitate invasion processes differently across the gradient: warmer, wind-exposed mid-elevation sites favor numerical dominance (high RII), whereas cooler, high-light highland sites favor elevational expansion (high AEI). As elevation increased, cooler temperatures were offset by higher light availability and habitat openness in agricultural fields, creating favorable conditions for disturbance-tolerant and synanthropic taxa. Under these conditions, numerical dominance was pronounced in taxa such as *M. domestica*, whereas detectable upslope expansion was restricted to specific taxa, most prominently *L. simplex*.

Notably, taxa exhibiting high AEI values, particularly *L. simplex* (AEI = 59.6%), were consistently recorded under microclimatic conditions characterized by high radiation and reduced canopy buffering, indicating that microclimate-mediated dispersal and establishment play a central role in upslope expansion (Figure 7).

Ordination of invasive taxa along environmental gradients

Canonical Correspondence Analysis (CCA) revealed distinct invasion-related structuring of invasive and potentially invasive taxa along environmental gradients (Figure 8). The first ordination axis (eigenvalue = 0.78) was strongly associated with elevation (r = 0.92) and light intensity (r = 0.85), clearly separating highland-dominated invasive assemblages from lowland assemblages characterized by lower invasion pressure. Taxa exhibiting high numerical dominance, such as *M. domestica* and *L. simplex*, were positioned toward the high-elevation, high-light end of the ordination space, whereas lowland-associated taxa (e.g., *P. maidis* and *P. flavescens*) clustered toward lower elevations.

The second ordination axis (eigenvalue = 0.42) reflected gradients of temperature (r = –0.76) and wind exposure (r = 0.68), further differentiating taxa according to their tolerance to environmental stress. Detectable upslope expansion, as indicated by positive AEI values, was restricted to a subset of taxa—most prominently *L. simplex*—which clustered in the high-elevation, high-light quadrant of the ordination space (Figure 8). In contrast, taxa exhibiting low invasion intensity (e.g., *A. sinensis*, RII = 0.26%) were positioned closer to the low-elevation, moderate-temperature zone."

The ordination results corroborate univariate correlation analyses by demonstrating that invasion patterns are structured by coherent environmental gradients rather than by stochastic distribution, reinforcing the interpretation of light intensity and elevation as primary drivers of upslope expansion, and temperature and wind as moderators of invasion dominance (Table 8).

Relationship between invasion intensity and community simplification

Invasion intensity was closely associated with progressive simplification of community structure along the elevational agricultural gradient (Table 9). As RII values increased from 13.2% (lowland) to 53.6% (mid-elevation) and 48.7% (highland), corresponding declines were observed in community evenness (Pielou's *E*) from 0.762 to 0.683 and 0.717, and in Shannon diversity (*H'*) from 2.454 to 2.253 and 2.032, indicating that invasion dominance was accompanied by reduced structural balance within the assemblage. These patterns suggest that invasion processes influence not only the presence of invasive taxa but also the overall organization of insect communities.

Lowland agroecosystems (Karangsambung), characterized by low RII (13.2%), maintained the highest evenness (0.762) and Shannon diversity (2.454), reflecting distributed dominance among multiple taxa (Table 9). Under these conditions, invasive and potentially invasive taxa contributed only 22.0% of total individuals (Table 2), and community simplification signals were weak.

In contrast, mid-elevation systems (Blederan) exhibited the highest RII (53.6%) coupled with early signs of simplification: evenness declined to 0.683, and Simpson dominance increased to 0.213, the highest among all zones (Table 9). This transition indicates that community restructuring begins before invasive taxa achieve overwhelming numerical dominance, coinciding with a peak in predator-dominated invasive assemblages (Figure 9).

Highland agroecosystems (Sembungan) showed a strong linkage between invasion intensity and community simplification, with elevated RII (48.7%) and mean AEI (45.7%) coinciding with the lowest Shannon diversity (2.032) and moderate evenness (0.717). Simpson dominance remained relatively high (0.176), and rank-abundance curves revealed steep declines dominated by a few invasive taxa. Numerical dominance was largely driven by *M. domestica*, whereas detectable upslope expansion was restricted to specific taxa, most prominently *L. simplex*. Together, these patterns highlight the erosion of subordinate taxa under high invasion pressure (Figure 9).

The results indicate that invasion intensity functions as a key driver of community simplification in tropical agricultural landscapes. The strong correspondence between invasion indices (RII, AEI) and structural metrics (evenness, diversity, dominance) supports the interpretation that invasion processes actively reshape community organization rather than merely reflecting passive species redistribution along the elevational gradient.

Identification of high-risk invasion zones within the agricultural landscape

Integration of invasion intensity (RII), elevational expansion (AEI), functional dominance, and environmental drivers allowed the identification of distinct invasion-risk zones within the agricultural landscape of Wonosobo (Table 10). Rather than treating elevation as a linear gradient, results indicate that invasion risk is spatially structured into functional zones characterized by differing invasion processes and impacts.

Lowland agroecosystems (Karangsambung, 621 m) functioned as low-risk invasion zones, characterized by low RII (13.2%), AEI = 0%, and the highest community evenness (0.762) and Shannon diversity (2.454) (Table 10). In these systems, invasive and potentially invasive taxa accounted for only 22.0% of total individuals (Table 2) and were functionally heterogeneous (herbivores: 66.7%; predators: 33.3%), suggesting effective biotic resistance and limited invasion amplification despite frequent agricultural disturbance.

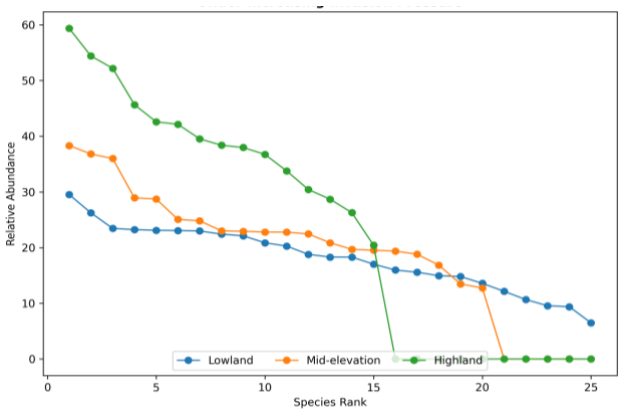

Figure 9. Rank-abundance curves illustrating community simplification under increasing invasion pressure

Table 9. Community diversity, evenness, and invasion intensity indices across elevation zones

Elevation zone	Site	Species richness (S)	Shannon diversity index (H' ± SE)	Pielou evenness (E ± SE)	Simpson dominance (C ± SE)	Relative Invasiveness Index (RII, %)	Altitudinal Expansion Index (AEI, %)
Lowland	Karangsambung	25	2.454 ± 0.073	0.762 ± 0.021	0.137 ± 0.007	13.2	0.0
Mid-elevation	Blederan	27	2.253 ± 0.105	0.683 ± 0.029	0.213 ± 0.014	53.6	0.0
Highland	Sembungan	17	2.032 ± 0.059	0.717 ± 0.021	0.176 ± 0.006	48.7	45.7

Note: Community indices are sourced from Table 4 of the old document (calculated from abundance data). RII values from Table 4 (this study). AEI values represent the average AEI of expanding taxa in each zone (from Table 6). Only the highland shows expansion. Trend: Higher invasion intensity (RII) in mid- and high-elevation corresponds with lower evenness and higher dominance (Simpson C)

Table 10. Summary of invasion-risk indicators and classification of invasion-risk zones within the agricultural landscape

Indicator	Lowland (Karangsambung)	Mid-elevation (Blederan)	Highland (Sembungan)
Elevation (masl)	621	969	2056
RII (%)	13.2	53.6	48.7
AEI (%)	0.0	0.0	45.7
Dominant Functional Group(s)	Herbivores (66.7%)	Predators (77.1%)	Saprophages (64.4%) and Detritivores (34.8%)
Shannon Diversity (H')	2.454 (highest)	2.253	2.032 (lowest)
Community Evenness (E)	0.762 (highest)	0.683	0.717
Simpson Dominance (C)	0.137 (lowest)	0.213 (highest)	0.176
Key Environmental Drivers	Higher temperature, moderate light	Moderate temperature and light	High light, high wind, low temperature
Invasion Risk Classification	Low-risk invasion zone	Transitional invasion zone	High-risk invasion zone
Rationale	Low invasion pressure, high diversity and evenness, minimal expansion.	High RII but no elevational expansion; early functional shift toward predators; moderate diversity	High RII and AEI; strong functional homogenization toward decomposers; reduced diversity and high dominance

Note: RII and AEI are primary indicators of invasion intensity and expansion. Functional homogenization (shift toward saprophages/detritivores) is a key marker of high invasion risk. Environmental drivers support invasion success in highlands (high light, open habitats). Management implication: Highland zones require priority intervention; mid-elevation zones are critical for early detection and prevention

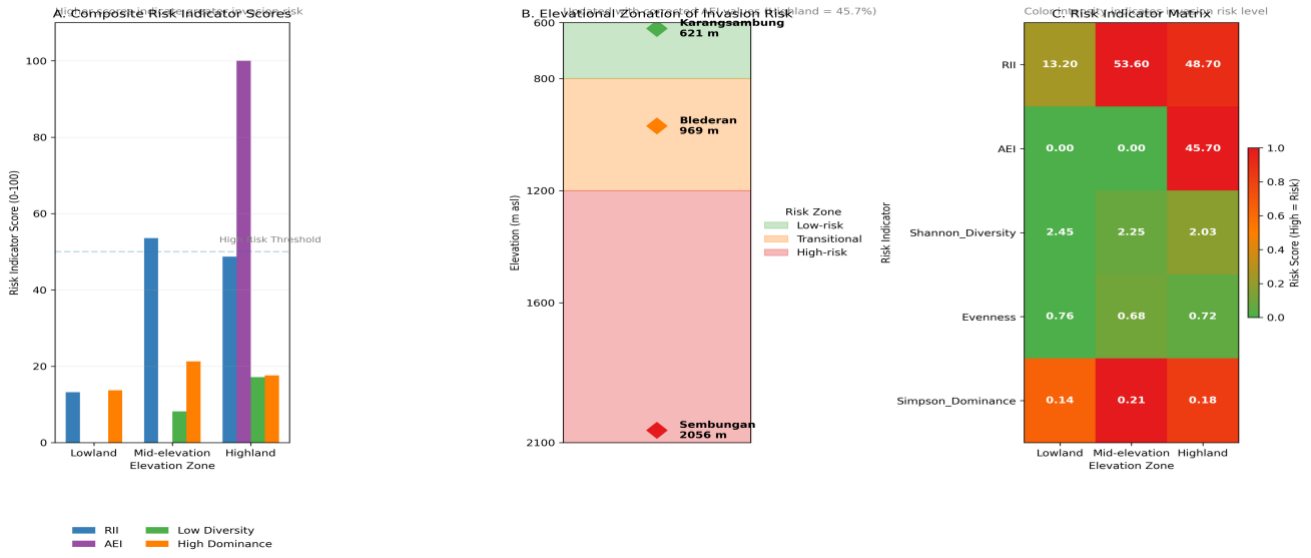

Figure 10. Identification of invasion-risk zones along the elevational agricultural gradient

Mid-elevation agroecosystems (Blederan, 969 m) emerged as transitional invasion zones with the highest RII (53.6%) but AEI = 0% (Table 10). These areas exhibited early functional reorganization toward predator dominance (77.1% of invasive individuals), moderate diversity (H′ = 2.253), and the highest Simpson dominance (C = 0.213). The coexistence of invasive taxa such as *P. flavescens* (RII contribution: 38.40%) and resident species indicates that mid-elevation systems represent critical gateways where invasion trajectories may be redirected through management intervention (Figure 10).

Highland agroecosystems (Sembungan, 2056 m) were identified as high-risk invasion zones, combining moderately high RII (48.7%) with positive mean AEI (45.7%), pronounced functional homogenization (saprophages + detritivores: 99.2%), and community simplification reflected by the lowest Shannon diversity (2.032) (Table 10). Invasive taxa such as *M. domestica* and *L. simplex* numerically dominated highland assemblages, whereas detectable upslope expansion (AEI = 38.7-59.6%) was restricted to specific taxa, most prominently *L. simplex*. Environmental conditions characterized by high light intensity (strongly correlated with AEI, r = +0.99), habitat openness, and reduced biotic resistance further amplified invasion risk (Figure 10). Zoning analysis demonstrates that invasion risk in tropical agricultural landscapes is spatially heterogeneous and elevation-dependent, providing an empirical basis for prioritizing invasion monitoring and management actions across mountain agroecosystems.

Discussion

Altitudinal gradients as invasion filters rather than biodiversity gradients

Altitudinal gradients are traditionally interpreted as biodiversity gradients shaped by climatic constraints, productivity, and habitat heterogeneity (Rahbek 1995; Hodkinson 2005). The results of this study, however, suggest that within the tropical agricultural landscapes of Wonosobo, elevation may function more prominently as an invasion filter than as a simple determinant of species richness. Along the Wonosobo gradient, increasing elevation was associated with strengthened invasion dominance, higher Relative Invasiveness Index (RII) values, and pronounced upslope expansion signals, while overall species richness declined (Table 9). This contrasting pattern indicates that elevational gradients can regulate invasion processes through selective filtering, even as taxonomic diversity decreases.

This invasion-filtering role arises from the interaction between abiotic stress and anthropogenic habitat modification. While lower temperatures and increased wind exposure at higher elevations are often assumed to constrain insect colonization, agricultural practices such as canopy opening, organic matter accumulation, and reduced structural complexity may counteract these constraints. Similar patterns have been reported in tropical and subtropical agroecosystems, where disturbance-tolerant insects exploit open highland environments despite climatic harshness (Davis et al. 2000; Pauchard et al. 2009; Seebens et al. 2017). In such systems, elevation does not act as a strict barrier but instead filters species based on ecological plasticity and disturbance tolerance.

Comparative studies from mountain regions in Southeast Asia, East Africa, and the Andes indicate that invasive insects and other arthropods increasingly penetrate higher elevations under conditions of land-use intensification and climate variability (Lenoir et al. 2008; Seipel et al. 2012; Alexander et al. 2015). These findings align with the observed dominance of synanthropic and saprophagous taxa at higher elevations in Wonosobo, suggesting that invasion filters favor generalist strategies over specialized adaptations. Consequently, elevation-mediated invasion filtering leads to functional homogenization and dominance amplification rather than to the maintenance of diverse assemblages.

Reframing altitudinal gradients as invasion filters rather than biodiversity gradients has important implications for invasion ecology in tropical agroecosystems. It emphasizes that invasion risk may intensify upslope even where overall species richness declines, challenging the assumption that high-elevation systems are inherently resistant to biological invasions. This perspective provides a more accurate ecological interpretation of invasion dynamics in mountain agricultural landscapes undergoing rapid environmental and land-use change.

Upslope expansion and early warning signals of mountain invasion

Upslope expansion of insects along altitudinal gradients represents one of the clearest early warning signals of emerging biological invasions in mountain ecosystems. In this study, elevated Altitudinal Expansion Index (AEI) values among several invasive and potentially invasive taxa indicate that insect distributions in the Wonosobo agricultural landscape are extending beyond historically documented elevational limits. Such expansion reflects a dynamic invasion process rather than stochastic dispersal, particularly when combined with consistent spatial occurrence and increasing dominance at higher elevations.

Mountain ecosystems were long considered refugia from biological invasions due to low temperatures, strong environmental filtering, and reduced propagule pressure. However, recent studies increasingly challenge this assumption, showing that land-use change, agricultural intensification, and climate variability can facilitate upslope invasion across diverse taxa (Lenoir et al. 2008; Pauchard et al. 2009; Alexander et al. 2015; Seebens et al. 2017). Insects, owing to their high dispersal capacity and rapid population turnover, are especially responsive to such changes. The detection of upslope expansion in synanthropic and saprophagous taxa in Wonosobo aligns with reports from tropical mountain agroecosystems in Africa, South America, and Southeast Asia, where invasive insects increasingly colonize higher elevations.

The application of AEI in this study provides a quantitative framework for identifying early-stage invasion processes before they manifest as overwhelming dominance or ecological damage. Taxa exhibiting high AEI values but moderate RII values may represent incipient invaders whose expansion is underway but whose impacts

are not yet fully realized. Similar early-warning approaches have been advocated in invasion ecology to prioritize monitoring and intervention efforts (Parker et al. 1999; Seebens et al. 2017). Importantly, AEI captures spatial displacement independently of abundance, allowing detection of expansion even in relatively low-density populations.

From a management perspective, recognizing upslope expansion as an early warning signal is critical for mountain agroecosystems. Once invasive insects establish and dominate high-elevation systems, eradication becomes increasingly difficult. Therefore, integrating elevational expansion metrics such as AEI into routine monitoring may enhance the capacity to anticipate and mitigate future invasion risks under ongoing environmental change.

Functional homogenization under increasing invasion pressure

Functional homogenization is a hallmark outcome of biological invasions, particularly in disturbed agroecosystems where environmental filtering favors generalist and disturbance-tolerant taxa. The results of this study demonstrate that increasing invasion intensity along the elevational gradient in Wonosobo is accompanied by a marked shift in functional composition, characterized by the dominance of saprophagous and other generalist functional groups and the decline of regulation-oriented taxa such as predators and pollinators. This pattern indicates that invasion processes restructure communities not only taxonomically but also functionally.

Similar functional shifts have been widely reported in invaded agricultural and semi-natural systems, where invasive insects disproportionately contribute to decomposition and herbivory at the expense of trophic regulation (Davis et al. 2000; Blackburn et al. 2011; Seebens et al. 2017). Studies from tropical coffee agroforests, highland vegetable systems, and temperate croplands show that invasion-driven dominance of generalist taxa often leads to reduced functional redundancy and weakened ecosystem resilience (Philpott et al. 2008; Perfecto and Vandermeer 2010; Tscharntke et al. 2012). The strong association between high RII values and functional skewness observed in Wonosobo aligns with these findings and underscores the ecological significance of invasion pressure beyond species replacement.

Functional homogenization was most pronounced in highland agroecosystems, where upslope expansion and dominance amplification coincided. These systems exhibited simplified functional profiles dominated by saprophagous and detritivorous taxa, reflecting the combined influence of habitat openness, organic matter accumulation, and reduced biotic resistance. Comparable patterns have been documented in mountain agricultural landscapes undergoing intensification, where high-elevation environments increasingly resemble lowland disturbed systems in terms of functional composition (Alexander et al. 2015; Guo et al. 2018).

Importantly, functional homogenization under invasion pressure has cascading implications for ecosystem services. The decline of predatory and pollinating taxa may reduce biological control and pollination efficiency, increasing reliance on chemical inputs and further reinforcing disturbance-driven invasion loops (Tscharntke et al. 2012; Seebens et al. 2017). In this context, the observed functional reorganization in Wonosobo represents not only an ecological shift but also a warning signal of declining agroecosystem sustainability. Addressing invasion-driven functional homogenization, therefore, requires management strategies that restore structural complexity and support functionally diverse assemblages.

Microclimatic mediation of invasion success in tropical agroecosystems

Microclimatic conditions play a central mediating role in determining invasion success within tropical agroecosystems, particularly along altitudinal gradients where abiotic stress and habitat modification interact. Results from this study indicate that invasion intensity and elevational expansion are closely associated with microclimatic drivers such as temperature, light intensity, and wind exposure. Rather than acting as direct constraints, these factors modulate invasion processes by influencing insect physiology, dispersal behavior, and habitat suitability.

High light intensity and habitat openness emerged as key facilitators of invasion dominance and upslope expansion in Wonosobo. Open agricultural fields at higher elevations reduce canopy buffering, leading to increased radiation and microclimatic variability that favor disturbance-tolerant and synanthropic insects. Similar mechanisms have been reported in tropical and subtropical agroecosystems, where increased light availability enhances flight activity, reproductive output, and colonization success of invasive insects (Hodkinson 2005; Pauchard et al. 2009; Guo et al. 2018). These conditions may compensate for lower temperatures typically associated with higher elevations, effectively relaxing climatic barriers to invasion.

Temperature gradients also played a significant role in mediating invasion patterns. Although lower temperatures at higher elevations can limit development rates of many insects, taxa exhibiting high AEI values appear to possess broad thermal tolerance or behavioral adaptations that enable persistence under cooler conditions. Comparable upslope shifts linked to thermal adaptation have been documented in mountain insects worldwide, particularly under scenarios of climate variability and warming (Lenoir et al. 2008; Alexander et al. 2015). In agricultural contexts, microclimatic heterogeneity generated by crop structure and management practices further modifies these thermal effects, creating localized refugia for invasive taxa.

Wind exposure, while generally considered a dispersal barrier, may also facilitate passive transport of lightweight or highly mobile insects across elevational zones. Studies have shown that wind-assisted dispersal can contribute to rapid range expansion in agricultural pests and synanthropic insects (Liebhold et al. 2012). Collectively, these findings highlight that microclimate mediates invasion success not through single-factor effects but via complex interactions that reshape invasion filters along tropical mountain agroecosystems.

Mid-elevation agroecosystems as transitional invasion zones

Mid-elevation agroecosystems represent critical transitional zones in invasion dynamics, functioning as ecological gateways where invasive and range-expanding insects accumulate before achieving dominance at higher elevations. In the Wonosobo agricultural landscape, mid-elevation systems exhibited intermediate values of invasion intensity (RII), detectable elevational expansion signals (AEI), and early functional reorganization. These characteristics suggest that mid-elevation environments facilitate the initial establishment and amplification of invasive taxa, rather than serving merely as passive conduits between lowland and highland systems.

The transitional role of mid-elevation zones has been documented across diverse mountain agroecosystems, where moderate climatic stress, heterogeneous land use, and intermediate disturbance levels create conditions favorable for invasion establishment (Davis et al. 2000). Such environments often combine sufficient propagule pressure from lowlands with reduced biotic resistance compared to intact highland ecosystems, allowing invasive taxa to expand spatially and adapt to novel conditions. Studies from tropical coffee agroforests and vegetable production systems have similarly identified mid-elevation belts as invasion hotspots and stepping stones for upslope expansion (Philpott et al. 2008; Perfecto and Vandermeer 2010; Alexander et al. 2015).

In Wonosobo, mid-elevation agroecosystems supported a mixture of resident and expanding taxa, reflecting functional and compositional overlap with both lowland and highland assemblages. This overlap likely enhances invasion success by providing ecological continuity and reducing dispersal barriers. Moreover, agricultural management practices at mid-elevation as mixed cropping, moderate canopy cover, and organic input use-may inadvertently promote invasion by increasing habitat heterogeneity while maintaining sufficient disturbance (Tscharntke et al. 2012; Guo et al. 2018).

From a management perspective, recognizing mid-elevation agroecosystems as transitional invasion zones is crucial. Interventions targeting these zones may prevent the progression of invasion fronts toward high-risk highland systems. Monitoring invasion indices and functional shifts at mid-elevation can therefore provide early warning signals and strategic entry points for invasion mitigation before dominance amplification occurs at higher elevations.

Implications for agroecosystem resilience and biological regulation

The observed increase in invasion intensity and functional homogenization along the elevational gradient has important implications for agroecosystem resilience and the maintenance of biological regulation. Resilience in agricultural systems is closely linked to functional diversity, redundancy, and the presence of regulation-oriented taxa such as predators and parasitoids that suppress pest populations. In this study, high invasion pressure-particularly in highland and transitional mid-elevation systems-was associated with reduced functional balance and increased dominance of saprophagous and generalist taxa, suggesting a weakening of intrinsic regulatory mechanisms.

Invasion-driven dominance can undermine biological regulation by displacing or suppressing native predators and parasitoids through competition, habitat alteration, or trophic decoupling. Similar outcomes have been reported in invaded agroecosystems worldwide, where increases in invasive insects correlate with reduced efficacy of natural enemies and higher pest outbreak frequency (Liebhold et al. 2012; Tscharntke et al. 2012). The decline in regulation-oriented functional groups observed in Wonosobo is therefore likely to translate into reduced stability of pest control services, particularly under conditions of continued disturbance and habitat simplification. Similar linkages between agricultural management practices, farmer behavior, and insect community structure have been documented in other Indonesian agroecosystems, such as cocoa plantations in West Sumatra, where management intensity influences both pest and beneficial insect assemblages (Rosalia et al. 2022). Comparable management-driven effects have also been reported from rice agroecosystems in South Sulawesi, where integrated pest management reduced *Scirpophaga innotata* populations while maintaining higher abundances of natural enemies, underscoring the role of management practices in sustaining biological control functions (Rahmawasiah et al. 2022).

Agroecosystem resilience is further compromised when invasion processes interact with environmental stressors such as climatic variability and land-use intensification. In mountain agricultural landscapes, reduced resilience may manifest as increased sensitivity to pest invasions, yield instability, and reliance on chemical inputs. Studies from tropical and subtropical systems demonstrate that invasion-induced functional simplification can trigger feedback loops, where pesticide use further disrupts community structure and facilitates additional invasions (Perfecto and Vandermeer 2010; Tscharntke et al. 2012).

The implications extend beyond pest regulation to other ecosystem services, including pollination and nutrient cycling. Although pollinating taxa were not dominant among invasive groups, their reduced representation under high invasion pressure raises concerns about service co-decline. Maintaining agroecosystem resilience, therefore, requires strategies that counteract invasion-driven homogenization, such as increasing structural complexity, enhancing habitat heterogeneity, and supporting functionally diverse assemblages. These findings underscore that invasion dynamics should be explicitly integrated into agroecological management frameworks aimed at sustaining long-term productivity and ecological stability (Seebens et al. 2017; Altieri 2018).

Methodological contributions and analytical limitations

This study offers a methodological contribution by integrating invasion-oriented indices with environmental ordination to examine invasion dynamics along an elevational agricultural gradient. The combined use of the Relative Invasiveness Index (RII) and the Altitudinal Expansion Index (AEI) enables a process-based assessment that moves beyond traditional diversity metrics. RII

captures dominance and spatial occurrence of invasion-relevant taxa, while AEI detects spatial displacement beyond historical elevational limits, allowing early identification of expansion processes before overt ecological impacts occur. Similar index-based approaches have been advocated in invasion ecology to prioritize dominance and spread over species counts (Parker et al. 1999; Blackburn et al. 2011).

The integration of these indices with Canonical Correspondence Analysis (CCA) further strengthens inference by explicitly linking invasion patterns to environmental drivers. This multivariate framework facilitates the identification of invasion filters and amplification zones along complex gradients, an approach increasingly recommended for invasion studies in heterogeneous landscapes (Legendre and Legendre 2012; Alexander et al. 2015). By restricting analyses to invasive and potentially invasive taxa, the methodology avoids redundancy with biodiversity-focused assessments and aligns analytical resolution with the study's invasion-centered objectives.

Several limitations should be acknowledged. First, the analysis is based on a single sampling period, which constrains inference regarding the temporal dynamics of invasion. Seasonal variation may influence the abundance and detectability of invasive taxa, particularly in tropical agroecosystems with pronounced phenological cycles. Second, historical elevational baselines were derived from published literature and global databases, which may vary in spatial resolution and sampling intensity. While a conservative interpretation of AEI was applied to mitigate this uncertainty, some expansion signals may reflect gaps in historical documentation rather than recent shifts.

Finally, invasion indices such as RII and AEI are proxies for ecological impact and should not be interpreted as direct measures of ecosystem damage. Their strength lies in detecting relative patterns and early warning signals rather than quantifying absolute effects. Future studies integrating multi-season sampling, experimental validation, and direct impact assessments would further refine invasion-risk evaluation in tropical mountain agroecosystems (Liebhold et al. 2012; Seebens et al. 2017).

Management relevance and invasion-risk prioritization

The identification of invasion-risk zones along the elevational agricultural gradient of Wonosobo provides a practical foundation for invasion management and prioritization. By integrating invasion intensity (RII), elevational expansion (AEI), functional reorganization, and environmental drivers, this study moves beyond descriptive assessments and offers a risk-based framework that can inform targeted intervention. Such prioritization is essential in tropical agroecosystems, where resources for monitoring and control are often limited and management actions must be strategically allocated.

Highland agroecosystems, characterized by strong invasion dominance, pronounced functional homogenization, and consistent upslope expansion signals, should be prioritized as high-risk invasion zones. In these systems, management efforts should focus on reducing habitat openness, limiting organic waste accumulation, and restoring structural complexity to enhance biotic resistance. Similar strategies have been recommended in invaded mountain agroecosystems worldwide, where increasing habitat heterogeneity has been shown to suppress invasive taxa and stabilize community structure (Perfecto and Vandermeer 2010; Tscharntke et al. 2012; Altieri 2018).

Mid-elevation agroecosystems represent strategic intervention zones, where early invasion signals are detectable but dominance amplification has not yet fully occurred. Targeted monitoring and rapid response in these transitional zones may prevent the progression of invasion fronts toward highland systems. Early detection approaches emphasizing range expansion metrics, such as AEI, have been widely advocated as cost-effective tools for invasion management (Parker et al. 1999). In practical terms, this may include periodic monitoring of invasion-relevant taxa, adjustment of crop management practices, and promotion of landscape features that support native predators and competitors.

Lowland agroecosystems, while exhibiting lower invasion risk, remain important sources of propagule pressure. Management in these areas should aim to reduce the spread of invasive taxa through improved sanitation, regulation of organic inputs, and coordination among farmers to limit dispersal pathways. Coordinated, landscape-scale approaches are increasingly recognized as critical for effective invasion control in agricultural systems (Blackburn et al. 2011; Liebhold et al. 2012).

Overall, prioritizing invasion management based on elevation-specific risk enhances the efficiency and effectiveness of intervention strategies. By explicitly linking ecological indicators with management relevance, this study provides a scalable framework for invasion-risk prioritization in tropical mountain agroecosystems under ongoing environmental and land-use change.

In conclusion, this study demonstrates that invasion dynamics in tropical agricultural landscapes of Wonosobo are strongly structured by elevation and associated microclimatic conditions. Of the 692 insect individuals recorded, 295 individuals (42.6%) belonged to nine invasive or potentially invasive taxa, indicating substantial invasion pressure across the landscape. Invasion intensity, quantified using the Relative Invasiveness Index (RII), peaked at mid-elevation systems (53.6%), followed by highland systems (48.7%), and was lowest in lowland systems (13.2%), confirming that invasion dominance does not increase linearly with altitude. Elevational range expansion, assessed using the Altitudinal Expansion Index (AEI), was detected exclusively in highland agroecosystems, with mean AEI values of 45.7% and a range of 38.7-59.6%. Detectable upslope expansion was restricted to specific saprophagous Diptera, most prominently *Leucostoma simplex*, which was recorded up to 856 m above its historically documented upper elevational limit. Along the elevational gradient, functional composition shifted from herbivore-dominated assemblages in lowland systems to predator-dominated assemblages at mid-elevation, and ultimately to saprophage–detritivore-dominated assemblages at high elevation, indicating functional homogenization under increasing invasion pressure. Environmental analyses

identified elevation and light intensity as primary drivers of upslope expansion, whereas temperature and wind exposure were more closely associated with invasion dominance. Overall, elevational gradients in tropical agricultural landscapes function as invasion filters rather than biodiversity gradients, with mid-elevation systems acting as transitional invasion hotspots and highland systems representing high-risk zones for invasion-driven community simplification.

ACKNOWLEDGEMENTS

We would like to thank local farmers in Wonosobo District, Central Java, Indonesia, for their cooperation and support during field sampling.

REFERENCES

Adnan BA, Kurniawati T, Trianto M. 2024. Diversity and abundance of soil arthropods in the terrestrial area of Situ Lengkong Panjalu, West Java, Indonesia. Jurnal Biodjati 9 (1): 66-79. DOI: 10.15575/biodjati.v9i1.33980.

Alexander JM, Diez JM, Levine JM. 2015. Novel competitors shape species' responses to climate change. Nature 525: 515-518. DOI: 10.1038/nature14952.

Altieri MA. 2018. Agroecology: The science of sustainable agriculture. CRC Press, Boca Raton. DOI: 10.1201/9780429495465.

Andriani DM, Setianingsih M, Susilo, Metiani, Darma AP. 2017. Keanekaragaman dan pola penyebaran insekta permukaan tanah di Resort Cisarua Taman Nasional Gunung Gede Pangrango Jawa Barat. Jurnal Pendidikan Biologi dan Biosains 1 (1): 24-30. DOI: 10.29405/bioeduscience/24-30111179. [Indonesian]

Bauer T. 2024. *Coccinella septempunctata* (seven-spotted lady beetle). Animal Diversity Web, University of Michigan Museum of Zoology. https://animaldiversity.org/accounts/Coccinella_septempunctata/

Belioka MP, Achilias DS. 2024. The effect of weathering conditions in combination with natural phenomena/disasters on microplastics' transport from aquatic environments to agricultural soils. Microplastics 3 (3):518-538. DOI: 10.3390/microplastics3030033.

Blackburn TM, Pyšek P, Bacher S, Carlton JT, Duncan RP, Jarošík V, Wilson JRU, Richardson DM. 2011. A proposed unified framework for biological invasions. Trends Ecol Evol 26 (7): 333-339. DOI: 10.1016/j.tree.2011.03.023.

CABI. 2024. Invasive Species Compendium. Wallingford, UK: CAB International. Available at: https://www.cabidigitallibrary.org.

CBD [Convention on Biological Diversity]. 2002. Guiding principles for the prevention, introduction, and mitigation of impacts of alien species that threaten ecosystems, habitats, and species. Convention on Biological Diversity, COP 6 Decision VI/23.

CBD [Convention on Biological Diversity]. 2023. Indonesia - country profile: biodiversity facts. Convention on Biological Diversity. Accessed 29 Nov 2025. https://www.cbd.int/countries/profile

Corbet PS. 1999. Dragonflies: Behavior and Ecology of Odonata. Cornell University Press, Ithaca.

Crosskey RW. 1976. A taxonomic conspectus of the Tachinidae (Diptera) of the Oriental Region. Bulletin of the British Museum (Natural History), Entomology Series, Supplement 26: 1-357.

Davis MA, Grime JP, Thompson K. 2000. Fluctuating resources in plant communities: A general theory of invasibility. J Ecol 88: 528-534. DOI: 10.1046/j.1365-2745.2000.00473.x.

Fajarfika R. 2020. Keanekaragaman dan dominansi serangga pada agroekosistem tanaman tomat (*Lycopersicum esculentum* Mill.). Jurnal Agro Wiralodra 3 (2): 68-73. DOI: 10.31943/agrowiralodra.v3i2.51. [Indonesian]

Gani RA, Purwanto S, Sukarman S. 2021. Karakteristik tanah vulkanik di Kabupaten Wonosobo dan pengelolaannya untuk pertanian. Jurnal Tanah dan Iklim 45 (1):1-11. DOI: 10.21082/jti.v45n1. [Indonesian]

GBIF. 2024. Global Biodiversity Information Facility. https://www.gbif.org.

Gul S, ur Rehman F, Taj MK, Gul S, Khan MA, Taj I, Khan S. 2024. The house flies, *Musca domestica*, as a mechanical vector and its management to control in Quetta City, Balochistan. Pak-Euro J Med Life Sci 7 (3): 437-448. DOI: 10.31580/87hj0c23.

He Q, Jiang X, Zhang Y. 2024. The gains and losses of cultivated land requisition-compensation balance: Analysis of spatiotemporal trade-offs and synergies in ecosystem services using Hubei Province as a case study. Land 13 (10): 1641. DOI: 10.3390/land13101641.

Heong KL, Aquino GB, Barrion AT. 1991. Arthropod community structures of rice ecosystems in the Philippines. Bull Entomol Res 81 (4): 407-416. DOI: 10.1017/S0007485300031977.

Hodkinson ID. 2005. Terrestrial insects along elevation gradients: Species and community responses to altitude. Biol Rev 80 (3): 489-513. DOI: 10.1017/S1464793105006767.

iNaturalist. 2024. iNaturalist.org species database. https://www.inaturalist.org.

ITIS. 2024. Integrated Taxonomic Information System. https://www.itis.gov.

Kumar P, Thakur TS, Deepika, Sharma N. 2022. Diversity studies on insect pests of high-altitudinal transitional zones of the North-western Himalayas. Nusantara Bioscience 14 (2): 203-210. DOI: 10.13057/nusbiosci/n140211.

Legendre P, Legendre L. 2012. Numerical Ecology. 3rd ed. Elsevier, Amsterdam.

Leksono AS. 2017. Ekologi Arthropoda. Universitas Brawijaya Press, Malang. [Indonesian]

Lenoir J, Gégout JC, Marquet PA, de Ruffray P, Brisse H. 2008. A significant upward shift in plant species optimum elevation during the 20th century. Science 320: 1768-1771. DOI: 10.1126/science.1156831.

Liebhold AM, Brockerhoff EG, Garrett LJ, Parke JL, Britton KO. 2012. Live plant imports: The major pathway for forest insect and pathogen invasions of the US. Front Ecol Environ 10:135-143. DOI: 10.1890/110198.

Lukvitasari L, Triwidodo H, Rizali A, Buchori D. 2021. Pengaruh lokasi terhadap serangan lalat puru *Cecidochares connexa* (Macquart) pada tumbuhan eksotik invasif *Chromolaena odorata* (L.) King and Robinson dan interaksinya dengan komunitas serangga lokal. Jurnal Entomologi Indonesia 18 (2):127-137. DOI: 10.5994/jei.18.2.127. [Indonesian]

Nault LR. 1990. Evolution of an insect pest: Maize and the corn planthopper, *Peregrinus maidis* (Hemiptera: Delphacidae). American Entomologist 36: 165-175.

Parker IM, Simberloff D, Lonsdale WM, Goodell K, Wonham M, Kareiva PM, Williamson MH, Von Holle B, Moyle PB, Byers JE, Goldwasser L. 1999. Impact: Toward a framework for understanding the ecological effects of invaders. Biological Invasions 1: 3-19. DOI: 10.1023/A:1010034312781.

Pauchard A, Kueffer C, Dietz H, Daehler CC, Alexander J, Edwards PJ, Arévalo JR, Cavieres LA, Guisan A, Haider S. 2009. Ain't no mountain high enough: Plant invasions reaching new elevations. Frontiers in Ecology and the Environment 7 (9): 479-486. DOI: 10.1890/080072.

Perfecto I, Vandermeer J. 2010. The agroecological matrix as an alternative to the land-sparing/agriculture intensification model. Proc Nat Acad Sci USA 107: 5786-5791. DOI: 10.1073/pnas.0905455107.

Philpott SM, Arendt WJ, Armbrecht I, et al. 2008. Biodiversity loss in Latin American coffee landscapes: Review of the evidence on ants, birds, and trees. Conserv Biol 22 (5): 1093-1105. DOI: 10.1111/j.1523-1739.2008.01029.x.

Pont AC. 1977. Family Muscidae. In: Delfinado MD, Hardy DE (eds). A Catalogue of the Diptera of the Oriental Region. Vol. 3. Suborder Cyclorrhapha (excluding Division Aschiza). University Press of Hawaii, Honolulu.

Quinn GP, Keough MJ. 2002. Experimental Design and Data Analysis for Biologists. Cambridge Univ Press, Cambridge.

Rahbek C. 1995. The elevational gradient of species richness: A uniform pattern? Ecography 18: 200-205. DOI: 10.1111/j.1600-0587.1995.tb00341.x.

Rahmadhani SE, Salsabila S, Andrianto R, Rosyida SH, Ainia Q, Dewangga A, Setyawan AD. 2025. Diversity and potential invasiveness of insects in agricultural landscapes of Wonosobo, Central Java, Indonesia. Asian J Agric 9: 663-677. DOI: 10.13057/asianjagric/g090234.

Rahmawasiah, Abadi AL, Mudjiono G, Rizali A. 2022. The effect of integrated pest management on *Scirpophaga innotata* population and

natural enemies on rice fields in South Sulawesi, Indonesia. Biodiversitas 23 (9): 4510-4516. DOI: 10.13057/biodiv/d230917.

Rentz DCF. 1996. Grasshopper Country: The Abundant Orthopteroid Insects of Australia. University of New South Wales Press, Sydney, Australia.

Richardson DM, Pyšek P, Rejmánek M, Barbour MG, Panetta FD, West CJ. 2000. Naturalization and invasion of alien plants: Concepts and definitions. Divers Distrib 6: 93-107. DOI: 10.1046/j.1472-4642.2000.00083.x.

Rosalia S, Yonariza, Syahrawati M. 2022. Effect of farmers' behavior in cocoa management on insect diversity in Salayo Cocoa Plantation, West Sumatra, Indonesia. Biodiversitas 23 (10): 5064-5073. DOI: 10.13057/biodiv/d231013.

Seebens H, Blackburn TM, Dyer EE, Genovesi P, Hulme PE, Jeschke JM, Pagad S, Pyšek P, Winter M, Arianoutsou M, et al. 2017. No saturation in the accumulation of alien species worldwide. Nat Commun 8:14435. DOI: 10.1038/ncomms14435.

Seipel T, Kueffer C, Rew LJ, Daehler CC, Pauchard A, Naylor BJ, Alexander JM, Edwards PJ, Parks CG, Jakobs G, McDougall K, Walsh N. 2012. Processes at multiple scales affect the richness and similarity of non-native plant species in mountains around the world. Global Ecol Biogeography 21: 236-246. DOI: 10.1111/j.1466-8238.2011.00664.x

Shannon CE, Wiener W. 1949. The Mathematical Theory of Communication. Univ Illinois Press, Urbana.

Skidmore P. 1985. The Biology of the Muscidae of the World. Series Entomologica. Springer, Dordrecht.

Sofian M, Haryanto H, Fauzi MT. 2023. Keragaman serangga hama dan musuh alami pada tanaman cabai rawit (*Capsicum frutescens* L.) di Kecamatan Labuhan Haji Kabupaten Lombok Timur. Jurnal Ilmiah Mahasiswa Agrokomplek 2: 349-361. DOI: 10.29303/jima.v2i3.3564. [Indonesian]

Tscharntke T, Klein AM, Kruess A, Steffan-Dewenter I, Thies C. 2005. Landscape perspectives on agricultural intensification and biodiversity-ecosystem service management. Ecol Lett 8 (8): 857-874. DOI: 10.1111/j.1461-0248.2005.00782.x.

Vincent M. 2024. *Forficula auricularia* (European earwig). Animal Diversity Web, University of Michigan Museum of Zoology. https://animaldiversity.org/accounts/Forficula_auricularia/

Zumpt F. 1965. Myiasis in Man and Animals in the Old World. Butterworths, London, UK.